kOMUNIKÁCIE
COMMUNICATIONS

A - OPERATION AND ECONOMICS

ON-SITE TRAFFIC MANAGEMENT EVALUATION AND PROPOSALS TO IMPROVE SAFETY OF ACCESS TO WORKPLACES A125
J. Paľo, O. Stopka

ELECTRIFICATION OF PUBLIC TRANSPORT BUS FLEET: IDENTIFICATION OF BUSINESS AND FINANCING MODELS A137
G. Dydkowski, J. Gnap, A. Urbanek

FUZZY-LOGIC APPROACH TO ESTIMATE THE PASSENGERS' PREFERENCE WHEN CHOOSING A BUS LINE WITHIN THE PUBLIC TRANSPORT SYSTEM A150
V. Naumov, B. Zhamanbayev, D. Agabekova, Z. Zhanbirov, I. Taran

EXTERNAL ECONOMIC EFFECTS OF AIR TRANSPORT DEVELOPMENT DUE TO THE LIBERALIZATION A158
O. Ovsak, M. Vysotska

IMPROVEMENT OF THE LOGISTIC PROCESSES USING THE REVERSE LOGISTICS CONCEPT A174
Z. Łukasik, A. Kuśmińska-Fijałkowska, S. Olszańska

THE IMPACT OF INFRASTRUCTURE SPENDING ON ECONOMIC GROWTH: A CASE STUDY OF INDONESIA A184
M. Syadullah, D. Setyawan

OPTIMIZING THE CHOICE OF MEANS OF TRANSPORT USING OPERATIONAL RESEARCH A193
P. Gorzelanczyk, H. Tylicki, T. Kalina, M. Jurkovič

B - MECHANICAL ENGINEERING

A DATA-DRIVEN METHOD FOR VEHICLE SPEED ESTIMATION B165
A. Bonfitto, S. Feraco

DIAGNOSTICS OF THE ON-VEHICLE SHOCK ABSORBER TESTING B178
M. Guzek, P. Zdanowicz

LABORATORY TESTS OF THE CONTROL OF THE CHILD SEATS USING METHOD FOR THE VIBRATION COMFORT OF CHILDREN TRANSPORTED IN THEM B187
A. Zuska, E. Szumska

ASSESSMENT OF THE CONSTRUCTIONALITY OF THE STRUCTURE IN THE ASSEMBLY PROCESSES B200
J. Matuszek, T. Seneta, Ľ. Dulina, E. Bigošová

FUZZY LOGIC METHOD FOR THE SPEED ESTIMATION IN ALL-WHEEL DRIVE ELECTRIC RACING VEHICLES B117
A. Bonfitto, S. Feraco, M. Rossini, F. Carlomagno

RESEARCH ON CURVILINEAR MOTION OF AUTOMOBILE WITH THE APPLICATION OF ON-BOARD CAN BUS DATA B211
H. Sar, M. Brukalski, K. Rokicki

THEORETICAL AND EXPERIMENTAL STUDY OF OPERATION OF THE TANK EQUIPMENT FOR ULTRASONIC PURIFICATION OF THE INTERNAL COMBUSTION ENGINE EXHAUST GASES B219
A. Kadyrov, A. Ganyukov, I. Pak, B. Suleyev, K. Balabekova

NUMERICAL SIMULATION OF TEMPERATURE DISTRIBUTION IN THE GAS TURBINE BLADE B227
D. Jakubek

DYNAMIC BEHAVIOR OF THE FULL-CAR MODEL IN THE J-TURN MANEUVER BY CONSIDERING THE ENGINE GYROSCOPIC EFFECTS B237
A. Shahabi, A. H. Kazemian, S. Farahat, F. Sarhaddi

C - ELECTRICAL ENGINEERING

DRONE CONTROL USING THE COUPLING OF THE PID CONTROLLER AND GENETIC ALGORITHM C75
M. Elajrami, Z. Satla, K. Bendine

E - MANAGEMENT SCIENCE AND INFORMATICS

RTK KINEMATIC POSITIONING ACCURACY WITH DOUBLE PHASE DIFFERENCE OF SIS GNSS SIGNALS E35
L. Setlak, R. Kowalik

E1 SIGNAL PROCESSING OF THE GALILEO SYSTEM IN THE NAVIGATION RECEIVER E46
L. Setlak, R. Kowalik

F - SAFETY AND SECURITY ENGINEERING

STUDY ON A BRAIN-CONTROLLED PNEUMATIC ACTUATOR TO ASSIST EMERGENCY BRAKING OF A VEHICLE F49
R. Dindorf, J. Takosoglu, P. Wos

ANALYSIS OF VEHICLE MOVING PARAMETERS IN VARIOUS ROAD CONDITIONS F58
R. Jurecki, T. Stańczyk

CLASSIFICATION OF THE SOCIO-PSYCHOLOGICAL ASPECTS OF PROTECTING SOFT TARGETS: A CASE STUDY FOR EVACUATION OF THE RAILWAY TERMINALS F71
A. Šplíchalová, T. Karásek, T. Apeltauer

THE METHODOLOGY TO EVALUATE A RESCUE AND TRAINING PHANTOM FOR THE ROAD RESCUING ORGANIZED BY POLICE OFFICERS AS EXEMPLIFIED BY CRASH KELLY F83
P. Gromek, M. Nepelski

ASSESSMENT OF STATIC RESILIENCE OF OBJECTS IN THE RAIL TRANSPORT F96
Z. Dvořák, N. Chovančíková, K. Hoterová, M. Szatmári

TRANSPORT RISK IDENTIFICATION AND ASSESSMENT F109
J. Kubáňová, I. Kubasáková

PREVENTION OF MAJOR ACCIDENTS OF MOBILE RISK SOURCES F116
K. Mäkká, K. Kampová, J. Dworzecki

ON-SITE TRAFFIC MANAGEMENT EVALUATION AND PROPOSALS TO IMPROVE SAFETY OF ACCESS TO WORKPLACES

Jozef Paľo[1,*], Ondrej Stopka[2]

[1]Department of Road and Urban Transport, Faculty of Operation and Economics of Transport and Communications, University of Zilina, Zilina, Slovak Republic
[2]Department of Transport and Logistics, Institute of Technology and Business in Ceske Budejovice, Ceske Budejovice, Czech Republic

*E-mail of corresponding author: jozef.palo@fpedas.uniza.sk

Resume
Transport is a phenomenon currently used in almost every sector. That is why attention is to be paid to transport safety, which should not only be addressed in relation to situation in cities or urban areas, but it is also necessary to deal with transport safety in larger enterprises where motor traffic encounters non-motorized traffic. The authors elaborated a similar research study. The introductory two sections analyze the current situation in terms of identifying bottlenecks of the traffic organization on the industrial site and possible separation of motor from non-motorized traffic to ensure safe access to workplaces and improve safety of transport on the site. In the most important part of the study, the obtained results are presented, wherein the "load" of the individual entry and exit points is specified. Thereafter, based on the acquired data, particular solutions related to transport safety with appropriate discussion are proposed.

Article info
Received 17 September 2020
Accepted 19 October 2020
Online 24 March 2021

Keywords:
traffic management,
transport safety,
access to workplace,
manufacturing enterprise

Available online: https://doi.org/10.26552/com.C.2021.3.A125-A136

ISSN 1335-4205 (print version)
ISSN 2585-7878 (online version)

1 Introduction

Transport safety represents a fundamental issue for any state or region and public, as well as private, authorities concerned are confronted with a problem of identifying a certain location wherein the specific safety restrictions and improvement measures are to be undertaken [1]. The very aspects associated with the three elements of transport safety; i.e. driver, vehicle, transport infrastructure and its surroundings, are often evaluated and investigated by implementing a variety of advanced information systems and technologies and have an influence on the particular consideration of transport safety and quality [2-3].

Transport safety will continue to be a crucial issue for each society, especially for l the ow-income states. The most relevant aspects affecting a road safety level and hence, may be considered to be key attributes in the context of introducing specific safety measures are as follows [4-7]:

- parameters of route (foundation, slopes, curves, gradients, designed parameters for vehicles and so forth),
- parameters of an entrance to the area concerned (access point),
- parameters of vehicles,
- infrastructure maintenance level,
- infrastructure network saturation degree,
- location visibility,
- long-term and short-term weather conditions,
- drivers and population features,
- previous statistics of drivers associated with transport safety in the given territory,
- preferences and special requirements.

Analogous topics have been addressed in a series of publications presented by numerous authors. For instance, the subject of the traffic safety in terms of social and economic aspects, such as working conditions, job strain and driving accidents, is emphasized in [8] by Useche at al. by Meszaros et al. [9] and by Malka et al. [10].

As far as another similar aspect is concerned, literature sources [11-12] deal with an issue of traffic safety systems in water transport, while Jurkovic et al. designed an advanced technology to increase navigation safety encompassing a system for monitoring the life functions of a crew member, as well as a position of the vessel towards the fairway/shore [11], whereas Wang et al. [12] tried to eliminate a risk of occupational hazards and thus improve safety conditions when strengthening hazard knowledge and enhancing safety behavior for water port employees.

This is an open access article distributed under the terms of the Creative Commons Attribution 4.0 International License (CC BY 4.0), which permits use, distribution, and reproduction in any medium, provided the original publication is properly cited. No use, distribution or reproduction is permitted which does not comply with these terms.

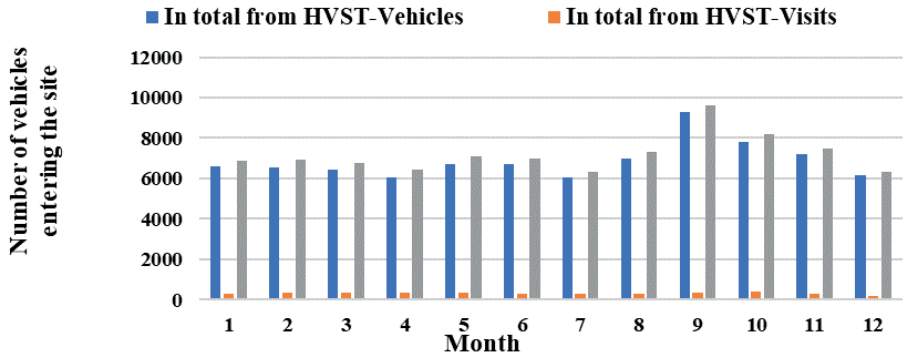


Figure 1 *Number of vehicles entering the site through the main entrance in the reference period*

Table 1 *Daily average of vehicles entering the site through the main gate (HVST-overall)*

day of the Week	Monday	Tuesday	Wednesday	Thursday	Friday	Saturday	Sunday	total daily average for 5 days of the week in the reference period
total daily average in the reference period	303.7	333.75	334.82	317.4	277.6	43.8	39.1	313.6

On the other hand, in publications [6, 13-14], a topic concerning an effect of a human factor on generating the traffic congestions is analyzed. Lizbetin and Bartuska were focused on creation of the traffic congestions, specifically on urban roads, wherein they confirm that the driver reaction (perception) time affects a number as well as an extent of such congestions [6]. In relation to manuscript [13], Kubanova and Poliakova highlighted importance of scheduling the truck-driver time, as one of the essential elements associated with the transport safety. As for Useche et al., their practical research study [14] investigates a relation between the stress-creating work conditions of bus-rapid-transport drivers and risky driving behaviors, as well as looks into whether fatigue entails a factor intermediating a relationship between these two attributes.

Even Posuniak et al. elaborated related publication, in which they presented the restraint safety systems for children (i.e. booster seats) when carrying in vehicles [15]. In particular, they conducted several experiments when utilizing child dummies under simulated traffic circumstances to better comprehend an impact on both the traffic dynamics and kinematics of the technology being applied.

And last but not least, description of different techniques for vehicle data detection used when the road traffic counting, during the largest traffic survey conducted in the Czech Republic, focused mainly on the traffic safety data, is outlined in article compiled by Hanzl et al. [16].

2 Data and methods

The objective of this manuscript is to analyze the current state on the specific industrial site regarding the traffic organization, identify potential bottlenecks in this particular regard and thereafter, propose possible scenarios in terms of separating motor from non-motorized traffic, as well as streamlining parking situation in order to secure safe access to individual workplaces and enhance transport safety on this site.

To this end, as alternative methods to be applied, following recommendations for their implementation into the examined industrial site are presented in the next sections of this research study: a) classification of roads and pathways on the site to secure better traffic management resulting in a more favorable orientation of drivers and pedestrians; b) design of a new parking area for heavy trucks to eliminate traffic jams currently emerging on the main road); c) design of new parking bays allowing vehicles to wait for handling while not obstructing the free passage of other vehicles; d) separation of road transport from pedestrians; i.e. establishment of a new pathway method for more convenient orientation of employees.

As for the access to workplace, regarding the examined enterprise, the main entrance (hereinafter referred to as HVST) is designed for employees, contractors, visitors and vehicles up to 3.5 tones. Persons enter the site through turnstiles 1 to 5 at the gate and only one person passes through in the car - the driver. The modified data set includes a breakdown of incoming vehicles into vehicles of visitors (hereinafter referred to as HVST-Visits) and other vehicles (hereinafter referred to as HVST-Vehicles) [17].

During the reference (examined) period, it was identified that about the same number of vehicles entered the site through the main entrance, which is over 6,000 vehicles per month, with a daily average of more than 200 vehicles (see Figure 1). However, these

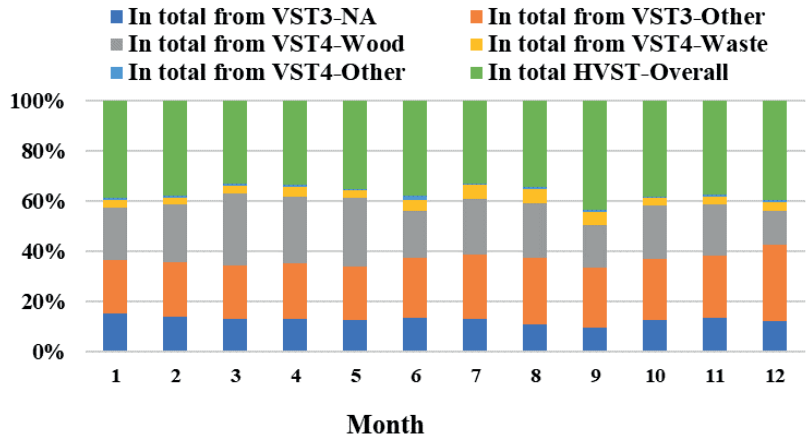


Figure 2 *Percentage of vehicles per site entrance investigated in the reference period*

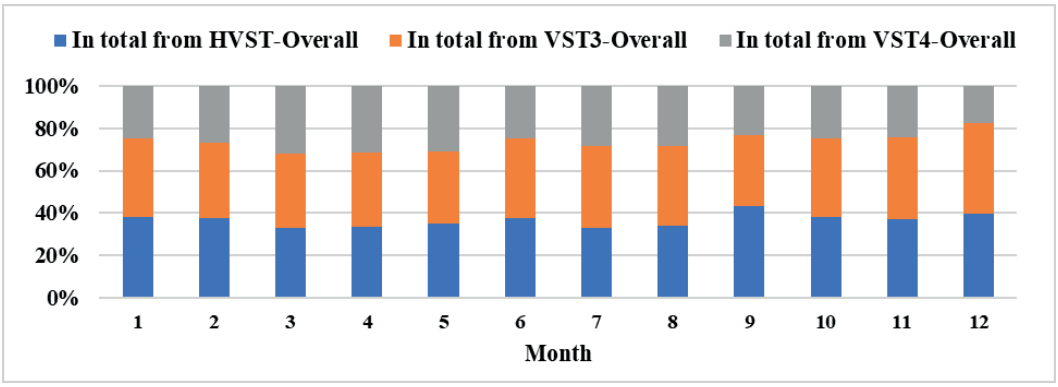


Figure 3 *Percentage of the sum of all the vehicles per site entrance investigated in the reference period*

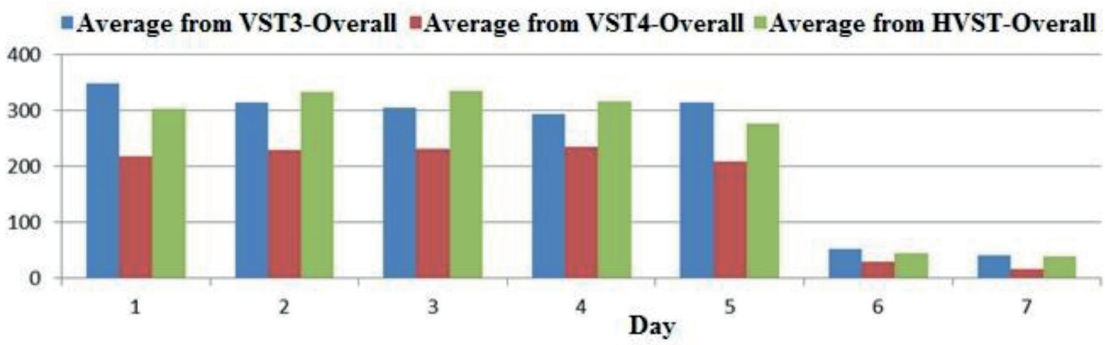


Figure 4 *Daily average of vehicles per site entrance investigated in the reference period by day*

values are affected by a significant decline in vehicles on Saturday and Sunday.

That is why the daily average of vehicles passing through the main entrance every day of the week is also provided (see Table 1). The daily average in the reference period was 300 vehicles from Monday to Friday with Tuesday and Wednesday (330 vehicles) being the busiest days and with a partial decline on Monday (300 vehicles) and especially on Friday (280 vehicles). The average on Saturday and Sunday was 40 vehicles.

In addition to the main entrance, two other entrance gates on the site, identified as entrance 3 (in figures and tables, referred to as VST3) and entrance 4 (in figures and tables, referred to as VST4) of the enterprise, were considered. Based on the processed data, Table 2 provides statistical evaluation of those entrances during the reference period [18-19]. As far as the number of vehicles during the reference period is concerned, entrance 3 with a total of 86,535 vehicles was the most occupied, followed by the main entrance with 86,347 vehicles and entrance 4 with a total of 62,820 vehicles.

The percentage of vehicles entering the site per entrance and month of the reference period is shown in Figures 2 and 3.

The overall data shows that this percentage does not even change with the day of the week [19].

The daily average of vehicles entering the site through the entrances investigated on each day of the week is shown in the following Figure 4. The average of 300 vehicles enter the site through entrance 3 and

Table 2 *Number of vehicles entering the site through the entrances investigated*

month	VST3-NA	VST3-other	VST3-overall	VST4-wood	VST4-waste	VST4-other	VST4-overall	HVST-vehicles	HVST-visits	HVST-overall
01	2,770	3,846	6,616	3,747	560	163	4,470	6,592	293	6,885
02	2,587	4,002	6,589	4,269	514	178	4,961	6,571	339	6,910
03	2,681	4,440	7,121	5,857	640	125	6,622	6,419	351	6,770
04	2,552	4,249	6,801	5,079	829	113	6,021	6,058	363	6,421
05	2,569	4,391	6,960	5,577	620	120	6,317	6,734	369	7,103
06	2,546	4,399	6,945	3,486	778	316	4,580	6,690	310	7,000
07	2,513	4,945	7,458	4,300	1,087	120	5,507	6,059	271	6,330
08	2,394	5,652	8,046	4,684	1,204	232	6,120	7,006	312	7,318
09	2,147	5,328	7,475	3,741	1,228	171	5,140	9,266	341	9,607
10	2,783	5,177	7,960	4,641	597	157	5,395	7,787	381	8,168
11	2,687	5,032	7,719	4,072	646	124	4,842	7,177	312	7,489
12	2,003	4,842	6,845	2,177	586	102	2,845	6,147	199	6,346
in total	30,232	56,303	86,535	51,630	9,289	1,921	62,820	82,506	3,841	86,347

Table 3 *Number of personnel using the access points at a distance of less than 500 m*

no.	description	distance from the main entrance in meters	number of employees using the given entrance			
			shift 1	shift 2	shift 3	shift 4
5	PM 16 - material preparation plant	100	22	10	6	6
6	channel storage system of finished goods PS 16/17	145	6	6		
1	finished goods store	200	30	11		
37	electric motor store	200	2			
8	treatment plant for PS 7 - processing machine hall	217	31	20	8	8
2	PS 1 - preparation plant	218	23	12		
7	administrative building of the timberyard + workshops	260	5	0		
10	timberyard - decortication and cutting machines ANDRITZ	409	22	11	11	
12	near mechanical workshops	477	5	0		
11	sanitation facilities	478	3	0		
13	mechanical workshops	500	23	2		
		total	172	72	25	14

the main entrance daily from Monday to Friday and the average of over 200 vehicles through entrance 4.

3 Use of the main entrances to the site by pedestrians

A breakdown of workplaces by distance from the main entrance was based on the available data [13]. Table 3 shows workplaces at a distance of less than 500 m from the main entrance - a total of 11 workplaces. Table 4 shows workplaces at a distance of 500 m to 1,000 m from the main entrance - 10 workplaces. Table 5 shows workplaces at a distance of more than 1,000 m from the main entrance - 10 workplaces. Two "unattended" workplaces and two workplaces with zero number of employees were not included in calculations. In addition, the office building (3) with the largest number of employees (300) of all the workplaces was not considered, since this building is not accessed through the main entrance [20]. In addition, the administrative building (97) was not considered, since it is used for training of contractors - the west entrance from the parking lot or the east entrance to the site for the foreign language courses.

Consequently, tabular data is presented graphically for all the shifts (see Figure 5).

Based on the analysis of the input data (number of employees, the expected financial investments, etc.), a proposal may be made to prioritize repairs/

Table 4 *Number of personnel using the access points at a distance of 500 m to 1,000 m*

no.	description	distance from the main entrance in meters	number of employees using the given entrance			
			shift 1	shift 2	shift 3	shift 4
14	mechanical maintenance workshops	550	17	6		
15	chemical store	600	1	1		
17	COV - chemical water treatment plant	650	1	1	1	
16	celpap warehouses + new cafeteria	680	5	0		
18	COV - operations building	740	32	7	7	
19	control room of the cooking plant	760	15	5		
20	administrative building of the pulp mill	900	36	2		
21	boiler house (RK1 + KB)	972	38	12	12	
27	workshops and locker room	997	4	1		
28	water treatment plant	1,000	5	2		
		total	154	37	20	0

Table 5 *Number of personnel using the access points at a distance of more than 1,000 m*

no.	description	distance from the main entrance in meters	number of employees using the given entrance			
			shift 1	shift 2	shift 3	shift 4
25	paper processing plant PM18	1,300	65	30		
26	solo packaging	1,300	25	8		
23	paper making machine hall PM 18	1,400	31	11	9	9
31	warehouses	1,400	3			
33	porter's lodge - entrance CIII	1,400	3	3		
34	finished goods store PM 18	1,400	13	6		
32	spare part store	1,500	6			
35	dock and workshop	1,550	3	0		
30	fire station - SD-pallets	1,600	17	12	4	
36	entrance gate for vehicles	1,954	4			
		total	170	70	13	9

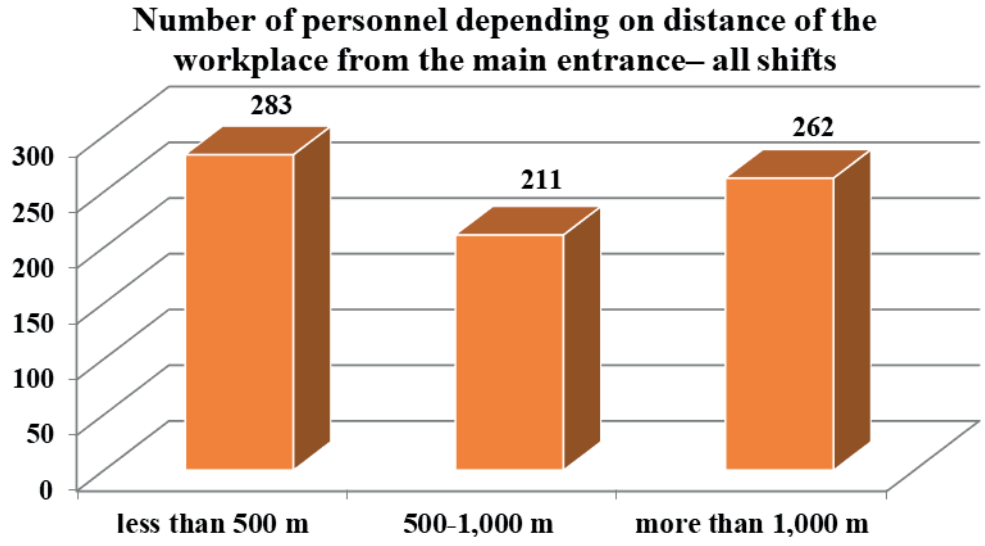


Figure 5 *Number of personnel depending on distance of the workplace from the main entrance - all shifts*

Table 6 *Workplaces with more than 20 employees*

no.	description	distance from the main entrance in meters	number of employees using the given entrance			
			shift 1	shift 2	shift 3	shift 4
25	paper processing plant PM18	1,300	65	30		
21	boiler house (RK1 + KB)	972	38	12	12	
20	administrative building of the pulp mill	900	36	2		
18	COV - operations building	740	32	7	7	
23	paper making machine hall PM 18	1,400	31	11	9	9
8	treatment plant for PS 7 - processing machine hall	217	31	20	8	8
1	finished goods store	200	30	11		
26	solo packaging	1,300	25	8		
13	mechanical workshops	500	23	2		
2	PS 1 - preparation plant	218	23	12		
10	timberyard - decortication and cutting machines ANDRITZ	409	22	11	11	

Table 7 *Number of pedestrians and vehicles moving through the main entrance and entrance 3 during week*

	pedestrians		vehicles				
day of the week	VST1 01	VST1 02	VST1 /P	VST1 /O	VST3 /P	VST3 /O	Total
1	1,135	1,070	314	314	384	359	3,576
2	1,217	1,143	319	342	371	334	3,726
3	1,253	1,195	336	349	374	356	3,863
4	1,333	1,226	345	368	303	263	3,838
5	1,085	1,056	269	263	287	273	3,233
6	578	574	39	36	48	37	1,312
7	13	52	29	32	46	29	201
total	6,614	6,316	1,651	1,704	1,813	1,651	19,749
weekly average Monday-Friday	1,204.6	1,138	316.6	327.2	343.8	317	

constructions of pavements leading to the workplaces at a distance of less than 500 m, or the most occupied roads. In the next stage, the workplaces at a distance of over 500 m, or cycling solutions for workplaces at a distance of more than 1,000 m can be provided.

4 Use of the existing roads and pavements by pedestrians

To evaluate how the existing roads and pavements are used by pedestrians, workplaces with more than 20 employees in the first shift were selected. The largest number of employees is in the PM18 Paper Processing Plant (25). There are 65 employees in the first shift and this also applies to the second shift with 30 employees as illustrated in Table 6. The most occupied part of the road accounts for 160 employees in the first shift. This road should be prioritized to take into consideration a possible construction of a separate pavement [10].

Table 6 does not include workplaces where the roads investigated are not used and workplaces with less than 20 employees in the first shift.

5 Analysis of the most occupied access points for vehicles and pedestrians

The data obtained from an analysis of the most occupied access points for vehicles and pedestrians is provided here. Persons who access the site through the main entrance are hereinafter referred to as VST1 01 and persons who exit the site through the main entrance as VST1 02 and cars entering (P) or exiting (O) the site.

Table 7 summarizes values concerning a number of pedestrians and vehicles entering and exiting the site through the main entrance and entrance 3 during one selected week. Figure 6 depicts all the values regarding a number of pedestrians and vehicles entering and exiting the site through the main entrance and entrance 3 by days [21-23].

The analysis identifies the largest number of

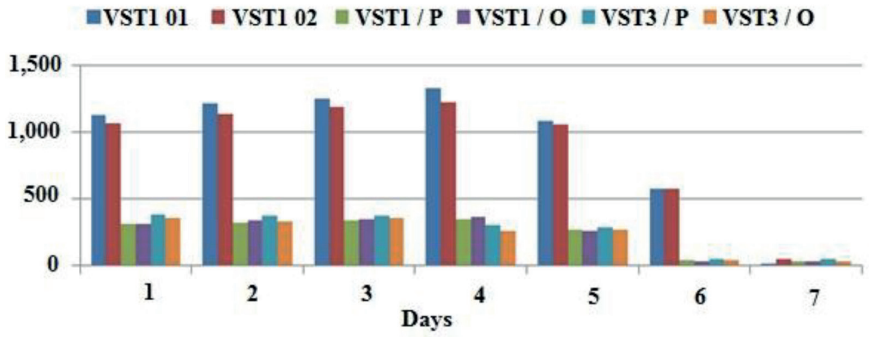


Figure 6 *Number of pedestrians and vehicles entering and exiting the site through the main entrance and entrance 3 - by days*

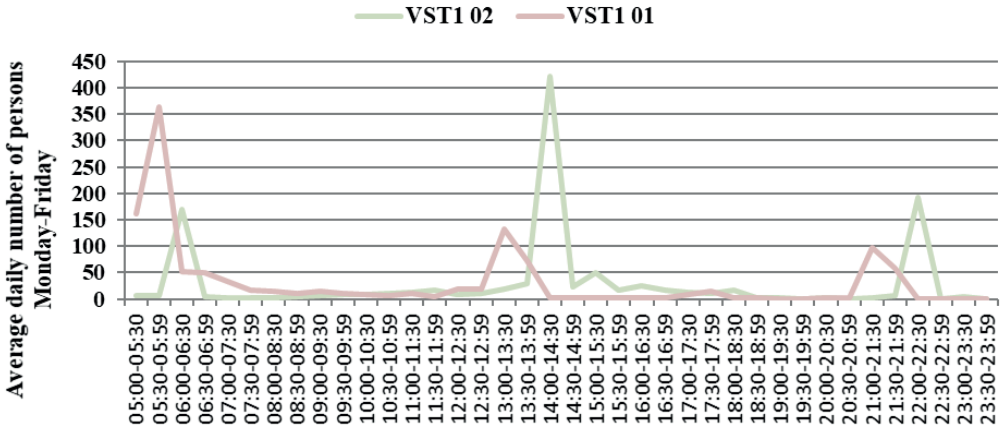


Figure 7 *Average daily number of persons entering (01) and exiting (02) the site through the main entrance from Monday to Friday*

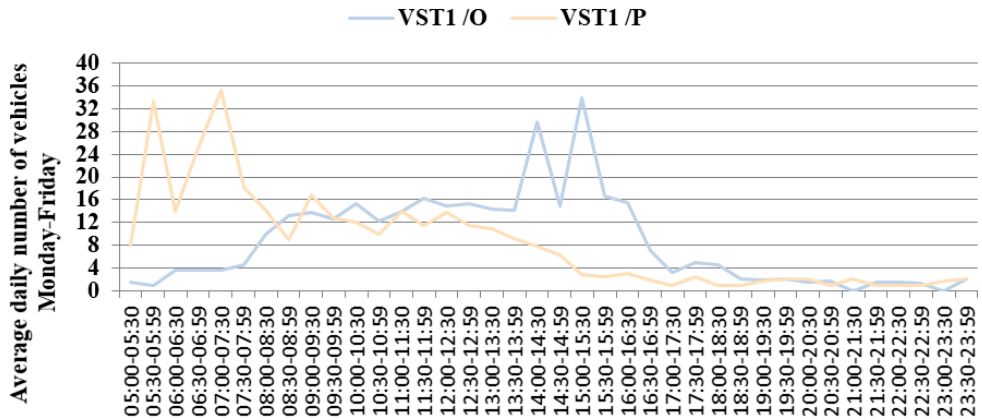


Figure 8 *Average daily number of vehicles entering (P) and exiting (O) the site through the main entrance from Monday to Friday*

persons with a weekly entry/exit average from Monday to Friday, namely persons who access the site - 1,204.6 and persons who exit the site - 1,138. The daily average is more than 300 vehicles entering and exiting the site through the main entrance and entrance 3.

Consequently, this data was analyzed in more detail at 30-minute intervals to determine the most exposed times regarding the number of persons who access the site through the main entrance. The most occupied time was specified the shift turnover at 5-7 a.m. where more than 600 people entered the site and 1-2 p.m. with more than 200 people, followed by 9-10 p.m. with more than 150 people. In regard to exit the site, more than 160 people left at 6-6.30 a.m., more than 500 people at 1:30-3:30 p.m. and more than 190 people at 10-10:30 p.m.

The detailed results obtained, i.e. quantification of average daily values, are depicted in Figures 7 to 9.

As for the access through the main entrance, more than 100 vehicles on average entered the site between 5:30 and 7:30 a.m.; later, this number decreased and stagnated until 2 p.m. Thereafter, this number dropped rapidly. Regarding the exit of the site, most of the

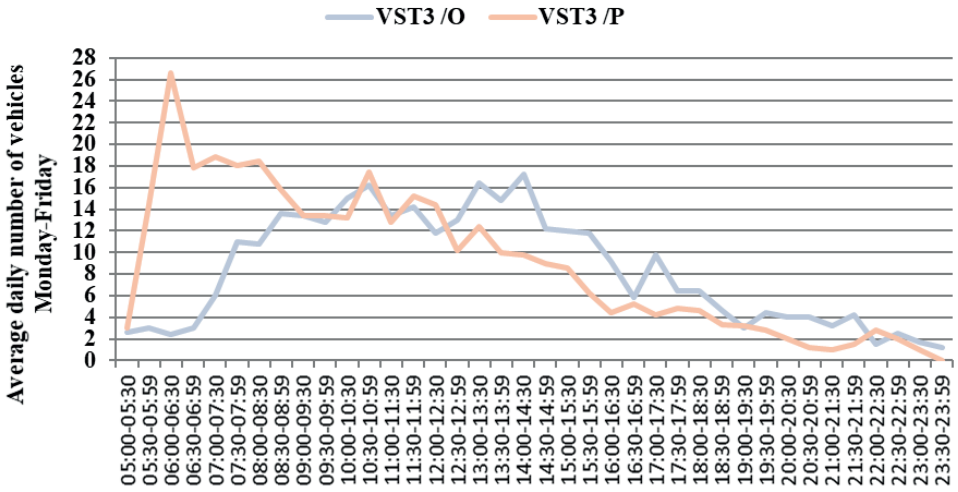


Figure 9 *Average daily number of vehicles entering (P) and exiting (O) the site through entrance 3 from Monday to Friday*



Figure 10 *Proposed parking area for heavy trucks nearby entrance 3*

vehicles left the site at 2-3:30, specifically more than 75.

Concerning the access through entrance 3, most of the vehicles (more than 40) entered the site between 5:30 and 7:30 a.m. Then, the average was of 18 vehicles in 30 minutes until 8:30 a.m. and later, more than 10 vehicles in 30 minutes until 1:59 p.m. After 2:00 p.m., the number of vehicles entering the site decreased and stagnated until the end of the day. In terms of exiting the site, the number of vehicles increased starting at 7 a.m., with the first peak from 10.30 to 10:59 a.m. - more than 16 vehicles in 30 minutes with a similar number of vehicles exiting the site again between 1:00-1:30 and 2:00-2:30 p.m.

6 Proposals to improve transport and discussion

This section consists of specific scenarios set towards improving the current state related to transport safety.

A. Systematic Marking of On-site Roads and Pathways

Considering the differentiation among different road functions and in a view of existing and expected traffic intensity and safety, for the examined manufacturing enterprise, it is recommended to classify roads and pathways on the site in order to provide easier orientation and traffic management. It will require, for example, to assign names and characteristics and determine main and secondary roads and provide markings of important building numbers for on-site roads, e.g. loading points and so on. The systematic markings will support a possible incorporation of roads in navigation solutions, better orientation of drivers and other similar benefits [16, 24].

B. Parking of Trucks Waiting in Front of Entrance 3

Vehicle queues currently occur because of trucks waiting for entering the site on the existing road in front of entrance 3. The idea of moving trucks entering loading points on the site to public car parks near the industrial site is rather difficult. There is not a suitable parking place downtown for a larger number of heavy trucks. Nearby petrol stations do not have a sufficient capacity to play the role of a parking lot [25].

To this end, a temporary or permanent parking area for heavy trucks (see Figure 10) is suggested to be used/built on the side of the current porter's lodge III. The very parking area should be dimensioned to allow enough space in order to avoid queues on the existing

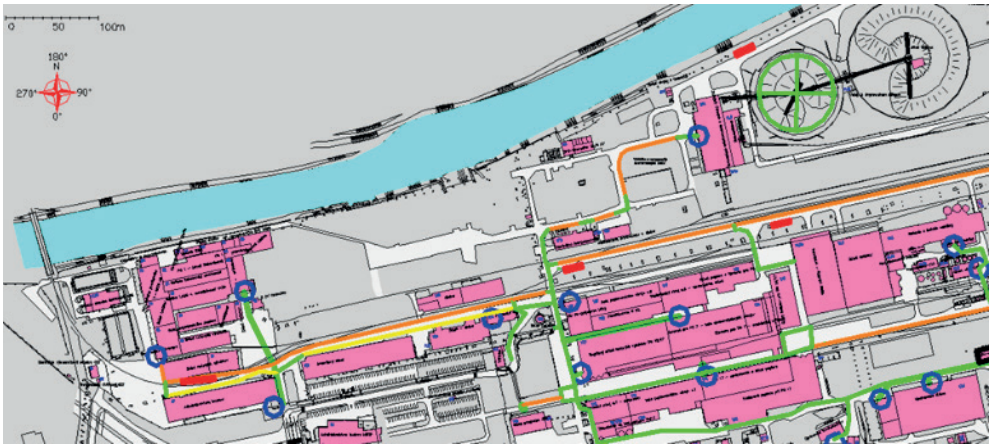


Figure 11 *Recommended location for parking bays for trucks*

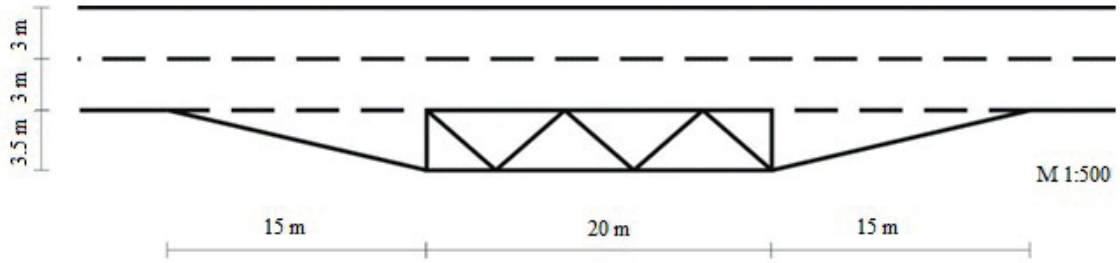


Figure 12 *Scenario of a parking for articulated vehicles*

road. Better material storage management in this area can create an additional space for a new parking area [26].

An alternative scenario for the heavy trucks parking area along the road (the main access to the town) is to build a parallel parking lot, which should eliminate traffic jams that currently emerge on the main road [19, 27].

C. Parking Bays on the Site

Currently, trucks are sometimes waiting for loading or unloading on several on-site roads. A solution would be to create parking bays allowing vehicles to wait for handling while not obstructing free passage of other vehicles (see Figure 11).

Parking areas for the road vehicles are designed in compliance with the technical standard STN 736056 where, however, dimensions for parking of articulated vehicles are not specified. Figure 12 illustrates a designed parking bay for such trucks. The width of the parking bay may also be reduced to 3 m.

D. Separation of Road Transport from Pedestrians

The current situation in terms of marking of sidewalks (pathways) was mapped based on the visual inspection of the industrial site. These are ensured by diagonal stripes, so called zebras along some roads. The current marking for pedestrians has many disadvantages such as it starts or leads to "nowhere" which may confuse pedestrians, as well as implementation of diagonal stripes is not appropriate with respect to form (confused with pedestrian crossings). That is why a new pathway design is to be implemented for employees who come to and leave work as well as those intervening between workplaces on the site [28-29].

To introduce the new horizontal road surface markings in the main transport area, it is recommended to use parallel stripes, each of 125 mm wide, for marking of the areas for pedestrians. In accordance with the standard STN 736110 [29], an one-way pedestrian lane should have a width of 0.75 m, i.e. the recommended width of the pavement should be 1.50 m for both directions. At crossing points where pedestrians have to cross the roads, it is recommended to apply diagonal stripes, or a dashed line [29]. As far as marginal points of sidewalk are concerned, a horizontal pedestrian sign may be marked at the beginning and at the end, or at regular distances (approx. 20 m) to highlight a reserved pedestrian area [30].

The safest scenario is to separate pedestrians so that pathways on the main pedestrian diagonals are situated on a separate body in the adjacent area and secondary pathways are situated in the main traffic area and provided with the suggested horizontal road surface markings [31].

7 Conclusions

The transport safety on the industrial site could be increased by implementing at least some of the above recommendations, in particular in relation to motor and

non-motorized traffic, above all with the emphasis on pedestrian traffic. It would also be reasonable to improve, streamline and simplify the movement of vehicles on on-site roads and thus put towards shortening the time-period of stay of trucks on the site.

In general, safety can be defined as a circumstance without a real threat or danger. Nevertheless, it has different specifications depending on the industry or situation. With regard to transportation, safety is referred to as creating conditions for minimizing conflicts and disturbances of the traffic flow in a certain mode of transport.

As for the specific proposals to be implemented in the industrial site being investigated, they can be summarized as follows:

- classification of roads and pathways on the site to secure better traffic management resulting in a more favorable orientation of drivers as well as other psychological-positive benefits,
- construction of a new parking area for the heavy trucks in front of entrance 3 (see Figure 10) to avoid queues on the existing road (i.e. to eliminate traffic jams that currently emerge on the main road),
- construction of the new parking bays allowing vehicles to wait for handling while not obstructing free passage of other vehicles (see Figure 11),
- implementation of a new pathway design for employees so that pathways on the main pedestrian diagonals are situated on a separate body in the adjacent area and secondary pathways are situated in the main traffic area and provided with the suggested horizontal road surface markings.

Aforementioned definition could also be regarded as a formulation of the objective addressed in this research study that tried to meet with the proposed scenarios - to minimize or eliminate traffic conflict situations on the industrial site in the examined manufacturing enterprise.

Acknowledgment

Contribution has been prepared based on the grant: VEGA no. 1/0436/18 - Externalities in road transport, an origin, causes and economic impacts of transport measures.

This manuscript was supported within realization of the research project entitled "Autonomous mobility in the context of regional development LTC19009" of the INTER-EXCELLENCE program, the VES 19 INTER-COST subprogram.

References

[1] MUIR, C., NEWNAM, S., NEWSTEAD, S., BOUSTRAS, G. Challenges for safety intervention in emergency vehicle fleets: a case study. *Safety Science* [online]. 2020, **123**, 104543. ISSN 0925-7535. Available from: https://doi.org/10.1016/j.ssci.2019.104543

[2] POLIAKOVA, B., SEMANOVA, S. The use of transport processes modelling in the freight transport company. In: 21th International Scientific on Conference Transport Means 2017: proceedings. 2017. ISSN 1822-296X, p. 913-918.

[3] CABAN, J., DROZDZIEL, P., VRABEL, J., SARKAN, B., MARCZUK, A., KRZYWONOS, L., RYBICKA, I. The research on ageing of glycol-based brake fluids of vehicles in operation. *Advances in Science and Technology-Research Journal* [online]. 2016, **10**(32), p. 9-16. ISSN 2299-8624. Available from: https://doi.org/10.12913/22998624/65113

[4] BERGLAND, H., PEDERSEN, P. A. Efficiency and traffic safety with pay for performance in road transportation. *Transportation Research Part B: Methodological* [online]. 2019, **130**, p. 21-35. ISSN 0191-2615. Available from: https://doi.org/10.1016/j.trb.2019.10.005

[5] JAGELCAK, J., KIKTOVA, M., STOPKOVA, M. The application of the verified gross mass of intermodal loading units in the conditions of the Slovak Republic. *Nase More* [online]. 2018, **65**(4), p. 218-223. Available from: https://doi.org/10.17818/NM/2018/4SI.10

[6] LIZBETIN, J., BARTUSKA, L. The influence of human factor on congestion formation on urban roads. *Procedia Engineering* [online]. 2017, **187**, p. 206-211. ISSN 1877-7058. Available from: https://doi.org/10.1016/j.proeng.2017.04.366

[7] VIVODA, J. M., PRATT, S. G., GILLIES, S. J. The relationships among roadway safety management practices, collision rates and injury rates within company fleets. *Safety Science* [online]. 2019, **120**, p. 589-602. ISSN 0925-7535. Available from: https://doi.org/10.1016/j.ssci.2019.07.033

[8] USECHE, S. A., GOMEZ, V., CENDALES, B., ALONSO, F. Working conditions, job strain and traffic safety among three groups of public transport drivers. *Safety and Health at Work* [online]. 2018, **9**(4), p. 454-461. ISSN 2093-7911. Available from: https://doi.org/10.1016/j.shaw.2018.01.003

[9] MESZAROS, F., MARKOVITS-SOMOGYI, R., BOKOR, Z. Modelling and multi-criteria optimization of road traffic flows considering social and economic aspects. *LOGI - Scientific Journal on Transport and Logistics* [online]. 2012, **3**(1), p. 70-82. ISSN 1804-3216, eISSN 2336-3037.

[10] MALKA, R. A., LEIBOVITZ-ZUR, S., NAVEH, E. Employee safety single vs. dual priorities: When is the rate of work-related driving accidents lower? *Accident Analysis and Prevention* [online]. 2018, **121**, p. 101-108. ISSN 0001-4575. Available from: https://doi.org/10.1016/j.aap.2018.08.020

[11] JURKOVIC, M., KALINA, T., TURCAN, R., GARDLO, B. Proposal of an enhanced safety system on board of the inland vessel. *MATEC Web of Conferences* [online]. 2017, **134**, 00022. eISSN 2261-236X. Available from: https://doi.org/10.1051/matecconf/201713400022

[12] WANG, Y., ZHAN, S., LIU, Y., LI, Y. Occupational hazards to health of port workers. *International Journal of Occupational Safety and Ergonomics* [online]. 2017, **23**(4), p. 584-588. ISSN 1080-3548, EISSN 2376-9130. Available from: https://doi.org/10.1080/10803548.2016.1199501

[13] KUBANOVA, J., POLIAKOVA, B. Truck driver scheduling of the rest period as an essential element of safe transport. In: 20th International Scientific on Conference Transport Means 2016: proceedings. 2016. ISSN 1822-296X, pp. 22-26.

[14] USECHE, S. A., ORTIZ, V. G., CENDALES, B. E. Stress-related psychosocial factors at work, fatigue and risky driving behavior in bus rapid transport (BRT) drivers. *Accident Analysis and Prevention* [online]. 2017, **104**, p. 106-114. ISSN 0001-4575. Available from: https://doi.org/10.1016/j.aap.2017.04.023

[15] POSUNIAK, P., JASKIEWICZ, M., KOWALSKI, K., DABROWSKI, F. Child restraint systems: problems related to the safety of children transported in booster seats (without integral safety belts). In: 11th International Scientific and Technical Conference on Automotive Safety: proceedings. 2018.

[16] HANZL, J., BARTUSKA, L., LUPTAK, V. Traffic counts on roads in the Czech Republic. In: 23rd International Scientific Conference on Transport Means 2019: proceedings. 2019. ISSN 1822-296X, p. 1346-1350.

[17] MAKAROVA, I., SHUBENKOVA, K., BUYVOL, P., MAVRIN, V., GINIYATULLIN, I., MAGDIN, K. Safety features of the transport system in the transition to industry 4.0. *The Archives of Automotive Engineering - Archiwum Motoryzacji* [online]. 2019, **86**(4), p. 79-99. eISSN 2084-476X. Available from: https://doi.org/10.14669/AM.VOL86.ART6

[18] OLUWASEYI, J. A., ONIFADE, M. K., ODEYINKA, O. F. Evaluation of the role of inventory management in logistics chain of an organisation. *LOGI - Scientific Journal on Transport and Logistics* [online]. 2017, **8**(2), p. 1-11. ISSN 1804-3216, eISSN 2336-3037. Available from: https://doi.org/10.1515/logi-2017-0011

[19] CERNICKY, L., KALASOVA, A., MIKULSKI, J. Simulation software as a calculation tool for traffic capacity assessment. *Communications - Scientific Letters of the University of Zilina* [online]. 2016, **18**(2), p. 99-103. ISSN 1335-4205, eISSN 2585-7878. Available from: http://komunikacie.uniza.sk/index.php/communications/article/view/338

[20] RANI, H. A., ISYA, M., IQBAL, M. Risk level analysis of work safety and health on national road routine maintenance project using self-management system. *IOP Conference Series: Materials Science and Engineering* [online]. 2018, **674**(1). ISSN 1757-899X, eISSN 1757-8991. Available from: https://doi.org/10.1088/1757-899X/674/1/012013

[21] CHOVANCOVA, M., KLAPITA, V. Modeling the supply process using the application of selected methods of operational analysis. *Open Engineering* [online]. 2017, **7**, p. 50-54. eISSN 2391-5439. Available from: https://doi.org/10.1515/eng-2017-0009

[22] STERNAD, M., SKRUCANY, T., JEREB, B. International logistics performance based on the DEA analysis. *Communications - Scientific Letters of the University of Zilina* [online]. 2018, **20**(4), p. 10-15. ISSN 1335-4205, eISSN 2585-7878. Available from: https://doi.org/10.26552/com.C.2018.4.10-15

[23] DROZDZIEL, P., KOMSTA, H., KRZYWONOS, L. Repair costs and the intensity of vehicle use. *Transport Problems*. 2018, **8**(3), p. 131-138. ISSN 1896-0596.

[24] WISHART, D., SOMORAY, K., EVENHUIS, A. Thrill and adventure seeking in risky driving at work: the moderating role of safety climate. *Journal of Safety Research* [online]. 2017, **63**, p. 83-89. ISSN 0022-4375. Available from: https://doi.org/10.1016/j.jsr.2017.08.007

[25] FEDORKO, G., MOLNAR, V., HONUS, S., NERADILOVA, H., KAMPF, R. The application of simulation model of a milk run to identify the occurrence of failures. *International Journal of Simulation Modelling* [online]. 2018, **17**, p. 444-457. ISSN 1726-4529. Available from: https://doi.org/10.2507/IJSIMM17(3)440

[26] YORK BIGAZZI, A., ROULEAU, M. Can traffic management strategies improve urban air quality? A review of the evidence. *Journal of Transport and Health* [online]. 2017, **7**, p. 111-124. ISSN 2214-1405. Available from: https://doi.org/10.1016/j.jth.2017.08.001

[27] KUBASAKOVA, I., JAGELCAK, J. Logistics system just-in-time and its implementation within the company. *Communications - Scientific Letters of the University of Zilina* [online]. 2016, **18**(2), p. 109-112. ISSN 1335-4205, eISSN 2585-7878. Available from: http://komunikacie.uniza.sk/index.php/communications/article/view/340

[28] KAMPF, R., HITKA, M., LIZBETINOVA, L. Direction of the corporate culture in Slovak and German transport companies from a top managers' perspective. *Periodica Polytechnica Transportation Engineering* [online]. 2019, **47**, p. 213-219. ISSN 0303-7800, eISSN 1587-3811. Available from: https://doi.org/10.3311/PPtr.11166

[29] ONDRUS, J., KARON, G. Video system as a psychological aspect of traffic safety increase. In: 17th International Conference on Transport Systems Telematics TST 2017: proceedings. Vol. 715. 2017. p. 167-177.
[30] GNAP, J., POLIAK, M., SEMANOVA, S. The issue of a transport mode choice from the perspective of enterprise logistics. *Open Engineering* [online]. 2019, **9**(1), p. 374-383. eISSN 2391-5439. Available from: https://doi.org/10.1515/eng-2019-0044
[31] MORAVCIK, L., JASKIEWICZ, M. Boosting car safety in the EU. In: 11th International Scientific and Technical Conference on Automotive Safety: proceedings. 2018.

ELECTRIFICATION OF PUBLIC TRANSPORT BUS FLEET: IDENTIFICATION OF BUSINESS AND FINANCING MODELS

Grzegorz Dydkowski[1], Jozef Gnap[2,*], Anna Urbanek[1]

[1]Department of Transport, University of Economics in Katowice, Katowice, Poland
[2]Department of Road and Urban Transport, Faculty of Operation and Economics of Transport and Communications, University of Zilina, Zilina, Slovakia

*E-mail of corresponding author: jozef.gnap@fpedas.uniza.sk

Resume
The paper presents possible models of electric buses purchase financing, taking into account purchase prices higher now than in the case of traditional buses. During the research, the solutions used on several continents and in many countries were analysed, including the USA, China and many European countries. The qualitative research methods were used, focusing less on the describing and dimensioning the current state and more on creating and presenting theories and the implementation proposals themselves. As a result, it also allowed to include issues related to applicability and implications of formulated solutions for managerial practice.

Article info
Received 21 September 2020
Accepted 26 November 2020
Online 26 March 2021

Keywords:
electromobility,
electric buses,
financing,
financing public transport

Available online: https://doi.org/10.26552/com.C.2021.3.A137-A149

ISSN 1335-4205 (print version)
ISSN 2585-7878 (online version)

This is an open access article distributed under the terms of the Creative Commons Attribution 4.0 International License (CC BY 4.0), which permits use, distribution, and reproduction in any medium, provided the original publication is properly cited. No use, distribution or reproduction is permitted which does not comply with these terms.

1 Introduction

Introduction of the city servicing by electric buses, not only within the scope limited to a few lines and as a pilot project, but to a significant extent of carried out transport, will require financing to be ensured - both for procurement of buses themselves, as well as of the necessary infrastructure. The financing of infrastructure and buses purchase are related projects, in terms of time and scope they must proceed in such a way that services provision would be possible; however, the financing methods and sources may differ. As a rule, the infrastructure is managed and financed by the public entities and from public funds - various level budgets, depending on its purpose and function carried out in a given country system. The vehicles financing and purchase in most cities worldwide was and is the domain of operators themselves (these entities do not need involvement of public capital), because as a rule it is them, who are obliged to ensure means of transport necessary to provide services. Electric buses are now significantly more expensive than traditional ones, i.e. driven by internal combustion engines. Anyway, the charging infrastructure and purchase of buses themselves do not comprise all the expenditures. An assumption may be made that for many years operators will be using both traditional buses with combustion engines and electric buses. This will result in a necessity to maintain the hitherto technical facilities for traditional buses and to provide additional equipment and also to employ people qualified to service and repair electric buses, which will also increase the costs [1].

Electric buses are more environment friendly at the place of service provision, hence significant external benefits are achieved. Apart from benefits, related to emissions cutting, reduction of dependence on liquid fuels is important, as well. Crude oil markets feature limited stability, there are numerous tensions and disturbances in some of extracting it countries [2], moreover there are numerous indications that the era of fossil fuels comes to an end due to their deposits depletion - at the current consumption rate the resources are estimated at approx. 40 years. Obviously, the Earth has still significant oil resources in shale and bituminous sands, in the Arctic, Amazonia and under oceans bottom (at great depths), but the costs of their extraction will be much higher than the extraction of reservoirs today. Thus, one can say that the era of cheap oil comes to an end [3].

When introducing electric buses to operation it is difficult to assume that the necessary additional funds will be obtained from growing revenues on sales of services; quite opposite - the spatial development of cities, population concentration in big cities and processes proceeding there cause the urban public transport to be more and more capital intensive, which results in growing demand for public financing [4-6].

Table 1 *Purchase prices and estimated usage time of buses [8]*

technology	capital expenditure (EUR)	depreciation (years)
diesel euro VI	230,000	10
CNG euro VI	270,000	10
PHEV euro VI	445,000	10
electric (with battery)	502,500	10
electric (with battery leased)	475,000	10

Table 2 *Forecast of battery prices (EUR/kWh) depending on demand for electric buses in Europe [1]*

battery price for buses (EUR/kWh)	2016	2018	2020	2022	2024	2026	2028	2030
low demand in European e-bus	510	333	269	224	194	167	146	129
high demand in European e-bus	510	333	262	204	160	122	102	85
variation low vs. high demand			-3%	-9%	-18%	-27%	-30%	-34%

Their limited range and time necessary to recharge the battery add to that, reducing the time during which they can be used to serve lines.

As an assumption, the service users pay for the service of moving and this service - understood as location change within a specific time - not necessarily depends on the fact whether a passenger moves by a bus with a combustion engine, or a bus with an electric motor. Obviously, in the case of electric buses it is emphasised that the motor operation is quieter and thereby the noise level lower, vibrations are smaller than those generated by combustion engines, there is no exhaust gas emission, especially when the bus approaches and waits on a stop, as well as the very feeling of moving by a zero-emission and modern vehicle [1]. However, these factors not necessarily cause a significant increase in the number of passengers using the public transport. Individual methods of movement, primarily by cars, remain the competition all the time. In the case of increased prices of the public transport services it is necessary to take into account a decline of demand for those services and an increased number of movements by cars, which in practice may cancel the reduction of environmental impact, which is expected to be achieved as a result of electric buses introduction to operation. Of course, one can refer to ecological awareness, however, it is not necessarily considered when making decisions about a method to move. It is proved by a significant share of journeys by private cars in cities and ineffectiveness of numerous tools, which for years were used trying to reduce the car traffic.

2 Materials and methods

2.1 Background of the research

The difference of prices between the electric and combustion buses depends on the world's region, the size of single procurement order, equipment, battery size and hence range, applied design solutions, guarantee conditions and other factors. Numerous analyses emphasise the fact that an electric bus is now roughly twice more expensive than a traditional bus with a combustion engine (Table 1) [7-8]. This is now the basic barrier to the order sizes growth [9], another barrier is the fact that external costs are not entirely or only to a small extent taken into account as evaluation criteria in the bidding procedures for vehicles purchase [1].

The zero-emission nature of electric buses affects expectations of their widespread use in cities, which in turn is related to the necessity of incurring high financial expenditures. Thus, a question arises to what extent it is possible to acquire additional funds, because of the better management of possessed resources and urban transport management, so that substantial purchases could be financed, at the same time additionally burdening the public budgets in a limited way. Each additional public expenditure means either funds originating from the better management of the existing resources or giving up other public tasks, or an increase in the tax burden now or in the future. Therefore, considerations should be broader, to what extent an increase in the public sector operation effectiveness is possible and how to finance vehicles purchases, so that the created solution would provide funds, but also would result in effective use of the purchased vehicles.

A part of available analyses forecast and expect that - with increasing amounts of purchases and further technology development - purchase prices of ecologically clean vehicles will decline, including primarily electric buses. Attention is drawn to the fact that the batteries and solutions for electricity charging management and electricity consumption are new and innovative ones and with the increasing demand and thereby production size the unit manufacturing cost will be going down. Table 2 presents the forecast of battery prices (EUR/kWh).

According to economic forecasts, assuming a scenario of high demand, it is expected that the battery prices will decrease to about 1/3 of current prices over the next 10 years. In addition, the lower operation and maintenance costs of electric buses are emphasised, which should result from a simpler structure of driving units and lower costs related to consumption of energy

Table 3 *Overview of the TCO per technology [8]*

	diesel	CNG	PHEV	BEV (opportunity charging)		BEV (depot charging)	
				with battery	lease	with battery	lease
fuel cost (EUR/km)	0.43	0.29	0.33	0.10	0.10	0.10	0.10
maintenance cost (EUR/km)	0.42	0.53	0.28	0.23	0.23	0.23	0.23
battery lease (EUR/km)	-	-	-	-	0.14	-	0.14
battery replacement (EUR/km)	-		0.002	0.013	-	0.025	-
insurance costs (EUR/km)	0.09	0.09	0.09	0.09	0.09	0.09	0.09
tax cost (EUR/km)	-	-	-	-	-	-	-
Subsidies	-	-	-	-	-	-	-
operational expenditures 10 years (EUR/km)	0.93	0.91	0.70	0.42	0.55	0.44	0.55
capital expenditures bus	184,719	216,844	357,391	403,571	381,485	403,571	381,485
infrastructure + maintenance	2,509.37	5,120.48	8,618.18	83,773.96	83,773.96	24,435.24	24,435.24
TCO 10 years (EUR/km)	1.24	1.27	1.32	1.24	1.33	1.18	1.23

to drive vehicles. All that should cause that the total costs of ownership (TCO), calculated as the cost of purchase and then operating costs of electric buses, in the future will be comparable to traditional buses [8, 10]. The study conducted by Hooftman et al. [8] shows that the unit TCO for 10 years usage may be similar for different technologies (Table 3). When calculating financial flows the residual value of bus batteries may be taken into account, which could be used within the so-called second life, i.e. in energy storage facilities [11]. Apart from the higher expenditures for the purchase, the electric buses operation is related also to such risks as batteries durability and possible decline of their capacity, which over time can affect buses capability to carry out transport on a hitherto transport line.

Research carried out in various countries pursues development of a new model - method for vehicles purchase financing, in particular electric buses [12-16]. Obviously, the well-known assets financing methods are used, but realities related to specific investments - which in this case are electric buses - are considered [17]. The basic problem when considering the investment issues consists in answering a question, how to invest, i.e. what should be the origin of funds and how they should be directed, since a good investing system should ensure:

- effective use of funds allocated for investments,
- effective operation of fixed assets acquired as a result of investment activity,
- stimulation of reaching the structure of transport market assumed by the public authorities.

In most cases operators are publicly owned - by municipalities, intermunicipal unions, or other public administration entities; that depend on solutions adopted in a specific country. They operate as commercial companies, with entities from the public finance sector as shareholders or stockholders, or pursuant to regulations indented for public sector entities. Operators also include entities with private capital involvement [18]. It is necessary, as far as possible, to create equal access conditions to the capital for electric buses purchase, both for entities from the public and private sector.

2.2 Methods

The paper focuses the consideration on the method of electric buses financing, so that the financing model would take into account peculiarities related to the new solution implementation. This issue is a challenge on all the continents or in all the countries introducing electric buses [9]. It is also necessary to examine, to what extent systemic solutions could cause that bigger amounts of funds, indispensable to engage by urban public transport operators, not necessarily burden budgets from which the urban public transport investments and services are financed - for example in the case of acquiring the non-repayable external funds, which co-finance now and in the future projects of electric buses implementation. At the same time, it is necessary to consider that external funds, originating from the European Union budget, are obtained from various tax burdens and only their flow is diversified.

Basic information sources used during the research comprise comprehensive studies from the field of public

sector finance, analyses, communications, assessments and transport development scenarios, documents related to the transport development policy and strategy and the best practice examples, as well. Apart from published materials, websites of the European Union institutions, scientific and research centres, governments and local authorities of various states of the world, were used.

Taking into account the subject and the aim of the study, qualitative research methods were used. Recognizing the significant importance of quantitative methods and observing the far-reaching domination of quantitative research in economic sciences, it should be noted that the quantitative research primarily provides answers to basic questions related to the number and frequency of solutions or allows to draw conclusions about the entire population based on the studied sample. In the quantitative research, the aim is to determine the quantitative dependencies of the studied phenomena, paying particular attention to the correctness of the determined variables and the measurement logic [19]. This attitude allows for establishing facts, quantifying the existing state and checking statistical relationships, but it is limited in creating theories and formulating proposals [20]. It is the qualitative methods that focus less on the frequency of the solutions or phenomena studied and more on the description, presentation and development of theories and related good practices. Qualitative methods allow obtaining answers to basic questions - why and how a given phenomenon takes place, as these methods aim to understand and determine the motives of such actions and behaviour [21]. The created theory is general to a certain degree and there are reservations in terms of its practical application. The main role of qualitative research is to create theories, using experience of the researchers involved in this process. At the same time, it is believed that qualitative methods have a significant potential, since, by using data and examples of social processes, they can provide a lot of information and explanations for the formulated theories and also allow the theory to be generalized to those elements of phenomena that are not subject to quantification [22]. Thus, the theoretical testing using case studies can be assumed. It is also worth paying attention to the fact that the qualitative research is not easier to conduct than the quantitative research and in the past it fulfilled and continues to play an important role in cognitive processes.

Taking into account the above, this paper is dominated by methods characteristic of qualitative research, in particular:

- method of critical literature review and document analysis, allowing e.g. to assess the condition of knowledge in the field of public sector functioning and assets financing, in particular fixed assets [23],
- methods of analysis and synthesis allowing to look for and learn about the influence of various environmental factors and to assess the existing solutions and to generalise and draw conclusions.

The chosen methods were influenced by the subject of research and the purpose of the research. The purchase and implementation of electric buses for operation is a relatively new issue, in many cities the implementation cases are pilot projects. The number or frequency of such or other solutions implemented is not crucial from the point of view of formulated proposals and theories created. It can be added that implementation projects take place simultaneously on several continents and in many countries, including the USA, China and many European countries. In terms of the public bus transport, these countries differ in the division of tasks between the public and private sectors and the adopted principles of urban transport financing. The lack of the well-established methods of financing and more pilot implementation projects result in the search for solutions that are not common but efficient ones, allowing to popularize the zero-emission means of transport and at the same time to spend public funds economically.

3 Results

3.1 The issue of thrift and effective funds spending in the public sector

The public sector is stronger and stronger present in the daily life, it manifests in multitude of public institutions, a significant number of persons employed and increasingly broad scope of services provided by this sector. Hence there is an ever-stronger need to look for solutions under which the provision of public services of increasingly high standards will be ensured and at the same time this will not require engaging by the public sector of higher and higher funds. Actions aimed at improving efficiency and effectiveness of the public sector functioning should proceed at the same time in many areas. It is possible to mention improvement in the public entities and services management, innovation implementation, provision of services with use of modern technologies, management of public services prices and charges and increasingly better, competent staff [24].

In general, the public sector provides services, which would not be provided in the expected scope and at expected prices by private entities. The public services are frequently provided at prices that do not cover the costs of their provision - lower prices are set on purpose, to increase the demand [25-26] and accessibility of such services, because this results - or according to the assumption should result - in benefits to the society as a whole. Table 4 presents the structure of the main funding sources for urban public transport operating costs in a selection of cities.

Figure 1 presents the cost-coverage ratios for fare revenues and public subsidies in a selection of cities in 2018. The size of each ball represents the relation between the volume of the annual costs of the public

Table 4 *Main funding sources for urban public transport operating costs in a selection of cities in 2012 [27]*

city and metropolitan area	coverage by fare revenues (%)	coverage by public subsidies (%)	coverage by other revenues (%)
Amsterdam	38.4	61.6	-
Barcelona	48.9	51.1	-
Berlin	55.6	44.4	
Brussels	44.9	29.5	25.6
Budapest	33.2	50.0	16.8
Cadiz	72.4	26.4	1.2
Copenhagen	54.6	45.4	-
Helsinki	51.3	48.7	-
London	67.6	32.4	-
Lyon	28.1	24.4	47.5
Madrid	40.1	59.9	-
Montreal	44.8	55.2	-
Paris	38.5	20.6	40.9
Prague	30.8	69.2	-
Stockholm	38.8	44.3	16.9
Stuttgart	57.3	42.7	-
Turin	30.7	69.3	-
Vilnius	48.9	35.7	15.4
Warsaw	38.6	61.4	-

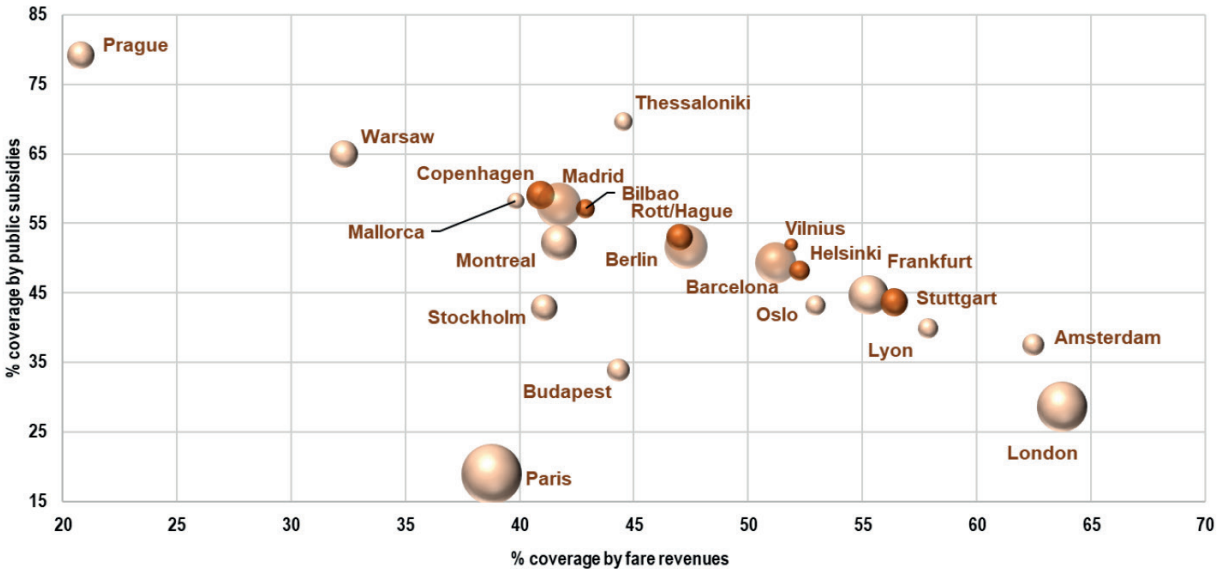


Figure 1 *Coverage by public subsidies vs coverage by fare revenues per PTA area inhabitants in 2018 [28]*

transport operations and the population of the Public Transport Authority (PTA) area (costs/total inhabitants). The share of the public funds in public transport financing is at a significant level, the average level of public subsidies coverage ratio is 50% [28].

Frequently, such goods are also made available free of charge, the education or health care services could be used as examples, because an assumption is made that the current civilisation and economic development should guarantee accessibility to such services, irrespective of the economic status. The criterion of exclusivity is another criterion deciding whether the public or private sector is to be responsible for ensuring of a given good provision. Attention should be drawn to the fact that in the case of the urban and regional transport, or transport services in general, the exclusivity is possible, hence if someone does not pay for the service, it is possible to limit the possibility of its use by assumption. So, it is difficult to refer to the necessity of public financing, like it is the case for goods/services,

in which the exclusivity cannot be ensured (e.g. national defence, local roads).

The setting of prices below the cost of selected services rendering, or ensuring the free access to a part of services, causes that it becomes necessary to ensure such solutions during their provision, which will feature hallmarks of effective. The services, to which access is free, can be rendered by the service provider on a lower level of quality - because the user receives them for free, so (s)he should not make complaints in the field of quality, on the other hand the users can notify demand on the level much higher than their needs and the motive can originate only from the fact that anyhow they are free [5, 29].

At services financing from public funds the issue of justice is raised - a situation occurs, in which funds are redistributed. As a result of tax burdens and later on financing services by funds originating from taxes, people who do not use a specific good, are paying for it, as well. The public financing of urban transport may be an example - public funds originate because of tax burdens also from those, who do not use the urban public transport. Obviously, it is possible to state that due to the public financing of the urban public transport the urban environment is improved and that means benefits to everybody, but this is also relative, to what extent the public financing of the urban public transport increases the demand and to what extent it is only social support for selected social groups, which should obtain such support directly and not by means of prices of urban public transport services. In addition, the effectiveness of support, provided via prices of the public transport services, is debatable - for example not all the elderly persons are poor people, requiring additional financial support.

In general, it should be stated that the term of justness is very relative and vague, more philosophical than economic [30]. However, justice is being sought in many decisions of the public sector, including in the urban public transport, especially in decisions related to entitlements to concessionary and free travelling. However, for practical applications it seems logical to adopt the following rules:

1. The user pays, it is possible to add costs or prices verified by a competitive market. So the costs should be incurred by the users of a specific solution.
2. Benefits can be direct or indirect, e.g. the use of services or only benefiting from the fact that the increase in the demand for such services results, say, in the environmental values improvement.
3. The aid or improvement to the situation of people worst-off, unless it leads to a significant fall in effectiveness or big wastefulness.

Public financing means financing from taxes and high taxes mean, among other things, limitation of the freedom of choice. Decisions on funds spending are made by local, regional, national, or EU level authorities and not independently by specific service users. Such decisions are not always consistent with current preferences and expectations, but, in the situation of the high tax burdens, possibilities of individual choices diminish. The expectations and preferences differ depending among other things on the age, e.g. during the studies or after graduation it is necessary to concentrate funds to purchase or rent an apartment and its indispensable equipment.

Various attitudes to economy of funds spending, depending on whose funds are spent and whose needs satisfied, are noticed in the literature [31]. In a situation when people pay from their own funds for their needs, rational funds spending is then visible. However, if a specific good is financed from other people's funds - other entities or public funds, then, in general, less weight is given to the amount of expenditure. The worst is the situation, when from other people's funds we finance other people's needs and this frequently occurs in the public sector, then the expenditure rationality and effectiveness may be objectively lower [31].

Public funds, hence in general originating from tax burdens, in many cases can be considered nobody's funds; the relationship between the expenditure rationality and later on - in longer - or shorter-time horizon - is not necessarily seen between the amount or even increase in the tax burden. Obviously, all the time via legal regulations, inter alia the obligation of management openness and spending public funds in a purposeful and thrifty way, stipulated in the Act of 27 August 2009 on Public Funds [32], the duty to carry out open competitive tender procedures prior to contract awarding, stipulated in the Act of 29 January 2004 on the Public Procurement Law [33], or even responsibility for the thriftlessness resulting from provisions of the Act of 06 June 1997 on Penal Code [34], rational and effective spending of public funds is sought for. However, via legal regulations, guidelines, or other standards, the effectiveness will not be obtained like in the situation when the direct user pays and expects then a good in accordance with his/her preferences and the entity providing a specific good is subject to market verification.

3.2 Public sector as the entity financing and providing goods and services

The public sector provides goods or carries out tasks considered basic, having special importance for the community functioning or conditioning the fulfilment of its basic needs. The scope of such tasks is related to a level of the social and economic development and conditioned by financial capabilities of public budgets. The existence of state, society and its elements' needs (e.g. local population) is an objective phenomenon and their non-fulfilment threatens the existence of society (e.g. national defence, natural environment protection) and of state (e.g. inefficient administration). So, an objective fact of the existence of society and of

institutions, which are its products (e.g. state, local government authorities), decides about the existence of collective needs [35]. It is possible to mention among tasks, or collective needs considered basic, the health care, social welfare, or education. However, it is difficult to classify the public transport services as such.

Existence of the public interest, which could be accomplished due to such an intervention, is primarily mentioned among premises for regulatory activities undertaken by the public sector. In particular the point is to allocate in a more democratic and efficient way the resources, to ensure accessibility of selected goods - public goods and to increase the market effectiveness [36]. The pursuit of increasingly more democratic and effective allocation of resources means, first of all, the limitation of non-renewable resources use and, what is important in the case of transport activities, reduction of the negative external effects of transport (exhaust gas emission, noise, accidents). It also includes supporting the public transport, because the negative external effects, calculated per transported person, differ in the case of movements carried out by personal cars and means of public transport [37-40]. To reduce the social costs of transport and to trigger the behaviour, in which rare resources are used thriftily, it is proper to apply the "'user pays" principle. This means charging the users, at least partly, with external costs originated due to the movements and generation of adverse effects in the environment. Identification of the external costs level remains the issue, which - depending on the place of activity, surroundings and other factors - are different and also ensuring of the fees collection in such a way as to connect the amount of fee with amount of the generated external costs. It is natural that the goods users are not willing to pay voluntarily for the negative effects of their activity, transferred onto third persons or goods consumed collectively. Therefore, only regulatory actions, through burdening with external costs, can contribute to reduction of undesirable external effects of the carried out transport activity. Another issue, related to an economical use of rare resources, is the fact that processes occurring on the markets would not always ensure proper supply, situations of selected goods overproduction are possible, e.g. oversupply of public transport services, hence services utilising rare resources (liquid fuels, environmental pollution) during their provision. The limitation of such situations is expected through the public administration intervention [37].

Attention should be also drawn to the fact that, deliberately or not, the market role limitation and thereby limitation of decisions on provided services, made by direct users, results in funds transfers/redistribution between various social groups. As a result, persons not using a specific service are also burdened (via tax burdens or other obligatory charges [41]) with the costs [37], which takes place, e.g. in the situation of subsidising from public funds the passenger transport by urban and regional public transport. Moreover, redistribution of funds occurs in the urban or regional public transport during the provision of transport services to areas of small passenger flows (e.g. city outskirts) and thereby generating a substantial deficit of funds and this service is financed by the revenue from more loaded lines/areas (city centres), where selected lines could be even profitable. This fact is not considered at the prices setting, especially criteria of their diversification. Hence, a part of regulatory activities may be explained also as an indirect form of taxation.

4 Sources and financing models of electric buses purchase - discussion of study results

4.1 Investment financing from operators depreciation and profits and directly by municipalities/organisers

Depreciation charges and accumulated profits should be included among basic financing sources of entities fixed assets. By their nature, depreciation charges should constitute the basic source of replacement investments financing. The investing of entities profits should be a supplementary financing source of simple reproduction and as a rule - the source of expanded reconstruction. However, in the case of the public services provision, which are usually provided below costs, i.e. the obtained revenues are lower than own costs of entities, the financial result and hence profits, if any, depend on the amount of public financing. Hence, one can talk here primarily about depreciation as a source of assets reconstruction. In this solution:

- the size of investments is adjusted to the size of service sales,
- the decision about investing is made by an operator, but also by organisers, who decide about requirements set to operators, which is reflected in provisions comprised by the contracts,
- the operator is the owner of assets acquired as a result of investing based on depreciation and possibly profit, so the issues of improper care of the acquired assets are limited,
- operators obtain higher accumulation more effectively and are in a position to allocate more funds to development.

In the case of the public sector operators, it is necessary to apply solutions of funds management control, e.g. via the ownership supervision, since one can encounter unused investment possibilities and/or consumption of achieved profit, in a direct form or through costs inflation. A possible solution consists of privatisation of the urban public transport operators. Another issue, limiting investment possibilities, is a situation of inappropriate cost structure and too small depreciation, amount of which does not allow even for a simple reproduction. This can result from the

following reasons:

- operators use depreciated assets and overestimation of the fixed assets value deviates from the price increase on the market,
- technical progress, market and environmental protection requirements cause (electric buses case) that means of production available on the market have better design solutions and thereby a higher price.

Because of the aforementioned reasons a part of investments must be based on retained earnings, or on repayable or non-repayable financing sources. However, it is worth drawing attention to the fact that the profit is burdened with an income tax. Hence the profit generation by operators implies the necessity to pay out a part of funds in the form of corporate income tax (in Poland to the state budget, from which only a small part feeds municipality budgets). An urban public transport is financed from public funds and just the amount of this financing decides about operators profitability. So, the investing from profits does not guarantee an effective use of funds assigned to investments. That means that depreciation and obtained profits, if any, have limited usefulness in the case of the capital-intensive development investments, e.g. electric buses purchase and must be supported by other solutions. The financing of investments from depreciation and achieved profits requires that the entity financing urban public transport approves an increased amount of the co-financing for the transport services provision and hence in its nature it boils down to financing purchases from the public budgets funds, however, in a system of funds flow through the operator carrying out the transport.

For the purchase needs of electric buses - more expensive that traditional buses - a system was created in which operators finance purchases in a mixed solution. They buy an electric bus, but without a battery - the cost of which is a significant part of the bus price - at a price similar to a price of a traditional bus purchase, but they use batteries on a principle of leasing [1, 9, 18]. This solution may be favourable for a number of reasons. First - the purchase order price of an electric bus does not differ significantly from the purchase price of a traditional bus, which means that the purchase may be financed from the depreciation fund and at the moment of purchase it does not disturb the entity's financial management. Another premise is the fact that battery financing is distributed over time and the leasing instalment paid may be included in costs, moreover, funds for its financing at least a part can originate from a decrease of electric bus operating costs as compared with a traditional bus. One can refer here to the lower electricity costs against fuel costs and also lower costs of maintenance and repairs - because of a simpler design of many components of the electric bus drive. Obviously, depending on the country and level of liquid fuels and electricity prices and also of those energy carriers purchase system, existing there, the costs reductions and thereby benefits obtained from such a solution will differ. In addition, one more benefit is obtained - risks related to potential reduction of battery durability or its parameters, below figures specified in the contract, are on the lessor's side.

Solutions consisting in a direct purchase of vehicles from budgetary funds by a municipality or another public unit and handing them over to the operator for use are also possible. An advantage of such a solution consists of using for investments all the funds allocated to this purpose, without limitations related to income tax burdens. Moreover, on this level vehicles may be purchased altogether for a few operators, because of which - due to economies of scale - unit prices may be lower. This solution may be preferred also in the case of acquiring the external co-financing. It is necessary to emphasise that in such a solution the link between the actual economic efficiency of the operator and its development possibilities is broken. Moreover, in a situation where transport in a given area is carried out by a few or a dozen or so bus operators, a problem originates of equal, as a rule, operators access to purchased vehicles. No privileged access, e.g. for publicly owned operators, shall be applied here, because the market costs verification would be lost. Another issue is the fact that operators are released this way (those acquiring vehicles in such a way) from the obligation to achieve appropriate accumulation Since the non-repayable handing over of fixed assets creates a problem of their efficient operation. As a result, an unjustified increase in the investments demand can occur. It will result from reduction of expenditures on the current maintenance of the received asset, leading thereby to its premature wear, resulting from the fact that the received asset did not cost the operator anything.

Another method of investment projects financing in commercial law companies consists in increasing the equity through shares issuing or additional equity contributions of hitherto and new shareholders. The increased amount of equity, available to the company, increases its investment possibilities, which in turn enables introducing the zero-emission vehicles and expansion of the scope of services provided, in accordance with the demand. The basic advantage of the solution consists of a possibility to introduce significant amounts of equity to operators, without inconveniences related to passing funds through the P&L account. The issue of capital availability is the main disadvantage.

Assuming the public ownership of operators carrying out the transport it is possible - apart from electric buses purchase - to indicate other situations, as well, in which the public entities will be interested in injecting capital to operators, i.e.:

- expansion of provided services scope due to land development and origination of the new traffic origins and destinations served by the public transport,
- change of the ownership structure and owners

influence on a given entity management,
- improvement in the entity competitiveness, its financial standing and in the future selling shares or stocks to non-municipal entities.

Attention is drawn to the fact that in the case of many owners, existence of various opinions can appear related to the capital injection need. This will result from a diversified financial situation of public entities, various needs and preferences in the field of allocation and thereby spending the funds available, as well as adopted standards of population needs satisfying in the field of the urban public transport. In addition, limitations related to public aid issues should be considered.

4.2 External financing sources

External financing sources may be divided into repayable and non-repayable. Obviously, the non-repayable ones are the most attractive, they allow to co-finance purchases - most often a significant part of the total funds spent on the investment, without the obligation to return them. A possibility to obtain the non-repayable co-financing occurs most frequently during the implementation of projects, which are not profitable and, at the same time, as a result of which substantial external benefits may be achieved, e.g. related to the environmental protection, as in the case of zero-emission public transport [42]. Special-purpose funds are created, or programmes under which such funds are acquired. Funds and programmes may be national or created within larger integration groups, e.g. the European Union.

In the situation, in which it is not possible to use the non-repayable financing, the financing from repayable sources remains. Credit is one of repayable investment financing sources. The use of credit for investment financing enables obtaining the effect of financial leverage. Operators, increasing their capital, increase assets and as a result can increase their profits. Other advantages of credit use include:
- possibility to incur substantial capital expenditures in a relatively short time,
- investments are implemented directly by the operator, who is most interested in rationality and rightness of purchases made,
- purchased goods are owned by the operator, which provides premises for due care of them and does not violate the balance between expenditures on goods purchase and their maintenance.

Credit is now pretty seldom used by operators to finance investments. It results, among other things, from concerns related to a high credit costs and, as a result, to financial costs growth. Another reason, in the case of projects resulting in benefits in the field of environmental protection, is the fact of non-repayable funds availability.

The use of credit each time requires an analysis taking into account:
- the amount of capital expenditure,
- the inflation rate and credit interest rate,
- possibility to achieve, as a result of investment, operating costs cutting,
- increased services supply and their improved quality.

The credit may be taken by operators or owners - e.g. public sector entities. If credit is taken by owners, it is possible to release the non-repayable financing by these entities.

In addition, bonds may be used, apart from the credit. Bonds can be issued both by the public sector entities, e.g. municipal bonds [43] and by operators. The bond issuer may commit to provide specified services to the bonds holder. Basic advantages of bonds use may include:
- substantial expansion of the scope of potential lenders; bonds may be purchased both by financial institutions and banks and by other enterprises and private individuals, as well,
- bonds give an opportunity to acquire substantial capital, frequently impossible to obtain under a bank loan,
- it is possible to force the bond issuer to provide the bond holder with specific benefits,
- the payment for services may be partially made using bonds.

It is necessary to emphasise that in the case of bonds purchase, e.g. by a public transport organiser, a mutual dependence between the organiser and bond issuer, i.e. operator, occurs. On the other hand, however, the organiser buying bonds can secure itself against an excessive rise in provided services price, by the use of indexed bonds.

The next source of acquiring new vehicles from outside consists in operation of vehicles owned by others, e.g. according to the leasing rules. The carrier (lessee) then uses vehicles for the payment of the leasing rate. Financial efficiency of this project depends on the contract signed by and between the carrier and the lessor, since the object of leasing can be shown in lessor's or lessee's assets. Attention is also drawn to the fact that a lessor may be a transport organiser, as well as entities operating in accordance with commercial rules. An electric bus, but also - what was emphasised before - electric bus batteries, may be the object of leasing. Leasing is considered an attractive financing tool, allowing to reduce the funds spent at the beginning of a purchase project and to distribute costs over time.

4.3 Applicability of research results and implications for managerial practice

There are different organizational and ownership solutions in the urban public transport in cities

worldwide. Involvement of the public administration varies, from the direct provision of services by public entities to being a regulator and commissioning the provision of services and, in some cases, also the management of urban transport. There are also different financing systems of investments and ongoing operations of municipal public transport services. However, irrespective of this, the formulated rules for implementation and financing of electric buses can be applied in various organizational systems of public transport. The key criteria used in their formulation included significant environmental benefits in cities resulting from the zero-emission of electric vehicles and the search for effective solutions to spend the funds, applicable to private entities. The same is valid especially for the public entities, as they spend public funds and at the same time there is no market verification of the services provision costs. Thus, the proposed solutions, as based on the principles of economic and effective spending of funds, are not limited to specific organizational solutions and are not limited to selected countries or cities. For example, they are used both in deregulated and privatized public transport in some cities - for example in the United Kingdom, or in publicly owned and privatized management - like in France, as well as in public entities of urban transport, e.g. in Germany, Poland or Slovakia.

Intensification of purchases and implementation of electric buses, as currently more expensive vehicles than traditional buses, require actions at the levels of transport policy, urban public transport management and the provision of transport services. At the level of the transport policy and the management of public urban transport systems, those require creating programmes and funds that can be used for non-returnable financing of purchases of the zero-emission vehicles. Moreover, when entrusting the provision of services (whether by way of an open competitive procedure or by direct entrustment), the assessment criteria should take into account minimization of the environmental impact and CO_2 emissions in addition to the rate or subsidy to the operating work unit. This will allow the environmental benefits to be balanced against increased public funding. Operators' activities should focus on several directions. The first one is associated with the maximum use of purchased electric buses, despite the increased downtime related to battery recharging. This means directing these vehicles to lines with significant maintenance times, moreover, lines running mainly in the city centres, where environmental aspects are of the greatest importance. The second direction is related to use at purchasing of such financial solutions, which costs will be as low as possible. This means, as far as possible, use of external, non-returnable sources of financing, or, if such are not available, interest-free (no-costs) credits related to environmental protection, irrespective of the previous battery lease solutions with which buses are equipped.

5 Conclusions

Introduction of the city servicing by electric buses means not only challenges related to the manufacturing technology of buses, batteries used by them and their range, creation of battery charging infrastructure and appropriate technical facilities in entities operating such vehicles, but ensuring the appropriate funds, as well, since all those require involvement of substantial funds, including the purchase of electric buses themselves. Services of the urban public transport are public services and the revenue obtained on their sales does not cover the incurred costs - co-financing from public funds is used here, most frequently originating from municipality budgets. Electric buses, as the zero-emission vehicles, allow to obtain the significant external benefits, hence involvement of public funds is advisable and because of buses high costs of purchase - indispensable. Use of the public funds in a special way should obligate to spend funds purposefully and thriftily. It is necessary to show here the search for solutions allowing for effective management of transport and tariffs, ticket inspections and effective recovery of additional charges, as well as implementation of innovations improving the other areas of organisers and operators activity, so that the obtained savings and free funds could be used for emission reduction.

When performing the financial analyses and assessments of electric buses implementation it is suggested to consider the costs incurred during the whole period of vehicles operation and not only those related to their purchase. This criterion should be taken into account and not only at the stage of the feasibility studies preparation, but, if possible, during the bids evaluation in tenders for the new buses procurement, as well. However, the purchase price was taken so far as a significant criterion of entity's choice at procurement of vehicles.

The depreciation write-offs should be the basic source of financing the replacement investments by the bus operators. Adhering to this principle has many advantages, the volume of purchases results from the actual needs related to transport services, more efficient operators have greater accumulation and therefore more funds can be spent on investment purchases and development and the operator is the owner of the property, which eliminates problems of the proper care for the acquired property. However, there is a problem with undertaking development investments and those in which the market and environmental protection requirements force the purchase of vehicles at a significantly higher price - and this is today the case of electric buses. The operators should then assign their profit and when it is not generated, it becomes necessary to use external sources - returnable or non-returnable. In the case of returnable sources, it will be necessary to obtain the higher subsidizing of services provision from public funds.

Prices of electric buses are much higher than of traditional ones, hence the depreciation funds, established by operators, is not sufficient. It is advisable - to a possible extent - to use the non-repayable funds during the procurement, which are aimed at supporting the low-emission transport and modernisation of the transport potential of the urban public transport. Bus purchases may originate also from repayable funds, e.g. a loan or bond issue, where a part of the credit costs may be also refinanced from funds related to the environmental protection and transport modernisation. In addition, the leasing solutions for batteries used by buses are attractive; in this way the demand for funds is reduced at the moment of procurement, as well as the risk of improper quality and durability of the battery itself.

Irrespective of funding sources themselves, it is necessary to implement solutions, in which the purchased vehicles will be effectively used so that the very fact of acquiring means of transport at prices lower than the market ones would not result in deterioration of their care, e.g. pursuing the service costs cutting. It is also necessary to ensure financing of provided services and carrying out an appropriate financial-accounting policy, so that after those means wear, the depreciation charges in the next cycle would allow to buy the next batteries and buses themselves.

References

[1] Electric buses arrive on time. Marketplace, economic, technology, environmental and policy perspectives for fully electric buses in the EU. A study by Transport and Environment [online] [accessed 2020-06-01]. November 2018. Available from: https://www.transportenvironment.org/sites/te/files/publications/Electric%20buses%20arrive%20on%20time.pdf

[2] U. S. Energy Information Administration. Short-Term Energy Outlook (STEO) Independent Statistics and Analysis [online] [accessed 2020-03-01]. February 2020. Available from: https://www.eia.gov/outlooks/steo/

[3] NOWICKI, M. Undepletable energy in the light of depletable minerals / Niewyczerpywalna energia w swietle wyczerpywalnych kopalin (in Polish). Institute for Market Economy Research, Centre for Energy Strategies / Instytut Badan and Gospodarka Rynkowa, Centrum Strategii Energetycznych [online] [accessed 2020-03-01]. December 2012. Available from: https://cse.ibngr.pl/niewyczerpalna_energia_w_swiecie_wyczerpywalnych_kopalin/

[4] RUIZ-MONTANES, M. Financing public transport: a spatial model based on city size. *European Journal of Management and Business Economics* [online]. 2017. **26**(1), p. 112-122 [accessed 2020-04-01]. ISSN 2444-8494. Available from: https://doi.org/10.1108/EJMBE-07-2017-007

[5] DYDKOWSKI, G., TOMANEK, R., URBANEK, A. Tariffs and toll collection systems in municipal public transport / *Taryfy i systemy poboru oplat w miejskim transporcie zbiorowym* (in Polish). Katowice: Wydawnictwo Uniwersytetu Ekonomicznego w Katowicach, 2018. ISBN 978-83-7875-440-4.

[6] ORBEA, J., CASTELLANOS, S., ALBUQUERQUE, C., SCLAR, R., PINHEIRO, B. Adapting procurement models for electric buses in Latin America. *Transportation Research Record: Journal of the Transportation Research Board* [online]. 2019, **2673**(10), p. 175-184 [accessed 2020-03-10]. ISSN 0361-1981, eISSN 2169-4052. Available from: https://doi.org/10.1177/0361198119846097

[7] WYSZOMIRSKI, O., WOLEK, M., JAGIELLO, A., KONIAK, M., MARTLOMIEJCZYK, M., GRZELEC, K., GROMADZKI, M. Electromobility in the public transport, Guide for local governments, public enterprises and private carriers. Practical aspects of implementation / Elektromobilnosc w transporcie publicznym. Przewodnik dla jednostek samorzadu terytorialnego, przedsiebiorstw uzytecznosci publicznej i prywatnych przewoznikow. Praktyczne aspekty wdrazania (in Polish) [online] [accessed 2020-03-10]. Special report. Warsaw: Polish Development Fund and Polish Alternative Fuels Association, 2018. Available from: http://pspa.com.pl/assets/uploads/2018/12/raport_PFR_elektromobilnosc_w_transporcie_S.pdf

[8] HOOFTMAN, N., MESSAGIE, M., COOSEMANS, T. Analysis of the potential for electric buses [online] [accessed 2020-03-10]. A study accomplished for the European Copper Institute. Vrije Universiteit Brussel. Available from: https://leonardo-energy.pl/wp-content/uploads/2019/02/Analysis-of-the-potential-for-electric-buses.pdf

[9] Pay as you save for clean transport. Instrument Analysis. Global Innovation Lab for Climate Finance, September 2018 [online] [accessed 2020-03-10]. Available from: https://climatepolicyinitiative.org/wp-content/uploads/2018/10/PAYS-for-Clean-Transport_Instrument-Analysis.pdf

[10] Directive (EU) 2019/1161 of the European Parliament and of the Council of 20 June 2019 amending Directive 2009/33/EC on the promotion of clean and energy-efficient road transport vehicles. Official Journal of the European Union L/188/116 [online] [accessed 2020-03-10]. Available from: https://eur-lex.europa.eu/legal-content/EN/TXT/PDF/?uri=CELEX:32019L1161&from=EN

[11] Electric bus fleets in Europe. Three turbulent effects that will dominate in the rapid electrification of our public transport. Perspectives, March 2019 [online] [accessed 2020-04-10]. Available from: https://www.accuracy.com/wp-content/uploads/2020/01/Perspectives-Print-Electric-bus-v1_anglais.pdf

[12] LI, X., CASTELLANOS, S., MAASSEN, A. Emerging trends and innovations for electric bus adoption - a comparative case study of contracting and financing of 22 cities in the Americas, Asia-Pacific and Europe. *Research in Transportation Economics* [online]. 2018. **69**, p. 470-481 [accessed 2020-11-10]. ISSN 0739-8859. Available from: https://doi.org/10.1016/j.retrec.2018.06.016

[13] SIOSHANSI, F., WEBB, J. Transitioning from conventional to electric vehicles: The effect of cost and environmental drivers on peak oil demand. *Economic Analysis and Policy* [online].2019, **61**(C), p. 7-15. ISSN 0313-5926. Available from: https://doi.org/10.1016/j.eap.2018.12.005

[14] JATTIN, M. G. *Financial mechanisms for electric bus*. Germany, Eschborn: Deutsche Gesellschaft fur Internationale Zusammenarbeit (GIZ) GmbH on behalf of the Federal Ministry for Environment, Nature Protection and Nuclear Safety of the Federal Republic of Germany, 2019.

[15] LI, X., GORGUINPOUR, C., SCLAR, R., CASTELLANOS, S. How to enable electric bus adoption in cities worldwide. A guiding report for city transit agencies and bus operating entities. Washington DC: World Resources Institute Ross Center, 2019 [online] [accessed 2020-11-10]. Available from: https://wrirosscities.org/research/publication/how-enable-electric-bus-adoption-cities-worldwide

[16] SCLAR, R., GORGUINPOUR, C., CASTELLANOS, S., LI, X. Barriers to adopting electric buses. Washington DC: World Resources Institute Ross Center, 2019 [online] [accessed 2020-11-10]. Available from: https://wrirosscities.org/sites/default/files/barriers-to-adopting-electric-buses.pdf

[17] MILLER, J., MINJARES, R., DALLMANN, T., JIN, L., Financing the transition to soot - free urban bus fleets in 20 megacities. Confederazione Svizzera: The International Council on Clean Transportation, Climate and Clean Air Coalition to Reduce Short-Lived Climate Pollutants, 2017 [online] [accessed 2020-04-10]. Available from: https://theicct.org/sites/default/files/publications/Soot-Free-Bus-Financing_ICCT-Report_11102017_vF.pdf

[18] MOON-MIKLAUCIC, CH., MAASSEN, A., LI, X., CASTELLANOS, S., Financing electric and hybrid-electric buses: 10 questions city decision-makers should ask. Working Paper. World Resources Institute, October 2019 [online] [accessed 2020-04-10]. Available from: https://wrirosscities.org/sites/default/files/financing-electric-hybrid-electric-buses.pdf

[19] RUSSELL BERNARD, H. *Social research methods: qualitative and quantitative approaches*. Los Angeles, London, New Delhi, Singapore, Washington D.C.: Sage Publications, Inc., 2013. ISBN 978-1412978545.

[20] MINTZBERG, H. An emerging strategy of "direct" research. *Administrative Science Quarterly* [online]. 1979, **24**, p. 582-589 [accessed 2020-11-10]. ISSN 0001-8392. Available from: https://doi.org/10.2307/2392364

[21] SHAH, S., CORLEY, K. Building better theories by bridging the qualitative-quantitative divide. *Journal of Management Studies* [online]. 2006, **43**(8), p. 1821-1835 [accessed 2020-11-10]. eISSN 1467-6486. Available from: https://doi.org/10.1111/j.1467-6486.2006.00662.x

[22] BITETKINE, A. Prospective case study design. qualitative method for deductive theory testing. Organizational Research Method. Sage Publications, 2007 [online] [accessed 2020-11-10]. Available from: https://citeseerx.ist.psu.edu/viewdoc/download?doi=10.1.1.117.8867&rep=rep1&type=pdf

[23] BOWEN, G. A. Document analysis as a qualitative research method. *Qualitative Research Journal* [online]. 2009, **9**(2), p. 27-40 [accessed 2020-11-10]. ISSN 1443-9883. Available from: https://doi.org/10.3316/QRJ0902027

[24] DYDKOWSKI, G., OKON, J. Partnerstwo publiczno-prywatne jako narzedzie korzystania z kapitalow prywatnych i efektywnej realizacji zadan publicznych. *Studia Ekonomiczne. Zeszyty Naukowe Uniwersytetu Ekonomicznego w Katowicach*. 2017, **316**, p. 57-69. ISSN 2083-8611.

[25] GNAP, J., KONECNY, V., POLIAK, M. Elasticity of demand in mass passenger transport. *Journal of Economics*. 2006. **54**(7). p. 668-684. ISSN 0931-8658. eISSN 1617-7134.

[26] URBANEK, A. Public transport fares as an instrument of impact on the travel behaviour: an empirical analysis of the price elasticity of demand. In: SUCHANEK, M. (ed) *Challenges of urban mobility, transport companies and systems* [online]. TranSopot 2018. Springer Proceedings in Business and Economics. Cham: Springer, 2019. ISBN 978-3-030-17743-0. p. 101-113. Available from: https://doi.org/10.1007/978-3-030-17743-0_9

[27] TURRO, M., PONS, A., SAURI, S., PENYALVER, D., BUSQUETS, M., GUTBERLET, T., KRITZINGER, S. Pilot project study on innovative ways of sustainably financing public transport. Final Report. Cenit, Prognos, COWI, European Commission, Directoriate general for Mobility and Transport, 2018 [online] [accessed 2020-04-10]. Available from: https://www.emta.com/spip.php?article267&lang=en

[28] EMTA Barometer 2020 - Based on 2018 data, Paris [online] [accessed 2020-06-16]. Available from: https://www.emta.com/spip.php?article267&lang=en

[29] DYDKOWSKI, G., GNAP, J., Premises and limitations of free public transport implementation. *Communications - Scientific Letters of the University of Zilina* [online]. 2019, **21**(4), p. 13-18. ISSN 13364205, eISSN 2585-7878. Available from: https://doi.org/10.26552/com.C.2019.4.13-18

[30] DYDKOWSKI, G. The application of just distribution theories to financing integrated systems of regional and urban public transport. *Scientific Journal of Silesian University of Technology. Series Transport* [online]. 2018, **100**, p. 23-33. ISSN 0209-3324. Available from https://doi.org/10.20858/sjsutst.2018.100.3

[31] FRIEDMAN, M., FRIEDMAN, R. *Free to choose: a personal statement*. New York and London: Harcourt Brace Jovanovich Inc., 1980. ISBN 0-15-133481-1.
[32] Act of 27 August 2009 on Public Finance, Unified text: Dz. u. of 2019, item 869, 1622, 1649 and 2020 / Ustawa z dnia 27 sierpnia 2009 roku o finansach publicznych, Tekst jednolity Dz. u. 2019, poz. 869, 1622, 1649, 2020 (in Polish) [online] [accessed 2020-04-10]. Available from: http://prawo.sejm.gov.pl/isap.nsf/download.xsp/WDU20091571240/U/D20091240Lj.pdf
[33] Act of 24 January 2004 - Public Procurement Law, unified text Dz. u. of 2019, item 1843 / Ustawa z 24 stycznia 2004 r. Prawo zamowien publicznych. Tekst jednolity Dz. u. z 2019, poz. 1843 (in Polish) [online] [accessed 2020-04-10]. Available from: http://prawo.sejm.gov.pl/isap.nsf/download.xsp/WDU20040190177/U/D20040177Lj.pdf
[34] Act of 6 June 1997 on Penal Code, unified text Dz. u. of 2018, item 1600, 2077 / Ustawa z dnia 6 czerwca 1997 r. kodeks karny, tekst jednolity Dz. u. z 2018 roku, poz. 1600, 2077 (in Polish) [online] [accessed 2020-04-10]. Available from: http://prawo.sejm.gov.pl/isap.nsf/DocDetails.xsp?id=WDU19970880553
[35] OWSIAK, S. *Public finance. Theory and practice* / *Finanse publiczne. Teoria i praktyka* (in Polish). Warsaw: PWN, 2005. ISBN 978-83-011-5732-6.
[36] KAMERSCHEN, D. R., MCKENZIE, R. B., NARDINELLI, C. *Economics* / *Ekonomia* (in Polish). Gdansk: Fundacja Gospodarcza NSZZ Solidarnosc, 1999. ISBN 83-00-03545-1.
[37] TOMANEK, R. *Competitiveness of urban transport* / *Konkurencyjnosc transportu miejskiego* (in Polish). Katowice: Wydawnictwo Akademii Ekonomicznej, 2002. ISBN 83-7246-199-6.
[38] VAN ESSEN, H., SCHROTEN, A., OTTEN, M., SUTTER, D., SCHREYER, CH., ZANDONELLA, R., MAIBACH, M., DOLL, C. External costs of transport in Europe. CE Delft, INFRAS Fraunhofer ISI, September 2011 [online] [accessed 2020-04-10]. Available from: https://www.cedelft.eu/publicatie/external_costs_of_transport_in_europe/1258
[39] BECKER, U. J., BECKER, T., GERLACH, J. The true costs of automobility: external costs of cars overview on existing estimates in EU 27. Technische Universitat Dresden [online] [accessed 2020-04-10]. Available from: https://stopclimatechange.net/fileadmin/content/documents/move-green/The_true_costs_of_cars_EN.pdf
[40] External costs of transport in Central and Eastern Europe. OECD, Central European Initiative, Austrian Federal Ministry of Agriculture, Forestry, Environment and Water Management, Paris, Trieste, Vienna [online] [accessed 2020-05-10]. Available from: http://www.oecd.org/greengrowth/greening-transport/29403950.pdf
[41] POLIAK, M., SEMANOVA, S., MRNIKOVA, M., KOMACKOVA, L., SIMURKOVA, P., POLIAKOVA, A., HERNANDES, S. Financing public transport services from public fonds. *Transport Problems* [online]. 2017, **12**(4). p. 61-72. eISSN 2300-861X. Available from: https://doi.org/10.20858/tp.2017.12.4.6
[42] GLOTZ-RICHTER M., KOCH H. Electrification of public transport in cities (Horizon 2020 ELIPTIC Project). *Transportation Research Procedia* [online]. 2016, **14**. p. 2614-2619 [accessed 2020-11-10]. ISSN 2352-1465. Available from: https://doi.org/10.1016/j.trpro.2016.05.416
[43] CASALE, M., MAHONEY, B. Paying for electric buses. financing tools for cities and agencies to Ditch Diesel. U.S. PRIG Education Fund, Fall 2018 [online] [accessed 2020-06-10]. Available from: https://uspirg.org/sites/pirg/files/reports/National%20-%20Paying%20for%20Electric%20Buses.pdf

FUZZY-LOGIC APPROACH TO ESTIMATE THE PASSENGERS' PREFERENCE WHEN CHOOSING A BUS LINE WITHIN THE PUBLIC TRANSPORT SYSTEM

Vitalii Naumov[1,*], Baurzhan Zhamanbayev[2], Dinara Agabekova[3], Zhumazhan Zhanbirov[4], Igor Taran[5]

[1]Faculty of Civil Engineering, Cracow University of Technology, Cracow, Poland
[2]Kazakh Academy of Transport and Communications, Almaty, Kazakhstan
[3]Eurasian Technological University, Almaty, Kazakhstan
[4]Central-Asian University, Almaty, Kazakhstan
[5]Department of Transport Management, Dnipro University of Technology, Dnipro, Ukraine

*E-mail of corresponding author: vnaumov@pk.edu.pl

Resume

For the developed system of public transport, the passengers, as the customers, have a variety of alternatives when choosing the transport mode or even the route for the given mode of public transport. The estimation of the passengers' preference is the key task for transportation planners for solving the wide range of optimization problems in the field of public transport. A methodology for estimation of the passengers' preference when choosing the bus line within a public transport system is developed in this paper. The proposed approach is based on the fuzzy-logic mathematical apparatus and uses the surveys' data to calculate the membership functions defining the passengers' preference. The case study of the passengers' survey, held in Talas (Kazakhstan), is used to illustrate the developed methodology.

Article info

Received 10 November 2020
Accepted 8 December 2020
Online 29 April 2021

Keywords:

public transport,
preference estimation,
fuzzy sets,
membership function

Available online: https://doi.org/10.26552/com.C.2021.3.A150-A157

ISSN 1335-4205 (print version)
ISSN 2585-7878 (online version)

1 Introduction

The passengers' preference is the fundamental feature that conditions the choice of possible alternatives by travelers within an existing transport system [1]. These alternatives to be chosen by the transport system users, usually refer to the modes of transport or the travel routes (transport lines in the case of a public transport system).

The traditional approach to model the travelers' preferences when selecting the mean of transport and trip path is based on the utility theory and, in practice, supposes the estimation of the utility function on the grounds of some empirical information.

The utility theory application in practical transportation studies may be found in recent publications [2-9]. The paper [2] compares different model specifications of travel time reliability in public transport route choices, the considered models are estimated based on empirical observations and used in order to evaluate the utility function. The authors of the paper [3] propose the mode choice model for public transport that integrates structural equation and discrete choice models with categorized latent variables; the objective of the presented study was to develop an improved disaggregate model that better ex-plains travel behavior within the public transport system. The study [4] uses empirical data of university students' transport choices in the Bilbao area, the authors illustrate how the utility that individuals get from the mode of transport can be modeled and estimated based on this information. The model described in publication [5] allows bicycle-sharing system operators to plan services more effectively by examining the impact of travel distance, land use, built environment and access to public transportation infrastructure on users' destination preferences: the authors of the paper propose to generate utility profiles as a function of distance and other attributes. Authors of [6] propose the approach to evaluate the passengers' comfort based on the preference survey where crowding levels are presented as illustrations; the survey data are used by the authors to estimate discrete choice models and obtain a subjective evaluation of passenger density through the parameters of the utility function. The study [8] depicts the study case of using the EVA mode choice model in the city of Ljubljana, Slovenia; the authors have designed the stated preference survey and estimated different types of utility functions; the utility functions obtained based on the survey results are used further as initial data for the PTV Visum software to simulate the operation of the city transport system.

This is an open access article distributed under the terms of the Creative Commons Attribution 4.0 International License (CC BY 4.0), which permits use, distribution, and reproduction in any medium, provided the original publication is properly cited. No use, distribution or reproduction is permitted which does not comply with these terms.

The results of the assessment of the travelers' preference are used for modelling the demand for transport services [10-11], but also for optimization of transport processes [12-13], as well as for designing and simulation of the transport system [14-16].

As far as the traveler preference cannot be determined unequivocally (as it depends on the big number of non-deterministic parameters with the values assessed subjectively by different persons), the fuzzy logic mathematical apparatus is widely used to define the preferences of passengers and their satisfaction with the provided transport services [17-20]. The authors of the paper [17] have developed an approach combining characteristics of the analytic hierarchy process, entropy weight method and the fuzzy comprehensive evaluation method to improve the accuracy of passenger satisfaction evaluation for public transport. A similar methodology is described in [18]: the authors propose a decision support model for measuring the public transport level by using a combination of the fuzzy logic and the analytic hierarchy process. A method, used to evaluate the passenger satisfaction with the public transportation system that is based on the Pythagorean fuzzy sets and multi-objective optimization, is described in [19]. A method to describe the travel comfort characteristics with synthetic indices, based on the individual comfort indices of travel components, is proposed in [20]; the authors use a fuzzy approach to evaluate the conditions of travelers' comfort.

This paper contributes to direction of using the fuzzy logic for assessment of the travelers' preferences. The aim was to develop a simple but reliable method that uses the travelers' survey data to calculate the membership functions describing the basic preferences of the passengers of a public transport system: pricing, comfortability and travel speed.

2 Proposed method of the passenger preferences assessment

The carrier's goal is the most complete coverage of the existing and potential market, for which it is necessary to attract passengers moving from and to the points covered by the public transport route. If the fulfillment of the passenger's need for movement is possible in the only way - by using one accessible bus route, then the carrier gets the maximum possible share of this market sector. However, if the need for travel can be realized in more than one way (the trip can be implemented by more than one route in the public transport system), the passenger has a choice. In this case, there will be a conflict situation between carriers who can potentially serve the same trip. Depending on the strategy chosen by the carrier, the passenger gives preference to the corresponding route.

The assignment of a trip to public transport routes depends on preferences of passengers, but also on importance of this trip for the carrier (meaning that the carrier determines the strategy of behavior depending on the attractiveness of a particular trip).

Passenger preferences when choosing a route depend on three main indicators: delivery speed (travel time), comfort and the price of services. All of these parameters are determined to some extent by the bus model. The delivery speed depends on the design features (however, the traffic speed is also affected by the congestion of the road network and the methods of organizing traffic). Comfortability directly depends on the passenger capacity of the bus, the design features of the cabin and vehicles' suspension. The price of the service is determined based on the cost of the provided transport services, which depends on the performance characteristics of a particular bus model. Thus, we can claim that the preferences of passengers when choosing a particular route depend on the bus models used by carriers.

It is convenient to describe the degree of preference by passengers of a particular bus model by means of a fuzzy subset that characterizes the belonging of a given bus model to the set of optimal models. In this case, the degree of preference for different origin-destination (O-D) pairs, or for the same O-D pair at different hours of the day (day of the week), can differ significantly. For example, for O-D pairs associated with the sleeping areas of a city, the significance of the travel speed is different depending on the time of day. In general, each O-D pair can be associated with different subgroups of consumers of transport services, based on the purpose of the trip, while the composition of the O-D pairs will determine the type of a membership function.

If the preference by the criterion of the travel speed is described with the membership function μ_V, by criterion of the travel comfort - with function μ_K and by criterion of the travel price - with function μ_T, where $\mu_V \in [0;1], \mu_K \in [0;1], \mu_T \in [0;1]$, then the general preference of a passenger can be expressed through a fuzzy subset μ, which is a combination of subsets μ_V, μ_K and μ_T:

$$\mu = w_V \cdot \mu_V + w_K \cdot \mu_K + w_T \cdot \mu_T, \quad (1)$$

where: w_V, w_K and w_T are weight coefficients for the membership functions of the travel speed, comfortability and the tariff, respectively.

To assess the preferences of passengers, it is necessary to determine the type of membership functions of a fuzzy subset of optimal bus models and standardize them for the main groups of passengers. In order to determine the membership functions, use of methodology for analyzing the results of an expert survey is proposed. For this, the following stages should be performed by a researcher:

1. Collecting the data and calculating significance of features for the respondents divided into main social groups of travelers (e.g., students, retirees, etc.).

2. Estimating the sufficiency of the collected data.
3. Assessing the consistency of the respondents' opinions.
4. Evaluating the empirical values of the membership functions for categories of the features' significance per each social group represented in the respondent's sample.
5. Evaluating the functional dependencies that approximate the membership functions (at this stage, the quality of the obtained mathematical models should be checked and the rescaling of the dependencies can be performed).

At the first stage, respondents (public transport customers) are invited to assess the significance of the level of tariffs, comfort and travel speed based on a 10-point scale. When processing the questionnaires for each of the characteristics, the features' significance z_i for the respondents is determined in unit fractions as follows:

$$z_i = \frac{B_i}{B_V + B_K + B_T}, \tag{2}$$

where: B_i is the number of points given by a respondent to the i-th feature: $B_i \in \{B_V; B_K; B_T\}$;
B_V, B_K and B_T are the grades given by the passengers to travel speed, comfortability and the tariff, respectively.

At the second stage, after a preliminary assessment of the respondents' opinions, the sufficiency of the number of interviewed respondents should be assessed. For this, the average sampling error Δ_i must be estimated according to the significance of the i-th characteristics to passengers participated in the survey [21]:

$$\Delta_i = \sqrt{\frac{1}{N \cdot (N-1)} \cdot \sum_{j=1}^{N} (z_{ij} - \bar{z}_i)^2}, \tag{3}$$

where: $\bar{z}_{ij}$ is the average value of the i-th feature's significance for a passenger; N is the number of respondents (passengers interviewed).

The required (sufficiently big) size N_i^* of the sample for the i-th feature is estimated in the following way [21]:

$$N_i^* = \frac{N}{N \cdot \frac{d_i^*}{3} + 1}, \tag{4}$$

where: d_i^* is the ratio of the sampling error margin to the standard deviation of the studied values (the features' significance for the passengers):

$$d_i^* = \frac{\Delta_i}{\sigma_i}, \tag{5}$$

where: σ_i is the standard deviation for the significance of the i-th feature.

At the third stage, it is proposed to assess the consistency of the respondents' opinions using the Kendall's coefficient of concordance W [21]:

$$W = \frac{12 \cdot S}{N^2 \cdot (M^3 - M)}, \tag{6}$$

where: S is sum of squares of deviations of all the rank estimates of each object of examination (the preference feature) from the corresponding mean value; M is the number of the objects of expertise (the preference features being assessed by the respondents).

The closer the concordance coefficient value to 1, the better is the consistency of the respondents' opinions. If the W value is less than 0.5, the number of the respondents participated in the survey should be increased.

At the fourth stage, based on the survey's data, it is proposed to define the passenger's preference as the membership function μ_{ijk} for the i-th social group by the j-th feature in the k-th category in the following way:

$$\mu_{ijk} = \frac{N_{ijk}}{\max\limits_{k} N_{ijk}}, \tag{7}$$

where: N_{ijk} is the number of respondents of the i-th social group who rated the j-th feature as a value in the k-th range defining the corresponding category.

Finally, at the fifth stage, it is proposed to estimate the analytical form of the membership functions based on the pairs of empirical values and the corresponding categories $\langle \mu_{ijk}, k \rangle$. The functional dependences may be assessed for each of the features (tariff, comfort and travel speed) by using the least squares method for the polynomial model reflecting the shape of the dependence:

$$\mu_i(k) = \sum_{p=0}^{P} a_{ip} \cdot k^p, \tag{8}$$

where: k is the ordinal number of the category for the i-th feature described by the membership function μ_i; a_{ip} are the coefficients of the polynomial model defining the functional dependence; P is the complexity of the polynomial model.

It should be noted that the polynomial models fitted to the empirical data must be complex enough to provide the desired quality of estimations, e.g. the highest degree of the polynomial must be big enough to guarantee the value of the determination coefficient at least at the level of 95 % (in practice, the higher is the polynomial model's complexity, the better is the model's fitness to the empirical data).

The coefficients a_{ip}^* of the polynomial models for determining the dependences of the membership functions on the natural values of the selected features (tariff, comfort level and travel speed) can be determined from the ratio:

$$a_{ip}^* = a_{ip} \cdot \left(\frac{K}{\max f_i} \right)^j, \tag{9}$$

where: $\max f_i$ is the maximum value of the i-th feature; K is the number of the defined categories of the

Table 1 *Results of the conducted survey*

range of the indicator's significance	number of respondents		
	tariff level	comfort level	speed level
adults of working age			
0…0.1	11	2	4
0.1…0.2	26	22	17
0.2…0.3	27	28	22
0.3…0.4	28	30	26
0.4…0.5	38	48	61
total in group	130	130	130
students			
0…0.1	1	4	2
0.1…0.2	12	52	13
0.2…0.3	48	70	15
0.3…0.4	30	17	52
0.4…0.5	91	39	100
total in group	182	182	182
retirees			
0…0.1	1	1	2
0.1…0.2	2	2	11
0.2…0.3	6	21	26
0.3…0.4	21	26	28
0.4…0.5	48	28	11
total in group	78	78	78
total in survey	390	390	390

Table 2 *Calculation results for the sufficient number of respondents*

parameter	feature		
	tariff level	comfort level	speed level
standard deviation	0.0107	0.0113	0.0074
average error of the sample	0.0005	0.0006	0.0004
margin of the sample's error	0.0016	0.0017	0.0011
the ratio of the sample's error margin to the standard deviation	0.1527	0.1527	0.1527
statistically sufficient number of respondents	371	371	371

feature's significance for the traveler (the bigger is the number of categories, the more precise estimation of the membership functions' dependencies will be obtained).

3 Case study: estimation of passengers' preference in Talas, Kazakhstan

The passenger preference survey was conducted in October 2019 in the city of Talas (Taraz), Kazakhstan. Within the conducted survey 390 inhabitants were interviewed and the following social groups were identified: adults of working age, students and pensioners (retirees). The division of the respondents on the subsets representing the mentioned social groups was conditioned by the existing pricing policy: the ticket price for students is partly refunded, adults pay the full price and retirees can use the public transport system under conditions of a full refund of the travel costs. Furthermore, the representatives of the listed social groups have different average incomes; this factor conditions the trip preferences of the passengers including the route and transport choice preferences. Children were not considered as the respondents in the conducted survey, as they usually do not travel alone and, as a consequence, do not make the trip choice decisions by themselves.

The survey was conducted at the bus stops of the Talas public transport system. The respondents answered the group of questions related to their social status (age, source of income, the average income, etc.). In addition, the respondents were asked to assess their

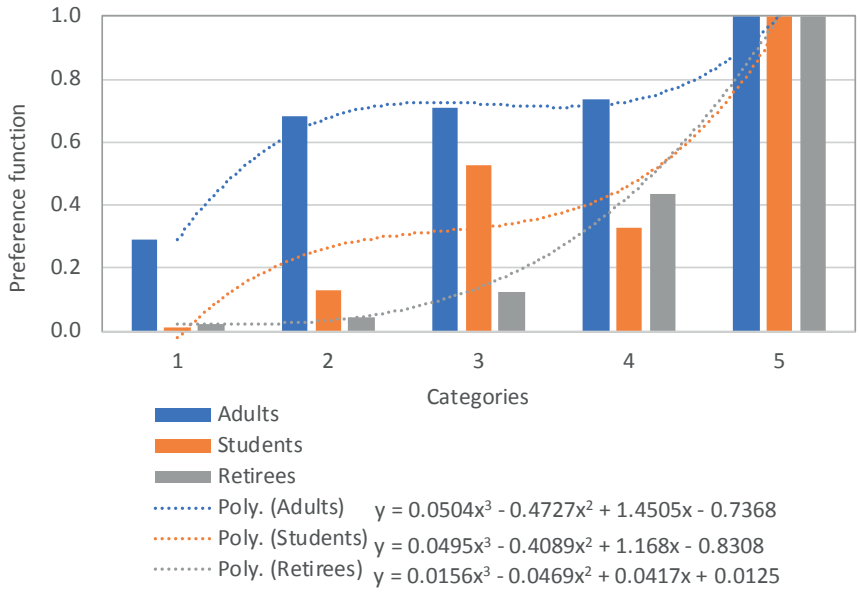


Figure 1 *Polynomial models for the tariff membership functions*

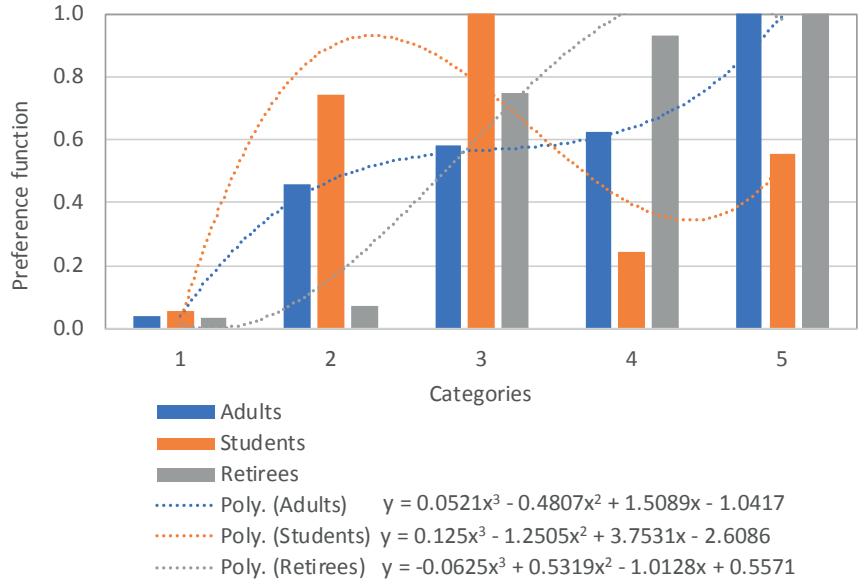


Figure 2 *Polynomial models for the comfort membership functions*

preference related to the transport line choice for three basic features: the level of tariff, comfortability and travel speed. For each feature, the grade was assigned according to a 10-points scale (the more preferable is the transport line's feature, the higher is the grade). Based on grades given by each respondent, the features' significance was calculated by using Equation (2).

After processing the survey results, it was stated that the value z_i for i-th feature is not greater than 0.5. To study the preferences of passengers, 5 ranges were defined in the range of possible values of the significance with a step of 0.1:

- 1 category: the features' significance z_i in the range [0; 0.1];
- 2 category: the features' significance z_i in the range (0.1; 0.2];
- 3 category: the features' significance z_i in the range (0.2; 0.3];
- 4 category: the features' significance z_i in the range (0.3; 0.4];
- 5 category: the features' significance z_i in the range (0.4; 0.5].

All respondents were divided into three groups according to social status, after which the preferences were investigated for each attribute in each of the groups. Results of the survey are presented in Table 1.

Results of calculation of a sufficient number of respondents for each feature of the passengers' preference are shown in Table 2.

As can be seen from Table 2, a sufficient number of respondents is smaller than the number of respondents who took part in the survey. It means that the analyzed

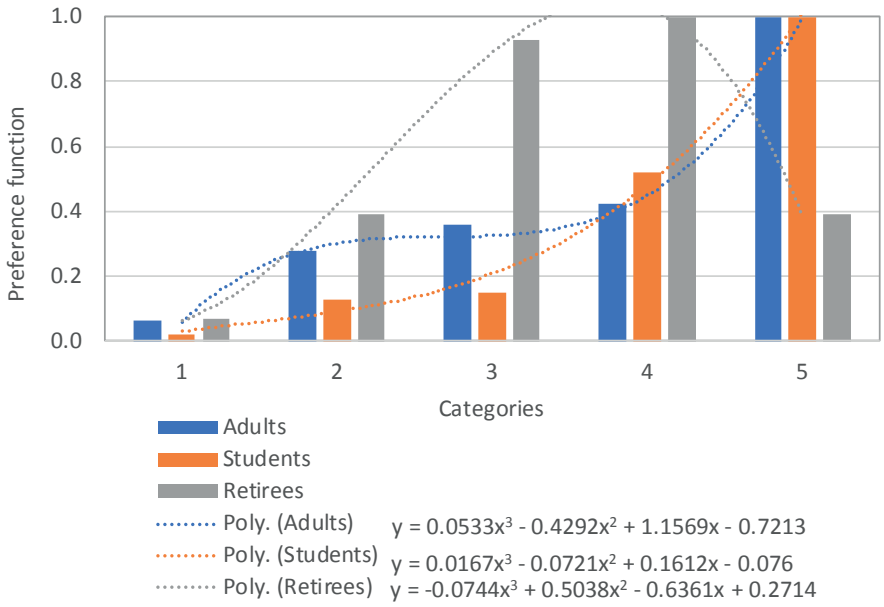


Figure 3 *Polynomial models for the travel speed membership functions*

Table 3 *Coefficients of polynomial models representing the membership functions*

degree of the polynomial p	categories of passengers					
	adults		students		retirees	
	a_{ip}	a^*_{ip}	a^*_{ip}	a^*_{ip}	a_{ip}	a^*_{ip}
tariff membership function						
3	0.0504	1.87e-06	0.0495	1.83e-06	0.0156	5.78e-07
2	-0.4727	-5.25e-04	-0.4089	-4.54e-04	-0.0469	-5.21e-05
1	1.4505	4.84e-02	1.168	3.89e-02	0.0417	1.39e-03
0	-0.7368	-7.37e-01	-0.8308	-8.31e-01	0.0125	1.25e-02
comfort membership function						
3	0.0521	6.51e+00	0.125	1.56e+01	-0.0625	-7.81e+00
2	-0.4807	-1.20e+01	-1.2505	-3.13e+01	0.5319	1.33e+01
1	1.5089	7.54e+00	3.7531	1.88e+01	-1.0128	-5.06e+00
0	-1.0417	-1.04e+00	-2.6086	-2.61e+00	0.5571	5.57e-01
travel speed membership function						
3	0.0533	5.33E-05	0.0167	1.67E-05	-0.0744	-7.44E-05
2	-0.4292	-4.29E-03	-0.0721	-7.21E-04	0.0538	5.38E-04
1	1.1569	1.16E-01	0.1612	1.61E-02	-0.6361	-6.36E-02
0	-0.7213	-7.21E-01	-0.076	-7.60E-02	0.2714	2.71E-01

Table 4 *Ranges of indicator values by categories*

category	tariff (KZT)	comfort level	travel speed (km/h)
1	25…50	0.0…0.2	0…10
2	50…75	0.2…0.4	10…20
3	75…100	0.4…0.6	20…30
4	100…125	0.6…0.8	30…40
5	125…150	0.8…1.0	40…50

sample is big enough to ensure the statistical significance of the membership functions being estimated.

The value of the coefficient of concordance, based on the results of a questionnaire, according to Equation (6), is equal to 0.827, which indicates a high agreement of opinions of respondents who participated in the survey.

4 Results and discussion

Using the standard MS Excel functions, the trend models for the membership functions as the third-degree polynomial models were defined. The third power of the polynomial models was accepted as the satisfactory precision, as far as determination coefficient for the obtained models was not lower than 0.90. A better approximation could be performed, if the higher power of polynomial models were applied; however, that may lead to overestimation of the functional dependencies representing the membership functions.

The polynomial models of the membership functions representing features of the passengers' preference depending on the categories of values are shown in Figures 1-3.

Results of calculations for the polynomial models coefficients, to determine the dependence of the membership function on the value of the corresponding feature, are shown in Table 3.

When calculating the coefficients a_{ip}^{*}, values of natural indicators presented in Table 4 were considered.

The polynomial models in their recalibrated form may be used for assessment of the passengers' preferences based on the features' values presented in the corresponding units (not on their significance for the public transport users). However, the features' values should be contained in the range of possible values shown in Table 4.

To evaluate the membership function μ, depicting the final preference of passengers, the weight coefficients for each of the selected features must be determined. Values of the weight coefficients, as the arithmetic mean values of z_i for all respondents, were defined. In accordance with the survey data, the following values were obtained w_V = 0.321, w_K = 0.322 and w_T = 0.357. As it can be noted, the selected preference features were evaluated by the respondents almost equally, although the tariff was assessed as a bit more significant feature.

It should be underlined that the functional dependencies described in this paper represent preferences of the public transport system customers in the Talas city. There is no evidence that these models may be used for assessing the preferences of the public transport users in other regions. However, the presented methodology is transferable and can be implemented for the survey-based studies of transport preferences in any system of public transport.

5 Conclusions

The proposed approach makes possible determining the shape of membership functions of a fuzzy subset of optimal bus models for the main categories of passengers. The obtained functional dependencies describing the membership functions allow researchers to estimate the preferences of passengers for specific origin-destination pairs. Results of evaluating the passenger preferences are the initial data for solving a wide range of problems in the field of transport planning, such as defining utility functions for the route-choice and mode-choice tasks in the advanced simulation models of a city transport system, choosing strategies of transport companies servicing a public transport system, assessing the quality of services provided within a city public transport system, etc.

The considered example of assessing passenger preferences, based on the results of a survey in the Talas city, suggests that the developed approach is a convenient tool using which a statistically significant assessment of passenger preferences can be obtained with minimal effort. Special attention, however, should be paid to the design of a survey used as initial data in the proposed method: the number of respondents representing considered social groups should correspond to the existing proportion of these groups in the city population. Furthermore, the number of respondents should be big enough to ensure the statistical significance of the models for assessing the passengers' preferences.

As directions for the further research, one should mention checking the conformity of the obtained polynomial models based on survey data in other cities, as well as using a bigger number of categories when calculating empirical values of membership functions. Another issue to be solved in the future concerns the complexity of the polynomial models approximating the membership functions, although in the case-study described in this paper the third-degree polynomial models have guaranteed the satisfactory precision.

References

[1] ORTUZAR, J. D., WILLUMSEN, L. G. *Modelling transport*. 2. ed. John Wiley & Sons, Ltd., 2011. ISBN 978-0-470-76039-0.

[2] SWIERSTRA, A. B., VAN NES, R., MOLIN, E. J. E. Modelling travel time reliability in public transport route choice behaviour. *European Journal of Transport and Infrastructure Research* [online]. 2017, **17**(2), p. 263-278. ISSN 1567-7141. Available from: https://doi.org/10.18757/ejtir.2017.17.2.3194

[3] CHEN, J., LI, S. Mode choice model for public transport with categorized latent variables. *Mathematical Problems in Engineering* [online]. 2017, **2017**, 7861945. ISSN 1024-123X. Available from: https://doi.org/10.1155/2017/7861945

[4] BILBAO-UBILLOS, J., FERNANDEZ-SAINZ, A., HEIDENREICH, N., SPERLICH, S. Flexible estimation of transport demand functions: recommendations for public policy makers. *Transportation Letters* [online]. 2015,

7(5), p. 241-251. ISSN 1942-7867. Available from: https://doi.org/10.1179/1942787514Y.0000000046

[5] FAGHIH-IMANI, A., ELURU, N. Analysing bicycle-sharing system user destination choice preferences: Chicago's Divvy system. *Journal of Transport Geography* [online]. 2015, **44**, p. 53-64. ISSN 0966-6923. Available from: https://doi.org/10.1016/j.jtrangeo.2015.03.005

[6] BATARCE, M., MUNOZ, J. C., ORTUZAR, J. D. D., RAVEAU, S., MOJICA, C., RIOS, R. A. Use of mixed stated and revealed preference data for crowding valuation on public transport in Santiago, Chile. *Transportation Research Record* [online]. 2015, **2535**, p. 73-78. ISSN 0361-1981. Available from: https://doi.org/10.3141/2535-08

[7] QUAN, Z., WEITIAO, W. T. Research on the critical attributes of travel mode choice utility function. *Advanced Materials Research* [online]. 2013, **790**, p. 515-521. ISSN 1022-6680. Available from: https://doi.org/10.4028/www.scientific.net/AMR.790.515

[8] STRNAD, I., ZURA, M. Genetic algorithms application to EVA mode choice model parameters estimation. *International Journal of Mathematical Models and Methods in Applied Sciences* [online]. 2011, **5**(3), p. 533-541. ISSN 1998-0140.

[9] ROORDA, M. J., PASSMORE, D., MILLER, E. J. Including minor modes of transport in a tour-based mode choice model with household interactions. *Journal of Transportation Engineering* [online]. 2009, **135**(12), p. 935-945. ISSN 0733-947X. Available from: https://doi.org/10.1061/(ASCE)TE.1943-5436.0000072

[10] BATARCE, M., IVALDI, M. Urban travel demand model with endogenous congestion. *Transportation Research Part A: Policy and Practice* [online]. 2013, **59**, p. 331-345. ISSN 0965-8564. Available from: https://doi.org/10.1016/j.tra.2013.12.006

[11] NAUMOV, V., Modeling demand for passenger transfers in the bounds of public transport network. *Advances in Intelligent Systems and Computing* [online]. 2019, **879**, p. 156-163. ISSN 2194-5357. Available from: https://doi.org/10.1007/978-3-030-02305-8_19

[12] BORJESSON, M., FUNG, C. M., PROOST, S., YAN, Z. Do buses hinder cyclists or is it the other way around? Optimal bus fares, bus stops and cycling tolls. *Transportation Research Part A: Policy and Practice* [online]. 2018, **111**, p. 326-346. ISSN 0965-8564. Available from: https://doi.org/10.1016/j.tra.2018.03.023

[13] NAUMOV, V. Optimizing the number of vehicles for a public bus line on the grounds of computer simulations. In: 5th IEEE International Conference on Models and Technologies for Intelligent Transportation Systems MT-ITS 2017: proceedings [online]. 2017. ISBN 978-150906484-7, p. 176-181. Available from: https://doi.org/10.1109/MTITS.2017.8005661

[14] AMOROSO, S., MIGLIORE, M., CATALANO, M., GALATIOTO, F. A demand-based methodology for planning the bus network of a small or medium town. *European Transport - Trasporti Europei*. 2010, **44**, p. 41-56. ISSN 1825-3997.

[15] MILLER, J. S., HOEL, L. A., DALTON, T. F., MCCRAY, D. R. Linking transportation planning to program implementation. *Journal of Urban Planning and Development* [online]. 2008, **134**(2), p. 88-95. ISSN 0733-9488. Available from: https://doi.org/10.1061/(ASCE)0733-9488(2008)134:2(88)

[16] NAUMOV, V., SAMCHUK, G. Class library for simulations of passenger transfer nodes as elements of the public transport system. *Procedia Engineering* [online]. 2017, **187**, p. 77-81. ISSN 1877-7058. Available from: https://doi.org/10.1016/j.proeng.2017.04.352

[17] ZHANG, X., LIU, H., XU, M., MAO, C., SHI, J., MENG, G., WU, J. Evaluation of passenger satisfaction of urban multi-mode public transport. *PLoS ONE* [online]. 2020, **15**(10), e0241004. ISSN 1932-6203. Available from: https://doi.org/10.1371/journal.pone.0241004

[18] UTAMA, D. N., ROKHMAN, A. N., PUTRI, N., RIANGGA, A., FAUZI, R. R. Fuzzy-AHP based decision support model for assessing public transport service. *International Journal of Emerging Trends in Engineering Research* [online]. 2020, **8**(8), p. 4185-4192. ISSN 2347-3983. Available from: https://doi.org/10.30534/ijeter/2020/25882020

[19] LI, X.-H., HUANG, L., LI, Q., LIU, H.-C. Passenger satisfaction evaluation of public transportation using Pythagorean fuzzy MULTIMOORA method under large group environment. *Sustainability* [online]. 2020, **12**(12), 4996. ISSN 2071-1050. Available from: https://doi.org/10.3390/su12124996

[20] KISGYORGY, L., TOTH, J. Fuzzy analysis of comfort along travel chains. *Transport* [online]. 2020, **35**(2), p. 203-212. ISSN 1648-4142. Available from: https://doi.org/10.3846/transport.2020.12634

[21] EASTERLING, R. G. *Fundamentals of statistical experimental design and analysis*. John Wiley & Sons, Ltd., 2015. ISBN 978-1-118-95463-8.

EXTERNAL ECONOMIC EFFECTS OF AIR TRANSPORT DEVELOPMENT DUE TO THE LIBERALIZATION

Oksana Ovsak*, Maryna Vysotska

Department of Management of Enterprises Foreign Economic Activity, Faculty of Transport, Management and Logistics, National Aviation University, Kyiv, Ukraine

*E-mail of corresponding author: ovsak@i.ua

Resume

The paper is devoted to research of the impact of gradual liberalization of aviation market on the country's air transport industry development and on formation of external economic components of the country's GDP connected to it directly: export and import of air transport services. The study of the relationship between the operation indicators of air transport and formed external economic effects has been conducted using comparative, correlative and regression analysis based on the statistical data of Ukraine, which has its own air transport industry and is on the path of aviation liberalization. A strong dependence of the export of air transport services on the total number of international flights and its passengers was revealed. This determines the feasibility of tracking the external economic effects in the design of changes on directions and means of further development of country's air transport sector.

Article info

Received 30 July 2020
Accepted 17 December 2020
Online 30 April 2021

Keywords:

aviation transport,
liberalization,
export,
import,
GDP,
external economic effects,
operation indicators of air transport

Available online: https://doi.org/10.26552/com.C.2021.3.A158-A173

ISSN 1335-4205 (print version)
ISSN 2585-7878 (online version)

This is an open access article distributed under the terms of the Creative Commons Attribution 4.0 International License (CC BY 4.0), which permits use, distribution, and reproduction in any medium, provided the original publication is properly cited. No use, distribution or reproduction is permitted which does not comply with these terms.

1 Introduction

In the recent decades many studies have been conducted to explore the impact of the air transport industry on the world economy and the economic system of the country involved. Well-known world aviation organizations, such as the International Civil Aviation Organization (ICAO), the International Air Transport Association (IATA), the Air Transport Action Group (ATAG), the European Regional Science Association (ERSA) publish annual reports, hold world conferences to inform the world community about the state and problems of global air transport development, reveal the specifics of its activities in the regional and national context, assess its impact on the economy and make development forecasts [1-4]. Problems of the aviation services market development are also cared of by the World Trade Organization (WTO) [5].

As a mode of transport, air transport contributes to development of the local economy, which receives primary, secondary, tertiary and perpetual effects [6]. Activity of the air transport companies works to increase the GDP of the involved country due to direct, indirect, catalytic and induced impact [1-5]. At the same time, with the growth of the GDP, the demand for air transport services is growing as an important component of the tourism business [5-7]. Like other modes of transport, there is a relationship between the growth of air transport enterprises' activity and the country's GDP [1, 6, 8-11], as well as regions [12]. The methodology for estimation of the economic (income) and social (employment) impact of the air transport on the national economy was presented in the research of Dimitrios and Maria [7], where all the quantifications of the socioeconomic impacts on the data of the Greek economy have been made.

Liberalization of air transportation is a steady trend in the world's civil aviation. Liberalization of air transportation is the gradual expansion of the established norms of air traffic regulation in the Chicago Convention, which has been signed in 1944 and the creation of special aviation regimes, which were called "open skies" [5-6]. Creation of the EU single aviation market put an end to the system of air services agreements between EU Member States [13]. Other countries are liberalizing aviation market by progressive expanding the terms of bilateral agreements on existing bilateral air services agreements between countries. Such agreements determine whether airlines can freely set tariffs (whether approval by the other party is required), how many airlines can provide transportation services and carrying capacity (capacity of air transportation services, e.g. volumes, frequency of air transportation, types of aircraft).

Liberalization has led to substantial economic and traffic growth due to increased competition and efficiency gains in the airline industry and positive externalities to the overall economy [6, 9, 12, 14-16]. Gillen, et al. [17]

have provided fundamental investigations and have developed a model that provides measures of distribution of the gains and losses across the consumers and airlines of each country involved in the bilateral air transport agreement. In liberalized markets, there is a significant increase in traffic due to lower airline tariffs with increased competition [7-8, 14-15, 18]. Liberalization allowed for greater choice and more competitive prices for the travelling public. It arises positive externalities to the overall economy by stimulation of growth and employment opportunities, trade promotion and better transport and logistics services [15]. However, these impacts are not uniform across countries. The high competition leads to a change in composition of airlines operating in the country's aviation market, especially for small countries, whose national airlines are not leaders in minimum costs. The financial performance of aviation companies directly depends on the volume characteristics of aviation traffic [19]. This situation leads to their shift from the market and dominance of the world low-cost leaders [14-15, 18, 20]. As it was stated at the ICAO World Aviation Forum in 2015, liberal environment has led to the sustainable development of international air transport [14]. An example is the rapid development of the low-cost carrier AirAsia Group Berhad (AAGB), which is a powerful transnationaly integrated structure. In particular, researchers in [12] have found that global GDP, regional GDP, regional GDP per capita and population growth are the most correlated factors for the economic development of AAGB.

Today, the issue of determining the impact of further liberalization on development of a certain national economy and its air transport industry remains unresolved. This is a research from the economical point of view and from the perspective of searching for effectiveness and the optimal decision making while aviation market liberalizing. The example given is the nation of Ukraine, which has its own air transport industry and is on the path of aviation liberalization.

2 Liberalization of aviation market and air transport development of Ukraine

Nowadays, the basis of agreements about air traffic between Ukraine and other countries are bilateral air service agreements (ASA). Aviation communication between Ukraine and EU is regulated based on the bilateral air service agreements (ASA) with all the member states and Horizontal Agreement with the European Commission on certain aspects of air services. The last one has been developed by European Commission as a model agreement that liberalizes air services between the EU and third countries, called „horizontal" [13]. The EU also provides setting up open aviation areas (so called "open skies") with key partners to further liberalise certain markets on the bilateral basis by European Common Aviation Area (ECAA) agreement between the EU and third countries [21]. In essence, it is a „free trade area" for aviation, in particular in matters of flight safety, passenger protection, air carrier liability, environmental protection, competition and state aid. A major step forward in the liberalisation of EU-US air traffic was marked with provisional application in March 2008 of the EU-US Air Transport Agreement. This agreement introduced new commercial freedoms for EU and US airlines and a unique framework for regulatory cooperation in the field of transatlantic aviation [22]. In Europe the first such agreements were concluded with the countries of the Western Balkans and Morocco in 2006. In 2010 similar agreements were signed with Georgia and Jordan. In June 2012 an agreement was signed with Moldova. In general, the ECAA agreements have been concluded with the EU, Albania, Bosnia and Herzegovina, the Republic of Macedonia, Montenegro, Serbia, Kosovo, Norway, Iceland, Liechtenstein, Switzerland, Morocco, Georgia, Israel, Jordan and Moldova. According to the ECAA agreement, the air carriers guided by the common law on licensing and market access, competition, non-discrimination, flight safety and state aid have the right to operate within the EU. After signing such an agreement, the countries incorporate the EU norms into their national legislation in the field of air transport management. According to the ECAA Agreement, the air carriers have the right to operate within the EU guided by the common law on licensing and market access, competition, non-discrimination, flight safety, state aid. After signing such an agreement countries incorporate the EU norms into their national legislation in the field of air transport management [21]. The Agreement with Ukraine was also based on the "horizontal" agreement, but it has been later expanded due to the presence of a large-scale aviation industry in Ukraine. Negotiations on signing the Agreement lasted from 2007 to 2013. The initialing of the ECAA agreement took a place on November 28, 2013 at the Ukraine-EU Summit in Vilnius. However, the signing of the Agreement has not taken place so far. The ASAs, as the main basis of regulation about air traffic between Ukraine and EU, designate airlines that are granted the right to operate flights on all the routes between countries. At present, Ukraine has concluded 70 ASAs on scheduled air services, 26 of which have been concluded between Ukraine and EU member states. Before 2002 such ASA had made the designation of airlines which are owned and controlled by nationals of that signatory EU Member State. However, in November 2002, the Court of Justice of the European Union (CJEU) found that such designation was discriminatory and was in breach of the EU law. Consequently, each EU Member State is required to grant equal market access for routes to destinations outside the EU to any EU carrier with an establishment in its territory [21]. Thus, the ASAs between the EU Member States and third countries, including Ukraine, have been amended to reflect this legal requirement.

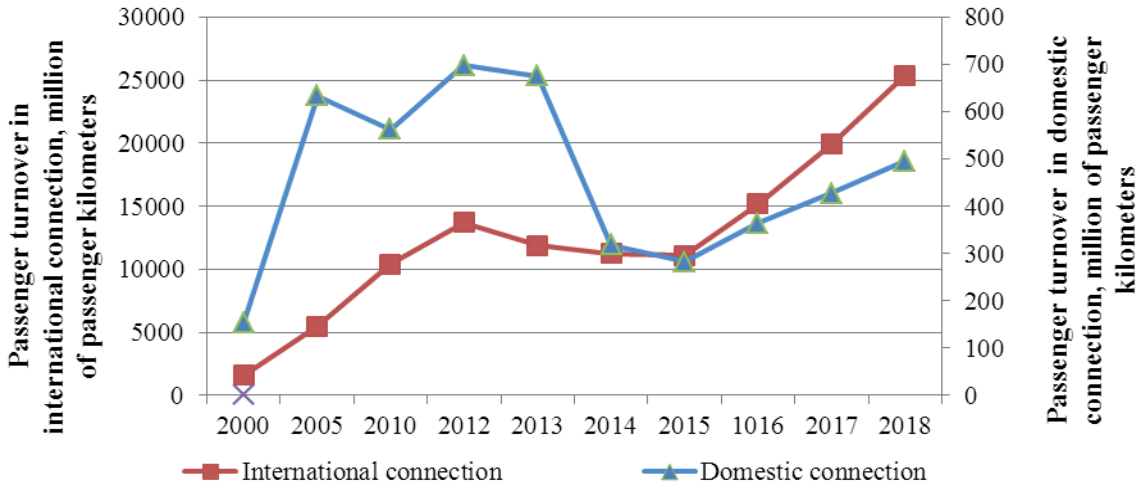


Figure 1 *Passenger turnover of air transport of Ukraine by types of services, [24-25]*



Figure 2 *Dynamics of passenger transportation volumes by Ukrainian airlines, [24-25]*

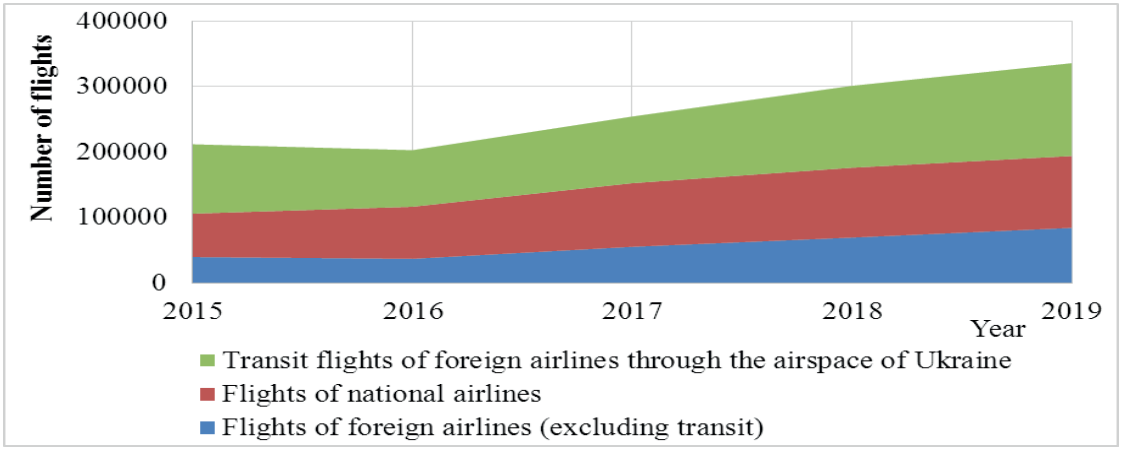


Figure 3 *Flights of domestic and foreign airlines in the airspace of Ukraine between 2015 and 2019, based on [26, 30-32]*

Thus, the low-cost companies, which were assigned to fly to Ukraine from the EU member states that did not have national airlines, were granted a wide access to Ukraine due to liberalization [18, 23]. In the course of progressive liberalization in the ASAs, there was a gradual increase in the number of designated carriers and frequency of flights on international routes.

As of 2018, air transportation in Ukraine was carried out by 34 national airlines, which performed 100.3 thousand commercial flights, which was 7.8% higher than in 2017, with an annual increase by 18.7% in the number of passengers and international passenger traffic by 27%. As shown in Figure 1, in 2016 there has been a 36% increase in international passenger traffic for the first time since the decline in 2013 due to the bankruptcy of the national airline - the monopolist "Aerosvit" and the redistribution of rights to international routes. In 2017 passenger turnover increased by 31%.

Since 2015, after the decline, the number of

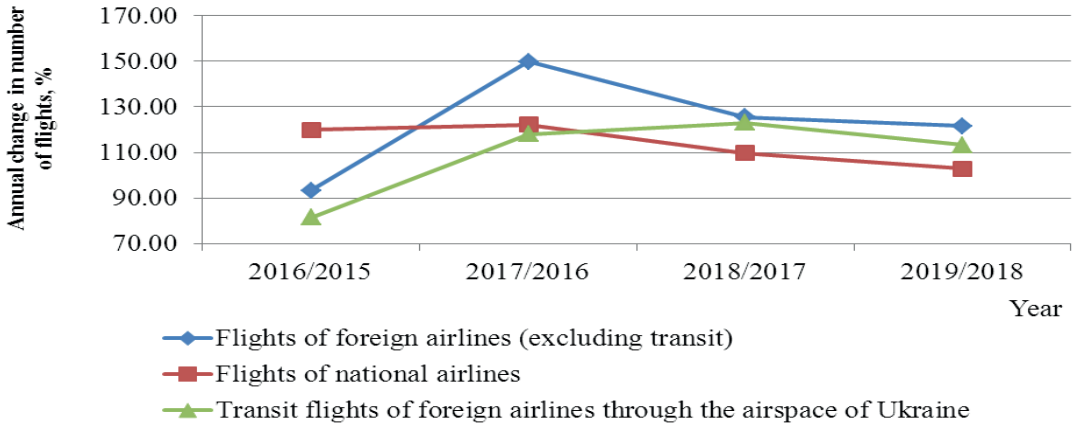


Figure 4 *The annual changes in the number of flights of domestic and foreign airlines in the airspace of Ukraine between 2015 and 2019, based on [26, 30-32]*

passengers carried on international flights of national airlines (scheduled and charter flights) has grown significantly: in 2016 by 31.6%, in 2017 by 28.6% and in 2018 the growth slowed down to 19.5%, as shown in Figure 2.

As of 2018, more than the half (54.2%) of all the passenger traffic of domestic airlines are international scheduled services. They were operated by 10 national airlines to 46 countries and the number of passengers who used their services increased by 16.4% and amounted to 6796.2 thousand people [26-27]. Moreover three of the national airlines, namely "Ukraine International Airlines", "Wind rose" and "Dniproavia", are parts of a strategic alliance based on joint ownership, which allows to improve the level of services in operational activities by providing aircraft in use, assigning slots at airports, providing convenient connections of routes [28]. As it was estimated by Oleshko and Heiets [29], the share of Ukraine in the global volume of aviation passenger traffic is not significant, but "despite the instability of the military, political and economic situation in the state, the growth rate of air traffic in the Ukrainian segment of the global aviation market is optimistic for predicting the future development of air transportation in Ukraine" [29, p. 5]. This is confirmed by analysis of changes in the number of flights of domestic and foreign airlines in the airspace of Ukraine between 2015 and 2019 as well as their annual rates (Figure 3, 4), performed in this article.

Thus, as shown in Figures 3 and 4, since 2016 there has been a positive trend of increasing the number of flights of both domestic and foreign airlines, as well as the number of transit flights of the latter. Since 2016, there has been a gradual slowdown in the growth rate of domestic airlines. At the same time, the growth rate of the number of flights of foreign airlines in the airspace of Ukraine slowed down slightly over the next two years after a rapid growth in 2017 by almost 50%. Due to liberalization and expansion of bilateral interstate agreements on air services between Ukraine and other countries, in 2019 the number of flights of foreign airlines in the airspace of Ukraine increased by 21.5%, while national airlines - only by 3% [31].

The observed trends indicate a significant development of the air transportation market due to the growth of activity of both Ukrainian airlines and foreign ones, which positively affects the business activity of Ukrainian airports. Thus, in January 2020 passenger traffic through the airports of Ukraine increased by 15.3% including international traffic with almost 17% compared to January 2019 [31].

To assess the level of aviation market liberalization, the Secretariat of the WTO has proposed the use of the Air Liberalization Index - (ALI), which is calculated based on the terms of bilateral air services agreements between countries [5]. At the beginning of 2017 the highest value of ALI calculated under the agreements of Ukraine with 54 other countries was at the level of 27, which corresponded to the average level [33]. By the end of 2019 the State Aviation Service of Ukraine decided to expand the conditions of operation of airlines under bilateral agreements, which governed air services of Ukraine with other countries, in particular, to increase the number of designated carriers and frequencies [34].

Since the liberalization of Ukraine's aviation market is not inherently a goal, but mostly a tool of ensuring Ukraine's integration into European airspace, there is a need to investigate its impact on Ukraine's economy through the study of the macroeconomic effects, namely the external economic effects of air transport development due to the liberalization.

3 Methodology for external economic effects of air transport development assessment

3.1 Analysis background and definitions

In general, the main effect on society from negotiated changes in bilateral air transport agreements or their removal is in providing more choices to air travel in terms of quantity, quality and fares, giving access to

the most efficient airlines to liberalized air transport market. This effect ensures the growth of air traffic and due to the direct, indirect, induced and catalytic effects it influences the economies of countries that have implemented the air transport liberalization. Thus, the direct impact of air transport is manifested in the direct creation of working places in airlines and airports, in handling companies that provide ground maintenance of aircraft and passengers in airport terminals and in the provision of air navigation services. In creation of jobs to ensure the production of goods needed to serve passengers on board and aircraft at the airport (food, service), in other words, there is an indirect economic impact of air transport in related industries. The induced impact is realized due to the ability of air transport to generate additional demand for jobs in other sectors of the economy, such as consumer goods companies, retail stores, restaurants, financial insurance institutions, i.e. due to the multiplier effect. The catalytic influence of the air transport is realized in its ability to facilitate the interaction of economic agents in implementation of business processes, ensuring development of the non-related businesses. The air transport has such impact on the travel business and international trade in particular. It is known that the direct, indirect, induced and catalytic effects of the air transport industry created approximately 65.5 million jobs worldwide in 2018, for comparison, 29 million jobs had been created as of 2005 (the growth of 226 %) [2]. The global economic impact of aviation (direct, indirect, induced and catalytic) is estimated at 2.7 trillion US dollars by experts, which is equivalent to 3.6 % of the world's gross domestic product (GDP), for comparison, such an impact amounted to 2.960 billion US dollars as of 2005, which accounted for 8 % of the world's GDP and was equivalent to the total GDP of the United Kingdom [1-2, 4]. The ACARE study estimates that air transport contributes 2.6 % of the EU GDP, as it was indicated in the Eurocontril report [35]. According to studies of the impact of the air transport on the EU economy, the overall economic effect through investment and underlying productivity have been more significant, increasing the GDP by 4 % [35].

In turn, the GDP growth stimulates growth in demand for the air transport services [5-9, 12]. The methodology for assessing the air transport socio-economic impact on national economy is presented in the detailed research in [7], where all the quantifications of the abovementioned effects have been made on the Greek economy' data. The studies on the impact of liberalization of the air transport on airline competition and air passenger traffic, on airports' development, on the economy of the territories adjacent to airports and on the regional economy, have also been conducted [5-6, 8-9, 14-18, 20]. The economic gains that US air transport receives from negotiated changes in bilateral agreements, or their removal, has been examined by Button and Taylor in [6], mainly focusing on the economic benefits in terms of employment generation. While considering the overall economic effects from freer trade in the air transportation services they have underlined the existence of incremental economic costs and benefits resulting from the policy change, such as the following: changes in the tax revenues and expenditures, "trade exports and imports and the balance of trade, in employment objectives: number and quality of jobs, development of tourism and related industries cost of travel to the business and tourist client" [6, p. 7].

In this study was assumed that for the country's air transport market the first direct effect of liberalization is growth of the international aviation traffic due to lower tariffs with the growth of the aviation network routes, as a result of competitive positioning of airlines and airports. The activity of national airlines in providing international air transportation is related to the consumption and provision of services to both residents and non-residents of the country. It enters into contractual relations with foreign air navigation services, airports, handling companies, airlines, ticket agencies and travel agencies, as well as the country's air navigation service, it's domestic airports and handling companies (residents) provide auxiliary services to foreign airlines - non-residents as regulated by the The Manual on Statistics of International Trade in Services, items 3.95-3.105 [36]. Accordingly, results of the external economic activity of aviation enterprises of the country are reflected in the articles „exports and imports of air transport services". Thus, values of exports and imports of the air transport services of the country can be considered as consequences of the external economic activity of its aviation enterprises. They represent the external economic effects that the country acquires from development of its air transport. Accordingly, the difference between the export and import of a country's air transport services (ATS) can be regarded as a net external economic effect from development of the country's air transport, the volume of which is a component of the country's net export' formation and therefore the GDP. In addition, the total trade in aviation services reflects the overall international economic business activity of aviation enterprises - residents, involved in the provision of international air transportation. Changes in the structure of air traffic (in the volume of passenger air traffic, in the number and ratio of flights of national and foreign airlines) affect the value of exports and imports of the air transport services. Values of exports of the air transport services (ATS' exports) of the country are formed by aviation enterprises provided aviation transportation services (passenger, cargo and auxiliary services) for the non-residents [36-38].

The methodological approach used in earlier studies of the impact of the development of air transport on the GDP of a country, region and the world, is based on assessment of number of jobs created by aviation enterprises and their contribution to GDP [1-4, 7-8]. The direct contribution to the GDP was calculated

Table 1 *Nomenclature of used abbreviations*

abbreviation	term
GDP	gross domestic product
ATS	air transport services
NA	national airlines
NA Pax	the number of international flights' passengers of national airlines
IF Pax	the total number of passengers on international flights
IF Pax DEP	the number of passengers departing from Ukrainian airports in international traffic
IF Pax ARR	number of passengers arriving to Ukrainian airports in international traffic
IFNA	number of international flights of national airlines
IFFA	number of international flights of foreign airlines
Total IF	total number of international flights to and from Ukrainian airports

Table 2 *GDP (million US dollars) and international trade of air transport services of Ukraine (thousand US dollars), [39-41]*

indicator	2008	2009	2010	2011	2012	2013	2014	2015	2016	2017	2018
GDP	179992	117228	136419	163160	175781	183310	131805	90615	93270	112154	130832
export of ATS	1231100	1111100	1181900	1501100	1510700	1333178	1071263	853619	882840	1091775	1221611
import of ATS	542400	338800	447600	685982	641300	643550	431038	466938	357465	452397	695720

Table 3 *Passenger traffic at the airports of Ukraine, thousands of people, [24-25]*

indicator	2008	2009	2010	2011	2012	2013	2014	2015	2016	2017	2018
IF Pax DEP	4087.3	3534.0	4148.5	5050.8	5733.0	6356.4	4777.3	4718.2	5663.6	7318.5	9115.2
IF Pax ARR	4087.6	3534.3	4148.1	5050.2	5741.4	6344.3	4727.0	4703.1	5630.9	7272.6	9142.3

Table 4 *International transportation of passengers by air, thousands of people, [24-25]*

indicator	2008	2009	2010	2011	2012	2013	2014	2015	2016	2017	2018
NA Pax	4934.8	4135.9	5144.3	6328.5	6820.9	6900.3	5826.6	5679.6	7475.3	9614.5	11446.1
IF Pax	8174.9	7068.3	8263.7	10030.6	11474.4	12700.7	9504.3	9421.3	11294.5	14591.1	18257.5

by multiplying the number of employees of aviation enterprises by their average wage (before tax). With this approach, the contribution of all the aviation transport to the socio-economic development of a country or region is assessed regardless of the sources of its formation, that is, regardless of the activity of which aviation entities, national or foreign, such indicators of socio-economic development were achieved.

The purpose of the methodology approach used in this research is the footprint analysis of the air transport development due to liberalization in terms of external economic effects on the national economy. The presented concept of assessing the external economic effects of air transport development can be used in addition to the methods used by ICAO, IATA [1-4], Button and Taylor [6], Dimitrios et al. [8], for a more complete assessment of the impact of air transport on the country's economy. The methodology used here can also be applied to identify additional external economic effects from liberalization of the country's air transport, due to its complex relationship with other sectors of the economy. The presence, of not only direct, but other types of influence of the air transport as well, was mentioned above.

Authors here relied on open sources of air transport 'statistics on indicators of air traffic and volumes of international trade to conduct investigation of their impact on formation of the external economic effects of Ukraine air transport services development. The study of the air traffic impact on the export and import of the air transport services was carried out by correlation and regression analysis.

4 Statistical data and methods of analysis

Quantification of aviation transport external economic effects was conducted based on the statistical reporting of Ukraine, the standards of which for collection and accounting of statistical reporting, in particular in the field of transport, meet the international standards, including the EU [36-38]. Further in the article for some terms abbreviations are used, as presented in Table 1.

Table 2 presents the statistical information from open sources on the GDP and volumes of international trade in aviation transport services of Ukraine. Tables 3-5 reveal statistical data on indicators of operational

Table 5 *Number of international flights (IF) to and from airports of Ukraine (flights), [24-25]*

indicator	2008	2009	2010	2011	2012	2013	2014	2015	2016	2017	2018
IFNA	57000	49401	62361	70928	70187	68152	55973	50713	63396	75117	83027
IFFA	55261	52490	56712	60939	70170	71213	51548	43900	41804	54983	69054
total IF	112261	101891	119073	131867	140357	139365	107521	94613	105200	130100	152081

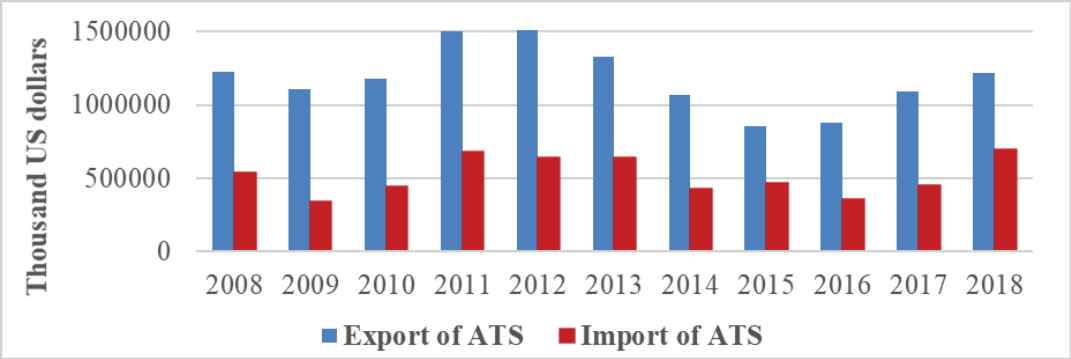


Figure 5 *Dynamics of export and import of the air transport services of Ukraine from 2008 to 2018, based on Table 2*

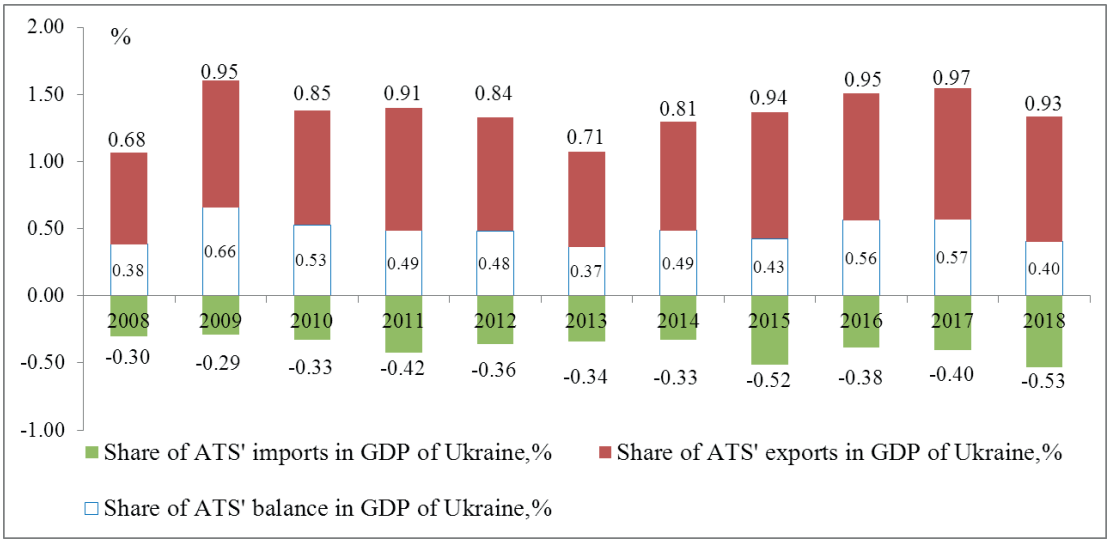


Figure 6 *Value of shares of exports, imports and balance of the air transport services of Ukraine in GDP for the period 2008-2018, %, based on Table 2*

activity of the air transport of Ukraine for the period between 2008 and 2018, systematized from statistical reporting of Ukraine [24-25].

The IF Pax, the total number of passengers on international flights (both national and foreign airlines), was obtained by summing up the number of passengers arriving at Ukrainian airports and departing from them. In the context of research on relationship between the ATS' export (import) and operational indicators of the air transport, methods of regression and correlation were used. The correlation and regression analyses were for absolute and relative values of x variables. The variables were chosen as follows: dependent (explained) variable Y as ATS' export (import) and independent (explanatory) variable X as operation indicator of the air transport: IFNA, IF, NA Pax, IF Pax. The correlation (r) and determination (R^2) coefficients were calculated using the Microsoft Excel software package. To determine the correlation strength, the following criteria were identified: strong dependence (if $0.8 \leq |r| < 1$), medium dependence (if $0.3 \leq |r| < 0.8$) and weak dependence (if $0 < |r| < 0.3$.

5 Results and discussions

Figure 5 shows the dynamics of export and import of air transport services in Ukraine from 2008 to 2018, which formed the direct external economic effects of Ukraine's air transport, respectively, export represented a positive effect and import was a negative one in terms of impact on the total trade of air transport services of Ukraine.

Figure 6 presents values of shares of the exports, imports and balance of the air transport services of Ukraine in the GDP, for the period 2008-2018,

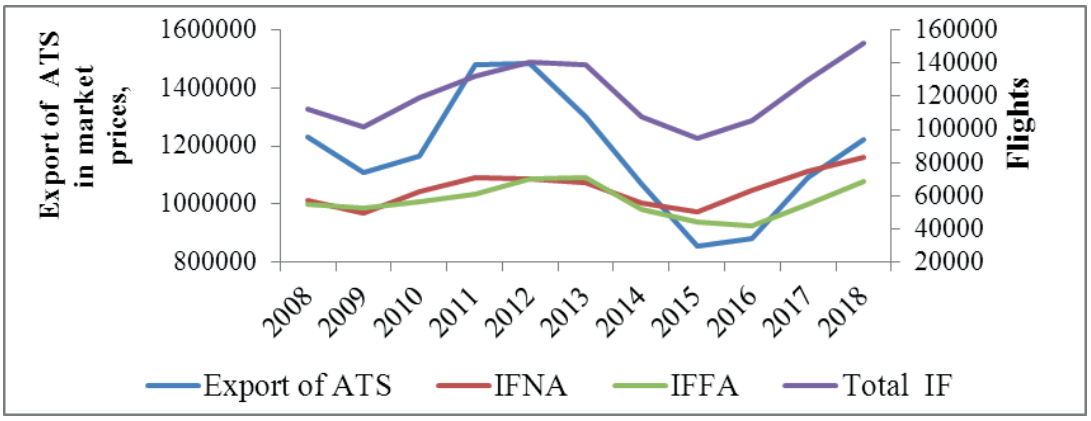


Figure 7 *Relationship between the ATS' export and number of passengers on international flights of national, foreign airlines and the total number of passengers on international flights to and from Ukraine' airports for a period of 11 years, based on Tables 2 and 5*

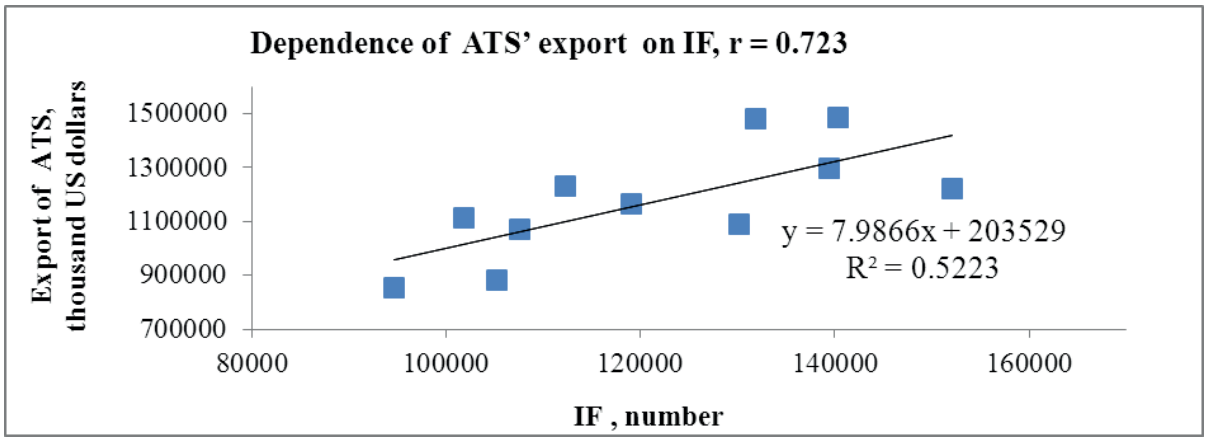


Figure 8 *Dependence of the ATS' export on the total number of international flights to and from Ukraine' airports for a period of 11 years*

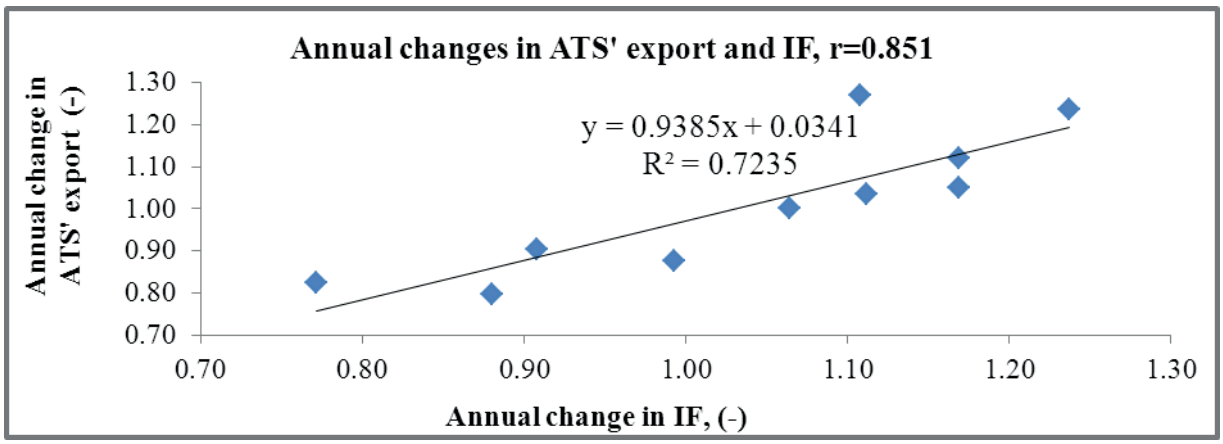


Figure 9 *Dependence of the annual rates of changes in the ATS' export from annual rates of changes in number of international flights to and from Ukraine' airports*

calculated based on Table 1. Thus, for 11 years of the study, the ATS' exports ranged between 0.68% of GDP and 0.97% of GDP and ATS'imports - between 0.3% of GDP to 0.53% of GDP. The balance of air transport services, respectively, ranged between 0.37 and 0.49% of Ukraine's GDP.

According to results of 2018, the IATA experts estimated that about 1.1% of Ukraine's GDP had been generated by the air transport and foreign tourists arriving by air [3]. In comparison to that value, the contribution of exports (+ 0.93%) and imports (-0.53%) to Ukraine's GDP was quite significant. The further study was focused on assessing the impact of the air transport volumes on formation of direct external economic effects.

The relationship between the dynamics of the ATS' exports and of the air traffic, represented by the number of international flights of national airlines (IFNA), foreign

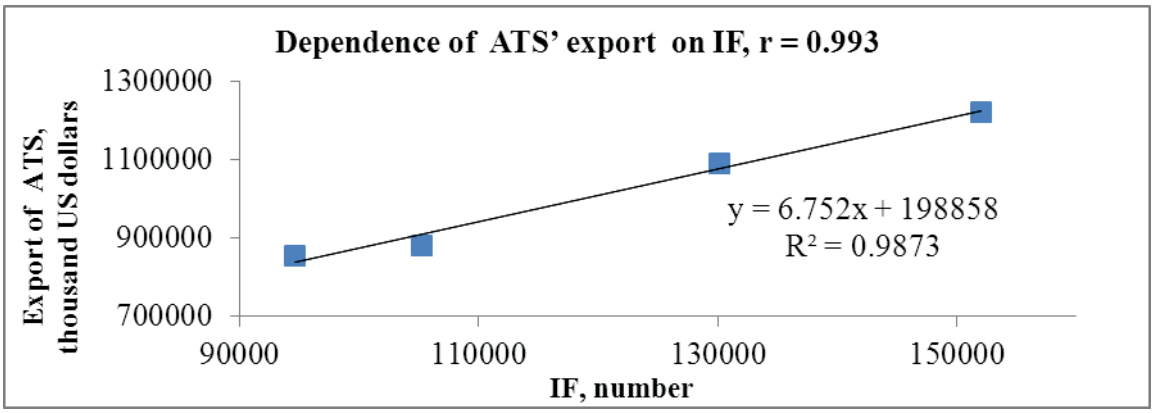
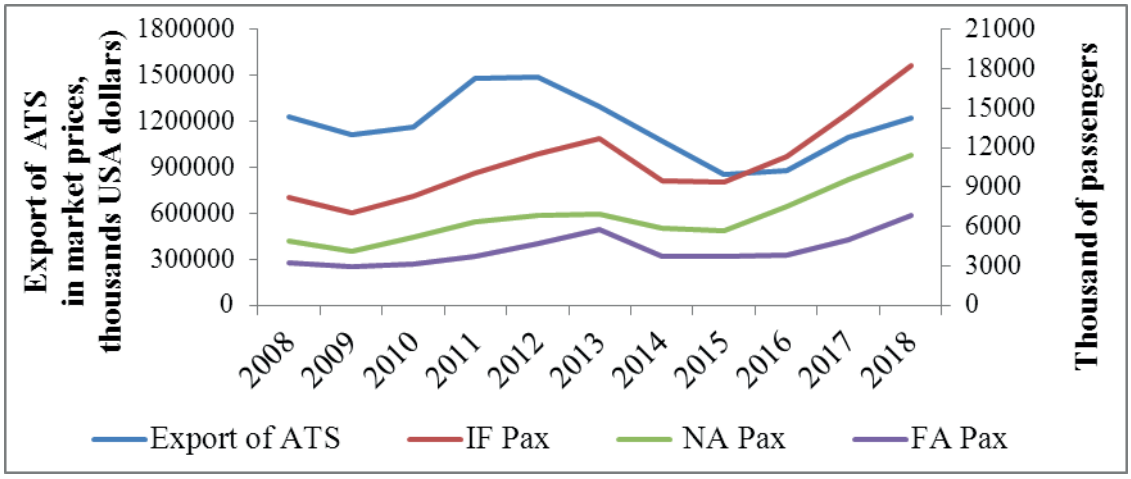


Figure 10 *Dependence of the ATS' export on the total number of international flights to and from Ukraine' airports for the period 2015-2018*



Source: Table 1, 3

Figure 11 *Relationships between the ATS export and the number of passengers on international flights arriving at and departing from Ukrainian airports over the eleven-year period, based on Tables 2 and 4*

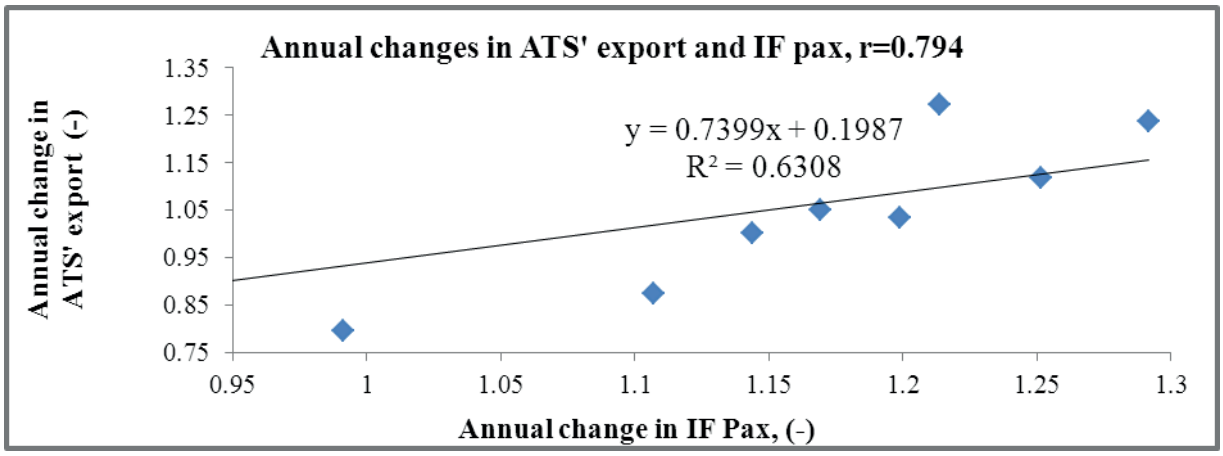


Figure 12 *Relationship between annual changes in the ATS' export and total number of passengers of international flights (IF Pax)*

airlines (IFFA) and the total number of international flights to and from the airports of Ukraine (Total IF) for a period of 11 years are clearly raced in Figure 7.

As can be seen from Figure 7 there was a positive relationship between the ATS export and the number of flights of both domestic and foreign airlines and the total number of international flights. In this study was used the total number of international flights. Results of the correlation analysis between the absolute values of the ATS' exports on the total number of international flights to and from Ukraine presented in Figure 8, had shown the presence of a sufficiently average dependence with the correlation coefficient r = 0.723. However, the coefficient of determination R^2 was equal to 0.52, which indicated that the model built in Figure 8 was not statistically significant.

Dependence of annual rates of changes in the ATS' export from annual rates of changes in the number of international flights to and from Ukraine' airports, considered as strong (r = 0.845), which indicated the statistical significance of the variable IF. However, the coefficient of determination of the constructed trend R^2 was equal to 0.43, which indicated that the constructed model cannot be considered statistically significant, as presented in Figure 9. At the same time, for the data of four years of observations (2015-2018), correlated - regression analysis of the dependence of ATS' exports on IF Pax, gave a correlation coefficient r = 0.993 and determined Fisher's criterion F = 77.5, which was much higher than the corresponding tabular value, which indicated the statistical significance of the model presented in Figure 10.

Figure 11 presents a study of the relationship between export from the ATS and the number of passengers carried on international flights of national and foreign airlines and their total number of flights that began and ended at Ukrainian airports, excluding the direct transit passengers.

As can be seen from Figure 11, there were a positive relationships between the ATS export and the number of passengers on international flights of both domestic and foreign airlines and the total number of passengers on international flights. Results of the study of the relationship between the absolute values of the ATS' export and IF Pax, using correlation analylis showed very weak correlation (r = 0.119), while identified a strong relationship between the annual changes in their values (r = 0.794), as shown in Figure 12.

That is, the IF Pax variable was statistically significant. However, for this case, the linear regression model is not statistically significant, due to the low value of the Fisher test (F = 1.7), which is less than the corresponding tabular value at the value of the significance level α = 0.05.

At the same time, for the data of four years of observations (2015-2018), correlation-regression analysis of the dependence of ATS'exports on IF Pax, gave a correlation coefficient r = 0.987 and determined Fisher's criterion F = 29.1, which was much higher than the corresponding tabular value (Figure 13). A similar regression-correlation analysis of the dependence of the annual change of ATS 'export on the annual change of IF Pax, based on observational data from 2015-2018, revealed a correlation coefficient r = 0.998 and Fisher's criterion F = 38 (Figure 14). These results showed the statistical significance of linear regression models for dependencies for 2015-2018.

Thus, the liberalization of the Ukrainian aviation

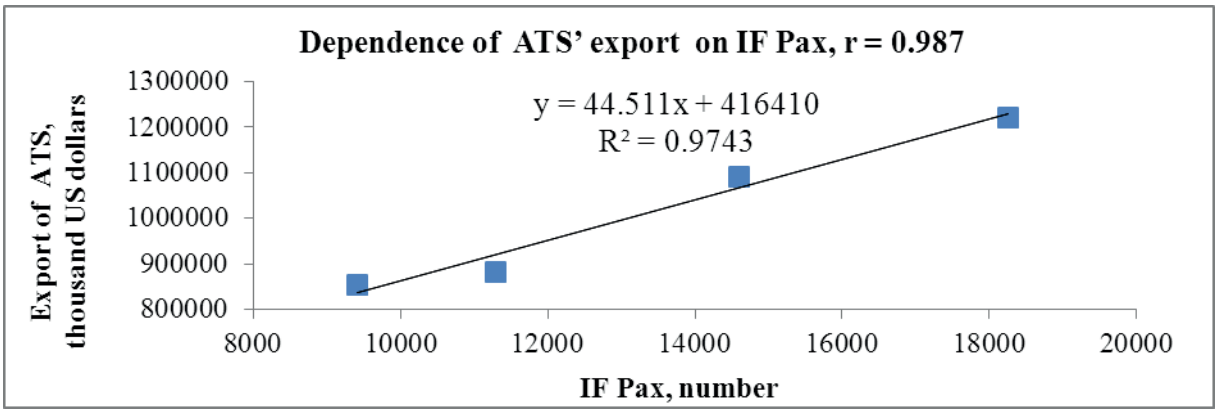


Figure 13 *Relationship between the ATS' export and the total number of passengers on international flights (IF Pax) for a period 2015-2018*

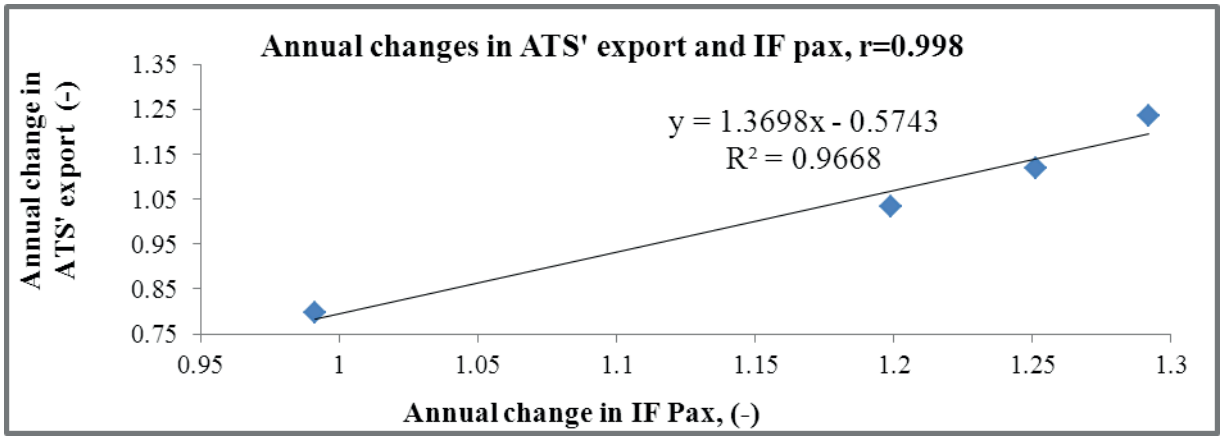


Figure 14 *Relationship between annual changes in the ATS' export and total number of passengers of international flights (IF Pax) for the period 2015-2018*

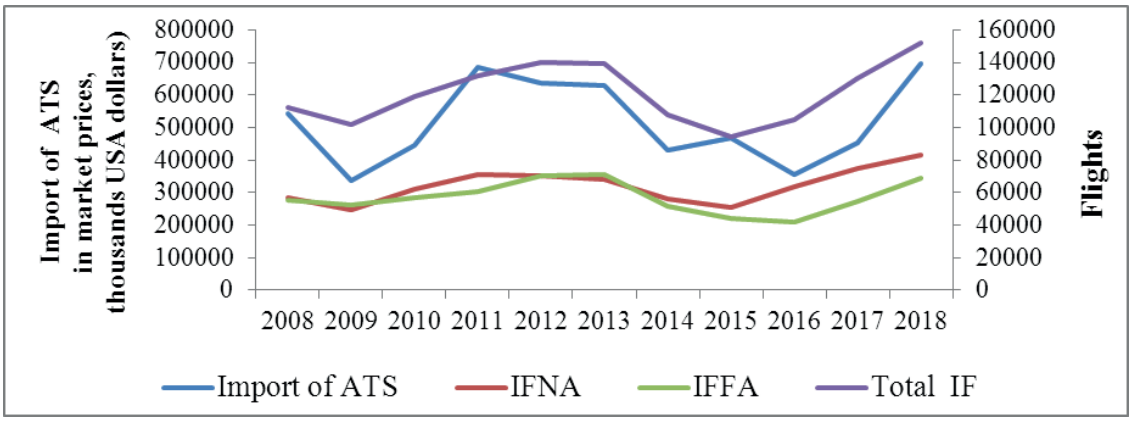


Figure 15 *Import of air transport services (ATS) and the number of international flights of national airlines, foreign airlines and the total international flights to and from Ukraine' airports, based on Tables 2 and 5*

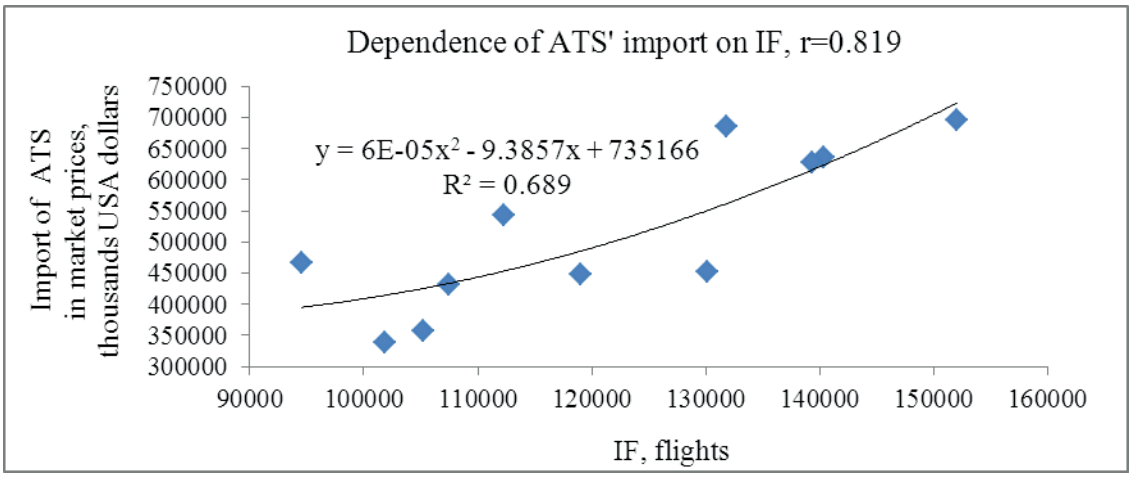


Figure 16 *Dependence of the ATS' import on the total number of international flights to and from Ukraine' airports*

market, which actually developed in the period 2015-2018, significantly increased the statistical significance of variables of the air traffic (number of international flights, their passengers, annual rate of change) for models of ATS'export. Therefore, to predict the value of the ATS exports and annual changes in ATS exports, one can focus on the constructed linear regression models shown in Figures 14 and 15.

As can be seen from the visual observation of Figure 15, there were a positive relationships between ATS' import and the number of flights of both national and foreign airlines and the total number of international flights.

As the simulation showed, a confident average dependence of the ATS' import on the total number of international flights has been revealed when both absolute and relative changes of indicators were analyzed. Dependence of the ATS' import on quantity of international flights to and from Ukraine' airports, can be considered as strong (r = 0. 819). The coefficient of determination showed that for 69% of cases the value of ATS' exports was determined by function of the IF dependence, presented in Figure 16. Correlation-regression modeling of this dependence, performed based on observations from 2015-2018, showed that the IF variable was statistically significant (r = 0.789) and the model was statistically significant (R^2 was equal to 0.97), in 97% of cases, the import of the ATS was determined by the function presented in Figure 17.

Figure 18 presents a study of the relationship between the import from the ATS and the number of passengers on international flights of Ukrainian airlines, foreign airlines and the total number of international flights.

As can be seen from Figure 18, there was a positive relationship between the ATS import and the number of passengers on international flights of both domestic and foreign airlines and the total number of passengers on international flights. The correlation coefficients showed that there were the weak dependence of the ATS' import from the total number of passengers on international flights of national airlines and from the number of passengers on total international flights (0.423 and 0.512).

Results of the study of the relationship between annual rates of changes in the ATS' import and annual rates of changes in the total number of passengers on international flights of national airlines and annual rates of changes in the number of passengers on total international flights, showed average correlation (r = 0.703 and 0.717), while the accuracy of selection of the regression equations was about 50%, which indicated

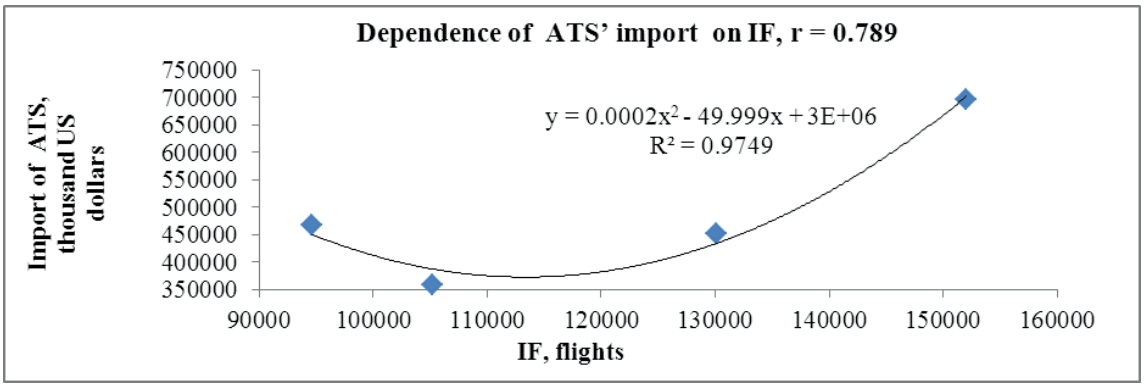


Figure 17 *Dependence of the ATS' import on the total number of international flights to and from Ukraine' airports for 2015-2018*

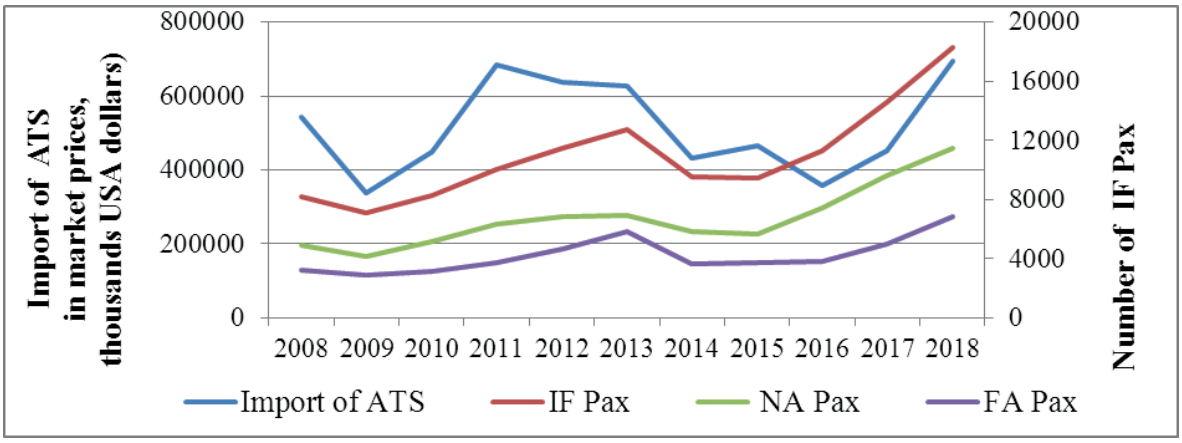


Figure 18 *The relationship between import from ATS and the number of passengers on international flights, based on Tables 2 and 4*

Table 6 *Dependence of the ATS' import and ATS' export on IF, NA Pax, IF Pax*

	IF	NA Pax	IF Pax
export of ATS	0.723	-	0.119
import of ATS	0.818	0.423	0.512

Table 7 *Dependence of the annual rates of changes in the ATS' import and ATS' export on annual rates of changes in IF, NA Pax, IF Pax*

	IF	NA Pax	IF Pax
export of ATS	0.851	-	0.94
import of ATS	0.672	0.703	0.717

that the model could not be considered statistically significant. The correlation-regression modeling, based on data for the period 2015-2018, showed similar results. The results of correlation analysis for a period of 11 years are presented in the Tables 6 and 7.

Due to the significant difference between the absolute values of endogenous and exogenous variables, it was found that the correlation between some of them was more pronounced in the analysis of their annual rates of change. The analysis of the correlation coefficients between the annual growth rates of the ATS' exports and the indicators of air traffic revealed a strong dependence of the ATS' exports on number of passenger flights and passengers of such flights. The correlation between values of the ATS' imports and aviation traffic indicators was more pronounced in the analysis of their annual rates of change and can be assessed as a confident average. So, the main conclusion is that the gradual liberalization of the aviation market of Ukraine has led to an increase in the number of passenger flights and passengers on such flights, which directly affected the increase in export earnings from the air transport services.

To continue the discussion, it should be noted that the proposed methodological concept for assessment of external economic effects of the air transport development allows to understand the mechanism of its influence on the formation of national economy indicators much better, as well as to track the impact of air traffic

due to the development of air transport, in particular, liberalization, on formation of the external economic effects of the national economy. The advantage of the proposed methodological approach is in availability of data for assessing the external economic effects, both direct and additional. The proposed concept for assessing the external economic effects of the development of air transport can be used for a more complete assessment of the impact of air transport on the country's economy as additional to the methods used by ICAO, IATA [1-4], Button and. Taylor [6] and Dimitrios et al. [8].

As the study showed, there has been a gradual increase in the magnitude of external economic effects due to introduction of the liberalization conditions in bilateral air services agreements between Ukraine and other countries since 2015. The analysis of the relationship between the external economic effects of Ukraine's air transport development and air traffic indicators revealed a strong dependence of positive external economic effects of the air transport development on the total number of international flights to and from Ukraine's airports. Similar results for airports were reported by researchers Button and Taylor [6], who, while studying a relatively large number of US airports, found that the international air transport stimulated additional growth of business activity and new jobs in the area adjacent to the airports.

Thus, according to results of the research confirmed that here was a significant positive relationship between the traffic volumes and liberalization of the aviation market, as it was indicated in [6, 8, 14, 15, 17, 18]**.** The strong dependence of the positive external economic effects of the air transport development in Ukraine on the air traffic volume indicates the feasibility of further liberalization of the aviation market. At the same time, the additional study of factors and peculiarities of formation of import of the air transport services is required, taking into account its growth over the last year of the research. The limitations in conducting this research were associated with difficulty of obtaining the detailed data on activities of enterprises belonging to different statistical groups of the air transport industry (airlines, airports, handling companies, air navigation services). The identified relationships of the external economic effects of the air transport development from such parameters of air traffic as the number of international flights and the number of passengers of international flights, do not exclude influence of other indicators of the air transport operations, their relationship and aggregate action. Formation of magnitude of the ATS exports and imports is influenced by such variables as volume of air traffic (passenger and cargo flights, number of transported passengers and cargo), air traffic structure (domestic and foreign airlines), price level, tax burden, values of airport charges, the cost of slots, the level of aviation tariffs and other indicators that affect activities of aviation entities in a competitive environment.

6 Conclusions

The growth of the air traffic affects the GDP valueand contributes to development of the country's economy due to liberalization of the air transport taking into account its direct, indirect, induced and catalytic impact. Changes in the air traffic structure, which occur due to the redistribution of traffic between the domestic and foreign airlines, have an impact on the formation of export and import of air transport services in the country. One can determine the external economic effects that a country acquires from its liberalization, while observing the dynamics of components of the international trade in the air transport services, when changing the indicators of air traffic. The numerical example was Ukraine, which has its own air transport industry and is on the path of aviation liberalization. The prevalence of a direct positive external economic effects of the air transport development over a negative ones was revealed during the study period between 2008 and 2018. The value of the ATS' exports in recent years of research formed an average of 0.95 % of Ukraine's GDP. The study has found that the gradual liberalization of the aviation market of Ukraine led to an increase in international traffic, which was directly reflected in the increase in the export earnings from air transport services. The strong dependence of the positive external economic effects of the air transport development in Ukraine on volume of the air traffic indicated the feasibility of further liberalization of the aviation market. The presented methodological approach on taking into account the external economic effects of the air transport development through further liberalization and the findings can be used by the country's aviation administration in developing the management decisions on the feasibility of structural changes in the air transport sector and areas for improving the transport policy, including aviation infrastructure.

Acknowledgement

This article is published within realization of the project UA No. 92/11.02.03 „Study of the export potential of the aviation complex of Ukraine" of the Department of Management of Enterprises' Foreign Economic Activity of the Faculty of Transport, Management and Logistics, National Aviation University.

Author contributions

Oksana Ovsak: conceptualization, methodology, data curation, investigation, visualization, writing original draft preparation, writing - reviewing and editing.

Maryna Vysotska: conceptualization, supervision, validation.

References

[1] The economic and social benefits of air transport [online] [accessed 2020-02-03]. Available from: https://www.icao.int/Meetings/wrdss2011/Documents/JointWorkshop2005/ATAG_SocialBenefitsAirTransport.pdf

[2] Aviation benefits report 2019 [online] [accessed 2020-02-05]. Available from: https://www.icao.int/sustainability/Documents/AVIATION-BENEFITS-2019-web.pdf

[3] The importance of air transport to Ukraine [online] [accessed 2020-01-15]. Available from: https://www.iata.org/en/iata-repository/publications/economic-reports/ukraine--value-of-aviation

[4] Aviation: benefits beyond borders 2014 report - Air Transport Action Group, April 2014. [online] [accessed 2019-12-23]. Available from: http://aviationbenefits.org/media/26786/ATAG__ AviationBenefits2014_FULL_LowRes.pdf

[5] PIERMARTINI, R., ROUSOVA, L. Liberalization of air transport services and passenger traffic - 2008 WTO Staff Working Papers ERSD-2008-06, World Trade Organization (WTO), Economic Research and Statistics Division [online]. [accessed 2020-05-13]. Available from: https://www.wto.org/english/res_e/reser_e/ersd200806_e.pdf

[6] BUTTON, K. J.; TAYLOR, S. International air transportation and economic development. In: 40th Congress of the European Regional Science Association: „European Monetary Union and Regional Policy": proceedings [online] [accessed 2020-05-12]. Louvain-la-Neuve: European Regional Science Association (ERSA). Available from: https://www.econstor.eu/bitstream/10419/114969/1/ERSA2000_483.pdf

[7] DIMITRIOS, D., MARIA, S. Assessing air transport socio-economic footprint. *International Journal of Transportation Science and Technology* [online]. 2018, **7**, p. 283-290 [accessed 2020-02-17]. ISSN 2046-0430. Available from: https://doi.org/10.1016/j.ijtst.2018.07.001

[8] DIMITRIOS, D., MOURMOURIS, J., SARTZETAKI, M. Quantification of the air transport industry socio-economic impact on regions heavily depended on tourism. *Transportation Research Procedia* [online]. 2017, **25**, p. 5242-5254. ISSN 2352-1465. Available from: https://doi.org/10.1016/j.trpro.2018.02.051

[9] LAKSHMANAN, T. R., CHATTERJEE, L. R. Economic consequences of transport improvements. *Journal of Transportation Research at the University of California*. 2005, **26**, p. 28-34. ISSN 2169-3536.

[10] CIGU, E, AGHEORGHIESEI, D. T., GAVRILUA (VATAMANU) A. F., TOADER, E. A. Transport infrastructure development, public performance and long-run economic growth: a case study for the EU-28 countries. *Sustainability* [online]. 2018, **11**(1), p. 1-22 [accessed 2020-02-12]. eISSN 2071-1050. Available from: https://doi.org/10.3390/su11010067

[11] GNAP, J., KONECNY, V., VARJAN, P. Research on relationship between freight transport performance and GDP in Slovakia and EU countries. Preliminary communication. *Nase More: International Journal of Maritime Science and Technology* [online]. 2018, **65**(1), p. 32-39 [accessed 2020-04-03]. ISSN 0469-6255, e-ISSN 1848-6320. Available from: https://doi.org/10.17818/NM/2018/1.5

[12] WU, C. Y., HEIETS, I., SHVINDINA, H. Business model management of low-cost: in a search for impact-factors of performance (case of AirAsia group airlines). *Marketing and Management of Innovations* [online]. 2020, **2**, p. 354-367 [accessed 2020-07-08]. ISSN 2218-4511, eISSN 2227-6718. Available from: http://doi.org/10.21272/mmi.2020.2-26

[13] European Commission and U. S. Transatlantic Airline Alliances. Competitive issues and regulatory approaches. 2010.

[14] Air transport liberalization and the economic development of the countries - ICAO Assembly, 39th session [online] [accessed 2020-04-23]. 2016. Available from: https://www.icao.int/Meetings/a39/Documents/WP/wp_189_en.pdf

[15] OUM, T. H., ZHANG, A., FU, X. Air transport liberalization and its impacts on airline competition and air passenger traffic. *Transportation Journal* [online]. 2010. **49**(4), p. 371-390 [accessed 2020-04-15]. ISSN 0041-1612. Available from: https://doi.org/10.2307/40904912

[16] CHAOUK, M., PAGLIARI, R., MOXON, R. The impact of national macro-environment exogenous variables on airport efficiency. *Journal of Air Transport Management* [online]. 2020, **82**, 101740 [accessed 2020-04-23]. ISSN 0969-6997. Available from: https://doi.org/10.1016/j.jairtraman.2019.101740

[17] GILLEN, D., HARRIS, R., OUM, T. H. Measuring the economic effects of bilateral liberalization air transport. *Transportation Research Part E: Logistics and Transportation Review* [online]. 2002, **38**(3-4), p. 155-174 [accessed 2020-05-18]. ISSN 1366-5545. Available from: https://doi.org/10.1016/S1366-5545(02)00003-0

[18] HEIETS, I. The impact of air service agreement liberalization: the case of Ukraine. In: 11th International Conference Modern Problems of Global Processes in the World Economy: proceedings. 2017. ISBN 50-4258-364-0, p. 16-17

[19] STOPKA, O., BARTUSKA, L., CABAN, J., KAPUSTINA, L. M. Proposal of the functional system for the airline companies financial situation assessment. *Communications - Scientific Letters of the University of Zilina* [online]. 2019, **21**(1), p. 3-8 [accessed 2020-05-18]. ISSN 1335-4205, eISSN 2585-7878 Available from: https://doi.org/10.26552/com.C.2019.1.3-8

[20] Impact of international air service liberalisation on Chile [online] [accessed 2020-05-25]. Available from: https://www.iata.org/en/iata-repository/publications/economic-reports/chile-benefits-from-further-liberalization/

[21] Council Regulation (EC) No 411/2004 of 26 February 2004 repealing Regulation (EEC) No 3975/87 and amending Regulations (EEC) No 3976/87 and (EC) No 1/2003, in connection with air transport between the community and third countries (text with EEA relevance) [online]. [accessed 2020-05-03]. Available from: https://eur-lex.europa.eu/legal-content/en/TXT/?uri=CELEX:32004R0411

[22] GASPARI, F. The EU air transport liberalization and re-regulation. *International and Comparative Law Review* [online]. 2011, **11**(2), p. 7-42 [accessed 2020-05-06]. ISSN 2464-6601. Available from: https://doi.org/10.1515/iclr-2016-0102

[23] OLESHKO, T., HEIETS, I., PAVLIUK, Y. Characteristics and analysis of development of low-cost airlines in Ukraine. *Problems of Systemic Approach in the Economy* [online]. 2018, **6**(68), p. 153-158. ISSN 2520-2200 [accessed 2020-04-26]. Available from: https://doi.org/10.32782/2520-2200/2018-6-24

[24] Transport and Communications of Ukraine 2012 (in Ukrainian) [online] [accessed 2019-12-11]. Available from: http://www.ukrstat.gov.ua/druk/publicat/Arhiv_u/08/Arch_tr_zb.htm

[25] Transport and Communications of Ukraine 2018 [online] [accessed 2019-12-11]. Available(in Ukrainian). from: http://www.ukrstat.gov.ua/druk/publicat/kat_u/2019/zb/08/zb_tr2018pdf.pdf

[26] State enterprise of air traffic services of Ukraine „Ukraerorukh“ (in Ukrainian) [online] [accessed 2019-12-25]. Available from: https:////uksatse.ua/index.php?s=7fafa5d747ed52968 70f4e285d3e17df&act=Part&CODE=247&id=450

[27] OVSAK, O. P., LISKOVYCH, N. Y. Macroeconomic aspects of the impact of air transport development on the economy of Ukraine (in Ukrainian). *Black Sea Economic Studies* [online]. 2019, **48**, p. 133-141 [accessed 2020-05-03]. ISNN 2524-0897, eISSN 2524-0900. Available from: https://doi.org/10.32843/bses.48-22

[28] KYRYLENKO, O., RIAZANOVSKA, V. NOVAK, V. Strategic airline alliances as a special form of company integration. *Baltic Journal of Economic Studies* [online]. 2019, **5**(1), p. 75-80 [accessed 2020-02-12]. ISSN 2256-0742, eISSN 2256-0963. Available from: https://doi.org/10.30525/2256-0742/2019-5-1-75-80

[29] OLESHKO, T., HEIETS, I. Perspectives of the air transportation market in Ukraine. *Aviation* [online]. 2018, **22**(1), p. 1-5 [accessed 2020-05-24]. ISSN 1648-7788, eISSN 1822-4180. Available from: https://doi.org/10.3846/aviation.2018.1855

[30] The volume of air navigation services provided to UkSATSE in 2019 increased by 11,5% / Obsyah nadanykh Ukraerorukhom aeronavihatsiynykh posluh u 2019 rotsi zbil'shyvsya na 11,5 %. (in Ukrainian) [online] [accessed 2020-01-06]. Available from: http://uksatse.ua/index.php?s=203f51197ddfa2715bb51336e9de5350&act=Part&CODE=247&id=512

[31] On-line information on key performance indicators of the aviation industry for January 2020 / Operatyvna informatsiya shchodo osnovnykh pokaznykiv diyalnosti aviatsiynoyi haluzi za sichen 2020 roku (in Ukrainian) [online] [accessed 2020-02-16]. Available from: https://avia.gov.ua/pro-nas/statistika/operativna-informatsiya/.

[32] OVSAK, O. P, LISKOVICH, N. Y., NAZARENKO, O. P. Ukraine on the path of aviation liberalization (in Ukrainian). *Market Infrastructure* [online]. 2020, **40**, p. 3-13 [accessed 2020-05-18]. eISNN 2519-2868. Available from: https://doi.org/10.32843/infrastruct40-1

[33] MATSENKO, O. M., HEYETS, I. O., MYRONOVA, Y. V., SKRYPKA, Y. O. Strategic directions of airspace liberalization between Ukraine and the EU / Stratehichni napryamy liberalizatsiyi povitryanoho prostoru mizh Ukrayinoyu ta YES (in Ukrainian). *The Mechanism of Economic Regulation* / *Mekhanizm rehulyuvannya ekonomiky* [online]. 2018, **3**, p. 66-78 [accessed 2019-12-12]. ISSN 1726-8699. Available from: https://doi.org/10.21272/mer.2018.81.06

[34] Information on the decisions taken by the Commission to consider the rights to operate the routes / Informatsiya shchodo pryynyatykh rishen Komisiyi z roz·hlyadu pytan shchodo prav na ekspluatatsiyu povitryanykh liniy (in Ukrainian) [online] [accessed 2020-01-17]. Available from: https://avia.gov.ua/informatsiya-shhodo-prijnyatih-rishen-komisiyi-z-rozglyadu-pitan-shhodo-prav-na-ekspluatatsiyu-povitryanih-linij-14/

[35] COOPER, A., SMITH, P. The Economic catalytic effects of air transport in Europe. Final report. Oxford Economic Forecasting, EEC/SEE/2005/004 [online] [accessed 2020-07-12]. 2002. Available from: https://www.eurocontrol.int/eec/public/standard_page/DOC_Report_2005_025.html

[36] MSITS 2010. Manual on statistics of international trade in services 2010 [online] [accessed 2020-11-23]. Available from: unstats.un.org/unsd/tradeserv/TFSITS/msits2010/M86%20rev1-white%20cover.pdf

[37] Air transport services - World Trade Organization [online] [accessed 2020-11-23]. Available from: https://www.wto.org/english/tratop_e/serv_e/transport_e/transport_air_e.htm#review1

[38] Statistics in respect of the carriage of passengers, freight and mail by air [online] [accessed 2020-05-26]. Available from: https://eur-lex.europa.eu/legal-content/EN/TXT/?qid=1589662698652&uri=LEGISSUM:l24059

[39] Ukraine's international trade in goods and services in 2016. Statistical collection (in Ukrainian) [online]

[accessed 2019-12-03]. Available from: http://www.ukrstat.gov.ua/druk/publicat/Arhiv_u/10/Arch_ztp_zb.htm
[40] GDP of Ukraine - International monetary fund [online]. Available from: https://www.imf.org/en/Countries/UKR#whatsnew
[41] Dynamics of international trade in services by types (in Ukrainian) [online] [accessed 2020-05-29]. Available from: http://www.ukrstat.gov.ua/operativ/operativ2008/zd/dseip/dseip2007_u.htm

IMPROVEMENT OF THE LOGISTIC PROCESSES USING THE REVERSE LOGISTICS CONCEPT

Zbigniew Lukasik[1], Aldona Kuśmińska-Fijalkowska[1,*], Sylwia Olszańska[2]

[1]Faculty of Transport, Electrical Engineering and Computer Science, Kazimierz Pulaski University of Technology and Humanities in Radom, Radom, Poland
[2]Chair of Logistics and Process Engineering, University of Information Technology and Management based in Rzeszow, Rzeszow, Poland

*E-mail of corresponding author: a.kusminska@uthrad.pl

Resume
Reverse logistics differs significantly from such fields as management of waste, of which the goal is, above all, efficient and effective collection and processing of waste. Therefore, it can be said that reverse logistics refers to such streams of flows in which it is possible to recover the value from discontinued products and situation, in which solution is contribution to a new supply chain. Therefore, in this aspect, the fundamental pillar is transport, in which the crucial element is management of transport process, above all, planning of changes improving this process to better control the degree of their execution.
In this article, the authors examined transport process in a real object in the context of improvement. As a result, practical aspects of planning and control of organization of transport were presented.

Article info
Received 9 September 2020
Accepted 4 October 2020
Online 19 May 2021

Keywords:
reverse logistics,
system approach,
logistics process

Available online: https://doi.org/10.26552/com.C.2021.3.A174-A183

ISSN 1335-4205 (print version)
ISSN 2585-7878 (online version)

1 Introduction

Transport is an inherent element of waste management system. Therefore, an integrated look at the concepts of management of the waste flows is important. As a result, increased interest in waste management is an effect of various interconnected actions [1-3]. Above all, it should be emphasized that all the tasks, connected with the waste management, fall within competences of logisticians [4-6]. In this aspect, a person managing transport must perceive organization of transport from the angle of execution of quantified partial tasks to achieve effective planning and execution of transport process [7-13]. A permanent goal in a transport enterprise is improvement of processes and as a result, implementation of effective methods of management to gain competitive advantage [14-17]. Therefore, the most advantageous is management of the transport process organization, as intentionally interconnected sequences of actions, transforming input state into output state, executing the plan of delivery of goods to clients in Just-in-Time and Door-to-Door system [18-21].

2 The subject, goal and the most important tasks of the reverse logistics

The reverse logistics is attractive showing both area of research and differences in determination of the scope of its application. There is also high compliance to the subject and tasks of the reverse logistics. The subject of reverse logistics is flow of waste and information connected with this flow. These flows should be configured in such a way to minimize harmful impact of waste on natural environment in the most functional and consistent way. To achieve it, one needs organizational, technical and financial coordination of the processes' course and logistic actions. The goal of reverse logistics is to combine the mentioned flows in time and space and by optimizing the costs of flows, guarantee proper condition of natural environment.

The scope of tasks of reverse logistics, resulting from the concept of the Reverse Logistics Association (RLA), is very significant in the aspect of the processes execution. Table 1 presents a list with the tasks of traditional logistics.

This is an open access article distributed under the terms of the Creative Commons Attribution 4.0 International License (CC BY 4.0), which permits use, distribution, and reproduction in any medium, provided the original publication is properly cited. No use, distribution or reproduction is permitted which does not comply with these terms.

Table 1 *Logistics and reverse logistics in accordance with concept of RLA*

supply chain - after - sales supply chain product life cycle				
logistics				reverse logistics
designing new products	material management	production and distribution	consumer/ recipient	after sales customer service
- designing, - development, - the changes of technologies, - designing electronic, integrated circuits, - mechanical projects, - prototypes, - launching new product.	- the relationships with the suppliers, - planning, - procurements, - planning of stocks, - productions of components.	- assembly of sub-assemblies, - assembly of finished goods, - production of assortment - integration - configuration, - final tests, - delivery to a client (distribution), - satisfaction of client's needs, - transport processes.		- customer service, - helpdesk, call centre, repair points - logistic services: • field service, • transport/ storage, • management of spare parts, • management of returned products, • management of exchange of products, - management of products with finished life cycle, - the actions connected with making client satisfied, - management of it processes, - recycling, - renovation/ tracking of products, - warranty support.

3 System approach in waste management

System approach is the key to understand logistics. This issue occurs on the spatial, organizational and information plane. Therefore, this approach requires comprehensive thinking due to connections and relations. This ideology is based on an assumption that all the actions in a specific enterprise that are involved in physical flow and storage of raw materials, semi-finished products, as well as finished goods, should be treated not as individual parts, but as a whole. As a result, application of the system approach in logistics helps to eliminate sub-optimization of solutions since the single elements of the system aim at such cooperation that is required in all the parts of comprehensively assessed logistic system [22].

It can also be said that a system is a set of interconnected components allowing to achieve established goal. In addition, while defining a logistic system, one should present a position of D. M. Lambert who considered the system starting from input elements, then their transformation and ending with output elements. The input elements include stocks, logistic material base and information, whereas the output element is a result of actions of the system with reference to products or services according to logistic orientation effective for the clients. The logistic system must be built in „the best way" (optimo modo) because the goal of its building is to guarantee the execution of logistic processes [23]. Above all, around this system, the connections between the elements of infrastructure have the character of flow of goods, people and information. In order to achieve the coordinated development, one should not only implement and improve effective methods of management, but one should take all the potential environmental factors affecting the human environment into account. Such factors include logistic functioning of integrated waste management system. In this aspect, integration means combination of particular elements of the system with use of tasks of modern logistics.

4 The application of reverse logistics within the scope of waste disposal and their reuse

A significant task of reverse logistics concerning waste disposal is planning the routes of the vehicles. The routes should be planned in an optimal way to provide efficient service for the towns/cities with the lowest possible costs of the waste collection, meeting also the requirements of transport congestion, frequency of service of stockpiles and minimization of negative impact on environment.

Two systems of waste collection were distinguished:

1) single-stage system - in this case, transport directly to a place of neutralization,
2) two-stage system - transport is provided with the of transhipment stations in which the waste is collected temporarily.

It is widely believed that the two-stage transport is much better than single-stage transport because it allows to increase economic efficiency and improve the efficiency and operating efficiency of the vehicles for waste collection. In addition, the two-stage transport is more profitable since the expenditure, incurred on the vehicles and transhipment station, quickly pay for itself.

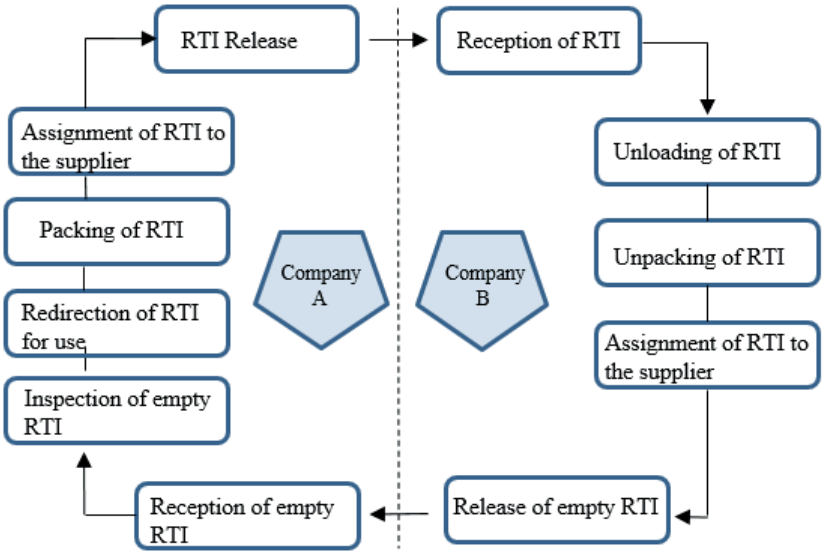


Figure 1 *The process of release and reception of returnable transport items*

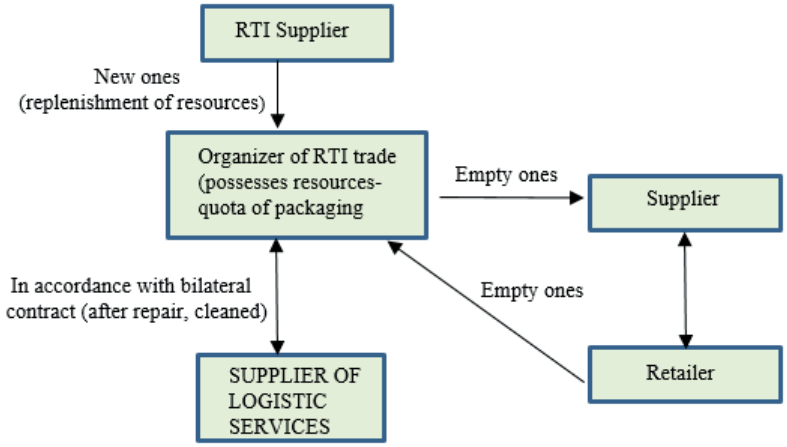


Figure 2 *Physical flows in the RTI system - Returnable Transport Items*

The types of selection of the transport means used in the waste management depend, above all, on a system of the waste collection, type of containers that are used and on whether waste for recycling is collected at the same time and in the same vehicle. The goals of organization and technique of the waste disposal should be:

- increasing multifunctionality of the fleet,
- constant improvement of the fleet,
- modernizing mechanization of the waste loading and as a result, reduction of the transport teams number,
- increasing the work comfort of the drivers.

To sum up, it may be concluded that execution of tasks of the reverse logistics within the waste disposal from the places of storage has significant impact on efficient functioning of the waste management logistic system.

Specific sections of path of life of the packaging are harmonized with subsequent processes. Above all, effective management of returnable transport items (RTI) is becoming increasingly important in modern supply chains (Figure 1) [24-25].

In the processes that include the rules of efficient management of returnable transport items, three basic entities are distinguished:

1. RTI producers,
2. suppliers,
3. customers.

Moreover, in some supply chains there are other entities, for example, logistic operator who is responsible for sending materials or for reception of returnable transport items from the customers [26].

In such a system of exploitation, an inherent element are the following problems, among others:

- lack of accurate control of the state of the packaging - the consequence is increased stocks,
- expensive production and return of the packaging - resulting in additional costs and risk of errors, slowing down the process,
- the processes of control of returnable transport items take much time that would be used in a different, much more profitable way.

Table 2 *Source data of the route Jaslo - Odense - Police - Jaslo, April 2020*

route	number of section	departure date	start of work	loading time (h)	hour of departure (h)	route	distance (km)	load (t)	pause time at the route (h)	arrival date	hour of arrival (h)	time of unloading (h)	time of loading (h)	end of work	total time of loading operations (h)	daily rest (h)	total fuel consumption (l)
	1	2020-04-20	6:00	1:00	07:00	Jaslo - Olszyna	605	24	00:50	2020-04-20	16:45			16:55	01:00	11:05	176
	2	2020-04-21	4:00		04:10	Olszyna - Odense (DN)	734	24	01:40	2020-04-21	15:40	01:10	01:00	17:50	02:10	12:10	211
1	3	2020-04-22	6:00	1:30	07:30	Odense (DN) - Police	675	24	00:50	2020-04-22	17:15	01:00		19:30	02:30	11:10	199
	4	2020-04-23	6:40		06:50	Police - Cracow	640	24	01:40	2020-04-23	18:20			18:30	00:00	11:10	188
	5	2020-04-24	5:40		05:50	Cracow - Jaslo	150	24		2020-04-24	08:30	04:00		13:00	04:00		43
				2:30		total	2 804		5:00			6:10	1:00		9:40:00	45:35:00	817
				1:15		average	560,8		1:15			2:03	1:00		1:56	11:23	163.4
				1:30		maximum	734		1:40			4:00	1:00		4:00	12:10	211
				1:00		minimum	150		0:50			1:00	1:00		0:00	11:05	43
				0:21		standard deviation	235		0:28			1:41	-		1:31	0:30	69
				28.3		standard deviation / average (%)	41.8		38.5			82.0	-		78.7	4.5	41.9

Table 3 Results of analysis of the route 1

number of section	date of departure	distance [km]	transport work [tkm]	time of transport [h]	time of ride [h]	time of work [h]	operational speed [km/h]	technical speed [km/h]	use factor of time of work [1]	fuel consumption [l]	combustion [l/100km]		traction with load [km]	traction without load [km]	combustion with load [l/km]	combustion without load [l/km]
1	2020-04-20	605	14 520	09:45	08:55	10:55	55.4	67.9	0.82	176	29.1		605	0	29.1	-
2	2020-04-21	734	17 616	11:30	09:50	13:50	53.1	74.6	0.71	211	28.7		734	0	28.7	-
3	2020-04-22	675	16 200	09:45	08:55	13:30	50.0	75.7	0.66	199	29.5		675	0	29.5	-
4	2020-04-23	640	15 360	11:30	09:50	11:50	54.1	65.1	0.83	188	29.4		640	0	29.4	-
5	2020-04-24	150	3 600	02:40	02:40	07:20	20.5	56.3	0.36	43	28.7		150	0	28.7	-
total		2 804	67 296	45:10:00	40:10:00	57:25:00	48.8	69.8	0.70	817	29.1	total	2804	0	29.1	
												(%)	100.0	0.0		

Therefore, the function of logistics in this aspect is limiting such problems. Therefore, the logistic management in this case was presented on Figure 2.

5 An analysis of transport process executed in the examined transport enterprise

The subject of analysis is a transport enterprise and transport processes executed in it. Examined enterprise provides transport services only by the road transport. The enterprise has decided to build competitive strategy to strengthen its position. Therefore, to single out their offer on the market, the managers have decided to extend transport potential for provision of services of transport of waste using specialized fleet. The managers also want to become a leader on the market of enterprises dealing with transport of waste. Therefore, the authors analysed executed transport processes in the aspect of efficiency. As a result, statistical analysis was conducted showing that time can be saved during the executed transport process.

Examined enterprise executes transport tasks both in a single-stage and two-stage system, however, most of the orders from the clients include execution of transport in a single-stage system. Because the superior attributes in organization of transport process include quality, time and costs, it is important for initial execution of a process, that is, from the moment of reception of a transport order to its final execution, to be coordinated and without delays. As a result, these actions lead to meeting the objectives of examined transport enterprise, because the minimization of costs and maximum profit are the most important for this enterprise.

The subject of analysis is **route 1**, executed in April 2020, where the return cargo is loaded in Police. This route consists of transport of three cargos:

- the first one on the route between Jaslo and Odense in Denmark,
- the second one on the route between Odense and Police,
- and the third one on the route between Police and Jaslo.

The source data are presented in a five-segment system and contain such information as: number of route, vehicle make, date, hour and place of departure, distance of drive, weight of cargo, date, hour and place of arrival, time of pauses on the route, time of loading operations, time of daily rest (Table 2).

Based on the source data, values of sums, average, maximal and minimum values, their standard deviation, if it was possible, were calculated and the value of standard deviation was compared with the average value in percentage terms. Directly from the monthly data, sums of distances, times of loading, unloading, pauses, daily rests, fuel consumption were calculated. Apart from the monthly sums, the average values of these parameters were calculated, their maximal and

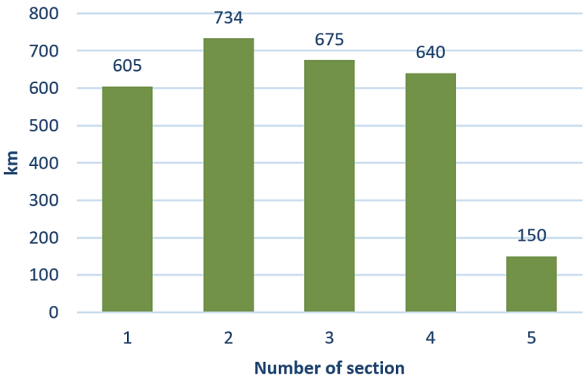


Figure 3 *Daily distances*



Figure 6 *Daily fuel consumption*

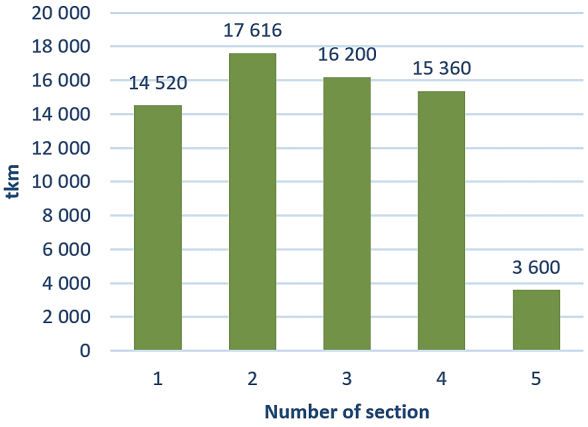


Figure 4 *Daily transport work*

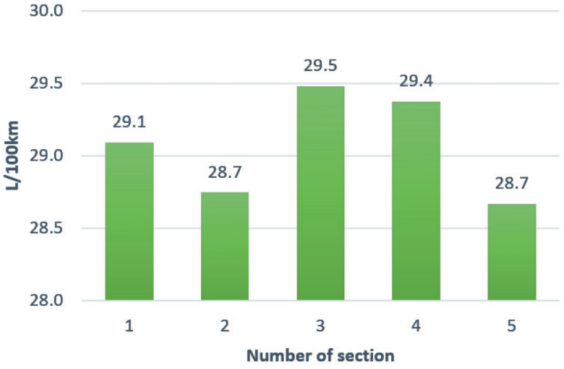


Figure 7 *Daily combustion*

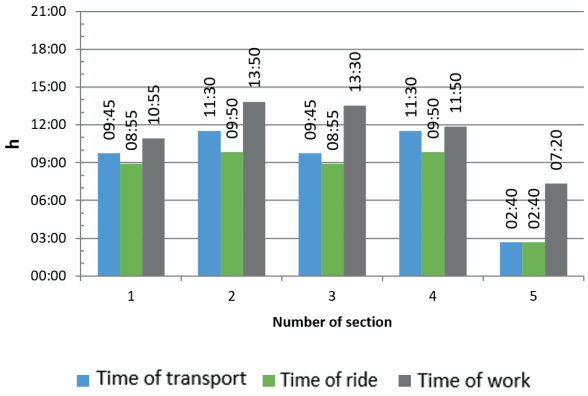


Figure 5 *Daily time of transport, ride and work*

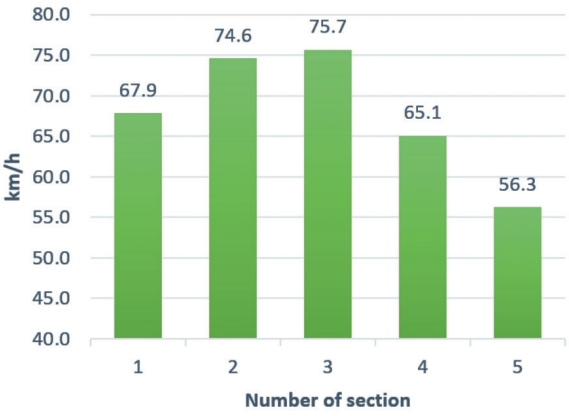


Figure 8 *Technical speed*

minimum values, standard deviation were determined and compared to average value. An analysis was conducted by calculating such rates as: transport work, time of transport, time of ride, time of work, operating speed, technical speed, fuel consumption (Table 3).

Results of analysis of the route 1, that is, daily distances, daily transport work, daily time of transport, ride and work, as well as daily fuel consumption, daily combustion and technical speed were presented in Figures 3 to 8.

Figure 3 shows daily distances of the route in km as a function of a section number. Diverse distances of the routes in subsequent days were observed. During the days 1, 2, 3, 4, these distances are between 605 and 734 km, therefore, they are similar to a maximum daily range. Therefore, in these sections, there is a risk of inability to reach a point of destination in the event of even minor disruptions of traffic flow. Whereas, on a day 5, daily length of the route is much shorter, 150 km, which results from the way of organization of the route.

Conducted analysis showed that daily transport work is diverse analogous to diversity of daily mileage (Figure 4).

Daily duration of transport is almost identical in all the sections of transport, because during the days: 1, 3, it is 9 h 45 min, whereas, in the sections 2, 4, it is 11 h 30

Table 4 *Improvement of the transport process with use of the monitoring system*

departure day	start of work (h)	time of loading (h)	hour of departure (h)	route	distance (km)	time of ride (h)	pause time at the route (h)	arrival day	hour of arrival (h)	time of unloading (h)	time of loading (h)	end of work (h)	time of work (h)	daily rest (h)	total fuel consumption (l)	time of ride on the section (h)	operational seped (km/h)	technical speed (km/h)
1	0:00	1:00	01:00	Jaslo - Olszyna	605	08:55	00:45	1	10:40			10:40	10:40	11:00	176	10:40	56.7	67.9
1	21:40		21:40	Olszyna - Odense (DN)	734	09:50	01:30	2	9:00	01:10	01:00	11:10	13:30	09:00	211	12:30	58.7	74.6
2	20:10		20:10	Odense (DN) - Police	675	08:50	00:45	3	5:45	01:00		6:45	10:35	11:00	199	10:35	63.8	76.4
3	17:45	1:30	19:15	Police - Cracow	640	09:50	01:30	4	6:35			6:35	12:50	09:00	188	12:50	49.9	65.1
4	15:35		15:35	Cracow - Jaslo	150	02:45		4	18:20	02:00		20:20	4:45		43	04:45	31.6	54.5
	2:30			total	2 804	40:10:00	4:30			4:10	1:00		52:20:00	40:00:00	817			
	1:15			average	560.8	8:02	1:07			1:23	1:00		10:28	10:00	163.4			
	1:30			maximum	734	9:50	1:30			2:00	1:00		13:30	11:00	211			
	1:00			minimum	150	2:45	0:45			1:00	1:00		4:45	9:00	43			
	-			standard deviation	235	2:59	0:25			0:32	-		3:26	1:09	69			
	-			standard deviation. / average (%)	41.8	37.2	38.5			38.6	-		32.9	11.5	41.9			

min, only in section 5, it is 2 h 40 min. Daily duration of drive is analogous to duration of transport. In the event of daily working time, there is high diversity in every section of the route (Figure 5).

Daily fuel consumption is diverse similarly to daily distances. However, in specific sections, small differences in fuel consumption can be observed, which can be caused by variability of the road conditions (Figure 6).

An analysis conducted by the authors showed that in section 3, there is the highest daily burning 29.5 L/100 km, whereas the lowest 28.7 L/100 km was found in section 5 (Figure 7).

The highest technical speed was recorded in section 3, which was 75.7 km/h and the lowest 56.3 km/h was in section 5 (Figure 8).

As a result of research conducted in a real object, the authors perceived the opportunity of improving the transport process by implementing innovative solutions.

6 Improvement of the transport process executed with use of an innovative monitoring system

Time of drive of analysed **route 1** is 40 hours and 10 minutes and it is divided into five working days. It should be checked whether application of the monitoring system should have impact on shortening the time of transport. In order to check the examined route 1, Table 4 was created. To simplify it, it was assumed that departure starts at 0:00 o'clock, but table allows to change the moment of departure. The set of data was also changed - time of loading and unloading, time of ride, pauses. Data are entered to the field of grey background, whereas, remaining data such as hours of departure, arrival, end of a working shift, time of work and day are not changed.

Shortening the time of execution of this transport to 4 days, while maintaining 5 working shifts is possible in the event of maintaining the standard worktime and driver's rest (Table 4). To sum up, in the route 1, time of drive can be shortened by 1 day. It generates savings because vehicle and driver can be used for an additional transport order.

Conducted analysis showed that the selected route is optimal. Alternative routes are longer, the roads are of the lower categories and require longer time of drive. Only in the run to Odense, change of route can be considered, that is, ride „there" through Police, which would shorten the time of drive through Germany and reduce the amount of remuneration of a driver because the number of hours paid according to German minimum rates would be lower. What is more, in the route 1, a place of a daily rest on the way back from Cracow can be changed to a town situated about 100 km closer. It would enable to avoid the ten-hour shift on the route between Police and Cracow, reducing it to about 8 hours and 30 minutes, whereas this distance can be covered on the next short shift to Jaslo. The prolonged unloading in Jaslo, lasting 4 hours is inexplicable. Obtained data showed that operation of unloading lasts on average about 2 hours, therefore, one can assume that there was some problems, for example, waiting for unloading.

7 Conclusions

A domain of reverse logistics is, above all, the processes in an integrated waste management system, of which inherent element is transport. Moreover, the use of logistics in the concept of the waste management processes gives many benefits, including unification of the processes of the waste streams flows and also, related to the flows, the correlated flow of information, which, as a result, allows to reduce the costs of service of the processes through effective use of resources.

The essence in a transport enterprise is provision of the high standard services, therefore, the managers often face the pressure of necessity of adjustment of the services to growing client-oriented market needs. Therefore, the forwarding agent should maximize the efficiency of executed transport process, which was shown in this article to maintain the high competitiveness level.

The authors of this article conducted research on transport process in a real object, which is one of the most important links of the supply chain in reverse logistics. As a result, they showed an improvement within the conducted transport process in reverse logistics. Therefore, due to the fact of multidimensionality of this problem, practical directions of actions adopted in the article aiming at improvement of planning and conducting of transport may be used by the forwarders in making decisions related to management of logistic processes. Furthermore, presented modern concept of management is becoming a driving force in rationalization of the actions in terms of flow of goods and information, as well as improvement of adopted strategy of conducting the transport processes directed towards, above all, duration, quality, flexibility and innovativeness.

References

[1] JANCZEWSKI, J. Automotive reverse logistics networks. Selected exemples (in Polish). *Zeszyty Naukowe Wyzszej Szkoly Humanitas. Zarzadzanie* [online]. 2016, **2**, p. 231-251. ISSN 1899-8658. Available from: https://doi.org/10.5604/18998658.1210118

[2] LIN, C., CHOY, K. L., HO, G. T. S., CHUNG, S. H., LAM, H. Y. Survey of green vehicle routing problem: past and future trends. *Expert Systems with Applications: An International Journal* [online]. 2014, **41**(4), p. 1118-1138. ISSN 0957-4174. Available from: https://doi.org/10.1016/j.eswa.2013.07.107

[3] LI, Y., LU, L. Research on B2C reverse logistics service quality evaluation system. In: 5th International Conference on E-Business and Applications ICEBA 2019: proceedings [online]. 2019. ISBN 978-1-4503-6262-7, p. 10-15. Available from: https://doi.org/10.1145/3317614.3317631

[4] ELMERINI, R., BENSLIMANE, M., ZOUADI, T. Reverse logistic optimization: application to the collect and the reuse of reusable containers. In: International Conference on Learning and Optimization Algorithms: Theory and Applications LOPAL ´18: proceedings [online]. 2018. ISBN 978-1-4503-5304-5, p. 1-5, art. no. 62. Available from: https://doi.org/10.1145/3230905.3230966

[5] HAUDER, V. A., BEHAM, A., WAGNER, S., AFFENZELLER, M. Optimization networks for real-world production and logistics problems. In: Genetic and Evolutionary Computation Conference Companion GECCO ´17: proceedings [online]. 2017. ISBN 978-1-4503-4939-0, p. 1411-1414. Available from: https://doi.org/10.1145/3067695.3092959

[6] CEMPIREK, V., NACHTIGALL, P., SIROKY, J. Security in Logistics. *Open Engineering* [online]. 2016, **6**(1), p. 637-641. eISSN 2391-5439. Available from: https://doi.org/10.1515/eng-2016-0082

[7] ULLRICH, C. A. Integrated machine scheduling and vehicle routing with time windows. *European Journal of Operational Research* [online]. 2013, **227**, p. 152-165. ISSN 0377-2217. Available from: http://dx.doi.org/10.1016/j.ejor.2012.11.049

[8] CAO, E., LAI, M., YANG, H. Open vehicle routing problem with demand uncertainty and its robust strategies. *Expert Systems with Applications* [online]. 2014, **41**, p. 3569-3575. ISSN 0957-4174. Available from: http://dx.doi.org/10.1016/j.eswa.2013.11.004

[9] CHE, Z. H., CHIANG, T.-A., HSIAO, K. H., CHEN, C. L., CHANG, J. Y. Cross-stage reverse logistics planning via a genetic algorithm. In: International Conference on Algorithms, Computing and Systems ICACS ´17: proceedings [online]. 2017. ISBN 978-1-4503-5284-0, p. 98-101. Available from: https://doi.org/10.1145/3127942.3127944

[10] GHANNADPOUR, S. F., NOORI, S, TAVAKKOLI-MOGHADDAM, R., GHOSEIRI, K. A multi-objective dynamic vehicle routing problem with fuzzy time windows: model, solution and application. *Applied Soft Computing* [online]. 2014, **14**, p. 504-527. ISSN 1568-4946. Available from: http://dx.doi.org/10.1016/j.asoc.2013.08.015

[11] PECENY, L., MESKO, P., KAMPF, R., GASPARIK, J. Optimisation in transport and logistic processes. *Transportation Research Procedia* [online]. 2020, **44**, p. 15-22. ISSN 2352-1465. Available from: https://doi.org/10.1016/j.trpro.2020.02.003

[12] OCALIR-AKUNAL, E. V. Decision support systems in transport planning. *Procedia Engineering* [online]. 2016, **161**, p. 1119-1126. ISSN 1877-7058. Available from: https://doi.org/10.1016/j.proeng.2016.08.518

[13] KAMPF, R. Optimization of delivery routes using the little´s algorithm. *Nase More* [online]. 2018, **65**(4), p. 237-239. ISSN 0469-6255, eISSN 1848-6320. Available from: https://doi.org/10.17818/NM/2018/4SI.13

[14] CEMPIREK, V., VRBOVA, P., ZAKOROVA, E. The possibility of transferring the transport performance on railway transport. *MATEC Web of Conferences* [online]. 2017, 134(2), 00006. eISSN 2261-236X. Available from: https://doi.org/10.1051/matecconf/201713400006

[15] FU, J., JENELIUS, E. Transport efficiency of off-peak urban goods deliveries: a Stockholm pilot study. *Cases Studies on Transport Policy* [online]. 2018, **6**(1), p. 156-166. ISSN 2213-624X, eISSN 2213-6258. Available from: https://doi.org/10.1016/j.cstp.2018.01.001

[16] PILLAC, V., GUERET, CH., MEDAGLIA, A. L. An event- driven optimization framework for dynamic vehicle routing. *Decision Support System* [online]. 2012, **54**(1), p. 414-423. ISSN 0167-9236. Available from: https://doi.org/10.1016/j.dss.2012.06.007

[17] SIMANOVA, L., STASIAK-BETLEJEWSKA, R. Monitoring and improvement of logistic processes in enterprises of the Slovak Republic. *LOGI - Scientific Journal on Transport and Logistics* [online]. 2019, **10**(1), p. 62-71. eISSN 2336-3037. Available from: https://doi.org/10.2478/logi-2019-0007

[18] PANDELIS, D. G, KARAMATSOUKIS, C. C., KYRIAKIDIS, E. G. Finite and infinite- horizon single vehicle routing problems with a predefined customer sequence and pickup and delivery. *European Journal of Operational Research* [online]. 2013, **231**(3), p. 577-586. ISSN 0377-2217. Available from: http://dx.doi.org/10.1016/j.ejor.2013.05.050

[19] LEI, H., LAPORTE, G., GUO, B. The vehicle routing problem with stochastic demands and split deliveries. *INFOR: Information Systems and Operational Research* [online]. 2012, **50**(20), p. 59-71. ISSN 0315-5986, eISSN 1916-0615. Available from: https://doi.org/10.3138/infor.50.2.059

[20] AZI, N., GENDREAU, M., POTVIN, J-Y. A dynamic vehicle routing problem with multiple delivery routes. *Annals of Operations Research* [online]. 2012, **199**, p. 103-112. ISSN 0254-5330, eISSN 1572-9338. Available from: https://doi.org/10.1007/s10479-011-0991-3

[21] CABAN, J., DROZDZIEL, P., KRZYWONOS, L., RYBICKA, I., SARKAN, B., VRABEL, J., Statistical analyses of selected maintenance parameters of vehicle of road transport companies. *Advances in Science and Technology Research Journal* [online]. 2019, **13**(1), p. 1-13. ISSN 2299-8624. Available from: https://doi.org/10.12913/22998624/92106

[22] KOCHANSKI, T. *Logistics as a concept of integrated management* (in Polish). Warszawa: Akademia Obrony Narodowej, 2003. ISBN 8388062697.

[23] DEMBINSKA-CYRAN, I., JEDLINSKI, M., MILEWSKA, B., *Logistics. Selected topics for studying the subject* (in Polish). Szczecin: Wydawnictwo Naukowe Uniwersytetu Szczecinskiego, 2001. ISBN 8372411956.

[24] Reusable Transport Items (RTI). Organizational Recommendations. EANCOM-Manual. Koln: Centrale fur Coorganisation GmbH, 2003.

[25] LYSENKO-RYBA, K. The impact of reverse logistics on customers satisfaction. In: *Logistics in management sciences. Part II* (in Polish). KAUF, S., PISZ, I. (eds.). Lodz - Waszawa: Wydawnictwo SAN, 2017. ISSN 2543-8190, p. 137-146. Available from: http://piz.san.edu.pl/docs/e-XVIII-8-2.pdf

[26] MICHNIEWSKA, K. *Recycling logistics in packaging* (in Polish). Warszawa: Wydawnictwo Difin, 2013. ISBN 9788376418384.

THE IMPACT OF INFRASTRUCTURE SPENDING ON ECONOMIC GROWTH: A CASE STUDY OF INDONESIA

Makmun Syadullah, Dhani Setyawan*

Fiscal Policy Agency, Ministry of Finance of the Republic of Indonesia, Jakarta, Indonesia

*E-mail of corresponding author: dhanisetyawan83@gmail.com

Resume

This paper aims to analyze the impact of infrastructure spending on economic growth in Indonesia, which includes investment in road, port and irrigation infrastructure. The period of observation was 2011-2018, which covered 29 provinces with consideration of data availability. This study employed the growth model with a panel data analysis, which analyze the relationship between the economic growth and government investment in infrastructure in the long run. The most essential finding in this study is that the economic growth is positively influenced by government investment in road, port and irrigation infrastructure. Road infrastructure investment has a significant positive impact and the effect occurs in the fourth year after infrastructure development. In comparison, port and irrigation infrastructure investment have a positive but not significant impact to other variables.

Article info

Received 20 November 2020
Accepted 23 December 2020
Online 19 May 2021

Keywords:

infrastructure investment,
economic growth,
transportation,
public investment,
agriculture

Available online: https://doi.org/10.26552/com.C.2021.3.A184-A192

ISSN 1335-4205 (print version)
ISSN 2585-7878 (online version)

This is an open access article distributed under the terms of the Creative Commons Attribution 4.0 International License (CC BY 4.0), which permits use, distribution, and reproduction in any medium, provided the original publication is properly cited. No use, distribution or reproduction is permitted which does not comply with these terms.

1 Background

Current development, including infrastructure development, will determine the future civilization. Infrastructure development will create more robust connectivity more evenly throughout the country. The availability of adequate infrastructure will minimize disparities between regions, reduce logistics costs and reduce the economic inequality between regions in Indonesia. Furthermore, infrastructure development will also improve community welfare.

The impact of infrastructure development on economy cannot be enjoyed directly. It takes at least a short amount of time to feel the effect. The study of measuring the performance of public infrastructure development on new economic growth was carried out around the 1990s [1]. Further, the study of relationship between the infrastructure development and economic growth was carried out in the period 1990-1995 [2]. In the next era, research on the impact of forest development on poverty became the focus of research. Various research findings show that results are very varied, even seem contradictory. According to [3], infrastructure measurement from the expenditure side is considered as the leading cause of conflicting research results compared to the size in terms of performance, which is due to various reasons. First, ignoring the contribution of infrastructure spending by the private sector and secondly, there are inconsistencies in infrastructure funding.

According to [4], there is a positive relationship between the economic growth and infrastructure spending. The availability of more significant infrastructure is a driver of economic growth. Investment in infrastructure will also encourage increased productivity and create externalities. Further, it also reduces transportation costs and production costs

China is one of countries that succeed in building infrastructure. The Chinese government spending on infrastructure is enormous in the hope that it will drive the economic growth. Many other countries are fascinated by China's infrastructure development policies. But the fact is, according to [5] that the infrastructure development in China is not much different from those of other countries. Chinese investment is generally in unproductive projects, which fail. The benefits expected at the beginning of growth were not realized; even the project was a burden to the economy, due to excessive investment in unproductive projects funded with debt. Further, results in debt buildup, economic fragility, unstable financial markets and expansion in the monetary sector. What happened in China must be a lesson for other countries.

In the era of President Joko Widodo, infrastructure development in Indonesia was a top priority, which can be proven from the portion of the financing in 2018, reaching around 18.6 % of total government expenditure. According to the performance report of the Ministry of Public Works and Public Housing , the output of road length increased, exceeding the target up to 3 times.

Will infrastructure development carried out massively in various regions in Indonesia have a positive impact on economic growth? This paper has analyzed the effect of infrastructure spending, specifically road, port and irrigation infrastructure on economic growth in Indonesia. The investment period analyzed is 2011-2018, which covers 29 provinces taking into account the availability of data.

2 Literature review

2.1 Definition of infrastructure

According to [6], infrastructure is defined as, "those services derived from the set of public work traditionally supported by the public sector to enhance private-sector production and to allow for household consumption". Meanwhile, according to [7] infrastructure is a physical system that provides transportation, irrigation, drainage, buildings and other public facilities, which are needed to meet basic human needs both social and economic conditions. Further [7] also defines infrastructure as a physical system that provides transportation, irrigation, drainage, buildings and facilities other public. This infrastructure is needed to meet basic human needs, both economic and social. In contrast, [8] defines infrastructure as a system that supports social and economic networks. Infrastructure is also a connector for the environmental system, where this system can be used as a basis for making policies.

Both central and regional governments provide infrastructure like public services to support and encourage the economic and social activities of the community. The provision of infrastructure is tailored to each region's needs so that it can improve the welfare of the city. Urban society requires different infrastructure from rural communities, as well as between regions industry with agriculture and coastal areas.

Infrastructure is non-exclusive (no one can be excluded), non-rival (consumption of an individual does not reduce the consumption of other individuals). Besides that, in general, marginal production costs are zero and cannot be traded (non-tradable).

Some types of infrastructure (such as toll roads) do not include pure public goods, even though the government provides them. The use of available goods is the non-rivalry and non-excludable rivalry. Rivalry in the sense that if someone uses an item, the item cannot be used by someone else. However, if on the contrary the goods were used by other people or used jointly, then the goods are public goods. The use of infrastructure is not directly charged, because the government provides the infrastructure as a support for social-economic activities.

Infrastructure, such as roads, education, health are the positive externalities. Providing support to these facilities can increase the productivity of all the inputs in the production process [9]. Positive externalities in infrastructure, in the form of increased production of companies and the agricultural sector, without having to raise input capital and labour, also increase the level of technology.

2.2 Infrastructure and growth

As a reference in analyzing economic growth models, the Solow growth model is often used. The model assumes that economic growth is influenced by three factors, namely savings, investment and population growth. Meanwhile, technological changes that describe the level of efficiency are assumed to be exogenous and are considered residuals. According to [10], the Solow Model is a growth model developed by Harrod-Domar, by adding labour and technology factors to the growth equation.

Infrastructure in the aggregate production function is considered as additional input [11]. The effect of public spending on development of the endogenous growth model was considered in [12]. Subsequent research was conducted by authors of [13] adding the private capital stock. Furthermore, the impact of infrastructure development on economic growth was examined in [14], as well. The results show a positive effect, a decrease in the number of poor people and an increase in the environment.

One important indicator that is often used to measure economic conditions in a country in a certain period is the Gross Domestic Product (GDP). Transportation facilities are needed to reduce the gap between consumers and producers. Thus, the means of transportation play a critical role as a means of connecting parties who need each other. Transport infrastructure plays a role in overcoming obstacles that disrupt the smooth flow of goods and people through the land, sea and air modes.

Some of the main variables that influence economic growth are the capital accumulation (including investment in land, physical equipment), human resources and technological progress. The capital accumulation would occur if a portion of the income received is reinvested to increase revenue in the future. This productive investment must be supported by investment in social and economic infrastructure, which includes the construction of roads, electricity supply, availability of clean water, irrigation channels, improvement of sanitation, construction of communication facilities and so on.

As a driver of economic growth, economic infrastructure plays a significant role. The intended economic infrastructure is public goods. As public goods, according to the theory of infrastructure, it has the character of an externality, because the government provides it and for each party that uses infrastructure does not pay directly.

Infrastructure development will have an economic

and social impact. The availability of adequate infrastructure can support economic activities and will affect the economic growth. According to [9], infrastructure has positive externalities because it can increase productivity in the production process. Positive externalities can take the form of increased production of companies and the agricultural sector without having to raise capital and labour input or also increase the level of technology.

Infrastructure is a link between various centres of economic activity and the surrounding area. In remote areas where the population is usually isolated, they live in poverty. Farmers have difficulty marketing their agricultural products, so they are burdened with high costs. As a result, the added value of agricultural products is low. Conditions like this are a barrier for poor people, on the one hand, infrastructure development will increase access for the community, on the other hand, it will make it easier for the government to overcome poverty. Improved access to infrastructure will reduce the costs of living and open opportunities for the poor to benefit from economic growth.

2.3 Previous research

One key to achieving higher and stable economic growth is availability of infrastructure. According to [15], many countries in Asia develop the necessary infrastructure, but rather focus on quantity rather than quality. To reduce the distance between regions and the link between national markets at low costs requires quality infrastructure [16].

Many research has been done on how the infrastructure investment affects economic growth. Authors of [11-12] use indicators of public capital to measure infrastructure as additional input in the production function of further research, while in [17] and [18] they use indicators of transportation, electricity and communication to measure infrastructure.

Transportation infrastructure is needed to achieve higher economic growth. This critical role of transportation infrastructure is used as a reason by many countries to build road infrastructure in disadvantaged areas to stimulate economic growth. Results of research supporting this reason are shown in [19] and [20] that the public infrastructure has an impact on increasing productivity and economic growth. Research on the effects of transportation infrastructure using indicators of road density in 48 U.S. states during the period 1960-1985 was conducted in [21]. The results show that the quantity and quality of highways have a positive impact on economic growth. Research with similar products was carried out in [22], which shows that economic growth is affected by the length of roads per thousand inhabitants, exports per capita, education expenditure per capita and physical capital stock per worker. The relationship between the economic growth and U-shaped urbanization is reversed. Economic growth will increase at a low rate of urbanization. However, when urbanization exceeds the threshold level, economic growth would decline.

Meanwhile, the port infrastructure also has a positive impact on economic growth. Authors of [23] show a positive relationship between the value-added in Chinese ports and regional economic development. This study contradicts the results of a previous study conducted in [24], which showed that ports have a declining effect on the economy.

Authors of [25] also researched the impact of port development on economic growth. Their research results led to conclusion that several companies in Hampton, United States, suffered losses due to port shortages. Meanwhile, according to results of [26], each million tons of net port throughput will create around 400-600 jobs in the Western European region. Meanwhile, according to [27], whenever there is a 10% increase in throughput at ports, the revenue will increase 6-20% of the regional GDP. At the same time, the surrounding areas will also enjoy an increase in income of approximately 5-18%.

Meanwhile, the development and management of irrigation infrastructure are closely related to national food security and economic politics in a country. Community access to irrigation infrastructure will have an impact on economic growth. With access to irrigation, the level of income and expenditure of the community will also increase. Thus, the irrigation infrastructure not only impacts income, output and welfare but can also contribute to poverty reduction, through the effects of income and consumption smoothing.

Research on the impact of irrigation infrastructure development on poverty alleviation was conducted in [28]. The results show that areas without irrigation infrastructure have high levels of poverty both in terms of income and consumption, while the lowest are in areas with adequate access to irrigation infrastructure.

2.4 Research methodology

The main problem faced with in the study of the impact of infrastructure investment on economic growth is the measurement of infrastructure investment. Various indicators to measure infrastructure investment have been used in several previous studies. Indicators of public capital are used iny [29-31]. Authors of [19] employed transportation, water and communication indicators. Road, telephone and electricity indicators are used byCanning in [20]. Meanwhile, physical capital stock indicators are used in [32-34].

Table 1 *Percentage of infrastructure budget allocation based on islands and Economic Growth 2010-2017 (Source: Ministry of Finance of the Republic of Indonesia)*

	road	port	irrigation	growth rate
Sumatera	20.80	12.09	23.40	2.83
Java	21.41	11.21	23.02	5.62
Kalimantan	4.30	7.23	6.07	2.76
Sulawesi	14.30	11.48	10.89	2.88
others	28.63	58.00	36.47	5.62

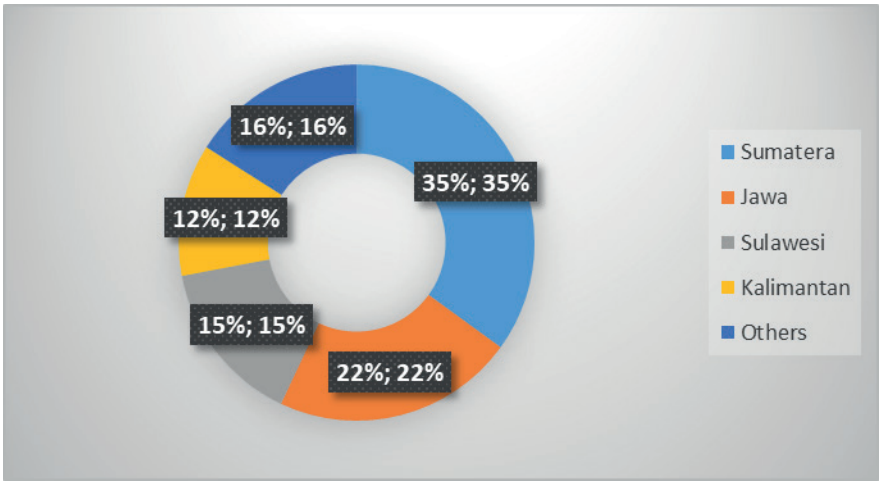


Figure 1 *Distribution of Road Length by Island in 2017 (Source: Central Bureau of Statistics of the Republic of Indonesia)*

In this paper, the infrastructure investment is proxied from central government investment in the province, which includes investment in roads, ports and irrigation. Given the unavailability of infrastructure investment data by local governments, both cities, districts and provinces, the acquisition is not taken into account. As data limitations, only 29 regions were selected out of 34 areas in Indonesia.

The problem that has the potential to interfere with the research results in this study is the geographical problem. Indonesia, with 34 provinces and 17,504 islands has different characteristics so that the economic growth rate of one region is different from the other areas. As a result, the central government investment in infrastructure in each region is also additional. This study ignores geographical problems.

The growth model used in this paper is a panel data analysis model developed by Canning and Pedroni in [9]. This model is used to analyze whether there is a relationship between economic growth and government investment in infrastructure in the long run. Government investment data per province for the period 2011-2017 and economic growth data were obtained from the Ministry of Finance and Statistics Agency. The model used here is:

$$EG = \beta 0 + \beta 1 \log(road) + \beta 2 \log(port) + \beta 3 \mathrm{Log}(irrigation), \quad (1)$$

where: E.G.: economic growth,
road: public investment in the road sector,
port: public investment in the port sector,
irrigation: public investment in the irrigation sector.

In this paper, the time element is included, to find out in what year infrastructure investment began to have an impact on economic growth. This study employs three tests to choose the best panel data regression model, namely: General Effects, Permanent Effects or Random Effects). The F Test (Chow Test), Hausman Test and Lagrange Multiplier Test (L.M.) were conducted, as well.

3 Data analysis and discussion

3.1 Development of infrastructure investment

One of the triggers for economic growth is infrastructure development. For this reason, in the context of building infrastructure, mostly road, port and irrigation infrastructure, government investment continues to increase from year to year. The road infrastructure investment increased from USD 1.06 billion in 2010 to USD 2.4 billion in 2017 or an average increase of 15.61 % per year. The port infrastructure investment increased from USD 78.4 million in 2010 to USD 422.3 million in 2017 or an average increase of 55.03 % per year. In comparison, irrigation

Table 2 *Development of Unloading and Loading at Ports for the 2010-2017 Period (million tons) (Source: Central Bureau of Statistics of the Republic of Indonesia)*

	domestic port		international port	
	uploaded	loaded	uploaded	loaded
2010	221.68	182.48	65.64	233.22
2011	284.29	238.94	78.84	376.65
2012	327.72	312.60	69.51	488.26
2013	336.06	303.88	89.51	510.70
2014	381.60	328.74	100.57	417.16
2015	318.68	296.17	98.52	342.66
2016	361.58	324.11	92.94	313.18
2017	409.34	334.11	105.49	272.40

infrastructure investment increased from Rp 208.7 million in 2010 to Rp 1.7 billion in 2017 or an average increase of 91.78 % per year.

The road infrastructure receives the largest investment allocation. In the observed period (2010-2017) the total portion of investment allocation for roads reached 65.99 %, irrigation 22.10 % and the smallest for ports was 11.91 %. While taking into account regional infrastructure needs, the total budget allocation for roads, ports and irrigation for Papua, Ambon, West Nusa Tenggara and East Nusa Tenggara in the period 2010-2017 reached 33.86 %, Java 20.55 %, Sumatra 20, 37 %, Sulawesi 13.58 % and Kalimantan 11.64 %. At the same time, the allocation based on the island and the type of infrastructure can be seen in Table 1.

When measured in terms of island size, investment allocations for the road, port and irrigation infrastructure do not yet reflect a sense of justice. The Java Island received the most considerable portion, reaching 20.55 %. In contrast, the area of Java was only 128,297 km^2 or 6.73 % of the land area of Indonesia, Papua, Ambon, West Nusa Tenggara and East Nusa Tenggara received allocations of 33.86 %. In contrast, the total area reaches 385,292 km^2 or 20.23 % of the land area of Indonesia. Sulawesi with an area of 174,600 km^2 or 9.17% of the land area of Indonesia received an allocation of 13.58 %. Kalimantan with an area of 743,330 km^2 or 39.02 % of the land area of Indonesia received a share of 11.64 %.

Meanwhile, Sumatra with an area of 473,481 km^2 or 24.85 % of the land area of Indonesia received an allocation of 20.37 %. However, if the factor of the population is one of the considerations, the investment allocation for infrastructure already reflects justice. Based on the projections of the Central Statistics Agency, in 2020 the number of residents living in Sumatra reached 21.89 %, Java 56.24 %, Kalimantan 6.19%, Sulawesi 7.3 5% and other regions 8.33 %. Investment allocation also considers natural conditions.

Along with the increasing number of cars and motorcycles, the allocation of investment for the road infrastructure has also increased. In the 2010-2017 period the number of vehicles and motorcycles nationwide nearly doubled, from 76.91 million units to 137.21 million units. The increase in transportation modes is driving an increase in the allocation of investment for roads. This investment is used to add new routes and repair damaged roads. National road length (not including tolls) in 2017 reached 539.41 thousand km^2, with distribution in Sumatra 35 %, in Java 22 %, Sulawesi 15 %, Kalimantan 12 % and other islands 16 % (see Figure 1). Based on the distribution of the length of the road, the allocation of road infrastructure investment has reflected the needs.

An increase in the port activity leads the government to increase investment in port infrastructure, or conversely, an increase in investment is that in the period 2010-2017, activities at ports, both uploaded and loaded at domestic and foreign ports, experienced relatively high growth (see Table 2). For domestic ports, uploading activity increased from 221.67 million tons to 409.34 million tons and packing activity has risen from 182.48 million tons to 334.11 million tons. As for international shipping, uploaded activity increased from 65.64 million tons to 105.49 million tons and loading activity rose from 233.22 million tons to 272.40 million tons.

Based on the area of the rice harvest, the allocation of infrastructure investment in irrigation does not seem to reflect the needs. Based on data from the Central Bureau of Statistics, the largest rice crop harvest area is in Java, which reaches 50.27% but receives only an allocation of irrigation infrastructure investment of 23.02 %. In comparison, other regions that have only 6.34 % paddy crop area received an irrigation infrastructure investment allocation of 36.47 %. The distribution of irrigation infrastructure investment allocations might consider other factors, such as ease of access to water. The availability of water in Java, in general, is more abundant compared to other islands so that the infrastructure development does not require high costs. The ease of accessing water is also reflected in the rice productivity. In

Table 3 *Data Panel Results*

variable	coefficient		
	t-1	t-2	t-4
C	183257.8	255307.7	-3979232.
road	-0.790838**	-1.762631*	2035645*.
port	0.144117	0.462570**	0.085962
irrigation	-0.414692	-0.357435**	0.013157
R-squared	0.522462	0.411494	0.672672
adjusted R-squared	0.448444	0.305370	0.613332

Note: * significant at the 5% level and ** significant at the 10% level

Java, the rice productivity per hectare reaches 5.69 tons, which is above the national average of 5.20 tons. In contrast, productivity on other islands is below the national average.

3.2 Data analysis and discussion

Based on the results of data processing, using the economic growth panel model, Table 3 shows that the random effects for t-4 are better to be used than the fixed effects (F.E.) and General Effects (C.E.), both at t-1 and t-2 levels.

Government investment in the road and irrigation sector in the first and second year has not had a positive impact on economic growth. In contrast, investment in ports has shown a positive effect. Government investment in the road, port and irrigation sector began to have a positive impact on economic growth in the fourth year; however, the only asset in the road sector had a significant impact. Other studies supporting this finding are [19-20], which show that the infrastructure investment has a positive effect on economic growth. However, previous research did not specify the type of infrastructure and in what year investment began to show a positive impact.

The results of this study imply that in the medium and long term, investment in public infrastructure has a positive impact on economic growth. However, a general problem associated with this study is that this model assumes the co-efficiency of cross-sectional homogeneity. It may be that the fact coefficient can vary between regions due to differences in geographical, institutional, social and economic structures. Bloch et al. found the results of this regression only represent an average relationship, which does not apply to each country in the sample, [35].

To connect the production and distribution activities with the end consumers requires adequate road transportation. The availability of roads is expected to bridge the gap, although the relationship between the two is open for debate. In Indonesia, the infrastructure network development has encouraged the growth and development of new businesses such as small industrial businesses, transportation services, building materials and so on. In addition, road access promotes the spread of action carried out by the government and the community, so that the involvement of the village community increases. The next impact of the rise and expansion of business is imposed by an increase in the real income of the community.

Previous studies, supporting the results of this study include [19]. Their results show the positive impact of investment in transportation and communication on economic growth. Boopen, in a study [36], analyzing the contribution of transportation investment to development in 38 Sub-Saharan African countries, concluded that transportation had been a contributor to the economic progress of these countries. Vlahinic Lenz et al. also proved that infrastructure plays an essential role in driving economic growth in Central and Eastern European Member States, [37]. In line with those findings, the results of [38] are the same for the case of East Asia.

The government, as a budget allocator hopes that the port infrastructure investment has economic benefits and impacts. Financial services cause impacts that can be measured directly in monetary terms. Meanwhile, the economic implications involve changes in infrastructure investment projects. After the benefits are measured, the effect can be observed. The results of this study indicate that government investment in the port infrastructure has a positive impact on economic growth, but not a significant one. The port infrastructure is one of the critical elements of the economy in Indonesia, which is an island nation. The insignificant impact of the port investment on growth is likely due to development of the port that has not been distributed evenly between provinces so that it has not been able to significantly cut the logistics costs.

Development of Indonesia's port cities on the coast continues to dominate. The towns that are still developing, urbanization is still high, minimum transportation costs for trade and land transportation infrastructure is still not right. Development of the port cities is increasingly shifting to the service sector, while the manufacturing industry is moving to hinterland cities or cities that do not have ports.

Thus, cities without ports continue to grow due to manufacturing sector activity.

The findings in this study are in line with the research results of [39]. In their research in Tunisia, authors concluded that the public investment in the service sector port infrastructure was the recipient of the most significant benefits from the port sector investment. Another study also showed that the port investment in China and Korea had a considerable impact on economic growth, [40]. Although the port investment in China has a positive effect on economic growth, there are real differences at various regional levels.

The government investment in irrigation infrastructure has a positive impact on economic growth, but the effect is not significant. Previous studies for cases in Indonesia support the findings in this study. According to [41], an increase in the contribution of the agricultural sector to economic growth does not have a significant impact on people's income per capita. Data from the Central Statistics Agency show that in the 2011-2018 period, the harvested area of rice increased from 8.095 million hectares to 11.38 million hectares. Still, the reverse rice production decreased from 65.76 million tons to 59.2 million tons. Thus, land productivity has reduced from 8.12 tons per hectare to 5.2 tons per ha.

In contrast to the findings of [41], the results of [42] research show that the road infrastructure, irrigation and markets together have a positive effect on added value in the agricultural sector. Findings in this study contradict the results of research in [43], which found the coefficient of the farming sector to be negative and significant to economic growth.

The further research, related to the insignificant positive impact of irrigation investment on economic growth, shown in this study, is needed. Research can be focused on the location where the government builds irrigation because the accuracy of location selection will determine the magnitude of the impact on economic growth. The report [44] for Sri Lanka can be used as a reference. According to [44], in areas that have adequate access to irrigation infrastructure, poverty levels are low, while the highest poverty is found in the regions that do not have the irrigation infrastructure.

4 Conclusions and recommendations

The most crucial finding in this study is that the government investment in the road, port and irrigation infrastructure began to show a positive impact on economic growth in Indonesia in the fourth year. However, only investment expenditure for roads has a significant effect. Based on these findings, it is recommended that the government develop policies should focus on developing roads that connect remote areas and maintain sustainable and applicable roads that would ensure reasonable access and flow in Indonesia.

The role of the port is significant, considering that Indonesia is an island nation. The port infrastructure can increase the supply, as well as increase the foreign exchange reserves and reduce the overall commodity prices. The port investment has a positive but not significant impact on economic growth, which is likely due to the uneven development of the port infrastructure, especially on small islands that have abundant natural resource potential. For this reason, the government should follow up on results of research by increasing investment in ports to serve interregional areas. It is hoped that the port development will not only produce economic benefits but also create a balance between various economic sectors and between regions.

Finally, in the context of investment in irrigation infrastructure, the most important implication of findings in this study is that the government should focus on irrigation development in areas that are still isolated, since the accuracy of location in building infrastructure would determine the magnitude of impact on the economic growth.

References

[1] HOLTZ- EAKIN, D., SCHWARTZ, A. E. Infrastructure in a structural model of economic growth. *Regional Science and Urban Economics* [online]. 1995, **25**(2), p. 131-151. ISSN 0166-0462. Available from: https://doi.org/10.1016/0166-0462(94)02080-Z

[2] CALDERON, C., SERVEN, L. Infrastructure and economic development in Sub-Saharan Africa. *Journal of African Economies* [online]. 2010, **19**(1), p. 13-87. ISSN 0963-8024, eISSN 1464-3723. Available from: https://doi.org/10.1093/jae/ejp022

[3] STRAUB, S. *Infrastructure and growth in developing countries: recent advances and research challenges*. Policy Research Working Paper No. 4460. The World Bank Development Research Department Research Support Team, 2008.

[4] ASCHAUER, D. A. The role of public infrastructure capital in Mexican economic growth. *Economia Mexicana. Nueva Epoca*. 1998, VII(1), p. 47-78. ISSN 1665-2045.

[5] ATIF, A., FLYVBJERG, B., BUDZIER, A., LUNN, D. Does infrastructure investment lead to economic growth or economic fragility? Evidence from China. *Oxford Review of Economic Policy* [online]. 2016, 32(3), p. 360-390. ISSN 0266-903X, eISSN 1460-2121. Available from: https://doi.org/10.1093/oxrep/grw022
[6] FOX, W. F. *Strategic options for urban infrastructure management (English)* [online]. Urban management programme policy paper; UMPP no. 17. Washington, D.C.: The World Bank, 1994. ISSN 1020-0215. Available from: http://documents.worldbank.org/curated/en/946371468765270932/Strategic-options-for-urban-infrastructure-management
[7] GRIGG, N. DAN FONTANE, D. G. Infrastructure system management and optimization. In: Internasional Seminar Paradigm and Strategy of Infrastructure Management: proceedings. 2000.
[8] KODOATIE, R. J. *Introduction to management: infrastructure / Pengantar manajemen: infrastruktur* (in Indonesian). Yogyakarta: Pustaka Pelajar, 2005. ISBN 979-3237-9.
[9] CANNING, D., P. PEDRONI. *The effect of infrastructure on long-run economic growth*. Department of Economics Working Papers. Williamstown, MA: Williams College, Department of Economics, 2004.
[10] TODARO, M. P., SMITH, S. C. *Economic development*. 9. ed. England: Pearson Education Ltd., 2006. ISBN 9780321485731.
[11] ARROW, K., KURZ, M. *Public investment, the rate of return and optimal fiscal policy*. Baltimore, MD: The Johns Hopkins University Press, 1970. ISBN 978-1-61726-030-8.
[12] BARRO, R. J. Government spending in a simple model of exogenous growth. *Journal of Political Economy* [online]. 1990, 98, p. 103-125. ISSN 0022-3808, eISSN 1537-534X. Available from: https://doi.org/doi:10.1086/261726
[13] FUTAGAMI, K., MORITA, Y., SHIBATA, A. Dynamic analysis of an endogenous growth model with public capital. *Scandinavian Journal of Economics* [online]. 1993, **95**, p. 607-625. ISSN 0347-0520, eISSN 1467-9442. Available from: https://doi.org/10.2307/3440914
[14] World Bank. World Development Report 1994: Infrastructure for development [online]. New York: Oxford University Press, 1994. Available from: https://openknowledge.worldbank.org/handle/10986/5977
[15] ISMAIL, N. W., MAHYIDEEN, J. M. The Impact of infrastructure on trade and economic growth in selected economies in Asia [online]. ADBI Working Paper Series No. 553. Tokyo, Japan: Asian Development Bank Institute, 2015. Available from: http://www.adb.org/publications/impact-infrastructuretrade-and-economic-growth-selected-economies-asia/
[16] Global competitiveness index - World Economic Forum [online] [accessed 2020-01-16]. 2014. Available from: http://www.weforum.org/reports
[17] SHAH, A. Dynamics of public infrastructure, industrial productivity and profitability. *Review of Economics and Statistics* [online]. 1990, **74**(1), p. 28-36. ISSN 0034-6535, eISSN 1530-9142. Available from: https://doi.org/10.2307/2109539
[18] UCHIMURA, K., GAO, H. *The importance of infrastructure on economic development*. Washington, DC: World Bank, Latin America and the Caribbean Regional Office, 1993.
[19] EASTERLY, W., REBELO, S. Fiscal policy and economic growth: an empirical investigation. *Journal of Monetary Economics* [online]. 1993, **32**(3), p. 417-458. ISSN 0304-3932. Available from: https://doi.org/10.3386/w4499
[20] CANNING, D. A database of world stocks infrastructure, 1950-1995. *World Bank Economic Review*. 1998, 12(3), p. 529-547. ISSN 0258-6770, eISSN 1564-698X.
[21] ASCHAUER, D. A. Highway capacity and economic growth. *Economic Perspectives*. 1990, 14(5), p. 14-24. ISSN 0164-0682.
[22] NG, C. P, LAW, T. H., JAKARNI, F. M., KULANTHAYAN, S. Road infrastructure development and economic growth. *IOP Conference Series: Materials Science and Engineering* [online]. 2019, **512**, 012045. ISSN 1757-8981, eISSN 1757-899X. Available from: https://doi.org/10.1088/1757-899X/512/1/012045
[23] DENG, P., LU, S., XIAO, H. Evaluation of the relevance measure between ports and regional economy using structural equation modelling. *Transport Policy* [online]. 2013, **27**, p. 123-133. ISSN 0967-070X. Available from: https://doi.org/10.1016/j.tranpol.2013.01.008
[24] JUNG, B.-M. Economic contribution of ports to the local economies in Korea. *The Asian Journal of Shipping and Logistics* [online]. 2011, **27**(1), p. 1-30. ISSN 2092-5212. Available from: https://doi.org/10.1016/S2092-5212(11)80001-5
[25] YOCHUM, G. R., AGARWAL, V. B. Economic impact of a port on a regional economy: note. *Growth Change* [online]. 1987, **18**(3), p. 74-87. eISSN 1468-2257. Available from: https://doi.org/10.1111/j.1468-2257.1987.tb00082.x
[26] BOTTASSO, A, CONTI, M, FERRARI, C, MERK, O, TEI, A. The impact of port throughput on local employment: evidence from a panel of European regions. *Transport Policy* [online]. 2013, 27, p. 32-38. ISSN 0967-070X. Available from: https://doi.org/10.1016/j.tranpol.2012.12.001
[27] BOTTASSO, A, CONTI, M, FERRARI, C, TEI, A. Ports and regional development: a spatial analysis on a panel of European regions. *Transportation Research Part A: Policy and Practice* [online]. 2014. 65, p. 44-55. ISSN 0965-8564. Available from: https://doi.org/10.1016/j.tra.2014.04.006

[28] HUSSAIN, I., HANJRA, M. A., TRIKAWALA, S., WIJERATNE, D. Impact of irrigation infrastructure development on dynamics of incomes and poverty econometric evidence using panel data from Sri Lanka. A collaborative research project initiated by the JBIC Institute, the Japan Bank for International Cooperation and undertaken by the International Water Management Institute (IWMI). 2003.
[29] ASCHAUER, D. A. Is public expenditure productive? *Journal of Monetary Economics* [online]. 1989, **23**(2), p. 177-200. ISSN 0304-3932. Available from: https://doi.org/10.1016/0304-3932(89)90047-0
[30] MUNNELL, A. Why has productivity growth declined? Productivity and public investment. *New England Economic Review*. 1990, **Jan**, p. 3-22. ISSN 0028-4726.
[31] KAMPS, CH. *The dynamic effects of public capital: VAR evidence for 22 OECD countries* [online]. Kiel Working Paper, No. 1224. Kiel: Kiel Institute for World, 2004. Available from: http://hdl.handle.net/10419/17768
[32] FEDDERKE, J. W., PERKINS, P., LUIZ, J. M. Infrastructural investment in long-run economic growth: South Africa 1875-2001. *World Development* [online]. 2006, **34**(6), p. 1037-1059. ISSN 0305-750X. Available from: https://doi.org/10.1016/j.worlddev.2005.11.004
[33] SAHOO, P., DASH, R. K. Infrastructure development and economic growth in India. *Journal of the Asia Pacific Economy* [online]. 2009, **14**(4), p. 351-365. ISSN 1354-7860, eISSN 1469-9648. Available from: https://doi.org/10.1080/13547860903169340
[34] SAHOO, P., DASH, R. K., NATARAJ, G. China's growth story: the role of physical and social infrastructure. *Journal of Economic Development* [online]. 2012, **37**(1), p. 53-75. ISSN 0254-8372. Available from: https://doi.org/10.35866/caujed.2012.37.1.003
[35] BLOCH, H, TANG, S. H. K. The role of financial development in economic growth. *Progress in Development Studies* [online]. 2003, 3(3), p. 243-251. ISSN 1464-9934, eISSN 1477-027X. Available from: https://doi.org/10.1191/1464993403ps063pr
[36] BOOPEN, S. Transport infrastructure and economic growth: evidence from Africa using dynamic panel estimates. *The Empirical Economics Letters*. 2006, 5(1), p. 37-52. ISSN 1681 8997.
[37] VLAHINIC LENZ, N., PAVLIC SKENDER, H., MIRKOVIC, P. A. The macroeconomic effects of transport infrastructure on economic growth: the case of Central and Eastern E.U. member states. *Economic Research-Ekonomska Istrazivanja* [online]. 2019, **31**(2018-1), p. 1953-1964. ISSN 1331-677X, eISSN 1848-9664. Available from: https://doi.org/10.1080/1331677X.2018.1523740
[38] SEETHAPALLI, K, BRAMATI, M. C., VERDES, D. *How relevant is the infrastructure to growth in east Asia?* [online]. World Bank Policy Research Working, Paper No. 4597. 2008. Available from: https://doi.org/10.1596/1813-9450-4597
[39] JOULE, T. A., ALLOUCHE, M. A. Impacts of seaport investment on economic growth. *Promet - Traffic and Transportation* [online]. 2016, **28**(4), p. 365-370. ISSN 0353-5320, eISSN 1848-4069. Available from: https://doi.org/10.7307/ptt.v28i4.1933
[40] JIANG, N. *Seaport investment and economic development in China*. Dalian, China: Dalian Marine University Press, 2010.
[41] MARYANINGSIH, N., HERMANSYAH, O., SAVITRI, M. The impact of infrastructure to Indonesian economy / Pengaruh infrastruktur terhadap pertumbuhan ekonomi Indonesia (in Indonesian). *Buletin Ekonomi Moneter dan Perbankan* [online]. 2014, **17**(1), p. 62-98. ISSN 1410-8046, eISSN 2460-9196. Available from: https://doi.org/10.21098/bemp.v17i1.44
[42] ELWA P, F., TAN, S., ACHMAD, E. The impact of infrastructure development to agriculture sector in Muaro Jambi / Pengaruh pembangunan infrastruktur terhadap pengembangan sektor pertanian di kabupaten Muaro Jambi (in Indonesian). *Jurnal Perspektif Pembiayaan dan Pembangunan Daerah* [online]. 2013, **1**(1), p. 29-34. ISSN 2338-4603, eISSN 2355-8520. Available from: https://doi.org/10.22437/ppd.v1i1.1339
[43] DEMURGER, S., Infrastructure development and economic growth: an explanation for regional disparities in China? *Journal of Comparative Economics* [online]. 2001, **29**(1), p. 95-117. ISSN 0147-5967. Available from: https://doi.org/10.1006/jcec.2000.1693
[44] HUSSAIN, I., HANJARA, M., THRIKWALA, S., WIJERATHNA, D., SHINKAI, N., SAWADA, Y. Impact of irrigation infrastructure development on dynamics of incomes and poverty: econometric evidence using panel data from Sri Lanka. JBICI Research Paper No. 32. Japan: JBIC, 2007.

OPTIMIZING THE CHOICE OF MEANS OF TRANSPORT USING OPERATIONAL RESEARCH

Piotr Gorzelanczyk[1,*], Henryk Tylicki[1], Tomáš Kalina[2], Martin Jurkovič[2]

[1]Stanislaw Staszic University of Applied Sciences in Pila, Pila, Poland
[2]Department of Water Transport, Faculty of Operation and Economics of Transport and Communications University of Zilina, Zilina, Slovak Republic

*E-mail of corresponding author: piotr.gorzelanczyk@puss.pila.pl

Resume
This study focuses on the issue of choosing a means of transport on the Pila-Warsaw route by four groups of recipients. Representative sample consists of a student, a family with two children, a business client and a pensioner. The choice of the means of transport depends on various criteria resulting from the preferences of the users of the means of transport. The following criteria emerged from the survey results as a priority: transport time, transport cost, comfort and safety of travel, availability of means of transport, necessity or absence of transfers, cost of luggage transport and punctuality of means of transport. Selected preferences were assigned weightings based on the evaluation of a panel of experts in the field of expertise. In order to select the means of transport to implement the transport task, multi-criteria optimization method was used.

Article info
Received 9 January 2021
Accepted 21 January 2021
Online 2 June 2021

Keywords:
means of transport,
multi-criteria optimization,
Pila-Warsaw

Available online: https://doi.org/10.26552/com.C.2021.3.A193-A207

ISSN 1335-4205 (print version)
ISSN 2585-7878 (online version)

This is an open access article distributed under the terms of the Creative Commons Attribution 4.0 International License (CC BY 4.0), which permits use, distribution, and reproduction in any medium, provided the original publication is properly cited. No use, distribution or reproduction is permitted which does not comply with these terms.

1 Introduction

Due to the rapid development of civilization, more and more people use private cars to quickly reach their destination, which is mainly work or school [1]. Over the last 10 years, the number of registered cars in Poland has increased by nearly 50% (Figure 1) [2]. Efficient and fast communication is very important due to the ability to easily change position and move from place to place in a short time. Many elements affect efficient communication. One of them is a means of transport adapted to our needs [3-4].

Effective communication with users depends on their activity. Within which one can distinguish their professional, social, existential, physical and other activity. The activity of the inhabitants depends, among other things, on the size of the city. One can meet other activities in the city and with others in the city. Various activities of the inhabitants influence their directions of mobility.

Mobility is defined differently by the authors of the publication. Szoltysek [6] treats mobility as a daily routine movement and activities resulting from the reorganization of personal life, which may include changing the place of residence or work. It can be equated with the movement and all the human activities performed by means of transport outside the place of residence [7-8]. On the other hand, Menes [9] presents mobility as mobility related to the daily movement of residents, mainly to work or school. The issue of mobility was also addressed in [10]. The author showed that the inhabitants of Poland mainly use the car, but quite often choose an active lifestyle, such as cycling or walking.

The mobility of residents depends, among others, on the road and rail infrastructure. The aim of the continuous expansion of road infrastructure is theoretically to reduce the traffic congestion and to adapt to the growing number of vehicles [11]. In addition, improving the road infrastructure may generate an increase in the level of motorization in the medium and long term, which in turn may lead to a new congestion [12].

The demand for travel is a product of individual human needs, for which each person decides to travel based on several factors. These individual decisions are complex and sometimes extremely difficult to define, as they involve many decisions about the destination, frequency and duration of the trip, the time of day the trip takes place, the destination and the chosen method of travel [13]. Moreover, these choices must be seen in the context of simultaneous choices, regarding car ownership, housing location, travel reason and end-of-journey activities [14]. This type of transport in the selection process is influenced by a number of factors directly and indirectly related to a number of decisions of an individual, which can be divided into three large groups: inherent characteristics of a person, route

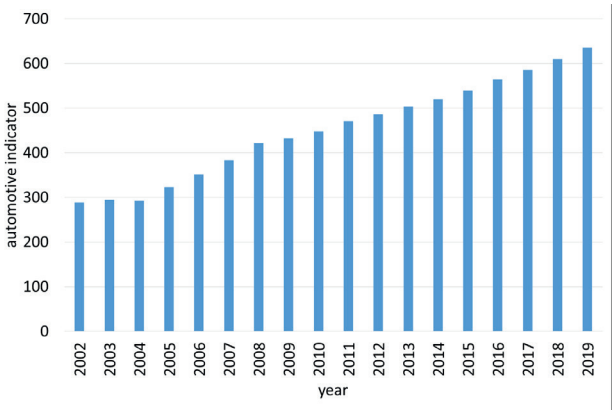


Figure 1 *Automotive index in 2002 ÷ 2019 [1,5]*



Figure 2 *Location of the city of Pila on the map of Poland [20]*

features and characteristics of the means of transport [15-16].

The cost of different modes of transport has been identified as one of the main determinants of the modal choice, along with the inherent time cost of each; The transport demand fluctuates with the time of day, with significant differences between peak and off-peak hours [16]; traffic congestion is a factor to consider and charges are generally higher [15]. In addition, when it comes to the financial costs of travel, aspects such as speed, privacy, personal taste, security and flexibility may play a role [17-18].

According to statistical data, 38 million people live in Poland. Pila is a city located in northwestern Poland in the Greater Poland Voivodeship (Figure 2). Currently, it has about 70000 inhabitants and its area is 102.68 km² [19-20]. The location of the city on the map of Poland is presented below [21-22]. Many residents move to the capital of Poland - Warsaw to rest, visit and it is related to business. They can choose a car, train, bus, or plane for this purpose. The question is which of these modes of transport is the best according to different criteria. The study specifies the method of choosing the means of transport by the inhabitants of Pila.

2 Method

Formulating the optimization task, as presented in studies [23-25], it is difficult to define one scalar quality function F, since acceptable solutions X can have many different properties whose values testify to the quality of the solution. Hence the need to formulate a multi-criteria optimization task with N quality indicators in the form of the F criterion function, which assigns it's a numerical assessment, in the form of the vector $F(x)$, to each acceptable solution $x \in X$, [26]. In the case of multi-criteria optimization, if there is a set of acceptable solutions $x_i \in X$ and there is a set of criteria $f_i \in F$ and a set of criteria dominated by f_i dominance relation $\Phi_i \in \Phi$, the optimization task is implemented according to the following algorithm [27-29]:

1. Normalization of the criterion space (space D^*),
2. Determining the coordinates of an ideal point d^{**},
3. Calculation of the norm value $|\cdot|$ with the parameter $p = 2$ (norm $|\cdot|$ is a measure of the distance of the results $d^* \in D^*$ from the ideal point d^{**} (r_i (D^*)),
4. Determining the optimal result x^o (e.g. $x^o = x_2$ it means that the object x_2 is the best according to the criterion function F).

3 Results

The decisive problem is the choice of means of transport on the route under consideration: Pila (center) - Warsaw (center), for the following groups of passengers:

- Family (two adults and two children, one of them up to 2 years old),
- Business customer,
- Student,
- Older person - pensioner.

The algorithm for obtaining the optimal means of transport for individual groups in accordance with studies [28-29] includes the following stages:

1. Determination of the set of acceptable solutions $x \in X$,
2. Determination of the criterion function for each area of action F,
3. Determination of the solutions of local optimization tasks, according to the "ideal point" method for each passenger group,
4. Determination of the global solution elements of the optimal solution.

The solution scheme for the optimization task of

Table 1 *Dominance relations* Φ

criterion / group of passengers	family	business customer	student	elderly person - pensioner
f_1 - travel time	min	min	min	min
f_2 - travel costs	min	min	min	min
f_3 - travel comfort	max	max	max	max
f_4 - travel safety	max	max	max	max
f_5 - availability of means of transport	max	max	max	max
f_6 - no transfers	min	min	min	min
f_7 - luggage costs	min	min	min	min
f_8 - punctuality of the means of transport	max	max	max	max

determining the optimal means of transport is proposed to be implemented according to the algorithm presented above, i.e.

1. Normalization of criterion space,
2. Determining the coordinates of an ideal point,
3. Calculation of the standard value $|\bullet|$ with the parameter $p = 2$,
4. Determining the optimal result x^o in the optimization task,

As a result, optimal solutions are obtained with specific weight values w_j depending on the distance $r_i(D^*)$.

The algorithmizing scheme for choosing the appropriate way of travel includes the stages, they are:

1. Determining the set of acceptable solutions X,
2. Determination of the criterion function F together with the dominance relation Φ,
3. Determining the optimal x^o solution.

4 Setting of acceptable solution

Firstly, acceptable X solutions are determined, including travel by one or more modes of transport. The set of acceptable solutions X then takes the form:

x_1 - car Pila - Warsaw
x_2 - Pila - Warsaw bus
x_3 - Pila - Warsaw train
x_4 - car Pila - Poznan, plane Poznan - Warsaw
x_5 - bus Pila - Poznan, plane Poznan - Warsaw
x_6 - Pila - Poznan train, Poznan - Warsaw plane
x_7 - car Pila - Poznan, train Poznan - Warsaw
x_8 - car Pila - Poznan, bus Poznan - Warsaw
x_9 - Pila - Poznan bus, Poznan - Warsaw train
x_{10} - Pila - Poznan train, Poznan - Warsaw bus

5 Determination of the criterion function

Passengers have different requirements for choosing the right means of transport, hence its selection depends on many criteria, which include transport costs, route, comfort, etc. In this case, the individual preferences of the passenger and his needs should also be taken into account, which should be met during the trip. These differences consist in different evaluation of criteria, e.g. depending on age, social groups or other preferences. For one of the groups safety may be the most important, for another the costs of transport. In this case, the passenger has the option of choosing a means of transport that will meet all or his most important expectations. The individual requirements are listed as elements of the criterion function, whose values will be different for each set of allowable solutions X. The criterion function F takes the form:

f_1 - travel time,
f_2 - travel costs,
f_3 - travel comfort,
f_4 - travel safety,
f_5 - availability of means of transport,
f_6 - no transfers,
f_7 - luggage cost,
f_8 - punctuality of the means of transport.

The algorithm presented at this stage is related to formulation and solution of the optimization task $< X, F, \Phi >$ for the choice of the means of transport.

Based on the above findings, determining the value of the criteria $f_j \in F$ is possible by calculating their values based on data obtained during the tests or by adopting them based on the expert knowledge. In developing the value of criteria for various acceptable solutions $x_j \in X$, values of criteria $f_j \in F$ and dominance relations Φ were adopted according to the second possibility [28-34] enriched with surveys. For the issues in question, depending on the groups of passengers, a different dominance relationship was adopted - Table 1.

Taking into account the dominance relations, a ranking of criteria for individual groups of passengers can be determined. The ranking of criteria was also corrected by means of surveys in 2020, which were preceded by a pre-test.

Based on Table 2, it can be concluded that for all the established user groups the most important are the travel time and safety. The least important, however, is the size of the luggage and the lack of transfers. The

Table 2 *Ranking of criteria for the considered groups of passengers*

family	business customer	student	elderly person - pensioner
travel time	travel time	travel time	travel time
travel safety	availability of means of transport	the costs of travel	travel safety
travel comfort	travel safety	availability of means of transport	travel comfort
the costs of travel	travel comfort	travel safety	no transfers
availability of means of transport	punctuality of the means of transport	punctuality of the means of transport	the costs of travel
punctuality of the means of transport	no transfers	travel comfort	punctuality of the means of transport
no transfers	luggage size	luggage size	luggage size
luggage size	the cost of travel	no transfers	availability of means of transport

Table 3 *Time of travel and number of transfers from Pila to Central Warsaw - by various means of transport [35-51]*

a set of acceptable solutions	travel time (h)	umber of transfers
x1 - Pila PKP / PKS car - Central Warsaw	4:32	0
x2 - bus Pila - Warsaw Central	6:44	0
x3 - train Pila - Warsaw Central	5:19-5:30	0
x4 - car Pila - Poznan, plane Poznan - Warsaw	Car Saw-Poznan Lawica 1:42 Airplane Poznan Lawica - Warsaw Okecie 1:00 + 1:00 - check-in Warsaw Okecie - Warsaw Central - city bus 0:20-0:28 Total time: 4:02-4:10	2
x5 - bus Pila - Poznan, plane Poznan - Warsaw	Bus Pila - Poznan Dworzec 1:40-1:52 Poznan Dworzec - Poznan Lawica 0:25-0:34 plane Poznan Lawica - Warsaw Okecie 1:00 + 1:00 - check-in for baggage and luggage Warszawa Okecie - Warsaw Central - city bus 0:20-0:28 Total time: 4:25-4:54	3
x6 - Pila - Poznan train, Poznan - Warsaw plane	Train Pila - Poznan Dworzec 1:21-2:09 Poznan Dworzec - Poznan Lawica 0:25-0:34 plane Poznan Lawica - Warsaw Okecie 1:00 + 1:00 - check-in Warszawa Okecie - Warsaw Central - city bus 0:20-0:28 Total time: 4:06-5:11	3
x7 - car Pila - Poznan, train Poznan - Warsaw	Car Pila-Poznan PKP / PKS 1:53 Train Poznan - Warsaw Central 2:54-6:33 Total time: 4:47-8:26	1
x8 - car Pila - Poznan, bus Poznan - Warsaw	Car Pila-Poznan PKP / PKS 1:53 Poznan PKP / PKS bus - Warsaw West 3:50 - 6:30 West Warsaw - East Warsaw - 0:08 train Total time: 5:51-8:31	2
x9 - Pila - Poznan bus, Poznan - Warsaw train	Bus Pila - Poznan Dworzec 1:40-1:52 Poznan - Central Warsaw train 2:54-6:33 Total time: 4:34-8:25	1
x10 - Pila - Poznan train, Poznan - Warsaw bus	Train Pila - Poznan Dworzec 1:21-2:09 Poznan PKP / PKS bus - Warsaw West 3:50 - 6:30 West Warsaw - East Warsaw - 0:08 train Total time: 5:19-8:47	2

Table 4 *Comparison of the travel costs with different means of transport [€] [35-51]*

a set of acceptable solutions / group of passengers	family	business customer	student	elderly person - pensioner
x1 - Pila PKP / PKS car - Central Warsaw	27	27	27	27
x2 - bus Pila - Warsaw Central	66	19	15	15
x3 - train Pila - Warsaw Central	50	19	9	13
class 1 class 2	38	14	7	10
x4 - car Pila - Poznan, plane Poznan - Warsaw				
economy class without luggage	147-270	54-95	54-95	54-95
economy class with luggage	194-317	70-111	69-110	69- 110
x5 - bus Pila - Poznan, plane Poznan - Warsaw				
economy class without luggage	154-284	51-94	50-93	49-92
economy class with luggage	201-331	67-110	66-108	65-107
x6 - Pila - Poznan train, Poznan - Warsaw plane	163-286	56-97	51-92	51-92
class 1 - economy class without luggage				
class 2 - economy class without luggage	155-282	53-95	49-91	49-91
class 1 - economy class with luggage				
class 2 - economy class with luggage	210-333	71-112	66-107	67-108
	202-329	68-111	65-106	65-107
x7 - car Pila - Poznan, train Poznan - Warsaw				
class 1	54-184	25-51	16-51	20-38
class 2	39-88	19-38	13-22	16-29
x8 - car Pila - Poznan, bus Poznan - Warsaw	42-62	17-26	16-25	17-26
x9 - Pila - Poznan bus, Poznan - Warsaw train				
class 1	54-184	25-51	16-51	20-38
class 2	39-88	19-38	13-22	16-29
x10 - Pila - Poznan train, Poznan - Warsaw bus				
class 1	56-76	18-27	13-22	15-24
class 2	48-71	15-25	12-21	13-23

exception is a business customer for whom the costs of travel are not a problem.

In order to facilitate the assessment of the abovementioned variants, the Tables 3-8 are presented in which individual variants of choices are characterized. The first is travel time and the associated number of transfers by various modes of transport.

Based on Table 3, it can be concluded that the shortest connection time from Pila to Central Warsaw is in the case of traveling to Poznan by car and then using the plane. The disadvantage of this solution is two transfers, in Poznan at the airport and in Warsaw the use of public transport to reach the railway station - Warsaw Central and amounts to 4:02 h. The longest minimum travel time, 6:44 h, occurs on the bus connection from Pila to Warsaw. The journey on the analyzed section can be from 4:02 h to 8:47 h and be without transfers, but it can also have 3 transfers when using the Pila - Poznan train and Poznan - Warsaw plane, where public transport in Poznan and Warsaw should be taken into account to and from the airport.

Noteworthy is the fact that when choosing an airplane, a passenger cannot only take flight time into account. In this case, one should also consider the time for check-in. In the case under consideration, it was assumed that this would be 1 h.

The car is the only means of transport by which one can reach the destination without changing. When choosing other means of transport, one must focus on transfers. In the analyzed case, from the city center to

Table 5 *Travel comfort by various means of transport*

criterion / means of transport	car	bus	train	plane
division into classes	individual passenger sensation	lack	class 1 and 2	none in domestic calls
	1	4	1	4
possibility of eating a meal while driving	yes, but it involves a break	lack	yes, but not on all the trains	yes
	3	4	2	1
air conditioning	in most cars occurs	most buses have one	occurs on some trains	yes
	2	2	3	1
it is possible to use the toilet while driving	no	yes, but not on all the buses	yes	yes
	4	3	1	1
space availability	no booking required	yes, but not on all the buses	yes, but not on all the trains	choosing a seat on the plane is charged extra
	1	2	2	2
the opportunity to rest while driving	yes	yes, depending on other passengers	yes, depending on other passengers	yes, depending on other passengers
	1	2	2	2
available space for 1 passenger	big	small	dependent on the train class	average
	1	4	2	3
sum	13	21	13	14

Warsaw, living outside the city center, one has to get to it using public transport or taxis. Sometimes one can get to the station on foot if one lives near the city center.

Table 4 presents a comparison of the travel costs with different options for choosing means of transport.

Analyzing Table 4, it turned out that the cheapest trip for a family is a car and amounts to 27€ and the most expensive by bus from Pila to Poznan and then by plane with additional luggage, which is reasonable with the family, amounting to 331 €. For the remaining groups studied, the cheapest was the direct train from Pila to Warsaw in class 2 and the most expensive by plane.

In Table 4, discounts for individual groups were considered when calculating travel costs. Thus, in the case of a Stalko bus ride: pensioner: receive 10%, senior 70+: 20%, student under 26: 20%, children under 6: 50%. The following discounts apply to Flixbus buses: 78% - children up to 4 years old who occupy a separate place, 37% - children over 4 years old. For other groups, Flixbus does not provide discounts.

Rail carriers apply statutory concessions, namely 51% discount for students under 26 years of age, children up to 4 years old – 100% discount, children aged 4-24 years – 37%. The above discounts apply only to transportation in Class 2. They do not apply in Class 1.

LOT Polish Airlines offer a 90% discount for infants and children up to 2 years old if they do not occupy a separate seat on the plane. The next discount applies to children aged 2-11 and amounts to 25%.

However, in public transport in Poznan, the Municipal Transport Board introduced the following discounts: a student receives 50%, children under 7 use free communication and children under 23 have a 50% discount. However, a pensioner over 70 uses communication free of charge.

Table 6 *Fatalities and injuries with the participation of individual means of transport [44-45]*

criterion / means of transport	car	bus	train	plane
number of fatalities	1682	48	31	0
number of injured, including:	22 271	1 153	24	0
number seriously injured	6160	253	15	0
number slightly injured	16111	900	9	0

Table 7 *Number of connections offered during the day [35-51]*

analyzed route	number of connections offered during the day
x_1 - car Pila PKP / PKS - Central Warsaw	100%
x_2 - bus Pila - Warsaw Central	1
x_3 - Pila - Warsaw Central train	3
x_4 - car Pila - Poznan, plane Poznan - Warsaw (6)	6
x_5 - bus Pila - Poznan (4), plane Poznan - Warsaw (6)	4
x_6 - Pila - Poznan train (18), Poznan - Warsaw plane (6)	6
x_7 - Pila car - Poznan, Poznan - Warsaw train (14)	14
x_8 - car Pila - Poznan, bus Poznan - Warsaw (9)	9
x_9 - Pila - Poznan bus (4), Poznan - Warsaw train (14)	4
x_{10} - Pila - Poznan train (18), Poznan - Warsaw bus (9)	9

In the case of public transport from Warsaw, Warsaw Public Transport has introduced the following discounts: children up to 7 years old free of charge, pupils and students up to 26 years old 50 % and people over 70 years old in Warsaw use public transport for free.

The Table 5 compares the comfort of traveling with different modes of transport. It assumed 6 most common factors that affect the subjective reading of a traveler. The best option was 1 and the worst 4. The means of transport that receives the least number of points can be considered the most comfortable.

Based on Table 5, the subjective assessments of the means of transport selected for analysis were presented in terms of comfort. Based on that, it can be concluded that a passenger car and a train turned out to be the most comfortable, in class 1. The bus was considered the least comfortable.

Another of the criteria discussed is the safety of means of transport. Data from 2019 were analyzed. Based on that, it can be concluded that the majority of the road incidents in the analyzed period were involving passenger cars, 324301 and buses 7922. Similarly, the largest number of road incidents were involving a car and buses, the same number of fatalities and injuries is recorded for these means of transport. The safest means of transport turned out to be an airplane in which there were no fatalities and injuries followed by train, bus. A passenger car turned out to be the least safe means of transport and the results differ significantly with respect to other means of transport. The data is presented in the Table 6.

Then the availability of a given means of transport was determined by checking the number of connections offered during the day on the tested section. The availability of the car as an individual means of transport was assumed as the maximum (100 %), since the passengers have the option of using it whenever they want. In addition to the car, the largest number of connections offered during the day, when connecting the car on the Pila - Poznan route and the Poznan Glówna - Warsaw Central train.

The number in brackets is the maximum number of connections per transport method. In addition, the field “L number of connections offered during the day “ does not include public transport, which runs very often and the train Warszawa Zachodnia - Warszawa Centralna, which is practically every now and then. These data are presented in Table 7.

Luggage size was also analyzed (Table 8). In this case, it was assumed that the traveler would carry a large suitcase measuring 690 x 440 x 250 mm, weight 20 kg. In all analyzed means of transport, the traveler can transport a suitcase for free, except for the plane, for which he must pay 15 € for each suitcase.

In the analyzed sets of acceptable solutions, the fee will be added in the following cases:

- x_4 - car Pila - Poznan, plane Poznan - Warsaw
- x_5 - bus Pila - Poznan, plane Poznan - Warsaw
- x_6 - Pila - Poznan train, Poznan - Warsaw plane

The punctuality of the means of transport in 2019 was also considered. A car is characterized by the greatest punctuality. It was assumed at 98 %, because there are unforeseen situations on the road, such as accidents or congestions, which extend the travel time.

The next punctual means of transport is the train. Based on the data published by the Office of Rail

Table 8 *Fee amount [27-43]*

type of transport	fee amount
car	without payments
train	without payments
bus	without payments
plane	hand luggage (1x 8 kg) - no fee checked baggage (1x 23 kg) - additional fee 15 €.
city transport board in Poznan	without payments
Warsaw public transport	without payments

Table 9 *Criteria values together with the dominance relation Φ for the Family - class 2 group with luggage on the plane*

	x_1	x_2	x_3	x_4	x_5	x_6	x_7	x_8	x_9	x_{10}	F
f_1	272	404	319	242	265	246	287	351	274	319	min
f_2	120	297.50	170.95	872.39	905.06	907.24	176.19	190.94	176.19	215.69	min
f_3	13	21	13	13.75	15.75	13.75	13	19	15	19	max
f_4	1682	48	31	420.5	12	7.75	443.75	456.5	35.25	43.75	max
f_5	1440	1	3	6	4	6	14	9	4	9	max
f_6	0	0	0	2	3	3	1	2	1	2	min
f_7	0	0	0	70	70	70	0	0	0	0	min
f_8	98	81	92.46	80.75	76.5	79.37	93.85	85.25	89.6	83.87	max

Table 10 *Criteria values together with the dominance relation Φ for the business customer - class 1 group with luggage on the plane*

	x_1	x_2	x_3	x_4	x_5	x_6	x_7	x_8	x_9	x_{10}	F
f_1	272	404	319	242	265	246	287	351	274	319	min
f_2	120	85	85	314.33	300.12	321.13	111.8	75.99	111.8	80.19	min
f_3	13	21	13	13.75	15.75	13.75	13	19	15	19	max
f_4	1682	48	31	420.5	12	7.75	443.75	456.5	35.25	43.75	max
f_5	1440	1	3	6	4	6	14	9	4	9	max
f_6	0	0	0	2	3	3	1	2	1	2	min
f_7	0	0	0	70	70	70	0	0	0	0	min
f_8	98	81	92.46	80.75	76.5	79.37	93.85	85.25	89.6	83.87	max

Table 11 *Criteria values along with the dominance relation Φ for the student - class 2 group with luggage on the plane*

	x_1	x_2	x_3	x_4	x_5	x_6	x_7	x_8	x_9	x_{10}	F
f_1	272	404	319	242	265	246	287	351	274	319	min
f_2	120	68	31.85	312.13	295.42	290.97	58.7	73.85	58.7	52.59	min
f_3	13	21	13	13.75	15.75	13.75	13	19	15	19	max
f_4	1682	48	31	420.5	12	7.75	443.75	456.5	35.25	43.75	max
f_5	1440	1	3	6	4	6	14	9	4	9	max
f_6	0	0	0	2	3	3	1	2	1	2	min
f_7	0	0	0	70	70	70	0	0	0	0	min
f_8	98	81	92.46	80.75	76.5	79.37	93.85	85.25	89.6	83.87	max

Transport data, train punctuality in 2019 was 92.46 %. In this case, it is worth noting that the punctuality threshold is 5 minutes and 59 seconds, which means that a train that is late, e.g. 5 minutes and 58 seconds, is considered punctual [52].

Bus (Flixbus -81 %) and public transport in Poznan (77.5 %) have less punctuality. This is mainly due to the weather conditions, season of the year and road conditions (e.g. road accidents, congestion) [53-54].

The plane has the lowest punctuality of the considered means of transport at the level of 75 %. This is mainly due to the exclusion of Dreamliner aircraft and the lack of airworthiness control in some European countries and renovation works at the Warsaw airport [55-57].

6 Determining the optimal solution

In order to solve the multi-criteria optimization task, a computer program "Multi-criteria optimization task 2017" was developed [27-28], which enables:

a) presentation of the set X_j and selection of elements $x_j \in X_j$;
b) presentation of the set F_j and selection, by the computer program operator, of elements $f_j \in F_j$ and dominance relations $\Phi_j \in \Phi$;
c) data entry according to two options: option 1 - manual data entry ($f_j \in F_j$ values), - option 2 - calculation of $f_j \in F_j$ values) based on data obtained during the experimental or simulation tests.
d) visualization of the optimization task solution (calculations and reporting - Tables 9-16).

Table 12 *Criteria values together with the dominance relation Φ for the group Elder - pensioner - class 2 with luggage on the plane*

	x_1	x_2	x_3	x_4	x_5	x_6	x_7	x_8	x_9	x_{10}	F
f_1	272	404	319	242	265	246	287	351	274	319	min
f_2	120	68	45.5	309.93	290.72	290.78	70.23	74.73	70.23	57.98	min
f_3	13	21	13	13.75	15.75	13.75	13	19	15	19	max
f_4	1682	48	31	420.5	12	7.75	443.75	456.5	35.25	43.75	max
f_5	1440	1	3	6	4	6	14	9	4	9	max
f_6	0	0	0	2	3	3	1	2	1	2	min
f_7	0	0	0	70	70	70	0	0	0	0	min
f_8	98	81	92.46	80.75	76.5	79.37	93.85	85.25	89.6	83.87	max

Table 13 *Visualization of the criteria solution for the Family group - class 2 with luggage in the plane*

f/x	x_1	x_2	x_3	x_4	x_5	x_6	x_7	x_8	x_9	x_{10}
f_1	272.00	404.00	319.00	242.00	265.00	246.00	287.00	351.00	274.00	319.00
min (f_1)	242.00									
f_1*	0.89	0.60	0.76	1.00	0.91	0.98	0.84	0.69	0.88	0.76
f_1**	0.60									
f_2	120.00	297.50	170.95	872.39	905.06	907.24	176.19	190.94	176.19	215.69
min (f_2)	120.00									
f_2*	1.00	0.40	0.70	0.14	0.13	0.13	0.68	0.63	0.68	0.56
f_2**	0.13									
f_3	13.00	21.00	13.00	13.75	15.75	13.75	13.00	19.00	15.00	19.00
max (f_3)	21.00									
f_3*	0.62	1.00	0.62	0.65	0.75	0.65	0.62	0.90	0.71	0.90
f_3**	1.00									
f_4	1682.00	48.00	31.00	420.50	12.00	7.75	443.75	456.50	35.25	43.75
max (f_4)	1682.00									
f_4*	1.00	0.03	0.02	0.25	0.01	0.00	0.26	0.27	0.02	0.03
f_4**	1.00									
f_5	1440.00	1.00	3.00	6.00	4.00	6.00	14.00	9.00	4.00	9.00
max (f_5)	1440.00									
f_5*	1.00	0.00	0.00	0.00	0.00	0.00	0.01	0.01	0.00	0.01
f_5**	1.00									
f_6	0.00	0.00	0.00	2.00	3.00	3.00	1.00	2.00	1.00	2.00
min (f_6)	0.00									
f_6*	1.00	1.00	1.00	0.00	0.00	0.00	0.00	0.00	0.00	0.00
f_6**	0.00									
f_7	0.00	0.00	0.00	70.00	70.00	70.00	0.00	0.00	0.00	0.00
min (f_7)	0.00									
f_7*	1.00	1.00	1.00	0.00	0.00	0.00	1.00	1.00	1.00	1.00
f_7**	0.00									
f_8	98.00	81.00	92.46	80.75	76.50	79.37	93.85	85.25	89.60	83.87
max (f_8)	98.00									
f_8*	1.00	0.83	0.94	0.82	0.78	0.81	0.96	0.87	0.91	0.86
f_8**	1.00									

Table 14 *Visualization of the criteria solution for a business customer group - class 1 with luggage on the plane*

f/x	x_1	x_2	x_3	x_4	x_5	x_6	x_7	x_8	x_9	x_{10}
f_1	272.00	404.00	319.00	242.00	265.00	246.00	287.00	351.00	274.00	319.00
min (f_1)	242.00									
f_1*	0.89	0.60	0.76	1.00	0.91	0.98	0.84	0.69	0.88	0.76
f_1**	0.60									
f_2	120.00	85.00	85.00	314.33	300.12	321.13	111.80	75.99	111.80	80.19
min (f_2)	75.99									
f_2*	0.63	0.89	0.89	0.24	0.25	0.24	0.68	1.00	0.68	0.95
f_2**	0.24									
f_3	13.00	21.00	13.00	13.75	15.75	13.75	13.00	19.00	15.00	19.00
max (f_3)	21.00									
f_3*	0.62	1.00	0.62	0.65	0.75	0.65	0.62	0.90	0.71	0.90
f_3**	1.00									
f_4	1682.00	48.00	31.00	420.50	12.00	7.75	443.75	456.50	35.25	43.75
max (f_4)	1682.00									
f_4*	1.00	0.03	0.02	0.25	0.01	0.00	0.26	0.27	0.02	0.03
f_4**	1.00									
f_5	1440.00	1.00	3.00	6.00	4.00	6.00	14.00	9.00	4.00	9.00
max (f_5)	1440.00									
f_5*	1.00	0.00	0.00	0.00	0.00	0.00	0.01	0.01	0.00	0.01
f_5**	1.00									
f_6	0.00	0.00	0.00	2.00	3.00	3.00	1.00	2.00	1.00	2.00
min (f_6)	0.00									
f_6*	1.00	1.00	1.00	0.00	0.00	0.00	0.00	0.00	0.00	0.00
f_6**	0.00									
f_7	0.00	0.00	0.00	70.00	70.00	70.00	0.00	0.00	0.00	0.00
min (f_7)	0.00									
f_7*	1.00	1.00	1.00	0.00	0.00	0.00	1.00	1.00	1.00	1.00
f_7**	0.00									
f_8	98.00	81.00	92.46	80.75	76.50	79.37	93.85	85.25	89.60	83.87
max (f_8)	98.00									
f_8*	1.00	0.83	0.94	0.82	0.78	0.81	0.96	0.87	0.91	0.86
f_8**	1.00									

The results of solution optimization task for $f_j \in F_j$ for all the studied travelers' groups indicate that in order to overcome flights Pila-Warsaw, the optimal solution, according to the criteria adopted, is use of the following means of transport: bus route Pila - Poznan and the aircraft on the route Poznan - Warsaw (Tables 17-20).

7 Discussion

Based on the calculations performed, it can be concluded that the solution to the optimization task for $f_j \in F_j$ for all the studied groups to travel the route from Pila to Warsaw, is to use the following means of transport: a bus on the Pila - Poznan route and an airplane on the Poznan - Warsaw route, assuming the above-mentioned criteria: time, cost, comfort, safety and availability of the means of transport. Taking into account the above assumptions, the next measure for the analyzed group of respondents should be the combination: the Pila - Poznan train, the Poznan - Warsaw plane, the Pila - Poznan car, the Poznan - Warsaw plane. It should be noted here that in solving the optimization problem, the plane appears despite the higher price and the greater number of transfers. The results would be completely different if there was an airport in the analyzed city and one would not have to travel to it 100 km. The least favorable means of transport for families, students and the elderly, was to travel by train to their destination. On the other hand, a business client, taking into account the adopted criteria, mainly due to the convenience and time of travel, should not use the bus to reach his destination.

Table 15 *Visualization of the criteria solution for the student - class 2 group with luggage on the plane*

f/x	x_1	x_2	x_3	x_4	x_5	x_6	x_7	x_8	x_9	x_{10}
f_1	272.00	404.00	319.00	242.00	265.00	246.00	287.00	351.00	274.00	319.00
min (f_1)	242.00									
f_1*	0.89	0.60	0.76	1.00	0.91	0.98	0.84	0.69	0.88	0.76
f_1**	0.60									
f_2	120.00	68.00	31.85	312.13	295.42	290.97	58.70	73.85	58.70	52.59
min (f_2)	31.85									
f_2*	0.27	0.47	1.00	0.10	0.11	0.11	0.54	0.43	0.54	0.61
f_2**	0.10									
f_3	13.00	21.00	13.00	13.75	15.75	13.75	13.00	19.00	15.00	19.00
max (f_3)	21.00									
f_3*	0.62	1.00	0.62	0.65	0.75	0.65	0.62	0.90	0.71	0.90
f_3**	1.00									
f_4	1682.00	48.00	31.00	420.50	12.00	7.75	443.75	456.50	35.25	43.75
max (f_4)	1682.00									
f_4*	1.00	0.03	0.02	0.25	0.01	0.00	0.26	0.27	0.02	0.03
f_4**	1.00									
f_5	1440.00	1.00	3.00	6.00	4.00	6.00	14.00	9.00	4.00	9.00
max (f_5)	1440.00									
f_5*	1.00	0.00	0.00	0.00	0.00	0.00	0.01	0.01	0.00	0.01
f_5**	1.00									
f_6	0.00	0.00	0.00	2.00	3.00	3.00	1.00	2.00	1.00	2.00
min (f_6)	0.00									
f_6*	1.00	1.00	1.00	0.00	0.00	0.00	0.00	0.00	0.00	0.00
f_6**	0.00									
f_7	0.00	0.00	0.00	70.00	70.00	70.00	0.00	0.00	0.00	0.00
min (f_7)	0.00									
f_7*	1.00	1.00	1.00	0.00	0.00	0.00	1.00	1.00	1.00	1.00
f_7**	0.00									
f_8	98.00	81.00	92.46	80.75	76.50	79.37	93.85	85.25	89.60	83.87
max (f_8)	98.00									
f_8*	1.00	0.83	0.94	0.82	0.78	0.81	0.96	0.87	0.91	0.86
f_8**	1.00									

8 Conclusions

Based on the research presented above, it can be stated that multi-criteria optimization is used in the task of choosing the means of transport on the analyzed route. In the analyzed example, on the Pila - Warsaw route, for all the examined groups (family, business client, student and elderly pensioner) it is reasonable to use two means of transport, namely: a bus on the Pila - Poznan route and an airplane on the Poznan - Warsaw route, despite not having the shortest time, nor the lowest ticket price, nor having too large a daily number of connections, the number of transfers and surcharges for luggage on the plane.

Analysis of results of the numerical experiment of solving the multi-criteria optimization task methodology showed the usefulness of the developed algorithm to determine the appropriate means of transport for carrying out the transport task. The advantage of the presented algorithm is also its universality, which allows it to be used to select elements of areas of operation of the broadly understood transport process.

Acknowledgement

This research is a result of the Project VEGA No. 1/0128/20: Research on the Economic Efficiency of Variant Transport Modes in the Car Transport in the Slovak Republic with Emphasis on Sustainability and Environmental Impact, Faculty of Operation and Economics of Transport and Communications, University of Zilina, 2020-2022.

Table 16 *Visualization of the criteria solution for the group Elder - pensioner - class 2 with luggage on the plane*

f/x	x_1	x_2	x_3	x_4	x_5	x_6	x_7	x_8	x_9	x_{10}
f_1	272.00	404.00	319.00	242.00	265.00	246.00	287.00	351.00	274.00	319.00
min (f_1)	242.00									
f_1*	0.89	0.60	0.76	1.00	0.91	0.98	0.84	0.69	0.88	0.76
f_1**	0.60									
f_2	120.00	68.00	45.50	309.93	290.72	290.78	70.23	74.73	70.23	57.98
min (f_2)	45.50									
f_2*	0.38	0.67	1.00	0.15	0.16	0.16	0.65	0.61	0.65	0.78
f_2**	0.15									
f_3	13.00	21.00	13.00	13.75	15.75	13.75	13.00	19.00	15.00	19.00
max (f_3)	21.00									
f_3*	0.62	1.00	0.62	0.65	0.75	0.65	0.62	0.90	0.71	0.90
f_3**	1.00									
f_4	1682.00	48.00	31.00	420.50	12.00	7.75	443.75	456.50	35.25	43.75
max (f_4)	1682.00									
f_4*	1.00	0.03	0.02	0.25	0.01	0.00	0.26	0.27	0.02	0.03
f_4**	1.00									
f_5	1440.00	1.00	3.00	6.00	4.00	6.00	14.00	9.00	4.00	9.00
max (f_5)	1440.00									
f_5*	1.00	0.00	0.00	0.00	0.00	0.00	0.01	0.01	0.00	0.01
f_5**	1.00									
f_6	0.00	0.00	0.00	2.00	3.00	3.00	1.00	2.00	1.00	2.00
min (f_6)	0.00									
f_6*	1.00	1.00	1.00	0.00	0.00	0.00	0.00	0.00	0.00	0.00
f_6**	0.00									
f_7	0.00	0.00	0.00	70.00	70.00	70.00	0.00	0.00	0.00	0.00
min (f_7)	0.00									
f_7*	1.00	1.00	1.00	0.00	0.00	0.00	1.00	1.00	1.00	1.00
f_7**	0.00									
f_8	98.00	81.00	92.46	80.75	76.50	79.37	93.85	85.25	89.60	83.87
max (f_8)	98.00									
f_8*	1.00	0.83	0.94	0.82	0.78	0.81	0.96	0.87	0.91	0.86
f_8**	1.00									

Table 17 *Values of distance r_j and weight values w_i for the Family group*

	x_1	x_2	x_3	x_4	x_5	x_6	x_7	x_8	x_9	x_{10}
r_i	1.7268	2.0507	2.0837	1.4796	1.4225	1.4387	1.8828	1.8760	1.8949	1.8539
w_i	0.1003	0.0982	0.0980	0.1018	0.1022	0.1021	0.0993	0.0993	0.0992	0.0995

Table 18 *Values of distance r_j and weight values w_i for the Business Customer group*

	x_1	x_2	x_3	x_4	x_5	x_6	x_7	x_8	x_9	x_{10}
r_i	1.5447	2.2005	2.1560	1.4929	1.4387	1.4520	1.8823	2.0309	1.8944	2.0063
w_i	0.1016	0.0976	0.0979	0.1019	0.1023	0.1022	0.0996	0.0986	0.0995	0.0988

Table 19 *Values of distance r_j and weight values w_i for the Student group*

	x_1	x_2	x_3	x_4	x_5	x_6	x_7	x_8	x_9	x_{10}
r_i	1.5019	2.0645	2.2021	1.4767	1.4204	1.4368	1.8372	1.8194	1.8496	1.8692
w_i	0.1016	0.0980	0.0971	0.1017	0.1021	0.1020	0.0994	0.0995	0.0994	0.0992

Table 20 *Values of distance r_j and weight values w_i for the group Older person - pensioner*

	x_1	x_2	x_3	x_4	x_5	x_6	x_7	x_8	x_9	x_{10}
r_i	1.5109	2.1191	2.2021	1.4804	1.4249	1.4412	1.8710	1.8695	1.8832	1.9347
w_i	0.1016	0.0978	0.0973	0.1018	0.1022	0.1021	0.0994	0.0994	0.0993	0.0990

References

[1] LUPTAK, V., DROZDZIEL, P., STOPKA, O., STOPKOVA, M., RYBICKA, I. Approach methodology for comprehensive assessing the public passenger transport timetable performances at a regional scale. *Sustainability* [online]. 2019, **11**(13), 3532. eISSN 2071-1050. Available from: https://doi.org/10.3390/su11133532

[2] Central register of vehicles and drivers - The number of means of transport in Poland [online] [accessed 2019-05-01]. Available from: http://www.cepik.gov.pl/statystyki

[3] POLIAK, M., POLIAKOVA, A., JASKIEWICZ, M., HAMMER, J. The need of public passenger transport integration. *Ekonomski pregled* [online]. 2020, **71**(5), p. 512-530 [accessed 2021-08-01]. Available from: https://doi.org/10.32910/ep.71.5.4

[4] DVORAK, Z., REHAK, D., DAVID, A., CEKEREVAC, Z. Qualitative approach to environmental risk assessment in transport. *International Journal of Environmental Research and Public Health* [online]. 2020, **17**(15), 5494. eISSN 1660-4601. Available from: https://doi.org/10.3390/ijerph17155494

[5] GORZELANCZYK, P. Influence of selected aspects of the technical condition of means of transport operating in Greater Poland on road safety. *Technical Sciences*. In press. ISSN 1505-4675, eISSN 2083-4527.

[6] SZOLTYSEK, J. *Creating mobility of city dwellers*. Warsaw: Wolters Kulwer, 2011. ISBN 9788326415494.

[7] ZALOGA, E., DUDEK, E. Selected problems of European society mobility. *Scientific Notebooks of the University of Szczecin, Problems of Transport and Logistic*. 2009, **9**, p. 99-109. ISSN 1640-6818.

[8] FLEJTERSKI, S., PANASIUK, A., PERENC, J., ROSA, G. *Contemporary economics of services*. Warsaw: PWN Scientific Publisher, 2008 ISBN 8301144882.

[9] MENES, E. Socio-economic aspects of the development of individual motorization in Poland. *Communication Review*., 2001, **1**. ISSN 0033-2232.

[10] GORZELANCZYK, P. Mobility of Polish residents. In: *Research and the Future of Telematics* [online]. Mikulski, J. (ed.). Switzerland: Springer, 2020. ISBN 978-3-030-59269-1, eISSN 978-3-030-59270-7. Available from: https://doi.org/10.1007/978-3-030-59270-7

[11] GARCIA-LOPEZ, M.-A. Urban spatial structure, suburbanization and transportation in Barcelona. *Journal of Urban Economics* [online]. 2012, **72**(2-3), p. 176-190. ISSN 0094-1190. Available from: https://doi.org/10.1016/j.jue.2012.05.003

[12] GORZELANCZYK, P., JURKOVIC, M., KALINA, T., SOSEDOVA, J., LUPTAK, V. Influence of motorization development on civilization diseases. *Transport Problems* [online]. 2020, **15**(3), p. 53-67. eISSN 2300-861X. Available from: https://doi.org/10.21307/tp-2020-033

[13] DYDKOWSKI, G., GNAP, J. Premises and limitations of free public transport implementation. *Communications - Scientific Letters of the University of Zilina* [online]. 2019, **21**(4), p. 13-18. ISSN 1335-4205, eISSN 2585-7878. Available from: https://doi.org/10.26552/com.C.2019.4.13-18

[14] MCFADDEN, D. The measurement of urban travel demand. *Journal of Public Economics* [online]. 1974, **3**(4), p. 303-328. ISSN 0047-2727. Available from: https://doi.org/10.1016/0047-2727(74)90003-6

[15] KONECNY, V., GNAP, J., SETTEY, T., PETRO, F., SKRUCANY, T., FIGLUS, T. Environmental sustainability of the vehicle fleet change in public city transport of selected city in Central Europe. *Energies* [online]. 2020, **13**, 3869. eISSN 1996-1073. Available from: https://doi.org/10.3390/en13153869

[16] DE DIOS ORTUZAR, J., WILLUMSEN, L. G. *Modelling transport*. 4. ed. Wiley, 2011. ISBN 978-0-470-76039-0, eISBN 978-1-119-99352-0.

[17] DE RUS, G., BETANCOR, O., CAMPOS, C., EUGENIO, J. L., SOCORRO, P., MATAS, A., RAYMOND, J. L., GONZALEZ SAVIGNAT, M., BREY, R., NOMBELA, G., BENAVIDES, J. Socioeconomic evaluation of the expansion of the Malaga airport. Working Paper of the project Socioeconomic and Financial Evaluation of Transportation Projects, Ministry of Development, CEDEX 2010 [online] [accessed 2016-02-20]. Available from: http://www.evaluaciondeproyectos.es

[18] BROMBERG, P. *Accessibility and mobility*. Colombia: Institute of Urban Studies - School of Architecture and Urbanism, National University of Colombia, 2000.

[19] ANDRES ROMERO LUCA TASCIOTTI FAYBER ACOSTA. Means of transportation choice for the residents of Villavicencio, Colombia: a quantitative analysis *Transportation Research Part F: Traffic Psychology and Behaviour* [online]. 2017, **44**, p. 134-144. ISSN 1369-8478. Available from: https://doi.org/10.1016/j.trf.2016.11.001
[20] Central Statistical Office [online] [accessed 2016-02-20]. Available from: www.stat.gov.pl
[21] GORZELANCZYK, P., PYSZEWSKA, D., KALINA, T., JURKOVIC, M. Analysis of road traffic safety in the Pila Poviat. *Scientific Journal of Silesian University of Technology. Series Transport* [online]. 2020, **107**, p. 33-52. ISSN 0209-3324, eISSN 2450-1549. Available from: https://doi.org/10.20858/sjsutst.2020.107.3
[22] Information about the city of Pila [online] [accessed 2016-02-20]. Available from: https://pl.wikipedia.org/wiki/Pila_(miasto)
[23] Map showing the location of the city of Pila in Poland [online] [accessed 2016-02-20]. Available from: https://www.google.pl/maps/@52.1782658,21.6247279,7.44z
[24] AMELJANCZYK, A. *Multi-criteria optimization.* Warsaw: WAT publisher. 1986.
[25] COYLE, J. J., BARDI, E. J., LANGLEY JR., C. J. *Logistic management.* Warsaw: Polish Economic Publisher, 2007. ISBN 9788320818642.
[26] JONAK, J., NIEOCZYM, A. *Logistics in the area of production and storage*. Lublin: Lublin University of Technology Publishing House, 2004. ISBN 9788379470228.
[27] STOPKA, O., STOPKOVA, M., KAMPF, R. Application of the operational research method to determine the optimum transport collection cycle of municipal waste in a predesignated urban area. *Sustainability* [online]. 2019, **11**(8), 2275. eISSN 2071-1050. Available from: https://doi.org/10.3390/su11082275
[28] Offer materials of the Institute of Logistics and Warehousing. Poznan [online] [accessed 2016-02-20]. Available from: http://www.ilim.poznan.pl/oferta/magazynowanie-oferta -ilim.html
[29] MINDUR, M. *Logistics, science - research - development*. Warsaw – Radom: Publisher of the Institute of Technology and Exploitation, 2017. ISBN 9788377894606.
[30] NIZINSKI, S., ZUREK, J. *General logistics*. Warsaw: Communication and Communication Publishing, 2011. ISBN 9788320618198.
[31] TYLICKI, H. Computer program "Multi-criteria Optimization Task 2017". Scientific and didactic materials of the Transport Department of the Polytechnic Institute. Pila: State Higher Vocational School, 2017.
[32] TYLICKI, H. Optimization of enterprise storage infrastructure. In: *Technology, exploitation, transport systems*. Radom: Buses Publishing House, 2015. ISSN 1509-5878.
[33] TYLICKI H., LATOS H. Elaboration of results of R&D works in the field of metal laser cutting production process and metal sheet warehouse automation. Scientific and didactic materials of the Department of Mechanical Engineering and Transport of the Polytechnic Institute. Pila: State Higher Vocational School, 2015.
[34] CURD, J. *Meters and logistic indicators.* Poznan: Logistics Library, 2003. ISBN 8387344915.
[35] LOT Polish Airlines [online] [accessed 2012-02-28]. Available from: https://www.lot.com
[36] Warsaw public transport [online] [accessed 2012-02-28]. Available from: https://www.wtp.waw.pl
[37] ZTCity Transport Board in Poznan [online] [accessed 2012-02-28]. Available from: https://www.ztm.poznan.pl
[38] Flixbus [online] [accessed 2012-02-28]. Available from: https://www.flixbus.pl
[39] PKP Intercity - Polish railway carrier [online] [accessed 2012-02-28]. Available from: https://www.intercity.pl
[40] Long-distance bus timetable [online] [accessed 2012-02-28]. Available from: https://www.busradar.pl/
[41] Bus timetable [online] [accessed 2012-02-28]. Available from: www.jakdojade.pl
[42] Timetable [online] [accessed 2012-02-28]. Available from: https://dworzeconline.pl/
[43] Timetable [online] [accessed 2012-02-28]. Available from: www.e-podroznik.pl
[44] PKS Pila [online] [accessed 2012-02-28]. Available from: https://pkspila.pl/
[45] PKP Timetable [online] [accessed 2012-02-28]. Available from: https://rozklad-pkp.pl/
[46] Maps [online] [accessed 2012-02-28]. Available from: https://www.targeo.pl/
[47] Telesfor [online] [accessed 2012-02-28]. Available from: https://www.telesfor.com.pl/
[48] Voyager Transport [online] [accessed 2012-02-28]. Available from: www. voyager-transport.pl
[49] Stalko [online] [accessed 2012-02-28]. Available from: https://www.stalko.net.pl/
[50] Flight booking [online] [accessed 2012-02-28]. Available from: https://book.lot.com
[51] Masovian Railways [online] [accessed 2012-02-28]. Available from: https://www.mazowieckie.com.pl/
[52] Train punctuality [online] [accessed 2012-02-28]. Available from: https://www.rynek-kolejowy.pl/mobile/na-ktorych-stacji-pociagi-spozniaja-sie-najczesarest-punktualnosc-za-2019-rok-95449.html
[53] Bus punctuality [online] [accessed 2012-02-28]. Available from: https://gloswielkopolski.pl/oto-najarest-punktualne-linie-autobusowe-w-poznaniu-top-6/ar/c1-14603547
[54] Bus delays [online] [accessed 2012-02-28]. Available from: https://www.transport-publiczny.pl/ consciousosci / flixbus-prawo-moze-utrudniac-niwelowanie-opoznien-63967.html
[55] Traffic incident search engine [online] [accessed 2012-02-28]. Available from: http://sewik.pl/

[56] Aircraft accident [online] [accessed 2012-02-28]. Available from: https://www.rynek-lotniczy.pl/ consciousosci / -2019- r- jednym-z-najysznenych-w-historii-lotnictwa-7565.html
[57] Aircraft delays [online] [accessed 2012-02-28]. Available from: https://www.rynek-lotniczy.pl/ consciousosci / lot-75-punktualnosc-w-roku-2019-7698.html

Project

Research and development of contactless methods for obtaining geospatial data for forest monitoring to improve forest management and enhance forest protection

is co-financed by the European Regional Development Fund

Project objective:

Creation of a long-term excellent research, development and innovation ecosystem in the field of geospatial information and communication technologies on the basis of an active partnership between the state and public research and development sector and the industrial sector.

Project description:

1. Development of the methodologies, procedures for processing large data sets (geospatial big data) obtained by the application of the most modern contactless technologies of ground and aeronautical remote sensing of the earth and research of the potential of their application in various areas (National Forest Centre).
2. Monitoring of changes in the landscape structure, evaluation of changes in forest ecosystems by research stationaries, monitoring of climate change in the nature reserves, application of dendrochronology methods in forestry (Comenius University in Bratislava).
3. Rationalization of mapping, forest condition identification, optimization of wild beasts management and forest management using progressive technologies of the earth remote sensing (Technical University in Zvolen).
4. Research of multidimensional evaluation system to support forestry (YMS, a.s.).
5. Research and development in the areas of environmental analysis of the properties of the air environment over the forest area and in the areas of ground survey of selected parts of the forest environment infrastructure (University of Žilina)

Beneficiary: National Forest Centre

In cooperation with:

University of Žilina
Technical University in Zvolen
Comenius University in Bratislava
YMS, a.s.

Contracted amount of the Non-Repayable Financial Contribution:

10 456 106,96 EUR

Project duration: 10/2019 – 06/2023

ITMS2014+ code: 313011V465

„This work was supported under the project of Operational Integrated Infrastructure: Research and development of contactless methods for obtaining geospatial data for forest monitoring to improve forest management and enhance forest protection, ITMS code 313011V465. The project is co-funding by European Regional Development Fund.“

EUROPEAN UNION
European Regional Development Fund
OP Integrated Infrastructure 2014 – 2020

MINISTRY
OF TRANSPORT
AND CONSTRUCTION
OF THE SLOVAK REPUBLIC

A DATA-DRIVEN METHOD FOR VEHICLE SPEED ESTIMATION

Angelo Bonfitto, Stefano Feraco*

LIM - Laboratorio Interdisciplinare di Meccatronica, Dipartimento di Ingegneria Meccanica e Aerospaziale (DIMEAS), Politecnico di Torino, Torino, Italy

*E-mail of corresponding author: stefano.feraco@polito.it

Resume

This paper presents a method based on Artificial Neural Networks for estimation of the vehicle speed. The technique exploits the combination of two tasks: a) speed estimation by means of regression neural networks dedicated to different road conditions (dry, wet and icy); b) identification of the road condition with a pattern recognition neural network. The training of the networks is conducted with experimental datasets recorded during the driving sessions performed with a vehicle on different tracks. The effectiveness of the proposed approach is validated experimentally on the same car by deploying the algorithm on a dSPACE computing platform. The estimation accuracy is evaluated by comparing the obtained results to the measurement of an optical sensor installed on the vehicle and to the output of another estimation method, based on the mean value of velocity of the four wheels.

Article info

Received 15 October 2020
Accepted 25 November 2020
Online 7 April 2021

Keywords:

vehicle speed,
artificial neural networks,
estimation,
regression,
classification,
road identification

Available online: https://doi.org/10.26552/com.C.2021.3.B165-B177

ISSN 1335-4205 (print version)
ISSN 2585-7878 (online version)

This is an open access article distributed under the terms of the Creative Commons Attribution 4.0 International License (CC BY 4.0), which permits use, distribution, and reproduction in any medium, provided the original publication is properly cited. No use, distribution or reproduction is permitted which does not comply with these terms.

1 Introduction

Automotive industry technologies witnessed a rapid evolution in the recent period, supported by the constant developments in the fields of electronics, actuation, automation and connectivity. Nowadays, commercial cars are highly performing and, at the same time, intelligent and sustainable [1]. Many benefits of the latest advancements are already tangible in terms of improved safety and comfort, reduction of the emissions and traffic congestions, lower stress for the car occupants and more confidence of the driver in a vehicle [2-3]. In this context, active strategies, relying on the real-time assessment of the vehicle dynamics assumes a crucial importance and the knowledge of the car states is a fundamental task, that is typically performed by direct measurement or, alternatively, by estimation and other indirect approaches [4]. However, some of the vehicle parameters (e.g. speed and sideslip angle) can be directly measured only with expensive, bulky and low robust devices, whose adoption in large production vehicles is not a viable solution. This motivates the considerable research effort that is recently being dedicated to investigation of alternative methods, such as the application of artificial intelligence to the assessment of vehicle dynamics [5-6]. In this paper, the attention is focused on estimation of the vehicle speed, a parameter that plays a key role in several active systems dedicated to control of the wheel slip, yaw rate and sideslip angle [7-8]. The direct measurement of the speed is commonly obtained using optical or GPS-based sensors [9]. However, these solutions may present some limitations according to the operating conditions. Optical sensors suffer problems of costs, size and sensitivity to dirt and environment conditions. On the other hand, the GPS-based sensors may be not sufficiently robust and reliable in specific atmospheric conditions as well as in situations with limited sky visibility, such as tunnels and urban environments with tall buildings. These problems can be partially overcome by analyzing signals coming from more satellites, using the Differential GPS technique or by exploiting two GPS antennas [10]. However, these approaches are still characterized by high signal latency time during the broadcasting of corrections. Typically, this latency is in the range of seconds, which might be far from the requirements of the active solutions implemented on board of a vehicle [11-12].

Alternative solutions are based on extraction of the speed information from vehicle analytical models [13]. A solution presented in [14] is based on e measurements of an Inertial Measurement Unit (IMU) using a slip detection estimator. This technique is typically implemented considering the unknown road condition as a bounded uncertainty and employing the estimated friction-independent tire forces for correcting the estimate. Nevertheless, the need for an accurate assessment of the road friction coefficient and of parameters related to the tires, which are highly time-varying, represents a relevant limitation of this

technique. Further approaches exploit the Kalman Filter (KF) [15], Adaptive Kalman Filter (AKF) [16] and its nonlinear versions, Extended Kalman Filter (EKF) [17] and Unscented Kalman Filter (UKF) [18]. Other methods rely on similar filter/observer-based techniques [19-20]. However, these model-based techniques may suffer accuracy problems if the reference model is inaccurate or unable to reproduce the vehicle dynamics in all the driving conditions. An alternative class of techniques is based on Fuzzy Logic (FL) [21-24], which is strongly dependent on the designer experience and requires a highly refined definition of the rules and membership functions [25]. Finally, a common solution computes the speed as the average of the velocity of the four wheels. Although simple and cheap, this method may result as inaccurate when one or more wheels are locking during a sudden braking or start spinning and skidding, i.e. while driving on wet or icy roads and during the extreme manoeuvres.

This paper proposes a method to estimate the vehicle speed by using artificial intelligence to mitigate the limitations of model-based techniques and have an effective solution also in conditions that are difficult to represent in the models. Specifically, the presented method exploits a combination of regression and classification Artificial Neural Networks (ANNs). As well known, ANN-based approaches do not rely on any model and, if the networks are appropriately trained, may guarantee good levels of accuracy and robustness, as demonstrated by the growing attention that these methods are gaining in several engineering fields [26-28]. To the author's knowledge, although the ANNs are widely documented as effective in executing system modeling and timeseries estimation, few research studies using the ANNs for the vehicle speed estimation are reported in the literature so far, since most of them rely on other techniques [29]. In this work, the proposed architecture includes two tasks: a) speed estimation computed by three parallel regression ANNs, dedicated to three different road conditions (dry, wet and icy road) and b) identification of the road condition with a pattern recognition neural classifier. The classifier output is used to select the correct estimation among the three outputs of the regression networks. Typically, the problem of the road condition detection is tackled with estimation of the friction coefficient with model-based approaches [30], regression ANNs [31-33], or exploiting the radar measurement [34-35]. In this study, on the contrary, the aim is not to provide the value of the friction coefficient, but the information of the class of the road condition: dry, wet or icy.

The ANNs' training datasets have been collected on a real vehicle, equipped with an optical sensor for acquisition of the reference speed, which is the target adopted during the supervised learning phase of the regression networks. Each regression network is trained with the dataset relative to the corresponding road condition. On the other hand, the input of the classifier is a single set of features extracted from the measured vehicle parameters and including all the road conditions. The validation of the method has been conducted experimentally on the same vehicle by deploying the designed algorithm on an auxiliary electronic control unit. The effectiveness of the approach is demonstrated by comparing the output of the estimator to the direct optical measurement and with another estimation computed as the average of the velocity of the four wheels. This estimation is extracted from an algorithm that was already deployed on the vehicle control unit.

The main contribution of this paper is the proposal of a data-driven method to estimate the vehicle speed. This approach has not been investigated yet in the literature and allows obtaining accurate results, if the training datasets effectively include all the significant behaviors of the vehicle in the widest possible set of handling manoeuvres and driving conditions. The good level of accuracy is quantified with the evidence obtained during the experimental validations. The results obtained on a high-performance vehicle allow highlighting the estimation behavior in extreme driving conditions.

The paper is structured as follows. The first section is dedicated to description of the vehicle setup and of the regression and classification tasks. Afterwards, the design of the neural networks for the speed estimation and for the road condition identification is illustrated. The last section presents the discussion of the experimental results obtained on the real vehicle in different driving conditions and in correspondence of road condition transients.

2 Estimation method and vehicle setup

The architecture of the proposed method is illustrated in Figure 1 and consists of two interconnected stages dedicated to the speed estimation and identification of the road condition. The former exploits three parallel Non-linear Autoregressive with Exogenous Input neural networks (NARX) and provides three outputs, one per each road condition: dry ($\hat{v}_{xD}$), wet ($\hat{v}_{xW}$) and icy ($\hat{v}_{xI}$).

The regression networks are fed with eight measurements listed in Table 1 (parameters 1 to 8) and trained with a supervised learning procedure using the speed measured by the optical sensor (v_x) as the target output.

Inputs from 5 to 8 are computed as

$$v_{ij} = \frac{1}{3.6} \cdot \frac{2\pi}{60} \cdot (\omega_{ij} \cdot \rho_i), \tag{1}$$

where i is F or R, in the case of front or rear wheels, respectively, j is L or R, in the case of left or right wheels, respectively, ω_{ij} is the angular speed of the ij-wheel, expressed in round per minutes and ρ_i is the wheel radius of the wheels, measured in meters. The total steering angle TS (input 4) is computed as the sum of the steering wheel angle (defined as the angle between

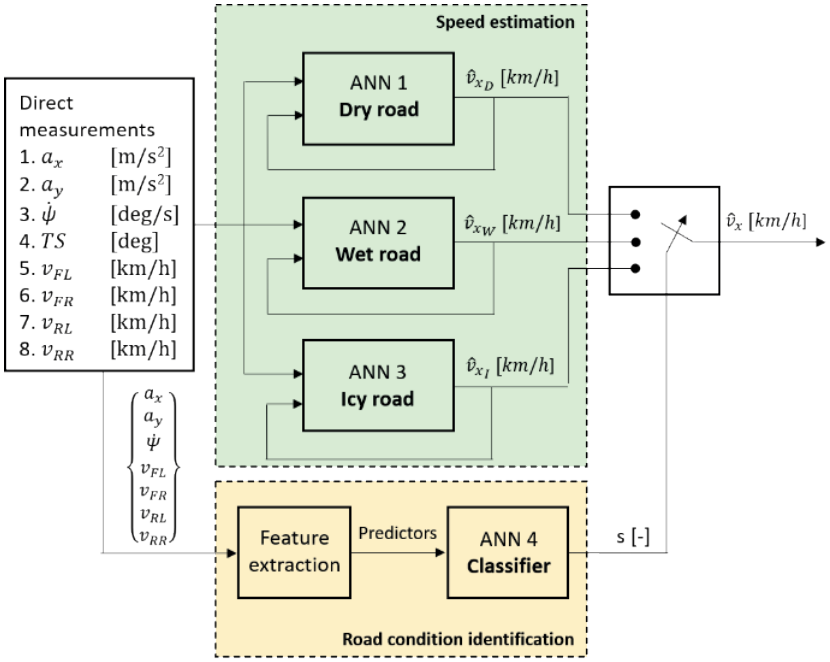


Figure 1 *Layout of the estimation algorithm. Based on the actual road condition, the correct output is selected by a switch driven by the road condition identification classifier (output S)*

Table 1 *Inputs of the estimation algorithm. R: parameters used for the three regression networks; C: parameters used for the classifier*

#	type	task	parameters	name	unit
1	input	R&C	long. acceleration	a_x	(m/s²)
2	input	R&C	lat. acceleration	a_y	(m/s²)
3	input	R&C	yaw rate	$\dot{\phi}$	(deg/s)
4	input	R	total steering angle	TS	(deg)
5	input	R&C	front left wheel speed	v_{FL}	(km/h)
6	input	R&C	front right wheel speed	v_{FR}	(km/h)
7	input	R&C	rear left wheel speed	v_{RL}	(km/h)
8	input	R&C	rear right wheel speed	v_{RR}	(km/h)
9	target	R	vehicle speed	v_x	(km/h)
10	target	C	class of the road	*D, W, I*	(-)

the vehicle's direction of motion and the steered wheel direction) and the active front steering input which is obtained from the electronic control unit of the vehicle.

The second stage allows identifying the road condition exploiting a classifier based on a pattern recognition feed-forward ANN. The classification process generates an output (s) allowing to select the correct estimation among the outputs of the three regression networks above described.

The datasets adopted for the training of the regression and classification networks are collected on an instrumented vehicle in different test tracks and road conditions. The vehicle is a four-wheel drive (4WD) sport car with a power-to-weight ratio of around 0.35 kW/Kg and a weight of about 1700 kg. The vehicle is equipped with standard inertial sensors and a two-axis optical sensor Correvit S-Motion from Kistler, which is exploited for the measurement of the speed and features a precision of ±0.5 km/h, declared by the manufacturer. A dSPACE MicroAutoBox is interfaced with the CAN-bus of the vehicle to allow collecting the training datasets in the design phase and deploying the designed algorithm for the experimental validation. The sampling rate of the data acquisition is 100 Hz.

The training dataset collection and experimental validation have been conducted in all the possible combinations of the different conditions that are reported in Table 2.

The following driving conditions have been explored in three different adherence conditions (dry, wet and icy road): different tire-road friction coefficients; summer and winter tires; new and used tires; tests performed with and without the active safety system; tests performed by selecting different car driving modes;

Table 2 *Possibilities of driving conditions, vehicle setup and manoeuvres used for the training dataset collection and experimental validation. (ESC: Electronic Stability Control)*

road condition	maneuver	esc status	driving setup
dry	handling	ON	normal
wet	double lane change	OFF	sport
icy	sine-sweep		racing
	sine steer		
	step steer		
	acceleration/braking		
	steady-state cornering		

Table 3 *Training parameters of the three regression neural networks. The networks have a single hidden layer*

road condition	dry	wet	icy
input buffer size d_x	2	3	2
feedback buffer size d_y	2	3	2
hidden layer size	40 neurons	60 neurons	40 neurons
training algorithm	Levenberg-Marquardt backpropagation		

tests performed with different driving styles and by professional and common drivers.

3 Design of the estimator

This section describes the design of the regression neural networks for the estimation of the speed and of the classifier for identification of the road condition.

3.1 Regression task for the vehicle speed estimation

A NARX ANN architecture is adopted for the regression task. This network allows modelling a discrete non-linear system. The output of the network is defined as:

$$y(n) = \varphi[y(n-1), y(n-2), \ldots, y(n-d_y); x(n-1), x(n-2), \ldots, x(n-d_x)], \quad (2)$$

where $x(n) \in \mathbb{R}$ and $y(n) \in \mathbb{R}$ are the inputs and outputs of the network at the discrete timestep n, respectively, d_x and d_y are the input and output buffer memory, respectively and φ is the non-linear model represented by the network.

During the regression procedure, the value of the dependent output signal $y(n)$ is regressed on the previous d_y values of the output signal considering previous d_x values of the independent (exogenous) input signal. In the proposed solution, the NARX is adopted in open-loop during the training process and in closed-loop during the estimation phase, i.e. when the network is deployed on the electronic unit in the real application. The target input is $y^*(n)$, which is provided to the ANN during the supervised training phase. The Hidden Activation Function (HAF) is a hyperbolic tangent sigmoid and the Output Activation Function (OAF) is a linear function. Table 3 reports the training parameters of the three networks, the number of neurons in the hidden layer and the input and feedback buffer size.

The networks are trained with the Levenberg-Marquardt backpropagation algorithm. These characteristics are the result of a trial and error procedure, since the design and training of a neural network does not follow a standard procedure, as discussed in detail in [36] and [37].

3.2 Classification task for the road condition identification

The road condition identification is performed by the two-layered (one hidden and one output layer) feed forward pattern recognition ANN. This architecture connects an input feature space to an output space of multiple pattern classes and it has been already presented in the literature to solve classification problems in different engineering fields [38-39]. After a trial and error procedure, the hidden layer has been designed with a size of 50 neurons. The HAF is a hyperbolic tangent sigmoid and the OAF is a normalized exponential function. The adopted training procedure is based on the Levenberg-Marquardt backpropagation algorithm.

The input of the classifier is a set of 64 predictors, extracted from seven of the acquired signals, namely longitudinal and lateral accelerations (a_x and a_y), yaw rate $\dot{\phi}$ and longitudinal speed of the four wheels ($v_{FL}, v_{FR}, v_{RL}, v_{RR}$) [6]. Features from 1 to 22 have a straightforward definition (mean, standard deviation, peak to RMS value and variance for the acquired signals). Features from 23 to 64 result from a spectral analysis performed on the input signals, where PSD stands for Power Spectral Density, computed using the

Table 4 *Summary of the conditions and estimation accuracy of the presented experimental cases. (ESC: Electronic Stability Control. MSE: mean square error of the proposed method, MSE_{AVG}: mean square error of the method based on the average of the four wheels' velocities)*

validation case	road condition	driving setup	esc	a_{xMAX} (m/s²)	a_{yMAX} (m/s²)	v_{xMAX} (km/h)	TS_{MAX} (deg)	$\dot{\phi}_{MAX}$ (deg/s)	MSE (km/h)	MSE_{AVG} (km/h)
Figure 4	dry	racing	OFF	7.4	12.4	107.9	553.5	97.5	0.217	15.721
Figure 5	wet	sport	OFF	6.7	10.1	172.2	153.1	40.1	0.003	4.172
Figure 6	icy	normal	ON	3.5	4.1	88.7	201.3	32.8	0.763	26.142

periodogram technique [40] by dividing the considered signal into multiple overlapping blocks and computing the average of their squared magnitude Fast Fourier Transforms (FFT) [41]. The average spectral power (features from 51 to 64) is computed as the integral of the PSD over the two adjacent frequency bands: 0.5 ÷ 1.5 Hz (frequency band 1) and 1.5 ÷ 5 Hz (frequency band 2). The predictors are collected in buffers with a time length of 2s and refilled with a frequency of 10 Hz, which is the output rate of the classifier and hence of the overall estimation output $\hat{v}_x$.

The set of predictors was selected by a trial and error procedure, performed to maximize the accuracy of the classification task. A more refined selection phase could be performed after a quantification of the influence of each predictor. This aspect is currently a hot research topic [42-43], nevertheless, this analysis is beyond the scope of the present study and would require a dedicated work.

4 Results and discussion

The results are presented in different driving and road conditions. This section is dedicated to the analysis of the estimation behavior in correspondence of road condition transients.

4.1 Speed estimation

The accuracy of the proposed method is evaluated by comparing the estimation ($\hat{v}_x$) to the measurement of the optical sensor mounted onboard the vehicle (v_x) and with a further estimation computed as the average of the velocity of the four wheels ($\hat{v}_{xAVG}$). The latter is an algorithm that was already deployed in the electronic control unit of the vehicle.

The more relevant experimental results are reported in the following figures. The graphs illustrate the comparison between v_x, $\hat{v}_x$ and $\hat{v}_{xAVG}$ in the subplot *a*, the absolute error of the two estimation methods with respect to the measured value in the subplot *b* ($\varepsilon_1 = \hat{v}_x - v_x, \varepsilon_2 = \hat{v}_{xAVG} - v_x$.) and behavior of the ANN input signals, specifically the longitudinal a_x and lateral a_y accelerations (subplot *c*), the total steering angle (subplot *d*), the wheels' speed (subplot *e*) and the yaw rate (subplot *f*). The main characteristics of the validation cases are summarized in Table 4, where *MSE* and MSE_{AVG} are the mean square error of the proposed method and of the method based on the average of the four wheels' velocity, respectively.

They are computed as follows:

$$MSE = \frac{1}{n}\sum_{i=1}^{n}(v_x(i) - \hat{v}_x(i))^2, \tag{3}$$

$$MSE_{AVG} = \frac{1}{n}\sum_{i=1}^{n}(v_x(i) - \hat{v}_{xAVG}(i))^2. \tag{4}$$

Figure 2 shows results obtained on a dry asphalt with the Electronic Stability Control (ESC) system off and the car set in the racing driving mode. At 20 s, a sine-sweep manoeuvre is performed with a frequency of *TS* increasing from 0.5 Hz to 1.5 Hz and the speed v_x equal to around 50 km/h. Three additional sine-sweep manoeuvres are performed at 40, 60 and 90 s and a step-steer manoeuvre is performed at 130 s, when the vehicle longitudinal speed goes to zero, while *TS* reaches -550 deg.

The speed is estimated accurately by the ANN-based algorithm. On the other hand, $\hat{v}_{xAVG}$ is affected by a relevant error at 155 s during a sudden braking, whereas the estimation of the proposed ANN-based method remains accurate. The error ε_2 (dashed line) presents high peaks confirming that the estimate provided by the wheels' velocity average may be not completely reliable during some extreme manoeuvres.

Figure 3 represents results obtained on a wet asphalt with the ESC system switched off and the car set in sport driving mode, during a lap on a handling circuit. During this acquisition, the driver has performed successive demanding manoeuvres, reaching 160 km/h and steering from -150 deg to 150 deg. The speed is estimated accurately by the proposed method, whereas the error ε_2 reaches peaks of 7 km/h.

Figure 4 shows results obtained on an icy asphalt with the ESC system enabled and the car set in normal driving mode. At the beginning of this acquisition, the driver performed a sine-sweep manoeuvre at an almost constant speed equal to about 40 km/h, while steering from -80 deg to 100 deg for about 30 s. The frequency of *TS* increases from 0.5 Hz to about 2 Hz during the sine-sweep manoeuvre. Afterwards, the driver performed a step-steer manoeuvre with *TS* equal to -200 deg, once the vehicle has reached a maximum speed equal to about 90 km/h. The speed is estimated accurately by the ANN-based investigated method.

On the contrary, the estimation $\hat{v}_{xAVG}$ is not accurate during the last manoeuvre, since the four wheels start skidding and blocking on the icy road surface, as represented in Figure 4.d. The absolute error ε_2 reaches 70 km/h in Figure 4.b during the last manoeuvre, while the error ε_1 is limited to less than 5 km/h in correspondence of demanding manoeuvres.

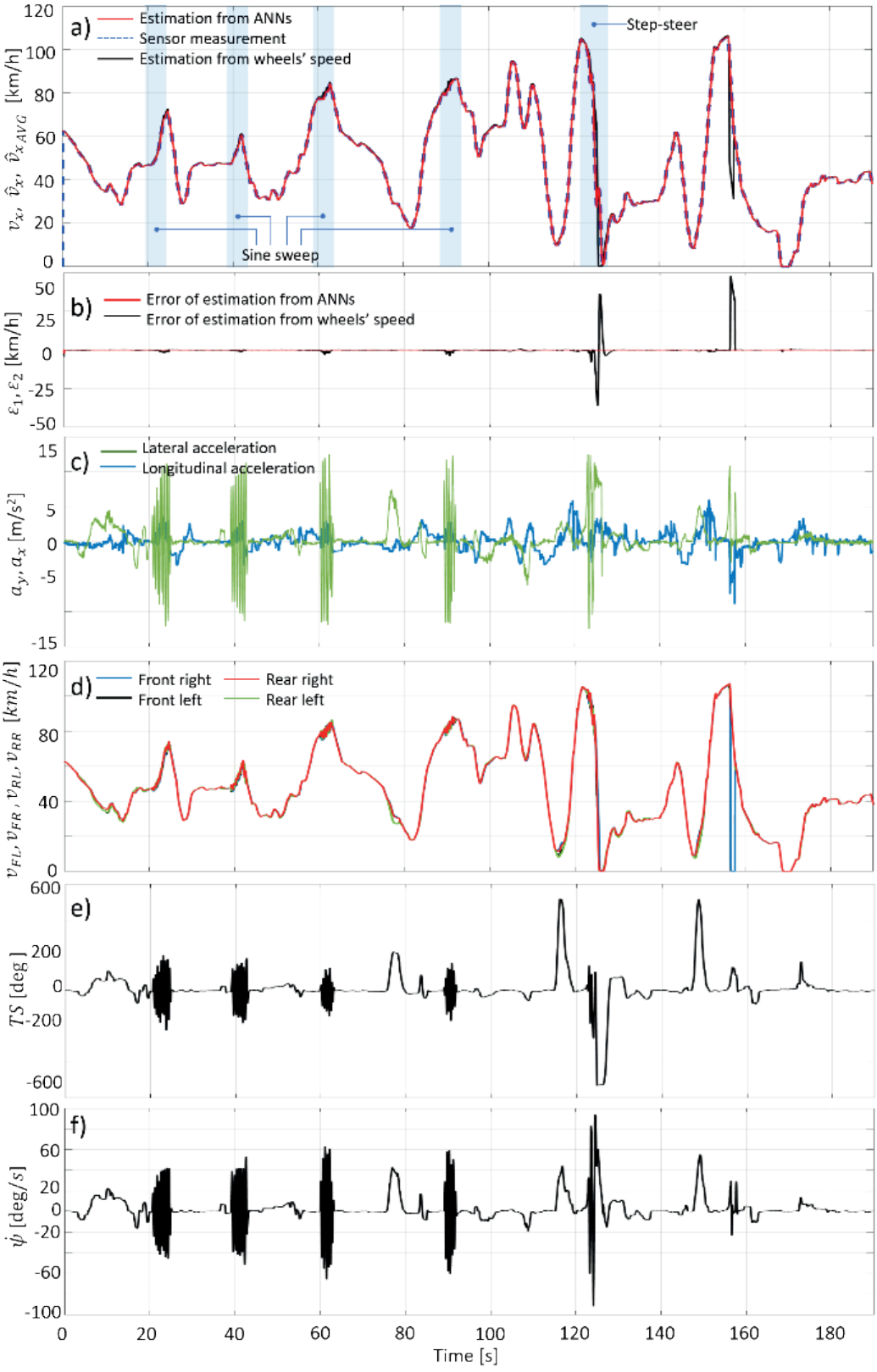


Figure 2 *Test 1. Dry road. a) Vehicle speed b) Absolute estimation errors. c) Longitudinal and lateral acceleration. d) Wheels' longitudinal speed. e) Total steering angle. f) Yaw rate. The commanded manoeuvres are highlighted in light blue areas*

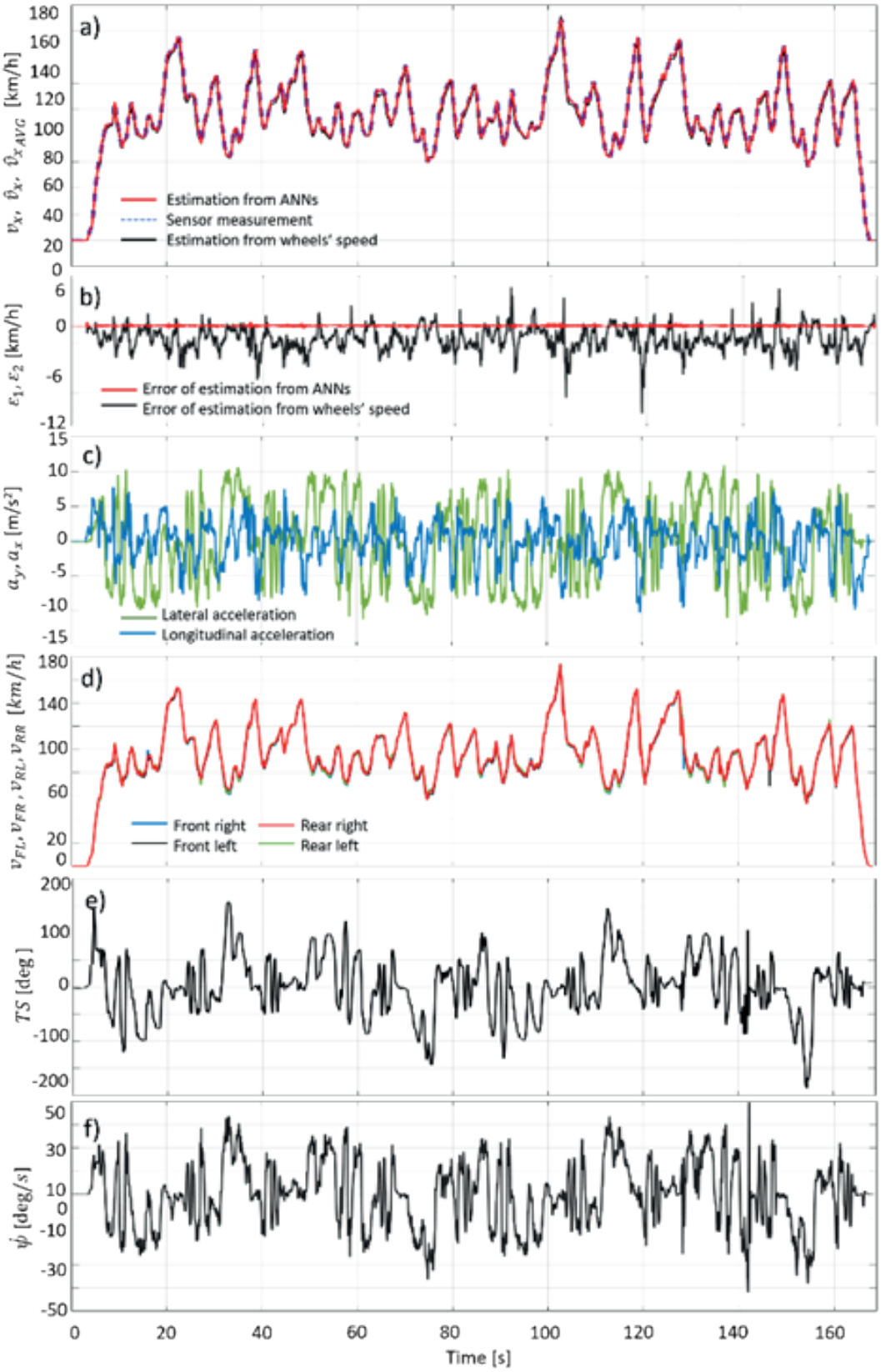


Figure 3 *Test 1. Wet road. a) Vehicle speed b) Absolute estimation errors. c) Longitudinal and lateral acceleration. d) Wheels longitudinal speed. e) Total steering angle. f) Yaw rate*

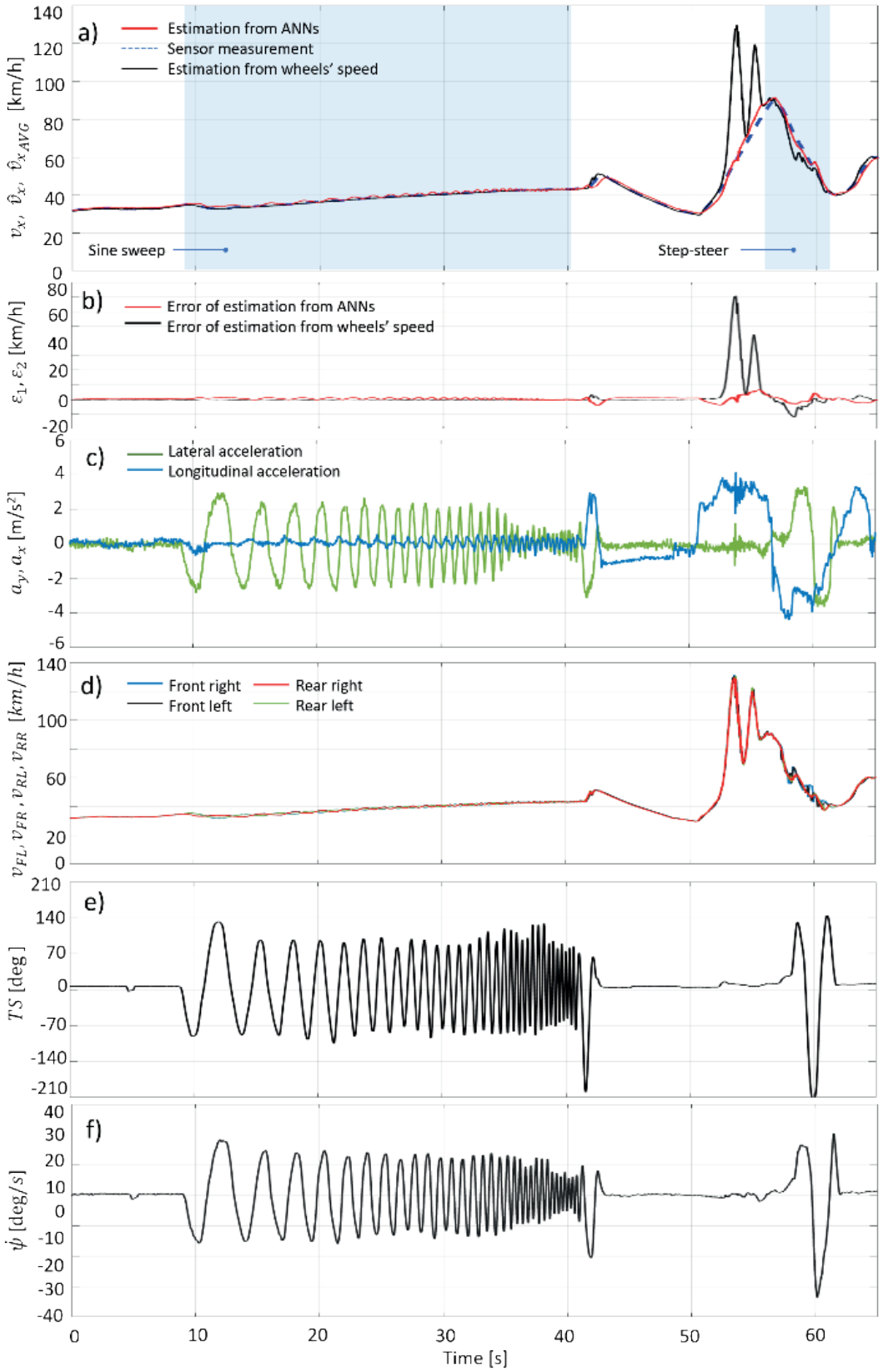


Figure 4 *Test 1. Icy road. a) Vehicle speed b) Absolute estimation errors. c) Longitudinal and lateral acceleration. d) Wheels longitudinal speed. e) Total steering angle. f) Yaw rate. The commanded manoeuvres are highlighted in light blue areas*

Classified road condition \ Actual road condition	Dry	Wet	Icy	
Dry	**37805** **CL:** 35.35%	**151** **CL:** 0.14%	**120** **CL:** 0.11%	
Wet	**114** **CL:** 0.11%	**25085** **CL:** 23.46%	**32** **CL:** 0.03%	
Icy	**104** **CL:** 0.1%	**10** **CL:** 0.01%	**43523** **CL:** 40.7%	
	N_D: **38023** α_{C_D} 99.43 %	N_W: **25246** α_{C_W} 99.36 %	N_I: **43675** α_{C_I} 99.65 %	N_{TOT}: **106944** $\alpha_{C_{TOT}}$ 99.5%

Figure 5 *Confusion matrix of the classifier for the road condition identification*

4.2 Road condition identification

The performance of the road condition identification is evaluated with a Confusion Matrix (*CM*) reported in Figure 5. The classified and actual road conditions instances are reported in the rows and columns, respectively. The values contained in the main diagonal cells indicate the correct classifications, whereas the off-diagonal cells report the number of the misclassifications. The data provided as input to the classifier are buffers with a duration of 2 seconds containing the features extracted in the classification process. These buffered data are overlapped with a time-shift of 0.1 s, thus the total number of input buffers (N_{TOT}) is 106944, equal to the sum of 38023 in dry (N_D), 25246 in wet (N_W) and 43675 in icy (N_I) acquisitions, corresponding to a total acquisition time of 10694.4 s.

For each cell, a classification rate *CL* is computed as the ratio between the number of cell instances $N_{i,j}$ and the total number of instances N_{TOT}:

$$CL_{i,j} = \frac{N_{i,j}}{N_{TOT}}. \tag{5}$$

The classification accuracy for each road condition is computed as follows:

$$\alpha_{C_D} = \frac{N_{1,1}}{N_D}, \alpha_{C_W} = \frac{N_{2,2}}{N_W}, \alpha_{C_I} = \frac{N_{3,3}}{N_I}, \tag{6}$$

for dry, wet and icy asphalt, respectively. The total classification accuracy is equal to 99.5 %, computed as

$$\alpha_{C_{TOT}} = \frac{N_{1,1} + N_{2,2} + N_{3,3}}{N_{TOT}}. \tag{7}$$

4.3 Validation during the road condition transients

Accuracy of the road conditions identification has been validated also in correspondence of the transient between the two different conditions: a) from dry to wet and from wet to dry and b) from wet to icy and from icy to wet.

Figure 6 reports the acquisition recorded with the car in normal driving mode and the ESC system disabled. During the initial part of the acquisition, the road is dry. Then, the road condition becomes wet at about 40 s. At around 80 s, the road is dry again. The output of the classifier S is reported in Figure 6 where the zoomed regions report the buffers along with the classification outputs. The second zoomed area is reported because it represents the occurrence of a misclassification. In this case, S indicates a wet road condition, although the asphalt is dry. However, this misclassification does not affect the longitudinal speed estimation, as represented in Figure 6.

In Figure 7, the results obtained during the road condition transient from wet to icy and from icy to wet are represented. The car has the ESC system enabled and is set in racing driving mode. The classification output S is reported in the zoomed portions. All the buffers are correctly classified and the final value of the estimation is accurate, as represented in Figure 7.

The number of misclassifications in correspondence of the road conditions change is very limited. This result has been achieved by reducing the length of the buffers considered for the feature extraction in the classification task. As a matter of fact, the larger the buffer, the higher is the possibility to incur in misclassifications. The high rate of classification output is also advantageous to limit the effect of estimation inaccuracies due to misclassifications. The estimation error is indeed recovered within the period of 0.1 s, corresponding to the output rate of the classifier. This motivates the absence of major estimation inaccuracies in correspondence of the misclassifications.

5 Conclusions

In this paper, a data-driven method for the vehicle speed estimation has been presented. The proposed technique exploits a combination of regression and

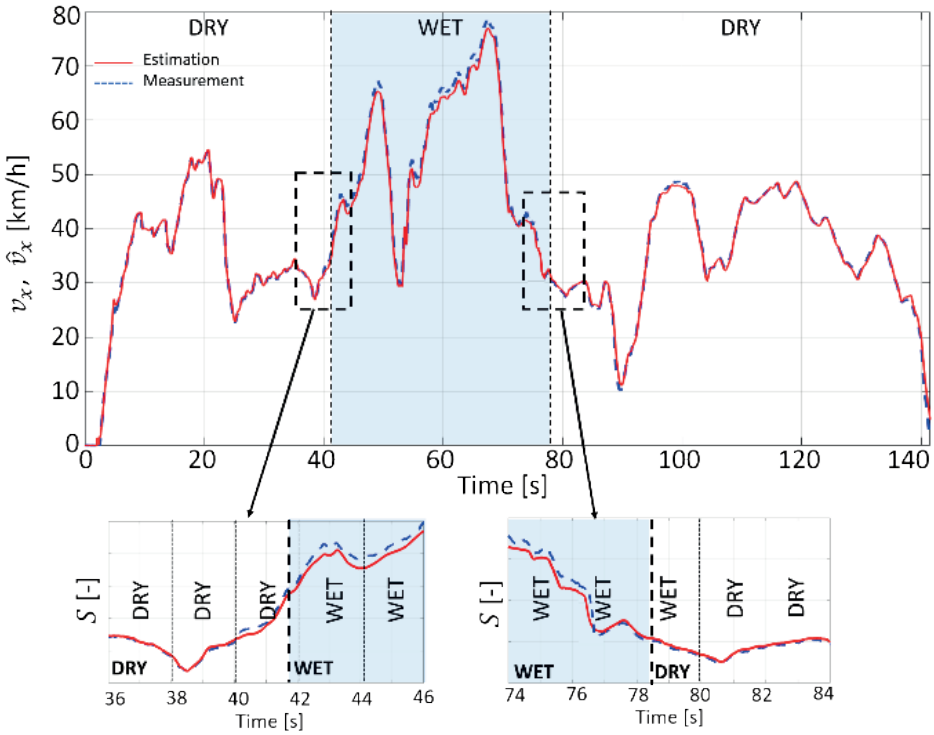


Figure 6 *Test performed in transient road conditions (dry-wet-dry). a) measured v_x (dashed) vs. estimated by the ANN-based algorithm $\hat{v}_x$ (solid) longitudinal speed. In the zoomed regions: ANN-based classifier's output S*

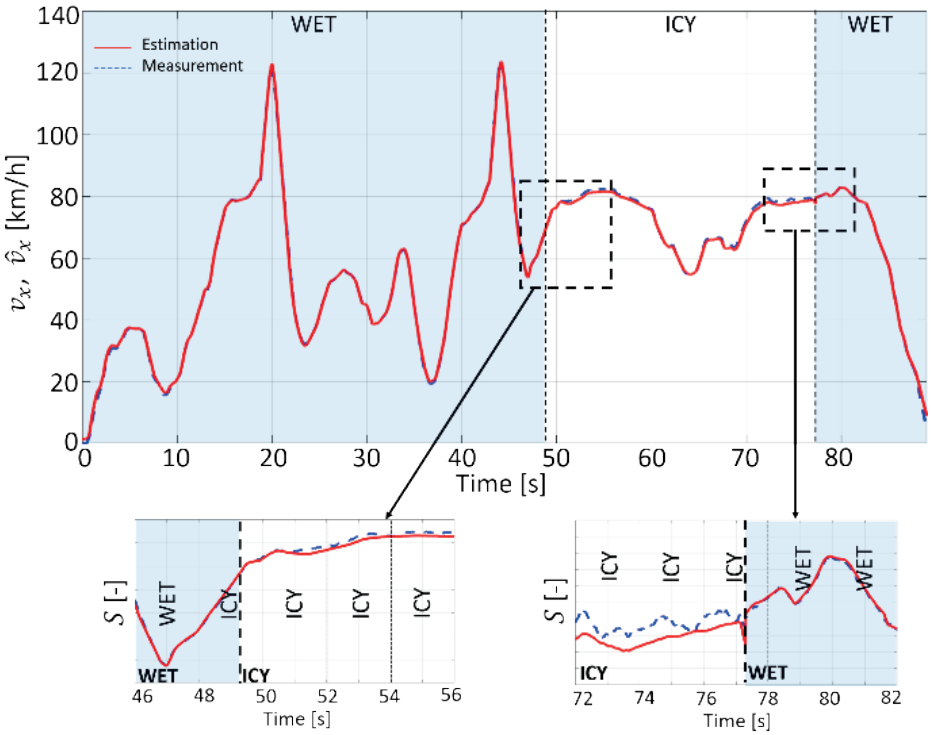


Figure 7 *Test performed in transient road conditions (wet-dry-wet). a) measured v_x (dashed) vs. estimated by the ANN-based algorithm $\hat{v}_x$ (solid) longitudinal speed. In the zoomed regions: ANN-based classifier's output S*

classification neural networks task to estimate the speed and identify the road condition. The solution is presented as a reliable alternative to existing methods to mitigate the limitations due to the model

representation. The performance of the method was evaluated experimentally in several driving conditions. The good match between the estimated and measured values of speed demonstrates the effectiveness of the method, also in correspondence of transients between different road conditions.

Acknowledgement

This work was developed in the framework of activities of the Interdepartmental Center for Automotive Research and Sustainable Mobility (CARS) of Politecnico di Torino (www.cars.polito.it).

References

[1] OKUDA, R., KAJIWARA, Y., TERASHIMA, K. A survey of technical trend of ADAS and autonomous driving. In: VLSI Technology, Systems and Application VLSI-TSA: proceedings [online]. IEEE. 2014. ISBN 978-1-4799-2776-0. Available from: https://doi.org/10.1109/VLSI-DAT.2014.6834940

[2] SHIBAHATA, Y., SHIMADA, K., TOMARI, T. Improvement of vehicle manoeuvreability by direct yaw moment control. *Vehicle System Dynamics* [online]. 1993, **22**(5-6), p. 465-481. ISSN 0042-3114, eISSN 1744-5159. Available from: https://doi.org/10.1080/00423119308969044

[3] LUCIANI, S., BONFITTO, A., AMATI, N., TONOLI, A. Model predictive control for comfort optimization in assisted and driverless vehicles. *Advances in Mechanical Engineering* [online]. 2020, **12**(11). ISSN 1687-8140, eISSN 1687-8140. Available from: https://doi.org/10.1177/1687814020974532

[4] FODOR, M., YESTER, J., HROVAT, D. Active control of vehicle dynamics. In: 17th Digital Avionics Systems Conference DASC: proceedings [online]. The AIAA/IEEE/SAE. Vol. 2. 1998. ISBN 0-7803-5086-3, p. I14/1-I14/8. Available from: https://doi.org/10.1109/DASC.1998.739865

[5] YIM, Y. U., OH, S. Y. Modeling of vehicle dynamics from real vehicle measurements using a neural network with two-stage hybrid learning for accurate long-term prediction. *IEEE Transactions on Vehicular Technology* [online]. 2004, **53**(4), p. 1076-1084. ISSN 0018-9545. Available from: https://doi.org/10.1109/TVT.2004.830145

[6] BONFITTO, A., FERACO, S., TONOLI, A., AMATI, N. Combined regression and classification artificial neural networks for sideslip angle estimation and road condition identification. *Vehicle System Dynamics* [online]. 2019, **58**(11), p. 1766-1787. ISSN 0042-3114, eISSN 1744-5159. Available from: https://doi.org/10.1080/00423114.2019.1645860

[7] CIROVIC, V., ALEKSENDRIC, D., SMILJANIC, D. Longitudinal wheel slip control using dynamic neural networks. *Mechatronics* [online]. 2013, **23**(1), p. 135-146. ISSN 0957-4158. Available from: https://doi.org/10.1016/j.mechatronics.2012.11.007

[8] MANNING, W. J., CROLLA, D. A. A review of yaw rate and sideslip controllers for passenger vehicles. *Transactions of the Institute of Measurement and Control* [online]. 2007, **29**(2), p. 117-135. ISSN 0142-3312, eISSN 1477-0369. Available from: https://doi.org/10.1177/0142331207072989

[9] BEVLY, D. M., GERDES, J. C., WILSON, C., ZHANG, G. The use of GPS based velocity measurements for improved vehicle state estimation. In: 2000 American Control Conference ACC: proceedings [online]. IEEE. 2000. ISSN 0743-1619, ISBN -7803-5519-9. Available from: https://doi.org/10.1109/ACC.2000.878665

[10] JANG, J., SUNG, S., LEE, Y. J. Improvement of differential GPS performance using range measurements between satellites. *International Journal of Aeronautical and Space Sciences* [online]. 2020, **21**(1), p. 201-209. ISSN 2093-274X, eISSN 2093-2480. Available from: https://doi.org/10.1007/s42405-019-00198-x

[11] SOLOMON, P. D., WANG, J., RIZOS, C. Latency determination and compensation in real-time GNSS/INS integrated navigation systems. International Archives of the Photogrammetry, Remote Sensing and Spatial Information Sciences 2011 ISPRS Workshop: proceedings [online]. Vol. XXXVIII-1/C22. 2011. p. 303-307. Available from: https://doi.org/10.5194/isprsarchives-XXXVIII-1-C22-303-2011

[12] WANG, Z., HAMEDI, M. YOUNG, S. Methodology for calculating latency of GPS probe data. *Transportation Research Record: Journal of the Transportation Research Board* [online]. 2017, **2645**(1), p. 76-85. ISSN 0361-1981, eISSN 2169-4052. Available from: https://doi.org/10.3141/2645-09

[13] KO, S. Y., KO, J. W., LEE, S. M., CHEON, J. S., KIM, H. S. Vehicle velocity estimation using effective inertia for an in-wheel electric vehicle. *International Journal of Automotive Technology* [online]. 2014, **15**(5), p. 815-821. ISSN 1229-9138, eISSN 1976-3832. Available from: https://doi.org/10.1007/s12239-014-0085-8

[14] HASHEMI, E., KHOSRAVANI, S., KHAJEPOUR, A., KASAIEZADEH, A., CHEN, S. K., LITKOUHI, B. Longitudinal vehicle state estimation using nonlinear and parameter-varying observers. *Mechatronics* [online]. 2017, **43**, p. 28-39. ISSN 0957-4158. Available from: https://doi.org/10.1016/j.mechatronics.2017.02.004

[15] KLOMP, M., GAO, Y., BRUZELIUS, F. Longitudinal velocity and road slope estimation in hybrid electric vehicles employing early detection of excessive wheel slip. *Vehicle System Dynamics* [online]. 2014, **52**(sup1), p. 172-188. ISSN 0042-3114, eISSN 1744-5159. Available from: https://doi.org/10.1080/00423114.2014.887737

[16] CHU, L., SHI, Y., ZHANG, Y., LIU, H., XU, M. Vehicle lateral and longitudinal velocity estimation based on adaptive Kalman filter. In: 3rd International Conference on Advanced Computer Theory and Engineering ICACTE: proceedings [online]. IEEE. 2010. Available from: https://doi.org/10.1109/ICACTE.2010.5579565

[17] CHU, L., XHANG, Y., SHI, Y., XU, M., OU, Y. Vehicle lateral and longitudinal velocity estimation using coupled EKF and RLS methods. *Applied Mechanic and Materials* [online]. 2010, **29-32**, p. 851-856. ISSN 1662-7482. Available from: https://doi.org/10.4028/www.scientific.net/AMM.29-32.851

[18] CHU, L., ZHANG, Y., SHI, Y., XU, M., LIU, M. Vehicle lateral and longitudinal velocity estimation based on unscented Kalman filter. In: 2nd International Conference on Education Technology and Computer: proceedings [online]. IEEE. 2010. ISSN 2155-1812. Available from: https://doi.org/10.1109/ICETC.2010.5529507

[19] MOAVENI, B., ABAD, M. K. R., NASIRI, S. Vehicle longitudinal velocity estimation during the braking process using unknown input Kalman filter. *Vehicle System Dynamics* [online]. 2015, **53**(10), p. 1373-1392. ISSN 0042-3114, eISSN 1744-5159. Available from: https://doi.org/10.1080/00423114.2015.1038279

[20] ZHAO, L., LIU, Z., CHEN, H. Design of a nonlinear observer for vehicle velocity estimation and experiments. *IEEE Transactions on Control Systems Technology* [online]. 2011, **19**(3), p. 664-672. ISSN 1063-6536, eISSN 1558-0865. Available from: https://doi.org/10.1109/TCST.2010.2043104

[21] GAO, X., YU, Z., XU, T. Longitudinal velocity estimation of electric vehicle with 4 in-wheel motors. In: SAE World Congress and Exhibition Vehicle Dynamics and Simulation: proceedings [online]. USA: SAE International. 2008. ISSN 0148-7191, eISSN 2688-3627, 2008-01-0605. Available from: https://doi.org/10.4271/2008-01-0605

[22] JIN, C., SHAO, L., LEX, C., EICHBERGER, A. Vehicle side slip angle observation with road friction adaptation. *IFAC PapersOnLine* [online]. 2017, **50**(1), p. 3406-3411. ISSN 2405-8963. Available from: https://doi.org/10.1016/j.ifacol.2017.08.593

[23] BASSET, M., ZIMMER, C., GISSINGER, G. L. Fuzzy approach to the real time longitudinal velocity estimation of a FWD car in critical situations. *Vehicle System Dynamics* [online]. 1997, **27**, p. 477-489. ISSN 0042-3114, eISSN 1744-5159. Available from: https://doi.org/10.1080/00423119708969343

[24] JIN, L., CHEN, P., ZHANG, R. AND LING, M. Longitudinal velocity estimation based on fuzzy logic for electronic stability control system. *Advances in Mechanical Engineering* [online]. 2017, **9**(5), p. 1-12. ISSN 1687-8140, eISSN 1687-8140. Available from: https://doi.org/10.1177/1687814017698662

[25] BONFITTO, A., FERACO, S., ROSSINI, M., CARLOMAGNO, F. Fuzzy logic method for the speed estimation in all-wheel drive electric racing vehicles. *Communications-Scientific Letters of the University of Zilina* [online]. 2021, **23**(2), p. B117-B129. ISSN 1335-4205, eISSN 2585-7878. Available from: https://doi.org/10.26552/com.C.2021.2.B117-B129

[26] BONFITTO, A., FERACO, S., AMATI, N., TONOLI, A. Virtual sensing in high-performance vehicles with artificial intelligence. In: International Design Engineering Technical Conferences and Computers and Information in Engineering Conference IDETC - CIE 2019: proceedings. Vol. 59216. American Society of Mechanical Engineers, 2019. p. V003T01A005.

[27] BONFITTO, A., FERACO, S., TONOLI, A., AMATI, N., MONTI, F. Estimation accuracy and computational cost analysis of artificial neural networks for state of charge estimation in lithium batteries. *Batteries* [online]. 2019, **5**(2), 47. eISSN 2313-0105. Available from: https://doi.org/10.3390/batteries5020047

[28] PROKHOROV, D. Neural networks in automotive applications. In: *Computational intelligence in automotive applications*. PROKHOROV, D. (ed.). Berlin, Heidelberg: Springer, 2008. ISBN 978-3-540-79257-4, p. 101-123.

[29] MARKEVICIUS, V., NAVIKAS, D., IDZKOWSKI, A., ANDRIUKAITIS, D., VALINEVICIUS, A., ZILYS, M. Practical methods for vehicle speed estimation using a microprocessor-embedded system with AMR sensors. *Sensors* [online]. 2018, **18**, 2225. eISSN 1424-8220. Available from: https://doi.org/10.3390/s18072225

[30] WANG, B., GUAN, H., LU, P., ZHANG, A. Road surface condition identification approach based on road characteristic value. *Journal of Terramechanics* [online]. 2014, **56**, p. 103-117. ISSN 0022-4898. Available from: https://doi.org/10.1016/j.jterra.2014.09.001

[31] LIU, C. S., HUEI, P. Road friction coefficient estimation for vehicle path prediction. *Vehicle System Dynamics* [online]. 1996, **25**(sup1), p. 413-425. ISSN 0042-3114, eISSN 1744-5159. Available from: https://doi.org/10.1080/00423119608969210

[32] AGUILAR, J. J. C., CARRILLO, J. A. C., FERNANDEZ, A. J. G., ACOSTA, E. C. Robust road condition detection system using in-vehicle standard sensors. *Sensors* [online]. 2015, **15**(12), p. 32056-32078. eISSN 1424-8220. Available from: https://doi.org/10.3390/s151229908

[33] NGWANGWA, H. M., HEYNS, P. S. Application of an ANN-based methodology for road surface condition identification on mining vehicles and roads. *Journal of Terramechanics* [online]. 2014, **53**, p. 59-74. ISSN 0022-4898. Available from: https://doi.org/10.1016/j.jterra.2014.03.006

[34] VIIKARI, V. V., VARPULA, T., KANTANEN, M. Road condition recognition using 24-GHz automotive radar. *IEEE Transactions on Intelligent Transportation Systems* [online]. 2009, **10**, p. 639-648. ISSN 1558-0016. Available from: https://doi.org/10.1109/TITS.2009.2026307

[35] ASUZU, P., THOMPSON, C. Road condition identification from millimeter-wave radar backscatter measurements. IEEE Radar Conference RadarConf18: proceedings [online]. IEEE. 2018. ISSN 2375-5318. Available from: https://doi.org/10.1109/RADAR.2018.8378522

[36] SHEELA, K. G., DEEPA, S. N. Review on methods to fix number of hidden neurons in neural networks. *Mathematical Problems in Engineering* [online]. 2013, **2013**, 425740. ISSN 1024-123X, eISSN 1563-5147. Available from: https://doi.org/10.1155/2013/425740

[37] GOODFELLOW, I., BENGIO Y., COURVILLE, A. *Deep learning*. Boston, USA: The MIT press, 2016. ISBN 978-0262035613.

[38] OU, G., MURPHEY, Y. L. Multi-class pattern classification using neural networks. *Pattern Recognition* [online]. 2007, **40**(1), p. 4-18. ISSN 0031-3203. Available from: https://doi.org/10.1016/j.patcog.2006.04.041

[39] BONFITTO, A., TONOLI, A., FERACO, S., ZENERINO, E. C., GALLUZZI, R. Pattern recognition neural classifier for fall detection in rock climbing. *Proceedings of the Institution of Mechanical Engineers Part P Journal of Sports Engineering and Technology* [online]. 2019, **233**(4), p. 478-488. ISSN 1754-3371, eISSN 1754-338X. Available from: https://doi.org/10.1177/1754337119850927

[40] WELCH, P. The use of Fast Fourier Transform for the estimation of power spectra: a method based on time averaging over short, modified periodograms. *IEEE Transactions on Audio and Electroacoustics* [online]. 1967, **15**(2), p. 70-73. ISSN 0018-9278, eISSN 1558-2582. Available from: https://doi.org/10.1109/TAU.1967.1161901

[41] RENAUDIN, V., SUSI, M., LACHAPELLE, G. Step length estimation using handheld inertial sensors. *Sensors* [online]. 2012, **12**, p. 8507-8525. eISSN 1424-8220. Available from: https://doi.org/10.3390/s120708507

[42] MANORANJAN, D., HUAN, L. Feature selection for classification. *Intelligent Data Analysis* [online]. 1997, **1**(1-4), p. 131-156. ISSN 1088-467X. Available from: https://doi.org/10.1016/S1088-467X(97)00008-5

[43] JANECEK, A., GANSTERER, W., DEMEL, M., ECKER, G. On the relationship between feature selection and classification accuracy. *Journal of Machine Learning Research: Workshop and Conference Proceedings of Machine Learning Research*. 2008, **4**, p. 90-105. ISSN 1938-7228.

DIAGNOSTICS OF THE ON-VEHICLE SHOCK ABSORBER TESTING

Marek Guzek, Piotr Zdanowicz*

Faculty of Transport, Warsaw University of Technology, Warsaw, Poland

*E-mail of corresponding author: piotr.zdanowicz@pw.edu.pl

Resume

The practical problems that usually come up during the on-vehicle testing of motor car shock absorbers have been discussed. Results of example tests carried out to the EUSAMA standard procedure were compared to the test results obtained with using newer methods, i.e. the phase angle method and half power bandwidth method (HPBM). The issue of incompatibility of the typical excitation applied by diagnostic suspension testers with one that often occurs in the road conditions has also been raised. It has also been shown that the wear of shock absorbers may affect the value of braking deceleration of cars with ABS (anti-lock braking system) when moving on uneven ground.

The main objective of the work was to assess usefulness and reliability of various diagnostic methods intended for the on-vehicle testing of car shock absorbers.

Article info

Received 17 September 2020
Accepted 6 November 2020
Online 8 April 2021

Keywords:

EUSAMA test,
phase angle method,
half power bandwidth method,
experimental tests,
simulation tests

Available online: https://doi.org/10.26552/com.C.2021.3.B178-B186

ISSN 1335-4205 (print version)
ISSN 2585-7878 (online version)

This is an open access article distributed under the terms of the Creative Commons Attribution 4.0 International License (CC BY 4.0), which permits use, distribution, and reproduction in any medium, provided the original publication is properly cited. No use, distribution or reproduction is permitted which does not comply with these terms.

1 Introduction

The technical condition of automotive shock absorbers is essential for vehicle motion safety and occupants' comfort. With development of the damping components of suspension systems, newer and better methods of diagnosing such parts are continuously sought. The "on-vehicle" tests are particularly useful thanks to their low costs and short duration time. Predominantly, "forced vibration tests" are used for this purpose [1-2]. At present, efforts are made in Europe to adopt an identical (standard) vibration excitation method for all the shock absorber testers. As one of the peculiarities of such a method, the stroke of the tester vibration plate is to be constant, equal to e.g. 6 mm, as it is in the case of the EUSAMA machines [1-7]. Unfortunately, such testers, which are the most popular, suffer from a major drawback: the final test result strongly depends on the tire inflation pressure, sprung mass, sliding friction in the suspension system, test conditions, and tester characteristics [1-2, 4, 6-8].

In consideration of the above, the authors decided to verify the reliability and usefulness of the phase angle method [8] and the half power bandwidth method (HPBM) [4] in relation to the classic EUSAMA test, the newer methods are based upon. This was the main objective of this work. At this opportunity, the issue of incompatibility of the typical excitation applied by diagnostic suspension testers with one that often occurs in the road conditions has also been addressed (see also [7]). It has been shown as well that the shock absorbers wear may affect the process of braking a car with the ABS when moving on uneven ground, which has been highlighted by e.g. the authors of [5].

2 Evaluation of the suspension system damping impact on the final results of the rig testing of shock absorbers by various methods

Usefulness and reliability of the diagnostic methods under consideration, used for the on-vehicle testing of motor car shock absorbers, was assessed on the grounds of measurement results obtained with using a prototype tester TUZ-1/E. A short description of the performed tests is presented in Table 1. In every test, a sinusoidal input was applied with a constant amplitude of 3 mm and a frequency declining from about 25 Hz to zero at a rate of 1 Hz/s; the outputs recorded were time histories of the vertical force under the tester vibration plate and of the vertical displacement and acceleration of the plate (necessary to eliminate the distorting impact of the inertial force of this exciter component, see also [6]). All the tests were carried out for the rear suspension system of an Opel Astra II (G) Van, in which the viscous damping was changed stepwise by applying 8 known damping levels γ, varying between 0.131 and 0.511 (see Table 2). Such tests were repeated twice, with the tire

Table 1 *Description of performed tests*

specification	method		
	EUSAMA	phase angle method	HPBM
tester and research object	TUZ-1/E and Opel Astra II (G) Van 		
excitation	for all tests: amplitude 3 mm, initial frequency 25 Hz, range 25 Hz→0; decrease 1 Hz/s		
measurement and processing	• vertical tire-plate force $N(t)$ • vertical plate acceleration $a(t)$ to correction plate inertia effect on vertical force $N(t)$	• vertical plate displacement $x(t)$ • vertical tire-plate force $N(t)$ • vertical plate acceleration $a(t)$ to correction plate inertia effect on vertical force $N(t)$ • frequency based on periods / half-periods $x(t)$	• vertical plate displacement $x(t)$ • vertical tire-plate force $N(t)$ • transformation to the frequency domain $N(\omega)$, $x(\omega)$ (by FFT); determination of frequency response function: $H(\omega)=N(\omega)/x(\omega)$
diagnostic parameter	EUSAMA indicator: $WE=N_{min}/N_{static}\cdot 100\%$	minimum difference value: $\Phi min = 180° - \varphi_{max}$ where: φ_{max} is maximum value of phase angle between x and N in the inter-resonance area	dimensionless dumping level θ based on frequency response function $H(\omega)$

Table 2 *Tested car and tests' conditions*

vehicle:	C-class car Opel Astra II (G) Van, car mass 1090 kg, "quarter" car sprung mass: 160 kg, "quarter" car unsprung mass: 35 kg	
tested vehicle part:	rear suspension	
variable:	dimensionless damping levels γ, 8 cases at range of 0.131 ÷ 0.511	
	the variable damping level was achieved by using (by replacing the original) a shock absorber with a variable damping characteristics	
car state case:	tire pressure p [MPa]	sliding friction Ats_1 [N]
• nominal	0.21	40
• reduced tire pressure	0.1	40
• increased sliding friction	0.21	250

inflation pressure being reduced from nominal 0.21 MPa to 0.1 MPa and the sliding friction in the suspension system being raised from 40 N (nominal value) to 250 N (value obtained by additional sliding friction damper in the suspension system; this situation may correspond to other cases of suspension design solutions, where the level of sliding friction in the suspension may be higher e.g. in suspensions with MacPherson struts or leaf springs); all the other vehicle parameters remained at their nominal levels.

In result of an analysis of results of the EUSAMA test (Figure 1), which were determined from the normal reaction at the tire-exciter contact point (instead of the force measured under the vibration plate, see also [6]), with the main test phase being extended to 25 s, the following has been found:

- The EUSAMA indicator value vs suspension damping curves have degressive shapes.
- For the car, with nominal sliding friction and standard tire inflation pressure, the diagnostic parameter changed here in a very narrow range (from 0 to about 20%).
- The growth of the sliding friction in the suspension system by 210 N could cause here the final test results to be overestimated by as much as 20 percentage points.
- The reduction of the tire inflation pressure from 0.21 MPa to 0.1 MPa could cause a considerable overestimation of the EUSAMA indicator value (even by more than 30 percentage points in this case).

The obtained tire pressure effect qualitatively

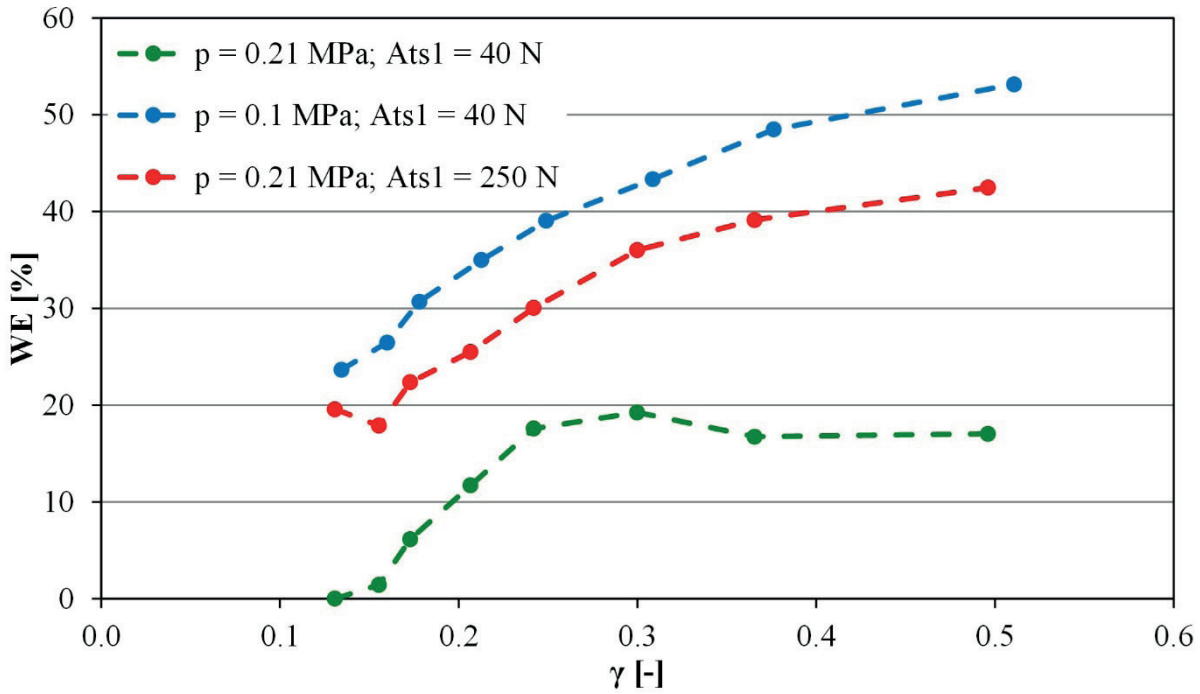


Figure 1 *Example results of diagnostic testing of the rear suspension system of an Opel Astra II (G) Van with using the EUSAMA method, for various levels of viscous damping in the shock absorber, at a nominal and reduced tire inflation pressure (p = 0.21 MPa and p = 0.1 MPa, respectively) and a nominal and raised sliding friction in the suspension system (Ats_1 = 40 N and Ats_1 = 250 N, respectively)*

confirms results known from the literature (see e.g. [1, 8]). The distorting effect of the sliding friction on the test result was presented in [2, 7], as well.

As mentioned in the introduction, the weaknesses of the EUSAMA method mentioned above are the source of search for the new methods. One of them is the phase angle method proposed in [8]. The evaluation criterion is the phase angle Φ between the input excitation (plate displacement) and the response in the form of a force in the tire-plate contact. Results of analogous tests for this method are shown in Figures 2 and 3. Figure 2 shows an example of histories of the phase angle value as a function of frequency for the test with a nominal shock absorber in very good condition (γ = 0.28). Figure 3 shows the criteria values for the assessment of the shock absorber wear - the minima Φ_{min} of the phase angle for different levels of damping in the tested rear suspension.

When usefulness of the phase angle method was assessed, the following was observed:

- At high values of the viscous damping and sliding friction in the suspension system, a minimum of the phase shift angle between the excitation and the tire-exciter contact force may be hardly noticeable or it does not exist at all (Figure 2).
- The minimum phase shift angle value vs suspension damping curves have the degressive shapes (Figure 3).
- For the car with nominal sliding friction and standard tire inflation pressure, the diagnostic parameter changed here in quite a wide range (from 0.4 rad to about 1.2 rad, see Figure 3).
- Reduction of the tire inflation pressure from 0.21 MPa to 0.1 MPa did not cause in this case any considerable changes in the final test results (Figure 3).
- Increase of the sliding friction in the suspension system for 210 N caused here the final test results to be overestimated by as much as 0.7 rad (Figure 3).
- During the test, the frequency drops to zero. However, assessment of the phase angle in the low-frequency area (here below 5÷7 Hz, see Figure 2), due to the highly distorted signals in this frequency range, turned out to be impossible to perform under the real measurement conditions (presence of the higher frequency components, as well as slack and friction in the system, resulted in local extremes, e.g. double maxima, minima, or transitions through the mean value level; as a result, it was not possible to determine the characteristic points on the waveforms and to determine the phase angle).

Summing up, this method shows significant advantages over the classic EUSAMA test (slight influence of tire pressure - see also [1, 8]), but unfortunately, influence of the sliding friction on the test result remains. It has also been shown that there may be situations when determination of the diagnostic parameter value may be impossible (e.g. with very high and low suspension damping).

The third considered method is the method proposed in [4] - the half power bandwidth method (HPBM). Here, too, analysis is performed in the frequency domain. The diagnostic parameter is the dimensionless damping coefficient θ determined based on the spectral function of the force response in the plate-tire contact in relation

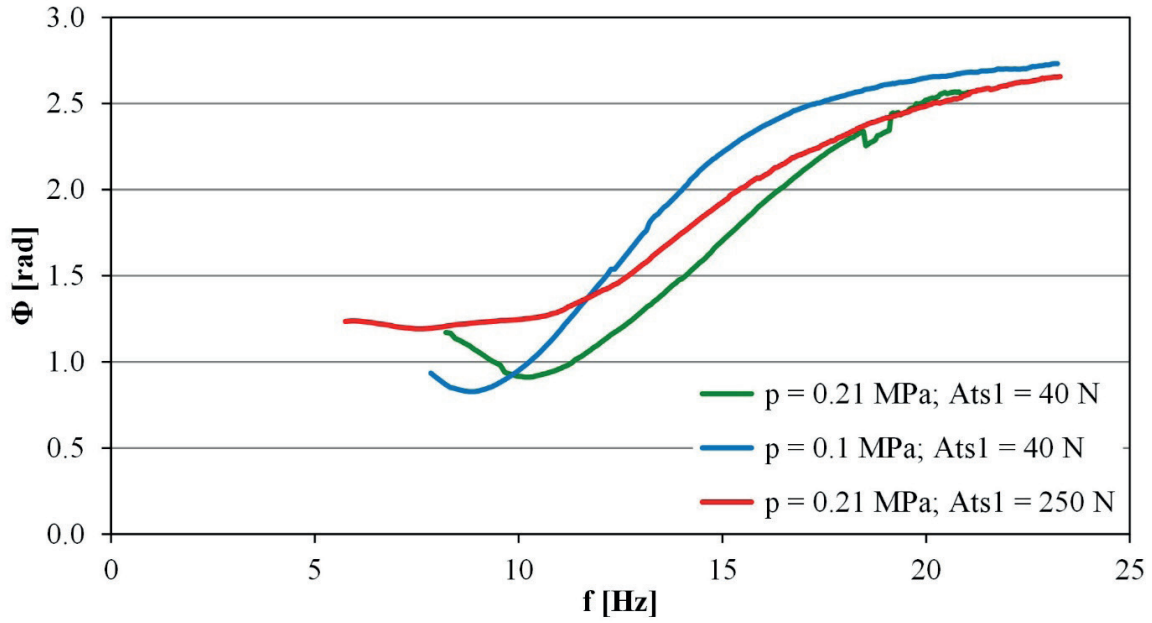


Figure 2 *Example results of diagnostic testing of the rear suspension system of an Opel Astra II (G) Van by the phase angle method, for a shock absorber in a very good condition, at a nominal and reduced tire inflation pressure (p = 0.21 MPa and p = 0.1 MPa, respectively) and a nominal and raised sliding friction in the suspension system (Ats_1 = 40 N and Ats_1 = 250 N, respectively)*

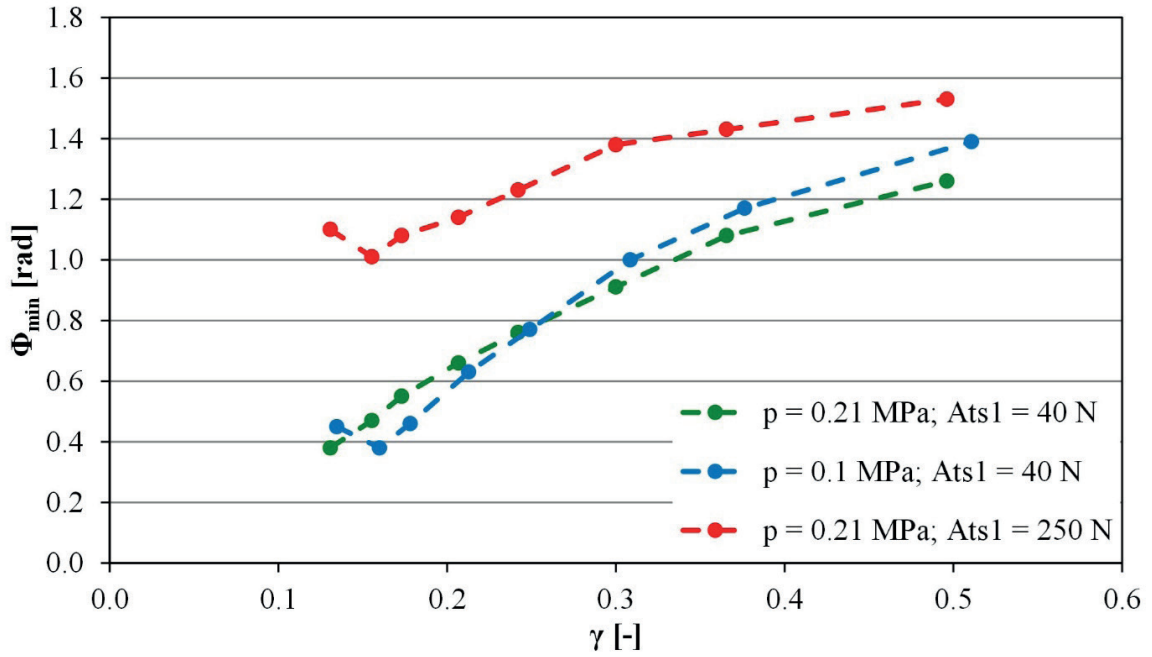


Figure 3 *Example results of diagnostic testing of the rear suspension system of an Opel Astra II (G) Van by the phase angle method, for various levels of viscous damping in the shock absorber, at a nominal and reduced tire inflation pressure (p = 0.21 MPa and p = 0.1 MPa, respectively) and a nominal and raised sliding friction in the suspension system (Ats_1 = 40 N and Ats_1 = 250 N, respectively)*

to the plate displacement. In the presented research, evaluation of the dimensionless damping coefficient using the HPBM method, the force signal recorded on the test rig was used (without eliminating the distorting impact of the force of inertia of the tester vibration plate). Based on appropriate measurements and calculations, the following was ascertained in this case (see Figure 4):

- Parameter θ quite well describes the actual condition of the shock absorber under test, except for excessive damping level (i.e. if $\gamma < 0.25$).
- For the high damping levels ($\gamma > 0.25$), the final results were markedly underestimated.
- The HPBM proved in this case to be rather insensitive to variations in the tire inflation pressure.
- Increase of the sliding friction in the suspension system for 210 N caused here the final test results to be clearly overestimated (even by more than 20 %).

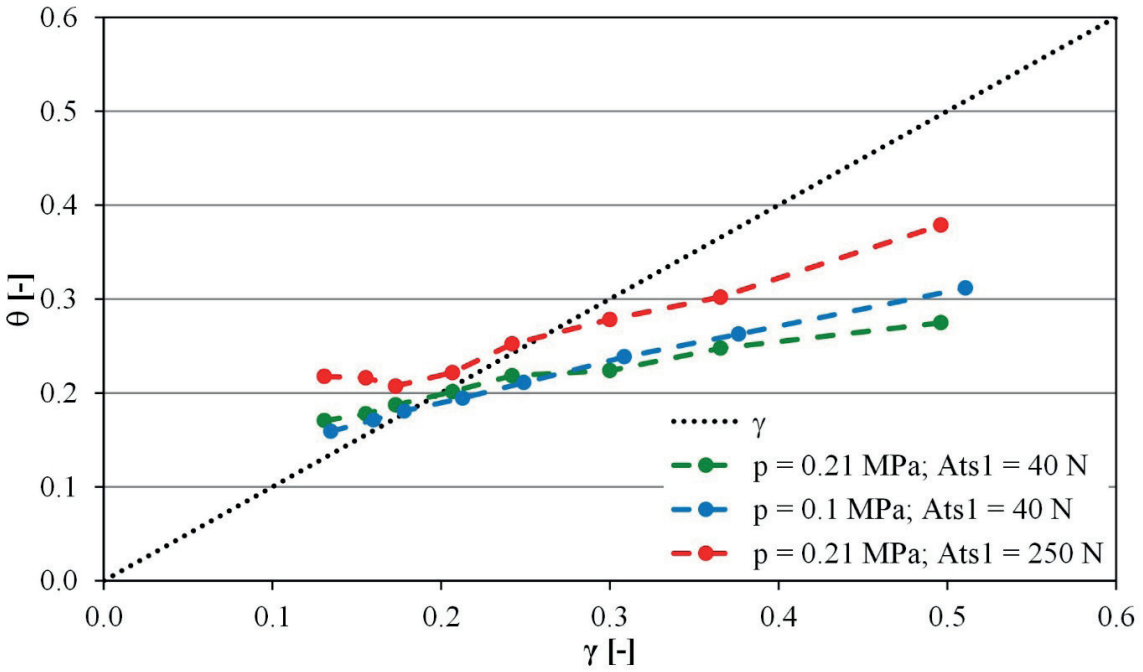


Figure 4 *Example results of diagnostic testing of the rear suspension system of an Opel Astra II (G) Van by the half power bandwidth method (HPBM), for various levels of viscous damping in the shock absorber, at a nominal and reduced tire inflation pressure (p = 0.21 MPa and p = 0.1 MPa, respectively) and a nominal and raised sliding friction in the suspension system (Ats_1 = 40 N and Ats_1 = 250 N, respectively)*

Summing up, based on the results shown, in the case of the HPBM method, we can talk about a slight influence of the tire pressure (see also [4]) and a significant influence of sliding friction. In addition, the method gave good results only in a narrow range of the viscous damping low levels.

3 Comparison, by simulation, of selected operating parameters of the motor car suspension system in a typical diagnostic test and in road conditions

To depict the differences in the vehicle suspension system functioning in a diagnostic test and real road operation conditions, simulation test results were used. This work was done on a front "quarter" of the Isuzu D-max motor vehicle. Although the two transverse arms were provided in the front suspension system of this vehicle, the system was characterized by relatively strong sliding friction force (Ats_1 = 158 N), typical for passenger cars with MacPherson struts.

In the simulations, a non-linear, experimentally verified "quarter-car" model was used (see Figure 5), where the sliding friction in the suspension system and smoothing properties of the tires and also tire separation from the ground ("lift-off") were taken into account (mathematical model - see also [2, 7]). Most of the model parameters had been previously identified in rig tests (main parameters - see Table 3). Only the shock absorber and tire damping were described in a linear form. The viscous damping in the suspension system was changed for the dimensionless coefficient of damping γ to vary from 0 to 0.5 in steps of 0.02 and the tire damping adopted was based on literature data.

Figure 6 shows results of a series of simulations in which the excitation was applied in a form analogous to the EUSAMA test. These are the obtained maximum and minimum values of viscous damping forces as a function of the EUSAMA indicator value (denoted here by "WE"). Due to the low amplitude (3 mm) and moderate frequency (10÷20 Hz) of excitation, at which the final test results are determined, rather low suspension deflection rates are obtained in the EUSAMA test, even if the shock absorbers under tests are worn out very badly. This situation occurs especially when the sliding friction in the suspension is sufficiently high. During such a diagnostic test, the maximum absolute values of the viscous damping force (meant as the force reduced to the vertical axis in the "quarter-car" model) very seldom exceed 500 N, even if the shock absorber condition is very good. One has to be aware of the fact that in the conditions where the EUSAMA test result is good, i.e. the EUSAMA indicator value is higher than 40 %, the amplitude of the viscous damping force only slightly exceeds the value of the force of sliding friction $Fts_{1min/max}$ in the suspension system. If, however, the half-cycle average values are used then the value of the viscous damping force amplitude may turn out to be markedly lower than the value of the sliding friction force. Hence, a statement may be made that the final result of the diagnostic EUSAMA shock absorber testing depends to a considerable degree on the frictional resistance in the suspension system (see also [7]).

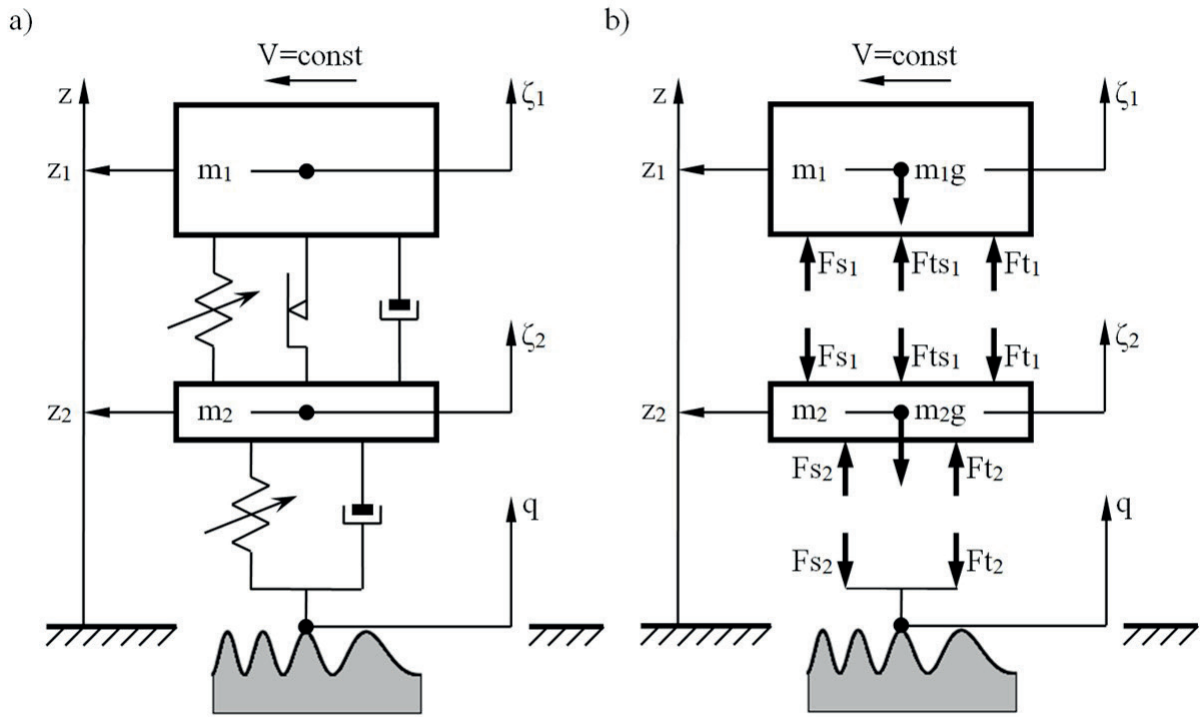


Figure 5 *Nonlinear "quarter-car" model with dry friction in the suspension system: a) general structure; b) system of forces; Fs_1 - elasticity force in the suspension system; Fs_2 - elasticity force in the tire; Ft_1 - viscous damping force in the suspension system; Ft_2 - damping force in the tire; Fts_1 - sliding friction force in the suspension system; m_1 - sprung mass; m_1g - weight of the sprung parts; m_2 - unsprung mass; m_2g - weight of the unsprung parts; q - input displacement; z_1 - coordinate of the centre of the sprung mass; z_2 - coordinate of the centre of the unsprung mass; ζ_1 - vertical axis of the system attached to the sprung mass; ζ_2 - vertical axis of the system attached to the unsprung mass*

Table 3 *Model and simulation parameters*

vehicle:	Isuzu D-Max, mass: 3011 kg
tested vehicle part:	front suspension
masses:	m_1 = 578 kg, m_2 = 69.5 kg
suspension and tire parameters:	nonlinear characteristics of spring elements, nonlinear characteristics of sliding friction, linear tire damping characteristic, for the presented test the linear shock-absorber damping characteristic was assumed; values and characteristics identified on real car
variable:	dimensionless damping levels γ, at range of 0 ÷ 0.5 (c = 0 ÷ 4531 Ns/m)
simulation condition:	car velocity: 25 m/s (90 km/h), excitation (road irregularities): EUSAMA tester sinusoidal signal or C class road by ISO [9] (taking into account the smoothing properties of the vehicle tires)
simulation model code:	Matlab-Simulink

Figure 7 shows the simulation results for the vehicle motion at a speed of 90 km/h on an average road (pavement category C, according to [9]). For the same vehicle, the suspension deflection rates will be much higher. In such suspension system operation conditions, the peak-to-valley values of the viscous damping forces in the shock absorber markedly increase (linearly, in rough terms) with growing relative damping in the suspension system. For the nominal values of vehicle parameters ($\gamma \approx 0.3$), the sliding friction resistance made here merely about 10 % of the viscous damping force in the suspension system and did not have any significant impact on the energy dissipation process of the vertical vehicle vibration. It can also be clearly seen that for the simulation of vehicle motion on an average road (pavement category C), the damping force generated by a nominal shock absorber would be three times as strong as that generated in the EUSAMA test (see also [7]).

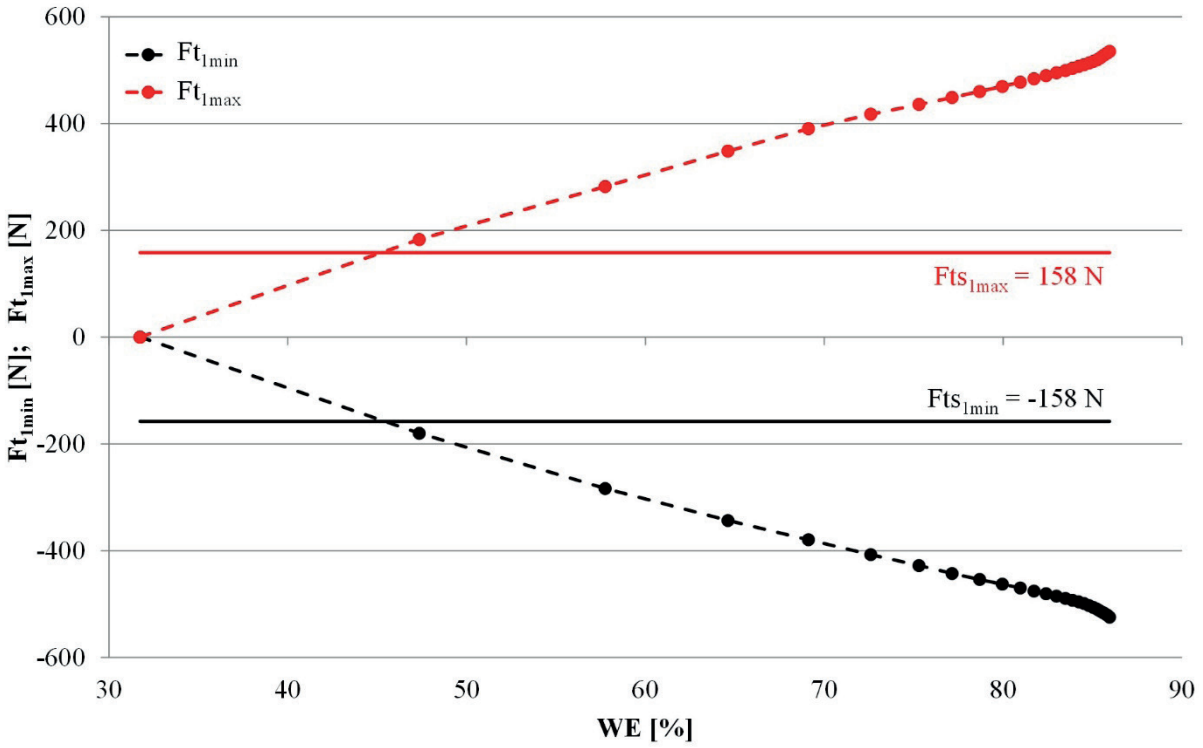


Figure 6 *Example extrema of the viscous damping forces (Ft_{1min} and Ft_{1max}) and sliding friction forces (Fts_{1min} and Fts_{1max}) in the suspension system for various values of the EUSAMA indicator (results of simulation tests with changes in the technical condition of the shock absorber in the front "quarter" of the Isuzu D-max motor vehicle)*

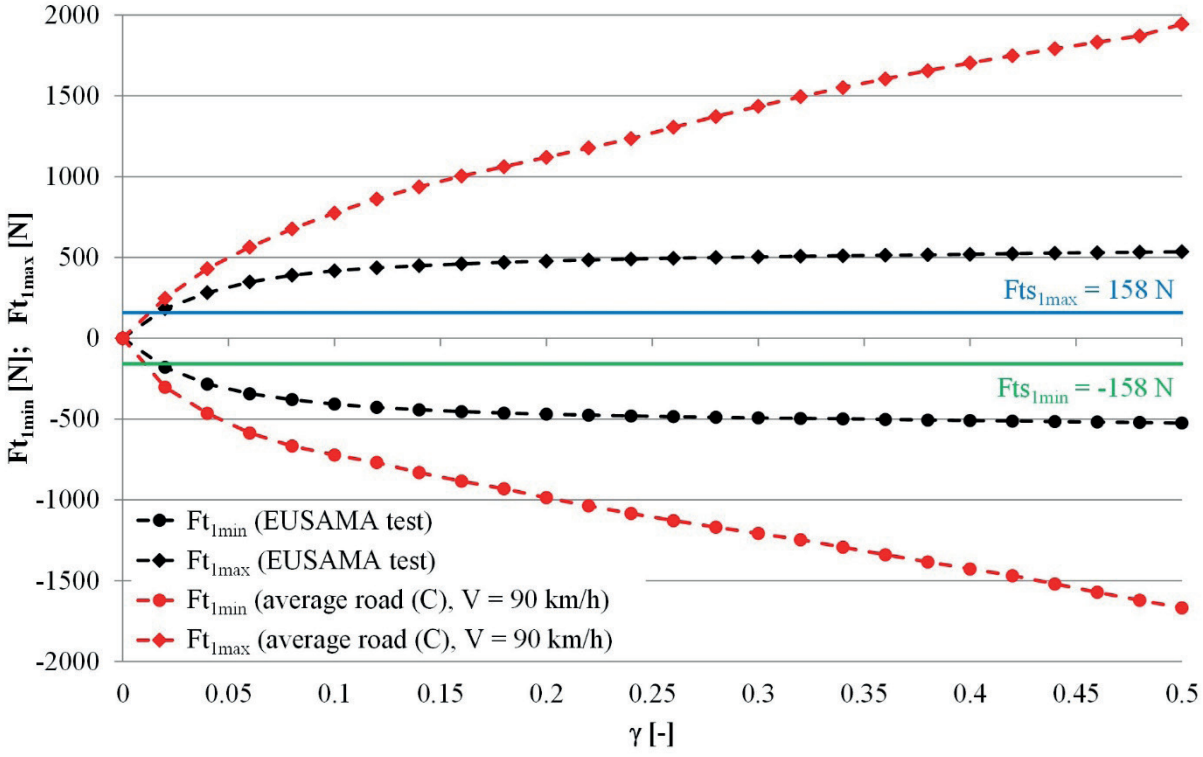


Figure 7 *Comparison of the example extrema of the viscous damping forces (Ft_{1min} and Ft_{1max}) and sliding friction forces (Fts_{1min} and Fts_{1max}) in the vehicle suspension system at various values of the dimensionless damping coefficient in the suspension system (results of a simulation of the EUSAMA test and a test of vertical vibration of the vehicle on an average road (C pavement category) for the front "quarter" of the Isuzu D-max motor vehicle)*

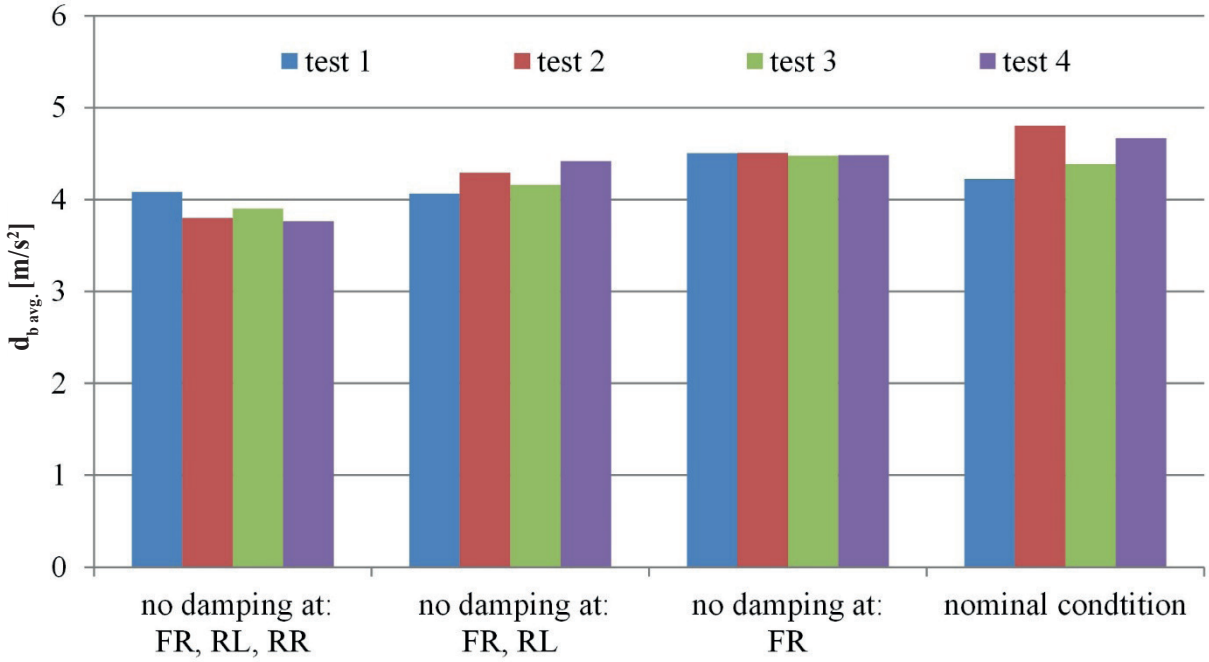


Figure 8 *Comparison of the average braking deceleration values recorded during the tests of an Opel Agila car on a test track section representing a double-track uneven tramway crossing, with various levels of the viscous damping in the car suspension system (FR - front right; RL - rear left; RR - rear right)*

4 Experimental evaluation of the impact of shock absorber wear on vehicle braking deceleration

Since the literature data (e.g. those provided in [5]) show a marked impact of the shock absorber condition on the course of the vehicle braking process, a decision was made to re-verify this information. With this end in view, 16 experimental tests were carried out on an Opel Agila 1.2 Twinport car provided with ABS (car mass ca. 1175 kg).

The tests of vehicle braking from an initial speed of about 50 km/h were carried out on a test track section representing a double-track tramway crossing with rails protruding about 20 mm above the road surface. The dry road pavement was made of concrete slabs, which were unevenly laid and, in consequence, additional vibration typical for crossings of this kind was excited.

The tests were carried out by a decelerometer CL-170 and with recording the braking deceleration and brake pedal force. This force deliberately exceeded the acceptable maximum so that the driver had a limited control over the course of the braking process. The instrument readings, subject to the final assessment, were the average braking deceleration values, determined for the main phase of the braking process. Every test was repeated three times, and 4 tests were carried out within each test series, during which the following vehicle options were examined:

- vehicle in its nominal condition;
- vehicle with no viscous damping in the front right (FR) wheel suspension system;
- vehicle with no viscous damping in the front right (FR) and rear left (RL) wheel suspension system;
- vehicle with no viscous damping in the front right (FR), rear left (RL), and rear right (RR) wheel suspension system.

When analyzing the measurement results presented in Figure 8, one can notice a moderate impact of the viscous damping in the vehicle suspension system on the vehicle braking deceleration value. For the vehicle with 3 shock absorbers damaged, the braking deceleration obtained was lower by about 0.5 m/s^2 to 1 m/s^2 in comparison to that obtained by the vehicle in its nominal condition.

5 Recapitulation and conclusions

The conducted research confirmed the information mentioned in the literature about the disruptive influence of the tire pressure [1, 8] and sliding friction [2, 7] on results of the standard diagnostic tests using the EUSAMA method. The presented results also show that the other analyzed methods (the phase angle method, HPBM) are less sensitive to the above-mentioned disturbances (in particular, lower influence of tire pressure), but also have their drawbacks. Among the diagnostic shock absorber testing methods discussed herein, the most promising one seems to be the phase angle method. On the other hand, the poorest opinion is deserved by the half power bandwidth method (HPBM), which intrinsically may only be used for estimation of the dimensionless damping coefficient in linear systems with one degree of freedom and with a low energy dissipation level. For the reliability and, simultaneously,

usefulness of the EUSAMA test to be raised, this method needs improving. A modification has already been proposed by one of the co-authors of this study, but it cannot be disclosed at present because of a patent application planned.

In all the methods, there is a problem because the excitation applied on a diagnostic test stand is incompatible with the one that often occurs in the real vehicle operation conditions. While the sliding friction in the suspension system can, so to say, "substitute" for the viscous damping during the diagnostic shock absorber test (making the test result satisfactory), it will definitely be insufficient to disperse the vertical vehicle vibration on a road.

The degree of shock absorber wear may have an impact on the course of the vehicle braking process, especially when the vehicle is provided with an ABS and is moving on an uneven ground.

References

[1] STANCZYK, T. L., JURECKI, R. Comparative analysis of testing methods of hydraulic shock absorbers / Analiza porownawcza metod badania amortyzatorow hydraulicznych (in Polish). *Zeszyty Naukowe Instytutu Pojazdow / Proceedings of the Institute of Vehicles* [online]. 2014, **4**(100), p. 25-45 [accessed 2020-08-07]. ISSN 1642-347X. Available from: http://www.zeszyty.simr.pw.edu.pl/artykuly/zn4(100)2014/025_045.pdf

[2] ZDANOWICZ, P. Assessment of the condition of vehicle's shock absorbers with taking into account the dry friction in the suspension system / Ocena stanu amortyzatorow pojazdu z uwzglednieniem tarcia suchego w zawieszeniu (in Polish). Doctoral dissertation. Warsaw: Warsaw University of Technology, Faculty of Transport, 2012.

[3] Recommendation for a performance test specification of an 'on-car' vehicle suspension testing system. Publication TS 02 76. Nottingham: European Shock Absorber Manufacturers Association, 1976.

[4] CALVO, J. A., DIAZ, V., SAN ROMAN, J. L. Establishing inspection criteria to verify the dynamic behaviour of the vehicle suspension system by a platform vibrating test bench. *International Journal of Vehicle Design* [online]. 2005, **38**(4), p. 290-306 [accessed 2020-08-07]. ISSN 0143-3369. Available from: https://doi.org/10.1504/IJVD.2005.007623

[5] CALVO, J. A., DIAZ, V., SAN ROMAN, J. L., GARCIA POZUELO, D. Influence of shock absorber wearing on vehicle brake performance. *International Journal of Automotive Technology* [online]. 2008, **9**(4), p. 467-472 [accessed 2020-08-07]. ISSN 1229-9138. Available from: https://doi.org/10.1007/s12239-008-0056-z

[6] LOZIA, Z., ZDANOWICZ, P. Simulation assessment of the impact of inertia of the vibration plate of a diagnostic suspension tester on results of the EUSAMA test of shock absorbers mounted in a vehicle. *IOP Conference Series: Materials Science and Engineering* [online]. 2018, **421**(2) [accessed 2020-08-07]. ISSN 1757-899X. Available from: https://iopscience.iop.org/article/10.1088/1757-899X/421/2/022018/pdf

[7] ZDANOWICZ, P. Comparative assessment of vertical vibrations of a vehicle on the road and during the EUSAMA test. *IOP Conference Series: Materials Science and Engineering* [online]. 2018, **421**(2) [accessed 2020-08-07]. ISSN 1757-899X. Available from: https://iopscience.iop.org/article/10.1088/1757-899X/421/2/022045/pdf

[8] TSYMBEROV, A. An improved non-intrusive automotive suspension testing apparatus with means to determine the condition of the dampers. *SAE Technical Paper* [online]. 1996, 960735 [accessed 2020-08-07]. ISSN 0148-7191. Available from: https://doi.org/10.4271/960735

[9] 1995 ISO 8608 Mechanical vibration. Road surface profiles. Reporting of measured data.

LABORATORY TESTS OF THE CONTROL OF THE CHILD SEATS USING METHOD FOR THE VIBRATION COMFORT OF CHILDREN TRANSPORTED IN THEM

Andrzej Zuska, Emilia Szumska, Damian Frej*

Department of Automotive Engineering and Transport, Kielce University of Technology, Kielce, Poland

*E-mail of corresponding author: frejdamian@gmail.com

Resume

The article presents results of the laboratory studies of the impact of the child seats mounting method on the vibration comfort of children transported in them. The tested child seats were mounted forward facing the rear seat of a passenger car. The A seat was fastened with the ISOFIX base, while the B seat was fastened with standard car seat belts. During the tests, values of the vertical vibrations were measured on the seat of the child seat, the rear seat of the vehicle and the ISOFIX base. It was noted that the analyzed system, may be characterized by two different vibration transmission chains, which depend on the child seat mounting system (classic seat mounting system and ISOFIX system). These studies show the negative impact of using the ISOFIX base, which is confirmed by the Root Mean Square (RMS) values and the Vibration Dose Value (VDV), determined for the "A" seat secured with the ISOFIX base that were higher than the RMS and VDV for the "B" classic mounted seat.

Available online: https://doi.org/10.26552/com.C.2021.3.B187-B199

Article info

Received 16 September 2020
Accepted 6 November 2020
Online 9 April 2021

Keywords:

vehicle safety,
vibrations,
child seat,
vibrating comfort

ISSN 1335-4205 (print version)
ISSN 2585-7878 (online version)

This is an open access article distributed under the terms of the Creative Commons Attribution 4.0 International License (CC BY 4.0), which permits use, distribution, and reproduction in any medium, provided the original publication is properly cited. No use, distribution or reproduction is permitted which does not comply with these terms.

1 Introduction

In many countries, transporting children in vehicles is possible only with use of appropriate seats, the purpose of which is to protect the children placed in them against the adverse effects of road accidents. The seats should be adjusted to the mass and height of a child. The choice of a child seat due to the rapidly changing anthropometric dimensions of a child should be vehicleried out with a particular vehicle. Proper placement and fastening of a child in the seat is the subject of many studies and scientific studies. Most scientists confirm that one of the main causes of serious injuries and even death of children involved in road accidents is incorrectly fastening the child in the seat. The paper [1] presents an analysis of accidents involving children up to the age of three, which occurred in the USA in 2011-2015. The authors found that more than half of the children involved in these accidents were not properly restrained in the vehicle seat. In the works [2-4] it was noted that improper installation of the seat in the vehicle may increase the risk of the child being injured in an accident. In order to meet social expectations, the authors of the work [5] developed an application for a smartphone, instructing how to properly install the vehicle seat in a vehicle. This application was subject to a questionnaire assessment, which shows that 100% of respondents found it useful and helpful.

A motor vehicle is a highly developed vibrating system, stimulated to vibrations by road surface irregularities and elements of the drive system such as the engine, clutch, gearbox, etc. Vibrations are particularly troublesome during the long journeys and may be a source of discomfort and have a negative impact on human health. Vibrations occurring while driving, depending on their amplitude, frequency and duration of impact, may affect the human body causing physical, physiological or psychological changes. Many scientific works and studies have confirmed the negative impact of vibrations on the human body. Examples can be found, among others in the works [6-8]. The permissible values of acceleration acting on an adult human have been the subject of many studies. For this purpose, both the measurement methods and the maximum vibration values themselves have been regulated by the International Standards Organization (ISO). The permissible values of vibrations affecting the human body are included in ISO 2631-1 [9] and British Standards BS 6841 [10]. Unfortunately, these standards apply only to adults and there are no appropriate standards by which to conduct research and assess the vibration comfort of children. For this purpose, the author of the work [11] proposed a method that allows to estimate the natural frequency of organs and parts of a child's body, based on data collected for an adult.

The concept of vibration comfort is associated with

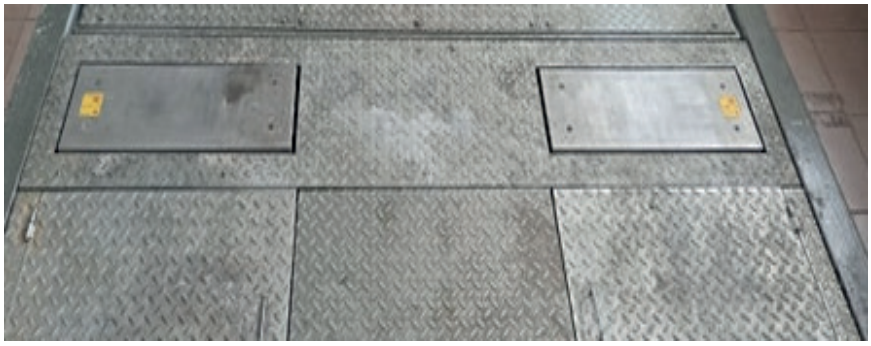


Figure 1 *View on the EUSAMA SA640*

Table 1 *Basic device parameters EUSAMA SA 640 [17]*

frequency of the generated vibrations	0 - 24 Hz
amplitude of generated vibrations	3 mm
the power of the engines	2x 2.5 kW
power protection	3 x 20 A

Table 2 *Technical parameters of child seats*

basic parameters	seat A avionaut aerofix	seat B avionaut pixel
dimensions (cm):		
height	73	44
width	43	58
depth	66	70
own mass (kg)	4	2.5
child's height (cm)	67-105	45-86
child's mass (kg)	up to17.5	up to13

the risk of mechanical vibrations while driving a vehicle. Driving on a road with a relatively smooth surface generates accelerations with a wide frequency range (4-80 Hz), which are transferred to the vehicle body. For travelers it is felt through vibrations of the floor or seats [12]. Driving on uneven roads is particularly uncomfortable for the passengers and the driver of the vehicle.

The topic of the ride comfort of adult vehicle users is now quite thoroughly explored, as opposed to the issue of the comfort of children traveling in vehicle seats. The work [13] presents the results of vibration tests vehicleried out with the use of two child seats while driving on roads with different surfaces. The results showed that the vibrations measured in the seat cushion turned out to be higher than the vibrations in the driver's seat. Similar conclusions were presented in [14]. The presented analysis covers the level of vibrations acting on a child sitting in a vehicle seat with use of a 3-year-old child's dummy and a driver represented by the HYBRID III dummy. The tests were vehicleried out on roads with two different surfaces. The results of the research showed that the vibration comfort of a child sitting in a vehicle seat is worse (by over 10%) compared to the vibration comfort of an adult sitting on a passenger seat in a passenger vehicle. The authors also noted that the incorrect way of mounting the seat has an impact on increase in acceleration in the vertical direction. Results of the research included in [15] show that the degree of wheel imbalance affects the vibration comfort of a child placed in a child safety seat during the journey.

In [16], the authors addressed the issue of ergonomic comfort (convenience) when designing child vehicle seats. The pressure of the child's body on the seat and backrest was analyzed. The result of the research is a model that will enable the manufacturers of vehicle seats to select the appropriate materials and the angle of the backrest to the child's body.

2 Research methodology

The experimental studies were conducted under laboratory conditions. During these tests, the wheels of the rear axle of the test passenger vehicle were made to vibrate using the measuring plates of the EUSAMA SA.640 device (Figure 1). The EUSAMA SA640 (Table 1) device is used to test shock absorbers using the EUSAMA method and is a part of the Bosch Beissbarth diagnostic line, but in these tests it acted as a vibration generator.



a) b)

Figure 2 *View of the ISOFIX base: a) the base with the stabilizing handle folded out, b) the base with the folded stabilizing handle*



a) *b)*

Figure 3 *View of the tested vehicle seats: a)seat for transporting children up to 17,5 kg - „A", b) seat for transporting children up to 13 kg - „B"*

The aim of the experiment was to measure and analyze propagation of the vertical vibrations in two subsystems. One of them consisted of a passenger vehicle rear seat and a child seat with a classic fastening system, while the second subsystem consisted of a rear seat and a child seat with an ISOFIX base.

The ISOFIX base (Figure 2) is a solution that allows you to quickly and securely mount the seat in the vehicle without use of the seat belts. It is attached to the metal ISOFIX brackets located in the gap between the backrest and the vehicle seat with two ISOFIX brackets. Additionally, in the front part of the base there is the so-called leg supporting the base against the floor of a vehicle.

During the experiment, on the left-hand side of the rear seat there was an Avionaut AeroFIX seat for fixing, with an ISOFIX base, while on the right-hand side there was an Avionaut Pixel seat mounted in a classic way, i.e. with 3-point seat belts. The technical specifications of the seats are presented in Table 2.

The „A" seat is Avionaut AeroFIX (Figure 3a), designed to transport children with a height of 67-105 cm and a mass of up to 17.5 kg. The seat has been designed so that one can also transport a child in a rearward-facing position. The height of a rearward-facing child, however, must not exceed 105 cm. The vehicle seat's own mass is 4 kg. The seat has a side protection system that protects the child from the side impacts.

The „B" seat is an Avionaut Pixel (Figure 3b), designed for transporting children mass up to 13 kg and height 45-86 cm. The vehicle seat's own mass is 2.5 kg. The seat is made of a composite material with the EPP ARPRO designation, which does not deform during an impact, but thanks to its flexibility it absorbs energy, distributing it evenly in its structure. The seat is mounted in the vehicle using the Avionaut IQ ISOFIX



a) *b)*

c) *d)*

Figure 4 *Location of three-way sensors during the testing: a) vehicle rear seat under the child seat, b) the seat child seat (gray), c) ISOFIX , d) the seat child seat (red)*

base, which is connected directly to the ISOFIX system available in the vehicle. The correct installation of the seat base is indicated by a sound signal. The child seat can also be attached to the rear seat of a passenger vehicle using the standard seat belts.

During the measurements, the child seats were loaded with a mass imitating the child's mass, which was 5 kg, 7.5 kg, 10 kg, 12.5 kg and 15 kg, respectively. Acceleration on the vehicle's rear seat, child seat base (ISOFIX) and on the seat of child seats were recorded using the three-way acceleration sensors. The location of the three-way sensors during the testing is shown in Figure 4. The sampling frequency of the recorded signal was 1024 Hz.

The vehicle, in which the seats were installed, belongs to the upper-middle class (E segment) and comes from 2009. It was equipped by the air suspension, which could assume four positions: raised, comfortable, automatic and dynamic. During the tests, the suspension was set to the comfort position. The measurements were vehicleried out for three different values of air pressure in the tires, which were respectively: 0.27 MPa, 0.31 MPa and 0.35 MPa.

3 Data analysis

Results of the measurements were used to determine the time courses of truncated accelerations and the indicators for assessing the vibration comfort. Examples of the time courses of vertical vibrations, recorded on the seats of the tested child seats, are shown in Figures 5 to 15. When comparing the time courses of acceleration for the A (red) seat and B (gray) seat, it should be stated that for all the load variants of the seats, the acceleration values recorded on the seat A were greater than on the B seat. The biggest difference between these accelerations was recorded when the seats were loaded with a mass of 5 kg. On the other hand, the smallest when they were loaded with a mass of 10 kg. Due to the low legibility of the recorded signals, additional indicators were used for their further analysis.

The RMS, VDV and SEAT indicators were used to analyze the propagation of vibrations in the tested child seats. Their values, which were determined for selected elements of the tested child seats, are summarized in Table 3. Values of these indicators are presented graphically in Figures 15 to 22. The main assessment

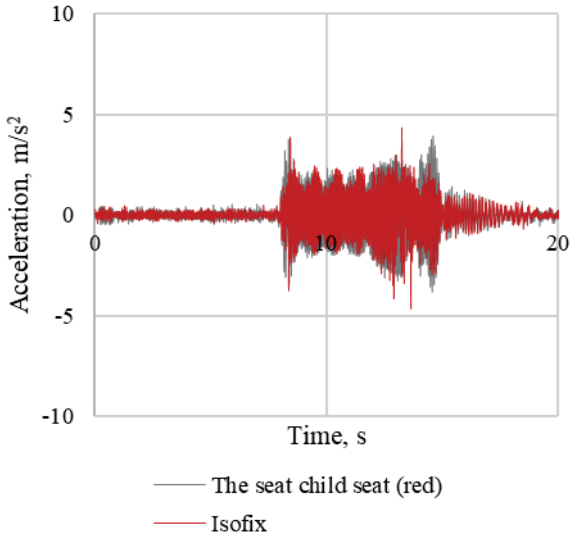


Figure 5 *Vertical accelerations recorded on the seat of the child seat A and on the ISOFIX base (air pressure in the tires 0.31 MPa, mass loading the child seat 15 kg)*

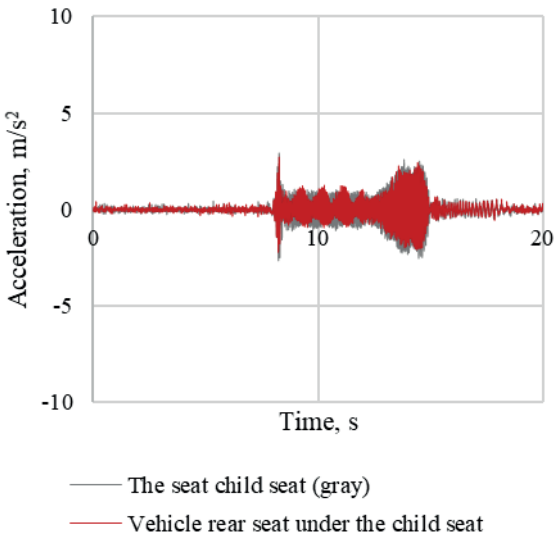


Figure 6 *Vertical accelerations recorded on the seat of the child seat B and the seat of the rear sofa under the seat (air pressure in the tires 0.31 MPa,mass loading the child seat 15 kg)*

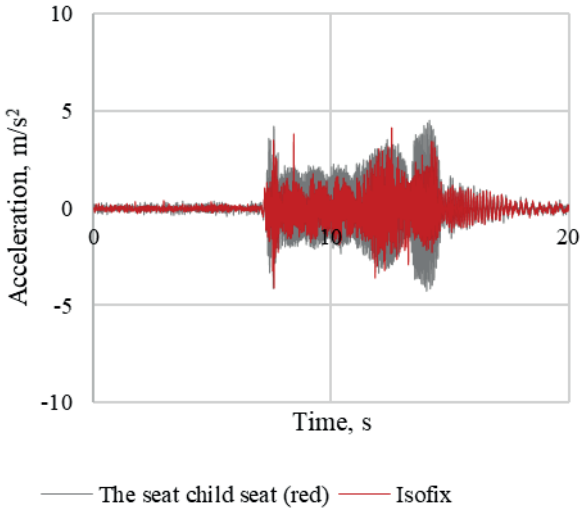


Figure 7 *Vertical accelerations recorded on the child seat A and ISOFIX base (air pressure in the tires 0.31 MPa, mass loading the child seat 12.5 kg)*

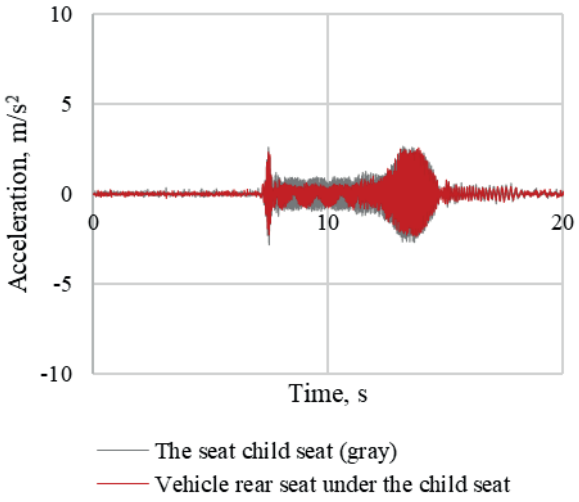


Figure 8 *Vertical accelerations recorded on the seat of the child seat B and the seat of the rear sofa under the seat (air pressure in the tires 0.31 MPa, mass loading the child seat 12.5 kg)*

of the impact of vibrations on vibration comfort while driving is the RMS value of accelerations acting in the direction of vertical - Equation (1). For accelerations *a(t)* registered as the stationary realization of the RMS stochastic process, it is the most common indicator of the vibration comfort assessment [17].

$$r.m.s = \left[\frac{1}{T}\int_0^T a^2(t)dt\right]^{\frac{1}{2}}, \quad (1)$$

where: *a(t)* - recorded as a function of time t, value of acceleration acting in the vertical direction, m/s², *T* - segment of the duration of the measurement, s.

The VDV (Vibration Dose Value) - Equation (2) indicator was developed for vibration analysis of the whole human body. The RMS and VDS values are not correlated with each other, because they accentuate the measured acceleration amplitudes in different ways. Both indicators do not estimate the impact of momentary shocks [17].

$$VDV = \left[\int_0^T a^4(t)dt\right]^{\frac{1}{4}}, \quad (2)$$

where: *a(t)* - the frequency massed acceleration as a function of in time, m/s²,
T - is the duration of measurement in s.

Using the accelerations recorded in selected points of the tested child seat, the SEAT index was determined. This index allows to assess the degree of damping of vibrations transmitted to the seat [5, 17]. This demonstrates the ability of the seat to damp vibrations

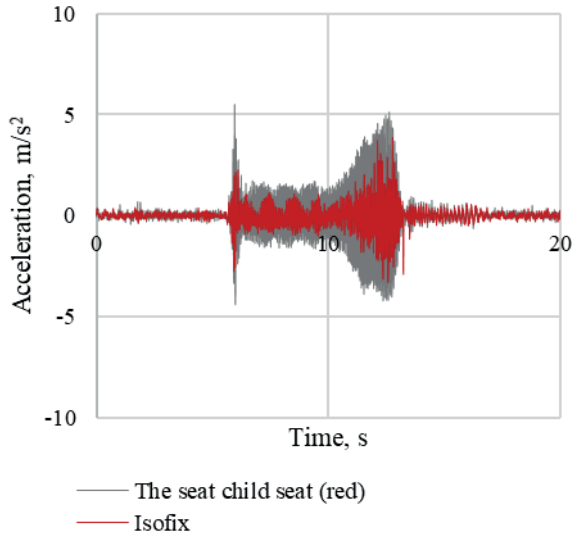


Figure 9 *Vertical accelerations recorded on the seat of the child seat A and on the ISOFIX base (air pressure in the tires 0.31 MPa, mass loading the child seat 10 kg)*

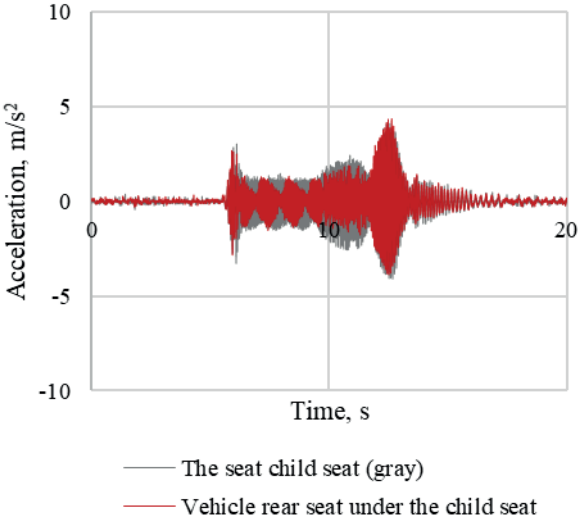


Figure 10 *Vertical accelerations recorded on the seat of the child seat B and the seat of the rear sofa under the seat (air pressure in the tires 0.31 MPa, mass loading the child seat 10 kg)*

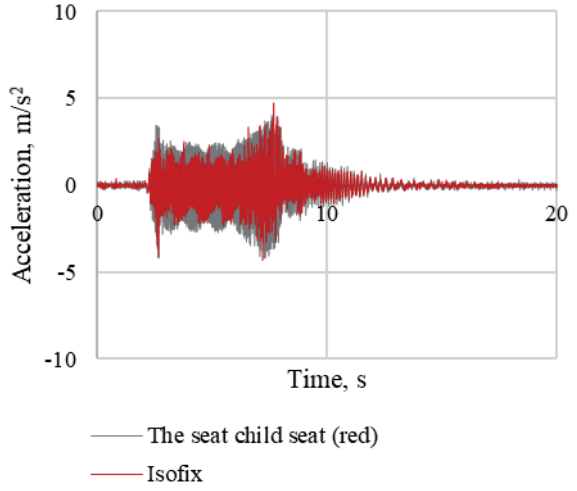


Figure 11 *Vertical accelerations recorded on the seat of the child seat A and on the ISOFIX base (air pressure in the tires 0.31 MPa, mass loading the child seat 7.5 kg)*

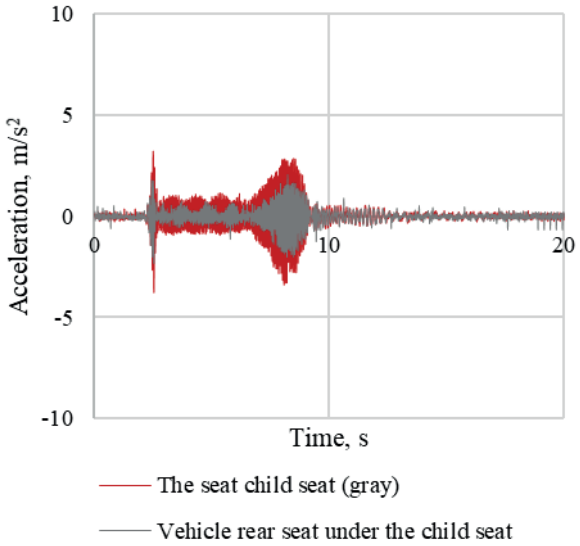


Figure 12 *Vertical accelerations recorded on the seat of the child seat B and the seat of the rear sofa under the seat (air pressure in the tires 0.31 MPa, mass loading the child seat 7.5 kg)*

in a vehicle in such a way as to protect the driver and passengers from excessive vibration. The SEAT value - Equation (3) is used to describe the vibration isolation of the vehicle seat [13, 17].

$$SEAT = \frac{V.D.V_F}{V.D.V_P}, \tag{3}$$

where: $V.D.V_F$ - Vibration Dose Value determined for the vehicle seat,
$V.D.V_P$ - Vibration Dose Value determined for the surface to which the vehicle seat is attached.

Indicator values RMS and VDV were designated for two seats, differing in design. Two different methods were used to mount them - the classic method and the ISOFIXsystem. The tests were vehicleried out for three different values of air pressure in the tires of the test vehicle. During the measurements, the seats were loaded with five different masss: 5kg, 7.5kg, 10kg, 12.5kg and 15kg. Two seats, three values of air pressure in the vehicle wheels and five different masses loading the tested seats, made it possible to conduct thirty different tests (fifteen for each seat). During these tests, the measured values were the vertical acceleration of the seat cushions, the acceleration of the rear seat of the vehicle and the acceleration of the ISOFIX base. Recorded waveforms of acceleration made it possible to determine the RMS and VDV.

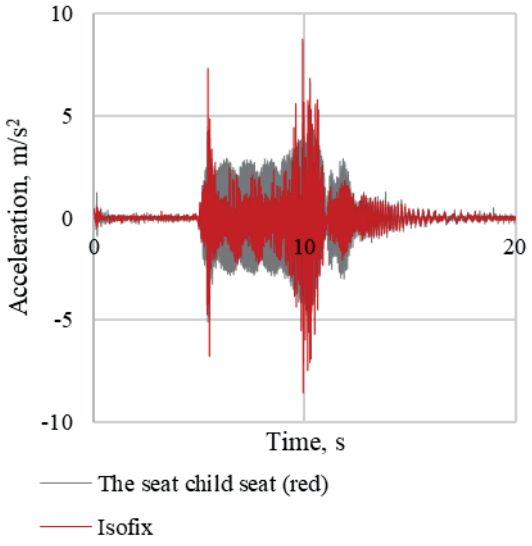


Figure 13 *Vertical accelerations recorded on the seat of the child seat A and on the ISOFIX base (air pressure in the tires 0.31 MPa, mass loading the child seat 5 kg)*

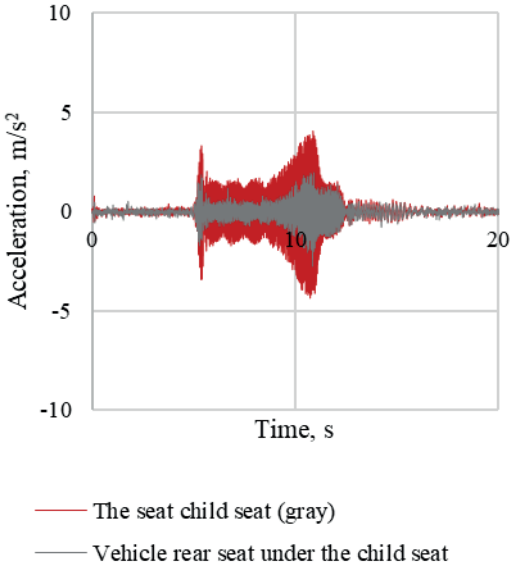


Figure 14 *Vertical accelerations recorded on the seat of the child seat B and the seat of the rear seat under the seat (air pressure in the tires 0.31 MPa, mass loading the child seat 5 kg)*

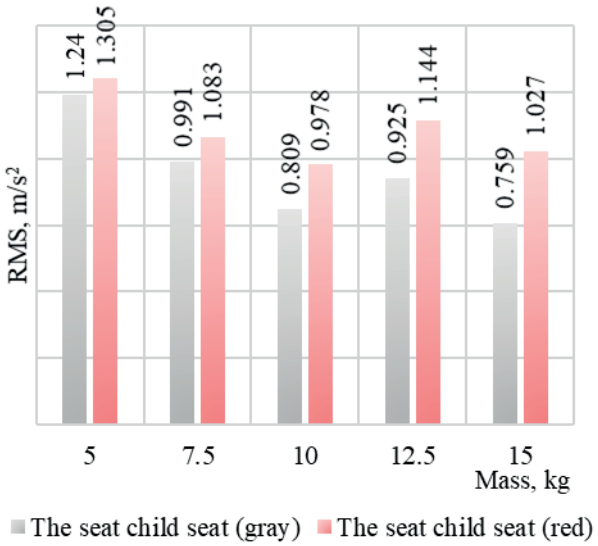


Figure 15 *RMS indicator for the seats of the tested child seats (air pressure in the tires 0.27 MPa)*

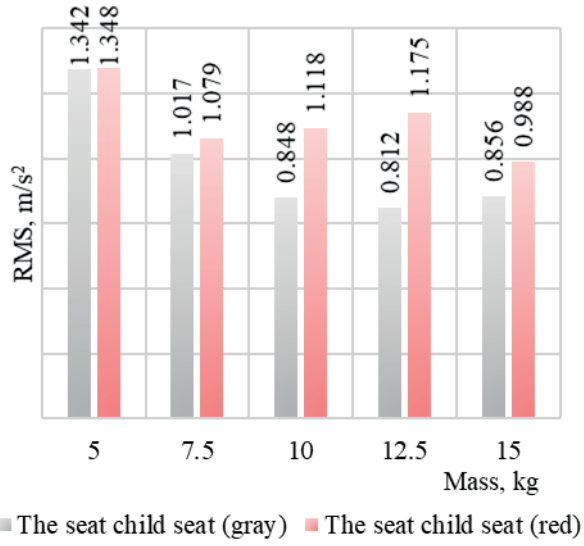


Figure 16 *RMS indicator for the seats of the tested child seats (air pressure in the tires 0.35 MPa)*

Values of RMS determined for the „A" seat mounted in the vehicle with the ISOFIX system are higher than the RMS for the classic „B" seat. The largest difference between the RMS values of the „A" seat and the RMS of the „B" seat, reaching 45%, was recorded only in one case, when the tested seats were loaded with a mass of 12.5 kg and the air pressure in the test vehicle wheels was 0.35 MPa. The influence of air pressure in the test vehicle wheels on the RMS value of the tested seats was insignificant. The vast majority of the RMS value increase for the tested vehicle seats under the influence of pressure increase did not exceed 10%.

Between the values of RMS determined for the „B" (gray) seat fitted in a classic way and the mass loading it, there is a high correlation and this relationship is significant. The correlation coefficient is -0.8 when the air pressure in the wheels of the tested vehicle was 0.31 MPa and increased to -0.86 when the air pressure in the wheels of the tested vehicle was 0.27 MPa. A negative value of the coefficient indicates a negative correlation. This means that the RMS value decreases as the mass loaded on the tested seat increases.

In the case of the „A" (red) seat fixed in the vehicle with the ISOFIX system, the correlation coefficient between the mass loaded on the seat and the RMS for one of the three test series is also high at -0.74. This value was obtained for tests during which the air pressure in the test wheels of the test vehicle was 0.35 MPa. In the

Table 3 *Values of RMS and VDV*

mass loading on the child seat, kg	pressure in tires, MPa	indicator	child seat „B”		child seat „A”	
			location of the acceleration sensor			
			vehicle rear seat under the child seat	the seat child seat	isofix	the seat child seat
5	0.27	RMS	0.543	1.240	0.978	1.305
		VDV	1.689	3.859	4.183	4.089
	0.31	RMS	0.577	1.304	1.075	1.316
		VDV	1.780	4.058	4.687	4.130
	0.35	RMS	0.626	1.342	1.222	1.348
		VDV	1.940	4.213	5.849	4.310
7.5	0.27	RMS	0.604	0.991	0.673	1.083
		VDV	2.036	3.156	2.295	3.409
	0.31	RMS	0.599	1.011	0.829	1.148
		VDV	2.056	3.234	2.843	3.636
	0.35	RMS	0.594	1.017	0.887	1.079
		VDV	2.045	3.237	3.553	3.517
10	0.27	RMS	0.644	0.809	0.655	0.978
		VDV	2.314	2.501	2.236	3.315
	0.31	RMS	0.768	0.943	0.901	0.977
		VDV	2.784	2.959	3.597	3.120
	0.35	RMS	0.641	0.848	0.966	1.118
		VDV	2.274	2.633	3.688	3.549
12.5	0.27	RMS	0.760	0.925	0.716	1.144
		VDV	2.874	3.124	2.353	3.666
	0.31	RMS	0.792	0.948	0.781	1.184
		VDV	2.946	3.161	2.610	3.789
	0.35	RMS	0.666	0.812	0.799	1.175
		VDV	2.413	2.667	2.749	3.756
15	0.27	RMS	0.616	0.759	0.743	1.027
		VDV	2.301	2.447	2.703	3.389
	0.31	RMS	0.765	0.939	0.861	0.998
		VDV	2.756	2.959	3.181	3.157
	0.35	RMS	0.627	0.856	0.917	0.988
		VDV	2.210	2.662	4.135	3.098

other two series, the correlation coefficient between the RMS of a seat „A” and the mass that weighs it on it is on a slightly lower level and ranges from -0.62 to -0.68. It proves a moderate correlation and a significant one.

The VDV values determined for the „A” seat, mounted in the vehicle with the ISOFIX system, are higher than the VDV values determined for the „B” seat, mounted in a conventional manner. These differences increase with increasing air pressure in the test vehicle wheels. The biggest difference between the VDV values of the „A” seat and the VDV of the „B” seat, reaching 40%, was recorded for the case when the tested seats were loaded with a mass of 12.5 kg and the air pressure in the test vehicle wheels was 0.35 MPa.

There is a high correlation between the VDV values determined for the „B” (gray) seat, mounted in a classic way and the mass that loads it and the relationship is significant. It amounted to -0.78 when the air pressure in the wheels of the tested vehicle was 0.27 MPa and increased to -0.85 when the air pressure in the wheels of the tested vehicle was 0.35 MPa. A negative value of the coefficient indicates a negative correlation. This means that the VDV value decreases as the mass loaded on the tested seat increases.

In the case of the „A” (red) seat, mounted in the vehicle with the ISOFIX system, the correlation coefficient for one of the three test series is also high at -0.78. This value was obtained for tests during which the air pressure in the test wheels of the test vehicle

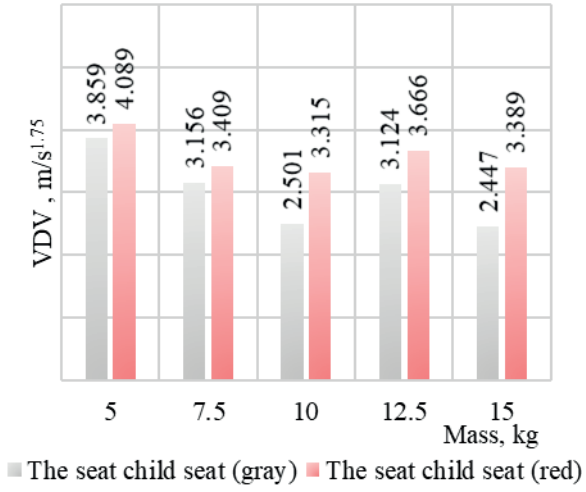


Figure 17 *The VDV indicator for the seats of the tested child seats (air pressure in the tires 0.27 MPa)*

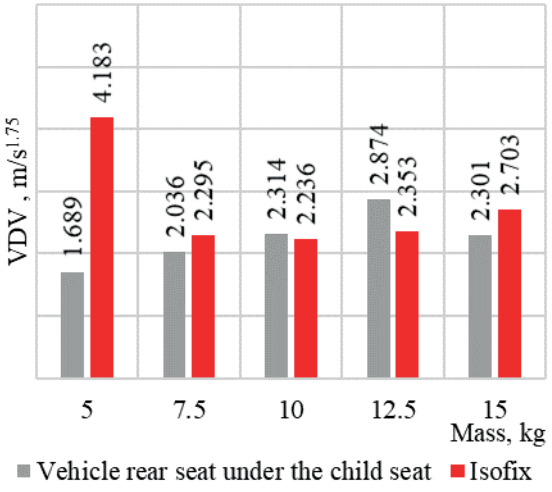


Figure 18 *The VDV indicator for the rear seat under the child seat and ISOFIX base (tire pressure 0.27 MPa)*

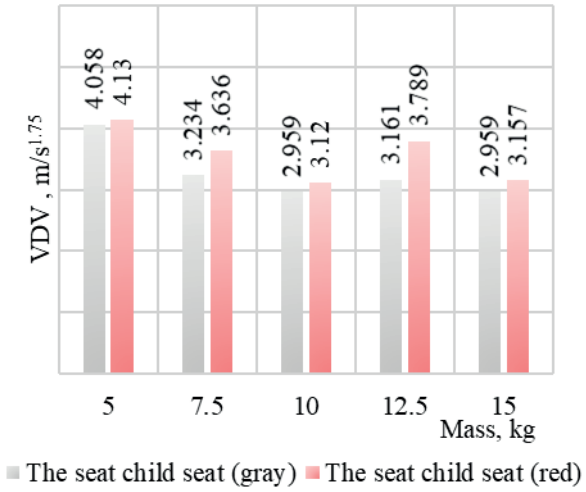


Figure 19 *The VDV indicator for the seats of the tested child seats (air pressure in the tires 0.31 MPa)*

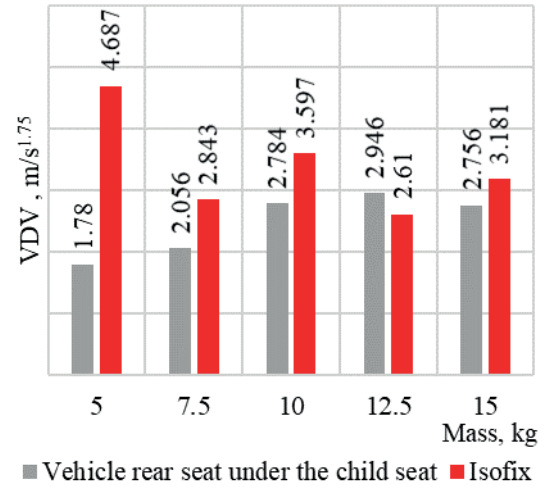


Figure 20 *The VDV indicator for the rear seat under the child seat and ISOFIX base (air pressure in the tires 0.31 MPa)*

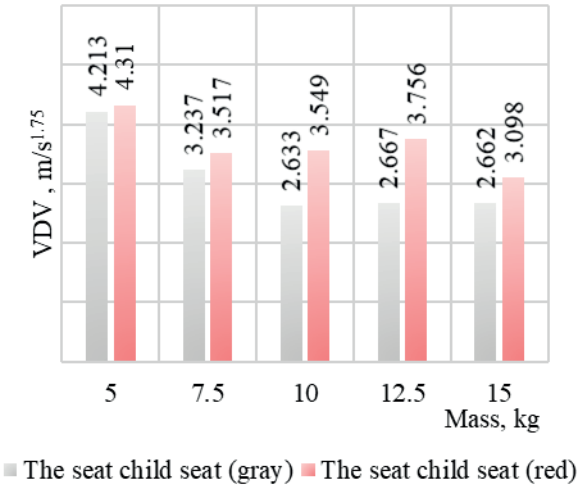


Figure 21 *The VDV indicator for the seats of the tested child seats (air pressure in the tires 0.35 MPa)*

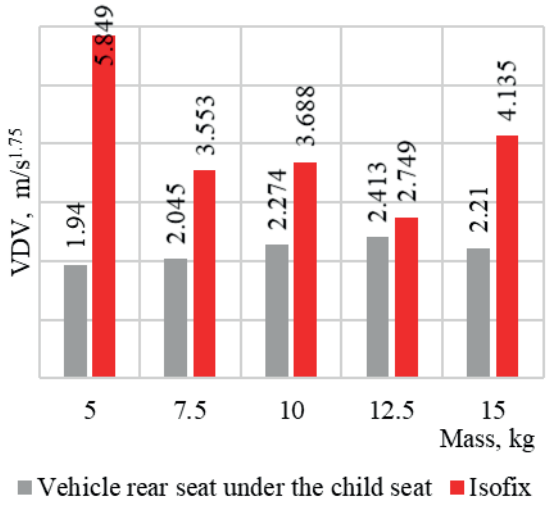


Figure 22 *The VDV indicator for the rear seat under the child seat and ISOFIX base (air pressure in the tires 0.35 MPa)*

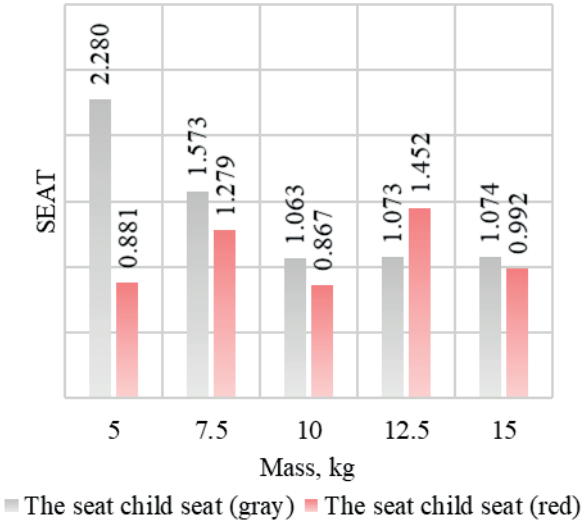


Figure 23 *The SEAT indicator (air pressure in the tires was 0.31 MPa)*

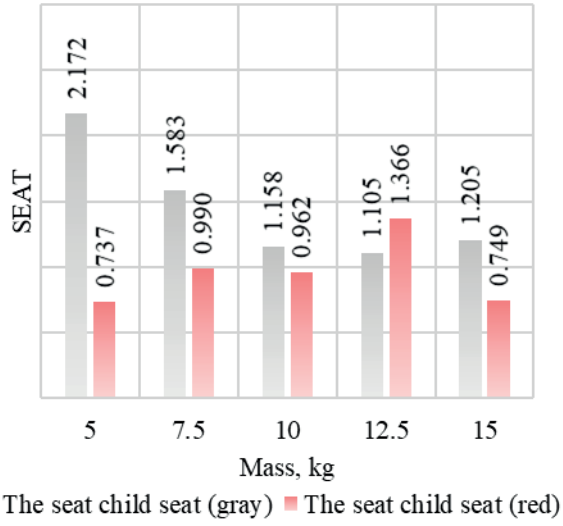


Figure 24 *The SEAT indicator (air pressure in the tires was 0.35 MPa)*

Table 4 *Correlation of the RMS indicator with the mass simulating the mass of a child (tire pressure 0.27 MPa)*

mass simulating the mass of a child	indicator RMS			
	vehicle rear seat under the child seat	the seat child seat B	isofix	the seat child seat A
5	0.543	1.240	0.978	1.305
7.5	0.604	0.991	0.673	1.083
10	0.644	0.809	0.655	0.978
12.5	0.760	0.925	0.716	1.144
15	0.616	0.759	0.743	1.027
correlation coefficient	0.598	-0.861	-0.517	-0.618

Table 5 *Correlation of the RMS indicatorwith the mass simulating the mass of a child (tire pressure 0.31 MPa)*

mass simulating the mass of a child	indicator RMS			
	vehicle rear seat under the child seat	the seat child seat B	isofix	the seat child seat A
5	0.577	1.304	1.075	1.316
7.5	0.599	1.011	0.829	1.148
10	0.768	0.943	0.901	0.977
12.5	0.792	0.948	0.781	1.184
15	0.765	0.939	0.861	0.998
correlation coefficient	0.871	-0.668	-0.801	-0.677

Table 6 *Correlation of the RMS indicator with the mass simulating the mass of a child (tire pressure 0.35 MPa)*

mass simulating the mass of a child	indicator RMS			
	vehicle rear seat under the child seat	the seat child seat B	isofix	the seat child seat A
5	0.626	1.342	1.222	1.348
7.5	0.594	1.017	0.887	1.079
10	0.641	0.848	0.966	1.118
12.5	0.666	0.812	0.799	1.175
15	0.627	0.856	0.917	0.988
correlation coefficient	0.447	-0.692	-0.847	-0.736

Table 7 *Correlation of the VDV indicator with the mass simulating the mass of a child (tire pressure 0.27 MPa)*

mass simulating the mass of a child	indicator VDV			
	vehicle rear seat under the child seat	the seat child seat B	isofix	the seat child seat A
5	1.689	3.859	4.183	4.089
7.5	2.036	3.156	2.295	3.409
10	2.314	2.501	2.236	3.315
12.5	2.874	3.124	2.353	3.666
15	2.301	2.447	2.703	3.389
correlation coefficient	0.750	-0.783	-0.560	-0.570

Table 8 *Correlation of the VDV indicator with the mass simulating the mass of a child (tire pressure 0.31 MPa)*

mass simulating the mass of a child	indicator VDV			
	vehicle rear seat under the child seat	the seat child seat B	isofix	the seat child seat A
5	1.780	4.058	4.687	4.130
7.5	2.056	3.234	2.843	3.636
10	2.784	2.959	3.597	3.120
12.5	2.946	3.161	2.610	3.789
15	2.756	2.959	3.181	3.157
correlation coefficient	0.875	-0.789	0.627	-0.660

Table 9 *Correlation of the indicator VDV with the mass simulating the mass of a child (tire pressure 0.35 MPa)*

mass simulating the mass of a child	indicator VDV			
	vehicle rear seat under the child seat	the seat child seat B	isofix	the seat child seat A
5	1.940	4.213	5.849	4.310
7.5	2.045	3.237	3.553	3.517
10	2.274	2.633	3.688	3.549
12.5	2.413	2.667	2.749	3.756
15	2.210	2.662	4.135	3.098
correlation coefficient	0.768	-0.853	-0.581	-0.783

was 0.35 MPa. In the other two series, the correlation coefficient between the VDV of the „A" seat and the mass loaded on it is somewhat lower. The correlation coefficient for these cases ranged from -0.57 to -0.66. It proves a moderate correlation and a significant one.

Results of the VDV indicator are presented in figures 17-22 Based on the recorded accelerations, the VDV of the ISOFIX base and the VDV of the rear seat were also determined. In twelve cases, the VDV values for the ISOFIX base are higher than the VDV values for the rear bench seat. Only in three cases the situation was reverse and the VDV for the rear seat seat was higher than the VDV for ISOFIX. The increase in pressure in the test vehicle wheels also increased the difference between the VDV of the ISOFIX base and the VDV of the rear seat.

Figures 23 and 24 show the results of the SEAT index for the tested child seats, taking into account the mass representing the mass of the child and the pressure in the tires of the vehicle used for the tests. In most cases, the SEAT index for the B (gray) seat is higher than for the „A" (red) seat. Only in one trial, in which the seats were loaded with a mass of 12.5 kg, the situation was the reverse and the SEAT values for the A (red) seat were higher than the SEAT values for the „B" (gray) seat.

Analyzing the correlation indexes included in Tables 4 to 9, it should be stated that with increase of the weight loading the seat, the value of the VDV index decreases. The correlation coefficient between the mass loaded on the seat and the VDV indicator „B" (gray) ranges from - 0.78 for the case when the pressure in the test vehicle wheels was 0.27 MPa to -0.85 when the pressure in the test vehicle wheels was 0.35 MPa. These values prove the high correlation and the significant dependence.

4 Conclusions

The subject of the research is part of the issue of the vibration comfort of children transported in child seats. The presented research is a part of a whole series of research vehicleried out by employees of the Department of Motor Vehicles and Transport of the Kielce University of Technology.

They concern the spread of vibrations in the following system: vehicle (vehicle floor) - vehicle seat - child seat. It was pointed out that the analyzed system may have two different vibration transmission chains, which depend on the child seat mounting system (classic seat mounting system and ISOFIX system). The paper presents the results of empirical tests vehicleried out at the EUSAMA SA.640 stand, which in these tests acted as a generator of vibrations with a frequency of 0 to 25 Hz. It is noteworthy that the seats were stabilized with the ISOFIX base. It separates the child seat from the rear seat cushion and the seat is attached more securely than with standard seat belts.

However, this method of fastening may cause a reduction in the vibration comfort of children vehicleried in the seat. The negative impact of separating the seats from the rear seat using the ISOFIX base is confirmed by the RMS and VDV determined for the „A" seat secured with the ISOFIX base that were higher than the RMS and VDV for the „B" classic mounted seat.

References

[1] LEE, G., POPE, C. N., NWOSU, A., MCKENZIE, L. B., ZHU, M. Child passenger fatality: child restraint system usage and contributing factors among the youngest passengers from 2011 to 2015. *Journal of Safety Research* [online]. 2019, **70**, p. 33-38. ISSN 0022-4375. Available from: https://doi.org/10.1016/j.jsr.2019.04.001

[2] BLAIR, J., PERDIOS, A., BABUL, S., YOUNG, K., BECKLES, J., PIKE, I., CRIPTON, P., SASGES, D., MULPURI, K., DESAPRIYA, E. The appropriate and inappropriate use of child restraint seats in Manitoba. *International Journal of Injury Control and Safety Promotion* [online]. 2008, **15**(3), p. 151-156. ISSN 1745-7300, eISSN 1745-7319. Available from: https://doi.org/10.1080/17457300802340980

[3] BROWN, J., FINCH, C. F., HATFIELD, J., BILSTON, L. E. Child restraint fitting stations reduce incorrect restraint use among child occupants. *Accident Analysis and Prevention* [online]. 2011, **43**(3), p. 1128-1133. ISSN 0001-4575. Available from: https://doi.org/10.1016/j.aap.2010.12.021

[4] CICCHINO, J. B., JERMAKIAN, J. S. Vehicle characteristics associated with LATCH use and correct use in real-world child restraint installations. *Journal of Safety Research* [online]. 2015, **53**, p. 77-85. ISSN 0022-4375. Available from: https://doi.org/10.1016/j.jsr.2015.03.009

[5] SCHWEBEL, D. C. TILLMAN, M. A, CREW, M., MULLER, M., JOHNSTON, A. Using interactive virtual presence to support accurate installation of child restraints: efficacy and parental perceptions. *Journal of Safety Research* [online]. 2017, **62**, p. 235-243. ISSN 0022-4375. Available from: https://doi.org/10.1016/j.jsr.2017.06.018

[6] KRAJNAK, K. Health effects associated with occupational exposure to hand-arm or whole body vibration. *Journal of Toxicology and Environmental Health, Part B arch* [online]. 2018, **21**(5), p. 320-334. ISSN 1093-7404, eISSN 1521-6950. Available from: https://doi.org/10.1080/10937404.2018.1557576

[7] QASSEM, W., OTHMAN, M. O., ABDUL-MAJEED, S. The effects of vertical and horizontal vibrations on the human body. *Medical Engineering and Physics* [online]. 1994, **16**(2), p. 151-161. ISSN 1350-4533. Available from: https://doi.org/10.1016/1350-4533(94)90028-0

[8] TROXEL, W. M., HELMUS, T. C., TSANG, F., PRICE, C. C. *Evaluating the impact of whole-body vibration (WBV) on fatigue and the implications for driver safety*. Santa Monica, Calif.: RAND Corporation, RR-1057-BOSE, 2015.

[9] ISO 2631-1: 1997 Mechanical vibration and shock. Evaluation of human exposure to whole-body vibration. Part 1: General requirements.

[10] BS 6841: 1987 Guide to measurement and evaluation of human exposure to whole-body mechanical vibration and repeated shock.

[11] WIECKOWSKI, D. An attempt to estimate natural frequencies of parts of the child's body / Proba oszacowania czestotliwosci drgan wlasnych czesci ciala dziecka (in Polish). *The Archives of Automotive Engineering - Archiwum Motoryzacji*. 2012, **55**(1), p. 61-74. ISSN 1234-754X, eISSN 2084-476X.

[12] WIECKOWSKI, D. Analysis domain of the time vertical vibration on account comfort child during ride in the vehicle / Analiza w dziedzinie czasu drgan pionowych ze wzgledu na komfort podrozowania dzieckaw samochodzie (in Polish). *Technical Transactions - Czasopismo Techniczne*. 2012,**10**(5-M), p. 73-91. ISSN 0011-4561, eISSN 2353-737X.

[13] GIACOMIN, J. Some observations regarding the vibrational environment in child safety seats. *Applied Ergonomics* [online. 2000, **31**(2), p. 207-215. ISSN 0003-6870. Available from: https://doi.org/10.1016/S0003-6870(99)00034-4

[14] WICHER, J., WIECKOWSKI, D. Influence of vibrations of the child seat on the comfort of child's ride in a vehicle / Wplyw drgan fotelika samochodowego na komfort podrozowania dziecka w samochodzie (in Polish). *Eksploatacja i Niezawodnosc*. 2010, **4**(48), p. 102-110. ISSN 1507-2711.

[15] FREJ, D., GRABSKI, P. The impact of the unbalanced rear wheel on the vibrating comfort of the child seat. *Transportation Research Procedia* [online]. 2019, **40**, p. 678-685. ISSN 2352-1465. Available from: https://doi.org/10.1016/j.trpro.2019.07.096

[16] LAI, H. - H., CHEN, CH. - H., CHEN, Y. - CH., YEH, J. - W., LAI, CH. F. Product design evaluation model of child vehicle seat using gray relational analysis. *Advanced Engineering Informatics* [online]. 2009, **23**(2), p. 165-173. ISSN 1474-0346. Available from: https://doi.org/10.1016/j.aei.2008.10.009

[17] FREJ, D., ZUSKA, A., CADGE, K. Analysis of vertical vibrations affecting a child transported in a child seat during a car passing over the release speed bump. *The Archives of Automotive Engineering - Archiwum Motoryzacji* [online]. 2019, **86**(4), p. 111-125. ISSN 1234-754X, eISSN 2084-476X. Available from: https://doi.org/10.14669/AM.VOL86.ART8

ASSESSMENT OF THE CONSTRUCTIONALITY OF THE STRUCTURE IN THE ASSEMBLY PROCESSES

Józef Matuszek[1], Tomasz Seneta[1], Ľuboslav Dulina[1], Eleonóra Bigošová[2,*]

[1]Department of Production Engineering, Faculty of Mechanical Engineering and Computer Science, University of Technology and Humanities in Bielsko-Biala, Poland
[2]Department of Industrial Engineering, Faculty of Mechanical Engineering, University of Zilina, Zilina, Slovakia

*E-mail of corresponding author: eleonora.bigosova@fstroj.uniza.sk

Resume
The paper presents the methodology of designing the production process of a new product from the point of view of the criterion of the assembly operations technology (Design for Assembly - DFA) in the automotive industry. The article describes methods and techniques used during the implementation of a new product into production. The impact of the methods on improving the assembly technology of a complex product is described. Suggestions for improving for unit and small series production are presented.

Article info
Received 12 November 2020
Accepted 29 November 2020
Online 14 April 2021

Keywords:
production process design,
construction manufacturability,
unit,
small-lot production

Available online: https://doi.org/10.26552/com.C.2021.3.B200-B210

ISSN 1335-4205 (print version)
ISSN 2585-7878 (online version)

This is an open access article distributed under the terms of the Creative Commons Attribution 4.0 International License (CC BY 4.0), which permits use, distribution, and reproduction in any medium, provided the original publication is properly cited. No use, distribution or reproduction is permitted which does not comply with these terms.

1 Introduction

To evaluate the technology of the assembly and defined guidelines for shaping the design process due to PDM (Product Data Management - PDM), different methods may be used. In the automotive industry, widely recognised methods known as DFA were proposed and described for the first time by G. Boothroyd and P. Dewhurst in 1983. The DFA methods are constantly being refined due to technical progress. They allow a more efficient evaluation of the possibility of reducing the number of product components and estimating the costs of machining processes and assembly of the analysed product. By introducing the DFA methods into the design process, the new product design team can propose improved design solutions, which are characterized by better indicators, simpler construction and components, which directly affect the simplification of assembly operations.

The most popular methods of the DFA practice are Lucas DFA, Boothroyd and Dewhurst (B & D), Hitachi AEM. [1-3].

Development of machining technology (thanks to the automation and extension of the possibility of making objects of complex construction), in connection with a significant share of manual work in the assembly processes of finished products, has led to a change in the approach to the production of new products. There has been a development of methods of determining the production costs. The share of assembly costs in the production costs of products has greatly increased [4-6]. The design process of the new product is shown in Figure 1.

The design process should be determined from the point of view of different usability criteria. The assessment is based on marketing and conceptual preparation; documentation - construction, production and organization; implementation of the production process; distribution; conditions for the operation and decommissioning of the product.

2 Proposal to modify the methods to assess the manufacturability design

2.1 Input assumptions

As a part of the work, based on analysing and comparing existing methods and algorithms to improve the product's technological efficiency, it was proposed to improve the abovementioned assessment methods.

The presented methods are focused on activities that reduce assembly times, which ultimately reduces the costs of assembly operations. An additional factor that reduces assembly times is the unification and standardization of product components, which can be

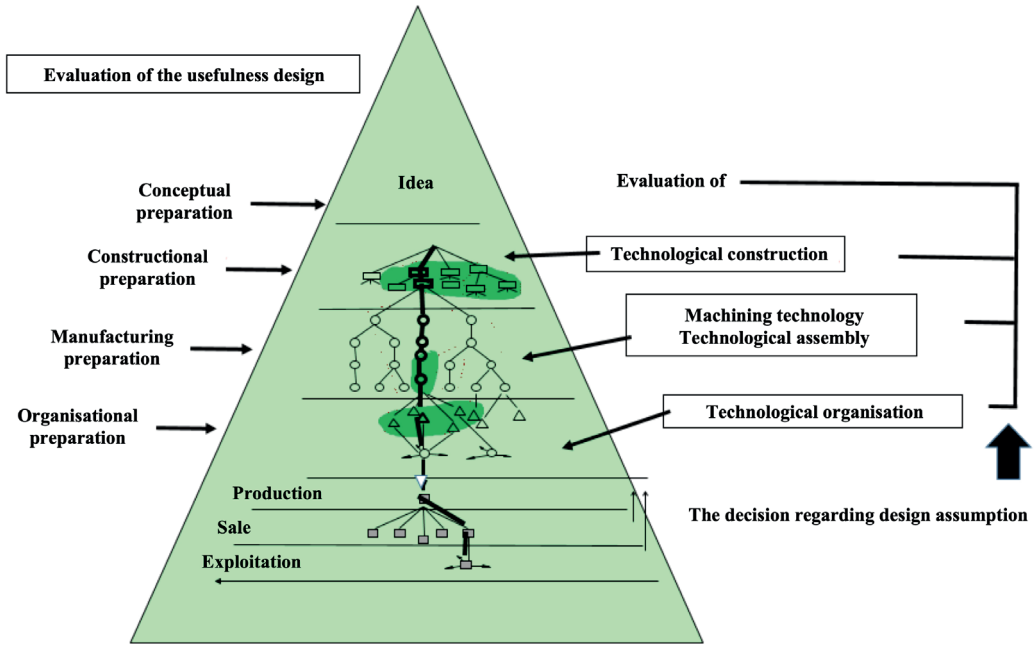


Figure 1 *The course of designing the production process of a new product [6]*

determined by an index of component unification. The unification of the product components allows, in turn, to rationalize production processes in the form of group processing applications. The proposed improvement of the above methods meets the development trends in the automotive industry consisting of continuous linear improvement of product design, use of components included in the assembly in many versions and brands of final products [7-8].

The presented methods of assessing manufacturability of the structure may also be used in the production of other products. As an example can be presented analysis of the structure's efficiency on the single-stage gear transmission used to drive devices installed on means of transport example (Figure 1) [9-11].

2.2 Modified Boothroyd Dewhurst DFA and Lucas DFA methods

The final stage in the Boothroyd & Dewhurst DFA method is calculation for which it is necessary to know the sum of the number of operations, the total time of the operation, the total costs of the operation, the theoretical minimum number of parts and the $DFMA_{index}$ [12-13].

In the Lucas DFA method, it is necessary to know the project performance indicator ($W_{ep} = DFMA_{index}$), manoeuvrability (W_{man}) and assemblability (W_{mon}). Determination of the abovementioned quantities to determine the effects of rationalization takes place before and after the assessment of technology [14].

Similarly, for a more detailed analysis, the authors propose to define the technological indicators for both above-mentioned methods, with a view to harmonising the components of the product and the possibility of using the group processing and increasing serial production. The structure efficiency index after analysis for unified and standardised components is:

$$Wtk_{UNK} = (C_{UNK}/C_t).100\% \quad (1)$$

where: Wtk_{UNK} - the structure efficiency index for unified and standardised components
C_{UNK} - the sum of unified and standardized assembly components,
C_t - total components.

The structure efficiency index after the analysis of component structure, enabling group processing is:

$$Wtk_{OG} = (C_{OG}/C_t).100\% \quad (2)$$

where: Wtk_{OG} - the structure efficiency index of component structure enabling group processing
C_{OG} - the sum of the components that can potentially be implemented using the group processing technologies in manufacturing processes,
C_t - total components.

3 Examples

3.1 The Boothroyd and Dewhurst DFA method

According to the Boothroyd & Dewhurst DFA method for the gear prototype design (Figure 1), the assembly process was defined, the fragment of which is presented in Tables 1-3. The DFMA indicator before making the change is [15]:

$$\mathrm{DFMA}_{\mathrm{index}} = (t_a \cdot L_o)/T_o, \quad (3)$$

for many parts, it can be assumed that: $L_o = A$ and where:
DFMAindex - the project performance indicator,
A - number of parts necessary for functioning of the product (it was assumed in the study that $L_o = A = C_t$),
t_a - assembly time of the basic ideal part (based on Boothoroyd; t_a = 3s),
T_o - total assembly time of the product).

$$DFMA_{index} = (3 \cdot L_o) / T_o, \quad (4)$$

where: L_o - the total number of operations to assembly ($L_o = A$),

For each assembled part and for each defined step of the assembly process, the following values were determined:

$$L_o = \Sigma l_{oi}, \; T_o = I_{man} + I_{mon} = \Sigma T_{man} + \Sigma T_{mon}, \quad (5)$$

where: l_{oi} - i-th assembly operation,
I_{man} - manipulation index for a given part of the product,
I_{mon} - assembly index for a given part of the product,
T_{man} - time manipulation index for the given product,
T_{mon} - assembly time for a given component of the product.

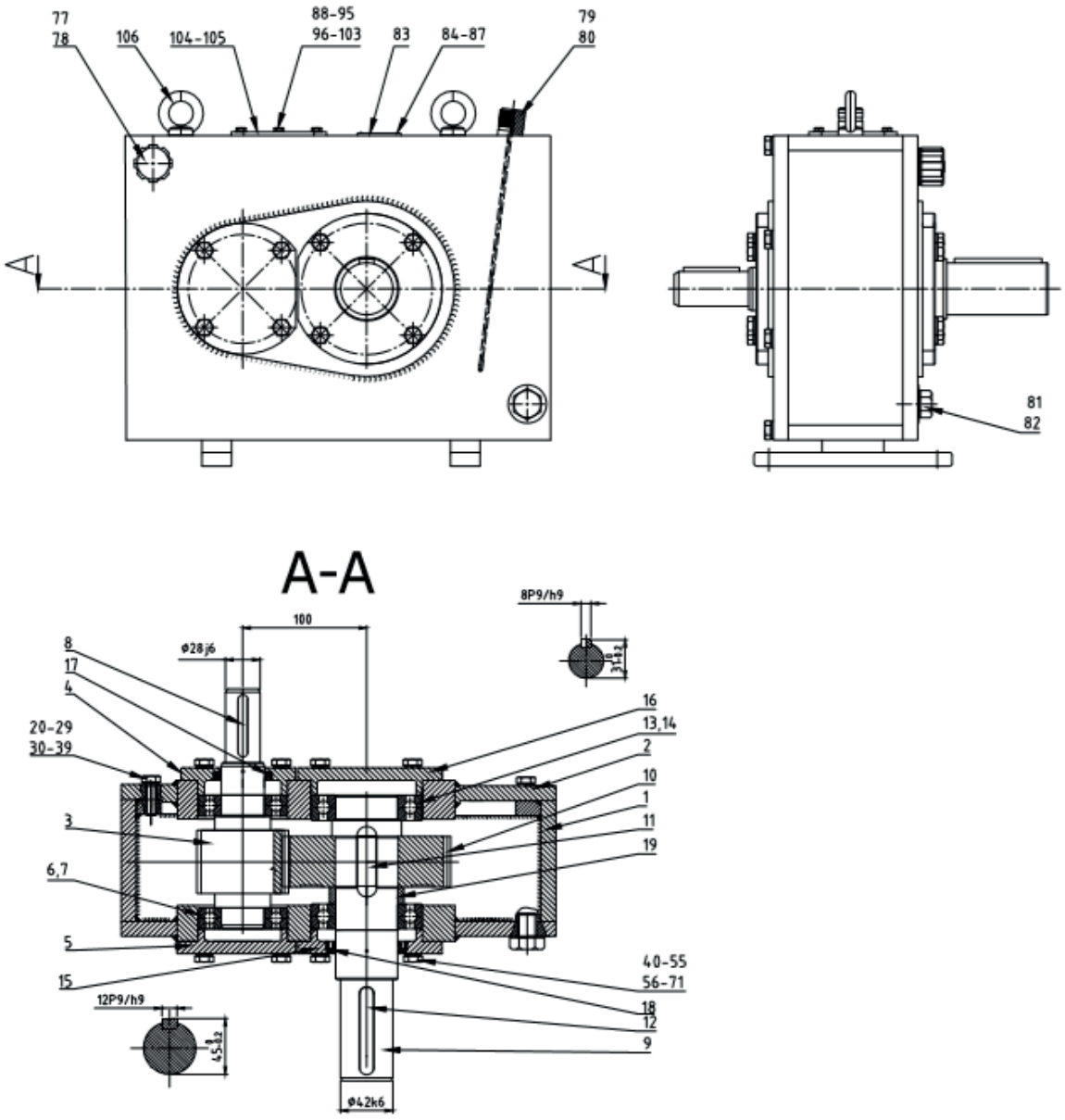


Figure 2 *Diagram of the gear unit being analysed*
1 - body, 2 - cover, 3 - pinion, 4 - pinion cover I, 5 - pinion cover II, 6- 7 - bearings pinion, 8 - pinion key, 9 - shaft, 10 - gear, 11 - gear key, 12 - shaft key, 13-14 - bearings shaft , 15 - shaft cover I, 16 - shaft cover II, 17 - pinion seal, 18 - shaft seal, 19 - spacer rings, 20-29 - body bolts, 30-39 - bolt washers to the body, 40-55 - cover bolts, 56-71 - bolt washers for covers, 72-76 - Monolith gasket, 77-78 - vent with cover gasket, 79-80 - oil gauge with gasket, 81 - oil plug, 82 - oil plug gasket, 83 - nameplate, 84-87 - rivet pin, 88-95 - sight glass screws, 96-103 - washers for sight glass screws , 104 - sight glass gasket, 105 - sight glass

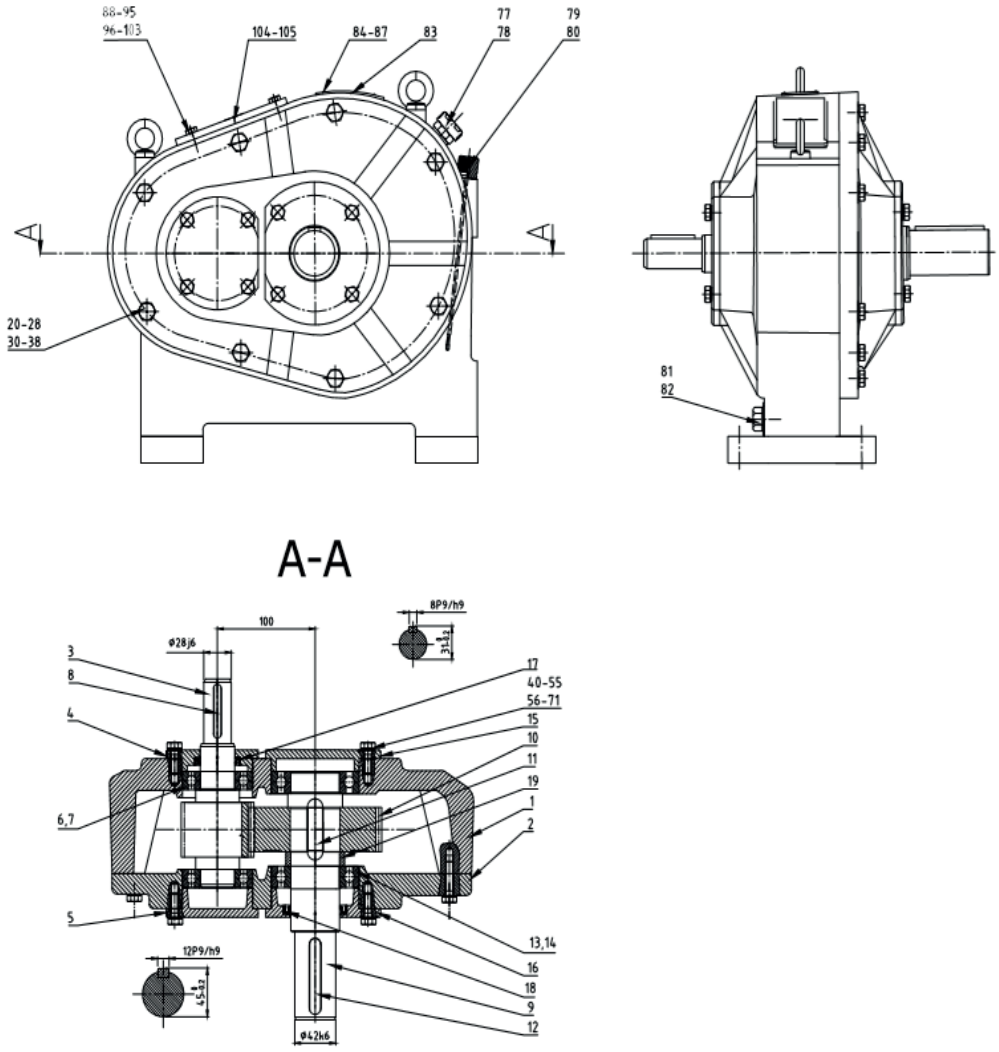


Figure 3 *Diagram of the gear unit analysed*
1 - body, 2 - cover, 3 - pinion, 4 - pinion cover I, 5 - pinion cover II, 6- 7 - bearings pinion, 8 - pinion key, 9 - shaft, 10 - gear, 11 - gear key, 12 - shaft key, 13-14 - bearings shaft , 15 - shaft cover I, 16 - shaft cover II, 17 - pinion seal, 18 - shaft seal, 19 - spacer rings, 20-29 - body bolts, 30-39 - bolt washers to the body, 40-55 - cover bolts, 56-71 - bolt washers for covers, 72-76 - Monolith gasket, 77-78 - vent with cover gasket, 79-80 - oil gauge with gasket, 81 - oil plug, 82 - oil plug gasket, 83 - nameplate, 84-87 - rivet pin, 88-95 - sight glass screws, 96-103 - washers for sight glass screws , 104 - sight glass gasket, 105 - sight glass

To improve the gear assembly technology, design of the proposed gear was changed (Figure 2). The change was adapted to the production conditions depending on the serial production. Limiting the scope of changes resulting from the serial production is forced by the costs of machining and assembly itself, which, with significant changes improving the technology of the structure, requires costly tooling (workshop aids) related to machining and assembly. Such changes are profitable in the conditions of mass production [16-18].

The gearbox dimensions result (Figure 2) from the ratio i = 1.95, the number of pinion teeth z_1= 22; the gear wheel z_2 = 43; the module m_n=3.00 mm, the tooth angle inclination β = 10°, the width of the teeth b = 15 m_n.

For the mass production, the material and form of the body were changed, from the welded structure to the cast structure with the division perpendicular to the axis of the shafts. This way, two bearing caps were eliminated, the remaining caps would be pressed in, thus eliminating washers and screws; the assembly of individual components was replaced for the assembly of assemblies that will only be mounted vertically using tooling. In unit and small-lot production similarly, it was proposed to change the body to a cast form, but the division of the body parallel to the shaft axis was kept. At the same time, the same construction form was used to assemble gears of different sizes (different transmitted powers) and different ratios, materials and forms of pinion and gear wheels were unified, ensuring constant unified inter-axle distances and unified different ratios at individual gear stages (from the same elements gears are also mounted in multi-stage gears); the diameters of bearing openings have been unified, - pinion units with mounted bearings, shaft with mounted gear wheel and bearings mounted on the shaft are mounted to the gear

Table 1 *Results of the technology analysis by the Boothroyd & Dewhurst method of the gearbox*

details of assembly and components				product data			
no.	description	initial assumption of the process	repetitions of activities	thickness (t mm)	size (s mm)	rotation alpha (°)	rotation beta (°)
1	main housing no.1	pick up	1	120	309	360	360
2	bearing no.6	press to main housing no.1	1	17	72	180	0
3	bearing no.13	press to main housing no.1	1	20	90	180	0
4	main shaft no.3	press to bearing no.6	1	37	194	360	0
5	slow-speed shaft no.9	pick up	1	28	216	360	360
8	spacer no. 19	assembly on shaft subassy	1	4	60	180	0
9	preheat gear no.9	preheat gear no.9 to 180 deg.	1				
10	shaft subassy	press to bearing no.14	1	136	216	360	360
11	cover no.2	pick up	1	25	288	360	360
12	bearing no.7	press to cover no.16	1	17	72	180	0
13	bearing no.14	press to cover no.15	1	20	90	180	0
18	spring washer z8.2	assem with screw	10	4	14	180	0
19	screw with washer	tighten cover no.2 to main housing	10	4	20	360	0
20	cover no.5	pick up	1	16	100	360	360
21	screw m8x20	pick up	4	4	20	360	0
22	spring washer z8.2	assem with screw	4	4	14	180	0
23	monolith seal	sealing	1				
24	screw with washer	tighten cover 5 to main housing no.1	4	4	14	180	0
	total number of parts/operations before changes		113				
for serial and mass production. after the change - 32 (theoretically 22), including unified elements - 23 (theoretically 13), including workpieces - 9, in group machining - 7 (theoretically also 9 and 7 respectively)							

body, washers, screws fastening covers to the body were unified, the whole series was unified gears, sight glasses and their fastening elements, workshop aids have been unified related to gear machining and assembly (e.g. bearing assembly, for sealing contact surfaces) [19-20].

Results of the technological analysis (for changes made for the mass production) are presented in Tables 1-3. In addition, the table provides data on transmission parts after a performance analysis for the conditions of the unit and small-lot production [21].

Based on the data set out in Tables 1-3, the following indicators of the gear structure design were obtained (the analyses assumed that $L_o = A = C_e$):

Indicator before the gear structure changes is (Figure 2):

$$DFMA_{wpz} = (3 \cdot A / T_{ipz}).100\% = \\ = (3 \cdot 105/683.19).100\% = 46\%. \quad (6)$$

Indicator after the changes for Unit and small-lot production:

$$DFMA_{wpo} = (3 \cdot A / T_{ipz}).100\% = \\ = (3 \cdot 85/683.19).100\% = 37\%. \quad (7)$$

After the changes for serial and mass production (Figure 3):

$$DFMA_{wpo} = (3 \cdot A / T_{ipz}) .100\% = \\ = (3 \cdot 32/683.19).100\% = 14\%. \quad (8)$$

Theoretical indicator (for the theoretical number of parts - 22, after inserting the push-fit connections and eliminating subsequent fasteners):

$$DFMA_{wpo} = (3 \cdot / T_{ipo}).100\% = \\ = (3 \cdot 22/683.19).100\% = 10\%, \quad (9)$$

where:
$DFMA_{wpz}$ - indicator before the gear structure changes,
$DFMA_{wpo}$ - indicator after changes made to the gear design,
S_{tpz} - number of A-type transmission components before changes,
S_{tpz} - number of A-type transmission components before the changes,
T_{ipz} - gearbox assembly time before structural changes,
T_{ipo} - gearbox assembly time after the structural changes.

According to calculations, it can be stated that the

Table 2 *Results of the technology analysis by the Boothroyd & Dewhurst method of the gearbox -Continue*

details of assembly and components				manoeuvrability		assemblability		operation time index
no.	description	initial assumption of the process	repetitions of activities	code	time index	code	time index	
1	main housing no.1	pick up	1	30	1.95	00	1.5	3.45
2	bearing no.6	press to main housing no.1	1	00	1.13	31	5.0	6.13
3	bearing no.13	press to main housing no.1	1	00	1.13	31	5.0	6.13
4	main shaft no.3	press to bearing no.6	1	88	6.35	41	7.5	13.85
5	slow-speed shaft no.9	pick up	1	30	1.95			1.95
8	spacer no. 19	assembly on shaft subassy	1	00	1.13	01	2.5	3.63
9	preheat gear no.9	preheat gear no.9 to 180 deg.	1			99	12.0	12.00
10	shaft subassy	press to bearing no.14	1	30	1.95	51	9.0	10.95
11	cover no.2	pick up	1	30	1.95			1.95
12	bearing no.7	press to cover no.16	1	00	1.13	31	5.0	6.13
13	bearing no.14	press to cover no.15	1	00	1.13	31	5.0	6.13
18	spring washer z8.2	assem with screw	10	05	1.84	06	5.5	73.40
19	screw with washer	tighten cover no.2 to main housing	10	10	1.5	38	6.0	75.00
20	cover no.5	pick up	1	30	1.95			1.95
21	screw m8x20	pick up	4	10	1.5			6.00
22	spring washer z8.2	assem with screw	4	05	1.84	06	5.5	29.36
23	monolith seal	sealing	1			99	12.0	12.00
24	screw with washer	tighten cover 5 to main housing no.1	4	10	1.5	38	6.0	30.00
total number of parts/operations before changes			113	total operating time before changes				683.19
for serial and mass production. after the change - 32 (theoretically 22), including unified elements - 23 (theoretically 13), including workpieces - 9, in group machining - 7 (theoretically also 9 and 7 respectively)				for piece and small batch production, after the change - 85, including unified elements - 71, including workpieces - 14, in group machining - 12				

results of the analysis for a cast iron gear body are better than the results of the analysis for a welded body gear. The DFMA project performance index should be as low as possible before the change it is 46% after changes depending on the production series 37% and 14% respectively.

3.2 Lucas DFA method

According to the Lucas DFA method, the same design of a single-stage gear prototype was analysed (Figure 1). For each assembled part and each defined step (Table 4 and 5) of the assembly process, the values of individual method indicators were determined. Results of the analysis for the assumed assembly process are presented in Tables 4 and 5. The table summarizes selected examples of operations assigning them an analysis of functionality (W_{ep}) (in the form of parts belonging to group *A* or *B*), manouvering (W_{man}), assemblability (W_{mon}) and additional operations. Data related to additional operations can be found in the Sec column [22].

The formula describing functionality W_{ep} is:

$$W_{ep} = L_{kA} / L_{kA} + L_{kB} = 23(23+82) = 0.22\ (22\%), \quad (10)$$

where: L_{kA} - number of components *A* (fulfilling the functions of a product),
L_{kB} - number of components *B* (characterised by a lack of product function e.g. rivets, washers).

Formula describing manoeuvring W_{man} is:

$$W_{man} = I_{man}/L_{kA} = 67.2/23 = 2.92, \quad (11)$$

where: I_{man} - manouvering index,
L_{kA} - number of components A.

Formula describing assemblability W_{mon} is:

$$W_{mon} = (W_m + W_d)/L_{kA} = 284.2/23 = 12.36, \quad (12)$$

Table 3 *Results of the technology analysis by the Boothroyd & Dewhurst method of the gearbox - Continue*

details of assembly and components				theoretical minimum number of parts/operations			
no.	description	initial assumption of the process	repetitions of activities	relative movement	another material	separation of parts	needed?
1	main housing no.1	pick up	1	N	N	Y	
2	bearing no.6	press to main housing no.1	1	Y	Y	Y	1
3	bearing no.13	press to main housing no.1	1	Y	Y	Y	1
4	main shaft no.3	press to bearing no.6	1	Y	N	Y	1
5	slow-speed shaft no.9	pick up	1	Y	N	Y	1
8	spacer no. 19	assembly on shaft subassy	1	N	N	N	0
9	preheat gear no.9	preheat gear no.9 to 180 deg.	1	N	N	N	0
10	shaft subassy	press to bearing no.14	1	Y	Y	Y	1
11	cover no.2	pick up	1	N	N	Y	1
12	bearing no.7	press to cover no.16	1	Y	Y	Y	1
13	bearing no.14	press to cover no.15	1	Y	Y	Y	1
18	spring washer z8.2	assem with screw	10	N	N	N	0
19	screw with washer	tighten cover no.2 to main housing	10	N	N	N	0
20	cover no.5	pick up	1	N	N	Y	1
21	screw m8x20	pick up	4	N	N	N	0
22	spring washer z8.2	assem with screw	4	N	N	N	0
23	monolith seal	sealing	1	N	Y	N	1
24	screw with washer	tighten cover 5 to main housing no.1	4	N	N	N	0
total number of parts/operations before changes			113	theoretical minimum number of parts/operations			22
for serial and mass production. after the change - 32 (theoretically 22), including unified elements - 23 (theoretically 13), including workpieces - 9, in group machining - 7 (theoretically also 9 and 7 respectively)				for piece and small batch production, after the change - 85, including unified elements - 71, including workpieces - 14, in group machining - 12			

where:
W_m - main activity indicator wherein, $W_m = L_{mA} + L_{mB} + L_{mC} + L_{mD} + L_{mE} + L_{mF}$,
W_d - indicator of additional activities, values making up the W_m and W_d parameters are specified in tables provided by the authors of the method,
L_{kA} - number of the type A parts.

Description of calculations presented above is presented in Table 4 and 5. In the example presented, the developed structure (Figure 1) is non-technological from the point of view of the possibility of implementation into production in conditions of high-volume production. In the applied assessment method, the project efficiency index was obtained at the level of W_{ep} = 22% (authors of publications [23-24] give a minimum value of 60%) and W_{man} = 2.92 and W_{mon} = 12.36 (where both indicators should be less than 2.5).

To improve the technology of the gearbox structure, the same changes were made as in the previously described method. Below are the indicators for the case of the unit and small-lot production, as well as for mass-production.

Based on the performed analysis, the number of parts of type A is 23 (L_{kA}), the number of type B is 62 (L_{kB}) for a piece and small series production.

Formulas describing functionality W_{ep} after the changes are:

$$W_{ep} = L_{kA} / L_{kA} + L_{kB} = 23(23+62) = 0.27\ (27\ \%). \quad (13)$$

Based on the new data, after the changes specified in Tables 4 and 5, the manoeuvring index I_{man} is:

$$I_{man} = L_{mA} + L_{mB} + L_{mC} + L_{mD} = 58, \quad (14)$$

where:
L_{mA} = 42,
L_{mB} = 7.7,
L_{mC} = 2.7,
L_{mD} = 5.6.

The formula for the manoeuvring factor W_{man} (W_d = 0) after the changes is:

$$W_{man} = I_{man} / L_{kA} = 58/23 = 2.52. \quad (15)$$

Table 4 *Results of the gear assembly technology analysis*

details of assembly and components				handling analysis				
no.	step of assembly	description	functional analysis	A	B	C	D	Sum
1	pick up	body no.1	A	3	0	0	0	3
2	pressing to body	bearing no.6	A	1	0.4	0	0	1.4
3								
4	pressing to body	bearing no.13	A	1	0.4	0	0	1.4
5								
6	pressing to bearing no.6	pinion shaft no.3	A	1	0	0.1	0.2	1.3
8	pick up	main shaft no.9	A	1	0	0.1	0.2	1.3
9	assembly	wedge 11	B	1	0	0	0.2	1.2
10	assembly on shaft subassy	gear 7	B	1	0.4	0.1	0.2	1.7
11	assembly on shaft subassy	spacer sleeve 19	B	1	0	0	0	1
13								
18								
55	assembly on shaft subassy	prismatic wedge 12	B	1	0	0	0.2	1.2
56	assembly to the body	vent 77	A	1	0	0.1	0.2	1.3
57	assembly to the body							
58	assembly to the body	oil indicator 79	A	1	0	0.1	0.2	1.3
59								
60	assembly to the body	plug 81	A	1	0	0.1	0.2	1.3
61	assembly to the body	sealing ring 82	A	1	0	0.1	0.2	1.3
63	pick up and setup	nameplate	B	1	0.2	0.1	0.2	1.5
64	riveting	rivet	B	1.5	0.2	0	0	1.7
65								
66								
82								
83				48	11	2.7	5.6	67.2
84								
		22%		2.92				
		project efficiency ratio				maneuverability index		

The formula for the main activity ratio W_m after the changes are:

$$W_m = L_{pA} + L_{pB} + L_{pC} + L_{pD} + L_{pE} + L_{pF} + Sec = 246.7 \quad (16)$$

where: $L_{pA} = 104$,
$L_{pB} = 1.9$,
$L_{pC} = 7.7$,
$L_{pD} = 15$,
$L_{pE} = 12$,
$L_{pF} = 7$,
$Sec = 99$.

The formula for assemblability factor W_{mon} after the changes is:

$$W_{mon} = W_m \ / \ L_{kA} = 246.7/23 = 10.73 \quad (17)$$

Based on the performed analysis, the number of parts of type A is 18 (L_{kA}), the number of type B is 14 (L_{kB}) for serial and mass production.

Formula, describing functionality W_{ep} after the changes, is:

$$W_{ep} = L_{kA} \ / \ L_{kA} + L_{kB} = 18(18+14) = 0.56 \ (56\ \%). \quad (18)$$

Based on the new data after the changes specified in Tables 4 and 5, the manoeuvring index I_{man} is:

$$I_{man} = L_{mA} + L_{mB} + L_{mC} + L_{mD} = 35.2, \quad (19)$$

where: $L_{mA} = 27$,
$L_{mB} = 4.3$,
$L_{mC} = 1.4$,
$L_{mD} = 3$.

Table 5 *Results of the gear assembly technology analysis - Continued*

no.		fitting analysis								
		A	B	C	D	E	F	sec.	sum	cumulative sum
1	pick up and place	1	0	0	0	0	0	0	1	1
2	pressing	1	0	0	0	0	0.7	0	1.7	2.7
3	baring position measure	1.3	0.1	0	1.5	0	0	1.5	4.4	7.1
4	pressing	1	0	0	0	0	0.7	0	1.7	8.8
5	baring position measure	1.3	0.1	0	1.5	0	0	1.5	4.4	13.2
6	pick up and hold down	1	0	0	0	0	0	0	1	14.2
8	pick up and place	1	0	0	0	0	0	0	1	18.6
9	assembly on shaft subassy	1	0	0	0	0.7	0	0	1.7	20.3
10	assembly on shaft subassy	2	0.1	0	0	0.7	0.7	0	3.5	23.8
11	assembly on shaft subassy	1	0.1	0	0	0	0	0	1.1	24.9
13										
18										
55	assembly on shaft subassy									
56	pick up and place	1	0	0	0	0.7	0	0	1.7	243.3
57	tightening	1	0	0	0	0	0	0	1	244.3
58	pick up and place	4	0.1	0	0	0	0	0	4.1	248.4
59	tightening	1	0	0	0	0	0	0	1	249.4
60	pick up and place	4	0.1	0	0	0	0	0	4.1	253.5
61	assembly on plug	1	0	0	0	0	0	0	1	254.5
63	pick up and place	1	0.1	0	0	0	0	0	1.1	255.6
64	pick up and place	2	0.1	0	0	0.7	0	0	2.8	262.5
65	riveting	2	0.1	0	0	0	0	0	2.1	264.6
66	additional rivets	4	0.1	0	0	0.7	0	0	4.8	269.4
82		2	0.1	0	0	0.7	0	12	14.8	284.2
83										284.2
84										284.2
		108	2.1	11	18	12	7	127		284.2
										284.2
	manouverity index				mounting index					12.36

The formula for the manoeuvring factor W_{man} after the changes is:

$$W_{man} = I_{man} \,/\, L_{kA} = 35.2/18 = 1.96. \quad (20)$$

The formula for the main activity ratio W_m after the changes is:

$$W_m = L_{pA} + L_{pB} + L_{pC} + L_{pD} + L_{pE} + L_{pF} + Sec = 112.8, \quad (21)$$

where:
$L_{pA} = 54$,
$L_{pB} = 1.4$,
$L_{pC} = 0$,
$L_{pD} = 7.5$,
$L_{pE} = 9.1$,
$L_{pF} = 6.3$,
$Sec = 35$.

The formula for the assemblability factor W_{mon} ($W_d = 0$) after the changes is:

$$W_{mon} = W_m \,/\, L_{kA} = 112.8/18 = 6.27. \quad (22)$$

According to calculations presented above, it can be stated that the analysis results for a cast iron gear body are better than the analysis results for a welded body gear. The W_{mon} project performance indicator should be as high as possible, before the change 22 %, after the change of 27 % and 56 %, respectively, according to the series production. The maneuvering and assemblability factors of W_{man} and W_{mon} should be as low as possible; before the change they are respectively 2.92 and 12.35, after the change they depend on the production series W_{man} = 2.52 and 1.96 and W_{mon} = 10.73 and 6.27.

The unification and batch processing ratios, for both methods before the redesigning, are as follows:

$$W_{unk} = 91 / \; 91+105 = 0.46 \; (46 \; \%). \quad (23)$$

After the redesign for the small lot production:

$$W_{unk} = 71/\ 71 + 85 = 0.45\ (45\ \%). \quad (24)$$

After the redesign for the mass production:

$$W_{unk} = 23/\ 23{+}32 = 0.42\ (42\ \%). \quad (25)$$

In the case of the gearboxes from the unification index (machining) before redesigning is:

$$W_{uno} = 5/5 + 14 = 0.26\ (26\ \%). \quad (26)$$

After the redesign for the small lot production:

$$W_{uno} = 12/12 + 14 = 0.46\ (46\ \%). \quad (27)$$

After the redesign for the mass production: (including theoretically):

$$W_{uno} = 7/2 + 7 = 078\ (78\%). \quad (28)$$

The presented results meet the assessment of the used production methods effectiveness in the production practice.

4 Conclusions and comments

The standard analysis of B&D and Lucas DFA is associated with a reduction in the number of parts that do not have a significant impact on the product's functions or their change consisting in improvement in terms of the assembly method. This change may be associated with an increase in manufacturing costs. In modified methods by introducing indicators unification and possibilities of group processing, it is possible to improve the design more accurately. Original methods are oriented towards the mass production. Modified methods improve original ones giving the possibility of use in production with smaller series, as well. Analysis of unification and group machining indicators allow for the unification of components and thus saving investment in machines and shorter overall assembly time. Their use can contribute to design of products with higher efficiency and lower production costs.

Proposals for modification of methods allow the analysis of the obtained values of the assembly efficiency assessment parameters, which also causes:

- shortening of times, elimination of errors, reduction of process costs,
- considering, in addition to assembly many other various factors, e.g. availability of spare parts, production seriality, production conditions in the form of equipment types, available assembly techniques, level of automation, the scope of external cooperation orders, etc.
- the use of methods for smaller series of manufactured products,
- stimulating a designer's creativity.

These two methods cannot be compared directly due to the different way of calculations. The following conclusions can be drawn from analysis of comparison of results obtained by both methods.

The Boothroyd-Dewhurst method is more stringent and is aimed at reducing/simplifying the components of the project. At the same time, in the case of production not qualified for the high-volume production, the result of such an assessment may be a product with a small number of components, but a very complicated form and, therefore, a high cost of processing and quality and other in the field of production organisation.

The Lucas method assesses the above project in a more balanced way. It enables the assessment of technology from the point of view of value of several parameters. Differences in relation to the intended goal between the two methods are not large. Both methods, together with complex proposals, allow universalisation of the presented methods and their application to conditions of the unit and small-lot production.

References

[1] ABDULLAH, A., POPPLEWELL, K., PAGE, C. J. A review of the support to tools for the process of assembly method selection and assembly planning. *International Journal of Production Research* [online]. 2003, **41**(11), p. 2391-2410 [accessed 2020-01-27]. ISSN 1366-588X. Available from: https://doi.org/10.1080/002075431000087265

[2] BOOTHROYD, G., DEWHURST, P. *Design for assembly*. *A designer´s handbook*. Amherst, Ma.: University of Massachusetts, Department of Mechanical Engineering, 1983.

[3] KNIGHT, W. A., BOOTHROYD, G. *Fundamentals of metal machining and machine tools*. 3. ed. Taylor and Francis Group: CRC Press, 2005. ISBN 978-157-444-659-3.

[4] BREYFOGLE, F. W. *Implementing six sigma.* 2. ed. New Jersey: John Wiley and Sons, 2003. ISBN 978-0471265726.

[5] EGAN, M. *Design for assembly in the product development process-a design theory perspective.* Thesis for the degree of licentiate of Engineering. Marina del Rey, 1997. ISBN 99-248946-85.

[6] DOCHIBHATLA, S. V. S., BHATTACHARYA, M., MORKOS, B. Evaluating assembly design efficiency: a comparison between Lucas and Boothroyd-Dewhurst methods. In: International Design Engineering Technical

Conferences and Computers and Information in Engineering Conference ASME 2017: proceedings. 2017. p. V004T05A012-V004T05A012.
[7] AHMAD, M. N., ADEERA, N., OSMAN MAZRAN, M. H., KHALID, M. The significant improvement on the design of pedestrian traffic light using Boothroyd Dewhurst design for assembly (DFA) method: a case study. *Journal of Advanced Research Design*. 2016, **25**(1), p. 11-19. eISSN 2462-1943.
[8] CHANG, T. C. *Expert process planning for manufacturing*. NY: Addison-Wesley Publishing Company, Inc., 1990. ISBN-13: 978-0201182972.
[9] MATUSZEK, J. *Production engineering /Inzynieria produkcji* (in Polish). Bielsko-Biala: Wydawnictwo Politechniki Lodzkiej Filii, 2000. ISBN 83-87087-97-1, p. 83-109.
[10] LIBERS, A., SREPPEL, A., SCHUTTERT, M., KALS, H. *Part classification for variant cost estimation*. In: 4th International Conference on Sheet Metal: proceedings. Vol. 2. SheMet, 1996. ISBN 903-650-804-5, p. 167-178.
[11] OHASHI, T., MIYAKAWA, S. The Hitachi assemblability evaluation method (AEM). In: 1st International Conference on Product Design for Assembly: proceedings. 1986.
[12] GREGOR, M., MATUSZEK, J. Production systems development trends / Tendencje projektowania systemow produkcyjnych (in Polish). *Mechanik* [online]. 2013, **7**, p. 231-238 [accessed 2020-01-27]. ISSN 0025-6552. Available from: http://www.mechanik.media.pl/pliki/do_pobrania/artykuly/2/4924_231_238.pdf
[13] MATUSZEK, J., SENETA, T. Algorithmisation of the new product implementation process in the conditions of mass production / Algorytmizacja procesu wdrazania nowegp produktu w warunkach wielkoseryjnej produkcji (in Polish). *Mechanik* [online]. 2016, **7**, p. 755-757 [accessed 2020-01-27]. ISSN 0025-6552. Available from: http://www.mechanik.media.pl/pliki/do_pobrania/artykuly/22/konferencja_158.pdf
[14] HERBERTSSON, J. Enterprise oriented design for manufacture - on the adaptation of DFM in an enterprise. Ph.D. thesis. LiTH, 1999.
[15] JAMES, A., GANDHI, O. P., DESHMUKH, S. G. Development of methodology for the disassemblability index of automobile system using a structural approach. *Proceedings of the Institution of Mechanical Engineers, Part D: Journal of Automobile Engineering* [online]. 2016, **231**(4), p. 516-535 [accessed 2020-01-27]. ISNN 0954-4070. Available from: https://doi.org/10.1177/0954407016656311
[16] PAN, L., CHO, H. J., PARK, J. I. Study on the design factors affecting the operating actions that can be used easily at the design stage. *Advanced Materials Research* [online]. 2015, **1061-1062**, p. 712-715 [accessed 2020-01-27]. ISSN 1662-8985. Available from: https://doi.org/10.4028/www.scientific.net/AMR.1061-1062.712
[17] MATUSZEK, J., SENETA, T. Evaluation of design manufacturability in new product production launches by Lucas DFA method. *Mechanik* [online]. 2017, **7**, p. 755-757 [accessed 2020-01-27]. Available from: http://www.mechanik.media.pl/pliki/do_pobrania/artykuly/22/2017_07_s0523_eng.pdf
[18] MATUSZEK, J., KOLOSOWSKI, M., KROKOSZ-KRYNKE, Z. *Cost accounting for engineers/Rachunek kosztow dla inzynierow* (in Polish). Warszawa: Polskie Wydawnictwo ekonomiczne, 2014. ISBN 978-83-208-2104-8, p. 215-247.
[19] SHETTY, D., ALI, A. A new design tool for DFA/DFD based on rating factors. *Assembly Automation* [online]. 2015, **35**(4), p. 348-357 [accessed 2020-01-27]. ISSN 0144-5154. Available from: https://doi.org/10.1108/AA-11-2014-088
[20] SHUKOR, A. I. A., ADAM, A. Evaluation of design efficiency using Boothroyd Dewhurst method for PCB drilling machine product. *International Journal of Simulation Systems, Science and Technology* [online]. 2018, **19**(5), p. 4.1-4.8 [accessed 2020-01-27]. ISSN 1473-8031, ISSN 1473-804x. Available from: https://doi.org/10.5013/IJSSST.a.19.05.04
[21] SWIFT, K. G., BOOKER, J. D. *Process selection from design to manufacture*. 2. ed. Oxford: Elsevier, 2003. ISBN 0 7506 5437 6.
[22] SWIFT, K., BROWN, N. *Design for assembly / manufacturing analysis practitioner's manual*. Version 10.5. Great Britain: University of Hull, 1994. ISBN 978-0-13-516569-0, p. 116-138.
[23] WIECEK, D., WIĘCEK, D. (2017). The influence of the methods of determining cost drivers values on the accuracy of costs estimation of the designed machine elements. In: International Conference on Information Systems Architecture and Technology: proceedings. Cham: Springer. 2017. p. 78-88.
[24] WIECEK, D., WIECEK, D., KURIC, I.: Cost estimation methods of machine elements at the design stage in unit and small lot production conditions. *Management Systems in Production Engineering* [online]. 2019, **27**(1), p. 12-17. eISSN 2450-5781. Available from: https://doi.org/10.1515/mspe-2019-0002

RESEARCH ON CURVILINEAR MOTION OF AUTOMOBILE WITH THE APPLICATION OF ON-BOARD CAN BUS DATA

Hubert Sar*, Mateusz Brukalski, Krzysztof Rokicki

Institute of Vehicles and Construction Machinery Engineering, Warsaw University of Technology, Warsaw, Poland

*E-mail of corresponding author: hubert.sar@pw.edu.pl

Resume

Modelling of vehicle's motion is one of the solutions applied in the research of automotive safety. There is always a discussion which model should be used for computer simulation. Models with higher number of degrees of freedom require identification of many parameters, which are usually difficult to obtain. So, very often relatively simple flat model of vehicle's motion is applied. It needs only such parameters as mass of a vehicle, location of centre of gravity from front and rear axle, yaw mass moment of inertia and side slip characteristics of the front and rear axle. In this paper the upper mentioned model was applied, considering different side slip characteristics of the front and rear axle. The scenario of vehicle's motion was based on random changes of steering wheel angle during the road test, recording signals from on-board CAN (Controller Area Network) bus of automobile simultaneously, which were further applied in simulation.

Article info

Received 16 September 2020
Accepted 7 November 2020
Online 15 April 2021

Keywords:

CAN bus data,
vehicle's motion modelling,
automotive safety,
side slip phenomenon,
computer simulation

Available online: https://doi.org/10.26552/com.C.2021.3.B211-B218

ISSN 1335-4205 (print version)
ISSN 2585-7878 (online version)

This is an open access article distributed under the terms of the Creative Commons Attribution 4.0 International License (CC BY 4.0), which permits use, distribution, and reproduction in any medium, provided the original publication is properly cited. No use, distribution or reproduction is permitted which does not comply with these terms.

1 Introduction

Research on automotive safety is conducted in a variety of ways. First, it may be investigation of driver's influence on the level of traffic safety, estimating reaction times on different disturbances generated on the road as mentioned in [1-4]. Moreover, research on vehicles' safety is analysed through the approach to automotive suspension's modelling, vertical vibrations of automobile's body as presented by [5-6], because the contact between tyres and road should be enough to transmit tangential forces resulting both from cornering, driving and braking forces. Vehicle's motion models are very sophisticated, including many interactions and many degrees of freedom, for example [7]. In turn, advanced tyre models are used, where interactions in three directions are included together with bending vibrations inside the tyre's structure [8]. Some papers refer to traffic safety through the analysis of post-accident investigation of traffic incidents as presented by [9]. Because of the vision systems development, they became helpful in researching vehicles' motion as depicted in [10]. Safety of heavy vehicles, for example firefighting automobiles, is discussed in [11], where the braking distance is considered. Very interesting approach can be found in [12], where the road profile estimation and vehicle model investigation are performed through the data from mobile devices. Computer simulation of automobile's motion is regarded as a cheap method of investigating its important properties. Of course, it must be preceded by the road measurements, applying suitable measurement equipment. Furthermore, adequate mathematical model of a vehicle must be applied. If a model is more sophisticated, it requires more parameters for identification. Thus, validation of such a model may be more problematic. Although, one can estimate some parameters of a model, but it should be done with relatively low error. Very often, for the rapid preparation of a simulation, a flat model of a vehicle, as presented in the article, is used. Another important issue are road measurement tests, for which it is necessary to apply adequate measurement equipment like data acquisition system and sensors. In this paper, data coming from the CAN (Controller Area Network) bus of a vehicle through special measurement card, was applied.

2 Data acquisition system

To be able to compare the measurement and simulation results, some signals had to be recorded, which also corresponded to the output signals of a model. Additionally, steering wheel angle signal and velocity of a vehicle were input signals of a model, which provided the basis for comparing the measurement results to the simulation results. Only velocity of a vehicle was taken outside the CAN bus. It was collected from simple 10 Hz



Figure 1 *GPS receiver QSTARZ BT-Q818XT 10Hz [13]*



Figure 2 *CAN bus data acquisition card [14]*

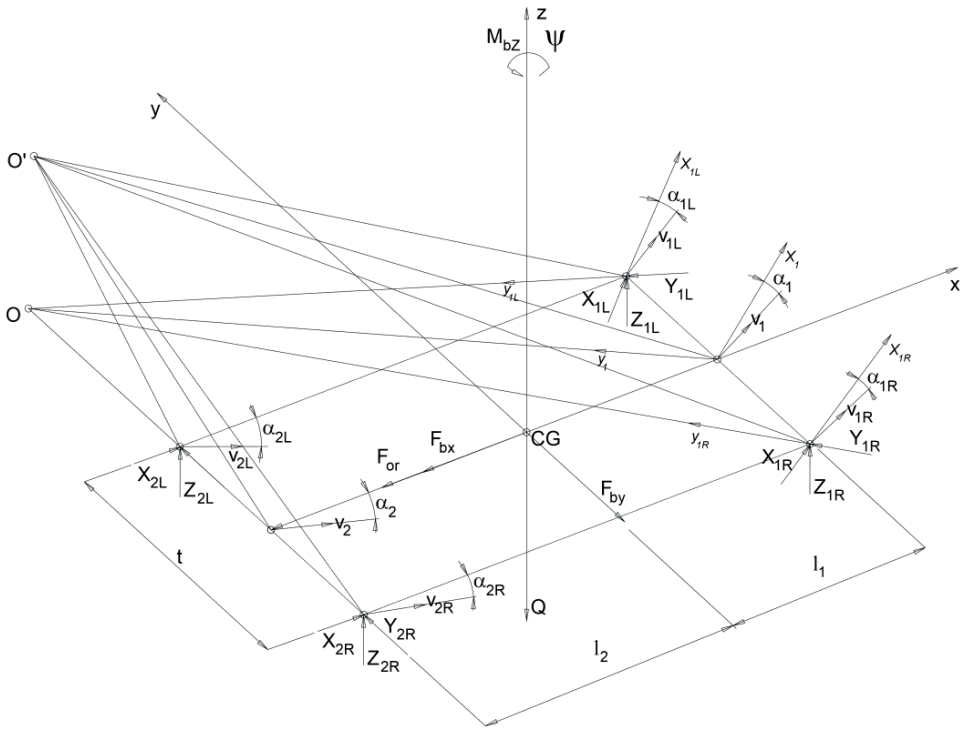


Figure 3 *Flat model of automobile for description of curvilinear motion of automobile*

GPS (Global Positioning System) receiver (see Figure 1). Other signals, typical for Electronic Stability Program (ESP), like lateral acceleration, yaw rate sensor and steering wheel angle, were recorded from the CAN bus through the special data acquisition measurement card (see Figure 2). It is important to say that this method of measurement is not a substitute for the professional data acquisition systems. The article only shows a new approach to road tests, applying cheaper measurement equipment, without necessity to buy new sensors and mount them inside a vehicle.

3 Mathematical description of vehicle's curvilinear motion

As already mentioned in the introduction, simple flat model of a vehicle (depicted in Figure 3) was applied in this paper. It included only a few inertial parameters as mass, its distribution between the front and rear axle, yaw mass moment of inertia. Of course, to perform the simulation, it needed two input signals - steering wheel angle and velocity of a vehicle. Additionally, it required an information about the side slip properties of the front and rear axle. Lateral forces and slip angles of the left and right part of front and rear axle are included separately in equilibrium equations of vehicle's model. The reason for this is that in the future it is planned to extend the model by applying the roll and pitch angle of vehicle body's motion. It will result in the changes of normal reaction forces between the road and a wheel, thus influencing lateral forces connected with side slip phenomenon.

Here are presented descriptions of symbols used in Figure 3 where:

X_i, Y_i, Z_i - (in capitals) reaction forces between left, right part of front or rear axle;

x, y, z - coordinate system connected with a vehicle;

x_i, y_i, z_i - (small letters) local coordinates' system of left, right side of front axle;

α_i - side slip angle of left, right side of front or rear axle;

v_i - resultant velocity of i-part of a vehicle;

Q - weight of a vehicle;

O - theoretical centre of vehicle's rotation;

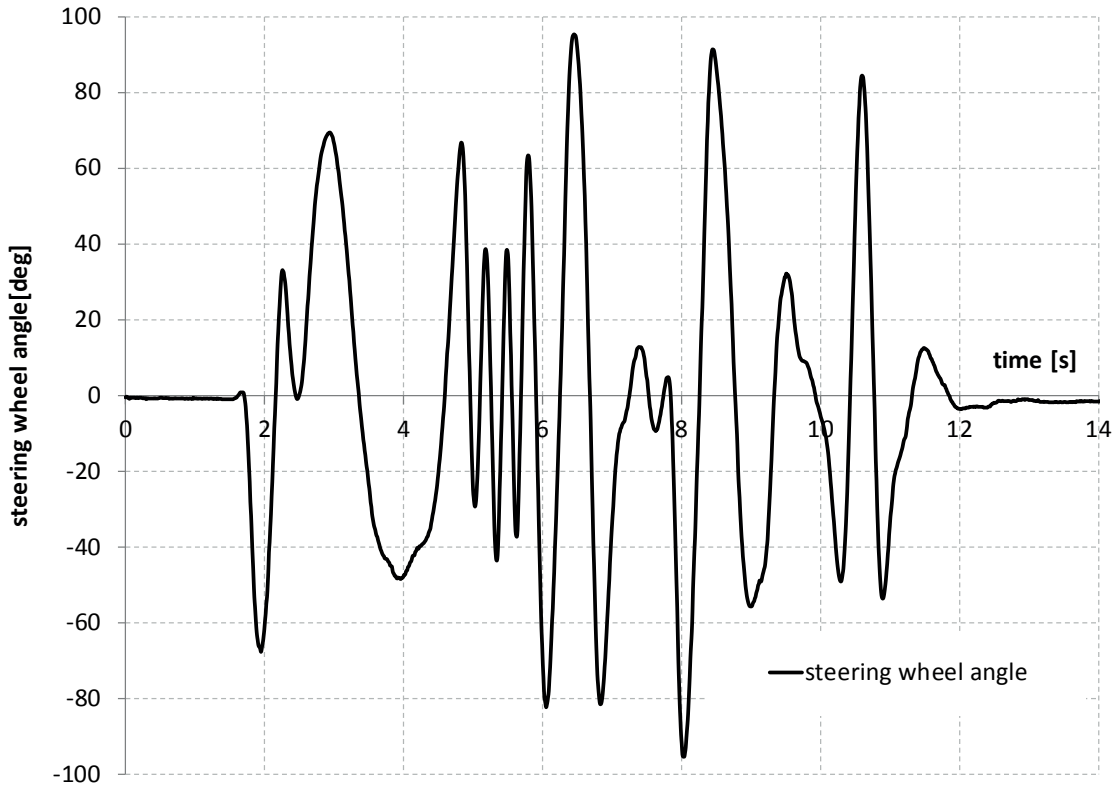


Figure 4 *The time course of the steering wheel angle of investigated vehicle*

O' - real centre of vehicle's rotation (including side slip phenomenon);
CG - centre of gravity;
M_{bz} - yaw torque of inertial resistance;
F_{by} - inertial lateral force;
ψ - yaw angle.

The steady-state condition of vehicle's motion in longitudinal direction, was assumed, as well. So that, forces F_{bx} and F_{or} were assumed as equal zero.

Equilibrium equations for the model presented in Figure 3 are presented below.

$$F_{by} = X_{1R}\cdot\sin\delta_{1R} + X_{1L}\cdot\sin\delta_{1L} + Y_{1R}\cdot\cos\delta_{1R} + \\ + Y_{1L}\cdot\cos\delta_{1L} + Y_{2R} + Y_{2L}, \tag{1}$$

$$m\cdot\dot{x}\cdot\phi + m\cdot\ddot{y} = X_{1R}\cdot\sin\delta_{1R} + X_{1L}\cdot\sin\delta_{1L} + \\ + Y_{1R}\cdot\cos\delta_{1R} + Y_{1L}\cdot\cos\delta_{1L} + Y_{2R} + Y_{2L}, \tag{2}$$

$$M_{bz} = X_{1L}\cdot\cos\delta_{1L}\cdot\frac{t}{2} - X_{1L}\cdot\sin\delta_{1L}\cdot l_1 - Y_{1L}\cdot \\ \cdot\cos\delta_{1L}\cdot l_1 - Y_{1L}\cdot\sin\delta_{1L}\cdot\frac{t}{2} - X_{1R}\cdot\cos\delta_{1R}\cdot\frac{t}{2} + \\ - X_{1R}\cdot\sin\delta_{1R}\cdot l_1 - Y_{1R}\cdot\cos\delta_{1R}\cdot l_1 + Y_{1R}\cdot\sin\delta_{1R}\cdot \\ \cdot\frac{t}{2} + X_{2L}\cdot\frac{t}{2} + Y_{2L}\cdot l_2 - X_{2R}\cdot\frac{t}{2} + Y_{2R}\cdot l_2, \tag{3}$$

$$I_z\cdot\ddot{\phi} = X_{1L}\cdot\cos\delta_{1L}\cdot\frac{t}{2} - X_{1L}\cdot\sin\delta_{1L}\cdot l_1 - Y_{1L}\cdot \\ \cdot\cos\delta_{1L}\cdot l_1 - Y_{1L}\cdot\sin\delta_{1L}\cdot\frac{t}{2} - X_{1R}\cdot\cos\delta_{1R}\cdot\frac{t}{2} + \\ - X_{1R}\cdot\sin\delta_{1R}\cdot l_1 - Y_{1R}\cdot\cos\delta_{1R}\cdot l_1 + Y_{1R}\cdot\sin\delta_{1R}\cdot \\ \cdot\frac{t}{2} + X_{2L}\cdot\frac{t}{2} + Y_{2L}\cdot l_2 - X_{2R}\cdot\frac{t}{2} + Y_{2R}\cdot l_2. \tag{4}$$

The inertial data of investigated vehicle (Hyundai Veloster 1.6 GDI MY2010) are:

mass of automobile m = 1419 kg, distance between front axle and centre of gravity l_1 = 1.089 m, distance between rear axle and centre of gravity l_2 = 1.561 m, average wheel track t = 1.560 m, average steering system ratio K_{sr} = 15.1.

Moment I_z was estimated using the following formula proposed by Heinz Burg [15] in 1982:

$$I_Z = 0.1269\cdot m\cdot L\cdot l_{12}\,. \tag{5}$$

where: length of automobile L = 4.22 m;
wheelbase l_{12} = 2.65 m.

After calculation using Equation (5) estimated yaw mass moment of inertia equals 2013 kg·m^2.

Finally, the value of I_z was rounded and assumed as I_z = 2100 kg·m^2.

In further part of the article, values of yaw angular velocity of automobile, its lateral velocity and lateral acceleration in the centre of gravity, are presented in a form of time courses, for random changes of steering wheel angle. They came both from the road measurements and simulations, together with steering wheel angle as the input signal of the mathematical model, of vehicle's motion. Additionally, in the case of lateral acceleration, it had to be filtered via the Butterworth filter, because of a noisy signal, which came from the CAN bus. As a result of filtration, harmonic components, characterized by 7 Hz and higher, were cut from the signal.

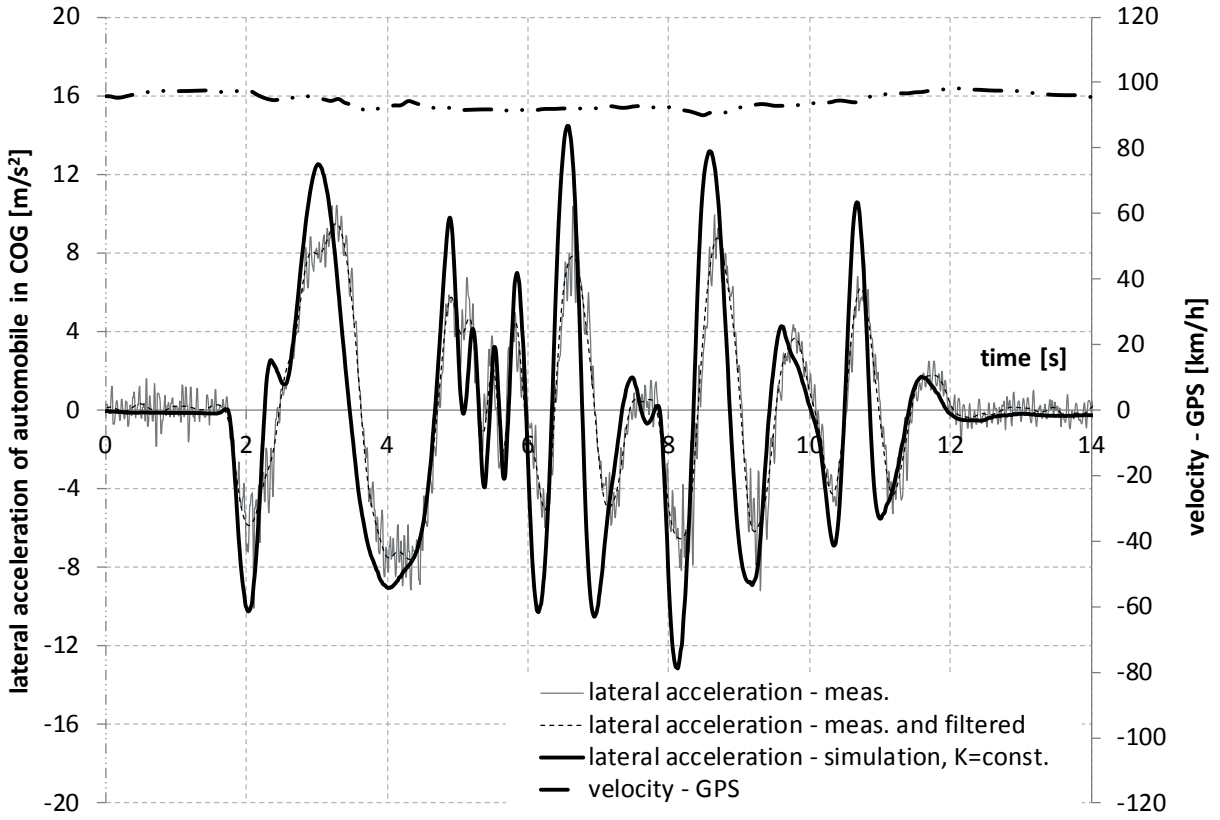


Figure 5 *The time course of the lateral acceleration in the centre of mass of investigated vehicle for the linear side slip characteristics*

First, the signal, which was common both for measurement and simulation, was the steering wheel angle. Its recorded time course is presented in Figure 4. It does not represent any normative road tests, but very narrow changes of the steering wheel angle. The road test was performed on Biala Podlaska airport.

Computer simulation of vehicle's curvilinear motion was performed for the two different equations describing the dependence between the lateral force and side slip angle of front and rear axle. It was done separately for the left and right side of each axle, because in the future the authors are planning to introduce more degrees of freedom in the model, among others the roll and pitch angle. It will generate changes of normal reaction forces and hence changes of tangential longitudinal and transverse forces between the axle and a road surface. The first Equation (6) is very simplified and includes very popular approach based on application of cornering stiffness coefficient K.

$$Y = K \cdot \alpha \,, \tag{6}$$

where:
Y - lateral reaction force between left or right part of front or rear axle and road surface,
α - side slip angle of the left or right part of front or rear axle and road surface;
K - cornering stiffness coefficient;
K_1 = 80000 N/rad, K_2 = 105000 N/rad.

The second type of Equation (7), describing the dependence between the lateral force and side slip angle, is represented by very popular Pacejka's Magic Formula [16] (MF). This non-linear dependence between the lateral force and side slip angle is important regarding higher values of the side slip angles, resulting from higher values of the steering wheel angle. In the case of the analysed test it was nearing ± 100 degrees.

$$\begin{aligned} Y = &-\mu \cdot Z \cdot \sin(C \cdot arctan(B \cdot \alpha - E \cdot (B \cdot \alpha + \\ &- arctan(B \cdot \alpha)))), \\ \mu = &\ 0.9\,. \end{aligned} \tag{7}$$

Here are given values of fitting constants for Magic Formula Equation (7), separately for front and rear axle: C_1 = 1.1, C_2 = 1.1, E_1 = -15, E_2 = -15, B_1 = 6.0, B_2 = 10.5.

Negative values of coefficients E_1 and E_2 are resulting from the sense of the lateral reaction forces vectors, acting from the ground on the front and rear axle.

In the presented version of the MF Equation (7), influence of the adhesion coefficient between the axle and a road surface - μ is included. Looking at Equation (7), lateral force Y is associated with normal reaction force Z. In this case the normal reaction forces are assumed as constant, but if the roll and pitch motion was unlocked in the model through adding additional equilibrium equations, that would assure the characteristics of force

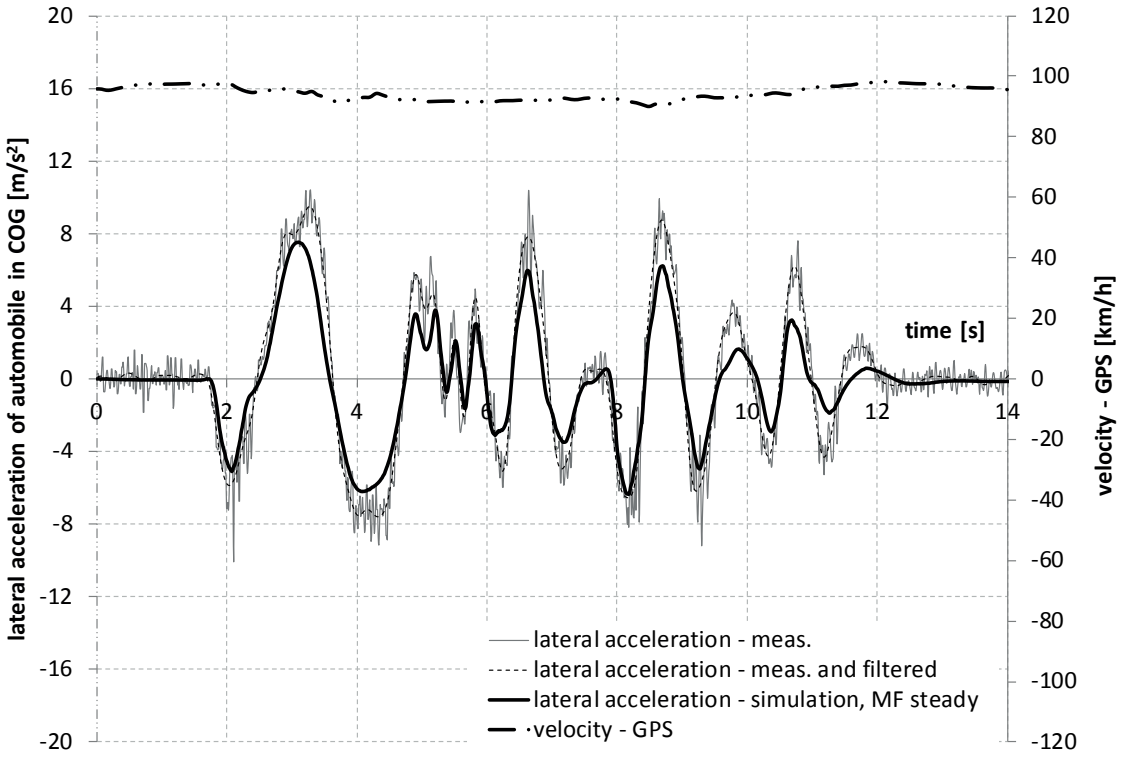


Figure 6 *The time course of the lateral acceleration in the centre of mass of investigated vehicle for the side slip characteristics described by Pacejka's Magic Formula*

Y as a function of angle α, each characteristics for different normal reaction force Z.

Figure 5 shows the lateral acceleration of automobile from measurements and from computer simulation with application of the most simplified side slip characteristics (see Equation (6)) - in this case linear. It means that dependence between the lateral force and side slip angle, generated by this force, is described only by the cornering stiffness.

In Figure 6 is depicted the time course of lateral acceleration of automobile, but for the non-linear side slip characteristics, defined by the Pacejka's Magic Formula - Equation (7). As can be seen, this description of the dependence between the lateral force and side slip angle results in better adjustment of the simulation in comparison to the measurement.

To conclude about the differences between simulation and measurement results of lateral acceleration, the following Equation (8) was used.

$$D_{i_a_y} = \frac{a_{ysim_i} - a_{ymeas_i}}{a_{ymeas_i}} \cdot 100\%, \tag{8}$$

where:

$D_{i_a_y}$ - difference in percentages between the simulated and measured lateral acceleration for i-point of simulation;

a_{ysim_i} - simulated lateral acceleration for i-point of simulation;

a_{ymeas_i} - measured lateral acceleration for i-point of simulation.

Then, for 14 seconds of simulation the standard deviation of the difference $D_{i_a_y}$ was calculated. It was shown below for two different formulas describing the dependence between lateral force and side slip angle:

- for Equation (6): $\sigma_{D_{i_a_y}} = 1074\%$,
- for Equation (7): $\sigma_{D_{i_a_y}} = 281\%$.

In analogy to the lateral acceleration, in Figure 7 is depicted the time course of yaw angular velocity of automobile on the background of the yaw velocity recorded from the CAN bus. In the case of the most simplified (linear) dependence between the lateral force and slip angle, values of simulated yaw velocity are a bit too high compared to the measured values. In the case of Figure 8, where for the dependence between the lateral force and a slip angle the Magic Formula was applied, the simulated course of yaw velocity is a bit below the measured values.

Like the comparison of simulated and measured values of lateral acceleration, here are presented the standard deviations of differences calculated for the yaw velocity using Equation (9):

$$D_{i_\dot{\phi}} = \frac{\dot{\phi}_{sim_i} - \dot{\phi}_{meas_i}}{\dot{\phi}_{meas_i}} \cdot 100\%, \tag{9}$$

where:

$D_{i_\dot{\phi}}$ - difference in percentages between simulated and measured yaw velocity for i-point of simulation;

$\dot{\phi}_{sim_i}$ - simulated yaw velocity for i-point of simulation,

$\dot{\phi}_{meas_i}$ - measured yaw velocity for i-point of simulation.

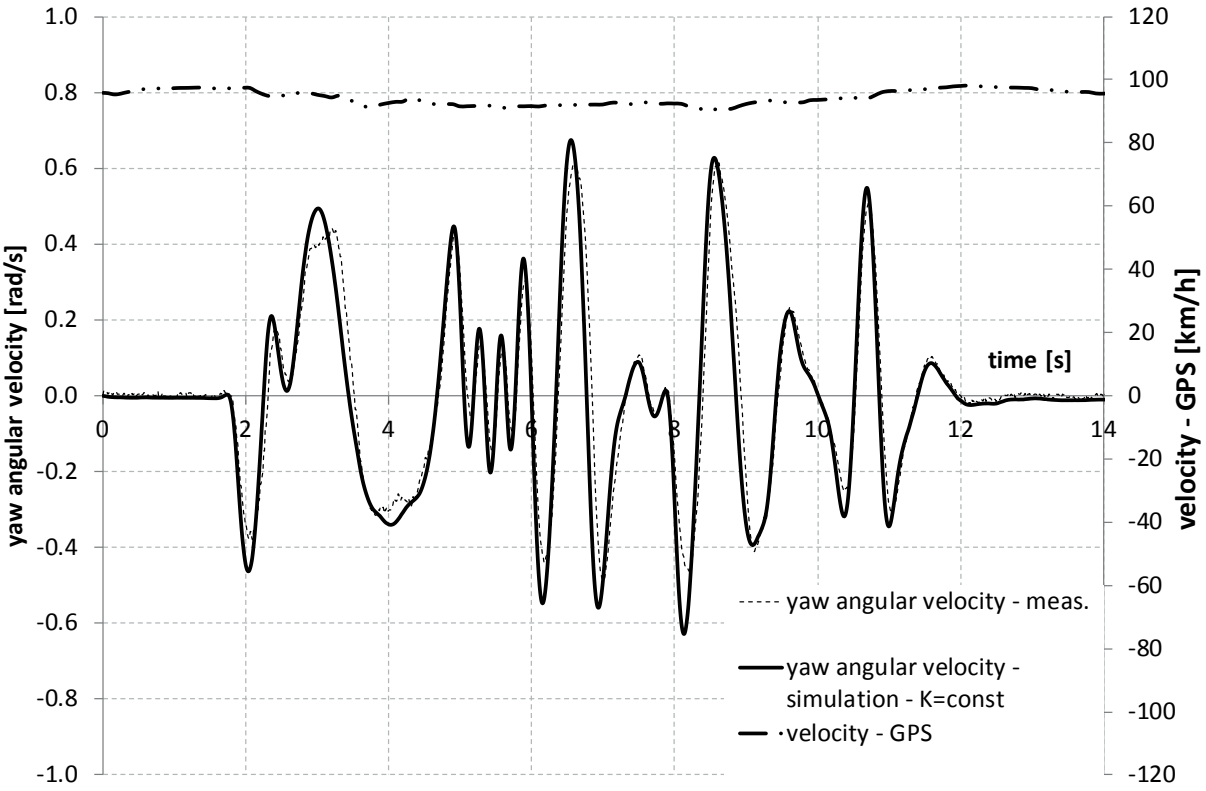


Figure 7 *The time course of the yaw angular velocity of investigated vehicle for the linear side slip characteristics*

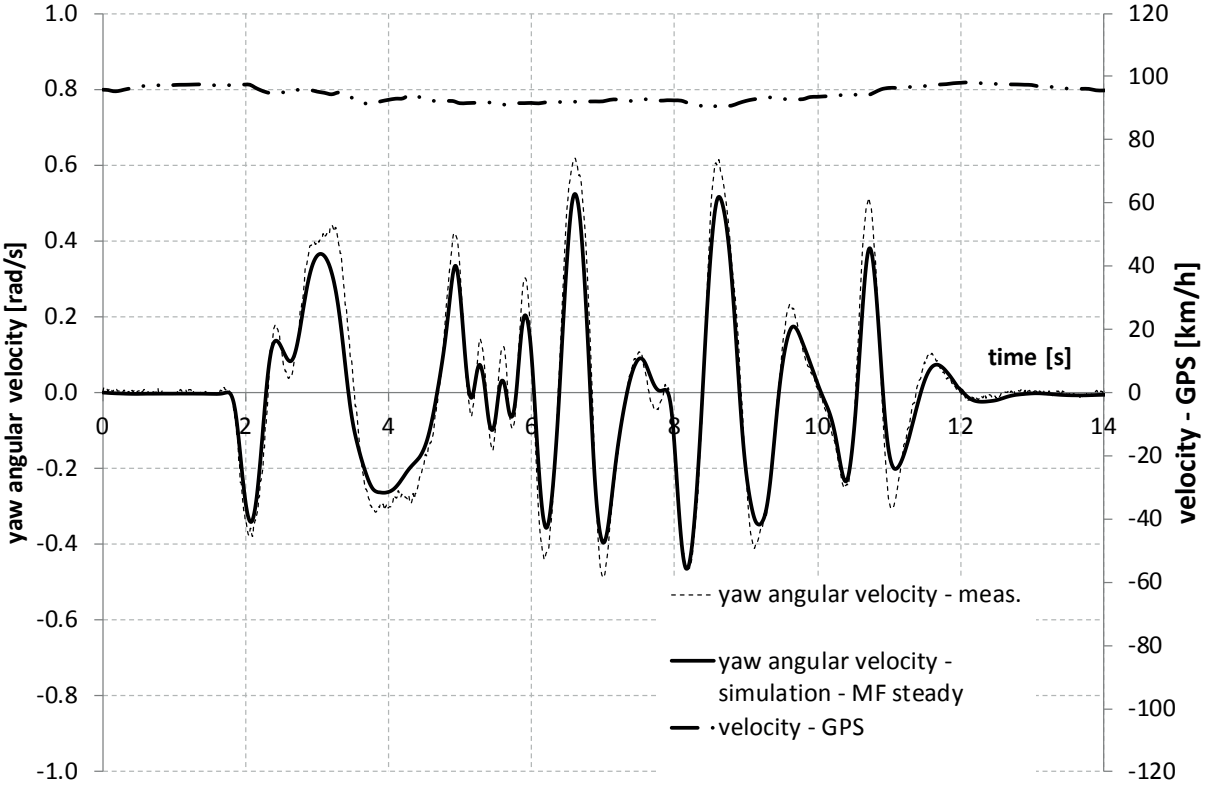


Figure 8 *The time course of the yaw angular velocity of investigated vehicle for the side slip characteristics described by Pacejka's Magic Formula*

In analogy to the lateral acceleration, for 14 seconds of simulation the standard deviation of the difference $D_{i_\dot{\phi}}$ was calculated. It is presented below for the two different equations of dependence between the lateral force and a side slip angle:

- - for Equation (6):
  $\sigma_{D_{i_\dot{\phi}}} = 845\%$,
- - for Equation (7):
  $\sigma_{D_{i_\dot{\phi}}} = 591\%$.

In the future it is planned to more precisely obtain all the model's parameters with the application of an optimization method like neural networks or random method like Monte Carlo algorithm. Including more DOFs (degrees of freedom) in the motion model would improve the quality of simulation results, but that is planned in the future. In particular, changes of the vertical load of the wheels will be performed in the future works. Moreover, improvement of the model will be possible because of unlocking roll and pitch motion of vehicle's body.

4 Conclusion

Application of a simple flat model of vehicle's curvilinear motion requires relatively low number of identified parameters. Such a model was applied in this paper as well as the results of road tests, which came from recording signals typical for electronic stability program (ESP). It was done through the special CAN bus measurement card and own data management-acquisition software made in LabView environment. Presented method of the measurement is not an alternative for dedicated measurement equipment. In the future, the method of collecting data from the CAN bus should be compared to simultaneously recorded signals using the traditional equipment in terms of possible phase shifts between the individual signals from the CAN bus, which is dedicated for information interchange between the electronic modules of a vehicle. However, it is justified to improve the presented method recording the signals, which are important if concerning lateral dynamics' problems of automobiles and automotive safety.

References

[1] JURECKI, R. Influence of the scenario complexity and the lighting conditions on the driver behaviour in a car-following situation. *Archiwum Motoryzacji* [online]. 2019, **83**(1), p. 151-173 [accessed 2020-07-10]. eISSN 2084-476X. Available from: https://doi.org/10.14669/AM.VOL83.ART11

[2] JURECKI, R., POLIAK, M., JASKIEWICZ, M. Young adult drivers: simulated behaviour in a car-following situation. *Promet - Traffic and Transportation* [online]. 2017, **29**(4), p. 381-390 [accessed 2020-07-10]. ISSN 0353-5320, eISSN 1848-4069. Available from: https://doi.org/10.7307/ptt.v29i4.2305.

[3] JURECKI, R. S., STANCZYK, T. L., JASKIEWICZ, M. J. Driver's reaction time in a simulated, complex road incident. *Transport* [online]. 2017, **32**(1), p. 44-54 [accessed 2020-07-10]. ISSN 1648-4142, eISSN 1648-3480. Available from: https://doi.org/10.3846/16484142.2014.913535

[4] JURECKI, R. S., STANCZYK, T. L. Driver reaction time to lateral entering pedestrian in a simulated crash traffic situation. *Transportation Research Part F: Traffic Psychology and Behaviour* [online]. 2014, **27**, p. 22-36 [accessed 2020-07-10]. ISSN 1369-8478. Available from: https://doi.org/10.1177/107754631247291610.1016/j.trf.2014.08.006

[5] MAKOWSKI, M., KNAP, L. Reduction of wheel force variations with magnetorheological devices. *Journal of Vibration and Control* [online]. 2014, **20**(10), p. 1552-1564 [accessed 2020-07-10]. ISSN 1077-5463, eISSN 1741-2986. Available from: https://doi.org/10.1177/1077546312472916

[6] MAKOWSKI, M., ZALEWSKI, R. Vibration analysis for vehicle with vacuum packed particles suspension. *Journal of Theoretical and Applied Mechanics* [online]. 2015, **53**(1), p. 109-117 [accessed 2020-07-10]. ISSN 1429-2955, eISSN 2543-6309. Available from: https://doi.org/10.15632/jtam-pl.53.1.109

[7] LOZIA, Z. Rollover thresholds of the biaxial truck during motion on an even road. *Vehicle System Dynamics* [online]. 1998, **29**(sup1), p. 735-740 [accessed 2020-07-10]. ISSN 0042-3114, eISSN 1744-5159. Available from: https://doi.org/10.1080/00423119808969601

[8] YU, X., HUANG, H., ZHANG, T. A theoretical three-dimensional ring based model for tire high-order bending vibration. *Journal of Sound and Vibration* [online]. 2019, **459**, p. 114820 [accessed 2020-07-10]. ISSN 0022-460X. Available from: https://doi.org/10.1016/j.jsv.2019.06.027

[9] HAVAJ, P., The quality and the complete evidence securing during the traffic crime scene investigation and its relevance for evidence completion during the traffic accidents. *Communications - Scientific letters of the University of Zilina* [online]. 2018, **20**(4), p. 76-81 [accessed 2020-07-10]. ISSN 1335-4205, eISSN 2585-7878. Available from: https://doi.org/10.26552/com.C.2018.4.76-81

[10] LOKTEV, D. A., LOKTEV, A. A., SALNIKOVA, A. V., SHAFOROSTOVA, A. A. Determination of the dynamic vehicle model parameters by means of computer vision. *Communications - Scientific letters of the University of Zilina* [online]. 2019, **21**(3), p. 28-34 [accessed 2020-07-10]. ISSN 1335-4205, eISSN 2585-7878. Available from: https://doi.org/10.26552/com.C.2019.3.28-34

[11] SUDRYCHOVA, I., KUCZAJ, J., JANOSIK, L., POLEDNAK, P., JANOSIKOVA, I. Firefighting vehicles braking distance metering. *Communications - Scientific letters of the University of Zilina* [online]. 2019, **21**(3), p. 85-91 [accessed 2020-07-10]. ISSN 1335-4205, eISSN 2585-7878. Available from: https://doi.org/10.26552/com.C.2019.3.85-91

[12] XUE, K., NAGAYAMA, T., ZHAO, B. Road profile estimation and half-car model identification through the automated processing of smartphone data. *Mechanical Systems and Signal Processing* [online]. 2020, **142**, 106722 [accessed 2020-07-10]. ISSN 0888-3270. Available from: https://doi.org/10.1016/j.ymssp.2020.106722

[13] Bluetooth GPS Receiver [online] [accessed 2020-07-10]. Available from: http://www.qstarz.com/Products/GPS%20Products/BT-Q818XT-F.htm

[14] USB-8502 - CAN Interface Device [online] [accessed 2020-07-10]. Available from: https://www.ni.com/pl-pl/support/model.usb-8502.html

[15] BURG, H. Approximation of moments of inertia in passenger cars / Approximation von Tragheitsmomenten bei Personenkraftwagen (in German). *Der Verkehrsunfall*. 1982, **20**, p. 61-63. ISSN 0341-2210.

[16] PACEJKA, H. B. *Tire and vehicle dynamics*. Elsevier, 2012. ISBN 9780080970165, eISBN 9780080970172.

THEORETICAL AND EXPERIMENTAL STUDY OF OPERATION OF THE TANK EQUIPMENT FOR ULTRASONIC PURIFICATION OF THE INTERNAL COMBUSTION ENGINE EXHAUST GASES

Adil Kadyrov[1], Aleksandr Ganyukov[1], Igor Pak[1], Bahtiyar Suleyev[1], Kyrmyzy Balabekova[2,*]

[1]Department of Transport Equipment and Logistics Systems, Karaganda Technical University, Karaganda, Kazakhstan
[2]Department of Transport, Transport Equipment and Technologies, L. N. Gumilyov Eurasian National University, Nur-Sultan, Kazakhstan

*E-mail of corresponding author: 06_03_92@mail.ru

Resume
The article presents results of scientific and experimental studies of the authors on operation of the tank equipment for ultrasonic purification of exhaust gases of internal combustion engines designed to reduce environmental pollution.
The scheme of the experimental device implementing the principle of the tank equipment operation for ultrasonic cleaning of the motor vehicles exhaust gases is presented; the obtained experimental data of ultrasonic coagulation processes were processed and analyzed. Empirical relationships of the coagulation coefficient and its rate of change are derived from experimental data.

Article info
Received 5 November 2020
Accepted 14 December 2020
Online 7 May 2021

Keywords:
internal combustion engine,
exhausted gases,
tank equipment,
ultrasonic purification,
coagulation,
coagulation coefficient,
experiment

Available online: https://doi.org/10.26552/com.C.2021.3.B219-B226

ISSN 1335-4205 (print version)
ISSN 2585-7878 (online version)

1 Introduction

Motor vehicles are much more aggressive to the environment compared to other modes of the land transport. It is a powerful source of toxic substances. As the vehicle fleet increases, the level of harmful impact of motor vehicles on the environment increases intensively. Thus, while in the early 1980s the proportion of pollution introduced into the atmosphere by transport was on average equal to 20 %, it has now reached 50 % and continues to grow. For large cities and industrial centers, the share of motor transport in the total volume of pollution is much higher and reaches 70 % or more, which creates a serious environmental problem [1].

Solving environmental problems of transport requires development of the necessary mechanisms to protect the environment and adoption of scientifically based engineering and technical solutions to reduce the negative impact of transport facilities.

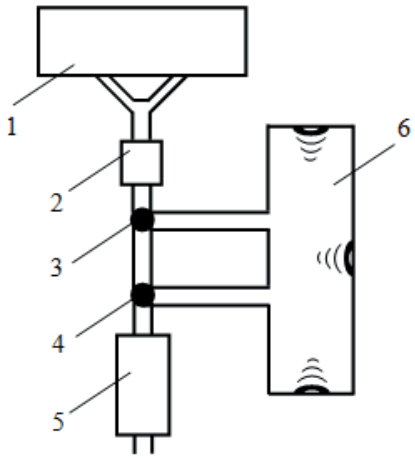
Reduction of harmful emissions of exhaust gases of internal combustion engine can be carried out by installation of various systems of neutralization and purification of exhaust gases operating on methods of liquid, thermal, catalytic neutralization, soot filters. A method for ultrasonic purification of exhaust gases is known. In order to reduce the concentration of toxic and polluting substances, it is proposed to equip motor vehicles with the tank equipment of cyclic action for ultrasonic purification of the motor vehicles exhaust gases, which is a tank with an ultrasonic generator and radiator mounted in it [2].

2 The tank equipment construction and principle of operation

During the development of equipment, the patents obtained by authors were used [3-4]. Diagram of connection of tank equipment for the ultrasonic purification of motor vehicles exhaust gases is shown in Figure 1.

The equipment operates in active and passive modes. In passive mode valves 3 and 4 pass exhaust gas from resonator 2 to muffler 5 bypassing the storage tank of equipment. During the engine warming-up, up-driving, acceleration or when the vehicle is driven to a stop, the device switches to the active mode - the inlet valve 3 is switched to the tank filling mode, the outlet valve of the device 4 closes the discharge from the storage tank and the gas is accumulated in the tank 6, that is, there is a temporary isolation of exhaust gases from emission into the atmosphere for the period

This is an open access article distributed under the terms of the Creative Commons Attribution 4.0 International License (CC BY 4.0), which permits use, distribution, and reproduction in any medium, provided the original publication is properly cited. No use, distribution or reproduction is permitted which does not comply with these terms.



1 - engine; 2 - resonator; 3 - inlet valve; 4 - outlet valve; 5 - muffler; 6 - tank ultrasonic purifying equipment

Figure 1 *Scheme of installation of tank equipment of ultrasonic purification of motor vehicle exhaust gases.*

of a stop for some time, after starting driving. At the same moment the ultrasonic device is switched on and ultrasonic coagulation of soot particles occurs in the containers, accompanied by their weighting and settling. After a pre-determined period of time, for example, when the bus is starting from the stop by a sufficient distance or when a certain pressure is reached in the tank set by the critical filling mode, the exhaust valve opens and the purified exhaust gas is released through the muffler 5 and any filtering device into the atmosphere.

The time of tank filling, its volume and strength characteristics are determined in the work [5].

The coagulation process is accelerated by exposure to ultrasound, which has a dispersing effect on emulsions and liquid sols and coagulating effect on aerosols (smoke, fog, dust).

Efficiency of the coagulation process increases when a standing wave occurs. Standing waves are a particular case of interference; two identical waves spread in opposite directions.

Exhaust gas consists of particles of different sizes. Depending on their magnitude and frequency of oscillations, the particles can follow sound oscillations and coagulate.

The first process takes place at low oscillation frequencies. When the oscillation frequency increases, there is an optimal frequency segment at which particles of different magnitude have different amplitude, collide with each other and coagulate. This kind of coagulation is called ortho-kinetic. When frequency increases, coagulation becomes hydrodynamic and it is performed due to friction. This process is described by the Bjerknes equations [6-9].

The degree of particle participation in sound oscillations in the case of standing sound wave is related to frequency of oscillations, radius of a particle and viscosity of environment; it is described by the following ratio [6-8]:

$$\frac{U_{ch}}{U_g} = \frac{1}{\left[(4\pi\rho r^2 f/9\eta)^2 + 1\right]^{1/2}}, \quad (1)$$

where: U_{ch}, U_g are the amplitudes of the particle and gas oscillations respectively;

ρ - density of the particle;

r - the radius of the particle;

f - frequency of gas oscillations under action of ultrasound;

η - dynamic viscosity.

This equation is derived from the Stokes law [6-9] and reflects the hydrodynamic coagulation.

The amplitude ratio will be smaller the higher the frequency and greater the radius of the particles. Therefore, depending on the degree of particle participation in gas oscillations, the value r^2f is determined. It is accepted to define the coefficient of fascination by the expression:

$$Z = \frac{\rho r^2 f}{\eta}. \quad (2)$$

The coagulation process for this device is described by the following dependencies.

When the ultrasonic generator is switched on:

$t = 0$; $PV = \text{const}$; $P = \text{const}$; $V = \text{const}$; $\rho = \text{const}$; $m = m_0$,

where t - time; P - pressure; V - volume; ρ - density; m - mass; m_0 - the initial mass.

During the ultrasonic generator operation:

$$t > 0; V = const; P = \tilde{P}(\rho, m); m = \tilde{m}(t).$$

Coagulation kinetics dependence, described by exponential dependence, is adopted as a coagulation model [10]:

$$n = n_0 \exp(-kt), \quad (3)$$

where n and n_0 are counting concentrations of gas

particles, respectively current at the initial moment;
k - coagulation coefficient.

Let it be assumed that the average concentration of gas and soot molecules is directly proportional to their masses and inversely proportional to the volume occupied. Then the total mass in the tank will be composed of the gas mass (m_G) and the soot mass (m_s):

$$m_0 = nm_G + (1-n)m_s. \tag{4}$$

From Equations (3) and (4), one obtains:

$$\frac{m_G}{V} = \frac{m_0}{V}e^{-kt}, \tag{5}$$

as:
$m_s = m_0 - m_G$,

then:

$$m_c = m_0 - m_0 e^{-kt} = m_0(1-e^{-kt}). \tag{6}$$

The pressure depending on the mass is determined as $P = \frac{mg}{S}$ where S - square, taking into account the gas mass $P = \frac{m_0 e^{-kt}}{S}g$.

The density of gas and soot taking into account their volumes will be equal to $\rho_g = \frac{m_0 e^{-kt}}{V}; \rho_s = \frac{m_0(1-e^{-kt})}{V_c}$, respectively.

The value of the drag coefficient is determined by expression:

$$Z = \frac{m_0 e^{-kt} r^2 f}{\eta}. \tag{7}$$

From Equation (6), the coagulation coefficient is determined as:

$$k = -\frac{\ln\left(1-\frac{m_c}{m_0}\right)}{t}. \tag{8}$$

The light transmission capacity of some volume of exhaust gas is directly dependent on the concentration of particulate matter contained therein, preferably soot, in a suspended state and it is due to the light absorption capacity of the particulate matter. The change in the light transmission capacity indicates the change in the soot concentration in the exhaust gas due to the deposition of soot particles on the bottom of the device.

The light absorption capacity can be estimated by the light flux absorption coefficient [2], determined as:

$$\beta_i = 1 - \alpha_i, \tag{9}$$

where α_i - is the degree of gas transparency α in the i-th time period determined by the ratio of illumination index E after gas injection into the i-th time period to illumination index prior to the gas injection.

$$\alpha_i = \frac{E_i}{E_{ish}}, \tag{10}$$

where i = 1…10.

Assuming that n and n_0 are counting concentrations of gas particles, respectively, they are current and at the initial moment are proportional to the light flux absorption degree β.

The coagulation coefficient is determined by formula:

$$k_i = -\frac{\ln\frac{\beta_i}{\beta_{i-1}}}{t}, \tag{11}$$

where i = 1…10;
t - time interval between readings, t = 60 s.

Based on the hypothesis of close correlation between the coagulation and gas transparency degree, one equates Equations (8) and (11):

$$-\frac{\ln\left(1-\frac{m_c}{m_0}\right)}{t} = -\frac{\ln\frac{\beta_i}{\beta_{i-1}}}{t}, \tag{12}$$

whence

$$m_c = m_0\left(1-\frac{\beta_i}{\beta_{i-1}}\right), \tag{13}$$

or

$$m_c = m_0\left(1-\frac{1-\alpha_i}{\alpha_{i-1}}\right) = m_0\left(1-\frac{1-\frac{E_i}{E_{ish}}}{1-\frac{E_{i-1}}{E_{ish}}}\right). \tag{14}$$

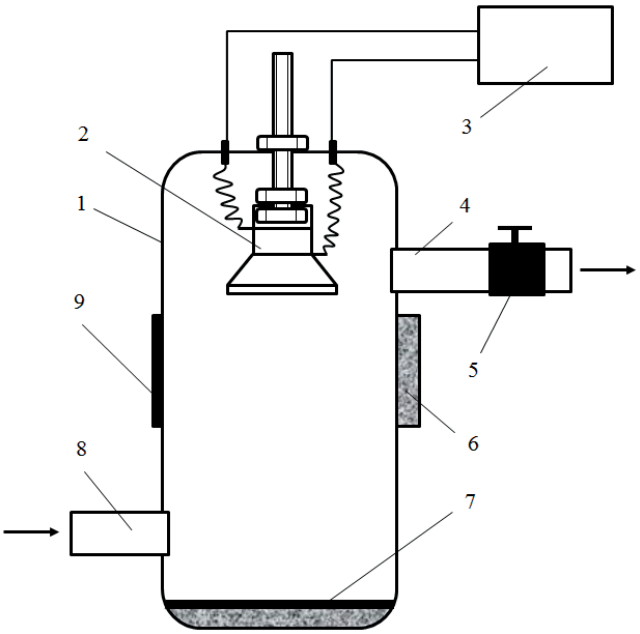
Thus, knowing the amount m_0 that can be determined from the volume of the tank and gas density, in order to determine the amount m_c, it is necessary to determine the ratio $\frac{\beta_i}{\beta_{i-1}}$ through the corresponding illumination values.

The device that detects this value is necessary, which is a transparent container, a light source, and an illumination sensor.

For experiments an experimental device was created for the ultrasonic purification of exhaust gases (Figure 2) consisting of a light-transmitting tank 1, an inlet 8 and an outlet 4 branch pipe with a valve 5, an ultrasonic radiator 2 and an ultrasonic generator 3, an ultrasonic wave reflector 7 [2].

The most effective frequencies of ultrasonic waves for the process of the soot particles coagulation of the internal combustion engines exhaust gases are in the frequency range from 15 to 30 kHz [6-7]; the frequency of ultrasonic generator of experimental device - 28 kHz, radiation power - 100 W.

The device is filled with exhaust gas through an inlet pipe 8, which in turn is connected to the exhaust pipe of the automobile. A faucet 5 is installed on the outlet branch pipe 4, which is closed after the installation is filled with exhaust gas. Under the action of ultrasonic waves, created by ultrasonic generator 3 and radiator



1 - light-transmitting tank; 2 - ultrasonic radiator; 3 - ultrasonic generator; 4 - outlet branch pipe; 5 - faucet; 6 - a light source; 7 - an ultrasonic wave reflector; 8 - inlet branch pipe; 9 - lux-meter.

Figure 2 *Experimental device for ultrasonic cleaning of exhaust gases*

Table 1 *The results of the experiments*

seconds	illumination index - E, lx		illumination change - ΔE, lx		transparency degree - α		degree of light flux absorption - β		coagulation coefficient - k	
	without ultrasound	with ultrasound	without ultrasound	with ultrasound	without ultrasound	with ultrasound	without ultrasound	with ultrasound	without ultrasound	with ultrasound
0	60	60			0.429	0.429	0.571	0.571		
60	66	80	5.64	20.00	0.469	0.571	0.531	0.429	0.0012	0.0048
120	70	90	4.82	9.91	0.503	0.642	0.497	0.358	0.0011	0.0030
180	73	95	2.18	5.18	0.519	0.679	0.481	0.321	0.0005	0.0018
240	76	101	3.00	5.64	0.540	0.719	0.460	0.281	0.0008	0.0022
300	77	105	1.00	4.45	0.547	0.751	0.453	0.249	0.0003	0.0020
360	79	109	2.27	3.73	0.564	0.778	0.436	0.222	0.0006	0.0019
420	80	113	0.91	3.64	0.570	0.804	0.430	0.196	0.0002	0.0021
480	82	116	2.55	3.00	0.588	0.825	0.412	0.175	0.0007	0.0019
540	84	118	1.27	2.45	0.597	0.843	0.403	0.157	0.0004	0.0018
600	85	120	0.91	1.64	0.604	0.855	0.396	0.145	0.0003	0.0013

2, processes of the soot particles coagulation are getting larger in exhaust gas, as a result of which soot particles are enlarged in size and mass and settle on the ultrasonic waves reflector's 7 surface. The purified exhaust gas is discharged to the atmosphere through the outlet branch pipe 4 after opening the faucet 5.

A lux-meter - 9 was used for the experiment. A light source - 6 was fixed on the opposite side. The entire structure was placed in a light-tight conduit to eliminate the effect of the external lighting change on results.

The experiments were carried out as follows. The device was filled with exhaust gas until the measured illumination decreased from 140 to 60 lx. The readings were taken at the frequency of 1 minute for 10 minutes without the ultrasonic generator being switched on and then a similar experiment was conducted with the ultrasonic generator turned on. The results of the experiments are shown in Table 1.

Graphs of the illumination index E (Figure 3), change of illumination ΔE (Figure 4) and coagulation coefficient - k dependences on the deposition time (Figure 5) are constructed.

Function of the coagulation coefficient dependence on time t is approximated according to the standard procedure described in [11] and [12]. The results are shown in Table 2.

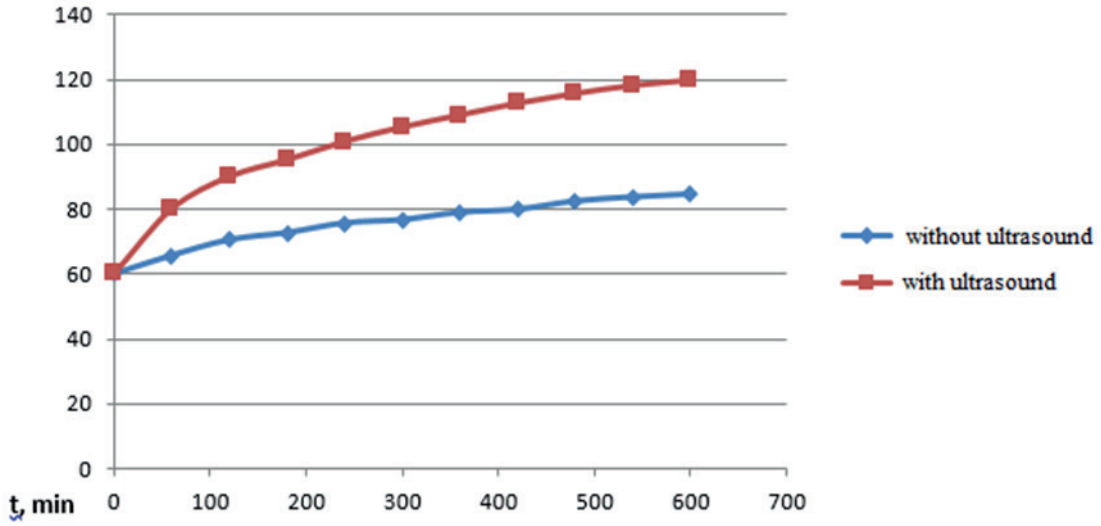


Figure 3 *Dependence of illumination index on deposition time*

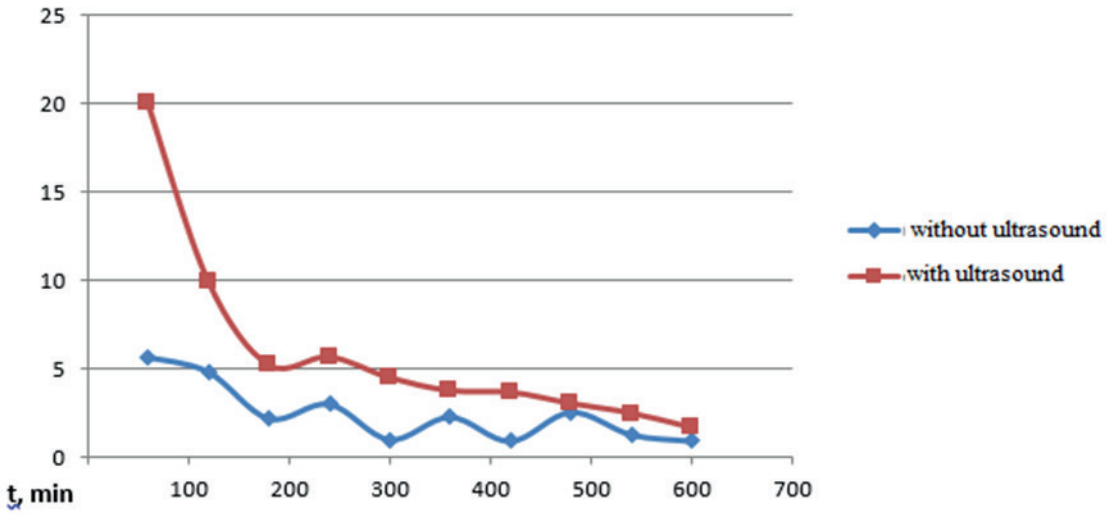


Figure 4 *Dependence of illumination index change on deposition time*

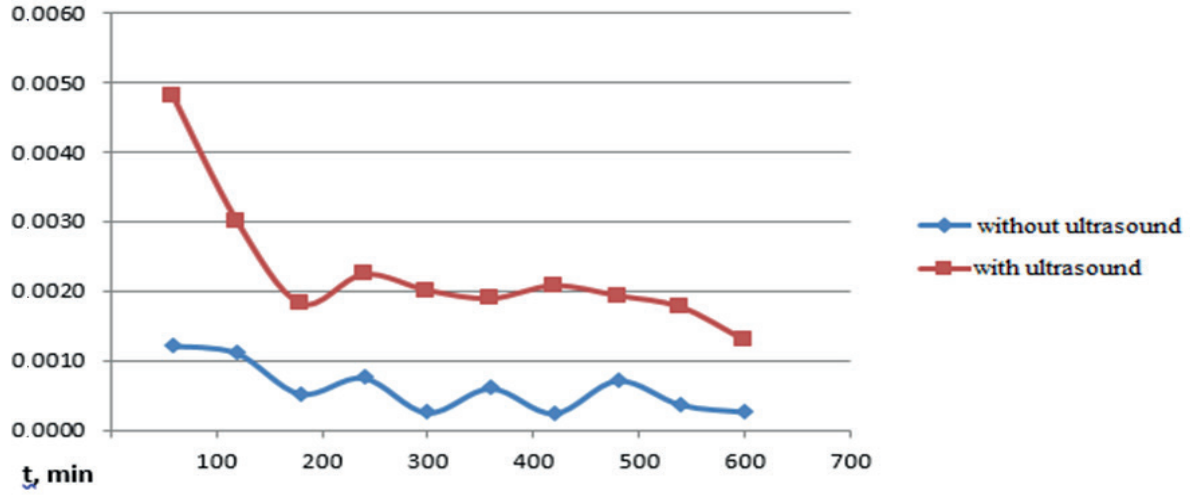


Figure 5 *Dependence of coagulation coefficient index on deposition time*

Table 2 *Results of approximation of the coagulation coefficient function of time*

regression	indicators	without ultrasound	with ultrasound
1	2	3	4
linear	dependence k=f(t)*10^{-4}	k = -0.0136364t + 10.60	k = -0.0402020t + 36.0666667
	linear pair correlation coefficient k=f (t) *10^{-4}	-0.7255863	-0.7429615
	determination coefficient	0.5264754	0.5519919
	average approximation error, %	45.4635773	19.6705412
quarter	dependence k=f(t)*10^{-4}	k = 0.0000442t^2 - 0.0428030t + 14.10	k = 0.0001473t^2 - 0.1374242t + 47.7333333
	correlation coefficient k=f (t) *10^{-4}	0.8086220	0.8501427
	determination coefficient	0.6538695	0.7227426
	average approximation error, %	38.3055195	18.8015330
cubic	dependence k=f(t)*10^{-4}	k = -0.0000002t^3 + 0.0002223t^2 - 0.0920778t + 17.4333333	k = -0.0000012t^3 + 0.0012994t^2 - 0.4562322t + 69.3
	correlation coefficient k=f (t) *10^{-4} of k=f (t) *10^{-4}	0.8356506	0.9732228
	determination coefficient	0.6983119	0.9471627
	average approximation error, %	36.1394885	8.2440902
degree	dependence k=f(t)*10^{-4}	k = 133.2196139$t^{-0.5768993}$	k = 232.5708630$t^{-0.4255949}$
	correlation coefficient	0.8073428	0.9193806
	determination coefficient	0.6518023	0.8452607
	average approximation error, %	35.4446902	11.8821493
indicative	dependence k=f(t)*10^{-4}	k = 10.6971362 · 0.9978466^t	k = 35.5964301 · 0.9984605^t
	correlation coefficient	0.7491687	0.7698100
	determination coefficient	0.5612538	0.5926074
	average approximation error,%	39.7408550	15.9516601
logarithmic	dependence k=f(t)*10^{-4}	k = 27.8815899 - 3.8848717 · ln t	k = 89.6447697 - 11.9255533 · ln t
	correlation coefficient	0.8083030	0.8824176
	determination coefficient	0.6533538	0.7786609
	average approximation error, %	37.8721412	15.1343431
hyperbolic	dependence k=f(t)*10^{-4}	$k = \frac{3.2191661 + 590.1396602}{t}$	$k = \frac{12.8257622 + 2043.2255254}{t}$
	correlation coefficient of k=f (t) *10^{-4}	0.7987887	0.9605531
	determination coefficient	0.6380633	0.9226623
	average approximation error, %	40.1251236	10.3018760
exponential	dependence k=f(t)*10^{-4}	$k = e^{2.3699761 - 0.0021557t}$	$k = e^{3.5722454 - 0.0015407t}$
	correlation coefficient	0.7491687	0.7698100
	determination coefficient	0.5612538	0.5926074
	average approximation error, %	39.7408550	15.9516601

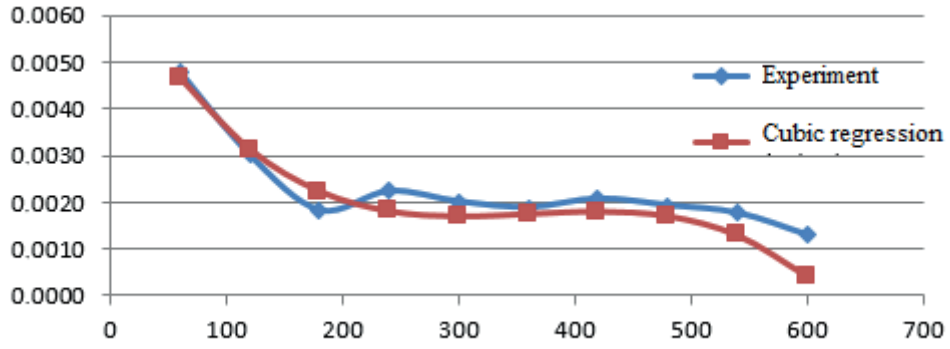


Figure 6 *Experimental and calculated graphs of coagulation coefficient dependence on time*

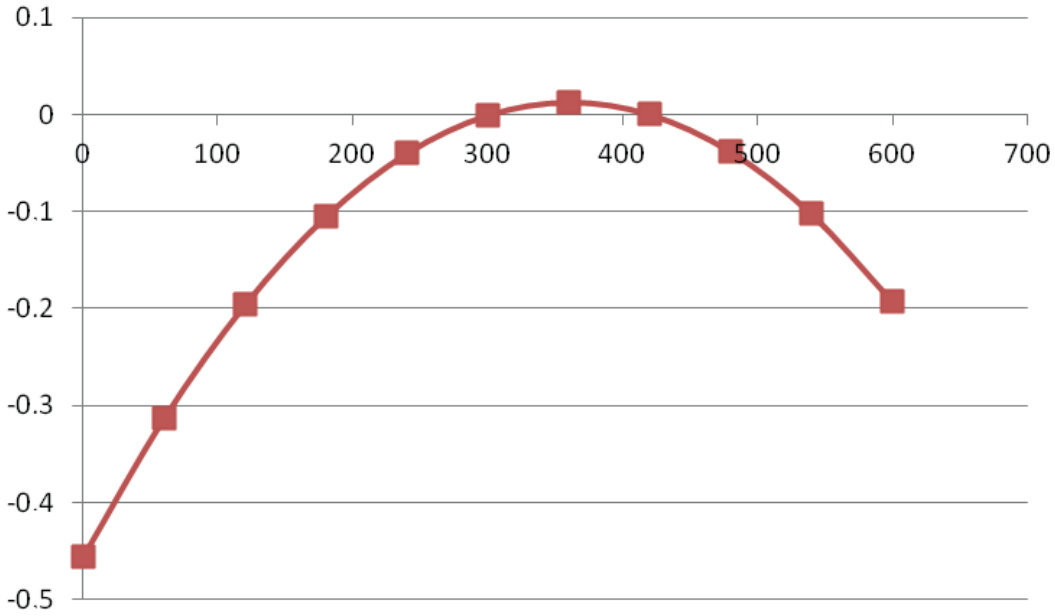


Figure 7 *Dependence of the coagulation coefficient change rate on time*

From analysis of Table 2 on the largest values of correlation coefficients, determinations and the smallest values of the average approximation error for the coagulation process using ultrasound, it is proposed to use the cubic regression equation:

$$k = (-0.0000012t^3 + 0.0012994t^2 - \\ -0.4562322t + 69.3)\cdot 10^{-4}. \quad (15)$$

Figure 6 shows graphs of dependencies k *(t)*, obtained from the experimental data and data calculated according to Equation (15).

Thus, the coagulation coefficient must be determined by Equation (15) and the soot mass by Equation (6).

The coagulation rate process is essential. Since Equation (15) has a significant determination factor, differentiation of the function is possible. Then, the coagulation rate was subjected to the following dependency:

$$\dot{k} = (-0.0000036t^2 + 0.0025988t - \\ -0 - 4562322)\cdot 10^{-4}. \quad (16)$$

Figure 7 shows a graph of the coagulation rate dependence on time.

3 Conclusions

The article confirms the possibility of using the exhaust gases in the isolation tank using ultrasonic generators. Using the assumptions that the average concentration of the gas molecules and soot particles is directly proportional to their masses and inversely proportional to their volumes, the ratio of these masses in the form of coagulation coefficient over time is obtained.

The assumption about close correlation between the coagulation and the degree of gas transparency was suggested, which made it possible to carry out the experiment based on determining the degrees of transparency and absorption of the light flux by the gas. The results of the experiment confirmed the analytical data.

The obtained results make it possible to use dependencies to determine the parameters and operation modes of the tank equipment for ultrasonic cleaning of motor vehicles exhaust gases depending on parameters of the ultrasonic generator and the tank volume by selection according to schedules.

Analytical and experimental studies make it possible to develop the methods of calculating the system of the tank equipment for ultrasonic cleaning of exhaust gases. This methodology includes dependencies for determining the parameters and operating modes of the system depending on parameters of the ultrasonic generator and the tank volume by selecting according to dependencies obtained in the article.

References

[1] EROKHOV, V. I. Toxicity of modern cars (methods and means of reducing harmful emissions to the atmosphere): textbook. Moscow: Forum: Infra-m, 2013. ISBN 978-5-911384-801-4.

[2] IBATOV, M. K., KADYROV, A. S., PAK, I. A., KADYROVA, I. A., ASKAROV, B. S. Results of experimental studies of operation of the tank equipment of ultrasonic purification of exhaust gases of motor vehicles (in Russian). *Ugol / Coal* [online]. 2020, **2**, p. 73-78. ISSN 0041-5790, eISSN 2412-8333. Available from: http://dx.doi.org/10.18796/0041-5790-2020-2-73-78

[3] IBATOV, M. K., KADYROV, A. S., BALABAYEV, O. T., ASKAROV, B. S., PAK, I. A. Device for ultrasonic purification of exhaust gases. Patent 3194 PK. 2018.

[4] IBATOV, M. K., KADYROV, A. S., PAK, I. A., ASKAROV; B. S. Device for exhaust gas isolation. *Bulletin*. 2012, **12**. ISSN 1609-1825.

[5] IBATOV, M. K., ALIYEV, S. B., BALABAYEV, O. T., ASKAROV, B. S. Main results of experimental studies of exhaust gas isolation of ICE of quarry locomotives. *Ugol / Coal* [online]. 2019, **7**, p. 28-30. ISSN 0041-5790, eISSN 2412-8333. Available from: http://dx.doi.org/10.18796/0041-5790-2019-7-28-30

[6] KHMELEV, V. N. Ultrasonic coagulation of aerosols. In: KHMELEV, V. N., SHALUNOV, A. V., SHALUNOVA, K. V., TSYGANOK, S. N., BARSUKOV, R. V., SLIVIN, A. N. (Eds.) Biysk: Biysk Institute of Technology, Altai State Technical University, 2010.

[7] BERGMAN, L. *Ultrasound and its applications in science and technology*. Moscow: Publishing House of Foreign Literature, 1957.

[8] BALDEV, R., RAJENDRAN, V., PALANICHAMI, P. *Applications of ultrasound*. Moscow: Technosphera, 2006. ISBN 5-94836-088-1.

[9] GALLEGO-JUAREZ, J. A., GRAFF, K. F. *Power ultrasonics: applications of high-intensity ultrasound*. 1. ed. Elsevier, 2014. ISBN 978-1-78242-028-6, eISBN 978-1-78242-036-1.

[10] KARDASHEV, G. A. *Fizicheskie metody intensifikatsii protsessov khimicheskoi tekhnologii / Physical methods of intensification of chemical technology processes* (in Russian). Moscow: Khimiya, 1990. ISBN 5-7245-0674-2.

[11] SHEROV, K. T., ALIKULOV, D. E. Control ruler for angles between planes of V-shaped guides. *Measurement Techniques* [online]. 2012, **55**(4), p. 397-399. ISSN 0543-1972, eISSN 1573-8906. Available from: https://doi.org/10.1007/s11018-012-9971-5

[12] SHEROV, K. T., SIKHIMBAYEV, M. R., NASAD, T. G., ABSADYKOV, B. N., IZOTOVA, A. S., OKIMBAYEVA, A. E., KUANOV, I. S. The research of the steel cutting blade reliability for thermo-frictional processing. *News of the National Academy of Sciences of the Republic of Kazakhstan. Series of Geology and Technical Sciences* [online]. 2020, **1**(439), p. 122-130. ISSN 2224-5278, eISSN 2518-170X. Available from: http://doi.org/10.32014/2020.2518-170X.15

NUMERICAL SIMULATION OF TEMPERATURE DISTRIBUTION IN THE GAS TURBINE BLADE

Dariusz Jakubek

Faculty of Mechanical Engineering, Cracow University of Technology, Cracow, Poland

*E-mail of corresponding author: darek.jakubek01@gmail.com

Resume

This paper concentrates on temperature distribution in the gas turbine blade equipped by the cooling holes system on transient heat transfer. The present study requires the specification of internal and external boundary conditions. The calculations had been done using both Crank-Nicolson algorithm, explicit and implicit methods, in which different heat transfer coefficients on internal cooling surfaces of the holes were applied. The value of coefficients has a direct and crucial impact on the final result. The heat transfer coefficient of cooling the working surface of the of heat pipes was 1600 W/(m2K). It was found that there were no significant differences of temperature distribution in comparison of results from explicit method in the Ansys analysis, Crank-Nicolson algorithm and implicit method in Matlab. The simulation is based on Finite Element Method, which uses the Crank Nicolson algorithm.

Article info

Received 27 September 2020
Accepted 7 December 2020
Online 24 May 2021

Keywords:

film cooling,
heat transfer,
gas turbine blade,
numerical method

Available online: https://doi.org/10.26552/com.C.2021.3.B227-B236

ISSN 1335-4205 (print version)
ISSN 2585-7878 (online version)

This is an open access article distributed under the terms of the Creative Commons Attribution 4.0 International License (CC BY 4.0), which permits use, distribution, and reproduction in any medium, provided the original publication is properly cited. No use, distribution or reproduction is permitted which does not comply with these terms.

1 Introduction

Development of materials and technology, used in the construction of turbine blades and cooling systems, contributed to an increase of combustion temperature of the fuel. Therefore, the first (and often the second) turbine stage is cooled by the air extracted from the compressor. The high compression ratios cause a significant increase in the temperature of the compressed air, which is approximately 1200 °F (649 °C). That causes the thermal stresses on cooperating elements - mainly gas turbine blades. To minimize the risk of premature material wear, solutions are used to reduce the temperature of the vanes in the form of cooling channels. The following section shows the main types of direct cooling:

1. Convection cooling,
2. Impingement cooling,
3. Film cooling,
4. Full-coverage film cooling,
5. Transpiration cooling.

An increase of the working medium temperature by 100 °F (56 °C) contributes to the increase of the power output by 8-13% and the increase of the overall efficiency 2-4% for a single system. The internal single-flow cooling used in the 1960's allowed the flue gas temperature to reach ~ 850 °C. Further development in the form of membrane cooling, combined with one-cycle air flow (1970's), increased the temperature resistance to over 1000 °C. This type of cooling works on the principle of radial air flow through the profiled channels of turbine blades and vanes. The radial flow through the channels provides multiple meandering air movement that removes the heat from the walls. This is currently the most widespread idea of cooling. The middle section is cooled by the forced convection, the air flows around the ribs that give off heat. The leading edge is also cooled by exhaust nozzles. The circulating air leaves the inner surface through the outlets at the trailing edge. Jet cooling is a part of the above solution. This is a type of high-efficiency convection cooling. The cooling air is directed, at a high speed, to the inner part - the front part of the blade. The high speed of the medium causes an increase in the heat transfer coefficient and thus a greater amount of heat is taken from the material [1-3].

Han et al. [4] performed an experimental investigation to study the effects of the hole pitch and the blowing ratio on the leading edge region film cooling performance of a twist turbine blade with three rows of film holes under rotating conditions.

Mishra and Sanjay [5] studied the radiative heat transfer of turbine blade cooling model and provided the unique performance maps for power utility designers.

Kamal-Omar et al. [6] undertook studies about the performance of a gas turbine, which depends on the air temperature and proved that the cooling systems are necessary to reduce the heat rate, as well as to increase the turbine's power output.

The major goal of Kim et al. [7] was to redesign

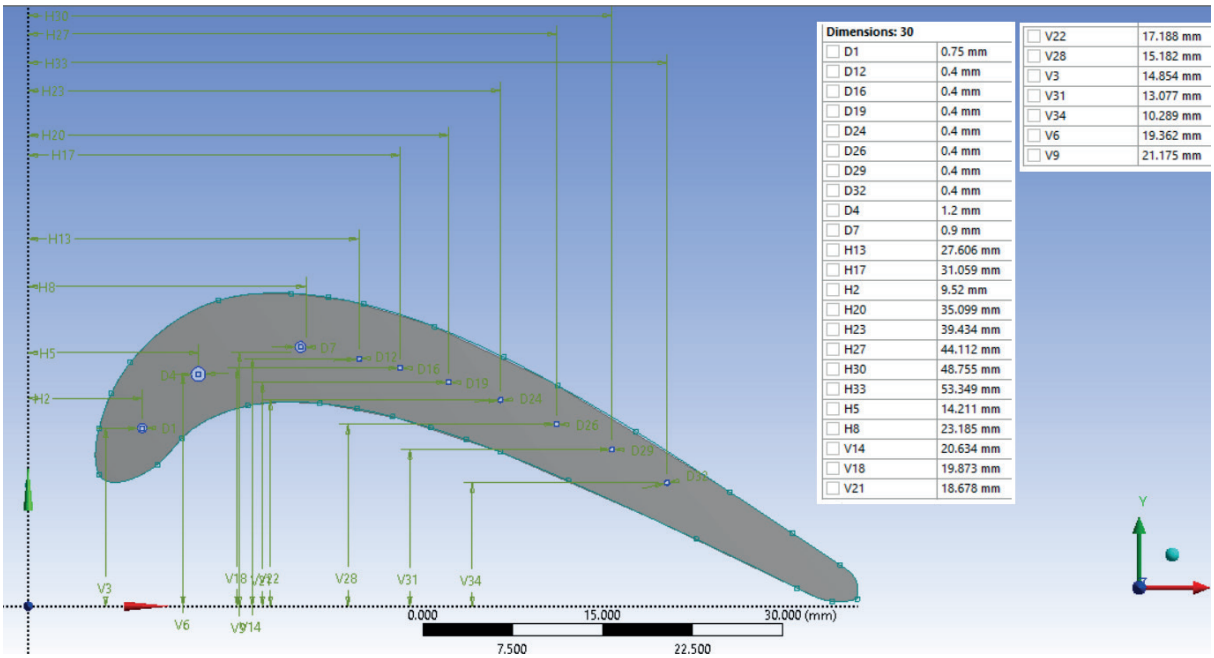


Figure 1 *The geometry model of the turbine blade used in simulation including all dimensions*

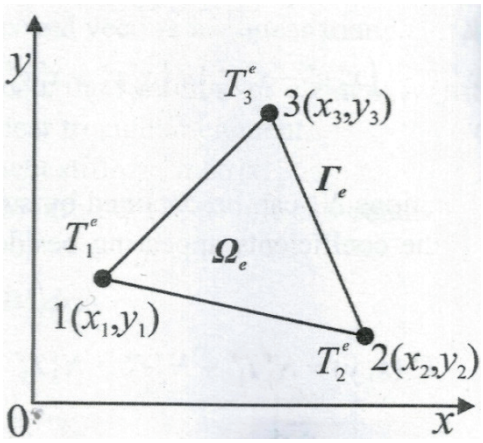


Figure 2 *The linear triangular element with three nodes [4]*

the internal cooling passage to reduce the pressure loss so that it does not demand increased coolant feed pressure. The high-fidelity numerical simulations predict improvement and, as a result, reducing the temperature of the turbine blade.

Baakeem, Orfi and Al-Ansary [8] achieved the optimum value of the cooled air temperature and presented the comparative study of widely used cooling methods by using mass and energy balance including mechanical vapor compression.

The research undertaken by Zhou et al. in [9] shows that film cooling effectiveness descends with the increasing blowing ratio. Numerical simulation proved that the blade middle-spane area has the thickest film cooling coverage.

He et al. [10] studied the cooling performances of three kinds of film holes (standard cylindrical film holes, transverse trenched and segmented trenched film holes). The research was undertaken with numerical method.

The film transfer cooling hole location and their dimension affect to film cooling system. It is proved by Zhou, Wang and Li [11] due to numerical investigation.

The major subject of Liu et al. paper [12] was modeling the film cooling flow of the turbine blade and compared results with developed method by adding end wall cooling part.

Wei et al. [13] performed the numerical simulation of effusion cooling mechanism by using different sizes of internal holes. During the modeling the inclination angle and the expansion angle were changing.

2 Numerical analysis

2.1 Problem formulation

The geometry of the turbine blade with cooling holes was created by using the Ansys software, the subject of this studies concentrates on the heat conduction by using the Finite Element Method application. The

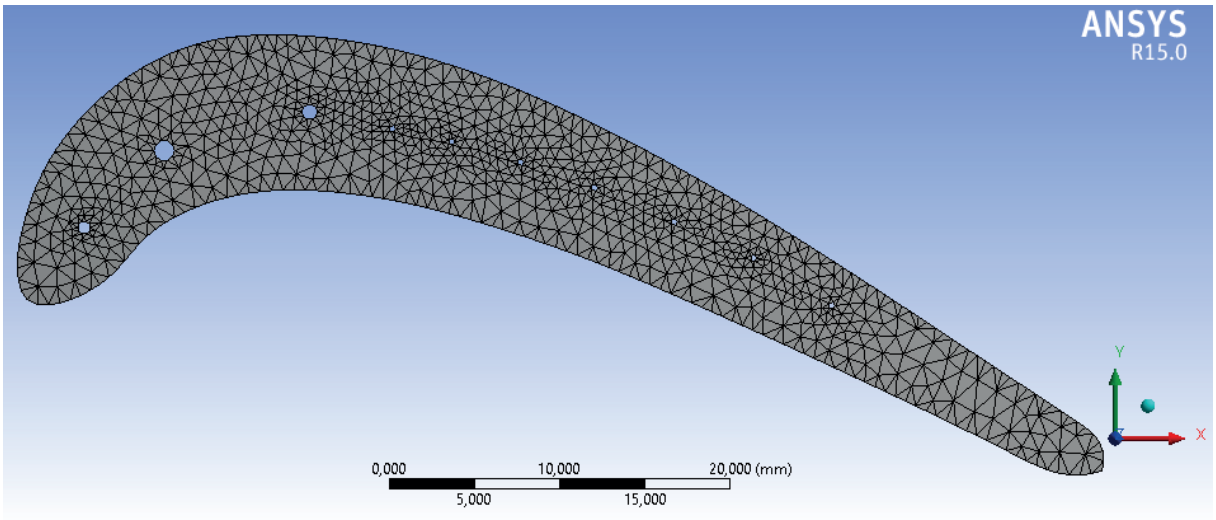


Figure 3 *The geometry model after discretization process [15]*

model considers the gas turbine blade with the cooling system. It had been managed by seven holes (Figure 1) through which the flowing air provides a decrease of temperature. All the dimensions and geometry are shown Figure 1.

The analysis considers the turbine blade cooled by the air passing through ten holes. The first three holes are marked as D1, D4 and D7, their dimensions are respectively 0.75 mm, 1.2 mm and 0.9 mm. The remaining holes have the same dimension - 0.4 mm.

The triangular method, used in the present analysis, consists of three nodes, therefore the temperature in the particular finite element was computed by using the temperatures in three nodes and shape function estimated in x, y coordinates. The example triangular element is shown in Figure 2.

The temperature within the triangular element Ω^e has been calculated by the function [14]:

$$T^e(x,y) = a_1^e + a_2^e x + a_3^e y\,. \tag{1}$$

The nodal coefficients (a_i^e) are obtained by solving the three linear equations, each one is corresponding with individual node in triangular finite element. The temperature changes in the x and y directions, therefore, in each equation the individual nodal coordinates are used. After calculations, one obtains the following three equations [15]:

$$a_1^e = \frac{1}{2A^e}[(x_2y_3 - x_3y_2)T_1^e + (x_3y_1 - x_1y_3)T_2^e \cdot \cdot (x_1y_2 - x_2y_1)T_3^e], \tag{2}$$

$$a_2^e = \frac{1}{2A^e}[(y_2 - y_3)T_1^e + (y_3 - y_1)T_2^e(y_1 - y_2)T_3^e], \tag{3}$$

$$a_3^e = \frac{1}{2A^e}[(x_3 - x_2)T_1^e + (x_1 - x_3)T_2^e(x_2 - x_1)T_3^e]. \tag{4}$$

A^e is considered as an area of a triangular element.

As a result of substitution of coefficients into the Equation (1), on obtains the shape functions for the three nodes of a finite element.

$$N_1^e = \frac{1}{2A^e}(a_1^e + b_1^e x + c_1^e y)\,, \tag{5}$$

$$N_2^e = \frac{1}{2A^e}(a_2^e + b_2^e x + c_2^e y)\,, \tag{6}$$

$$N_3^e = \frac{1}{2A^e}(a_3^e + b_3^e x + c_3^e y)\,. \tag{7}$$

2.2 Finite element model

To obtain the discrete model, the Ansys - Workbench software was used. The geometry model after discretisation is shown in Figure 3. The whole structure has been divided into the finite elements by the mapped face meshing method. That feature automatically determines a suitable amount of divisions on the edges. However, the automatic method generates the high density of nodes around the circularly shaped cooling holes, therefore, for the better nodes arrangement on the whole surface the upper and lower edge were divided by applying the solid number of divisions (120 - for the upper and lower edge of the blade). In this analysis, the triangular method was applied, hence the number of nodes and elements are respectively 960 and 1 633.

2.3 Boundary conditions

Applied boundary conditions are shown in Figure 4. The following analysis is considered as a heat transfer in two dimensions. The convective surface boundary conditions are defined in locations in yellow and red. The outer blade's surface is divided into two segments "out 1" and "out 2". The inner surface is divided into ten sections "in 1" - "in 10" The material parameters and meticulous description of values and their units are shown in Table 1. It contains the thermal conductivity

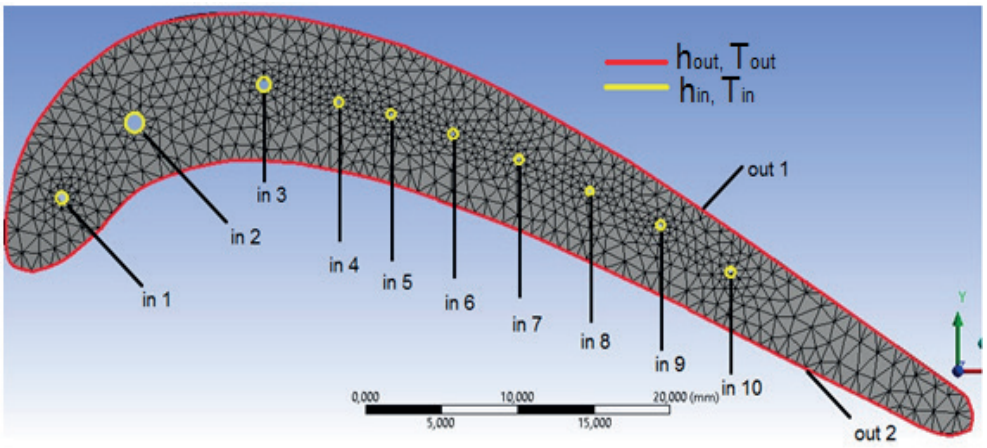


Figure 4 *Finite element method of the turbine blade with applied boundary conditions*

Table 1 *Parameters of the transient heat transfer in the present case*

parameter	units	value
thermal conductivity (k)	$\frac{W}{m \times K}$	6.92
density (ρ)	$\frac{kg}{m^3}$	4540
specific heat (c)	$\frac{J}{kg \times K}$	460
heat transfer coefficient in surfaces of turbine blade (h_{in}, h_{out})	$\frac{W}{m^2 \times K}$	400 - 5000/ 1600
temperature on turbine blade surfaces (t_{in}, t_{out})	°C	280 / 500
time step (δτ)	s	from 1x 10^{-4} to 1x 10^{-3}1x 10^{-3} s
initial temperature (t_0)	°C	22

of the blade (k); specific heat of material used in analysis (c), convective heat transfer coefficients h_{in}, h_{out}, volume of temperatures T_{in},T_{out}, time step (Δτ).

The high temperature in the compressor stages in aero engines is determined using titanium as a major component of material, which can withstand difficult conditions. The material used in simulation (Ti-6AL-2Sn-4Zr-2Mo) is characterized by superior stability in the long term application at temperature over 540 °C, therefore it is one of the most suitable material for compressor turbine blades, especially common in US in the jet engine applications [16-20].

2.4 Crank Nicolson method

The Crank-Nicolson method is used to solve calculations in numerical simulations related to the subject of the heat flow. The main second order partial differential equation (PDE) takes the following form:

$$A\frac{\partial^2 u}{\partial x^2} + B\frac{\partial^2 u}{\partial x \partial y} + C\frac{\partial^2 u}{\partial y^2} + D = 0\,, \tag{8}$$

where A, B *and*, C are independent variables of x, y, while D can be a function of x, y, u. Equation (8) is called a parabolic partial differential equation, when the quadratic equation B^2-4AC = 0. Below is a diagram describing the principle of operation of the discussed method. The calculation attempt was made to conduct the heat through the one-dimensional element. The general form of the equation takes the form [20-22]:

$$\alpha\frac{\partial^2 T}{\partial x} = \frac{\partial T}{\partial t}\,. \tag{9}$$

The method is based on the following differential scheme:

$$\left.\frac{\partial^2 T}{\partial x^2}\right|_{i,j} \approx \frac{1}{2}\left[\frac{T_{i+1}^{j} - 2T_i^j + T_{i-1}^j}{(\Delta x^2)} + \right. \\ \left. + \frac{T_{i+1}^{j+1} - 2T_i^{j+1} + T_{i-1}^{j+1}}{(\Delta x^2)}\right]. \tag{10}$$

The right part of the Equation (10) is the result of the arithmetic mean of the second degree derivative for position x at time j + 1 and j. Its main advantage is the more accurate result compared to the implicit method. This is due to the error of estimating the top for this method is O (Δt^2+ Δx^2).

$$\left.\frac{\partial T}{\partial}\right|_{i,j} \approx \frac{T_i^{j+1} - T_i^j}{\Delta t}\,, \tag{11}$$

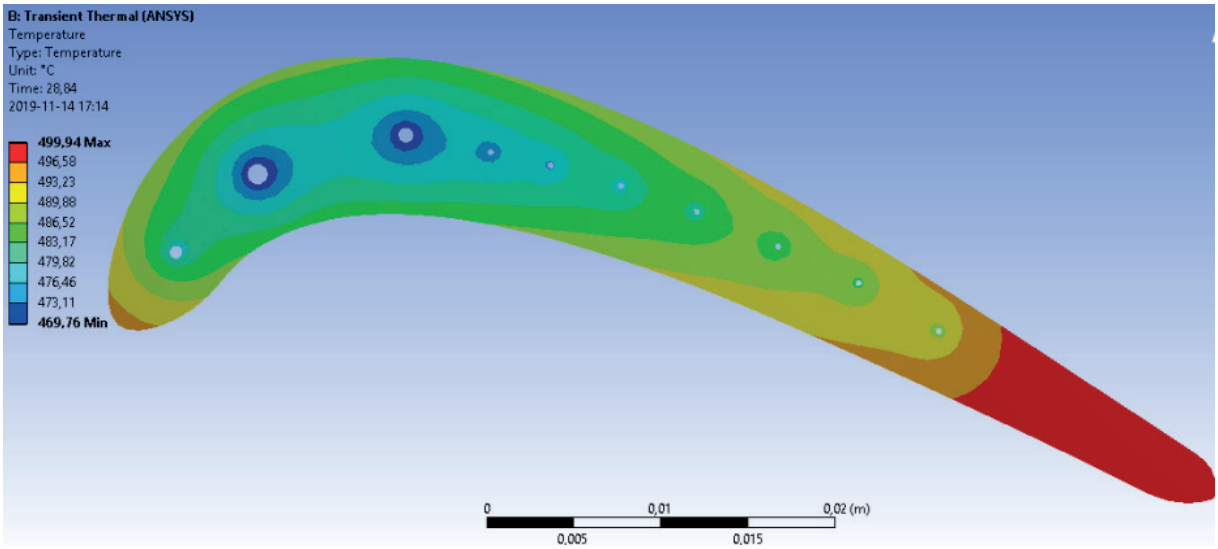


Figure 5 *Temperature distribution in the turbine blade for the heat transfer coefficient 400 W/(m²K)*

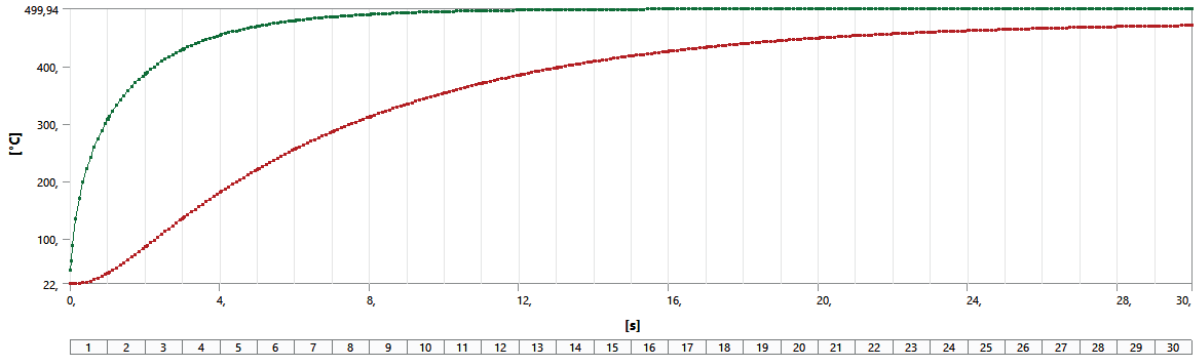


Figure 6 *The result of the transient thermal analysis for the model parameters given in Table 1 in Ansys software.*

$$\alpha\frac{1}{2}\left[\frac{T_{i+1}^{j}-2T_{i}^{j}+T_{i-1}^{j}}{(\Delta x)^2}+\right.$$
$$\left.+\frac{T_{i+1}^{j+1}-2T_{i}^{j+1}+T_{i-1}^{j+1}}{(\Delta x)^2}\right]=\frac{T_{i}^{j+1}-T_{i}^{j}}{\Delta t}. \quad (12)$$

The following equation is a linear equation, thanks to which one can calculate the temperature in all the nodes (except boundary conditions) at a given time.

$$-\lambda T_{i-1}^{j+1}+2(1+\lambda)T_{i}^{j+1}-\lambda T_{i+1}^{j}=$$
$$\lambda T_{i-1}^{j}+2(1-\lambda)T_{i}^{j}+\lambda T_{i+1}^{j}. \quad (13)$$

The Crank Nicolson method is an efficient technique of computing ordinary differential equations, which is based on the trapezoidal approximation to determine the temperature in nodes at time. Regarding the matrices and vectors, the formula is used:

$$\{T\}^{n+1}=\{T\}^{n}+\left[\begin{matrix}(1-\theta)\left\{\frac{dT}{d\tau}\right\}^{n}+\\+\theta\left\{\frac{dT}{d\tau}\right\}^{n+1}\end{matrix}\right]\Delta\tau, \quad (14)$$

$\{T\}^n$ - temperature vector at n time level,
$\{T\}^{n+1}$ - temperature vector at n+1 time level,
$\{dT\}^n$ - temperature derivative at n time level,
$\{dT\}^{n+1}$ - temperature derivative at n+1 time level.

The equation which was used to determine nodal temperatures by using global matrices **[M]** and **[K]** and vector of nodes **[f]** is (14).

3 Results

After the meshing procedure and applying all the boundary conditions, the temperature of the turbine blade was calculated in twenty-four different heat transfer coefficient. In the next step, the same geometry and all the conditions were used in the simulation to obtain the results in the Ansys-Workbench and Matlab software. The results are presented in plots below.

3.1 Transient thermal analysis

The plots and visualizations of the transient thermal analysis of the turbine blade in the Ansys software for parameters given in Table 1 are shown below.

The transient thermal analysis (Figures 5 and 6) for the step controls: maximum time step: 0.001 s; minimum time step: 0.0001 s, the heat transfer coefficient was 400

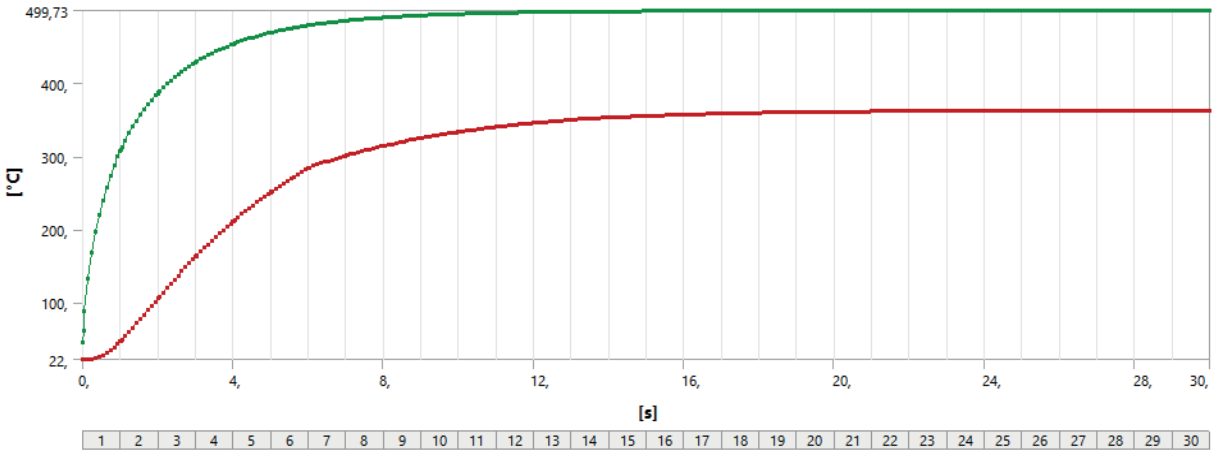


Figure 7 *The result of the transient thermal analysis for the model parameters given in Table 1 in Ansys software.*

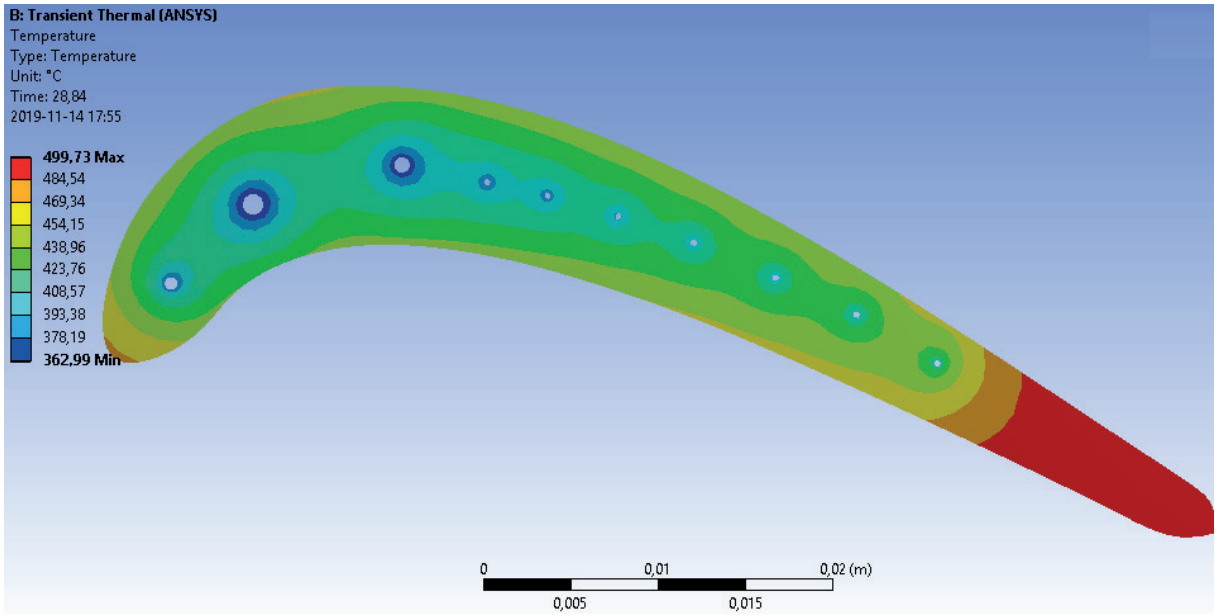


Figure 8*The visualization of transient thermal analysis for heat transfer coeficient 5000 W/(m²K), model in Ansys-Workbench software*

W/(m²K), the minimum and maximum temperature at the beginning of the calculation are respectively: 22.0 °C and 44.4 °C, at the last second of computing the minimum and maximum temperatures are respectively: 470.7 °C and 499.87 °C.

The analysis (Figures 7 and 8) for the step controls: maximum time step: 0.001 s; minimum time step: 0.0001 s, the heat transfer coefficient was 5000 W/(m²K), the minimum and maximum temperature at the beginning of the calculation are respectively: 22.0 °C and 45.4 °C, at the last second of computing the minimum and maximum temperature are respectively: 363.0 °C and 499.87 °C.

3.2 Crank-Nicolson method

The Crank-Nicolson soulutions for the model parameters given in Table 1, for the time step 0.001s, are shown in the plots below (Figures 9 and 10). The heat transfer coefficients, applied in simulations, are 400 W/(m²K) and 5000 W/(m²K), respectively. Results of calculations are the minimum and maximum temperatures of the turbine blade. At the beginning of the analysis, the temperatures are 20.8 ºC and 26.2 ºC, in both cases. At the last second of computing the minimum temperatures are 470.5 ºC for 400 W/(m²K) and 362.8 ºC for 5000 W/(m²K). The maximum temperature for both plots is 499.9 ºC.

3.3 Implicit method

The implicit solutions for the model parameters given in Table 1, for the time step 0.001s, are shown in the plots below (Figures 11 and 12). The heat transfer coefficients, applied in simulations, are 400 W/(m²K) and 5000 W/(m²K), respectively. At the beginning of analysis the temperatures are 21.8 ºC and 26.2 ºC in both cases. At the last second of computing the minimum

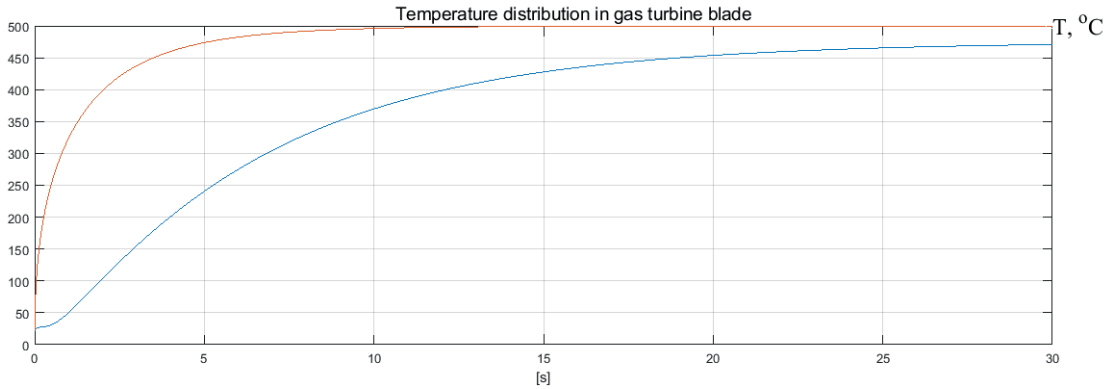


Figure 9 *The Crank-Nicolson solution for the model parameters given in Table 1, the heat transfer coefficient was 400 W/(m²K)*

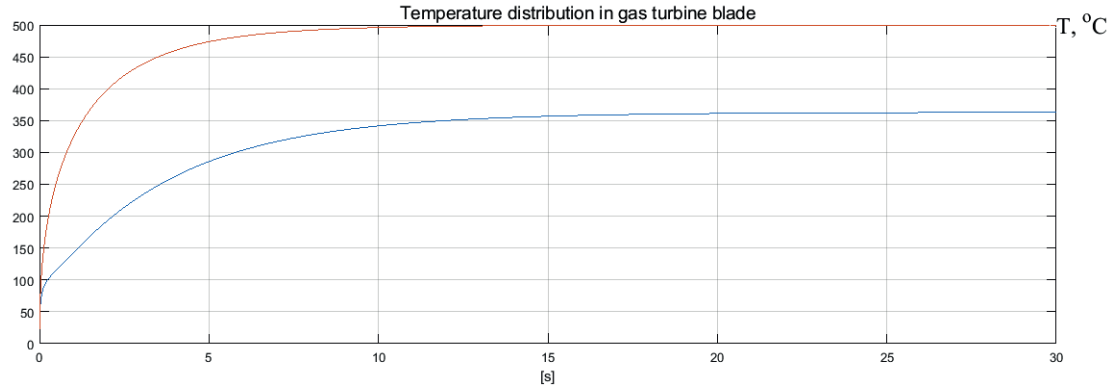


Figure 10 *The Crank-Nicolson solution for the model parameters given in Table 1, the heat transfer coefficient was 5000 W/(m²K)*

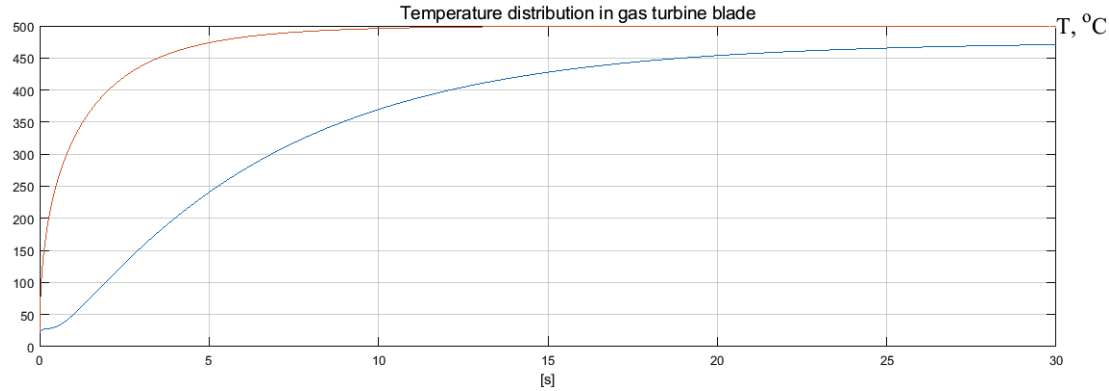


Figure 11 *The implicit calculation for the model parameters given in Table 1, the heat transfer coefficient was 400 W/(m²K)*

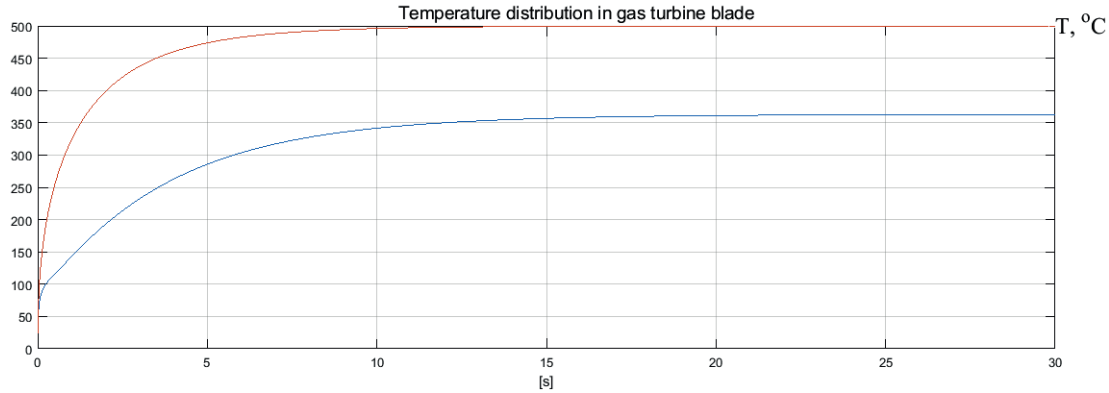


Figure 12 *The implicit calculation for the model parameters given in Table 1, the heat transfer coefficient was 5000 W/(m²K)*

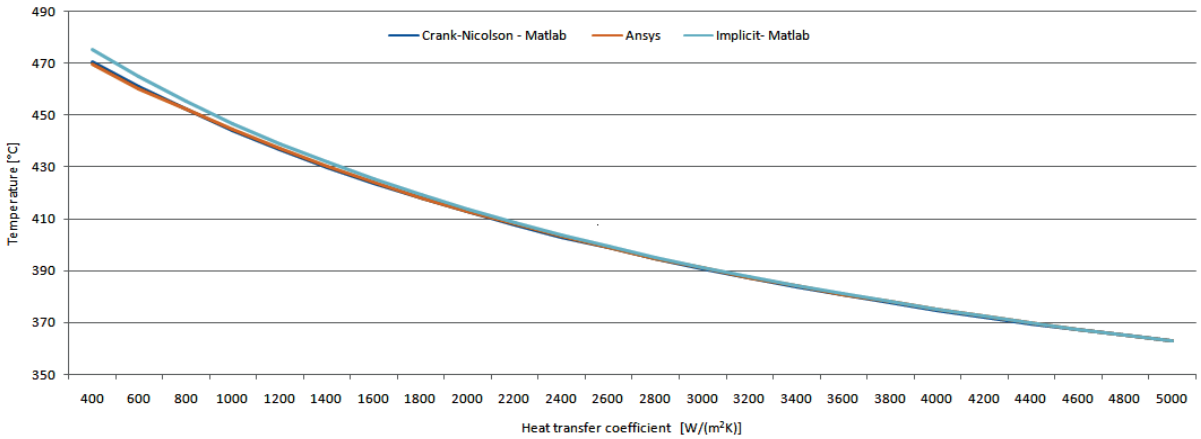


Figure 13 *The influence of the heat transfer coefficient on the final temperature based on the three calculation methods*

temperatures are 475.8 ºC for 400 W/(m²K) and 362.9 ºC for 5000 W/(m²K). The maximum temperature is 499.9 ºC in both cases.

4 Conclusions

The mathematical model of the turbine blade heat exchange was prepared by the three different methods. The optimal time step of calculation for Explicit and Implicit, Crank-Nicolson method were selected which gives convergent results, what is shown in the plot below (Figure 13).

- As the heat transfer coefficient increases the efficiency of the cooling holes rises as well, therefore the temperature of the turbine blade wall has been reduced.
- The smaller value of the heat transfer coefficient, the poorer cooling efficiency has occurred. The maximum temperature calculated in the hottest part of the blade was 499.9 °C, as a consequence the differences between the lowest and the highest point of temperature was only 30 °C.
- In the highest value of heat transfer coefficient, efficiency of the cooling holes is the most significant. The difference between the lowest and the highest point of temperature was 136 °C

The presented solution provides an effective way to reduce the temperature of the front part turbine blade (cooling area).

References

[1] BOYCE, M. P. An overview of a gas turbines. *Gas turbine engineering handbook.* 2. ed. Boston: Gulf Professional Publishing, 2011. ISBN 9780123838421, eISBN 9780123838438.

[2] XUE, S., NG, W.F. Turbine blade tip external cooling technologies. *Aerospace [online].* 2018, **5**(3), 90. eISSN 2226-4310. Available from: https://doi.org/10.3390/aerospace5030090

[3] GUPTA, A. *Vocational training report new turbine shop - block 15*. India: Bharat Heavy Electrical Limited, Mechanical Engineering Manav Rachna University, 2017.

[4] HAN, F., GUO, H., DING, X.-F., ZHANG, D.-W., LI, H.-W. Experimental investigation on the effects of hole pitch and blowing ratio on the leading edge region film cooling of a rotating twist turbine blade. *International Journal of Heat and Mass Transfer [online].* 2020, **150**, 119380. ISSN 0017-9310. Available from: https://doi.org/10.1016/j.ijheatmasstransfer.2020.119380

[5] MISHRA, S., SANJAY. Energy and exergy analysis of air-film cooled gas turbine cycle: Effect of radiative heat transfer on blade coolant requirement. *Applied Thermal Engineering [online].* 2018, **129**, p. 1403-1413. ISSN 1359-4311. Available from: https://doi.org/10.1016/j.applthermaleng.2017.10.128

[6] KAMAL, S. N. O., SALIM, D. A., FOUZI, M. S. M., KHAI, D. T. H., YUSOF, M. K. Y. Feasibility study of turbine inlet air cooling using mechanical chillers in Malaysia climate. *Energy Procedia [online].* 2017, **138**, p. 558-563. ISSN 1876-6102. Available from: https://doi.org/10.1016/j.egypro.2017.10.159

[7] KIM, CH., SON, CH. Rapid design approach for U-bend of a turbine serpentine cooling passage. *Aerospace Science and Technology [online].* 2019, **92**, p. 417-428. ISSN 1270-9638. Available from: https://doi.org/10.1016/j.ast.2019.05.019

[8] BAAKEEM, S. S., ORFI, J., AL-ANSARY, H. Performance improvement of gas turbine power plants by utilizing turbine inlet air-cooling (TIAC) technologies in Riyadh, Saudi Arabia. *Applied Thermal Engineering [online].* 2018, **138**, p. 417-432. ISSN 1359-4311. Available from: https://doi.org/10.1016/j.applthermaleng.2018.04.018

[9] ZHOU, Z., LI, H., WANG, H., XIE, G., YOU, R. Film cooling of cylindrical holes on turbine blade suction side near leading edge. *International Journal of Heat and Mass Transfer [online]*. 2019, **141**, p. 669-679. ISSN 0017-9310. Available from: https://doi.org/10.1016/j.ijheatmasstransfer.2019.07.028

[10] HE, W., DENG, Q., ZHOU, W., GAO, T., FENG, Z. Film cooling and aerodynamic performances of a turbine nozzle guide vane with trenched cooling holes, *Applied Thermal Engineering [online]*. 2019, **150**, p. 150-163. ISSN 1359-4311. Available from: https://doi.org/10.1016/j.applthermaleng.2019.01.002

[11] ZHOU, J., WANG, X., LI, J. Influences of effusion hole diameter on impingement/effusion cooling performance at turbine blade leading edge. *International Journal of Heat and Mass Transfer [online]*. 2019, **134**, p. 1101-1118. ISSN 0017-9310. Available from: https://doi.org/10.1016/j.ijheatmasstransfer.2019.02.054

[12] LIU, J. H., LIU, Y. B., LIU, L. Film cooling modeling of a turbine vane with multiple configurations of holes. *Case Studies in Thermal Engineering [online]*. 2018, **11**, p. 71-80. ISSN 2214-157X. Available from: https://doi.org/10.1016/j.csite.2018.01.001

[13] WEI, H., AI, J. L., ZU, Y. Q., DING, L. Heat transfer characteristics of fan-shaped hole effusion cooling for a constant hole exit width -numerical simulation and experimental validation. *Applied Thermal Engineering [online]*. 2019, **160**, 113978. ISSN 1359-4311. Available from: https://doi.org/10.1016/j.applthermaleng.2019.113978

[14] TALER J, OCLON, P. Finite element method in steady-state and transient heat conduction. In: *Encyclopedia of thermal stresses*. HETNARSKI, R. B. (ed.). Dordrecht, Holland: Springer, 2014. ISBN 978-94-007-2738-0, eISBN 978-94-007-2739-7.

[15] OCLON, P. Heat conduction equation for plane 2D problems. Numerical modeling of heat transfer and fluid flow processes with energy engineering applications. Cracow: Cracow University of Technology, 2015.

[16] BENINI, E. Materials for gas turbines - an overview. In: *Advances in gas turbine technology[online]*. BENINI, E. (ed.). Italy: IntechOpen, 2011. ISBN 978-953-307-611-9, eISBN 978-953-51-4411-3. Available from: https://doi.org/10.5772/664

[17] GURRAPPA, I., YASHWANTH, V. S., GOGIA, A. K. The selection of materials for marine gas turbine engines. In: *Efficiency, performance and robustness of gas turbines [online]*. VOLKOV, K. (ed.). United Kingdom: IntechOpen, 2012. ISBN 978-953-51-0464-3, eISBN 978-953-51-6191-2. Available from: https://doi.org/10.5772/2595

[18] GADDAM, R., SAFER, B., PEDERSON, R., ANTTI, M.-L. Study of alpha -case depth in Ti-6Al-2Sn-4Zr-2Zr-2Mo and Ti-6Al-4V. *IOP Conference Series: Materials Science and Engineering [online]*. 2013, **48**, 012002. ISSN 1757-8981, eISSN 1757-899X.Available from: https://doi.org/10.1088/1757-899X/48/1/012002

[19] Timet_DataSheets_6242 [online] [accessed 2019-09-07] Available from:http://www.timet.com/assets/local/documents/datasheets/alphaalloys/6242.pdf

[20] BEGUM, F., REDDY, V. V. R., RAMANJANEYULU, S. Design and thermal analysis of cooling of gas turbine blade through radial holes. *Materials Today: Proceedings [online]*. 2017, **4**(8), p. 7714-7722. ISSN 2214-7853. Available from: https://doi.org/10.1016/j.matpr.2017.07.106

[21] Holistic numerical methods [online] [accessed 2020-05-17]. Available from: http://nm.mathforcollege.com/topics/pde_parabolic.html

[22] WENG, Z., FENG, X., HUANG, P. A new mixed finite element method based on the Crank-Nicolson scheme for the parabolic problems. *Applied Mathematical Modelling [online]*. 2012, **36**(10), p. 5068-5079. ISSN 0307-904X. Available from: https://doi.org/10.1016/j.apm.2011.12.044

Annex - Nomenclature

nomenclature	meaning
Roman symbols	
A	area, m^2
C	specific heat capacity, J/(kg·K)
h	heat transfer coefficient, $W/(m^2K)$
h	enhanced heat transfer coefficient based on outer tube surface A_o, $W/(m^2K)$
k	thermal conductivity, W/(mK)
N_i	finite element shape function refferd to i-th node
T	temperature, °C
T_{in}	initial temperature, °C
x, y	Cartesian coordinates, m
-T	temperature as a function of place, x and time t
-α	thermal diffusivity obtained by equation $\alpha = \frac{k}{\rho C}$
-k	thermal conductivity
-C	specific heat
Matrices and vectors	
{f}	vector of nodal loads
{K}	stiffness matrix
{T}	vector of nodal temperatures
Greek symbols	
α	line search parameter; temperature coefficient
τ	time, s
ρ	density, $kg.m^{-3}$

DYNAMIC BEHAVIOR OF THE FULL-CAR MODEL IN THE J-TURN MANEUVER BY CONSIDERING THE ENGINE GYROSCOPIC EFFECTS

Ali Shahabi, Amir Hossein Kazemian*, Said Farahat, Faramarz Sarhaddi

Department of Mechanical Engineering, University of Sistan and Baluchestan, Zahedan, Iran

*E-mail of corresponding author: kazemian@eng.usb.ac.ir

Resume

This study presents a new dynamic modeling of a vehicle by considering the engine dynamics. By selecting the vehicle coordinate system as the reference frame, all the force-torque equations of the sprung mass and unsprung masses are derived in this coordinate system by using the Newton's equations of motion. Unlike the previous researches, in this work the sprung mass of the vehicle is not considered as a rigid body. The dynamics of the sprung mass components, such as gyroscopic effects of the engine crankshaft, is considered. In order to study the vehicle's dynamic behavior, in the J-turn maneuver, the governing equations of the full-car model are evaluated and validated by the numerical simulation method and ADAMS/Car software. Based on the results, the maximum roll angle and roll rate of a vehicle reach about 8 degrees and 40 degrees per second, respectively.

Article info

Received 19 November 2020
Accepted 13 January 2021
Online 7 June 2021

Keywords:

J-turn maneuver,
full-car model,
engine crankshaft,
dynamic behavior

Available online: https://doi.org/10.26552/com.C.2021.3.B237-B249

ISSN 1335-4205 (print version)
ISSN 2585-7878 (online version)

This is an open access article distributed under the terms of the Creative Commons Attribution 4.0 International License (CC BY 4.0), which permits use, distribution, and reproduction in any medium, provided the original publication is properly cited. No use, distribution or reproduction is permitted which does not comply with these terms.

1 Introduction

Safety assessment is one of the most important issues in the automotive industry. The safety of vehicles can be examined from two perspectives: the pre-crash safety and post-crash safety. Stability analysis is an important factor in the pre-crash safety and vehicle instability plays a major role in fatal crashes. Understanding the dynamic behavior of a vehicle in standard maneuvers can be effective in assessing its stability.

A set of experimental examinations was performed to evaluate the actual dynamic behavior of a vehicle in various standard maneuvers [1], from which the phase IV rollover tests of the National Highway Traffic Safety Administration (NHTSA) [2] can be pointed out. Cooperrider et al. [3] performed experiments to investigate tripped rollover, the results of which included five types of the curb-tripped rollover tests. In their researches, acceptable information was obtained through the minimum required speed for the rollover occurring, as well as the characteristics of the rollover phenomenon at different speeds. Labuda et al. [4] studied the simulation of wheeled vehicle dynamic regimes in laboratory conditions by considering the congruent courses of driving speeds. Sindha et al. [5] developed an experimental prototype along with its simulation to study the steer system on the vehicle stability improvement. Zhang et al. investigated the vehicle maneuverability and its lateral stability by experimental validations, [6]. Phanomchoeng and Rajamani [7] developed a new rollover index that can detect both tripped and untripped rollovers by experimental and simulation examinations. The purpose of computer simulations is to reveal the effect of systems and components on the dynamic behavior of a vehicle as much as possible. By using the computer simulations, this purpose can be reached much earlier in the targeting and initial design stages of a vehicle than for the actual prototype. Chen et al. [8] simulated the rollover dynamics, such as rollover speed thresholds of a vehicle in roundabouts. Loktev et al. [9] determined the geometric, kinematic and dynamic characteristics of a vehicle and its state parameters on the road by computer vision algorithms. Phalke and Mitra [10] simulated a quarter-car model to investigate the effect of damping coefficient, stiffness, sprung mass and velocity on ride comfort and road holding. Saga et al. [11] investigated possibilities of a fuzzy technique in a vehicle dynamic analysis by computer simulations. Kazemian et al. [12-13] presented the rollover index and new dynamics of suspension system in order to study the vehicle's dynamic behavior by computer simulations. Rajamani [14] and Gillespie [15] studied the vehicle dynamics and its subsystems such as tire in order to study on the vehicle's dynamic behavior, such as roll and yaw dynamics, by considering the dynamics' basics [16]. Pacejka [17-19] examined the tire characteristics, such

as its longitudinal and lateral forces and obtained the data, by mathematical expressions based on a formula. In vehicles, knowing the dynamic behavior of the engine elements, such as crankshaft, can be useful for obtaining the dynamic behavior of the vehicle [20-21]. The effect of static misalignment on the dynamic behavior of a main crankshaft bearing is examined by Lahmar et al. [22]. Ahmadabadi [23] proposed an application of lightweight vibration control strategy known as nonlinear energy sink (NES) to mitigate the undesired vibrations in engine crankshaft systems. Huang et al. [24] proposed a method for dynamic balance measurement and imbalance compensation of crankshaft assemblies. Moreover, basic researches of dynamic modeling have been reported in [25-28]

This study, by presenting a 15-DOF model of the vehicle dynamics, considers reducing the complexity of the model to the extent that it would be acceptable for the dynamic behavior of the vehicle studying and modeling the necessary subsystems, such as tire and engine, with sufficient accuracy. The tire is modeled with the Pacejka 89 model, which calculates the tire forces using the longitudinal and lateral slips. The moments due to the gyroscopic effect of engine rotation are taken into account in the equations and the final equations of motion of the vehicle were derived. The dynamic behavior of the 15-DOF presented model is validated by the ADAMS/Car software. Dynamic behavior and stability of a vehicle in the J-turn maneuver is simulated by the Newmark numerical method under the supervision of the NHTSA, [25].

2 Modeling and equations

In this research, the vehicle is considered as a set of lumped masses including the sprung mass and four unsprung masses as a set of wheels and tires. The unsprung masses are connected to the sprung mass by the spring and a damper. Each tire is assumed equivalent to a spring and a damper, parallel in the vertical direction. The number of degrees of freedom that are considered for the vehicle model is 15, out of which 6 DOFs are related to translation and rotation of the sprung mass. The next 4 DOFs are for vertical movement of the unsprung masses, which indicate the vertical movement of the suspension systems, while the following 4 DOFs are related to rotation of the wheels around their axes and 1 DOF is considered for steerability of the front wheels. For this set of masses, separate coordinate systems, such as fixed inertial coordinate system (O), sprung mass coordinate system (S), roll axis coordinate system (vehicle coordinates (V)) and wheel coordinate system (US), are considered. The direction of the coordinate systems, as shown in Figure 1, is in accordance with the SAE (Society of Automotive Engineers) standard [15]. In Figure 1 the sprung mass coordinate system is located at its center of gravity (CGS). The coordinate system located on the roll axis, which is the most important coordinate system and all variables are expressed in that system, is located at a point on the roll axis and below the center of gravity of the vehicle mass (VCG). It is also assumed that this coordinate system rotates only around the Z axis. To obtain the equations of wheels motion in the vertical direction and around their rotation axis for each wheel, a coordinate system is used at the center of rotation. According to coordinate systems and using the Newton's equations of motion, all equations of motion for the sprung and unsprung masses are obtained in the vehicle coordinate system. Therefore, for the sprung mass, the following Equations can be written:

$$\begin{aligned}&\omega_V^V=\{0\ 0\ \dot{\varphi}\}^T, V_V^V=\{V_x\ V_y\ 0\}^T,\\&\rho_{CGS}^V=\{l_s\ 0\ h_s\}^T,\\&V_{CGS}^V=\{V_x\ V_y\ V_z\}^T=\{V_x\ V_y\ \dot{Z}_{CGS}\},\end{aligned}\tag{1}$$

$$\begin{aligned}&\omega_S^V=\{\dot{\theta}\cos\phi\ \dot{\phi}\cos\theta\ \dot{\varphi}+\dot{\phi}\sin\theta+\dot{\theta}\sin\phi\}^T\\&\xrightarrow{\sin\phi=\phi=0,\cos\phi=1}\omega_S^V=\{\dot{\theta}\ \dot{\phi}\cos\theta\ \dot{\varphi}+\phi\sin\theta\}^T,\end{aligned}\tag{2}$$

$$V_S^V=V_{CGS}^V+\omega_S^V\times\rho_{CGS}^V\rightarrow V_S^V=\begin{Bmatrix}V_x+h_s\dot{\phi}\cos\theta\\V_y-h_s\dot{\theta}+l_s(\dot{\varphi}+\dot{\phi}\sin\theta)\\\dot{Z}_{CGS}-l_S\dot{\phi}\cos\theta\end{Bmatrix}.\tag{3}$$

Similarly, for the unsprung masses, next Equations are obtained:

$$\begin{aligned}&\omega_{usfR}^V=\{\omega_w\sin\delta_{fR}\ \omega_w\cos\delta_{fR}\ \dot{\varphi}\}^T,\\&\omega_{usfL}^V=\{\omega_W\sin\delta_{fL}\ \omega_W\cos\delta_{fL}\ \dot{\varphi}\}^T\\&\omega_{usrL}^V=\{0\ \omega_w\ \dot{\varphi}\}^T, \omega_{usrR}^V=\{0\ \omega_w\ \dot{\varphi}\}^T,\\&V_{CGusij}^V=\{V_x\ V_y\ \dot{Z}_{usij}\}^T\end{aligned}\tag{4}$$

$$\begin{aligned}&\rho_{usfR}^V=\{l_f\ t/2\ Z_{usfR}\}^T, \rho_{usfL}^V=\{l_f\ -t/2\ Z_{usfL}\}^T,\\&\rho_{usrL}^V=\{l_r\ -t/2\ Z_{usrL}\}^T, \rho_{usrR}^V=\{l_r\ t/2\ Z_{usrR}\}^T,\end{aligned}\tag{5}$$

$$V_{CGusij}^V=V_{CGusij}^V+\omega_{usij}^V\times\rho_{CGusij}^V\rightarrow V_{usfR}^V=\begin{Bmatrix}V_x+Z_{usfR}\omega_w\cos\delta_{fR}-\left(\frac{t}{2}\right)\dot{\varphi}\\V_y-Z_{usfR}\omega_w\sin\delta_{fR}+l_f\dot{\varphi}\\\dot{Z}_{usfR}+\omega_w\left(\frac{t}{2}\sin\delta_{fR}-l_f\cos\delta_{fR}\right)\end{Bmatrix},$$

$$V_{usfL}^V=\begin{Bmatrix}V_x+Z_{usfL}\omega_w\cos\delta_{fL}-\left(\frac{t}{2}\right)\dot{\varphi}\\V_y-Z_{usfL}\omega_w\sin\delta_{fL}+l_f\dot{\varphi}\\\dot{Z}_{usfL}+\omega_w\left(\frac{t}{2}\sin\delta_{fL}-l_f\cos\delta_{fL}\right)\end{Bmatrix},\tag{6}$$

$$V_{usrL}^V=\begin{Bmatrix}V_x+Z_{usrL}\omega_w+\left(\frac{t}{2}\right)\dot{\varphi}\\V_y+l_r\dot{\varphi}\\\dot{Z}_{usrL}-\omega_w l_r\end{Bmatrix},$$

$$V_{usrR}^V=\begin{Bmatrix}V_x+Z_{usrR}\omega_w+\left(\frac{t}{2}\right)\dot{\varphi}\\V_y+l_r\dot{\varphi}\\\dot{Z}_{usrR}-\omega_w l_r\end{Bmatrix}.$$

By placing velocities of Equations (1)-(3) in the Newton's linear momentum equation of the sprung mass, the force vector of the sprung mass in the vehicle coordinate system is obtained:

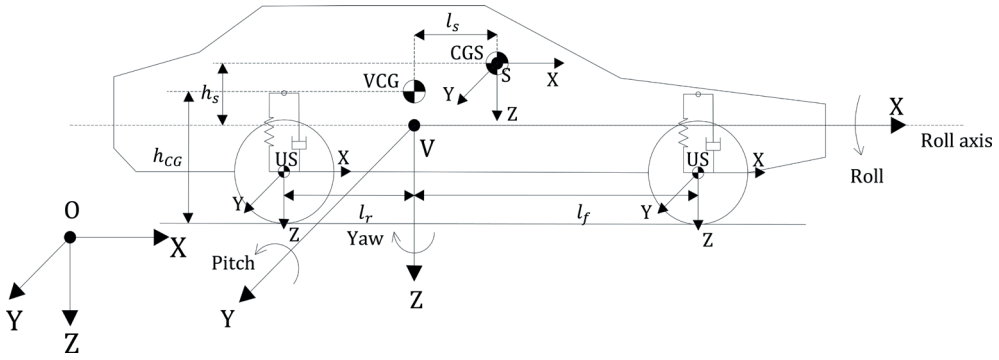


Figure 1 *Direction of the vehicle coordinate system according to the SAE standard*

$$F_S^V = m_S\left[\frac{d}{dt}V_S^V + \omega_V^V \times V_S^V\right] \rightarrow F_S^V = \begin{Bmatrix} \dot{V}_x + h_s\begin{pmatrix}\ddot{\psi}\cos\theta - \\ -\dot{\psi}\dot{\theta}\sin\theta\end{pmatrix} - \dot{\varphi}\begin{pmatrix}V_y - h_s\dot{\theta} + \\ l_s(\dot{\varphi} + \dot{\psi}\sin\theta)\end{pmatrix} \\ m_s\begin{Bmatrix} \dot{V}_y - h_s\ddot{\theta} + \\ + l_s\begin{pmatrix}\ddot{\varphi} + \ddot{\psi}\sin\theta + \\ + \dot{\varphi}\dot{\theta}\cos\theta\end{pmatrix} + \dot{\varphi}(V_x + h_s\dot{\psi}\cos\theta) \\ \ddot{Z}_{CGS} - l_s(\ddot{\psi}\cos\theta + \dot{\psi}\dot{\theta}\sin\theta)\end{Bmatrix}\end{Bmatrix}. \quad (7)$$

Similarly, for the unsprung masses the following Equations are obtained:

$$F_{usij}^V = m_{usij}\left[\frac{d}{dt}V_{usij}^V + \omega_V^V \times V_{usij}^V\right], \quad (8)$$

$$F_{usfR}^V = m_{usfR}\begin{Bmatrix} \dot{V}_x + \cos\delta_{fR}(\dot{Z}_{usfR}\omega_w + Z_{usfR}\dot{\omega}_w) - \\ \left(\frac{t}{2}\right)\ddot{\varphi} - \dot{\varphi}\begin{pmatrix}V_y - Z_{usfR}\omega_w\sin\delta_{fR} + \\ l_f\dot{\varphi}\end{pmatrix} \\ \dot{V}_y + \sin\delta_{fR}(\dot{Z}_{usfR}\omega_w + Z_{usfR}\dot{\omega}_w) - \\ l_f\ddot{\varphi} + \dot{\varphi}\begin{pmatrix}V_x - Z_{usfR}\omega_w\cos\delta_{fR} - \\ \left(\frac{t}{2}\right)\dot{\varphi}\end{pmatrix} \\ \dot{Z}_{usfR} + \dot{\omega}_w\left(\frac{t}{2}\sin\delta_{fR} + l_f\cos\delta_{fR}\right)\end{Bmatrix}, \quad (9)$$

$$F_{usfL}^V = m_{usfL}\begin{Bmatrix} \dot{V}_x + \cos\delta_{fL}(\dot{Z}_{usfL}\omega_w + Z_{usfL}\dot{\omega}_w) - \\ \left(\frac{t}{2}\right)\ddot{\varphi} - \dot{\varphi}\begin{pmatrix}V_y - Z_{usfL}\omega_w\sin\delta_{fL} + \\ l_f\dot{\varphi}\end{pmatrix} \\ \dot{V}_y + \sin\delta_{fL}(\dot{Z}_{usfR}\omega_w + Z_{usfL}\dot{\omega}_w) - \\ l_f\ddot{\varphi} + \dot{\varphi}\begin{pmatrix}V_x - Z_{usfR}\omega_w\cos\delta_{fL} - \\ \left(\frac{t}{2}\right)\dot{\varphi}\end{pmatrix} \\ \dot{Z}_{usfL} + \dot{\omega}_w\left(\frac{t}{2}\sin\delta_{fL} + l_f\cos\delta_{fL}\right)\end{Bmatrix}, \quad (10)$$

$$F_{usrL}^V = m_{usrL}\begin{Bmatrix} \dot{V}_x + \dot{Z}_{usrL}\dot{\omega}_w + \left(\frac{t}{2}\right)\ddot{\varphi} - \dot{\varphi} \\ (Vy + l_r\dot{\varphi}) \\ \dot{V}_y + l_r\ddot{\varphi} + \dot{\varphi}\begin{pmatrix}V_x + Z_{usrL} + \\ \left(\frac{t}{2}\right)\dot{\varphi}\end{pmatrix} \\ \ddot{Z}_{usrL} - \dot{\omega}_w l_r\end{Bmatrix}, \quad (11)$$

$$F_{usrR}^V = m_{usrR}\begin{Bmatrix} \dot{V}_x + \dot{Z}_{usrR}\dot{\omega}_w + \left(\frac{t}{2}\right)\ddot{\varphi} - \dot{\varphi} \\ (Vy + l_r\dot{\varphi}) \\ \dot{V}_y + l_r\ddot{\varphi} + \dot{\varphi}\begin{pmatrix}V_x + Z_{usrR} + \\ \left(\frac{t}{2}\right)\dot{\varphi}\end{pmatrix} \\ \ddot{Z}_{usrR} - \dot{\omega}_w l_r\end{Bmatrix}. \quad (12)$$

According to Equation (13), the total forces acting on the vehicle include the forces acting on all the sprung and unsprung masses:

$$F_V^V = F_S^V + F_{usij}^V = \begin{Bmatrix} m\dot{V}_x - m\varphi V_y + m_s\left[h_s(\ddot{\psi}\cos\theta - \right. \\ \left.\dot{\psi}\dot{\theta}\sin\theta + \dot{\varphi}\dot{\theta}) - l_s(\dot{\psi}\dot{\varphi}\sin\theta + \dot{\varphi}^2)\right] + m_{usf} \\ \begin{bmatrix}\cos\delta_f\begin{pmatrix}\omega_w(\dot{Z}_{usfR} + \dot{Z}_{usfL}) \\ + \omega_w(Z_{usfR} + Z_{usfL})\end{pmatrix} + \dot{\varphi}\omega_w\sin\delta_f \\ (Z_{usfR} + Z_{usfL}) - 2\dot{\varphi}^2 l_f\end{bmatrix} + \\ m_{usr}\begin{bmatrix}\omega_w(\dot{Z}_{usR} + \dot{Z}_{usL}) + \dot{\omega}_w(Z_{usR} + Z_{usL}) - \\ 2\dot{\psi}^2 l_r\end{bmatrix} + \\ m\dot{V}_y + m\dot{\varphi}V_x - m_s\begin{bmatrix}h_s(\ddot{\theta} - \dot{\psi}\dot{\varphi}\cos\theta) + l_s \\ (\ddot{\varphi} - \ddot{\psi}\sin\theta - \dot{\psi}\dot{\theta}\cos\theta)\end{bmatrix} + \\ m_{usf}\begin{bmatrix}-\sin\delta_f\begin{pmatrix}\omega_w(\dot{Z}_{usfR} + \dot{Z}_{usfL}) \\ + \omega_w(Z_{usfR} + Z_{usfL})\end{pmatrix} + \\ 2\ddot{\varphi}l_f + \dot{\varphi}\omega_w\cos\delta_f(Z_{usfR} + Z_{usfL})\end{bmatrix} + m_{usr} \\ [\dot{\varphi}\omega_w(Z_{usrR} + Z_{usrL}) + 2\ddot{\varphi}l_r]m_s\begin{bmatrix}\ddot{Z}_{CGS} - l_s \\ \begin{pmatrix}\ddot{\psi}\cos\theta - \\ \dot{\psi}\dot{\theta}\sin\theta\end{pmatrix}\end{bmatrix} + \\ m_{usf}[\ddot{Z}_{usfL} + \ddot{Z}_{usfR} - 2\dot{\omega}_w l_f\cos\delta_f] + m_{usr} \\ [\ddot{Z}_{usrL} + \ddot{Z}_{usrR} - 2\dot{\omega}_w l_r]\end{Bmatrix}. \quad (13)$$

where $m = m_s + 2m_{usf} + 2m_{usr}$ is the total mass of a vehicle. According to the Newton's angular momentum equation, the resultant of the torques, acting on the body, is equal to change of the body's angular momentum. If one writes this relation for the center of the vehicle's coordinate system, the distance of which to the center of the sprung mass coordinate system remains constant, Equation is obtained:

$$M_S^V = R_S^V M_S^S = R_S^V\frac{d}{dt}(I_S^S\omega_S^S). \quad (14)$$

where R_S^V is the matrix of coordinate transformation from the sprung mass coordinates to the vehicle coordinates (see Appendix 1). Assuming that values of inertia moments remain constant, with small rotation of the roll and pitch of a vehicle, on obtains:

$$M_S^V = I_S^V\dot{\omega}_S^V + \omega_S^V \times (I_S^V\omega_S^V), \quad (15)$$

where:

$$\dot{\omega}_S^V = \frac{d}{dt}\omega_S^V + \omega_V^V \times \omega_S^V = \begin{Bmatrix} \ddot{\theta} - \dot{\varphi}\dot{\psi}\cos\theta \\ \ddot{\psi}\cos\theta - \dot{\psi}\dot{\theta}\sin\theta + \dot{\theta}\dot{\varphi} \\ \ddot{\varphi} + \ddot{\psi}\sin\theta + \dot{\psi}\dot{\theta}\cos\theta \end{Bmatrix}. \quad (16)$$

Since the xy plane is a symmetry plane of the vehicle with a good approximation, so $I_{xy} = I_{yz} = 0$ and with ignoring the value of I_{xz}, the matrix of the sprung mass inertia moments is presented by:

$$I_S^V = \begin{bmatrix} I_{xx} & I_{xy} & I_{xz} \\ I_{yx} & I_{yy} & I_{yz} \\ I_{zx} & I_{zy} & I_{zz} \end{bmatrix} \rightarrow I_S^V = \begin{bmatrix} I_{xx} & 0 & 0 \\ 0 & I_{yy} & 0 \\ 0 & 0 & I_{zz} \end{bmatrix}. \quad (17)$$

By placing $\omega_S^V, \dot{\omega}_S^V$ and I_S^V, respectively, from Equations (2), (16) and (17) in Equation (15), one obtains:

$$M_S^V = \begin{Bmatrix} I_{xx}(\ddot{\theta} - \dot{\varphi}\dot{\psi}\cos\theta) + (I_{zz} - I_{yy})\times \\ (\dot{\varphi}\dot{\psi}\cos\theta + \dot{\psi}^2\theta\cos\theta) \\ I_{yy}(\ddot{\psi}\cos\theta - \dot{\psi}\dot{\theta}\sin\theta + \dot{\theta}\dot{\varphi}) + \\ (I_{xx} - I_{zz})(\dot{\psi}\dot{\theta}\sin\theta + \dot{\theta}\dot{\varphi}) \\ I_{zz}(\ddot{\varphi} + \ddot{\psi}\sin\theta + \dot{\psi}\dot{\theta}\cos\theta) + \\ (I_{yy} - I_{xx})\dot{\psi}\dot{\theta}\cos\theta \end{Bmatrix}. \quad (18)$$

To derive the equation of the unsprung mass angular momentum, similar to e equation of the sprung mass angular momentum (15), Equations (19)-(21) are obtained as follows:

$$M_{usij}^V = I_{usij}^V \dot{\omega}_{usij}^V + \omega_{usij}^V \times (I_{usij}^V \omega_{usij}^V), \quad (19)$$

$$\dot{\omega}_{usij}^V = \frac{d}{dt}\omega_{usij}^V + \omega_V^V \times \omega_{usij}^V \rightarrow \dot{\omega}_{usfR}^V = \begin{Bmatrix} \dot{\omega}_w \sin\delta_{fR} - \dot{\varphi}\omega_w \cos\delta_{fR} \\ \dot{\omega}_w \cos\delta_{fR} + \dot{\varphi}\omega_w \sin\delta_{fR} \\ \ddot{\varphi} \end{Bmatrix},$$
$$\dot{\omega}_{usfL}^V = \begin{Bmatrix} \dot{\omega}_w \sin\delta_{fL} - \dot{\varphi}\omega_w \cos\delta_{fL} \\ \dot{\omega}_w \cos\delta_{fL} + \dot{\varphi}\omega_w \sin\delta_{fL} \\ \ddot{\varphi} \end{Bmatrix}, \quad (20)$$
$$\dot{\omega}_{usrL}^V = \begin{Bmatrix} -\dot{\varphi}\omega_w \\ \dot{\omega}_w \\ \ddot{\varphi} \end{Bmatrix}, \dot{\omega}_{usrR}^V = \begin{Bmatrix} -\dot{\varphi}\omega_w \\ \dot{\omega}_w \\ \ddot{\varphi} \end{Bmatrix},$$

$$M_{usfR}^V = \begin{Bmatrix} I_{xxusf}(\dot{\omega}_w \sin\delta_{fR} - \dot{\varphi}\omega_w \cos\delta_{fR}) + \\ (I_{zzusf} - I_{yyusf})\dot{\varphi}\omega_w \cos\delta_{fR} \\ I_{yyusf}(\dot{\omega}_w \cos\delta_{fR} - \dot{\varphi}\omega_w \sin\delta_{fR}) + \\ (I_{xxusf} - I_{zzusf})\dot{\varphi}\omega_w \sin\delta_{fR} \\ I_{zzusf}\ddot{\varphi} + (I_{yyusf} - I_{xxusf})\times \\ \omega_w^2 \sin\delta_{fR}\cos\delta_{fR} \end{Bmatrix},$$
$$M_{usfL}^V = \begin{Bmatrix} I_{xxusf}(\dot{\omega}_w \sin\delta_{fL} - \dot{\varphi}\omega_w \cos\delta_{fL}) + \\ (I_{zzusf} - I_{yyusf})\dot{\varphi}\omega_w \cos\delta_{fL} \\ I_{yyusf}(\dot{\omega}_w \cos\delta_{fL} - \dot{\varphi}\omega_w \sin\delta_{fL}) + \\ (I_{xxusf} - I_{zzusf})\dot{\varphi}\omega_w \sin\delta_{fL} \\ I_{zzusf}\ddot{\varphi} + (I_{yyusf} - I_{xxusf})\times \\ \omega_w^2 \sin\delta_{fL}\cos\delta_{fL} \end{Bmatrix}, \quad (21)$$

$$M_{usrL}^V = \begin{Bmatrix} -I_{xxusr}\dot{\varphi}\omega_w + (I_{zzusr} - I_{yyusr})\dot{\varphi}\omega_w \\ I_{yyusr}\dot{\omega}_w \\ I_{zzusr}\ddot{\varphi} \end{Bmatrix},$$
$$M_{usrR}^V = \begin{Bmatrix} -I_{xxusr}\dot{\varphi}\omega_w + (I_{zzusr} - I_{yyusr})\dot{\varphi}\omega_w \\ I_{yyusr}\dot{\omega}_w \\ I_{zzusr}\ddot{\varphi} \end{Bmatrix}.$$

Considering that the coordinate center of a vehicle is a point that differs from the center of mass of the sprung and unsprung masses, the total torque applied to the vehicle can be calculated as [16]:

$$(H_Q)_{rel} = (H_G)_{rel} + \overline{\rho} \times m V_{rel}. \quad (22)$$

Equation (22) shows the angular torque around the desired point Q. According to the toques principle in which the sum of the torques of all the external forces of a system around the point Q must be equal to resultant torque around Q and the following Equation is obtained:

$$\sum M_Q = \sum M_G + \overline{\rho} \times \sum F. \quad (23)$$

By placing the vector of forces and torques in Equation (23) for the proposed vehicle model, one obtains:

$$M_V^V = M_S^V + M_{usij}^V + \rho_{CGS}^V \times F_S^V + \rho_{usij}^V \times F_{usij}^V. \quad (24)$$

By entering the force-torque equations (Equations (7), (9)-(12), (18) and (21)) in Equation (24), the torque components of the vehicle are obtained:

$$\begin{aligned} M_{VX}^V &= I_{xx}(\ddot{\theta} - \dot{\varphi}\dot{\psi}\cos\theta) + (I_{zz} - I_{yy})\times \\ &(\dot{\varphi}\dot{\psi}\cos\theta + \dot{\psi}^2\sin\theta\cos\theta) + 2I_{xxusf}\times \\ &(\dot{\omega}_w \sin\delta_f - \dot{\varphi}\omega_w \cos\delta_f) + 2(I_{zzusf} - I_{yyusf})\times \\ &\dot{\varphi}\omega_w \cos\delta_f - 2I_{xxusr}\dot{\varphi}\omega_w + 2(I_{zzusr} - I_{yyusr})\dot{\varphi}\omega_w - \\ &m_s h_s \begin{bmatrix} \dot{V}_y - h_s\ddot{\theta} + l_s(\ddot{\varphi} + \ddot{\psi}\sin\theta + \dot{\psi}\dot{\theta}\cos\theta) \\ + \dot{\varphi}(V_x + h_s\dot{\psi}\cos\theta) \end{bmatrix} + \\ &\frac{t}{2}\begin{bmatrix} m_{usf}(\ddot{Z}_{usfR} - \ddot{Z}_{usfL} + \dot{\omega}_w t\sin\delta_f) + \\ m_{usf}(\ddot{Z}_{usrR} - \ddot{Z}_{usrL} + \dot{\omega}_w t) \end{bmatrix} - m_{usf}\times \\ &\begin{bmatrix} Z_{usfR}\begin{pmatrix} \dot{V}_y - \sin\delta_f(\dot{Z}_{usfR}\dot{\omega}_w + Z_{usfR}\dot{\omega}_w) + \\ l_f\ddot{\varphi} + \dot{\varphi}\left(V_x + Z_{usfR}\omega_w\cos\delta_f - \frac{t}{2}\dot{\varphi}\right) \end{pmatrix} + \\ Z_{usfL}\begin{pmatrix} \dot{V}_y - \sin\delta_f(\dot{Z}_{usfL}\omega_w + Z_{usfL}\dot{\omega}_w) + \\ l_f\ddot{\varphi} + \left(V_x + Z_{usfL}\omega_w\cos\delta_f + \frac{t}{2}\dot{\varphi}\right) \end{pmatrix} \end{bmatrix} - \\ &m_{usr}\times \\ &\begin{bmatrix} Z_{usfL}\begin{pmatrix} \dot{V}_y - \sin\delta_f(\dot{Z}_{usfL}\dot{\omega}_w + Z_{usfL}\dot{\omega}_w) + \\ l_f\ddot{\varphi} + \dot{\varphi}\left(V_x + Z_{usfL}\omega_w\cos\delta_f - \frac{t}{2}\dot{\varphi}\right) \end{pmatrix} + \\ Z_{usfR}\begin{pmatrix} \dot{V}_y - \sin\delta_f(\dot{Z}_{usfR}\omega_w + Z_{usfR}\dot{\omega}_w) + \\ l_f\ddot{\varphi} + \left(V_x + Z_{usfR}\omega_w\cos\delta_f + \frac{t}{2}\dot{\varphi}\right) \end{pmatrix} \end{bmatrix}, \end{aligned} \quad (25)$$

$$\begin{aligned} M_{VY}^V &= I_{yy}(\ddot{\psi}\cos\theta - \dot{\psi}\dot{\theta}\sin\theta + \dot{\theta}\dot{\varphi}) + (I_{xx} - I_{zz}) \\ &(\dot{\psi}\dot{\theta}\sin\theta + \dot{\theta}\dot{\varphi}) + 2I_{yyusf}(\dot{\omega}_w\cos\delta_f + \dot{\varphi}\omega_w\sin\delta_f) + \\ &2(I_{xxusf} - I_{zzuf})\dot{\varphi}\omega_w\sin\delta_f + 2I_{yyusr}\dot{\omega}_w + m_s h_s[\dot{V}_x + \\ &h_s\ddot{\psi}\cos\theta - h_s\dot{\psi}\dot{\theta}\sin\theta + l_s(\ddot{\varphi} + \ddot{\psi}\sin\theta + \dot{\psi}\dot{\theta}\sin\theta) - \end{aligned}$$

$$
\begin{aligned}
&-\dot{\varphi}(V_y - h_s\dot{\theta} + l_s(\dot{\varphi} + \dot{\psi}\sin\theta))] - m_s l_s \times \\
&(\ddot{Z}_{CGS} - l_s\ddot{\psi}\cos\theta + l_s\dot{\psi}\dot{\theta}\sin\theta) + m_{usf} \times \\
&[2l_f\dot{\omega}_w\cos\delta_f - \ddot{Z}_{usfR} - \ddot{Z}_{usfL}] + m_{usr}l_r \times \\
&[2l_r\dot{\omega}_w\cos\delta_f - \ddot{Z}_{usrR} - \ddot{Z}_{usrL}] + m_{usf} \times [Z_{usfR} \times \\
&\left(\dot{V}_x + \cos\delta_f(\dot{Z}_{usfR}\omega_w + Z_{usfR}\dot{\omega}_w) - \frac{t}{2}\ddot{\varphi} - \right. \\
&\dot{\varphi}(V_y - Z_{usfR}\omega_w\sin\delta_f + l_f\dot{\varphi})) + Z_{usfL}(\dot{V}_x + \\
&\cos\delta_f(\dot{Z}_{usfL}\omega_w + Z_{usfL}\dot{\omega}_w) - \frac{t}{2}\ddot{\varphi} - \dot{\varphi} \times \\
&(V_y - Z_{usfL}\omega_w\sin\delta_f + l_f\dot{\varphi}))] + m_{usr}[Z_{usfL} \times \\
&\left(\dot{V}_x + \cos\delta_f(\dot{Z}_{usfL}\omega_w + Z_{usfL}\dot{\omega}_w) - \frac{t}{2}\ddot{\varphi} - \right. \\
&\dot{\varphi}(V_y - Z_{usfL}\omega_w\sin\delta_f + l_f\dot{\varphi})) + Z_{usfR}(\dot{V}_x + \\
&\cos\delta_f(\dot{Z}_{usfR}\omega_w + Z_{usfR}\dot{\omega}_w) - \frac{t}{2}\ddot{\varphi} - \dot{\varphi} \times \\
&(V_y - Z_{usfR}\omega_w\sin\delta_f + l_f\dot{\varphi}))],
\end{aligned}
\tag{26}
$$

$$
\begin{aligned}
&M_{VZ}^V = I_{ZZ}(\ddot{\varphi} + \ddot{\psi}\sin\theta + \dot{\psi}\dot{\theta}\cos\theta) + (I_{yy} - I_{xx}) \\
&\dot{\psi}\dot{\theta}\cos\theta + 2I_{zzusf}\ddot{\varphi} + 2(I_{yyusf} - I_{xxusf})\omega_w^2\sin\delta_f \times \\
&\cos\delta_f + 2I_{zzusr}\ddot{\varphi} + m_s l_s[\dot{V}_y - h_s\ddot{\theta} + l_s(\ddot{\varphi} + \\
&\ddot{\psi}\sin\theta + \dot{\psi}\dot{\theta}\cos\theta + h_s\dot{\psi}\dot{\varphi}\cos\theta + \dot{\varphi}\dot{V}_x)] + m_{usf} \times \\
&[l_f(2\dot{V}_y - \sin\delta_f((\dot{Z}_{usfR} + \dot{Z}_{usfL})\omega_w + \\
&(Z_{usfR} + Z_{usfL})\dot{\omega}_w) + 2l_f\ddot{\varphi} + \dot{\varphi}(2V_x + \omega\cos\delta_f \times \\
&(Z_{usfR} + Z_{usfL}))) + \frac{t}{2}(\cos\delta_f\omega_w(\dot{Z}_{usfR} + \dot{Z}_{usfL}) + \\
&\dot{\omega}(Z_{usfR} + Z_{usfL})) + t\ddot{\varphi} - \dot{\varphi}\omega_w\sin\delta_f \times \\
&(Z_{usfR} + Z_{usfL}))] + m_{usr}[l_r(2\dot{V}_y - (\dot{Z}_{usrR} + \dot{Z}_{usrL}) \times \\
&\omega_w + (Z_{usrR} + Z_{usrL})\dot{\omega}_w + 2l_r\ddot{\varphi} + \dot{\varphi}(2V_x + \omega_w \times \\
&(Z_{usrR} + Z_{usrL}))) + \frac{t}{2}(\omega_w(\dot{Z}_{usrL} + \dot{Z}_{usrR}) + \\
&\dot{\omega}_w(Z_{usrR} + Z_{usrL}) + t\ddot{\varphi} - \dot{\varphi}\omega_w(Z_{usrR} + Z_{usrL}))].
\end{aligned}
\tag{27}
$$

The left-hand side of Equations (13) and (25)-(27), which are the main equations of motion of the vehicle, includes the forces and torques of the external forces applied to the vehicle and an example of them is shown in Figures 2 and 3. Note that by considering the directions of the coordinate systems, these forces and torques are entered into the equations of motion of the vehicle.

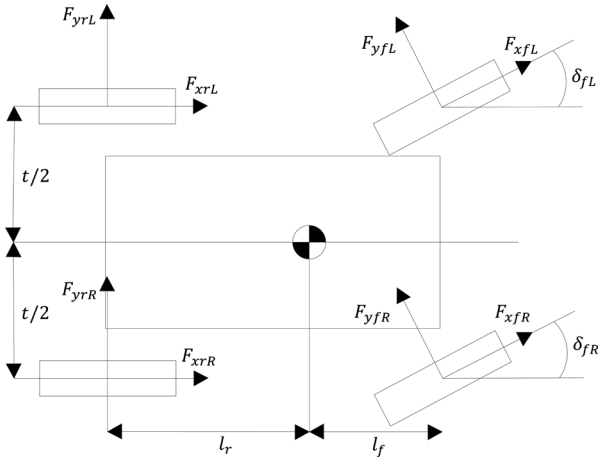


Figure 2 *External forces on the xy plane of vehicle coordinate system*

2.1 Equations of external forces

By writing the resultant of forces and torques applied to the vehicle, next two Equations are obtained:

$$
F_V^V = \begin{Bmatrix}
F_{xfR}\cos\delta_{fR} - F_{yfR}\sin\delta_{fR} + F_{xfL}\cos\delta_{fL} - \\
F_{yfL}\sin\delta_{fL} + F_{xrR} + F_{xrL} \\
F_{yfR}\cos\delta_{fR} + F_{xfR}\sin\delta_{fR} + F_{yfL}\cos\delta_{fL} + \\
F_{xfL}\sin\delta_{fL} + F_{yrR} + F_{yrL} \\
m_s g - k_{ij}(Z_n - Z_{usij}) - c_{ij}(\dot{Z}_n - \dot{Z}_{usij}) \\
n = 1,2,3,4
\end{Bmatrix}, \tag{28}
$$

where n shows the unsprung masses.

$$
M_V^V = \begin{Bmatrix}
\frac{t}{2}[-k_{fR}(Z_1 - Z_{usfR}) - k_{rR}(Z_4 - Z_{usrR}) + \\
k_{fL}(Z_2 - Z_{usfL}) + k_{rL}(Z_3 - Z_{usrL}) - c_{fR} \times \\
(\dot{Z}_1 - \dot{Z}_{usfR}) - c_{rR}(\dot{Z}_4 - \dot{Z}_{usrR}) + c_{fL} \times \\
(\dot{Z}_2 - \dot{Z}_{usfL}) + c_{rL}(\dot{Z}_3 - \dot{Z}_{usrL})] + h_{RCf} \times \\
(F_{yfR}\cos\delta_{fR} + F_{xfR}\sin\delta_{fR} + F_{yfL}\cos\delta_{fL} + \\
F_{xfL}\sin\delta_{fL}) + h_{RCr}(F_{yrR} + F_{yrL}) + \\
m_s g h_s\sin\theta \\
l_f[k_{fR}(Z_1 - Z_{usfR}) + k_{fL}(Z_2 - Z_{usfL})] - \\
l_r[k_{rR}(Z_4 - Z_{usrR}) + k_{rL}(Z_3 - Z_{usrL})] + \\
l_f[c_{fR}(\dot{Z}_2 - \dot{Z}_{usfL}) + c_{fL}(\dot{Z}_2 - \dot{Z}_{usfL})] - \\
l_r[c_{rR}(\dot{Z}_4 - \dot{Z}_{usrR}) + c_{rL}(\dot{Z}_3 - \dot{Z}_{usrL})] - \\
m_s g l_s\cos\phi + h_{RA}(F_{xfR}\cos\delta_{fr} - \\
F_{yfR}\sin\delta_{fR} + F_{xfL}\cos\delta_{fL} - F_{yfL}\sin\delta_{fL} + \\
F_{xrR} + F_{xrL}) \\
\frac{t}{2}(-F_{xfR}\cos\delta_{fR} + F_{yfR}\sin\delta_{fR} + \\
F_{xfL}\cos\delta_{fL} - F_{yfL}\sin\delta_{fL} - F_{xrR} + F_{xrL}) - \\
l_f(F_{yfR}\cos\delta_{fR} + F_{xfR}\sin\delta_{fR} + F_{yfL}\sin\delta_{fL} \\
+ F_{xfL}\sin\delta_{fL}) + l_r(F_{yrR} + F_{yrL})
\end{Bmatrix}. \tag{29}
$$

In Equations (28) and (29) Z_n is the displacement of a point of the sprung mass in the vertical direction above the unsprung masses, which is calculated according to Equation (30):

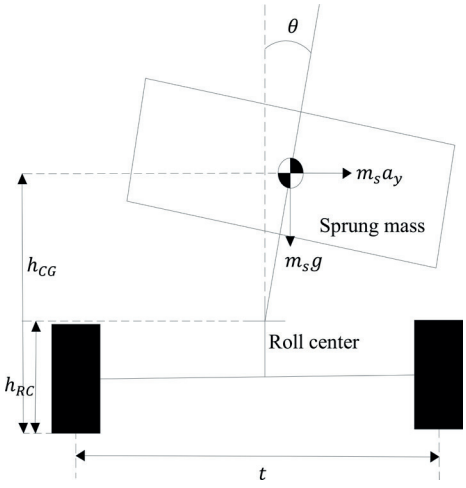


Figure 3 *Vehicle's roll dynamics with stationary roll center*

$$
\begin{aligned}
Z_1 &= Z_{CGS} + \frac{t}{2}\sin\theta - l_f \sin\phi,\\
Z_2 &= Z_{CGS} - \frac{t}{2}\sin\theta - l_f \sin\phi,\\
Z_3 &= Z_{CGS} - \frac{t}{2}\sin\theta + l_r \sin\phi,\\
Z_4 &= Z_{CGS} + \frac{t}{2}\sin\theta + l_r \sin\phi.
\end{aligned} \tag{30}
$$

2.2 Equations of engine rotating

Generally, in deriving equations of a vehicle, the sprung mass is considered as rigid. Now, if a part of the sprung mass has a rotation, relative to the vehicle coordinate system (such as the engine crankshaft), then it is necessary to enter the effect of that rotation in the force-torque equations that have been calculated so far. In this study, it is assumed that the rotating components are symmetric, so the product of inertia multiplications is zero. In this case, the rotation of these components will not create any force and therefore the force equation remains stable. However, if the rotational velocity of the rotating components or their moment of inertia are significant, then the gyroscopic moments, due to the angular momentum of the rotating component, are considerable and their effect must be considered in the torque equation. The gyroscopic moment is obtained according to:

$$
\sum M = \left(\frac{dH}{dt}\right)_S + \omega_s^V \times H,\; H = I_e^V \omega_e^V . \tag{31}
$$

In Equation (31) H is the angular momentum vector of the engine and the vector of the angular velocity of the engine in the vehicle coordinate system (ω_e^V) is considered according to:

$$
\omega_e^V = \left\{\dot\theta \;\; \dot\phi\cos\theta + \omega_e \;\; \dot\varphi + \dot\phi\sin\theta\right\}^T . \tag{32}
$$

In this study, the crankshaft coordinate axes are considered to correspond to the vehicle coordinate axes, in which case the product of the crankshaft inertia multiplications in the vehicle coordinates is also equal to zero. Thus:

$$
I_e^V = \begin{bmatrix} I_e & 0 & 0\\ 0 & I_{ae} & 0\\ 0 & 0 & I_e \end{bmatrix}. \tag{33}
$$

By placing Equations (32) and (33) in Equation (31), the gyroscopic moment vector in the vehicle coordinate system is obtained as:

$$
M_{Ve}^V = \begin{Bmatrix} I_e(\ddot\theta + \dot\phi^2\cos\theta\sin\theta + \dot\varphi\dot\phi\cos\theta) - \\ I_{ae}(\dot\phi\cos\theta + \omega_e)(\dot\phi\sin\theta + \dot\varphi) \\ I_{ae}(\ddot\phi\cos\theta - \dot\theta\dot\phi\sin\theta + \dot\omega_e) \\ I_e(\ddot\varphi + \ddot\phi\sin\theta) + I_{ae}\dot\theta(\dot\phi\cos\theta + \omega_e) \end{Bmatrix}. \tag{34}
$$

In Equation (34), ω_e is the angular velocity of the engine and I_{ae} is the crankshaft inertia moment around its rotation axis. In this study, the gyroscopic moment of the crankshaft is considered like other external torques and is added directly to the torque vector of external forces.

2.3 Wheels equations of motion

The wheel's equations of motion in the vertical direction are determined according to Equations (35)-(38). With writing the resultant of forces for each of the unsprung masses (Figure 4), one obtains:

$$
\begin{aligned}
\sum F_z = m_{usij}\ddot Z_{usij} \rightarrow\; & k_{fR}(Z_1 - Z_{usfR}) + c_{fR}(\dot Z_1 - \\
& \dot Z_{usfR}) + m_{usf}g - k_{tf}(Z_{usfR} - Z_{gfR}) - c_{tf}(\dot Z_{usfR} - \\
& \dot Z_{gfR}) = m_{usf}\ddot Z_{usfR},
\end{aligned} \tag{35}
$$

$$
\begin{aligned}
& k_{fL}(Z_2 - Z_{usfL}) + c_{fL}(\dot Z_2 - \dot Z_{usfL}) + m_{usf}g - \\
& k_{tf}(Z_{usfL} - Z_{gfL}) - c_{tf}(\dot Z_{usfL} - \dot Z_{gfL}) = m_{usf}\ddot Z_{usfL},
\end{aligned} \tag{36}
$$

$$
\begin{aligned}
& k_{rL}(Z_3 - Z_{usrL}) + c_{rL}(\dot Z_3 - \dot Z_{usrL}) + m_{usr}g - \\
& k_{tr}(Z_{usrL} - Z_{grL}) - c_{tr}(\dot Z_{usrL} - \dot Z_{grL}) = m_{usr}\ddot Z_{usrL},
\end{aligned} \tag{37}
$$

$$
\begin{aligned}
& k_{rR}(Z4 - Z_{usrR}) + c_{rR}(\dot Z_4 - \dot Z_{usrR}) + m_{usr}g - \\
& k_{tr}(Z_{usrR} - Z_{grR}) - c_{tr}(\dot Z_{usrR} - \dot Z_{grR}) = m_{usr}\ddot Z_{usrR}.
\end{aligned} \tag{38}
$$

2.4 The tire modeling

In this research, the model of Pacejka 89 (Magic Formula), which has the ability to estimate the lateral and longitudinal forces of the tire under the lateral and longitudinal slips, is considered [17-19]. This model receives variables such as vertical force of the wheel and longitudinal and lateral slips as input, while its output are the longitudinal and lateral forces of a tire. The longitudinal slip is considered based on Equations (39) and (40):

The longitudinal slip during the acceleration is:

$$
\alpha_x > 0 \rightarrow \sigma = 1 - (V_x / V_w). \tag{39}
$$

while the longitudinal slip during the braking is:

$$
a_x < 0 \rightarrow \sigma = (V_w / V_x) - 1. \tag{40}
$$

In Equations (39) and (40), $V_w = r_w\omega_w$ and the lateral slip angle is the difference between the direction of tire longitudinal axis and the direction of tire velocity vector in the xy plane (Figure 5). The lateral slip angles are obtained in the form:

$$
\begin{aligned}
\alpha_{fR} &= \arctan\left[(V_y + \dot\varphi l_f)/\left(V_x + \dot\varphi\frac{t}{2}\right)\right] - \delta_f,\\
\alpha_{fL} &= \arctan\left[(V_y + \dot\varphi l_f)/\left(V_x + \dot\varphi\frac{t}{2}\right)\right] - \delta_f,
\end{aligned} \tag{41}
$$

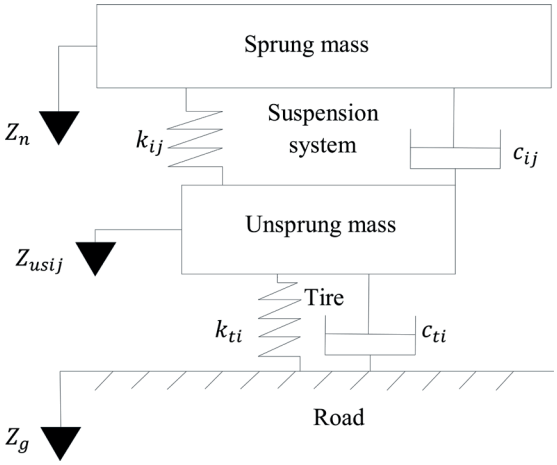


Figure 4 *Modeling of the unsprung mass*

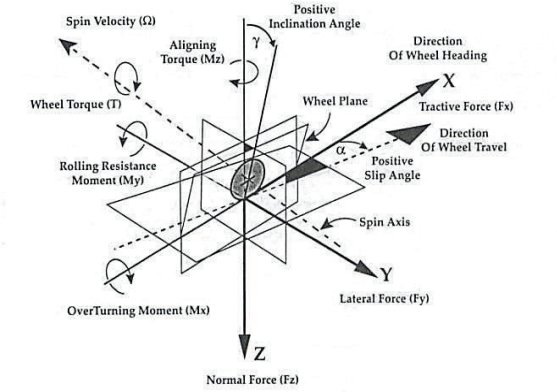


Figure 5 *Tire coordinates according to the SAE standard [17]*

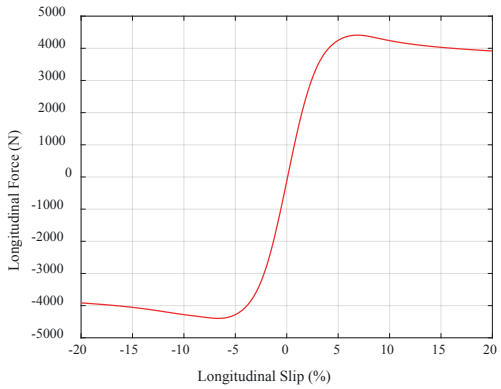


Figure 6 *Variation of the longitudinal force of the Magic Formula according to longitudinal slip*

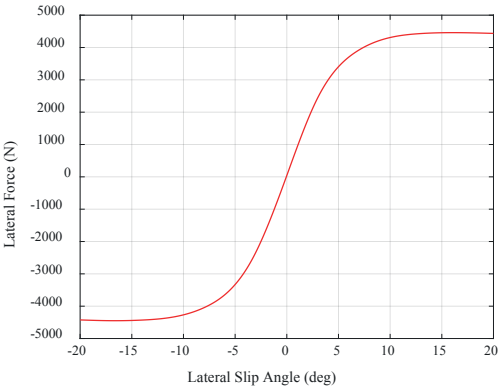


Figure 7 *Variation of the lateral force of the Magic Formula according to lateral slip angle*

$$\alpha_{fR} = \arctan\left[\left(V_y + \dot{\varphi} l_r\right)/\left(V_x + \dot{\varphi}\frac{t}{2}\right)\right],$$
$$\alpha_{fL} = \arctan\left[\left(V_y + \dot{\varphi} l_r\right)/\left(V_x + \dot{\varphi}\frac{t}{2}\right)\right]. \quad (42)$$

Therefore, the longitudinal and lateral forces of the tire are obtained according to Equations (43) and (44) by determining the longitudinal slip and lateral slip angle. In the appendix 1, the constants of the Magic Formula (Pacejka 89) are given and longitudinal and lateral forces of the Magic Formula are shown in Figures 6 and 7.

$$F_x = D\sin(C\arctan(BX_1 - E(BX_1 - \arctan(BX_1)))) + Sv, C = b_0, D = (b_1F_z^2 + b_2F_z),$$
$$BCD = (b_3F_z^2 + b_4F_z)e^{(-b_5F_z)}, B = BCD(C/D), \quad (43)$$
$$E = (b_6F_z^2 + b_7F_z + b_8), Sh = b_9F_z + b_{10},$$
$$Sv = 0, X_1 = \sigma + Sh,$$

$$F_y = D\sin(C\arctan(BX_1 - E(BX_1 - \arctan(BX_1)))) + Sv, C = a_0, D = (a_1F_z^2 + a_2F_z),$$
$$BCD = a_3\sin(\arctan(F_z/a_4))(1 - a_5|\gamma|),$$
$$B = BCD(C/D), E = (a_6F_z + a_7), \quad (44)$$
$$Sh = a_9F_z + a_{10} + a_8\gamma,$$
$$Sv = a_{11}F_z\gamma + a_{12}F_z + a_{13}, X_1 = \sigma + Sh.$$

3 Numerical method

By using the Newmark numerical method in the form of time integration [25], vehicle's dynamic behavior is simulated. In the Newmark methods family, at time of τ the vector of displacement (q), velocity $(\dot{q})$ and acceleration $(\ddot{q})$ are estimated by $E_{d+1}, \dot{E}_{d+1}$ and a_{d+1} at time of τ_{d+1}. The vehicle's displacement vector is selected as Equation (45) and the governing matrix-vector equations at time f $\tau = \tau_{d+1}$ can be changed to an estimated prescription as Equation (46).

$$q = \{X, Y, Z_{CGS}, \theta, \varphi, \phi, , Z_{usfR}, Z_{usjL}, Z_{usrR}, Z_{usrL}\}^T, \quad (45)$$

$$\Gamma(E_{d+1})a_{d+1} + G(E_{d+1}, \dot{E}_{d+1}) = \Lambda_{d+1}$$
$$E_0 = E(0), \dot{E}_0 = \dot{E}(0), \quad (46)$$
$$a_0 = -\Gamma^{-1}(E(0))G(E(0), \dot{E}(0)).$$

where, Γ is the inertia matrix and Γ and G are functions of the displacement and velocity, Λ is the vector of external excitations, E_0 is the initial displacement, $\dot{E}_0$ is the initial velocity and a_0 is the initial acceleration. Displacement and velocity can be predicted by:

$$\hat{E}_d = E_d + \Delta\tau \dot{E}_d + 0.5\Delta\tau^2(1-2\xi)a_d\,, \tag{47}$$

$$\hat{\dot{E}}_d = \dot{E}_d + (1-\eta)\Delta\tau a_d\,. \tag{48}$$

respectively, where $\Delta\tau = \tau_{d+1} - \tau_d$ is the time step size, ξ and η are the Newmark's algorithm parameters which show the accuracy of the algorithmic. Updated displacement and velocity are obtained from Equations (49) and (50), respectively:

$$E_{d+1} = \hat{E}_d + \xi\Delta\tau^2 a_{d+1}\,, \tag{49}$$

$$\dot{E}_{d+1} = \hat{\dot{E}}_d + \eta\Delta\tau a_{d+1}\,. \tag{50}$$

In order to obtain E_{d+1} and $\dot{E}_{d+1}$, an update of the acceleration must be known (a_{d+1}). By using method the Newton–Raphson for each time step and by placing Equations (49) and (50) into Equation (46), a_{d+1} is obtained from:

$$\Delta a^u_{d+1} + a^u_{d+1} = a^{u+1}_{d+1}\,, \tag{51}$$

$$J^u_{d+1}\Delta a^u_{d+1} = -\Gamma^u_{d+1}a^u_{d+1} - G^u_{d+1} + \Lambda_{d+1}\,, \tag{52}$$

where, d and u are the iteration number of the time step and Newton–Raphson method, $\Gamma^u_{d+1} = \Gamma(E^u_{d+1})$, $G^u_{d+1} = G(E^u_{d+1}, \dot{E}^u_{d+1})$ and J^u_{d+1} is the Jacobian matrix and is defined as:

$$J^u_{d+1} = \Gamma(E^u_{d+1}) + \xi\Delta\tau^2\left[\frac{\partial J^u_{d+1}a^u_{d+1}}{\partial E^u_{d+1}} + \frac{\partial G^u_{d+1}}{\partial E^u_{d+1}}\right] + \eta\Delta\tau\frac{\partial G^u_{d+1}}{\partial \dot{E}^u_{d+1}}. \tag{53}$$

The process of the Newmark method is shown in Figure 8.

4 Validation and simulation results

Several different test programs in the phase IV of the light vehicle rollover research program were reviewed and evaluated to select the most appropriate maneuver to investigate the rollover. According to Table 1, it can be seen that one of the best maneuvers is the J-turn test, which has obtained the highest score. Due to the fact that the vehicle is assumed to be perfectly symmetrical with respect to its xz plane, direction of the steering wheel angle (clockwise or counterclockwise) of Figure 9 has no effect on the maneuver results. The initial speed of the vehicle is shown in Figures 10 and 11 and the engine speed is 5000 rpms. During the J-turn maneuver, the passed trajectory by the vehicle is shown in Figure 12. By applying the steering wheel angle according to Figure 9, the Newmark numerical method and parameters of Table 2, the dynamic behavior of the vehicle is compared by ADAMS/Car software according to Figures 13 and 14. Based on the validation results, it is found that the 15-DOF presented model in this research simulates the vehicle's dynamic behavior with a good accuracy. According to the numerical results (Figures 13b, 14b, 15 and 16), by applying the steering input, the lateral acceleration reaches about -0.8 g and finally decreases with decreasing longitudinal velocity of a vehicle.

The maximum roll angle and roll rate of a vehicle reach about 8 º and 40 º/s. Moreover, the yow rate of the vehicle reaches a maximum of about - 41 º/s and then decreases to about -15 º/s and finally reaches about -35 º/s.

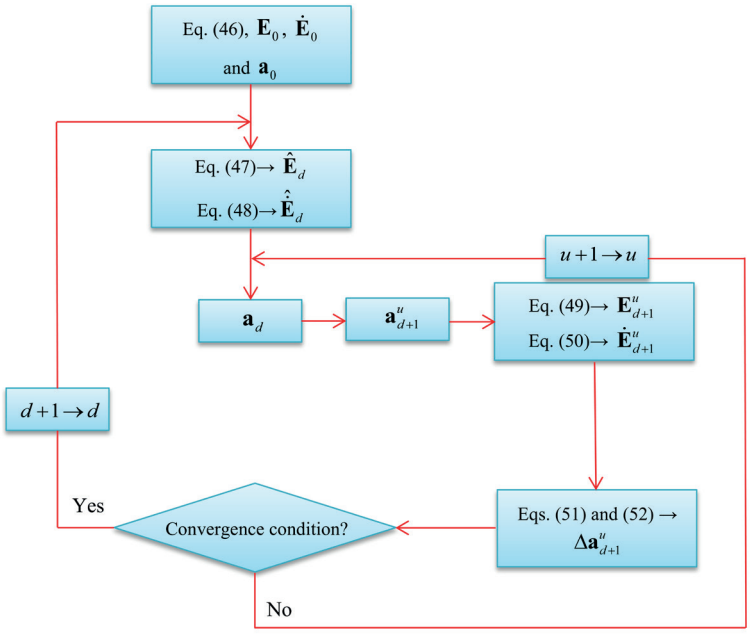
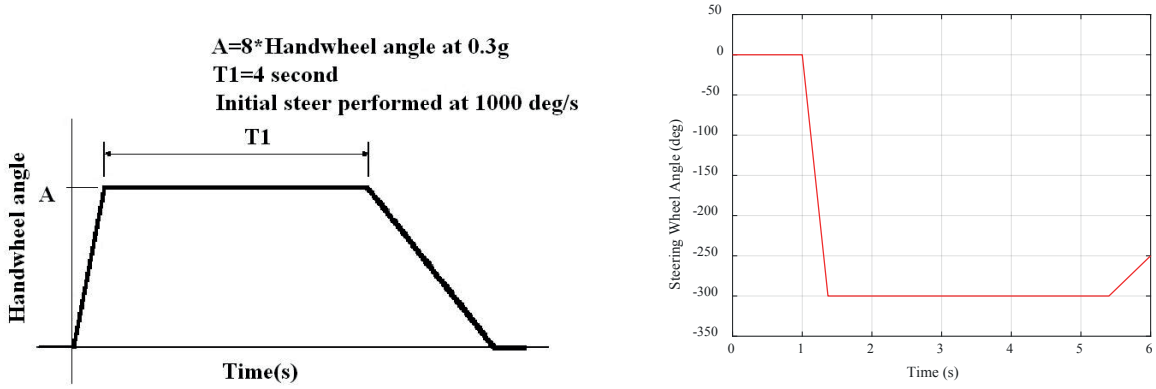


Figure 8 *Flowchart of the Newmark numerical method*



(a) (b)

Figure 9 *Schematics of the steering wheel angle of a vehicle in: (a) NHTSA J-turn maneuver [2] and (b) this study*

Table 1 *Comparison of different rollover maneuvers [2]*

assessment criterion	NHTSA J-turn	fishhook #1a	fishhook #1b	Nissan fishhook
objectivity and repeatability	excellent	excellent	excellent	good
performability	excellent	good	excellent	satisfactory
discriminatory capability	excellent	excellent	excellent	excellent
appearance of reality	good	excellent	excellent	good

Table 2 *System parameters of this study*

parameter	value	unit	parameter	value	unit
m_s	808	Kg	c_r	882.9	N.s/m
m_{usf}	2×31.5	Kg	I_x	298	Kg.m^2
m_{usr}	2×29.5	Kg	I_y	1243	Kg.m^2
h_{CG}	0.54	m	I_z	1130	Kg.m^2
h_{RA}	0.1	m	r_w	0.257	m
t	1.4	m	h_{RC}	0.1	m
l_f	0.945	m	h_s	0.45	m
l_r	1.4	m	I_{ae}	1.5	Kg.m^2
k_f	16	kN/m	k_{tf}	160	kN/m
k_r	15.4	kN/m	k_{tr}	154	kN/m
c_f	1414.3	N.s/m	ξ	0.25	-
c_t	0	N.s/m	η	0.5	-
l_s	0.35	m			

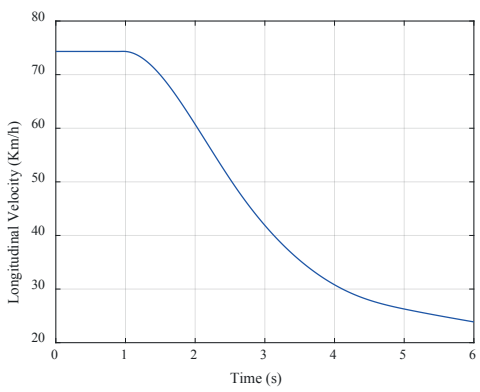


Figure 10 *The longitudinal velocity of the vehicle in the J-turn maneuver*

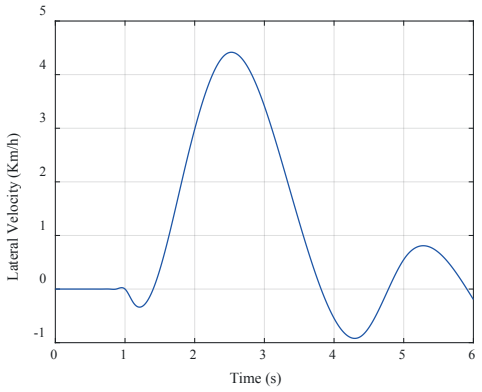


Figure 11 *The lateral velocity of the vehicle in the J-turn maneuver*

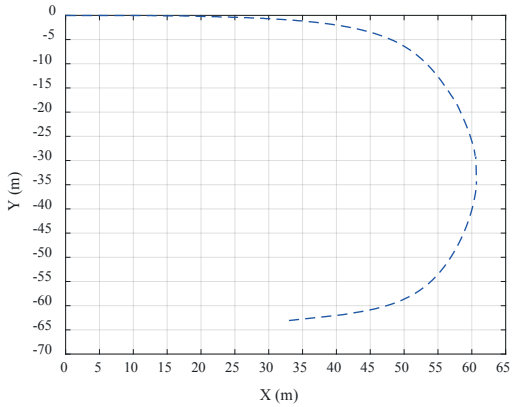
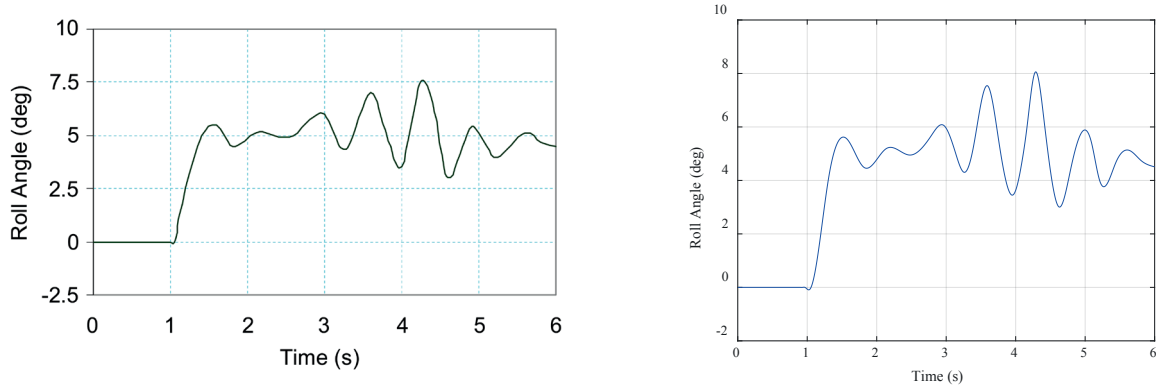
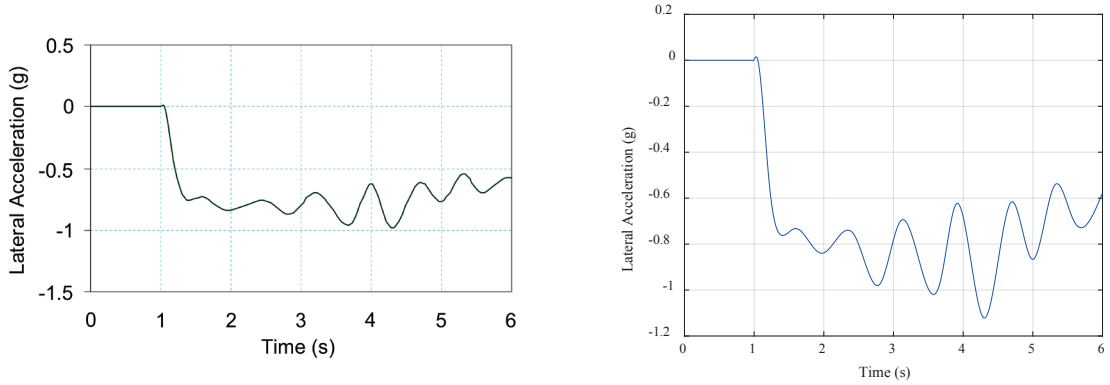


Figure 12 *Trajectory of a vehicle in the J-turn maneuver*



(a) *(b)*

Figure 13 *The roll angle of the vehicle in the J-turn maneuver: (a) ADAMS software and (b) this study*



(a) *(b)*

Figure 14 *The lateral acceleration of the vehicle in the J-turn maneuver: (a) ADAMS software and (b) this study*

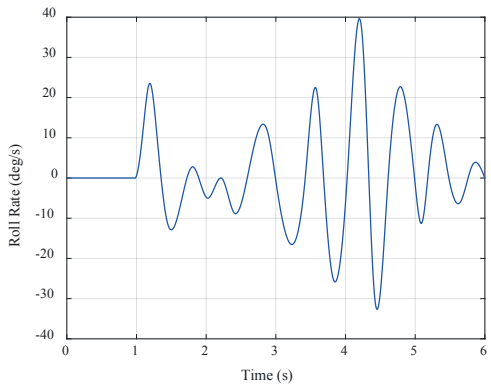


Figure 15 *The roll rate of the vehicle in the J-turn maneuver*

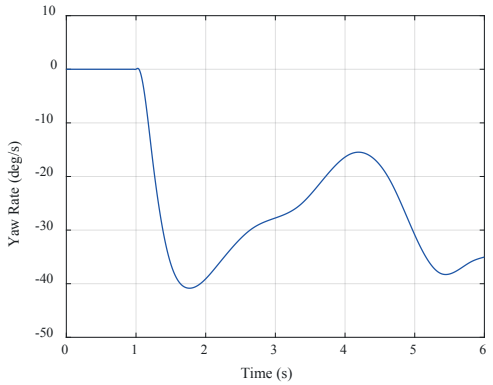


Figure 16 *The yaw rate of the vehicle in the J-turn maneuver*

5 Conclusions

This study presents the dynamics of a 15-DOF model of a vehicle by performing simulations to investigate the vehicle's dynamic behavior in the J-turn maneuver under the supervision of the phase IV of NHTSA's light vehicle rollover research program. Using the Newton's equations of motion, the equations of motion for the sprung and unsprung masses are all written in the vehicle coordinate system. In order to study the engine dynamics, the crankshaft coordinate axes are considered to correspond to the vehicle coordinate axes. Finally, the gyroscopic moment of the crankshaft is added directly to the torque vector of external forces and the governing equations are evaluated by numerical method of the Newmark. The tire is modeled with the Pacejka 89 model, which estimates the tire forces by using the longitudinal and lateral slips. By selecting the J-turn maneuver, the dynamic behavior of the presented 15-DOF model is validated by ADAMS/Car software. Based on the simulation results, it is found that the 15-DOF model, presented in this research, simulates the vehicle's dynamic behavior with a good accuracy. By applying the steering input the lateral acceleration reaches about -0.8 g and finally decreases with decreasing longitudinal velocity of the vehicle. The maximum roll angle and roll rate of the vehicle reach about 8 º and 40 º/s. The yaw rate of a vehicle reaches a maximum of about -41 º/s and then decreases to about -15 º/s and finally reaches about -35 º/s.

References

[1] HEYDINGER, G. J., HOWE, J. G. Analysis of vehicle response data measured during severe maneuvers. *SAE Technical Papers* [online]. 2000, **01**, 1644, p. 2154-2167. ISSN 0148-7191, eISSN 2688-3627. Available from: https://doi.org/10.4271/2000-01-1644

[2] FORKENBROCK, G. J., GARROTT, W. R., HEITZ, M., O'HARRA, B. C. A comprehensive experimental examination of test maneuvers that may induce on-road, untripped, light vehicle rollover [online]. Report DOT HS 809 513. Phase IV of NHTSA's Light Vehicle Rollover Research Program. NHTSA, 2002. Available from: https://moam.info/a-comprehensive-experimental-examination-of-test-maneuvers-_59b212851723ddddc6092afb.html

[3] COOPERRIDER, N. K., THOMAS, T. M., HAMMOUD, S. A. Testing and analysis of vehicle rollover behavior. *SAE Technical Papers* [online]. 1990, 900366, p. 518-527. ISSN 0148-7191, eISSN 2688-3627. Available from: https://doi.org/10.4271/900366

[4] LABUDA, R., KOVALCIK, A., REPKA, J., HLAVNA, V. Simulation of a wheeled vehicle dynamic regimes in laboratory conditions. *Communications-Scientific Letters of the University of Zilina* [online]. 2012, **14**(3), p. 5-9. ISSN 1335-4205, eISSN 2585-7878. Available from: http://komunikacie.uniza.sk/index.php/communications/article/view/753

[5] SINDHA, J., CHAKRABORTY, B., CHAKRAVARTY, D. System identification and lateral dynamics of the active tilt-controlled electric three wheeler. *Journal of Dynamic Systems, Measurement and Control* [online], 2020, **142**(9), 091001. ISSN 0022-0434. Available from: https://doi.org/10.1115/1.4046798

[6] ZHANG, J., WANG, H., ZHENG, J., CAO, Z., MAN, Z., YU, M., CHEN, L. Adaptive sliding mode-based lateral stability control of steer-by-wire vehicles with experimental validations. *IEEE Transactions on Vehicular Technology* [online]. 2020, **69**(9), p. 9589-9600. ISSN 0018-9545. Available from: https://doi.org/10.1109/TVT.2020.3003326

[7] PHANOMCHOENG, G., RAJAMANI, R. New rollover index for the detection of tripped and untripped rollovers. *IEEE Transactions on Industrial Electronics* [online]. 2012, **60**(10), p. 4726-4736. ISSN 0278-0046. Available from: https://doi.org/10.1109/TIE.2012.2211312

[8] CHEN, Y., ZHENG, X., PETERSON, A., AHMADIAN, M. Simulation evaluation on the rollover propensity of multi-trailer trucks at roundabouts. *SAE Technical Papers* [online]. 2020, **01**, 5005. ISSN 0148-7191, eISSN 2688-3627. Available from: https://doi.org/10.4271/2020-01-5005

[9] LOKTEV, D. A., LOKTEV, A. A., SALNIKOVA, A. V., SHAFOROSTOVA, A. A. Determination of the dynamic vehicle model parameters by means of computer vision. *Communications-Scientific Letters of the University of Zilina* [online]. 2019, **21**(3), p. 28-34. ISSN 1335-4205, eISSN 2585-7878. Available from: https://doi.org/10.26552/com.C.2019.3.28-34

[10] PHALKE, T. P., MITRA, A. C. Analysis of ride comfort and road holding of quarter car model by SIMULINK. *Materials Today: Proceedings* [online]. 2017, **4**(2), p. 2425-2430. ISSN 2214-7853. Available from: https://doi.org/10.1016/j.matpr.2017.02.093

[11] SAGA, M., LETRICH, M., KOCUR, R. An analysis of vehicle vibration with uncertain system parameters. *Communications-Scientific Letters of the University of Zilina* [online]. 2005, **7**(1), p. 16-21. ISSN 1335-4205, eISSN 2585-7878. Available from: http://komunikacie.uniza.sk/index.php/communications/article/view/1223

[12] KAZEMIAN, A. H., FOOLADI, M., DARIJANI, H. Rollover index for the diagnosis of tripped and untripped rollovers. *Latin American Journal of Solids and Structures* [online]. 2017, **14**(11), p. 1979-1999. ISSN 1679-7817. Available from: https://doi.org/10.1590/1679-78253576

[13] KAZEMIAN, A. H., FOOLADI, M., DARIJANI, H. Non-linear control of vehicle's rollover using sliding mode controller for new 8 degrees of freedom suspension model. *International Journal of Heavy Vehicle Systems* [online]. 2019, **26**(5), p. 707-726. ISSN 1744-232X. Available from: https://doi.org/10.1504/IJHVS.2019.101888

[14] RAJAMANI, R. *Vehicle dynamics and control* [online]. USA: Springer Science and Business Media, 2011. ISBN 978-1-4614-1432-2, eISBN 978-1-4614-1433-9. Available from: https://doi.org/10.1007/978-1-4614-1433-9

[15] GILLESPIE, T. D. *Fundamentals of vehicle dynamics*. 4. ed. Warrendale: Society of Automotive Engineers, 1992. ISBN 978-1-56091-199-9.

[16] MERIAM, J. L., KRAIGE, L. G. *Engineering mechanics: dynamics*. John Wiley and Sons, Inc., 2012. ISBN 9780470614815.

[17] PACEJKA, H. *Tire and vehicle dynamics*. 2. ed. Elsevier, 2005. ISBN 9780750669184, eISBN 9780080543338.

[18] BAKKER, E., PACEJKA, H. B., LIDNER, L. A new tire model with an application in vehicle dynamics studies. *SAE Technical Papers* [online]. 1989, 890087, p. 101-113. ISSN 0148-7191, eISSN 2688-3627. Available from: https://doi.org/10.4271/890087

[19] PACEJKA, H. B., BAKKER, E. The magic formula tire model. *Vehicle System Dynamics* [online]. 1992, **21**(S1), p. 1-18. ISSN 0042-3114. Available from: https://doi.org/10.1080/00423119208969994

[20] BURIAKOVSKYI, S., LIUBARSKYI, B., MASLII, A., POMAZAN, D., TAVRINA, T. Research of a hybrid diesel locomotive power plant based on a free-piston engine. *Communications-Scientific Letters of the University of Zilina* [online]. 2020, **22**(3), p. 103-109. ISSN 1335-4205, eISSN 2585-7878. Available from: https://doi.org/10.26552/com.C.2020.3.103-109

[21] ISKRA, A., BABIAK, M., KALUZNY, J. Identification of the combustion Engine resistance to motion torque components. *Communications-Scientific Letters of the University of Zilina* [online]. 2011, **13**(4), p. 12-15. ISSN 1335-4205, eISSN 2585-7878. Available from: http://komunikacie.uniza.sk/index.php/communications/article/view/871

[22] LAHMAR, M., FRIHI, D., NICOLAS, D. The effect of misalignment on performance characteristics of engine main crankshaft bearings. *European Journal of Mechanics-A/Solids* [online]. 2002, **21**(4), p. 703-714. ISSN 0997-7538. Available from: https://doi.org/10.1016/S0997-7538(01)01202-5

[23] AHMADABADI, Z. N. Nonlinear energy transfer from an engine crankshaft to an essentially nonlinear attachment. *Journal of Sound and Vibration* [online]. 2019, **443**, p. 139-154. ISSN 1095-8568. Available from: https://doi.org/10.1016/j.jsv.2018.11.040

[24] HUANG, T., ZHANG, J., CHEN, G, WANG, C. Dynamic balance two-dimensional measuring of crankshaft assembly in motorcycle engine. *IEEE Access* [online]. 2020, **8**, p. 133757-133766. ISSN 2169-3536. Available from: https://doi.org/10.1109/ACCESS.2020.3010171

[25] NEWMARK, N. M. A method of computation for structural dynamics. *Journal of the Engineering Mechanics Division* [online]. 1959, **85**(3), p. 67-94. ISSN 0044-7951, eISSN 2690-2427. Available from: https://cedb.asce.org/CEDBsearch/record.jsp?dockey=0011858

[26] REZAEI, V., SHAFEI, A. M. Dynamic analysis of flexible robotic manipulators constructed of functionally graded materials. *Iranian Journal of Science and Technology, Transactions of Mechanical Engineering* [online]. 2019, **43**(1), p. 327-342. ISSN 2228-6187. Available from: https://doi.org/10.1007/s40997-018-0160-2

[27] JANOT, A., WENSING, P. M. Sequential semidefinite optimization for physically and statistically consistent robot identification. *Control Engineering Practice* [online]. 2021, **107**, p. 104699. ISSN 0967-0661. Available from: https://doi.org/10.1016/j.conengprac.2020.104699

[28] ZHANG, Y., LIU, H., MA, T., HAO, L., LI, Z. A comprehensive dynamic model for pneumatic artificial muscles considering different input frequencies and mechanical loads. *Mechanical Systems and Signal Processing* [online]. 2021, **148**, p. 107133. ISSN 0888-3270. Available from: https://doi.org/10.1016/j.ymssp.2020.107133

Appendix 1

The transformation relation between the coordinate systems of the sprung mass and a vehicle, which results from the pitch and roll rotation, is obtained as follows:

$$R_S^V = \begin{bmatrix} \cos\phi & 0 & \sin\phi \\ 0 & 1 & 0 \\ -\sin\phi & 0 & \cos\phi \end{bmatrix} \begin{bmatrix} 1 & 0 & 1 \\ 0 & \cos\theta & -\sin\theta \\ 1 & \sin\theta & \cos\theta \end{bmatrix} = \begin{bmatrix} \cos\phi & \sin\phi\sin\theta & \sin\phi\cos\theta \\ 0 & \cos\theta & -\sin\theta \\ -\sin\phi & \cos\phi\sin\theta & \cos\phi\cos\theta \end{bmatrix} \tag{A.1}$$

Table A.1 *Constant values used in the Pacejka 89 tire model*

lateral constants	longitudinal constants
$a_0 = 1.65, a_1 = -34, a_2 = 1250,$	$b_0 = 2.37272, b_1 = -9.46, b_2 = 1490,$
$a_3 = 3036, a_4 = 12.8, a_5 = 0.00501,$	$b_3 = 130, b_4 = 276, b_5 = 0.0886,$
$a_6 = -0.02103, a_7 = 0.77394,$	$b_6 = 0.00402, b_7 = -0.0615, b_8 = 1.2,$
$a_8 = 0.002289, a_9 = 0.013442,$	$b_9 = 0.0299, b_{10} = -0.176$
$a_{10} = 0.003709, a_{11} = 19.1656,$	
$a_{12} = 1.21356, a_{13} = 6.26206$	

Appendix 2

nomenclature	meaning
a	acceleration and lateral constants of the Magic Formula
b	longitudinal constants of the Magic Formula
c	damping coefficient
F	force
h	height
H	angular momentum
I	moment of inertia
k	stiffness coefficient
m	mass
M	torque
r	radius
R	function of coordinate transformation
t	track width
V	velocity
Z	vertical displacement
α	lateral slip angle
γ	camber angle
δ	steering input
θ	roll angle
σ	longitudinal slip
φ	yaw angle
ϕ	pitch angle
ω	angular velocity
subscripts	meaning
ae	crankshaft
CG	center of gravity
e	engine
f	front
g	road
i	front and rear wheels (f, r)
j	right and left wheels (L,R)
L	left side
r	rear
R	right side
RA	roll axis
RC	roll center
s	sprung mass
t	tire
us	unsprung mass
V	vehicle
w	wheel
x	longitudinal direction
y	lateral direction
z	vertical direction

Project

Creation of a Digital Biobank to Support the Systemic Public Research Infrastructure

is co-financed by the European Union

Project objective:
Expansion and completion of research and innovation infrastructure and capacities for the development of excellence in research and innovation through the establishment of a data biobanking system and its integration into the international network of research infrastructures.

Project description:
The project is focused on the so-called digital banking of medical data that will be related to a specific sample of biological material. These are data from hospital information systems - clinical anonymized data, data from the laboratory information management system, data from the research information system and data from the PACS. The obtained data will be analysed bioinformatically, biostatistically and artificial intelligence algorithms can be applied to them. The digital biobank will also support the possibility of creating so-called digital pathology, which is a unique issue in the Slovak environment.

Beneficiary: University of Žilina

In cooperation with:
Ministry of Health of the Slovak Republic
Comenius University in Bratislava

Contracted amount of the Non-Repayable Financial Contribution:
11 590 338,03 EUR

Project duration: 06/2020 - 06/2023

ITMS2014+ code: 313011AFG4

This publication has been produced with the support of the Integrated Infrastructure Operational Program for the project: Creation of a Digital Biobank to Support the Systemic Public Research Infrastructure, ITMS: 313011AFG4, co-financed by the European Regional Development Fund.



EUROPEAN UNION
European Regional Development Fund
OP Integrated Infrastructure 2014 – 2020



MINISTRY
OF TRANSPORT
AND CONSTRUCTION
OF THE SLOVAK REPUBLIC

Project

Creation of a Digital Biobank to Support the Systemic Public Research Infrastructure

is co-financed by the European Union

Project objective:
Expansion and completion of research and innovation infrastructure and capacities for the development of excellence in research and innovation through the establishment of a data biobanking system and its integration into the international network of research infrastructures.

Project description:
The project is focused on the so-called digital banking of medical data that will be related to a specific sample of biological material. These are data from hospital information systems - clinical anonymized data, data from the laboratory information management system, data from the research information system and data from the PACS. The obtained data will be analysed bioinformatically, biostatistically and artificial intelligence algorithms can be applied to them. The digital biobank will also support the possibility of creating so-called digital pathology, which is a unique issue in the Slovak environment.

Beneficiary: University of Žilina

In cooperation with:
Ministry of Health of the Slovak Republic
Comenius University in Bratislava

Contracted amount of the Non-Repayable Financial Contribution:
11 590 338,03 EUR

Project duration: 06/2020 - 06/2023

ITMS2014+ code: 313011AFG4

This publication has been produced with the support of the Integrated Infrastructure Operational Program for the project: Creation of a Digital Biobank to Support the Systemic Public Research Infrastructure, ITMS: 313011AFG4, co-financed by the European Regional Development Fund.



EUROPEAN UNION
European Regional Development Fund
OP Integrated Infrastructure 2014 – 2020



MINISTRY
OF TRANSPORT
AND CONSTRUCTION
OF THE SLOVAK REPUBLIC

DRONE CONTROL USING THE COUPLING OF THE PID CONTROLLER AND GENETIC ALGORITHM

Mohamed Elajrami*, Zouaoui Satla, Kouider Bendine

Laboratory of Mechanical Structures and Solids, University Djillali Liabes of Sidi Bel Abbes, Sidi Bel Abbes, Algeria

*E-mail of corresponding author: eladjrami_mohamed@yahoo.fr

Resume

Due to their strong abilities and easy usage, unmanned aerial vehicles (UAVs) commonly named drones have found a place and merged in varieties of industrial sectors. These diversities of applications have encouraged researchers to involve new control algorithms that offer the drones to gain more maneuverability and flexibility. In this regard, the present study aims to propose a new PID controller with optimally selected gain values. The control algorithm has been used for the case of drones' type quadcopter. To this purpose, a state-space representation have been formulated based on the Newton Euler's rigid body method. As an enhancement of the performance of the control algorithm (PID) the parameters Kp, Ki and Kd have been selected thanks to an optimization search scheme based on a genetic algorithm. Various simulations were performed to test validity of the proposed model.

Article info

Received 18 July 2020
Accepted 2 December 2020
Online 20 April 2021

Keywords:

drone,
control,
PID,
genetic algorithm

Available online: https://doi.org/10.26552/com.C.2021.3.C75-C82

ISSN 1335-4205 (print version)
ISSN 2585-7878 (online version)

This is an open access article distributed under the terms of the Creative Commons Attribution 4.0 International License (CC BY 4.0), which permits use, distribution, and reproduction in any medium, provided the original publication is properly cited. No use, distribution or reproduction is permitted which does not comply with these terms.

1 Introduction

Unmanned air vehicles, shortly called UAVs, have found application in unlimited sectors ranging from military to civil world. They can serve in different areas, which include, but not limited to, capturing photos, monitoring pipelines and megastructures, inspection missions, neutral military targets. The UAVs nowadays are almost everywhere which results in an increasing interest in their designing, modeling and monitoring that led to a great enhancement in their performance. The UAVs range in shape, size, power-driven and control system, among this diversity, one comes across the well know Quadcopters. The Quadcopters by definition refer to a multi rotor helicopter that uses four rotors with propellers to provide lifting. Disregarding the fact that Quadcopters are not as fast as other types of UAVs, however, they provide a great advantage, which is mainly the Vertical Take-Off and Landing concept that turns to be critical in a specific type of missions and operations. Recently, a focus has been made on the Quadcopters, this interest has been motivated by the aforementioned advantages. Thus, a lot of papers have been dedicated to the modeling of Quadcopters. Some of the literature sources have offered various models for Quadcopters, which are diverse by their complexity and included parameters [1-6].

The main two approaches used to formulate the mathematical representative model are the Newton-Euler and Euler-Lagrange. Both approaches result in different types of models that range from the state-space representation to a transfer functions, which are later coupled with different control algorithms to reach the required maneuverability. The research community have investigated these approaches widely for more details about the formulations reader can refer to [7]. The authors proposed a mathematical model that relies on the Euler Newton formula and a simple PID controller for the case of quadcopter. The model steering angles were changed based on a fixed frame, which helps simplifying the final dynamic model, thus leading to an easy control of the drone [8]. Szabolcsi [9] introduces an analytic method with an enhanced PID and PI controllers for the case of the drone autopilot; the author's work was mainly based on MATLAB scripting. A method to fairly predict heading pitch and roll angle, using polynomial and logarithmic method, is presented in [10].

Obviously, the control algorithms are crucial for the UAV models development, they are considered as the brain that serves to control the structures and deliver the required path. Various techniques of control were tested for examined behavior of the UAV quadrotors, ranging from classical like PID to optimal like LQR, LQG [7] or fuzzy [11]. Each proposed controller has its advantage and a draw back. Optimal controllers, such as LQR and LQG, have a great performance and less noises. However, unfortunately, to be

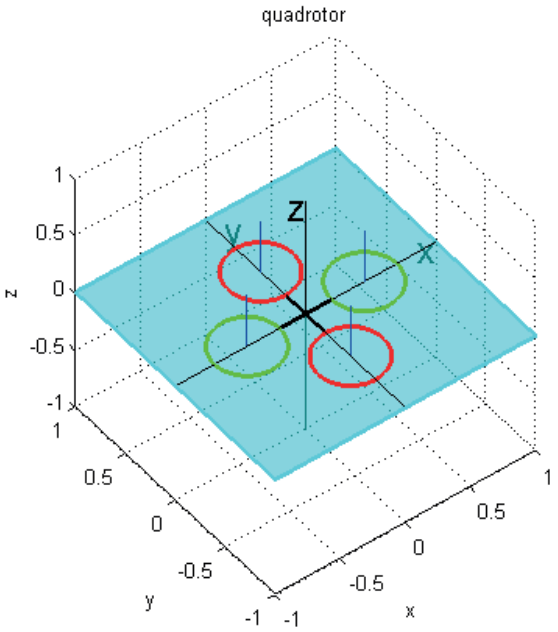


Figure 1 *Quadcopter and principal axes*

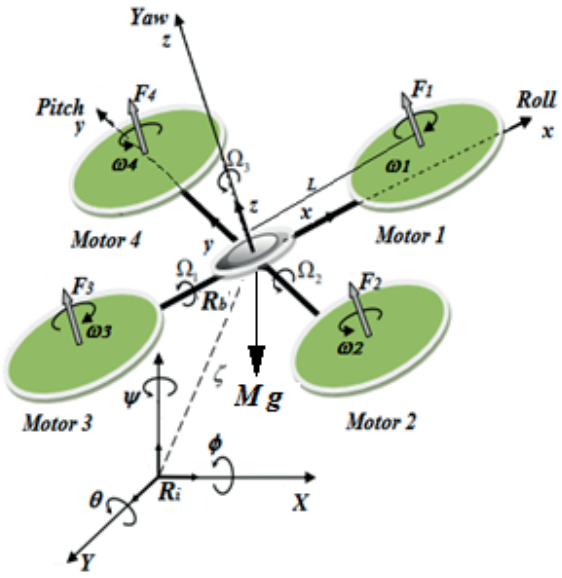


Figure 2 *The structure of quadrotor and relative coordinate systems*

used the model needed to be properly defined and mathematically formulated, which is not easy, especially when the models were of the complex type and also needed a parameters tunning. On the other hand, controllers like PID are extremely easy to implement and required no knowledge of the model. Sadly, the PID is less suitable for the nonlinear models and provide less performance. Generally, the choice of the controller is mainly driven by the used model and an enhancement is always needed to reach the desired performance and this paper is a contribution to that enhancement.

In terms of usability, both methods are fully accurate in simulation analysis but limited when it comes to the real-life models and the need for parameters' identification is crucial.

In this paper, the Newton Euler method has been used to formulate the state-space equation; the obtained equation involved six coordinates, which is then reduced to a more soft model that includes three main coordinates, which are the altitude z, steering angle (pitch), the direction of an arrangement parameter (Y coordinates). The state space equation is then coupled with a PID controller to easy monitor the drone. To improve the efficiency, the controller parameters were chosen based on a searching optimization scheme with help of the genetic algorithm (GA) in a way that has not been studied before. The angle has a range between

values 0 and 10 degrees and this leads to a significant simplification of the equation, as one can notice in the next section. The optimization objective function has been taken to be the minimum of the difference between the desired position and the actual one. Different scenarios have been discussed and a conclusion is formulated.

2 Mathematical formulation

A good mathematical model representation can help improving the controllability of the drone. One of the best formulation methods that proves to be efficient is the well-known Newton-Euler. Thus, the proposed model is based on this formulation and the following dynamic equation is written [8]:

$$\begin{bmatrix} MI_{3\times 3} & 0 \\ 0 & I \end{bmatrix} \begin{bmatrix} \dot{V} \\ \dot{\Omega} \end{bmatrix} + \begin{bmatrix} \Omega \times M\dot{\xi} \\ \Omega \times I\dot{\eta} \end{bmatrix} = \begin{bmatrix} F \\ \tau \end{bmatrix}. \tag{1}$$

The model (Figure 1) is represented by 12 state variables, describing the quadrotors dynamic behavior: the position $\xi = [XYZ]$, the linear velocity $V = [uvw]$ and, rotational angles $\eta = [\phi\theta\psi]$ (Roll, Pitch and Yaw) and angular velocities $\Omega = [\Omega_1\Omega_2\Omega_3]$. The vector (F,τ) stands for the applied forces and torques generated by the four motors rotation, while M is the quadcopter mass and M is the inertia.

Including the effect of the gravitational force and the vector of controller inputs are shown in Figure 2.

The dynamic model Equation (1) of a drone is driven using the Newton-Euler approach; a simplified mathematical model has been chosen [12]. The differential equation of motion of the modelled can be formulated as follows:

$$\begin{cases} \ddot{X} = (\sin\phi\sin\phi + \cos\phi\sin\theta\cos\phi)\dfrac{U_1}{M} \\ \ddot{Y} = (\sin\phi\cos\phi + \sin\phi\sin\theta\cos\phi)\dfrac{U_1}{M} \\ \ddot{Z} = -g + (\cos\phi\cos\theta)\dfrac{U_1}{M} \\ \ddot{\phi} = \dfrac{U_2}{I_{xx}} \\ \ddot{\theta} = \dfrac{U_3}{I_{yy}} \\ \ddot{\psi} = \dfrac{U_4}{I_{zz}} \end{cases}. \tag{2}$$

3 The control law

The PID algorithm is considered as the simplest controller, not just for its easy implementation, but for the high efficiency and reliability, as well. The PID controller can be formulated as follows [4]:

$$u(t) = K_p e(t) + K_i \int e(t)dt + K_d \dot{e}(t), \tag{3}$$

where:
K_p : is the proportional gain,
K_i : is the integral gain,
K_d : is the derivation gain.
$e(t)$: is the error given in the case of the drone by:

$$e(t) = s_p - p_v(t), \tag{4}$$

where:
s_p : is the setpoint or desired position,
$p_v(t)$: is the process variable at an instantaneous time according to s_p.

4 Results and discussion

To study the efficiency of the proposed methodology, a simulation study has been carried out using Matlab Simulink for 3 degrees of freedom. The model is presented in Equation (5). The physical parameters of the proposed quadcopter can be found in [13-14]. Three PID controllers are implemented to control the pitch, the altitude z and the y coordinates. To optimally choose parameters K_p, K_i and K_d a GA (genetic algorithm) optimization technique has been used to minimize the error between the desired drone position and the real one. After tuning the optimization algorithm, the following PID parameters were obtained:

$$\begin{cases} \ddot{Y} = (\sin\phi)\dfrac{U_1}{M} \\ \ddot{Z} = -g + (\cos\phi)\dfrac{U_1}{M} \\ \ddot{\phi} = \dfrac{U_2}{I_{xx}} \end{cases}. \tag{5}$$

After considering the pitch angle to take the values between 0 and 10 $(0 < \emptyset < 10)$, it is possible to linearize equation (5), by substituting $\sin\emptyset$ with $\emptyset$ and $\cos\emptyset$ with 1, which leads to Equation (6). Then the model can be easily designed as a block scheme using the Matlab Simulink, as shown in Figure 3.

$$\begin{cases} \ddot{Y} = (\phi)\dfrac{U_1}{M} \\ \ddot{Z} = -g + \dfrac{U_1}{M} \\ \ddot{\phi} = \dfrac{U_2}{I_{xx}} \end{cases}. \tag{6}$$

4.1 Optimization with genetic algorithm (GA)

To extract the needed PID parameters for the case of pitch angle controlling, each parameter was isolated separately to accelerate the solution calculation and the first parameter that has been optimized is the proportional gain K_p. As presented in Figure 4, the optimization results a value of proportional gain K_p equal

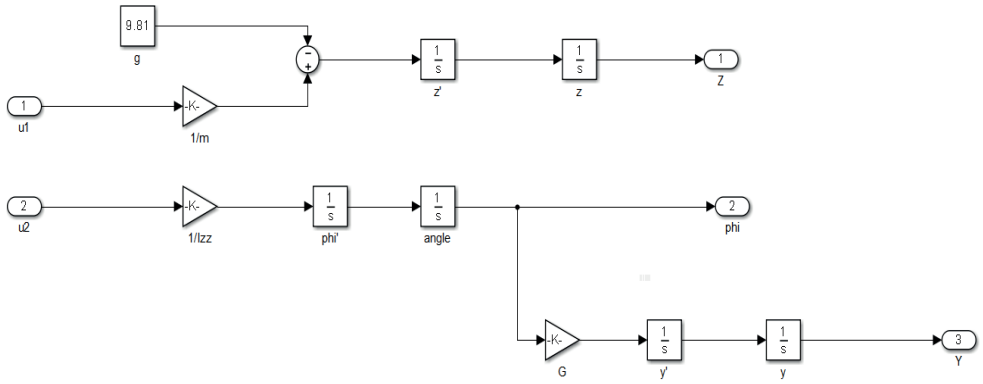


Figure 3 *The block diagram of a quadrotor with 3DDL*

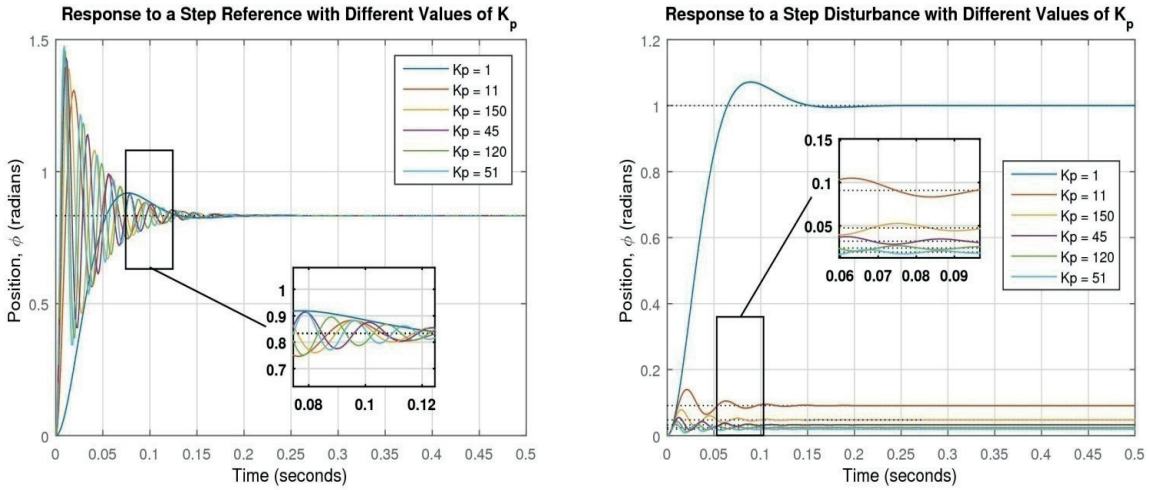


Figure 4 *Optimization of the K_p parameter of the PID controller of a pitch angle, K_p =150*

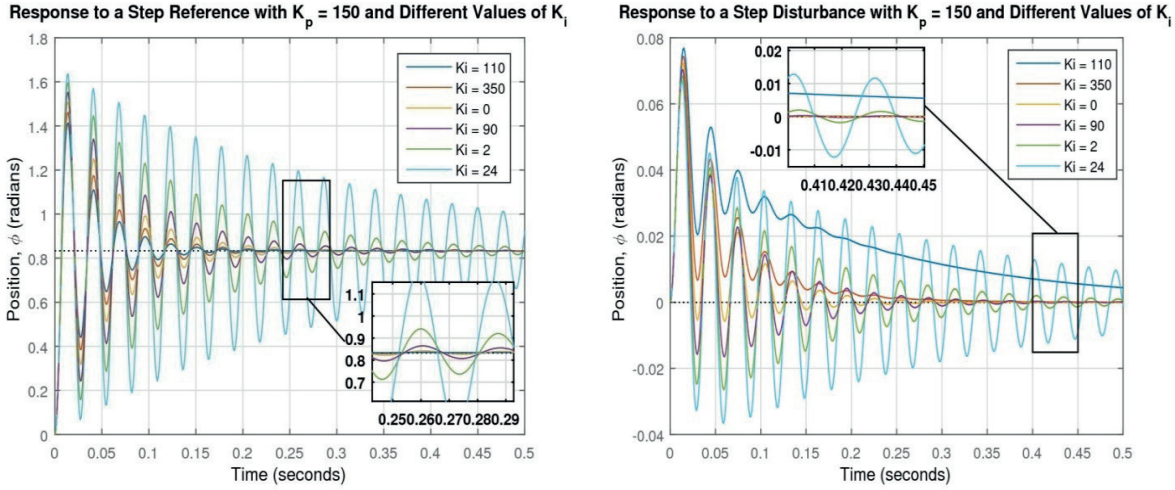


Figure 5 *Optimization of the K_i parameter of the PID controller of a pitch angle, K_i =0*

to 150. After, the first optimization the model shows some disturbance. Hence, an integral parameter has been plugged to reduce the resulting disturbance. The second optimization is then set, maintaining the K_p as 150 and optimizing the K_i gain for the set interval of [0, 350].

The integral control has successfully reduced the steady-state error to zero and test integral gains K_i ranging from 0 to 350, even when a step disturbance is present (Figure 5); that was the aim for accumulation of the integral term. For the reaction to

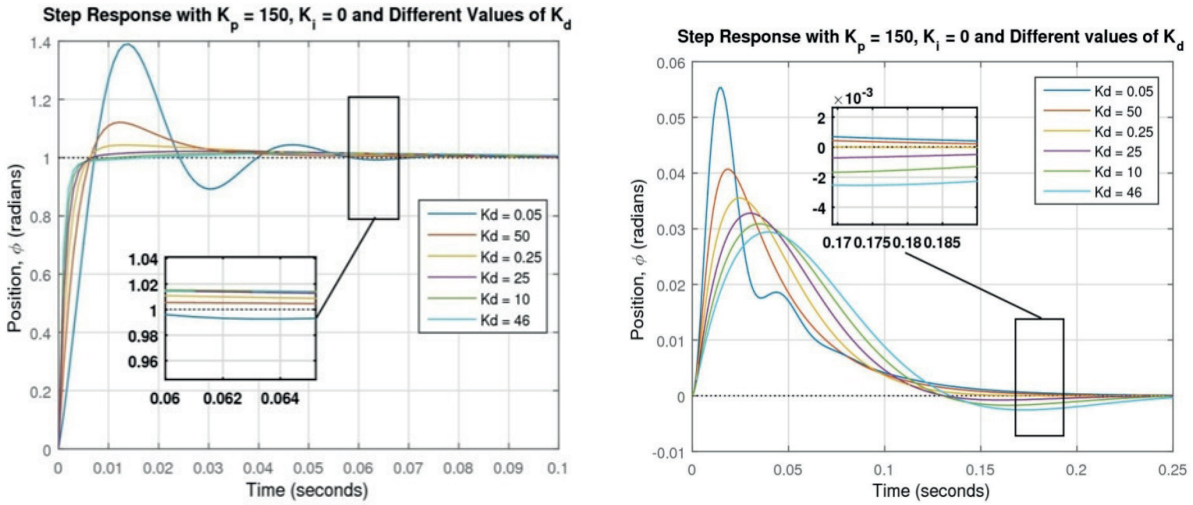


Figure 6 *Optimization of the K_d parameter of the PID controller of a pitch angle, K_d =50*

Table 1 *Optimization of parameters of the PID controller in the z and y directions*

parameters PID controller	*Kp*	*Ki*	*Kd*
PID in the z-direction	5	4	3
PID in the y-direction	0.3	0	10

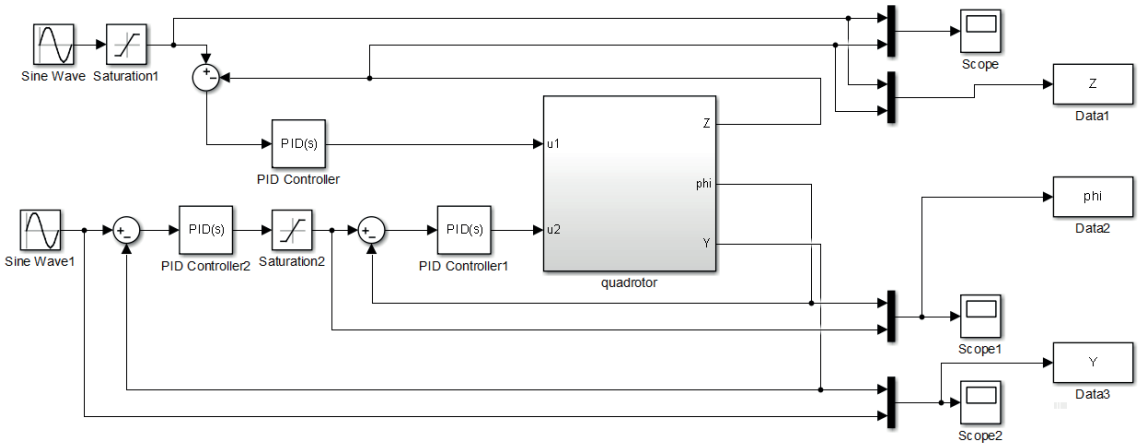


Figure 7 *The block diagram of the closed-loop system*

the step reference, all of the responses look similar to the amount of oscillation, increasing slightly as K_i is made it better, though, the response due to the disturbance changes considerably as the integral gain K_i is changed. Exclusively, the larger the value of K_i employed, the faster the error decays to zero. The best choice for a value of K_i will be K_i = 0 because the error due to the disturbance decays to zero quickly, however, the response to the reference has a longer settling time and more overshoot.

Introducing the term derivative to the control will help reducing the time needed for the stability and overshoot. Adding a derivative term to the console is the final step to reach the full working PID controller. The derivative gains that range from 0.05 to 50 were investigated by fixing the two proportional and integral terms with their previously selected values of an optimization K_p = 150 and K_i = 0.

Figure 6 also shows that when K_d = 50, the full requirements for the pitch angle control have been met.

In the same way, the values of the terms proportional to the integral and derivative of the two directions *z* and *y* are extracted, as shown in Table 1. There is an explanatory point since angle ∅ has a direct effect on *y*. Must first know The behavior of angle must be first known; thus it became known in advance in the field of simulation, which made it easy to study the behavior of *y*.

After including all the physical and the controller parameters and by using the aforementioned equations a Simulink block has been designed, as shown in Figure 7.

The proposed controller is tested with the following desired paths of the drone:

$$Z_{desired} = \sin(t), \tag{7}$$

$$Y_desired = \sin\left(\frac{1}{2} * t\right). \tag{8}$$

The model is run for time of 25 s. The obtained results are shown in Figures 8 to 10. Figure 8 presents the pitch angle variation over time. From the figure can be seen that there is a small error in the start of the simulation and that is because the controller is trying to catch the desired position. Once the actual position coincided with the desired one, the curve is stabilized, which is a proof of the proposed controller accuracy. The same observation is suitable for the y and z coordinate in Figures 8 and 9. For the better understanding of the proposed path, a 3D curve is presented in Figure 11. The figure reveals without doubts that the drone is following the same trajectory as the predicted one.

As a study of the performed optimization, the time needed to extract each PID parameter has been calculated and presented in table 2. It is worthy to note here that the used computer is with performance of the CPU i5 and 4G Ram. As it is clearly shown in Table 2, the required time for the whole optimization is indeed negligible.

5 Conclusion

The present study aims to provide a mathematical model with a simple control scheme for the case of a small quadrotor. The model is formulated using the Newton-Euler assumption and extracted

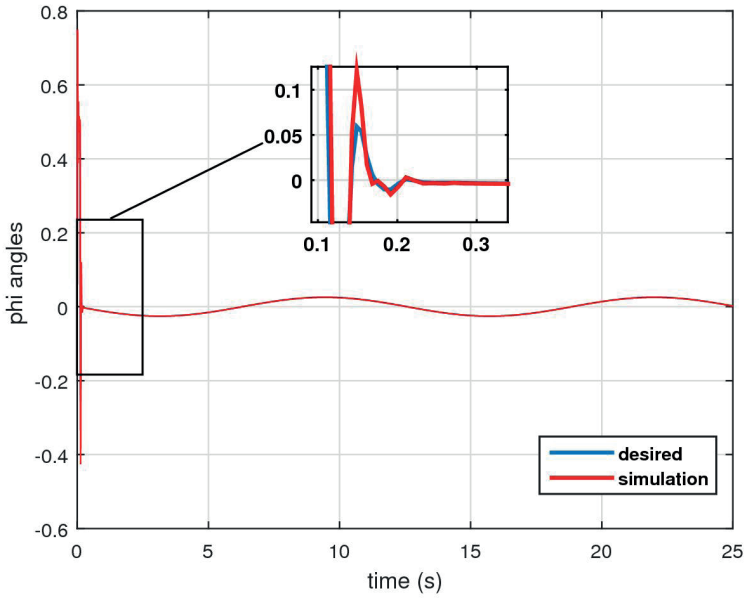


Figure 8 *The desired trajectory of the pitch angle and actual response*

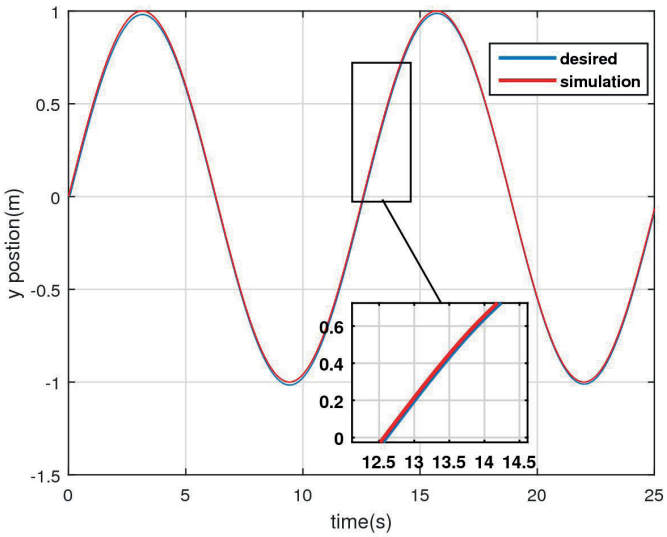


Figure 9 *The Y position response of the closed-loop system*

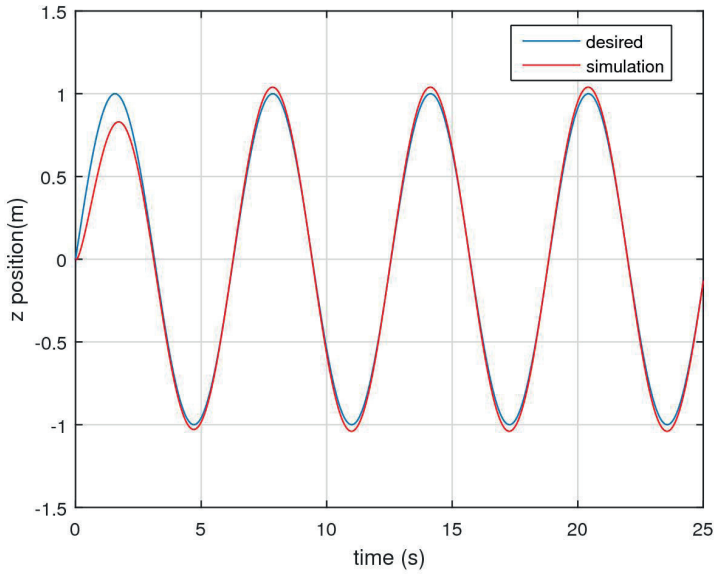


Figure 10 *Response of the closed-loop system to the desired trajectory of altitude*

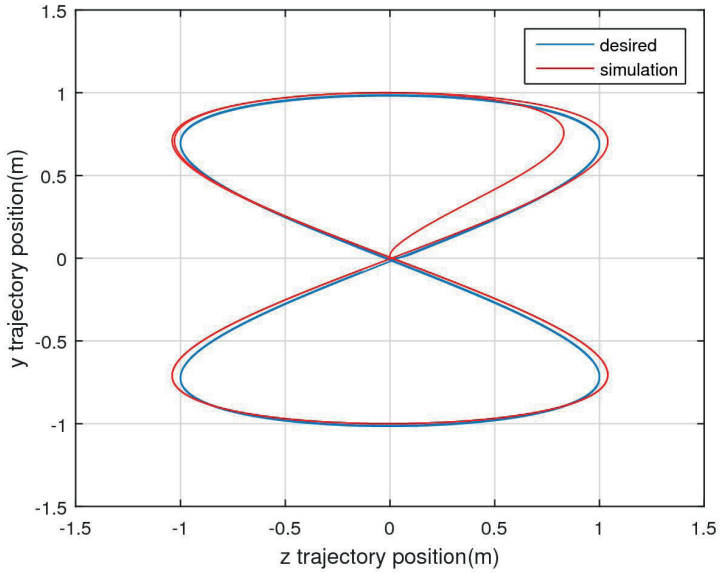


Figure 11 *The closed-loop system response with the PID trajectory 3D controllers*

Table 2 *The CPU time needed for the optimization routine*

parameters controller	∅ (s)	*z* (s)	*y*
CPU time for optimization of parameters PID	7731.605431	6605.553147	7533.582554
CPU time for simulation		1 815.246054	

based on a dynamic equation. To control the drone a PID algorithm has been designed with considering use of the best tuning parameters. The controller parameters have been selected using the Genetic Algorithm (GA) search optimization scheme.

To test the accuracy of the proposed model, a simulation study has been carried out for 25 s. The error between the desired and simulation trajectory is reduced successfully to a very low value for the three control parameters, as well as the altitude, which proves the robustness towards the stability and tracking of the proposed model.

The results of this paper show that this method of controlling the quadrotor has a very high performance to track the position path and hover and a good stability of this model.

References

[1] AL YOUNIS, Y., AL JARRAH, M. A., JHEMI, A. A. Linear vs. nonlinear control techniques for quadrotor vehicle. In: 7th Symposium of Mechatronics and its Applications ISMA 2010: proceedings. IEEE. 2010.

[2] MIAN, A. A., DAOBO, W. Nonlinear flight control strategy for an under actuated quadrotor aerial robot. In: 15th IEEE International Conference on Networking, Sensing and Control ICNSC: proceedings [online]. IEEE. 2008. ISBN 978-1-4244-1685-1. Available from: https://doi.org/10.1109/ICNSC.2008.4525351

[3] MAHONY, R., KUMAR, V., CORKE, P. Multirotor aerial vehicles modeling simulation and control of quadrotor. *IEEE Robotics and Automation Magazine* [online]. 2012, **19**(3), p. 20-32. ISSN 1070-9932. Available from: https://doi.org/10.1109/MRA.2012.2206474

[4] KOSZEWNIK, A. The parrot UAV controlled by PID controllers. *Acta Mechanica et Automatica* [online]. 2014, **8**(2), p. 65-69. eISSN2300-5319. Available from: https://doi.org/10.2478/ama-2014-0011

[5] JAMKHANDI, A. G., TULPULE, S., CHATURVEDI, A., CHARVET, J.-N. Controlling the position and velocity in space of the quad-rotor UAV AR. Drone using predictive functional control and image processing in open CV. In: 2012 International Conference on Signal Processing Systems ICSPS 2012: proceedings [online]. IPCSIT. Vol. 58. Singapore: IACSIT Press, 2012. Available from: https://doi.org/10.7763/IPCSIT.2012.V58.3

[6] SALIH, A. L., MOGHAVVEMI, M., MOHAMED, H. A. F., GAEID, K. S. Flight PID controller design for a UAV quadrotor. *Scientific Research and Essays*. 2010, **5**(23), p. 3660-3667. ISSN 1992-2248.

[7] ALTUG, E. Vision-based control of unmanned aerial vehicles with applications to an autonomous four-rotor a helicopter, quadrotor. Ph.D. thesis, University of Pennsylvania, 2003.

[8] SATLA, Z., ELAJRAMI, M., BENDINE, K., SALAH, M., POLAT, A. P, PI, PID controller designed for UAV Quadrotors trajectory. In: International Conference on Innovative Engineering Applications: proceedings. 2018.

[9] SZABOLCSI, R. Optimal PID controller-based autopilot design and system modelling for small unmanned aerial vehicle. *Review of the Air Force Academy* [online]. 2018, **3**(38), p. 43-58. ISSN 1842-9238. Available from: https://doi.org/10.19062/1842-9238.2018.16.3.6

[10] WIERZBICKI, D., KRASUSKI, K. Methods of predicting the heading, pitch and roll angles for an unmanned aerial vehicle. *Communications - Scientific Letters of the University of Zilina* [online]. 2020, **22**(2), p. 52-59. ISSN 1335-4205, eISSN2585-7878. Available from: https://doi.org/10.26552/com.C.2020.2.52-59

[11] AMIRKHANI, A., SHIRZADEH, M., KUMBASAR, T. Interval type-2 fuzzy cognitive map-based flight control system for quadcopters. International Journal of Fuzzy Systems[online]. 2020, **22**, p. 2504-2520. ISSN 1562-2479, eISSN 2199-3211. Available from: https://doi.org/10.1007/s40815-020-00940-8

[12] KHATOON, S., SHAHID, M., CHAUDHARY, H. Dynamic modeling and stabilization of quadrotor using PID controller. In: International Conference on Advances in Computing, Communications and Informatics ICACCI 2014: proceedings [online]. IEEE. 2014. p. 746-750. Available from: https://doi.org/10.1109/ICACCI.2014.6968383

[13] MOHAMMED, M. J., RASHID, M. T., ALI, A. A. Design optimal PID controller for quad rotor system. *International Journal of Computer Applications* [online].2014, **106**(3), p. 15-20. ISSN 0975-8887. Available from: https://doi.org/10.5120/18500-9565

[14] SATLA, Z., ELAJRAMI, M., BENDINE, K. Easy tracking of UAV using PID Controller. *Periodica Polytechnica Transportation Engineering* [online]. 2019, **47**(3), p. 171-177. ISSN 0303-7800, eISSN1587-3811. Available from: https://doi.org/10.3311/PPtr.10838

RTK KINEMATIC POSITIONING ACCURACY WITH DOUBLE PHASE DIFFERENCE OF SIS GNSS SIGNALS

Lucjan Setlak, Rafał Kowalik

Department of Avionics and Control Systems, Faculty of Aviation Division, Military University of Aviation, Deblin, Poland

*E-mail of corresponding author: r.kowalik@law.mil.pl

Resume

The article presents results of verification of the kinematic measurements usefulness for precise real-time positioning RTK in the local reference system. These measurements allow for continuous RTK measurements in the event of temporary interruptions in radio or internet connections, which are the main reason for interruptions in RTK kinematic measurements and cause a decrease in the reliability and efficiency of this positioning method. Short interruptions communication are allowed during the loss of the key correction stream from the local RTK support network, so the global corrections obtained from the geostationary satellite are used. The aim of the article was to analyze the accuracy of measuring the position of moving objects. Practical conclusions were formulated according to the research subject, the presented mathematical models, the experiment and the analysis of the obtained results.

Article info

Received 8 October 2020
Accepted 4 November 2020
Online 26 May 2021

Keywords:

real-time kinematic (RTK) positioning,
double signal difference,
GNSS system

Available online: https://doi.org/10.26552/com.C.2021.3.E35-E45

ISSN 1335-4205 (print version)
ISSN 2585-7878 (online version)

This is an open access article distributed under the terms of the Creative Commons Attribution 4.0 International License (CC BY 4.0), which permits use, distribution, and reproduction in any medium, provided the original publication is properly cited. No use, distribution or reproduction is permitted which does not comply with these terms.

1 Introduction

The key point of precise positioning of the Global Navigation Satellite Syste) (GNSS) is the ability to mitigate (reduce) all the potential source errors and interference in the system. All errors in the GNSS observations caused by signal propagation, the environment around the receiver and the equipment of the recipient, must be mitigated [1-4].

Limitation can be improved by modeling, estimating and creating individual combinations of station observations, as well as application of the differential mechanism of technique. Such errors of the analyzed observation are the subject of detailed considerations, included in the further part of this article.

2 Observations of the GNSS navigation system

The basic measurements recorded by the GNSS receiver are the differences in time or phase between the signals transmitted by the GNSS satellites and the reference signals generated inside the receiver. Signals of the GNSS system are transmitted at different frequencies, while the GNSS system receivers produce observable signals different from the signals of the navigation system [5-7]. Types of observation of the pseudorange code, carrier phase and *Doppler* phenomenon are discussed in the subsequent parts of individual subsections.

2.1 Model for determining the pseudorange

Unlike the terrestrial electronic distance measurements, the GNSS system uses an „one-way concept" in which satellite and receiver clocks are involved. Therefore, the ranges are affected by the satellite clock and receiver errors. Therefore, they are marked as pseudoranges. The GPS (Global Positioning System) receiver generates a copy of the pseudo-random code and compares it to that coming from the satellite [8-9].

The time offset is calculated by the autocorrelation function between the received pseudo-random code from the satellite and generated by the receiver. This type of shift includes the signal travel time and incorrect synchronization of satellite clocks and receivers. Pseudorange measurements usually have an accuracy of 1-10 meters.

The following is the equation for the observed pseudoranges [10-12]:

$$P^s_{r,j} = \rho^s_r + c(dt_r - dt^s) + I^s_{r,j} + \\ + T^s_r + b_{r,j} - b^s_j + \varepsilon^s_{r,j}, \quad (1)$$

where: superscript s - refers to a given satellite, subscript r - refers to the receiver, subscript

j - identifies the frequency, $P^s_{r,j}$ - is the pseudorange between the receiver r and the satellite j, ρ^s_r - is the geometric distance from the receiver r to the satellite s, including relativistic corrections, as well as the phase shift and variations, c - means the speed of light in vacuum.

In addition, dt_r and dt^s - these are receiver and satellite clock offsets relative to system time, $I^s_{r,j}$ - is the ionospheric delay in the signal path of the frequency j, T^s_r - is the tropospheric delay in the signal path, and $b_{r,j}$ and b^s_j - are the deviation of the receiver code r and the satellite s on the frequency j, respectively $\varepsilon^s_{r,j}$ - represents the effect of observational noise and all the non-modeled error sources, such as: satellite clock errors, predicted orbits and inaccuracies in ionospheric and tropospheric modeling, with the meter [m] being used for all the conditions.

In this work, pseudorange measurement is mainly used to obtain approximate or initial positions and construct ionosphere and geometry-free measurements.

2.2 Phases of SIS carrier signals

Observations of the carrier phase of the SIS signal (Signal in Space) are obtained by comparing phases between the signal transmitted by the satellite and a similar (analogous) signal generated by the receiver. The receiver registers a fraction of the satellite phase of the GNSS system and tracks changes in the received carrier phase, where the initial phase, called ambiguity, is unknown [13-14].

In order to use the phase observations, the so-called phase ambiguity must be resolved (analyzed). In addition, it should be noted that phase observations have noises of a few millimeters and are much more accurate than pseudoranges.

The carrier phase measurement equation can be written as [15-17]:

$$\lambda^s_j * \varphi^s_{r,j} = \rho^s_r + c*(dt_r - dt^s) - I^s_{r,j} + T^s_r + \lambda^s_j * \\ *N^s_{r,j} + d_{r,j} - d^s_j + e^s_{r,j}, \quad (2)$$

where: λ^s_j - is the satellite carrier wavelength s on the frequency j, $\varphi^s_{r,j}$ - is the carrier phase of the observation in cycles between the receiver r and the satellite s on the frequency j and ρ^s_r - means pseudoranges the geometric distance from satellite s to receiver r, containing not only relativistic corrections, but the phase shift and variations, as well, with $I^s_{r,j}$ - being the ionospheric advance of the carrier phase on a signal path on the frequency j scaled to a unit of length, having the same magnitude as for pseudorange measurements, but the opposite sign.

In addition, $N^s_{r,j}$ - is an integer ambiguity for a specific receiver-satellite pair with a frequency j, $d_{r,j}$ and d^s_j - are the deviation of the carrier phase of the receiver r and the satellite s on the frequency j and $e^s_{r,j}$ - represent the unmodified effects, modeling errors and measurement errors for the observation of the carrier phase, which are three or four orders of magnitude smaller than for the code measurements.

2.3 Doppler effect in SIS signals

The *Doppler* effect is a phenomenon of the frequency shift of the induced electromagnetic signal by the relative movement of the emitter in relation to the receiver.

In the first approximation, the *Doppler* change is given as [18-20]:

$$D^s_{r,j} = f^s_j - f^s_{r,j} = \frac{V_{\rho^s_r}}{c} f^s_j = \frac{V_{\rho^s_r}}{\lambda^s_j}, \quad (3)$$

where: $D^s_{r,j}$ - is the *Doppler* shift between the receiver r and the satellite s on the frequency j, f^s_j - means the frequency emitted j to the satellite s, $f^s_{r,j}$ - means the frequency j received from the satellite s, $V_{\rho^s_r}$ - is the relative speed along the distance line between the satellite s and the receiver r, and λ^s_j - is the carrier wavelength of the satellite s on the frequency j.

Equation (3) for the observed *Doppler* shift scaled to range speed is given as:

$$V_{\rho^s_r} = \lambda^s_j * D^s_{r,j} = \dot{\rho}^s_r + c*(\dot{dt}_r - \dot{dt}^s) + \varepsilon, \quad (4)$$

where: derivatives in relation to time are marked with a dot and ε - is a measurement error.

It should be noted that the *Doppler* shift is a by-product of both carrier phase measurements, independently observable and a measure of instantaneous range speed.

For example, when the satellite is moving towards the GNSS receiver, the *Doppler* shift is positive, so more *Doppler* counts are obtained when the range decreases.

3 Linear combinations of GNSS system observation

Several linear combinations of the GNSS primary carrier phase and code measurements are used in data analysis to eliminate or reduce some of the observation equation components. For example, a linear combination to remove the ionosphere effect can be created [21-22].

These types of combinations are listed and discussed later in this article. Parameter φ_j represents phase observations in cycles with a frequency j, while P_j - represents code observations in meters on a frequency j.

3.1 Linear combinations without influence of the ionosphere

The ionospheric delay, caused by the collapse of the GNSS electromagnetic signal, where propagation through the ionospheric layer in the atmosphere, is in the range of 6 - 150 [m]. A normal approach to eliminate ionospheric delay is created by a dedicated LC (Linear Combination) of GNSS observation. This kind of combination is called "ionosphere-free LC measurement".

For observation of the carrier phase of Equation (2) and observation of the Equation code (1), the combination without the influence of the ionosphere can be written as [23-25]:

$$\varphi_{LC} = \frac{f_1^2}{f_1^2 - f_2^2}\varphi_1 - \frac{f_1 * f_2}{f_1^2 - f_2^2}\varphi_2 \tag{5}$$

and:

$$P_{LC} = \frac{f_1^2}{f_1^2 - f_2^2}P_1 - \frac{f_2^2}{f_1^2 - f_2^2}P_2\,. \tag{6}$$

The ionospheric advance depends on frequency. The above Equations (5) and (6) eliminate the first-order ionospheric advance effect of the observation, which is widely used in the GNSS data processing [26-28]. The disadvantage of this linear combination is that noise from φ_1 and φ_2 measurements increases threefold and that ambiguities cannot be directly resolved as integers.

In the case of receivers that have two-phase capabilities, the LC combination is usually the preferred method in geodetic and atmospheric applications for estimating coordinates, tropospheric deceleration values and receiver clock deviation.

3.2 "Wide-Lane" linear combination

The „Wide-Lane" (WL) observation is a popular linear combination mainly used for ambiguity and can be described as:

$$\varphi_{WL} = \varphi_1 - \varphi_2\,. \tag{7}$$

The combination of the wavelength λ_{WL} measurements of the carrier phases $L1$ and $L2$ is 86 [cm]. This long wavelength simplifies the solution to the ambiguity. It is widely used in analysis of the GNSS stations more than several dozen kilometers apart. In the data pre-processing process, this type of solution can also be used to detect signal cycles.

3.3 Linear combination for determining the position of the moving objects

It should be noted that since the parameters φ_1 and φ_2 carry the same geometrical information, the number of independent positions can be constructed by subtracting φ_2, the carrier phase observation multiplied by the frequency ratio, from φ_1, which can be recorded as:

$$\varphi_{EX_{WL}} = \varphi_1 - \frac{f_1}{f_2}\varphi_2\,. \tag{8}$$

This type of linear combination eliminates geometry (orbits, position coordinates), troposphere and clock synchronization elements in equation with the carrier phase. In this way, it is often called a linear combination not related to geometry or *extra-wide-lane* (EWL/EX_WL). Because the combination of initial phase ambiguities remains, EX_WL can only represent a set of ionospheric delay variations during continuous tracking [29-30].

For the initial processing of GPS data, it is possible to construct a polynomial fit for EX_WL and to identify discontinuities such as cycle sections or outliers. However, in conditions of the high ionosphere activity, it is difficult to detect cycles slip with a linear ionospheric combination.

3.4 „MW Wide-Lane" linear combination

Observation of *wide-lane* MW (*Melbourne-Wübbena* combination) in Equation (7) still contains information about the position, with ionospheric effects and position information from *wide-lane* observations can be can be eliminated (removed), except that the ionosphere effects on the code and phase measurement are equal, but have opposite signs in Equation (1) and (2).

In the case where both code and phase information are available on two frequencies, observation without position and ionosphere is given in the form [31-32]:

$$\varphi_{MW_{WL}} = \varphi_1 - \varphi_2 - \frac{f_1 - f_2}{f_1 + f_2}\left(\frac{P_1}{\lambda_1} + \frac{P_2}{\lambda_2}\right). \tag{9}$$

This state, called the *Melbourne-Wübbena* combination, combines phase and code observations to eliminate ionospheric, geometric and clock effects and will be used to initiate ambiguities in the processing of the GNSS navigation system data. In addition, it should be noted that only multipath error and pseudorange noise are still included in the MW_WL observation, but can be reduced or eliminated by averaging many epochs.

4 Kinematic positioning based on multiple reference stations

This section primarily deals with the GNSS DD (double-difference) positioning approach based on multiple reference stations that are used to determine the baseline vectors between simultaneous observing receivers. Issues of this section focus on discussion of the GNSS DD positioning, with particular emphasis

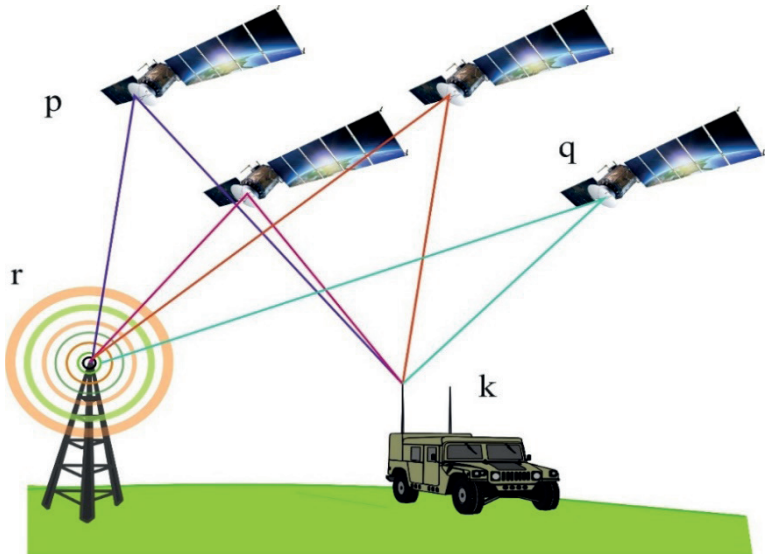


Figure 1 *Illustration for positioning the GNSS DD system*

on the analysis of observation equations for a single difference SD (single-difference) and DD. The challenge of DD positioning in a wide region was presented using the ultra-short and ultra-long base experiments. In addition, the kinematic positioning approach of many reference stations, based on apriori constraints, relates to the precise kinematic positioning of the GNSS system in a wide area.

At the final stage of consideration, solid *Kalman* filter theory is used to suppress the effect of outliers observations on trajectory estimates for air gravimetry.

4.1 Double-Difference positioning

The DD positioning is a classic GNSS system data processing method. This method is regularly used to eliminate or reduce errors between the satellite and the receiver. In addition, since observations of the carrier phase on satellites of the GNSS system can be used to determine the user's position even more precisely than by means of pseudorange measurements, in this part of this subsection the principle of DD carrier phase positioning is presented [33-35].

4.2 The principle of positioning the classic double difference

A simple example of positioning the DD (double difference) is shown in Figure 1, whereby p and q - mean the GNSS satellites, r - means the reference station and k - means the kinematic station.

According to observation of the carrier phase of Equation (2), the observations of the carrier phase of the reference of the station r and the kinematic station k to a common satellite p can be written as:

$$\lambda_j^p * \varphi_{r,j}^p = \rho_r^p + c*(dt_r - dt^p) - I_{r,j}^p + T_r^p + \lambda_j^p * \\ *N_{r,j}^p + d_{r,j} - d_j^p + e_{r,j}^p, \tag{10}$$

$$\lambda_j^p * \varphi_{k,j}^p = \rho_k^p + c*(dt_k - dt^p) - I_{k,j}^p + T_k^p + \lambda_j^p * \\ *N_{k,j}^p + d_{k,j} - d_j^p + e_{k,j}^p, \tag{11}$$

By creating a single difference, subtracting the measurement at the reference station from that at the kinematic station, the satellite clock dt^p and the satellite phase deviation d_j^p (which are common errors for both observers) are canceled by the following equation written in the form:

$$\lambda_j^p * \Delta\varphi_{k-j,r}^p = \Delta\rho_{k-r}^p + c * \Delta dt_{k-r} - \Delta T_{k-r}^p + \\ + \lambda_j^p * N_{k-rj}^p + \Delta dt_{k-r,j} + \Delta e_{k-r,j}^p, \tag{12}$$

where: operator Δ - indicates for example a single difference $\varphi_{k-j,r}^p$ marked as $\varphi_{k,j}^p - \varphi_{k,j}^p$.

It should be noted that if both antennas are close together, for example less than 10 [km] on the ground, the tropospheric delays are approximately the same, so that the differences in tropospheric delays ΔT_{k-r}^p are small and significantly reduced in Equation (12).

However, for medium and long baselines, the path of the signal traveling through the troposphere is different for each station, especially if the receivers are at different altitudes. This may be the case e.g. in mountainous regions or when an airplane approaches an airport. Thus, the tropospheric path delay is not canceled in positioning a single difference for medium and long baselines. Assuming that the kinematic station is close enough to the reference station, the path of the GNSS satellite signal through the ionosphere will be almost identical for the reference station and the kinematic station. Hence, the ionospheric delay can be significantly reduced and this summation can be made for distances up to about 1000 [km]. For long baselines, ionospheric delay can be eliminated for the first order approximation by creating a ionosphere-free dual frequency observation linear combination. In this

Table 1 *List of equipment selected from the IGS website*

station name	receiver type	antenna type
station 1	JPS LEGACY	LEIAR25.R4
station 2	JPS LEGACY	LEIAR25.R4

way, the differential ionospheric delay ΔI^{p}_{k-rj} can be neglected.

Therefore, in this case Equation (12) can be further simplified by writing it as [36-38]:

$$\lambda^{p}_{j} * \varphi^{p}_{k-j,r} = \Delta\rho^{p}_{k-r} + c * \Delta dt_{k-r} + \Delta T^{p}_{k-r} + \lambda^{p}_{j} * \\ * \Delta N^{p}_{k-r,j} + \Delta d_{k,j} - d_{k-rj} + e^{p}_{k-r,j}. \quad (13)$$

This type of differential processing is called „single difference positioning", namely the differential measurement of two receivers relative to a common satellite. The positioning of a single difference is applied to the satellite q with the signal frequency i, which is given as:

$$\lambda^{p}_{i} * \varphi^{p}_{k-i,r} = \Delta\rho^{p}_{k-r} + c * \Delta dt_{k-r} + \Delta T^{p}_{k-r} + \lambda^{p}_{i} * \\ * \Delta N^{p}_{k-r,i} + \Delta d_{k,i} - d_{k-ri} + e^{p}_{k-r,i}. \quad (14)$$

Assuming the same frequencies $j = i(\lambda^{p}_{j} = \lambda^{q}_{i})$ for satellite signals and using denotation $\nabla\Delta\,{}^{p-q}_{k-r} = \Delta\,{}^{p}_{k-r} - \Delta\,{}^{p}_{k-r}$, differentiating the two individual differential observations from Equation (13) and Equation (14), in the same places r and k, to two different GNSS system satellites p and q, give DD observation as:

$$\lambda^{p}_{i} * \nabla\Delta\varphi\,{}^{p-q}_{k-r,j} = \nabla\Delta\rho\,{}^{p-q}_{k-r} + \nabla\Delta T\,{}^{p-q}_{k-r} + \lambda^{p}_{j} * \\ * \nabla\Delta N\,{}^{p}_{k-r,j} + \nabla\Delta e\,{}^{p}_{k-r,j}. \quad (15)$$

The receiver clock error Δdt_{k-r} and carrier phase deviation $\Delta dt_{k-r,j}$ are typical errors in Equation (14) and Equation (15), so they can be reduced by positioning DD. Therefore, this is the main reason why the DD positioning is preferably used. However, if the frequencies of signals between the satellites of the GNSS system are different $(\lambda^{p}_{j} \neq \lambda^{q}_{i})$, as in the case of the Russian GLONASS system (Global Navigation Satellite System), the carrier phase polarization $\Delta dt_{k-r,j}$ and $\Delta dt_{k-r,i}$ cannot be canceled from Equation (15). Introducing the abbreviated notation, symbolically $\nabla\Delta\,{}^{p-q}_{k-r} = \Delta\,{}^{p}_{k-r} - \Delta\,{}^{q}_{k-r}$, the DD equation for the two different frequency satellites can be given as:

$$\lambda^{p}_{i} * \nabla\Delta\varphi\,{}^{p-q}_{k-r,j} = \nabla\Delta\rho\,{}^{p-q}_{k-r} + \nabla\Delta T\,{}^{p-q}_{k-r} + \lambda^{p}_{j} * \\ * \nabla\Delta N\,{}^{p-q}_{k-r,j} + \nabla\Delta e\,{}^{p-q}_{k-r,j}. \quad (16)$$

Based on the above, it should be noted that it is difficult to separate the carrier phase polarization $\Delta d_{k-r,j}i$ from the ambiguity parameter, so a „float" solution is used to determine the GLONASS system disturbances [39-40]. The procedure described above is called the „DD positioning", where the satellite orbit error, satellite clock error and receiver clock error have been reduced. For the short baselines, the remaining ionospheric and tropospheric delays can be neglected. For medium and long baselines, the combination of no ionosphere (LC) is used to eliminate the first order ionosphere path delays. The remaining tropospheric delay is reduced by estimating wet zenith delay parameters.

5 Static experiment based on a GPS+GLONASS system receiver

In order to test the accuracy, reliability of the algorithm and software in the experiment with static data, static observation data of the GNSS system was randomly selected for testing from the IGS (International GNSS Service) from April 1, 2019, used to increase the accuracy of aircraft positioning. The length of this baseline is approximately 190 [km]. Types of the receiver and antenna equipment are given in Table 1.

The number of the GPS, GLONASS and GPS + GLONASS system satellites is shown in Figure 2 as the blue, green and red lines, respectively, where station 2 was selected as the reference station [41-42]. In turn, station 1 was processed by the GNSS LAB using kinematic processing. Results were compared to the coordinates taken from the IGS website (http://www.igs.org) and in the final stage four diagrams were compared (diagram 1÷4).

Diagram 1: GPS was used separately to calculate the position of Station 1.

Diagram 2: The GLONASS system itself was used to calculate the position of Station 1.

Diagram 3: The integrated GPS and GLONASS system was used to calculate the position of Station 1.

Diagram 4: The integrated GPS and GLONASS system was used to calculate the position of Station 1 using VCE Helmert .

Differences between the „real values" and results of diagrams 1-4 are respectively shown in the following figures (Figures 3-6) as time series.

The above experiments, based on the kinematic processing of static data, illustrate the effectiveness, repeatability and stability of the proposed method in static data. Accuracy of the kinematic positioning of the GNSS system, based on the (single) GLONASS system itself, is slightly lower than the accuracy of only the GPS system. Combination of GPS and GLONASS is better

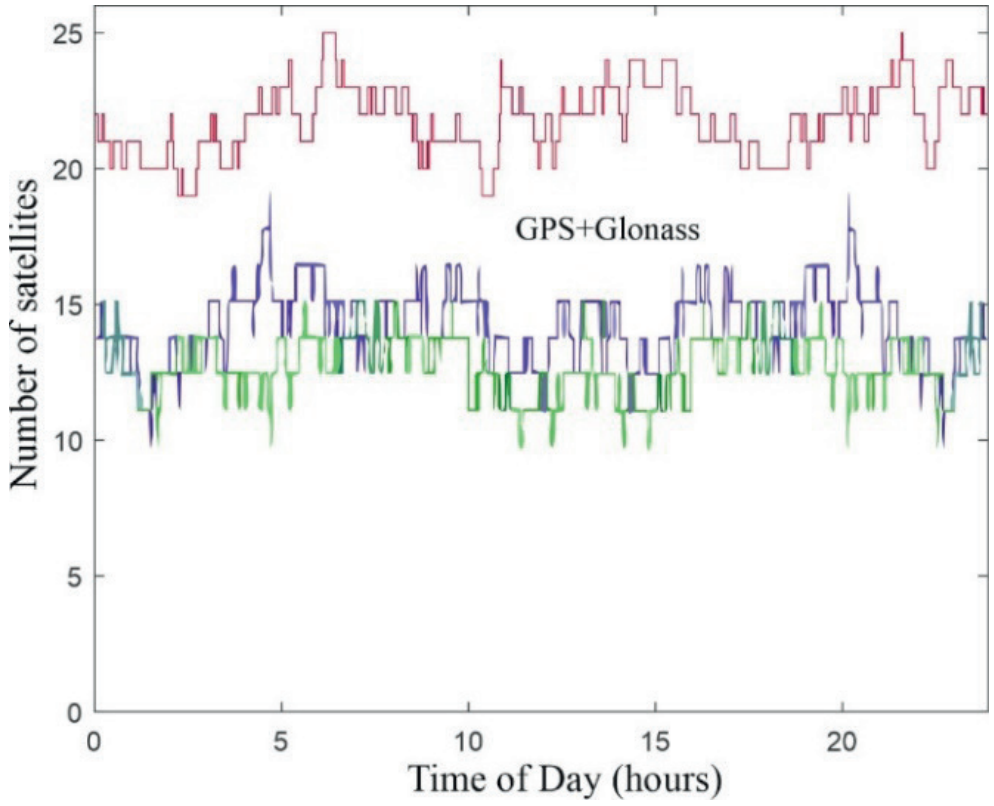


Figure 2 *Number of selected GPS (blue line), GLONASS (green line) and GPS + GLONASS (red line) satellites for the static experiment (IGS TITZ and FFMJ station on January 1, 2013)*

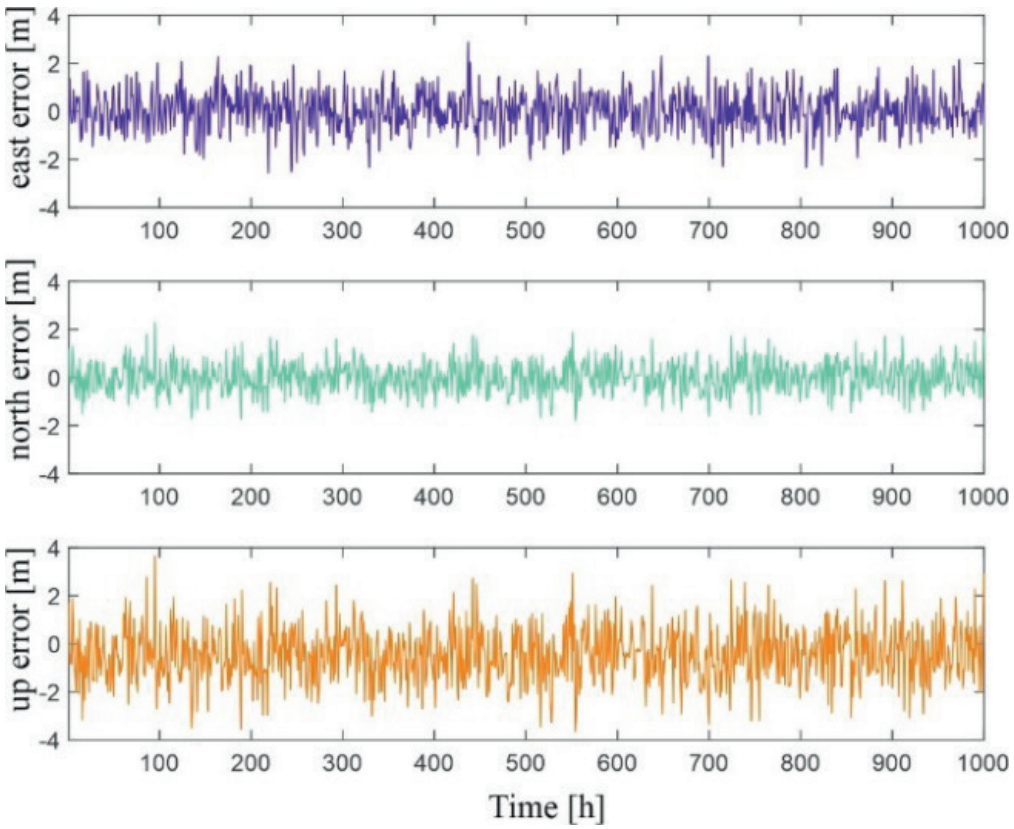


Figure 3 *Differences between the IGS result and results of GPS the kinematic system positioning for the TITZ - FFMJ baseline (diagram 1)*

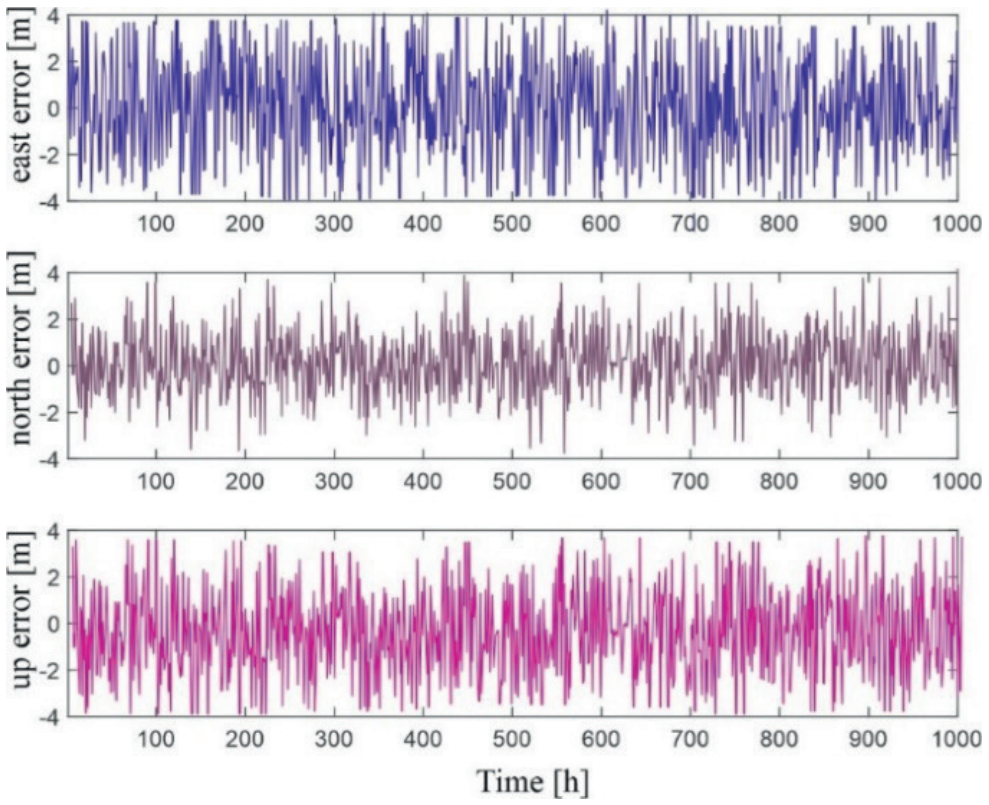


Figure 4 *Differences between the IGS result and results of the kinematic system positioning of the GLONASS system for the TITZ - FFMJ baseline (diagram 2)*

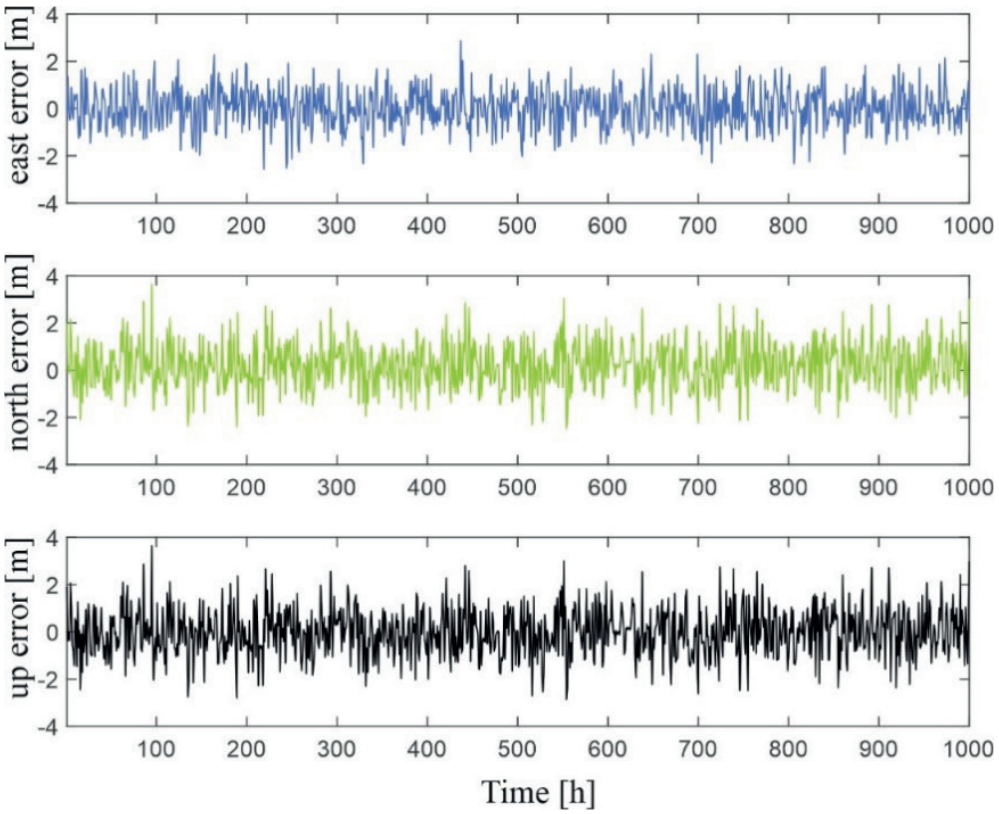


Figure 5 *Differences between the IGS result and results of the GPS + GLONASS kinematic positioning (with weights 1:1) for the base line TITZ- FFMJ (diagram 3)*

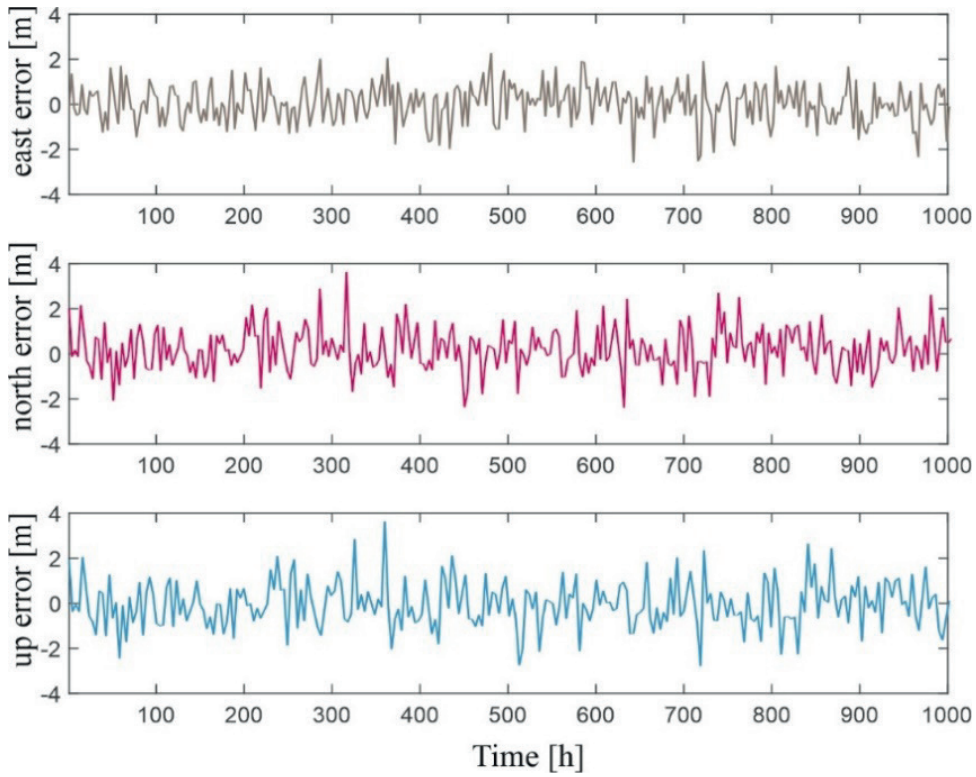


Figure 6 *Differences between the IGS result and results of the GPS + GLONASS kinematic positioning (with Helmert weights) for the TITZ - FFMJ baseline (diagram 4)*

Table 2 *Summary of results*

	average (m)	rms (m)	standard deviation (m)
		experiment 1	
X	2.38	1.84	1.75
Y	1.29	1.62	1.60
H	2.77	1.57	1.55
		experiment 2	
X	4.15	3.99	1.88
Y	3.32	3.19	1.87
H	4.08	3.97	1.67
		experiment 3	
X	2.51	2.25	1.60
Y	2.37	2.19	1.59
H	2.66	2.35	1.58
		experiment 4	
X	1.78	1.57	1.45
Y	3.85	3.42	1.74
H	3.95	3.68	1.68

(more efficient) than their use as individual systems and improves both accuracy and reliability.

It should be noted that the method based on estimation of the VCE Helmert variance component (Variance Component Estimation) can further increase the accuracy of integrated kinematic positioning (Figure 6).

Values of the average differences, maximum, minimum, as well as the RMS error and standard deviation are presented in Table 2.

The conducted research clearly shows that in the case of a localization system in which the systematic error is unknown, accuracy can be determined similarly to the precision, treating the whole as

a random variable. Differences in results are small, of the order of 3.5%. Although such a solution does not comply with recommendations in the normative regulations and the strict definition of accuracy according to ISO 5725-1, it may be an alternative form and in the case of location systems it allows to treat all the errors as random ones.

6 Conclusions

The presented work has shown that use of the GNSS system integration can improve accuracy and reliable positioning of the GNSS navigation system. In turn, since the Galileo system and the BeiDou satellite navigation system (BDS) have not yet reached full readiness, only the GPS systems and GLONASS were used in this article for research into the combination of multiple systems (Figures 3-6).

Creating the mathematical models and integrated system processing methodologies is valuable because it identifies key issues for connecting two or more GNSS positioning systems. Therefore, these are experiences that can be applied to other GNSS systems that can integrate the GPS system with Galileo, GLONASS, BDS or all four.

The work showed that accuracy of the kinematic positioning of the GNSS system, solely based on the GLONASS system as a single system, is slightly worse than just the GPS system. However, combination of the GPS and GLONASS is better than using them as individual systems and improves accuracy. At the final stage of this article, it was demonstrated that the VCE *Helmert* method can be used to estimate the weight of many GNSS observation data and can further improve the accuracy of the integrated kinematic positioning of this system.

The GNSS system kinematic positioning method is based on multiple kinematic stations on the same platform with apriori distance constraints and estimation of the common tropospheric delay parameter. In this new method, distances between the multiple GNSS antennas are known and used as apriori distance restrictions to improve accuracy of the state estimates.

In addition, it has been shown that since the characteristics of tropospheric delays in a small area are similar, for such many kinematic stations a common tropospheric delay parameter can be established, which can increase accuracy of the state estimates.

In summary, it can be stated that the kinematic positioning method using the integration of many GNSS systems based on estimation of *Helmert's* variance components is addressed to adjust the weights in a reasonable way to balance the input of many GNSS systems and improve accuracy of the GNSS navigation kinematic navigation system.

Results of the obtained research allow to formulate the following conclusions:

1. The precise GPS receiver, dedicated to aviation applications, allows for the guidance of objects with an accuracy of about 1 m, even without use of its own Differential Global Positioning System (DGPS) reference station, intended for accurate position determination, thanks to increasing accuracy of the GPS system through the introduced corrections to pseudo-ranges determined by the reference station.
2. The vicinity of tall buildings strongly interferes with the accuracy of the measurement, hence significant errors in guidance should be taken into account in the case of such obstacles.

References

[1] FENG, Y., WANG, J. Exploring GNSS RTK performance benefits with GPS and virtual galileo measurements. In: Institute of Navigation (ION) National Technical Meeting 2007: proceedings. 2007, p. 218-226.
[2] LANGLEY, R. B. The integrity of GPS. *GPS World*. 1999, **10**(3), p. 60-63. ISSN 1048-5104.
[3] HIGGINS, M. GNSS, CORS and positioning infrastructure: business and the future. In: 6th FIG Regional Conference: proceedings. 2007.
[4] WANG, J. Stochastic modelling for RTK GPS/Glonass positioning. *Navigation* [online]. 2000, **46**(4), p. 297-305. eISSN 2161-4296. Available from: https://doi.org/10.1002/j.2161-4296.1999.tb02416.x
[5] MIRSA, P., ENGE, P. Global positioning systems, signals, measurements and performance. Lincoln: Ganga Jamuna Press, 2004. ISBN 978-0970954428, p. 227-254.
[6] PRATT, M., BURKE, B., MISRA, P. Single-epoch integer ambiguity resolution with GPS-GLONASS L1-L2 data. In: ION GPS-98: proceedings [online]. 1999, p. 1-10. https://trid.trb.org/view/898384
[7] TEUNISSEN, P. J. G. The least-squares ambiguity decorrelation adjustment: a method for fast GPS integer ambiguity estimation. *Journal of Geodesy* [online]. 1995, **70**(1-2), p. 65-82. ISSN 0949-7714, eISSN 1432-1394. Available from: https://doi.org/10.1007/BF00863419.
[8] WANG, J., SATIRAPOD, C., RIZOS, C. Stochastic assessment of GPS carrier phase measurements for precise static relative positioning. *Journal of Geodesy* [online]. 2002, **76**(2), p. 95-104. ISSN 0949-7714. Available from: https://doi.org/10.1007/s00190-001-0225-6.
[9] XU, G. GPS theory, algorithms and applications. 1. ed. Berlin Heidelberg: Springer-Verlag, 2003. ISBN 978-3-540-67812-0.

[10] GRZEGORZEWSKI, M. Results of a research predicting the position of an aircraft during approach and landing using the bessel function. *Journal of Theoretical and Applied Mechanics*. 2013, **51**(4), p. 915-926. ISSN 1429-2955.

[11] WANG, Z., WU, Y., ZHANG, K., MENG, Y. Triple-frequency method for high-order ionospheric refractive error modelling in GPS modernization. *Journal of Global Positioning Systems* [online]. 2004, **4**(1-2), p. 291-295. ISSN 1446-3156. Available from: https://doi.org/10.5081/jgps.4.1.291

[12] WANNINGER, L., MAY, M. Carrier phase multipath calibration of GPS reference sites. In: 13th International Technical Meeting of the Satellite Division of the Institute of Navigation ION GPS 2000: proceedings. 2000, p. 132-144.

[13] ENGE, P., VAN DIERENDONCK, A. J. Wide area augmentation system [online]. In: *Global Positioning System: theory and applications*. *Vol II*. PARKINSON, B. W., ENGE, P., AXELRAD, P., SPILKER JR., J. J. (eds.). Washington D.C.: American Institute of Aeronautics and Astronautics, 1996. ISBN 978-1-56347-107-0, eISBN 978-1-60086-639-5, p. 117-142. Available from: https://doi.org/10.2514/5.9781600866395.0117.0142

[14] SAUER, K. Integrated high precision kinematic positioning using GPS and EGNOS observations. PhD thesis. London, UK: Department of Civil and Environmental Engineering, Imperial College, 2003.

[15] SETLAK, L., KOWALIK, R. Examination of the unmanned aerial vehicle. *ITM Web of Conferences* [online]. 2019, **24**, 01006. eISSN 2271-2097. Available from: https://doi.org/10.1051/itmconf/20192401006

[16] SCHMITZ, WYBBENA, M., BOETTCHER, G. G. Test of phase centre variations of various GPS antennas and some results. *GPS Solutions* [online]. 2002, **6**(1-2), p. 18-27. ISSN 1080-5370, eISSN 1521-1886. Available from: https://doi.org/10.1007/s10291-002-0008-4

[17] SCHUELER, T., HEIN, G.W., EISSFELLER, B. On the use of numerical weather fields for troposphere delay estimation in wide area augmentation systems. In: GNSS 2000: proceedings. 2000, p. 1077-1091.

[18] TEFERLE, F. N., ORLIAC, E. J., BINGLEY, R. M. An assessment of bernese GPS software precise point positioning using IGS final products for global site velocities. *GPS Solution* [online]. 2007, **11**, p. 205-213. ISSN 1080-5370, eISSN 1521-1886. Available from: https://doi.org/10.1007/s10291-006-0051-7

[19] TSUJII, T., WANG, J., DAI, L., RIZOS, C., HARIGAE, M., INAGAKI, T., FUJIWARA, T. KATO, T. A technique for precise positioning of high altitude platforms system (HAPS) using a GPS ground reference network. In: 14th International Technical Meeting of the Satellite Division of the Institute of Navigation ION-GPS-2001: proceedigs, 2001, p. 1017-1026.

[20] SETLAK, L., KOWALIK, R., SMOLAK, M. Doppler delay in navigation signals received by GNSS receivers. In: WSEAS Transactions on Applied and Theoretical Mechanics, 3rd International Conference on Applied Physics, System Science and Computers APSAC 2018: proceedings. 2018. Lecture Notes in Electrical Engineering. Vol. 574, p. 3-8.

[21] RYAN, S. Y., DATY, A. G., BRAIN, T. D. Investigation and comparison of horizontal protection level and horizontal uncertainty level in FDE algorithms. In: ION GPS 1996: proceedings. 1996, p. 1607-1614.

[22] ZANDBERGEN, DINWIDDY, R. S., HAHN, J., BREEUWER, E., BLONSKI, D. GALILEO orbit selection. In: 17th International Technical Meeting of the Satellite Division of The Institute of Navigation ION GNSS 2004: proceedings. 2004, p. 616-623.

[23] WIESER, A., BRUNNER, F. K. An extended weitht model for GPS phase observations. *Earth Planets Space* [online]. 2000, **52**, p. 777-782. ISSN 1880-5981. Available from: https://doi.org/10.1186/BF03352281

[24] STURZA, M. A. Navigation system integrity monitoring using redundant measurements. *Navigation* [online]. 1989, **35**(4). eISSN 2161-4296. Available from: https://doi.org/10.1002/j.2161-4296.1988.tb00975.x

[25] TEUNISSEN, P. J. G. Least-squares estimation of the integer GPS ambiguities. In: IAG General Meeting: proceedings. Section IV: Theory and Methodology. 1993.

[26] SETLAK, L., KOWALIK, R. Analysis, mathematical model and selected simulation research of the GNSS navigation receiver correlator. *MATEC Web of Conferences* [online]. 2018, **210**, p. 1-11. eISSN 2261-236X. Available from: https://doi.org/10.1051/matecconf/201821005008.

[27] HUGENTOBLER, U., DACH, R., FRIDEZ, P., MEINDL, M. *Bernese GPS software version 5.0*. Bern: Astronomical Institute University of Bern. 2007.

[28] PARKINSON, B. W., SPILKER Jr., J. J. *Global Positioning System: Theory and Applications. Vol. I. Progress in Astronautics and Aeronautics* [online]. Washington DC: American Institute of Aeronautics and Astronautics, 1996. ISSN 978-1-56347-106-3, eISSN 978-1-60086-638-8. Available from: https://doi.org/10.2514/4.866388

[29] PULLEN, S. P., PERVAN, B. S., PARKINSON, B. W. A new approach to GPS integrity monitoring using prior probability models and optimal threshold search. In: PLANS '94: proceedings. 1994.

[30] RAQUET, J. F. Development of a method for kinematic GPS carrier-phase ambiguity resolution using multiple reference receivers. PhD. Thesis. Calgary: University of Calgary, Department of Geomatics Engineering, 1998.

[31] REMONDI, B. W. NGS second generation ASCII and binary orbit formats and associated interpolation studies. In: 20th general assembly of the IUGG: proceedings. 1991.

[32] RICHERT, T., EL-SHEIMY, N. Optimal linear combinations of triple frequency carrier phase data from future global navigation satellite systems. *GPS Solutions* [online]. 2007, **11**(1), p. 11-19. ISSN 1080-5370, eISSN 1521-1886. Available from: https://doi.org/10.1007/s10291-006-0024-x

[33] ROTHACHER, M., SPRINGER, T. A., SCHAER, S., BEUTLER, G. Processing strategies for regional GPS networks. In: IAG General Assembly: proceedings. Springer, 1997.

[34] ENGE, P. K. The Global Positioning System: signals, measurements,and performance, *International Journal of Wireless Information Networks* [online]. 1994, **1**(2), p. 83-105. ISSN 1068-9605, eISSN 1572-8129. Available from: https://doi.org/10.1007/BF02106512

[35] ZHANG, W. Triple frequency cascading ambiguity resolution for modernized GPS and GALILEO. UCGE reports, No. 20228. Calgary: University of Calgary, Department of Geomatics Engineering, 2005.

[36] SETLAK, L., KOWALIK, R. Examination of multi-pulse rectifiers of PES systems used on airplanes compliant with the concept of electrified aircraft. *Applied Sciences* [online]. 2019, **9**(8), 1520. Available from: https://doi.org/10.3390/app9081520

[37] ZHANG, X. H., ANDERSON, O. B. Surface ice flow velocity and tide retrieval of the amery ice shelf using precise point positioning. *Journal of Geodesy* [online]. 2006, **80**(4), p. 171-176. ISSN 0949-7714, eISSN 1432-1394. Available from: https://doi.org/10.1007/s00190-006-0062-8

[38] YOUSIF, H., EL-RABBANY, A. Assessment of several interpolation methods for precise GPS orbit. *The Journal of Navigation* [online]. 2007, **60**, p. 443-455. ISSN 0373-4633, eISSN 1469-7785. Available from: https://doi.org/10.1017/S0373463307004250.

[39] SETLAK, L., KOWALIK, R. Analysis, mathematical model and simulation tests of the unmanned aerial vehicle control system. *ITM Web of Conferences* [online]. 2019, **24**, 01005. eISSN 2271-2097. Available from: https://doi.org/10.1051/itmconf/20192401005

[40] WYBBENA, G., SCHMITZ, M., MENGE, F., BODER, V., SEEBER, G. Automated absolute field calibration of GPS antennas in real time. In: International Technical Meeting of the Satellite Division of the Institute of Navigation ION-GPS-2000: proceedings. 2000, p. 2512-2522.

[41] WERNER, W., WINKEL, J. TCAR and MCAR options with GALILEO and GPS. In: ION GPS/GNSS 2003: proceedings. 2002.

[42] TEUNISSEN, P. J. G., DE JONGE, P. J., TIBERIOUS, C. C. J. M Performance of the LAMBDA method for fast GPS ambiguity resolution. *Navigation* [online]. 1997, **44**(3), p. 373-383. eISSN 2161-4296. Available from: https://doi.org/10.1002/j.2161-4296.1997.tb02355.x

E1 SIGNAL PROCESSING OF THE GALILEO SYSTEM IN THE NAVIGATION RECEIVER

Lucjan Setlak, Rafał Kowalik

Department of Avionics and Control Systems, Faculty of Aviation Division, Military University of Aviation, Deblin, Poland

*E-mail of corresponding author: r.kowalik@law.mil.pl

Resume

The subject of this article are issues related to the navigation system in the field of analyzing the processed signal in the GNSS system receiver. The main purpose of the work is to discuss the Galileo E1 signal processing methods in the GNSS navigation system receiver, supported by adapted research tools in terms of solving the research problem (analysis, model, simulation tests) and the mathematical apparatus used. Key studies are concentrated around the process of generating the navigation data, dispersing sequences and signal modulation. Thus, when designing a receiver, it is better to use the simulation signals than the real ones, since one can get more control over the properties of the received signal. In the final part of the work, in accordance with the subject of research, based on the developed appropriate research tools, observations and final conclusions were formulated, which have practical applications.

Article info

Received 8 October 2020
Accepted 24 November 2020
Online 26 May 2021

Keywords:

signal processing,
E1 signal,
Galileo system,
navigation system receiver

Available online: https://doi.org/10.26552/com.C.2021.3.E46-E55

ISSN 1335-4205 (print version)
ISSN 2585-7878 (online version)

This is an open access article distributed under the terms of the Creative Commons Attribution 4.0 International License (CC BY 4.0), which permits use, distribution, and reproduction in any medium, provided the original publication is properly cited. No use, distribution or reproduction is permitted which does not comply with these terms.

1 Introduction

In recent years, many efforts have been made to design and implement the Galileo signal simulator. This work presents simulations of the GNSS/Galileo navigation system transmitter signals via a graphical programming language, which is the Matlab/Simulink programming environment, with the same efficiency as text programming languages.

The GUI (Graphical User Interface) environment was used. In addition, use of a graphical programming language makes every part of the navigation system transmitter architecture very clear and much easier to understand and modify. The Galileo system receiver consists of four main components: acquisition, satellite tracking, digital processing and positioning efficiency. It is based entirely on the algorithms of the Matlab/Simulink program [1-2].

In addition, some of the decoding algorithms were previously developed for the GPS system technology, so everything had to be adjusted, including the navigation message. However, it should be noted that majority of the Galileo system algorithms have been recently developed.

Real Galileo signals taken from the GNSS navigation system receiver were used for the tests. These signals were helpful, among others in understanding the structure of navigational messages and obtaining parameters transmitted by the Galileo system signals. However, it should be mentioned that study encountered some inconvenience due to insufficient information on the system under consideration. Although there is a lot of information and publications in the field of the GPS, the Galileo system is still under development and some specifications have not been fully defined or have been left to ongoing improvement.

In the rest of this article, in accordance with the subject of the study, the issue of the positioning efficiency of the GNSS navigation system (Galileo) was considered from an aspect of an ideal and not ideal mathematical model of the pseudo-distance of the system [3-5].

2 Positioning performance

Navigation data consists of 4 types of data needed to perform positioning, i.e. ephemeris parameters necessary to indicate the position of the satellite relative to the receiver, time and clock correction parameters to calculate the pseudorange, service parameters for identifying satellites and signal quality and almanac parameters, indicating the positions of other satellites. After presenting the ephemeris, services and almanac parameters, it is time to delve into time parameters and clock correction. This is necessary to calculate the so-called pseudorange. Then the equations used to find the position of the satellite would be presented.

2.1 Pseudorange of the ideal model

The relative pseudorange is the distance (or time) between the two reference points. There is no absolute reference to time in the GNSS system. The only reference to time is the sampling frequency and the clock deviation of the receiver [6-8].

To determine its position, the receiver determines the distances from at least four satellites, as well as their positions at the time of broadcasting. Knowing the orbital parameters of the satellites, these positions can be calculated for any point in time. The pseudorange of each satellite is obtained by multiplying the speed of light by the time the signal traveled from the satellite to the receiver [9-11]. The ideal case for calculating the pseudorange is when there are no errors with the transmitter and receiver clock, ionosphere, troposphere or receiver noise. This case is calculated according to:

$$R_i(t_T,t_R) = |r_{si}(t_{Ti}) - r_R(t_R)| = \\ = \sqrt{(x_{si}-x_R)^2+(y_{si}-y_R)^2+(z_{si}-z_R)^2}, \quad (1)$$

where: $R_i(t_T,t_R)$ - the distance between the transmitter and the receiver, t_R - the moment of time when the received signal arrives at the receiver, t_{Ti} - the moment of time when the signal is sent by satellite i.

One can also define the delay associated with the satellite i, marked τ_i and written as:

$$R_i(t_T,t_R) = |r_{si}(t_{Ti}) - r_R(t_R)|\tau_i = \\ = \frac{R_i(t_T,t_R)}{c} = t_R - t_{Ti}. \quad (2)$$

At least 3 satellites are required to calculate position. A non-linear system of three equations with three unknowns must be solved.

2.2 Pseudorange of the non-ideal model

This is the real case where errors occur. The transmission time of the satellite i is:

$$t_{Ti} = t_{Ti}^{Galileo} + \Delta t_{Ti}, \quad (3)$$

where: Δt_{Ti} - satellite clock error.

The signals reach the receiver at the following moment, it can be written as:

$$t_R^{Galileo} = t_{Ti}^{Galileo} + \tau_i - \Delta t_1^{rel}, \quad (4)$$

where: Δt_i^{rel} - relativistic correction.

However, the moment measured by the receiver, taking into account the above Equation (4), can be presented in the following form:

$$t_R = t_R^{Galileo} + \Delta t_R + \Delta t_n = t_{Ti}^{Galileo} + \tau_i - \Delta t_i^{rel} + \\ + \Delta t_R + \Delta t_n, \quad (5)$$

where: Δt_R - receiver clock error, Δt_n - delay caused by the receiver measurement error due to the white noise. In contrast, the random variable has the same statistical properties for each satellite. Finally, taking into account Equation (3), the following form was obtained [12-14]:

$$t_R = t_{Ti} + \tau_i - (\Delta t_{Ti} + \Delta t_i^{rel}) + \Delta t_R + \Delta t_n. \quad (6)$$

It should be noted that Δt_R is common to all satellites. The delay τ_i is obtained by the sum of the geometric τ_i^{geo}, ionospheric Δt_i^{ion} and tropospheric Δt_i^{trop} delays, as shown in the following form:

$$\tau_i = \tau_i^{geo} + \Delta t_i^{ion} + t_i^{trop}. \quad (7)$$

The total delay between transmitter and receiver is:

$$\tau_i^{tot} = t_{Ri} - t_{Ti} = \tau_i - (\Delta t_{Ti} + \Delta t_i^{rel}) + \Delta t_R + \Delta t_n. \quad (8)$$

Replacing τ_i by Equation (7), the following form was obtained:

$$\tau_i^{tot} = \tau_i^{geo} + \Delta t_i^{ion} + \Delta t_i^{trop} - (\Delta t_{Ti} + \Delta t_i^{rel}) + \\ + \Delta t_R + \Delta t_n. \quad (9)$$

After calculating the total delay, it is possible to obtain a pseudorange by multiplying it by the speed of light c, resulting in [15-17]:

$$\rho_i = c\tau_i^{tot} = R_i + c\Delta t_i^{ion} + c\Delta t_i^{trop} - \\ - c(\Delta t_{Ti} + \Delta t_i^{rel}) + c\Delta t_R + c\Delta t_n. \quad (10)$$

where: R_i - the geometric distance and as already shown in Equation (1) of the ideal model, the geometric distance is calculated as follows:

$$R_i = R_i(t_{Ti}^{Galileo}, t_R^{Galileo}) = \left| r_{si}(t_{Ti}^{Galileo}) - r_R(t_R^{Galileo}) \right|, \quad (11)$$

$$R_i(t_{Ti}^{Gal}, t_R^{Gal}) = \sqrt{\begin{matrix}[x_{si}(t_{Ti}^{Gal}) - x_r(t_R^{Gal})]^2 + \\ +[y_{si}(t_{Ti}^{Gal}) - y_r(t_R^{Gal})]^2 + \\ +[z_{si}(t_{Ti}^{Gal}) - z_r(t_R^{Gal})]^2\end{matrix}}. \quad (12)$$

It should be noted that both the parameter Δt_R from Equation (10) and the parameter r_R from Equation (11) do not depend on the position of the satellites. The parameter Δt_R, i.e. the receiver clock error, is not known, so it can be treated as another unknown. Hence, four satellites are necessary to determine coordinates of the receiver and its clock error.

3 Linearization

To solve the obtained system of equations, it should be taken into account that it is non-linear. It should be linearized, assuming that the approximate position and

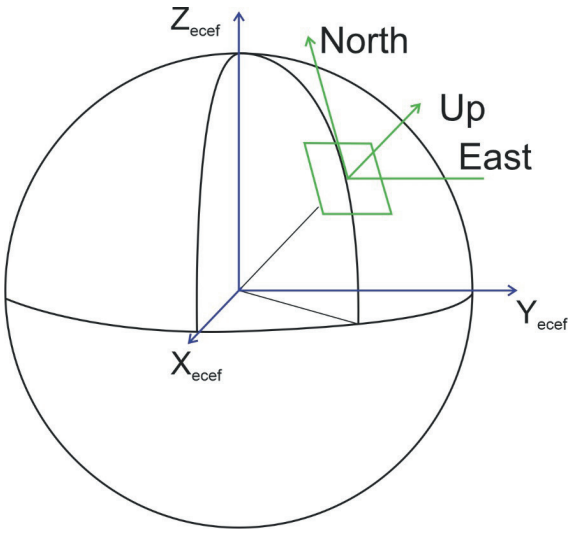


Figure 1 *Coordinate system used in the mathematical description*

approximate clock error are known. The pseudorange is derived from the following formula [18-20]:

$$\delta\rho_i = \frac{\delta\rho_i}{\delta x_R}\delta x_R + \frac{\delta\rho_i}{\delta y_R}\delta y_R + \frac{\delta\rho_i}{\delta z_R}\delta z_R + \frac{\delta\rho_i}{\delta w_R}\delta w_R \,, \quad (13)$$

where: $w_R = c\Delta t_R$.

In turn, partial derivatives can be written in the following forms:

$$\frac{\delta\rho_i}{\delta x_R} = \frac{-x_{S_i} - x_R}{R_i}, \quad (14)$$

$$\frac{\delta\rho_i}{\delta y_R} = \frac{-y_{S_i} - y_R}{R_i}, \quad (15)$$

$$\frac{\delta\rho_i}{\delta z_R} = \frac{-z_{S_i} - z_R}{R_i}, \quad (16)$$

$$\frac{\delta\rho_i}{\delta w_R} = 1. \quad (17)$$

Then it is defined as:

$$\delta_p = [\delta x_R \delta y_R \delta z_R \delta w_R]^T; \delta_p = [\delta\rho_1 \delta\rho_2 .. \delta\rho_K]^T, \quad (18)$$

$$A = \begin{pmatrix} a_{11} & a_{12} & a_{13} & 1 \\ a_{21} & a_{22} & a_{23} & 1 \\ .. & .. & .. & 1 \\ a_{K1} & a_{K2} & a_{K3} & 1 \end{pmatrix}, \quad (19)$$

where:
$a_{i1} = \frac{-x_{s_i} - x_R}{R_i}, a_{i2} = \frac{-y_{s_i} - y_R}{R_i}, a_{i3} = \frac{-z_{s_i} - z_R}{R_i}$
and $p = [x_R y_R z_R w_R]^T$ - specifies the extended vector with receiver error.

It can therefore be written in the following form:

$$\delta\rho = A\delta p. \quad (20)$$

The position of the receiver can be calculated iteratively. Regardless of whether an approximate extended position vector is available at the moment, the estimation can be improved as follows:

$$p^{(k)} = p^{(k-1)} + \delta p^{(k)}, \quad (21)$$

where: $\delta p^{(k)}$ - solution of the linear system.

However, due to the fact that it is possible to use more equations than unknown quantities, the solution will be the so-called the least squares method [21-23]:

$$\delta p^{(k)} = (A^{(k-1)T} A^{(k-1)})^{-1} A^{(k-1)T} \delta\rho^{(k-1)}, \quad (22)$$

where: $\delta\rho^{(k)} = \hat{\rho} - \rho^k$.

This process will continue until the condition is met $\delta p < 10^{-12}$.

3.1 Calculation of the satellite position

To obtain the position of the satellite in the Earth-related coordinate system ECEF (Earth-Centered Earth-Fixed), the issues considered in this section use all information obtained from ephemeris data.

The calculated average movement n_0, is the average angular velocity of the satellite:

$$n_0 = \frac{2\pi}{T} = \sqrt{\frac{\mu}{A^s}}, \quad (23)$$

where: μ - geocentric gravitational constant, A - semi-major -axis.

After obtaining the average movement in $\left[\frac{rad}{s}\right]$, the corrected average movement can be calculated [24-26]:

$$n = n_0 + \Delta n, \quad (24)$$

where: Δn - average movement difference from the calculated value.

The actual total time difference between time t and epoch t_{0_s} is t_k, which can be determined by the following:

$$t_k = t - t_{0s}, \tag{25}$$

where: t - is the Galileo system time.

The average anomaly can be determined from the following:

$$M = M_0 + nt_k, \tag{26}$$

where: M_0 - mean anomaly at reference time.

The Kepler equation for the eccentric E anomaly (can be solved by iteration) is defined as:

$$M = E - e\sin(E), \tag{27}$$

where: e - eccentricity.

The condition of relativistic correction can be obtained by:

$$\Delta t_r = FeA^{\frac{1}{2}}\sin(E), \tag{28}$$

where: $F = -2\mu^{\frac{1}{2}}/c^2$ - constant.

The satellite time correction (in seconds) is modeled by the following second order polynomial that defines parabola according to the following equation [27-29]:

$$\begin{aligned}\Delta t_{SV}(X) &= a_{f0} + a_{f1}(X)[t - t_{0C}(X)] + \\ &+ a_{f2}(X)[t - t_{0C}(X)]^2 + \Delta t_r,\end{aligned} \tag{29}$$

where: a_{f0}, a_{f1}, a_{f2} - SV *(Space Vehicle)* clock correction coefficients, t_{0C} - clock correction related to *Time of Week*, $(X) = (f_1, f_2)$ - frequency combination f_1 and f_1 used in the clock model.

The true anomaly is defined as:

$$\begin{aligned}v &= \tan^{-1}\left\{\frac{\sin(v)}{\cos(v)}\right\} = \tan^{-1}\times \\ &\times\left\{\frac{\sqrt{1-e^2}\sin(E)/(1-e\cos(E))}{(\cos(E)-e)/(1-e\cos(E))}\right\}.\end{aligned} \tag{30}$$

The argument of latitude can be determined from the formula:

$$u = v + \omega. \tag{31}$$

The argument of latitude correction is calculated as follows:

$$\delta u = C_{us}\sin(2\Phi) + C_{uc}\cos(2\Phi). \tag{32}$$

The radius vector correction is determined from the following formula:

$$\delta r = C_{rs}\sin(2\Phi) + C_{rc}\cos(2\Phi). \tag{33}$$

However, the inclination correction is determined from the following equation:

$$\delta i = C_{is}\sin(2\Phi) + C_{ic}\cos(2\Phi). \tag{34}$$

The anomaly at epoch t is the sum of the argument of latitude and its correction:

$$u = \Phi + \delta u. \tag{35}$$

The corrected radius vector is calculated from the formula:

$$r = A(1 - e\cos(E)) + \delta r. \tag{36}$$

In contrast, improved inclination is:

$$i = i_0 + \delta i + \left(\dot{i}\right)t_k. \tag{37}$$

Then the position in the orbital plane can calculated as follows:

$$x' = r\cos u, y' = r\sin u. \tag{38}$$

The right-ascension of the ascending node Ω is calculated as follows according to equation [30-32]:

$$\Omega = \Omega_0 + \left(\dot{\Omega}\right)t_k. \tag{39}$$

However, this result is obtained for the geocentric inertial coordinate system ECIS (Earth-Centered Inertial System). After receiving Ω, the next step to get the result in the ECEF system is:

$$\Omega = \Omega - \omega_E t_k - \omega_E t_{0s}, \tag{40}$$

where: ω_E - average angular velocity of the Earth.

Finally, to find the satellite position, the following form was obtained:

$$\begin{pmatrix} x \\ y \\ z \end{pmatrix} = \begin{pmatrix} x'\cos(\Omega) - y'\sin(\Omega)\cos(i) \\ x'\sin(\Omega) + y'\cos(\Omega)\cos(i) \\ y'\sin(i) \end{pmatrix}. \tag{41}$$

3.2 BOC modulation

The Galileo system signals are modulated using a new technique called BOC (Binary Offset Carrier) modulation. The BOC modulation was designed to modernize the GPS and Galileo systems to facilitate addition of other signals that have the same carrier frequency in the radio frequency bands, without interfering with other signals.

Advantages of the BOC modulation are: improvement of traditional GNSS system signal properties for better resistance to multi-path and interference with various types of noise and ensuring the spectral isolation between signals with the same carrier frequency.

The BOC modulated signal consists of a sinusoidal carrier, a rectangular subcarrier (*BOC*sin and *BOC*cos), a pseudo-random PRN code (Pseudorandom Noise) and a data sequence. The signal is presented as BOC

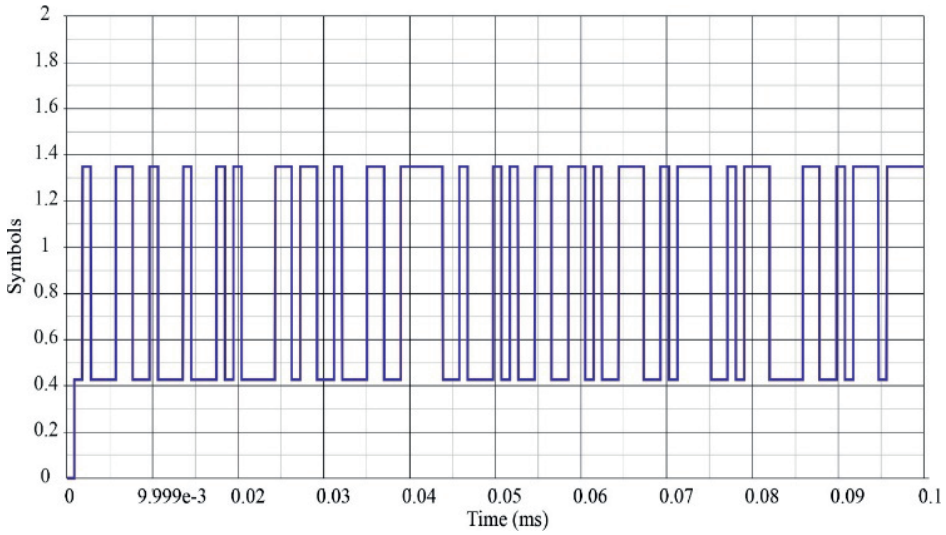


Figure 2 *CBOC subcarrier of B channel with BOC (1.1) and BOC (6.1)*

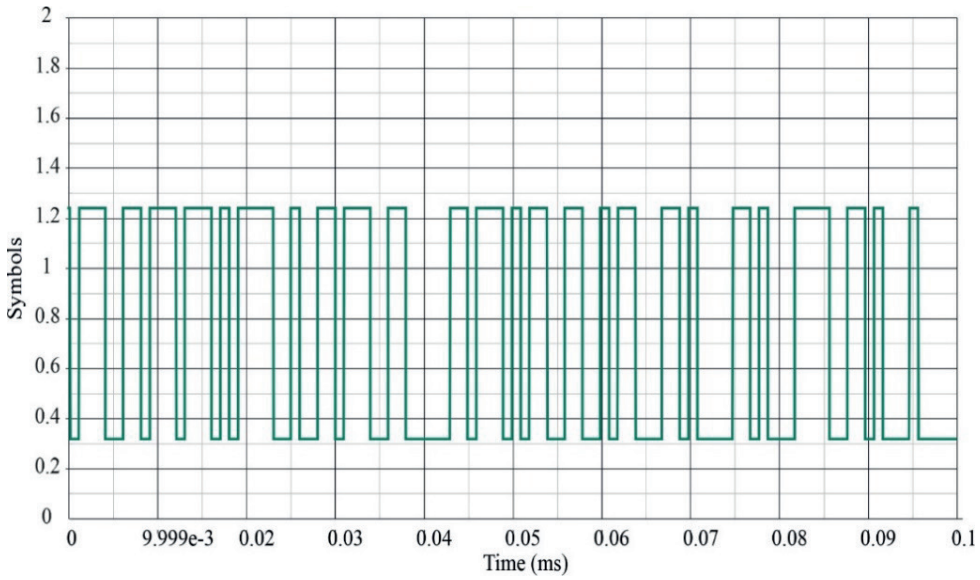


Figure 3 *CBOC subcarrier of C channel with BOC (1.1) and BOC (6.1)*

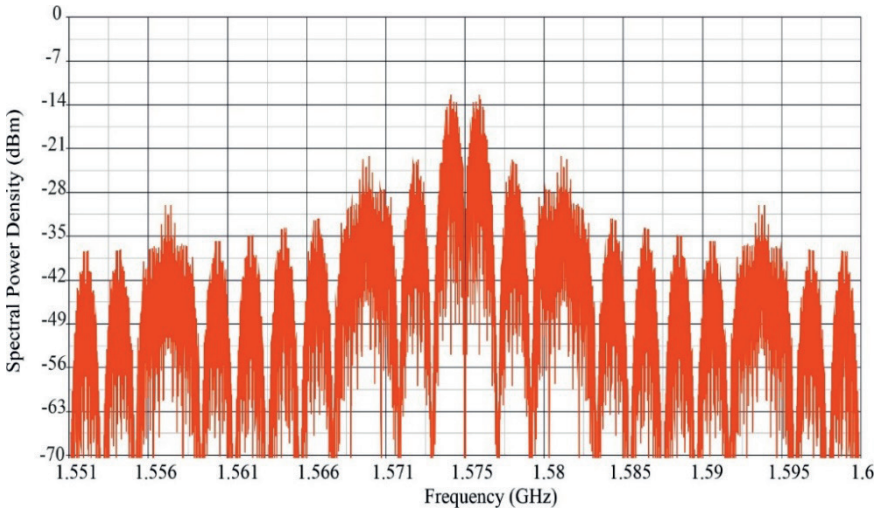


Figure 4 *Spectral power density of E1 signal for the CBOC modulation (1.6)*

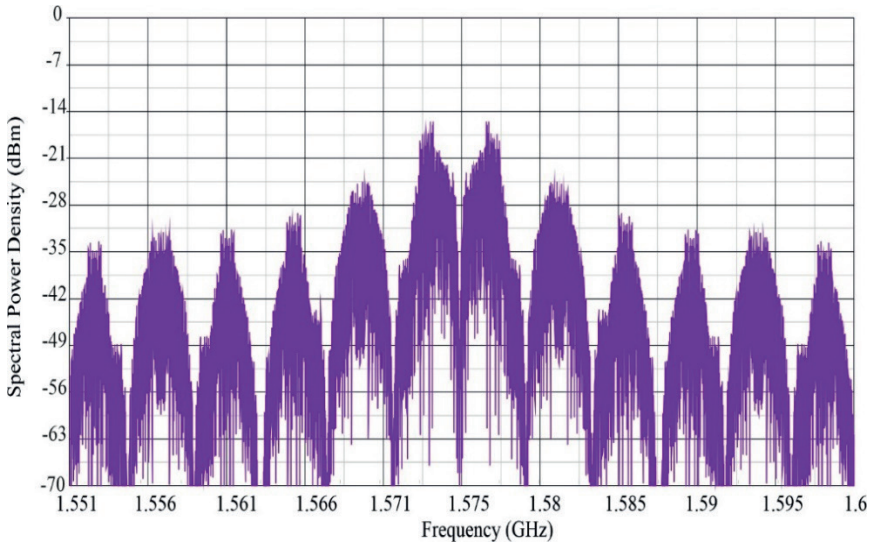


Figure 5 *Spectral power density of E1 signal for the CBOC modulation (6.2)*

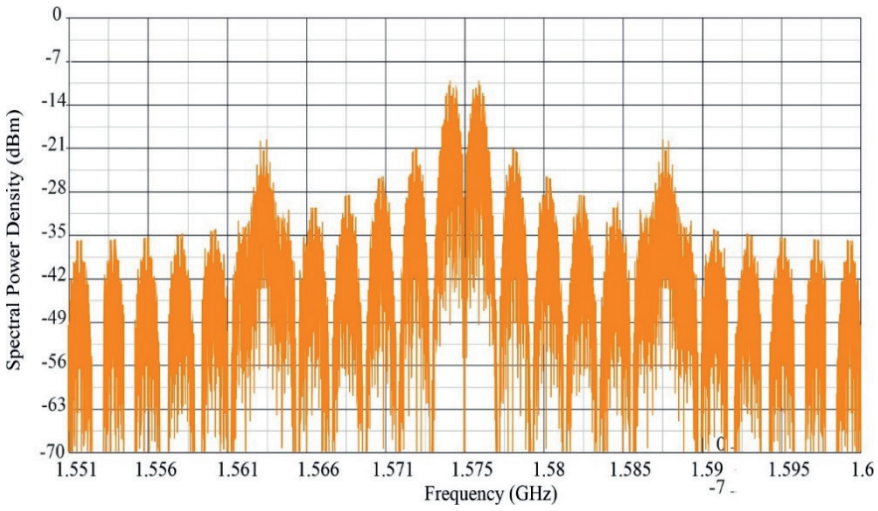


Figure 6 *Spectral power density of E1 signal for the CBOC modulation (12.1)*

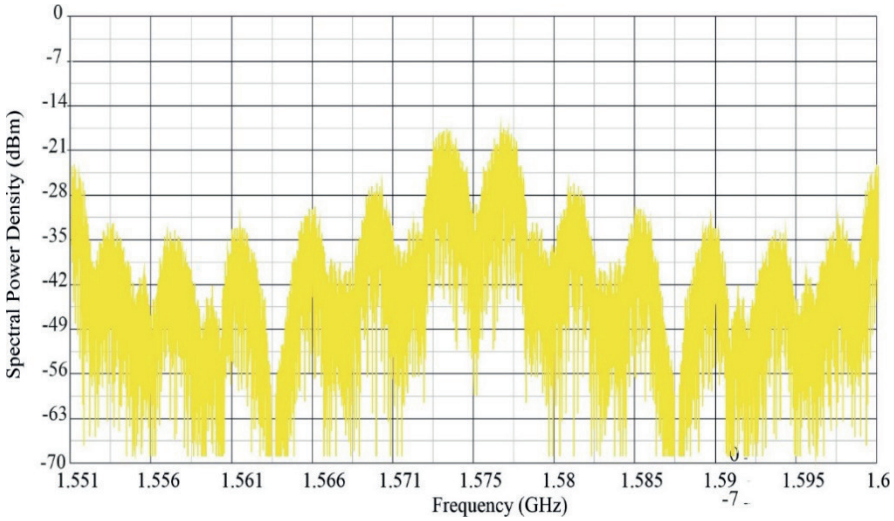


Figure 7 *Spectral power density of E1 signal for the CBOC modulation (2.20)*

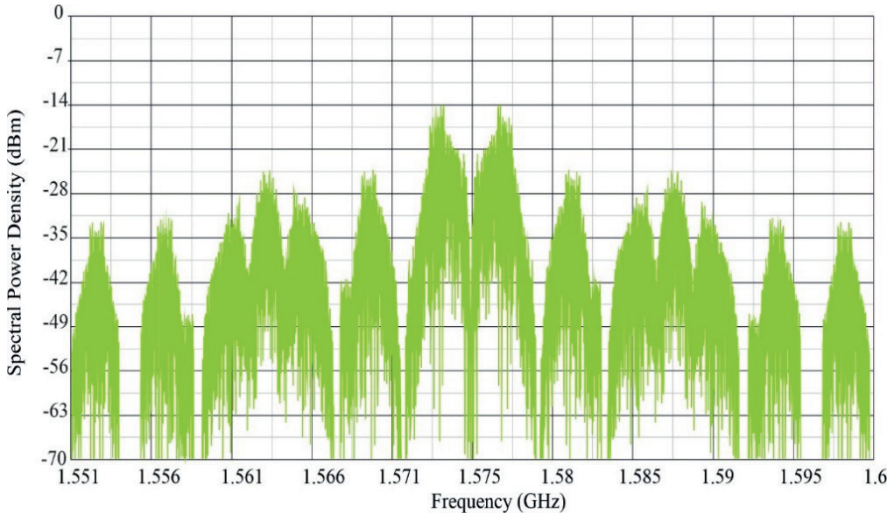


Figure 8 *Spectral power density of E1 signal for the CBOC modulation (2.12)*

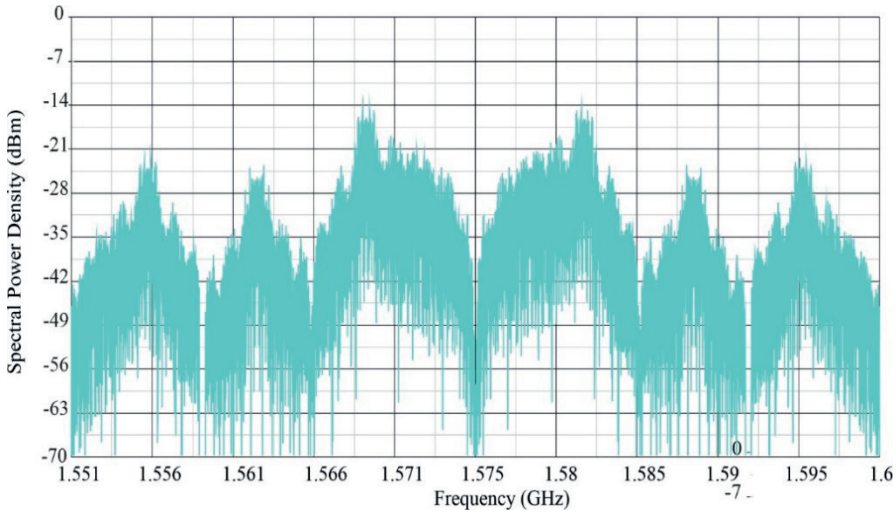


Figure 9 *Spectral power density of E1 signal for the CBOC modulation (6.12)*

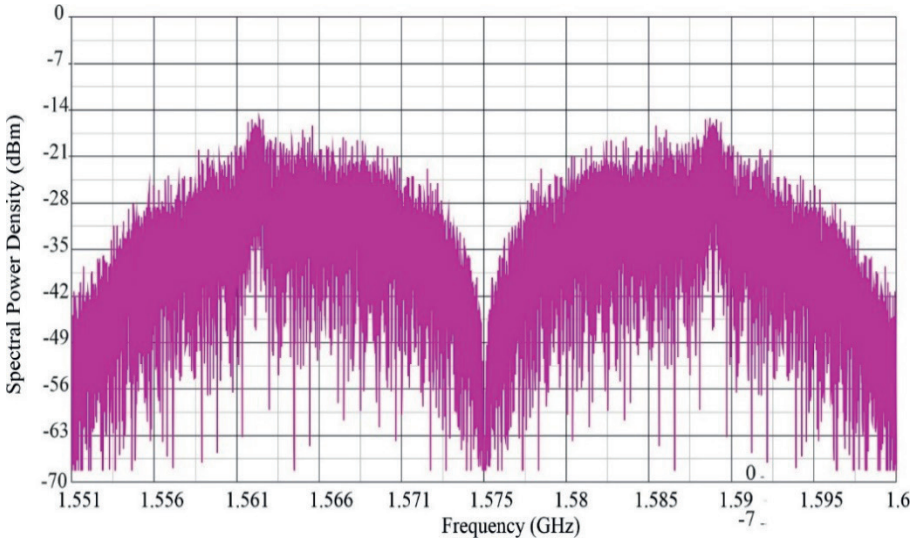


Figure 10 *Spectral power density of E1 signal for the CBOC modulation (12.12)*

(*m,n*). Two independent parameters *m* and *n* are used to concentrate the signal strength in specific parts of the spectrum to reduce interference with other signals [33-34].

Parameters *m* and *n* are defined as follows:

$$m = \frac{F_s}{F_0}, n = \frac{F_c}{F_0}, \tag{42}$$

where: F_s - defines the subcarrier frequency in [MHz], F_c - means transmission speed in [Mcps], F_0 - reference frequency F_0 = 1.023 [MHz] which is generated by the atomic clock on satellites.

4 Selected tests for the BOC modulation

Channels *B* and *C* are modulated by „Composite BOC" modulation (CBOC (6.1, 1/11)). CBOC modulation combines BOC (1.1) and BOC (6.1).

The CBOC modulation results from the multiplexing of the narrowband BOC signal (1.1), whose subcarrier frequency is 1.023 [MHz] and the transmission speed 1.023 [Mcps], with the wideband BOC signal (6.1), with the subcarrier frequency 6.138 [MHz] and the transmission speed 1.023 [Mcps].

The normalized CBOC power spectral density (6.1, 1/11) is obtained according to equation:

$$G_{CBOC}\left(6.1\frac{1}{11}\right)(f) = \frac{10}{11}G_{BOC}(1.1) + \\ + G_{BOC}(6.1)(f), \tag{43}$$

where: $G_{CBOC(m,n)}(f)$ - PSD (Packet-Switched Data) unit of BOC sinusoidal modulation.

Thus 1/11 of the power is allocated on the high frequency channel (BOC (6.1)). CBOC modulation for B and C channels can be illustrated by the following equations:

$$scB(t) = \alpha sc(t)_{BOC(1.1)} + \beta sc(t)_{BOC(6.1)}, \tag{44}$$

$$scC(t) = \alpha sc(t)_{BOC(1.1)} + \beta sc(t)_{BOC(6.1)}, \tag{45}$$

where: $\alpha = \sqrt{\frac{1}{10}}$ and $\beta = \sqrt{\frac{10}{11}}$.

Figures 2 and 3 show the generated CBOC subcarriers for $scB(t)$ and $scC(t)$ using the Matlab/Simulink environment.

Equations (46) and (47) identify *BOC*sin and *BOC*cos respectively:

$$BOC\sin: sc(t) = sign(\sin(2\pi Fst)), \tag{46}$$

$$BOC\cos: sc(t) = sign(\cos(2\pi Fst)), \tag{47}$$

where: F_s - subcarrier frequency.

It should be noted that the BOC modulation divides the spectrum into two main symmetrical layers focused on $\pm f_s$ [MHz] (subcarrier frequency) around the carrier frequency. The generated PSD from the SE1 signal is shown in Figures 4-10.

Figures 4-10, illustrate the signal spectra modulated by the composite CBOC method (*n,m*), differing in the occurrence of the main leaves representing the main band in which the transmission of the Galileo system radio signals is carried out and the shift, causing the use of additional band for other signal transmissions or services.

The above process is possible both by changing the transmission speed of the carrier wave *n* and the transmission speed of *m* chips. Based on the analysis of the spectra of the signal modulated on individual waveforms, it can be observed how the process of extending, adding a new band or its shift takes place for different values of *n* and *m*.

Especially valuable in this context is the signal power spectral density analysis E1 for the CBOC modulation (6.12) as shown in Figure 9, considering a candidate/pretender signal providing a wide frequency band E5a/E5b for the transmission of Galileo navigation signals.

It should be noted that the CBOC (6.12) signal is very interesting from the point of practical use because it provides spectral isolation between the two upper and lower bands of the same navigation signal. In this way it is possible to track each element separately or together.

5 Conclusions

The Power Spectral Density (PSD) for different types of BOC signal is shown. The analysis was carried out in this aspect comparing the BOC and CBOC modulations and then the method of generating the BOC signals was considered. In addition, the necessary tests and simulations of the process of generating CBOC (1.3), CBOC (12.1), CBOC (6.12) and CBOC (12.12) signals modulated with both sine and cosine subcarriers were performed using the Matlab/Simulink programming environment. The simulation tests were successful. Signal waveforms have been generated for channel *B* navigation data, *B* and *C* channel dispersing sequences and modulated *B* and *C* subcarrier channels.

The rectangular waveform of channel *C* dispersing sequence with primary and secondary code has a longer period than the dispersing sequence of channel *B* with only the basic code. The waveforms of modulated *B* and *C* subcarrier channels are essentially no different (Figures 1-2).

In general, graphical programming languages facilitate system design since they clearly define the relationship between the system modeling, simulation system and system implementation [35-36]. Since the Galileo system is still being developed and its improvements are expected, the *E*1 signal simulation shown in this work may contribute to facilitating the redesign of the transmitter and receiver.

In addition, the simulation model may have educational purposes due to the transparency of the design and algorithm simulation. The introduced model may also facilitate system implementation. Implementation tools available in the Matlab/Simulink module, such as „Code Composer Studio", can be used at the implementation stage.

On the other hand, since the transmitter design of most GNSS systems is similar, the simulation models introduced in this work can be used in design of the transmitter simulator, which will have a direct positive impact on the testing stages and checking the receiver.

References

[1] BONE, K., AKOS, D. *A Software-defined GPS and Galileo receiver; a single-frequency approach*. New York: Birkhauser. 2007. ISBN 978-0-8176-4390-4.

[2] GODET, J. Technical annex to Galileo SRD signal plans. STF annex SRD 2001/2003. Draft 1. July 2003.

[3] European Union. European GNSS (Galileo) open service signal. In: Space interface document. OS SIS ICD, Vol. 3, Issue 1, 2016.

[4] DE GAUDENZI, R., HOULT, N., BATCHELOR, A., BURDEN, G., QUINLAN, M. *Galileo signal validation development*. John Wiley & Sons, Ltd., 2000.

[5] AVILA-RODRIGUEZ, J.-A., PANY, T., HEIN, G. W. Bounds on signal performance regarding multipath-estimating discriminators. In: International Technical Meeting of the Institute of Navigation ION-GNSS 2006: proceedings. 2006.

[6] AVILA-RODRIGUEZ, J.-A., HEIN, G. W., WALLNER, S., SCHUELER, T., SCHUELER, E., IRSIGLER, M. Revised combined Galileo/GPS frequency and signal performance analysis. In: International Technical Meeting of the Institute of Navigation ION-GNSS 2005: proceedings. 2005.

[7] BAO-YEN TSUI, J. *Fundamentals of Global Positioning System receivers: A software approach*. 2. ed. John Wiley & Sons, 2005. ISBN 0-471-38154-3.

[8] European Space Agency / European GNSS Supervisory Authority, Galileo Open Service - Signal in Space Interface Control Document. OS SIS ICD, Issue 1.1, September 2010.

[9] HEIN, G. W., AVILA-RODRIGUEZ, J. A., WALLNER, S. The Galileo code and others. *Inside GNSS*. 2006, p. 62-74. ISSN 2329-2970.

[10] GRZEGORZEWSKI, M. Results of a research predicting the position of an aircraft during approach and landing using the bessel function. *Journal of Theoretical and Applied Mechanics* [online]. 2013, **51**(4), p. 915-926. ISSN 1429-2955.

[11] SETLAK, L., KOWALIK, R. Analysis, mathematical model and simulation tests of the unmanned aerial vehicle control system. *ITM Web of Conferences* [online]. 2019, **24**, 01005. eISSN 2271-2097. Available from: https://doi.org/10.1051/itmconf/20192401005

[12] KAPLAN, E. D. *Understanding GPS principles and applications*. 1. Ed. Artech-House Publishers, 1996. ISBN 9780890067932.

[13] FERNANDEZ-PRADES, C., AVILES, C., ESTEVE, L., ARRIBAS, J., CLOSAS, P. An open source galileo E1 software receiver. In: 6th ESA workshop on Satellite Navigation Technologies and European GNSS Signals and Signal Processing NAVITEC: proceeding, ESTEC, 2012.

[14] AVILA-RODRIGUEZ, J.-A. On optimized signal waveforms for GNSS. Ph.D. thesis. Neubiberg, Germany: University FAF Munich, 2007.

[15] DE LATOUR, A. Code tracking performance of PRS and M-code signals. In: 1st CNES workshop on Galileo signals: proceedings. 2006.

[16] WALLNER, S., AVILA-RODRIGUEZ, J.-A., HEIN, G. W., RUSHANAN, J. J. Galileo E1 OS and GPS L1C pseudo random noise codes - requirements, generation, optimization and comparison. In: International Technical Meeting of the Institute of Navigation ION-GNSS 2006: proceedings. 2006.

[17] RIES, L., LESTARQUIT, L., ISSLER, J-L., PRATT, A. R., HEIN, G., GODET, J., DONDL, P., COUTURIER, F., ERHARD, P., OWEN, J. I. R., LUCAS-RODRIGUEZ, R., MARTIN, J.-C. New investigations on wide band GNSS2 signals. In: European Navigation Conference GNSS: proceedings. 2003.

[18] SETLAK, L., KOWALIK, R., SMOLAK, M. Doppler delay in navigation signals received by GNSS receivers. In: WSEAS Transactions on Applied and Theoretical Mechanics, 3rd International Conference on Applied Physics, System Science and Computers APSAC 2018: proceedings. 2018. Lecture Notes in Electrical Engineering. Vol. 574, p. 3-8.

[19] IRSIGLER, M., AVILA-RODRIGUEZ, J.-A., HEIN, G. W. Criteria for GNSS multipath performance assessment. In: 18th International Technical Meeting of the Satellite Division of the Institute of Navigation ION GNSS 2005: proceedings. 2005.

Dear colleague,

Journal Communications - Scientific Letters of the University of Zilina are a well-established open-access scientific journal aimed primarily at the topics connected with the field of transport. The main transport-related areas covered include Civil engineering, Electrical engineering, Management and informatics, Mechanical engineering, Operation and economics, Safety and security, Travel and tourism studies. The full list of main topics and subtopics is available at: *http://komunikacie.uniza.sk/index.php/communications/topics*

Journal Communications - Scientific Letters of the University of Zilina are currently indexed by EBSCO and SCOPUS.

We would like to invite authors to submit their papers for consideration. We have an open-access policy and there are no publication, processing or other fees charged for published papers. Our journal operates a standard double-blind review procedure, the successful completion of which is a prerequisite for paper publication.

The journal is issued four times a year (in January, in April, in July and in October).

I would also like to offer you the opportunity of using already published articles from past issues as source of information for your research and publication activities. All papers are available at our webpage: *http://komunikacie.uniza.sk*, where you can browse through the individual volumes.

For any questions regarding the journal Communications - Scientific Letters of the University of Zilina please contact us at: *komunikacie@uniza.sk*

We look forward to future cooperation.

Sincerely

Branislav Hadzima
editor-in-chief

[20] HEIN, G. W., GODET, J., ISSLER, J.-L., MARTIN, J.-C., LUCAS-RODRIGUEZ, R., PRATT, T. The Galileo frequency structure and signal design. In: International Technical Meeting of the Institute of Navigation ION-GNSS 2001: proceedings. 2001.

[21] HEIN, G. W., GODET, J., ISSLER, J.-L., MARTIN, J.-C. ERHARD, P., LUCAS-RODRIGUEZ, R., PRATT, A. R. Status of Galileo frequency and signal design. In: ION GPS 2002: proceedings. 2002.

[22] ISSLER, J.-L., RIES, L., BOURGEADE, J.-M., LESTARQUIT, L., MACABIAU, C. Contribution of AltBOC to interference mitigation for civil aviation. In: 1st CNES Workshop on Galileo Signals: proceedings. 2006.

[23] IRSIGLER, M., HEIN, G. W., SCHMITZ-PEIFFER, A. Use of C-band frequencies for satellite navigation: benefits and drawbacks. *GPS Solutions* [online]. 2004. **8**(3), p. 119-139. ISSN 1080-5370, eISSN 1521-1886. Available from: https://doi.org/10.1007/s10291-004-0098-2.

[24] BORRE, K. The Galileo signals with emphasis on LI OS. In: Power Electronics and Motion Control Conference: proceedings. 2006.

[25] PEDROS, R. C., O'DROMA, M. Galileo signal generation simulation analysis. Limerick: Department of Computer and Electronic Engineering. University of Limerick, 2009.

[26] SETLAK, L., KOWALIK, R. Examination of the unmanned aerial vehicle. *ITM Web of Conferences* [online]. 2019, **24**, 01006. eISSN 2271-2097. Available from: https://doi.org/10.1051/itmconf/20192401006

[27] GAO, X. G., SPILKER, J., WALTER, T., ENGE, P., PRATT, A. R. Code generation scheme and property analysis of broadcast Galileo L1 and E6 signals. In: 19th International Technical Meeting of the Satellite Division ION GNSS 2006: proceedings, 2006.

[28] GAO, G., LORENZO, D., CHEN, D., LO, S., AKOS, D., WALTER, T., ENGE, P. Galileo GIOVE - a broadcast E5 codes and their application to acquisition and tracking. Stanford University. 2007, p. 1-11.

[29] HEIN, G. W., AVILA-RODRIGUEZ, J.-A., WALLNER, S., PRATT, A. R., OWEN, J., ISSLER, J., BETZ, J. W., HEGARTY, C. J., LENAHAN, S., RUSHANAN, J. J., KRAAY, A. L., STANSELL, T. A. MBOC: the new optimized spreading modulation recommended for Galileo L1 OS and GPS L1C. In: 2006 IEEE/ION Position, Location and Navigation Symposium: proceedings. 2006. ISBN 0-7803-9454-2. Available from: https://doi.org/10.1109/PLANS.2006.1650688.

[30] SETLAK, L., KOWALIK, R. Analysis, mathematical model and selected simulation research of the GNSS navigation receiver correlator. *MATEC Web of Conferences* [online]. 2018, **210**, p. 1-11. eISSN 2261-236X. Available from: https://doi.org/10.1051/matecconf/201821005008

[31] AVILA-RODRIGUEZ, J.-A., HEIN, G. W., WALLNER, S., ISSLER, J.-L., RIES, L., LESTARQUIT, L., DE LATOUR, A., GODET, J., BASTIDE, F., PRATT, T., OWEN, J. The MBOC modulation: the final touch to the Galileo frequency and signal plan. *Navigation* [online]. 2008, **55**(1). ISSN 0028-1522. Available from: https://doi.org/10.1002/j.2161-4296.2008.tb00415.x.

[32] JULIEN, O., MACABIAU, C., ISSLER, J.-L., RIES, L. 1-bit processing of composite BOC (CBOC) signals. In: ESA-CNES Workshop on GNSS Signals: GNSS Signal 2007: proceedings. 2007.

[33] PRATT, A. R., OWEN, J. I. R. Performance of GPS Galileo receivers using m-PSK BOC signals. In: International Technical Meeting of the Institute of Navigation ION-GNSS 2003: proceedings. 2003.

[34] REBEYROL, E., MACABIAU, CH., LESTARQUIT, L., RIES, L., ISSLER, J.-L., BOUCHERET, M. L., BOUSQUET, M. BOC power spectrum densities. In: National Technical Meeting of the Institute of Navigation ION-NTM 2005: proceedings. 2005.

[35] SETLAK, L., KOWALIK, R. Examination of multi-pulse rectifiers of PES systems used on airplanes compliant with the concept of electrified aircraft. *Applied Sciences* [online]. 2019, **9**(8), 1520. Available from: https://doi.org/10.3390/app9081520

[36] SOELLNER, M., ERHARD, P. Comparison of AWGN code tracking accuracy for alternative-BOC, complex-LOC and complex-BOC modulation options in Galileo E5-band. In: European Navigation Conference ENC-GNSS 2003: proceedings. 2003.

STUDY ON A BRAIN-CONTROLLED PNEUMATIC ACTUATOR TO ASSIST EMERGENCY BRAKING OF A VEHICLE

Ryszard Dindorf*, Jakub Takosoglu, Piotr Wos

Department of Manufacturing Engineering and Metrology, Faculty of Mechatronics and Mechanical Engineering, Kielce University of Technology, Kielce, Poland

*E-mail of corresponding author: dindorf@tu.kielce.pl

Resume

This article deals with the issue of safety within the road freight transport sector with regards to the securing of cargo on a vehicle. The first part of the article focuses on the legal framework that regulates this issue in the Czech Republic. The second part is based on a case study and survey conducted among drivers of the road freight transport vehicles into their awareness of what they understand is meant by securing and secure cargo. The case study was carried out in a specific transport company and includes an analysis of the current situation and concrete measures for improving safety while securing timber for transport.

Article info

Received 17 September 2020
Accepted 6 November 2020
Online 18 March 2021

Keywords:

road freight transport,
lashing and securing cargo,
safety,
case study

Available online: https://doi.org/10.26552/com.C.2021.3.F49-F57

ISSN 1335-4205 (print version)
ISSN 2585-7878 (online version)

This is an open access article distributed under the terms of the Creative Commons Attribution 4.0 International License (CC BY 4.0), which permits use, distribution, and reproduction in any medium, provided the original publication is properly cited. No use, distribution or reproduction is permitted which does not comply with these terms.

1 Introduction

Automotive manufacturers are currently trying to implement autonomous driving (ADV) technology. Along with the progress of innovative technology, new cases of using the ADV in means of transport will appear, which largely depend on the type of a vehicle and their location. According to press reports, the final ADV implementation plan is a car without a driver. However, in autonomous vehicles, various human intentions are incorrectly recognized. The human brain provides a lot of information about the driver's cognitive and emotional states that are associated with various road events [1]. Developing a brain-computer interface (BCI) strategy and automatic driving can bring benefits to car traffic safety [2]. The purpose of various studies is to use the brain (mind) in vehicle control systems or their particular mechanisms. Particular solutions, such as a brain-controlled car for people with disabilities, are also being considered. In paper [3], was presented a car for a disabled person, in which read brain signals and controls the car accordingly. The limitations of the BCI lead to poor vehicle control by the driver's brain. To improve efficiency and safety of a brain-controlled car, a novel assistant controller designed by using the model predictive control method was proposed [4]. The brain-controlled vehicles can provide a way for people with disabilities to improve their mobility. These are revolutionary changes in a society in which the distinction between abled and disabled driver will vanish. The driver-vehicle interface (DVI), based on electroencephalogram (EEG) signals, translates these signals into driving-related commands [5]. Chinese engineers from Nankai University in Tianjin have developed a system that can read brain signals and control a car accordingly. In paper [6], it was considered to develop a brain-driven car that would be very helpful for people with physical disabilities. The car works on the asynchronous mechanism of artificial intelligence. Several papers [7-8] considered developing an EEG-based brain-controlled car, that could be used by people with physical disabilities. At the same time, various brain states that were the result of different patterns of neural interaction were taken into account. Brain patterns are characterised by different brain wave frequencies, e.g. beta waves between 12 and 30 Hz are associated with concentration while alpha waves between 8 and 12 Hz are associated with relaxation and a state of mental calm [9]. The contractions of muscles within the head are also associated with unique wave patterns and isolating these patterns is a way to detect the driver's emotional states [10]. The emotional state of the driver directly affects the reaction time during the emergency braking. Based on the literature data, the pressure force and the reaction time of an abled driver during the emergency braking were analysed [11]. Manning [12] registered a mean peak force of 750 N while braking and found no statistical difference

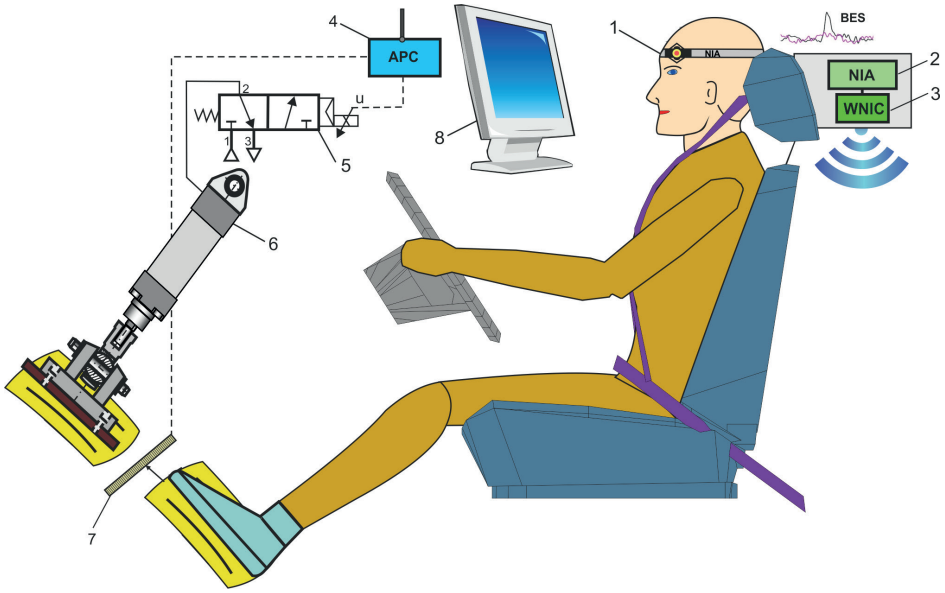


Figure 1 *Simulator for a pneumatically assisted emergency braking of a vehicle: 1 - headband with surface electrodes, 2 - neural impulse actuator (NIA), 3 - wireless network interface controller (WNIC), 4 - actuator position controller (APC), 5 - pneumatic control valve, 6 - pneumatic actuator assembly, 7 -sensor of a brake pedal deflection, 8 - monitor screen.*

between men and women. According to [13] average brake force in the emergency braking event was 796 N and the reaction time was 0.5 s. In the emergency braking event, the simulated average speed was 67 km/h. Furthermore, it was shown that in an emergency it is more common to push the brake pedal before using the clutch. It was also clearly stated that subjects who placed their foot higher up on the brake pedal produced a higher maximum brake force. People over the age of 50 produced maximum emergency braking force much more slowly than younger people. The papers [14-17] presents the results of research on the reaction time of drivers of motor vehicles in case of accident risk. These tests have been conducted on the driving simulator. The study in [18] aimed to determine how a driver's foot and ankle forces during a frontal vehicle collision depend on initial lower extremity posture and brake pedal force. Emergency Brake Assist (EBA) is a new technology being developed in vehicles [19]. The EBA, sometimes called Brake Assist (BA), detects danger and ensures as shortest braking distance as possible. Research conducted on the driving simulator revealed that more than 90% of drivers fail to brake with enough force when faced with an emergency. By interpreting the speed and force with which the brake pedal is pushed, the EBA system detects if the driver is trying to execute an emergency stop and if the brake pedal is not fully applied, the Anti-Lock Braking System (ABS) takes. Each car manufacturer has its own emergency braking system technology, but they all rely on some type of sensor input. Mostly speed with which a brake pedal is depressed. The EBA system is often combined with other brake systems like AEB, ESP and ABS.

The authors conducted a study on use of the bioelectric signals to control pneumatic systems [20]. This solution was used to safely control the pneumatic servo drives. The emergency stop of a pneumatic cylinder using “thoughts” was analysed. However, in paper [21] they presented a new design of a wearable orthosis of the elbow joint with a bi-muscular pneumatic servo-drive with control based on the recording of bioelectric signals. In this study, an innovative solution, involving use of the brain-controlled pneumatic cylinder to exert the pressure force on the foot brake pedal in the car, for a disabled driver during the emergency braking, was proposed. A pneumatic cylinder assembly has been adopted to exert the required pressure on the foot brake pedal. The pneumatic cylinder assembly is removable, so it can also be used for accurate and rapid testing procedures of brake systems, e.g. on car assembly lines. Further tests will be carried out in the real driving conditions. Then, the car will have additional equipment to ensure safe driving, such as obstacle detection and avoidance systems. If the developed braking assistance system becomes a cost-effective way and it will be possible to enable more functions. In the future, brain support for driving systems such as automatic navigation systems, automatic speed control mechanisms, traffic signals and signboard detection and automatic car starting mechanism will be analysed.

2 Simulator design solution

Simulator of authors' design solution for a pneumatically assisted emergency braking system of a vehicle, based on the driver's brain activity, is shown in Figure 1. The driver is seated in front of a monitor screen on which various road incidents affecting his emotional state are simulated. The neural impulse actuator (NIA), as a recording device, contains a headband with three surface electrodes, a control box and communication

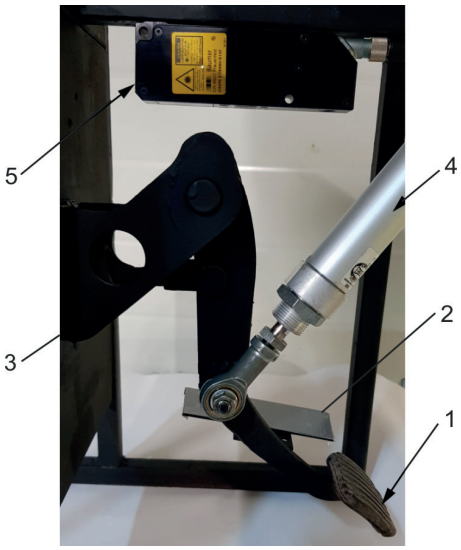


Figure 2 *View of the space of the dual foot brake pedals: 1 - primary foot brake pedal, 2 - secondary foot brake pedal, 3 - brake pedal mechanism, 4 - pneumatic actuator, 5 - laser sensor.*

software with a wireless network interface controller (WNIC). The NIA analyses bioelectric signals (BESs) induced by the driver brain activity, then decodes them into control signals sent by a WNIC to the actuator position controller (APC).

The NIA is a non-invasive device, which reads the BESs caused by the brain activity (as a result of brain waves, i.e. electroencephalogram signals (EEG) and by muscle tension inside the head (movement of the face and eyelids, clenching of jaws, pressing the tongue on the palate, etc. EMG - electromyography signals) [22]. The NIA device as a BCI improves the BESs to the form of control signals useful for controlling the pneumatic actuator. Effective control of the pneumatic control system with use of the NIA requires a snug fit of the sensors to readers of BESs, calibration of the device and training of the test participants (drivers). To test the use of biosignals and wireless communication in control of a pneumatically actuated foot brake pedal, a wireless network interface controller (WNIC) was built. A WNIC enables a high-fidelity control signal to be streamed to a Wi-Fi-connected device in real-time. The wireless communication does not distort the control signals and does not limit the movement of the driver while driving a car. The actuator position controller (APC) enables to control the movement of the pneumatic actuator by an electrical input signal task to a directional 3/2-way solenoid pilot operated valve. The 3/2 directional valve is always closed in the neutral position (NC normally closed), i.e. when the valve is not activated. Upon the electrical signal task, the valve opens and the actuator piston extends and presses on the secondary foot brake pedal (braking state). When the electric signal disappears, the cylinder piston retracts immediately (brake release state). The APC receives a feedback signal from the position transducer of the secondary brake pedal. The measuring system is designed to check the position of the brake foot pedal and protection against uncontrolled movement of the pneumatic actuator. The triangulation laser sensor, with an output signal in the range of 0-4.74 V, ensures the measurement of the pedal deflection up to 80 mm. Figure 2 shows the view of the dual foot brake pedals space in which a pneumatic actuator presses the foot brake pedal and the laser sensor measures the deflection of the brake pedal. The pressure force of the pneumatic cylinder on the secondary foot brake pedal is constant over the entire stroke range. In contrast, the primary foot brake pedal pressure, felt by the driver's foot, increases gradually but it will be significantly felt when the brake pedal reaches a height of 50% of the available deflection. Braking becomes effective only when the brake pedal deflection exceeds 60% of the available deflection,

2.1 Dual foot brake pedals

The dual control systems are installed in cars to ensure driving safety in special conditions. The dual control systems in the car relate especially to the auxiliary devices such as clutch pedals, brake pedals and acceleration pedals, which are located on the passenger side. Such dual control is installed mainly in driving schools, but it can also be useful for people who require checking while driving. The dual brake pedals themselves have been introduced to increase the safety standard and driving comfort for certified driver rehabilitation specialists, who supervise disabled drivers. The dual brake pedals can also be used by people who want to extend the training period in a family vehicle. In this case, the dual brake pedals are ideal for the long-term use beyond the training evaluation period, reducing risk and stress for both the driver and passenger. A disabled driver during the independent

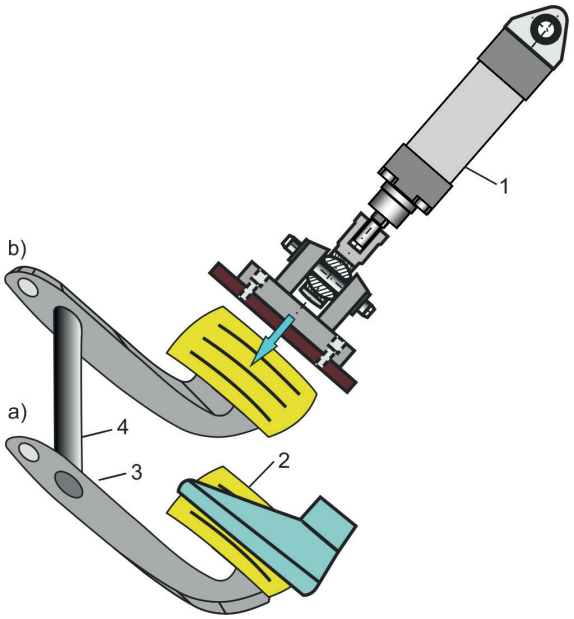


Figure 3 *Dual foot brake pedals: a) primary driver brake pedal, b) secondary brake pedal with pneumatic assistance, 1 - pneumatic actuator assembly, 2 - brake pedal pad, 3 - brake pedal arm, 4 - tubular shaft.*

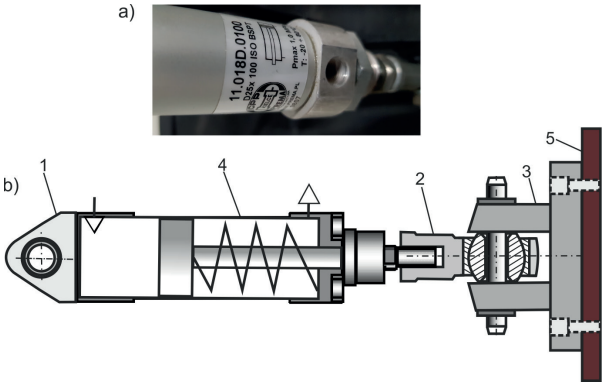


Figure 4 *Pneumatic actuator assembly: a) view of pneumatic actuator, b) design solution of an actuator assembly, 1 - pneumatic actuator (single-acting cylinder), 2 - spherical rod-end, 3 - cap-end female clevis, 4 - articulated male rear hinge, 5 - contact pad.*

driving can react to road hazards with some delay, especially during the emergency braking. A new solution of the dual foot brake pedals, consisting of the primary driver pedal and the secondary pedal pressed by the pneumatic actuator is shown in Figure 3. The primary foot brake pedal is rigidly connected to the secondary pedal by a tubular shaft. The driver presses his feet on the primary foot brake pedal while braking the vehicle under normal driving conditions. A spring returns the pedals to the upper (resting) position when the driver's foot is removed from the pedal. In the case of emergency braking, the pneumatic actuator presses the secondary brake pedal faster before the driver starts pressing the primary brake pedal with his foot. The secondary foot brake pedal is pressed by a pneumatic cylinder, which is controlled by the driver as a result of his brain activity during the emergency braking. When relaxing the driver, the pneumatic actuator releases the pressure on the secondary brake pedal. The dual braking system ensures greater driving safety because the secondary brake pedal is pneumatically pressed when the disabled driver cannot press the primary brake pedal in due time.

2.2 Pneumatic actuator assembly

The design solution of a pneumatic actuator assembly with mounting accessories is shown in Figure 4.

A standard pneumatic actuator ISO 6432 (Prema S.A., Poland), with the D = 25 mm piston diameter and the S = 100 mm stroke, was used. The pneumatic actuator used in the pneumatic assembly is a single-acting cylinder with a single-piston rod. In a single-acting actuator, compressed air is supplied only to one side of the piston surface. The other side is open to the atmosphere. The single-acting actuator uses compressed air energy only for the working stroke, movement in one direction. The return movement of the piston is effected by a built-in spring. The presented pneumatic actuator assembly is adapted to exert a specific pressure on the secondary foot brake pedal in a car. When selecting the stroke of the pneumatic actuator, it was assumed that the brake pedal sits 160 mm from the floor, when this distance is measured perpendicular to the front face of the pedal. As the brake pedal is pressed by the contact pad of the pneumatic actuator, it rotates through an arc. This angle can be up to 40° depending on the vehicle type. The total brake pedal deflection is 80 mm. The free displacement of the brake pedal, which may be around 6% of the available deflection, must be taken into account.

2.3 Neural impulse actuator

The neural impulse actuator (NIA) device by OCZ is a BCI type interface equipped by a neuro signal reader [23]. Signals, originating from the neural activity of the brain, are captured by the NIA in the form of electrical biopotentials, which occurred as a result of Alpha and Beta brain waves, movement of the facial muscles and eyelids. The NIA is a non-invasive device that was used as a brain-machine interface (BMI), that reads bioelectrical signals (BESs) caused by brain activity, muscle tension in the head and during eye movement. The NIA offers interpretation of the raw EEG (electroencephalography) and EMG (electromyography) data, as well as their translation into an understandable frequency spectrum.

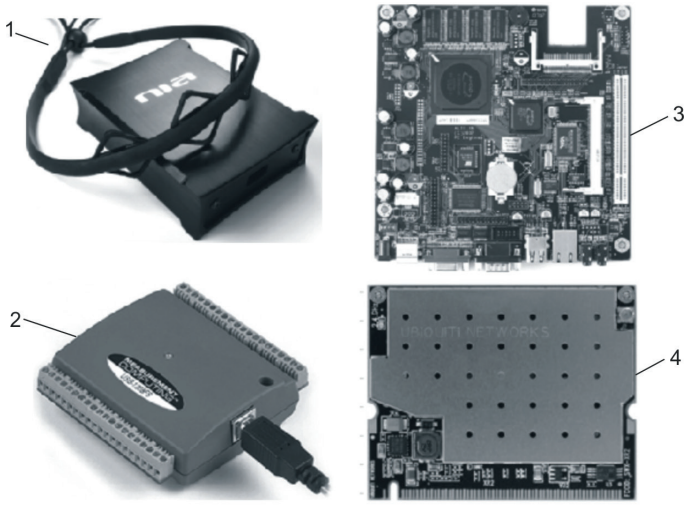


Figure 5 Control system: 1 - NIA set, 2 - data acquisition device, 3 - microcomputer board, 4 - wireless card

The EEG records a series of brain waves and EMG records muscle movement. The NIA is composed of a control box, client software and a headband with three diamond-shaped sensors, which are put on the driver's forehead. In the control box, recorded BES are analyzed, translated and sent to the NIA client software suite for further processing. The client software relays the binary impulse signals sent from the control box and passes them onto an executable program based upon the command specifications. The software provided with the NIA enables calibration and defining the control profiles creating applications. The rubber headband consists of three diamond-shaped conductor plates with BESs sensors based on carbon nanofibers (CNFs), that are bound to the forehead. Effective control of technical devices with use of the NIA requires a snug fit of the BESs sensors to the forehead, calibration of the device and training.

2.4 Simulator control system

The simulator control system consists of the NIA, microcomputer board ALIX.1D PC, data acquisition device MicroDAQ USB-1208FS and a wireless card Ubiquiti XR2 WiFi card (see Figure 5). The ALIX.1D system board is equipped by an AMD Geode 500 MHz processor and 256 MB of RAM. It is powered by a 12 V supply and has the low power consumption, in the range of 0.4 to 0.5 A. The software for the servo drive and controller was written using the LabVIEW environment. The task of the system board is to integrate the wireless card, IO port and the controller application. The Windows operating system has been installed on the memory card. Since the controller requires +24 V supply the device uses a step-down voltage regulator built on an LM2576 system to reduce the voltage to the required 12 V. The I/O port for the controller is the MicroDAQ USB-1208FS data acquisition module, connected with the controller board via a USB cable. This module includes 12-bit differential analogue inputs and 11-bit single-ended inputs. In the single-ended mode, a ±10 V measurement is possible, whilst in the differential mode, ±20 V. Two 12-bit analogue outputs are available for generating output signals. The output voltage range is 0 ÷ 4.096 V under a maximum load of 15 mA. Due to the low output voltage, a k_u = 2.5 preamplifier was installed on the controller to obtain a 10 V output signal. The preamplifier was built on the LM358 Op Amp system. Use of a rail-to-rail amp is connected with the asymmetric controller supply current.

Two applications were written, the first for communication between the NIA control box and the computer and the second for controlling the pneumatic actuator. Both applications were written using LabVIEW software. Data are sent via a wireless IT network, which enables the use of the TCP and UDP wireless transmission protocols. The TCP protocol ensures reliable delivery of data to the receiver using follow, confirm and retransmit functions for the data. The second UDP protocol has a simpler structure and is faster, but does not ensure the retransmission of lost data. For the position control of the pneumatic actuator, a PID controller was used, with tuning carried out by the Ziegler-Nichols method.

3 Biosignal processing

Currently, the tendency to use the bioelectric signals to control technical devices is increasing. The brain provides a lot of information about a person's physiological, emotional and cognitive states, which, when properly selected, can be used for various purposes. Brain activity accompanying their various states is reflected in the BES waves of varying range and frequency. Reading the BES is generally described in terms of its amplitude and frequency band. The amplitude of the EEG shows a great

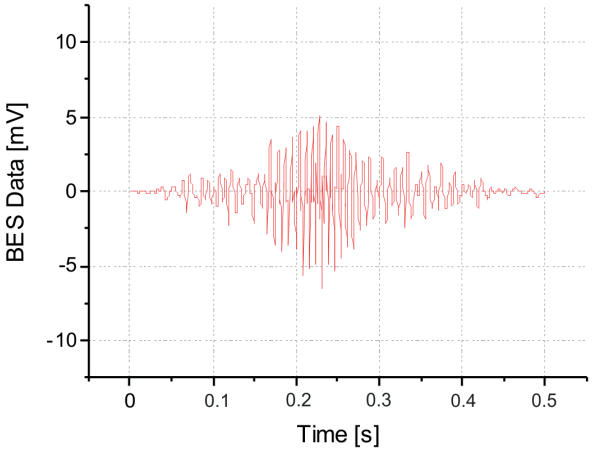


Figure 6 *Recorded time-dependent BESs spectrum activated by the muscle tension inside the head.*

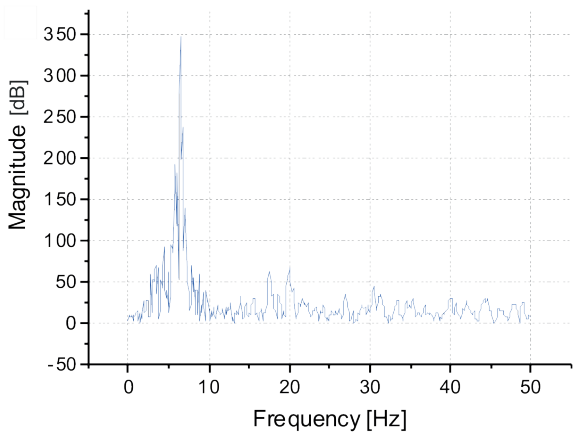


Figure 7 *Recorded BESs frequency spectrum activated by the muscle tension inside the head.*

deal of variability depending on external stimulation, as well as internal mental states. Electrodes located on the scalp register brain wave activity, which results in the user being able to issue commands by "thought". These electrodes also read muscle tension in the head area, which result from brain activity. The brain activity causes a change in biosignals that can be measured and used as control signals. Biosignals are space, time, or space-time records of a biological event such as a brain activity or a contracting muscle. The electrical and mechanical activity that occurs during the biological events produces signals that can be measured and analysed. Biosignals, therefore, contain useful information that can be used to understand the underlying physiological mechanisms of a specific biological event or system and that may be useful for technical. Basic methods of signal analysis, such as amplification, filtering, digitization, processing and storage, can be applied to many biological signals [24].

Once the NIA has captured the BESs, they are analysed and separated through the Fast Fourier transforms (FFT) into different frequencies to be translated into commands that the user defines as control signals to activate the pneumatic actuator of the secondary brake pedal. To obtain the extension of the actuator down (pressure force on the brake pedal) and retract the actuator up (release the pressure force on the pedal) control commands were selected, u = (down, up). Figure 6 shows the recorded time-dependent BES spectrum activated by muscle tension in the head. However, Figure 7 shows the recorded BES frequency spectrum activated by the muscle tension in the head.

There are two main problems during the detection, recording and decoding of the BESs to command signals. The first problem is the signal to noise ratio. The second problem is the noise signal defined as an electrical signal that is not a part of the desired BES. Research on the BESs shows that distinction of mental tasks can be carried out selectively in selected frequency bands. The measured BESs can be processed to eliminate noise or other possible interference. Initial biosignal processing usually involves signal filtration and removing noise and interference. At this stage, digital filters, spatial filters and signal whitening methods are used. These different approaches have been considered to perform the analysis in the frequency domain and to compute power spectral density (PSD) of the BES. Features, obtained using the discrete Fourier transform (DFT), illustrate the amplitude of the signal for individual frequency components, can be written as [25]:

$$X_i(k) = \sum_{n=0}^{M-1} x_i(n) w(n) e^{-j} \quad \omega_k{}^n 1 \le i \le K\,, \tag{1}$$

where x_i is the measured BES as the input variables, n is the number of the signal sample, M is the samples per segment, K is the smaller segment, $w(n)$ is the windows, ω_k is the discrete frequency of DFT, $\omega_k = 2\,\pi\,k/N$, k is the frequency bins, N is the number of samples, $N = M\,R$, R is the number of non-overlapping frames.

The power spectrum, according to the second modification made by Welch to Bartlett's method, is [26]:

$$P_i(k) = \frac{1}{M\,U}[X_i(k)]^2\,, \tag{2}$$

where U is the normalisation factor for the power spectrum in the window function $w(n)$:

$$U = \frac{1}{M}\sum_{n=0}^{M-1} w^2(n)\,. \tag{3}$$

Based on Equation (2), the main power spectrum in a frequency band for a limited time can be calculated as:

$$P_m(k) = \frac{1}{K}\sum_{i=1}^{K-1} P_i(k)\,. \tag{4}$$

For the real signals, due to the symmetry of the spectrum, it is sufficient to account for a half of the N/2 stripes only. It is known that the useful biosignal band is in the range from 0.5 Hz to 50 Hz. Due to the overall power spectrum, it is possible to identify a disturbance of the bio-potential baseline and distinguish it from increased brain activity. The BESs electrical potentials have both positive and negative voltage. To convert

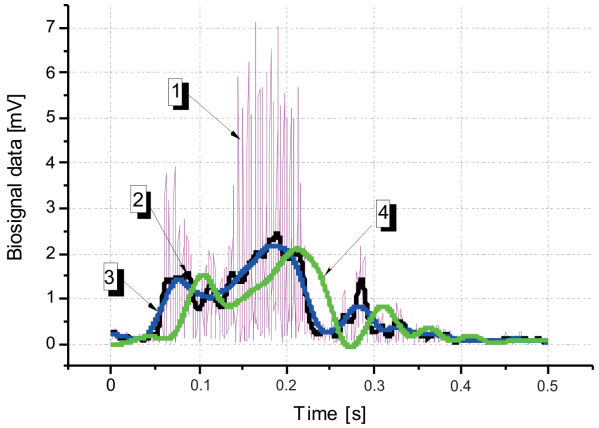


Figure 8 *Processing for smooth BES data: 1 - measured BES data (absolute value), 2 - FFT filter, 3 - Lowess method, 4 - Low-pass filter.*

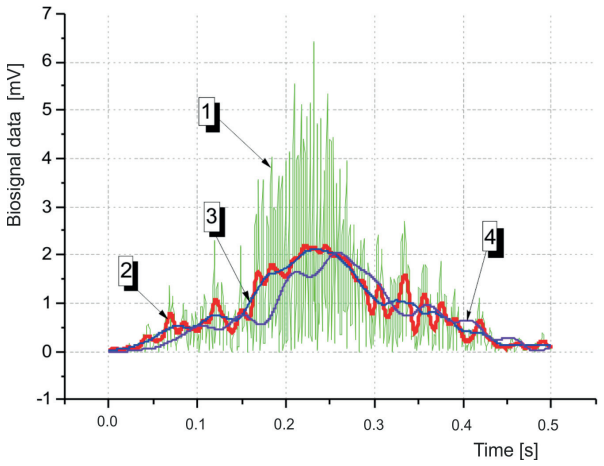


Figure 9 *Processing for the smooth BES data: 1 - measured BES data (absolute value), 2 - FFT filter, 3 - Lowess method, 4 - Low-pass filter.*

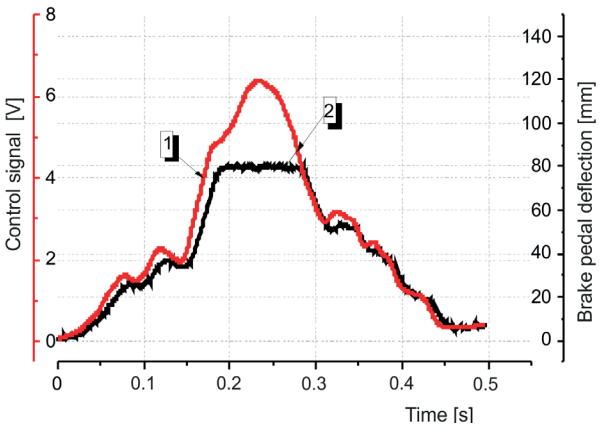


Figure 10 *Test results of emergency braking: 1 - control signal based on Lowess method filter, 2 - brake pedal deflections measured with a laser sensor.*

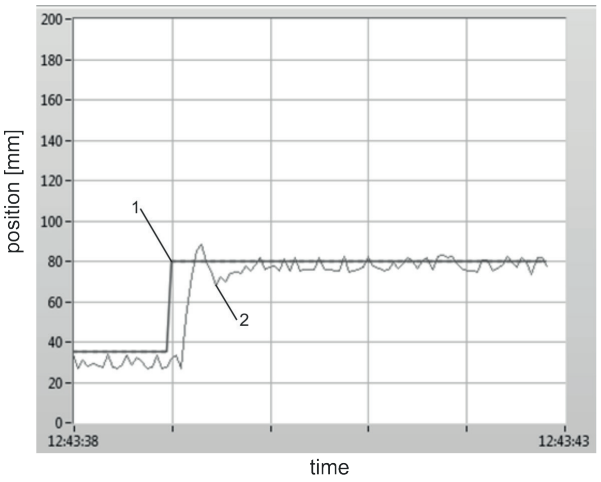


Figure 11 *Results of pneumatic actuator position control: 1 - set position, 2 - current position.*

the BES to a user control signal, all the negative amplitudes are firstly converted into positive amplitudes (see Figure 6). The negative peaks are transferred in a positive direction. In addition to transparency of the record, this action aims to obtain the ability to plot curves for the standard amplitude parameters, such as mean, peak - maximum and field values (the raw BES record has an average amplitude value equal to zero). To solve this problem, a unique part of the signal is minimized by using the digital smoothing algorithms that emphasize the main direction in which the biosignal travels. Peaks with excessive amplitude are trimmed and the biosignal is linearized. In addition, a digital smoothing algorithm was used. For smoothing the BESs data, an FFT filter, a low-pass filter (LF) and the Lowess method (LM) was used. The LM also is known as locally weighted polynomial regression (LWPR). The LWPR approximates nonlinear functions in large-dimension spaces with redundant and insignificant inputs. The effect of the BES data smoothing process is shown in Figure 8.

As a result of the driver's brain activity experiment, it was concluded that the BES with frequencies of up to 50 Hz and amplitudes of several mV, caused by muscle tension in the head, e.g. pressing the tongue against the palate or clenching of jaws with a bigger or smaller force, provides the best effects of the position control signals of the pneumatic actuator generation, that presses on the secondary foot brake pedal. Accuracy of the pneumatic actuator movement and the brake pedal deflection can be increased by the driver training on the driving simulator.

4 Emergency braking test

Results of the first tests on a brain-controlled pneumatic actuator to assist vehicle emergency braking have been published in a scientific letter [27]. The drivers' ability to generate biosignals at a sufficient level can be achieved through appropriate exercises. During the tests, the effect of various biosignals, decoded on the signals controlling the pressure force of the pneumatic actuator on the secondary brake pedal, was analyzed. Various driver activities generating biopotential were taken into account, such as eyeball movement, muscle movement on the forehead, or moving the jaw, heavy

thinking and relaxing, or closing the eyes. The best effects were obtained at pressing the tongue against the palate or clenching of jaws with a greater or lesser force. The time-dependent BES spectrum when the tongue is pressed to the palate and the smoothing process this spectrum is shown in Figure 9. Processed biosignals are amplified to input control signals in the range of 0-10 V, which are used to valve control of the pneumatic systems. Practical tests of control of the pneumatically assisted braking system that were carried out confirmed the assumptions of using the driver's brain activity for the emergency braking. Sample results of practical tests, carried out on the test stand, showing control signals based on the LM smoothing, are presented in Figure 10. The graphs in Figure 10 show that there is a delay between the control signal of the pneumatic actuator and the measurement signal of the brake pedal deflection, which affects the slowing down the braking of a vehicle. This delay is due to data acquisition and the process of generating and processing the control signal.

The reaction time t_r of the pneumatically assisted emergency braking is the sum of the processing time t_p of the biological signal (see Figure 9 based on the tests) and the stroke time t_s of the pneumatic actuator:

$$t_r = t_p + t_s = 0.23 + 0.01 = 0.24\,\text{s}\,. \tag{5}$$

The task of controlling the pneumatic actuator was not to precisely position it, but only to rapidly extend the piston rod. Figure 11 shows the position control results of a pneumatic actuator for a step input signal. The above graphs show that there is a delay between the value of the input signal and the actuator response. With a rapid increase in the control command, the delayed valve actuation and movement of the pneumatic actuator are always technically justified.

Tests carried out on the simulator confirmed that a brain-controlled pneumatic actuator can be used to assist the emergency braking of the vehicle.

5 Conclusions

In this study, the possibilities of using a driver's brain activity to pneumatically actuate a secondary foot brake pedal were analysed. The idea of this solution is to use the driver's brain activity for wireless remote control of the pneumatic actuator that exerts pressure on a secondary foot brake pedal during the vehicle emergency braking. For this purpose, a simulator according to authors' design solution, to test the pneumatically actuated foot brake pedal based on the driver's brain activity, was built. The simulator, equipped by the dual foot brake pedals, was used. A pneumatic actuator assembly was also designed, which has been adapted to exert pressure on the secondary foot brake pedal. The designed control system consists of devices for reading the bioelectric signals, analysing and decoding them into the control signals, as well as amplifying, transforming and wireless transmission of the control signals to the position controller of the pneumatic actuator. The recording device, the neural impulse actuator (NIA), reads and analyses the bioelectric signals (BESs), induced by the driver's brain activity, then decodes them into the control signals sent by wireless network interface controller (WNIC) to the actuator position controller (APC). As a result of the experiment, it was found that BESs artefacts are easy and stable to be recognized on the driver's head. As a result of the experiment, it was concluded that the biopotential artefacts caused by muscle tension in a driver's head, e.g. pressing the tongue against the palate or clenching of jaws with a greater or lesser force, generate bioelectric signals with a frequency of up to 50 Hz and an amplitude of several mV, which can be decoded into a command that control of the pneumatic actuator. The dual brake pedals are justified if it is necessary to increase the driving safety of the less experienced drivers, including disabled drivers, when an accompanying person cannot help them. During the emergency braking, the pneumatic actuator presses the secondary foot brake pedal. After using the pneumatic assistance, the driver's reaction time during the emergency braking is shortened, thus increasing driving safety. The driver's ability to use a pneumatically assisted secondary foot brake pedal by brain activity depends on training on a braking simulator. The main goal of the study was achieved, i.e. increased driving safety by shortening the driver's reaction time during emergency braking.

References

[1] FAIRCLOUGH, S. H., GILLEADE, K., NACK, L. E., MANDRYK, R. L. Brain and body interfaces: designing for meaningful interaction. In: SIGCHI Conference on Human Factors in Computing Systems: proceedings. 2011. ISBN 978-14503-0228-9, p.1-4.

[2] LI, W., DUAN, F. A human-vehicle collaborative simulated driving system based on hybrid brain-computer interfaces and computer vision. *IEEE Transactions on Cognitive and Developmental Systems* [online]. 2017, **10**(3), p. 1-13. ISSN 2379-8920, eISSN 2379-8939. Available from: https://doi.org/10.1109/TCDS.2017.2766258

[3] SOLANKE, P.B., PATIL, S.P., SHENDE, P.S. Mind-driven vehicle for disabled person using intelligent system. *International Journal of Innovative Studies in Sciences and Engineering Technology*. 2017, **3**(5), p. 38-42. ISSN 2455-4863.

[4] BI, L., WANG, M., LU, Y., GENETU, F. A. A shared controller for brain-controlled assistive vehicles. In: IEEE International Conference on Advanced Intelligent Mechatronics AIM: proceedings [online]. IEEE. 2016. ISBN 978-15090-206-6. Available from: https://doi.org/10.1109/AIM.2016.7576754

[5] BI, L., ZHANG, J., LIAN, J. EEG-based adaptive driver-vehicle interface using variational autoencoder and PI-TSVM. *IEEE Transactions on Neural Systems and Rehabilitation Engineering* [online]. 2019, **27**(10), p. 1-9. ISSN 1534-4320. Available from: https://doi.org/10.1109/TNSRE.2019.2940046

[6] NARESH, P., HARI BABU, A. V., SUDHAKA REDDY, M., SAI, P. Brain controlled car for disabled using artificial intelligence. *Journal of Advancement in Engineering and Technology* [online]. 2016. **3**(4), p. 1-3. ISSN 2348-2931. Available from: https://doi.org/10.5281/zenodo.999315

[7] SAIKRISHNA, D., EPHRAM, N., AHAMED, S., RAJESWARI, M. Brain controlled car for disabled using EEG. *International Journal for Research Trends and Innovation*. 2017, **2**(3), p. 83-88. ISSN 2456-3315.

[8] THILAGAVATHI, S., AKSHAYA, B., KUMUTHA RAJESWARI, G., PRIYANKA, K. Brain controlled car for disabled using blue brain technology. *International Journal of Pure and Applied Mathematics*. 2018, **119**(15), p. 1613-1618. ISSN 1314-3395.

[9] MAHMUD, M., HAWELLEK, D., VALJAMAE, A. Brain-machine interface based on EEG: extracted alpha waves applied to a mobile robot. In: ECSIS Symposium Advanced Technologies for Enhanced Quality of Life: proceedings. 2009. p. 28-31.

[10] TEPLAN, M. Fundamentals of EEG measurement. *Measurement Science Review*. 2020, **2**(2), *p. 1-11.* ISSN 1335-8871.

[11] SUMMALA, H. Brake reaction times and driver behavior analysis. *Transportation Human Factors* [online]. 2014, **2**(3), p. 217-226. ISSN 1093-9741. Available from: https://doi.org/10.1207/STHF0203_2

[12] MANNING, P., WALLACE, W. A., ROBERTS, A. K., OWEN, C. J.,. LOWNE, R. W. The position and movement of the foot in emergency manoeuvres and the influence of tension in the Achilles tendon. In: 41th Stapp Car Crash Conference: proceedings. 1997. ISBN 0-76-800033-5, p. 195-206.

[13] PALMERTZ, C., JAKOBSSON, L., KARLSSON, A. S. Pedal use and foot positioning during emergency braking. In: JRCOBJ Conference: proceedings. 1998. p. 135-146.

[14] JURECKI, R. S., JASKIEWICZ, M., GUZEK, M., LOZIA, Z, ZDANOWICZ, P. Driver's reaction time under emergency braking a car - research in a driving simulatory. *Eksploatacja i Niezawodnosc - Maintenance and Reliability*. 2012, **14**(4), p. 295-301. ISSN 1507-2711.

[15] JURECKI, R. S., STANCZYK, T. L, JASKIEWICZ, M. Diver's reaction time in a simulated, complex road incident. *Transport*. 2017, **32**(1), p. 44-45. ISSN 1648-4142.

[16] JURECKI, R. S., JASKIEWICZ, M. Analysis of road accidents in Poland over the last ten years. *Zeszyty Naukowe, Akademia Morska w Szczecinie*. 2012, **32**(104), p. 65-70. ISSN 1733-8670.

[17] JURECKI, R. S. An analysis of collision avoidance manoeuvres in emergency traffic situations. *The Archives of Automotive Engineering* [online]. 2016, **72**(2), p. 73-93. ISSN 1234-754X. e-ISSN 2084-476X. Available from: https://doi.org/10.14669/AM.VOL72.ART2

[18] HARDIN, E. C., SU, A., VAN DEN BOGER, A. J. Pre-impact lower extremity posture and brake pedal force predict foot and ankle forces during an automobile collision. *Journal of Biomechanical Engineering* [online]. 2005, **126**(6), p. 770-778. ISSN 1528-8951. Available from: https://doi.org/10.1115/1.1824122

[19] DAY, A. *Braking of road in vehicles.* Waltham, MA: Elsevier, 2014. ISBN 978-0-12-397314-6.

[20] MAZUR, S., DINDOR, R., WOS, P. Remote control of the electro-pneumatic servo drive using biosignals. *Technical Transactions, Mechanics*. 2013, **1-M**, p. 245-253. ISSN 0011-4561. e-ISSN 2353-737X.

[21] DINDORF, R., WOS, P. Using the bioelectric signals to control of wearable orthosis of the elbow joint with bi-muscular pneumatic servo-drive. *Robotica* [online]. 2020, **38**(5), p. 804-818. ISSN 0263-5747. Available from: https://doi.org/10.1017/S0263574719001097

[22] REYNOLDS, B., WAECHTER, A. *Brain-computer interfacing using the neural impulse actuator. A usability and statistical evaluation*. Los Angeles, CA: California Polytechnic State University, 2009.

[23] COAKLEY, E. Demonstrating realistic avatar control in a virtual environment through the use of a neural impulse actuator. MS Project: Neural avatar control. Final Report. Lake Forest, CA, 2010.

[24] ENDERLE, J. D., BRONZINO, J. D. *Introduction to biomedical engineering*. 3. ed. Burlington, MA: Elsevier, 2012. ISBN 978-0-12-374979-6.

[25] PAMPU, N. C. Study of effects of the short-time Fourier transform configuration on EEG spectral estimates. *Acta Technica Napocensis, Electronics and Telecommunications*. 2011, **52**(4), p. 26-29. ISSN 1221-6542.

[26] PROAKIS, J. G., MANOLAKIS, D. G. *Digital signal processing. Principles, algorithms and applications.* 3rd Ed. Upper Saddle River, NJ, USA: Prentice-Hall Inc., 1996. ISBN 0-13-394338-9.

[27] DINDORF, R., WOS, P. Analysis of the possibilities of using a driver's brain activity to pneumatically actuate a secondary foot brake pedal. *Actuators* [online], 2020, **9**(49), p. 1-13. ISSN 2076-0825. Available from: https://doi.org/10.3390/act9030049

ANALYSIS OF VEHICLE MOVING PARAMETERS IN VARIOUS ROAD CONDITIONS

Rafał Jurecki*, Tomasz Stańczyk

Faculty of Mechatronics and Mechanical Engineering, Kielce University of Technology, Kielce, Poland

*E-mail of corresponding author: rjurecki@tu.kielce.pl

Resume

The safety of road users is one of the priority issues raised by those involved in vehicle design, latest passive and active safety systems, traffic organization or driver education. Nowadays, an important road safety problem is the behaviour of drivers in emergency situations. In order to measurably estimate the driving quality, parameters such as velocity, acceleration, the way and frequency of using the control pedals are quite often used. This article describes how to assess driver's behaviour based on measurements taken on the road. The frequency of different acceleration ranges during the vehicle drive was determined based on the results obtained. For the arbitrarily adopted acceleration range of - 0.5 - 0.5 m/s^2, the driver's working time was over 77 percent on average, with the difference varying significantly between different route sections. Similarly, the study compares the driving times for other ranges of acceleration.

Article info

Received 18 September 2020
Accepted 3 November 2020
Online 24 March 2021

Keywords:

safety,
driver behaviour,
acceleration,
data acquisition system,
acceleration sensors

Available online: https://doi.org/10.26552/com.C.2021.3.F58-F70

ISSN 1335-4205 (print version)
ISSN 2585-7878 (online version)

This is an open access article distributed under the terms of the Creative Commons Attribution 4.0 International License (CC BY 4.0), which permits use, distribution, and reproduction in any medium, provided the original publication is properly cited. No use, distribution or reproduction is permitted which does not comply with these terms.

1 Introduction

Research on drivers regarding improvement of the road safety is performed in many research centres. Over the years, there have been various references to the way the driver's behaviour is defined and modelled. Due to a large number of factors that can determine the way drivers behave and drive, this topic is still relevant. This is even more important since nowadays driving is a quite common activity. At the same time, e impact of the road traffic, which generates many threats in the present world, makes the topic related to attempts to increase safety in this area very important. Many efforts are being made to implement tests and analyses to detect certain driver behaviour relationships that may have a direct impact on the road safety. Three methodological aspects are identified in [1] as being important in analysis of the road accidents. They covered reliability of accident predictors, time period for accidents used as dependent variable and culpability for accidents. To be able to predict the ability of drivers to drive safely, tests were performed in a driving simulator to determine the visual sensitivity, defined as the ability to respond quickly to various visual stimuli [2].

Therefore, there are many publications in which the driving process is analysed. These tests concern both attempts to determine the driver's profile, personality traits and the ability (aptitude) to drive. Many of them refer to three main aspects of the driving efficiency, namely physical and mental fitness, as well as knowledge, skills and attitude of the driver.

The dominant aspect of the tests is assessment of the mental fitness while driving. They analyse the mental, intellectual and personality traits of drivers. This test range is described in publications where the following are tested: driver response time [3-7], driver perception quality, stereoscopic and stereometric vision. The mental acuity, vision after dark and glare sensitivity, fatigue, eye-hand coordination [8-10] is particularly crucial in the case of elderly people. Very important parameters determining the driver is experience, ability to assess the velocity of vehicles in motion, selected memory features. The listed features of drivers and their mode of operation are tested in various environments, both real (standard road or test section) and virtual, such as in a simulator, station-based environments [11].

Many publications analyse the way of driver behaviour in terms of harmful emissions and the level of driving economy [12-16]. In the literature related to driver studies, there are equally broad descriptions of studies performed with participation of people with physical disabilities [17], or mental disorders [18], e.g. Parkinson's disease [19]. One of the important factors determining the driver behaviour is also whether they are under the influence of alcohol or other active substances, such as drugs [20-21].

The driver behaviour tests by many researchers are aimed at determining certain parameters of their behaviour in selected road situations. Tests may be

carried out on the driver response time [22-24] or the way they undertake defensive manoeuvres [10, 25], as well as on certain indicators facilitating a wider analysis of driver behaviour. Examples of such indicators include headway or time to collision.

There are currently popular studies on influence of various devices on the way the driver reacts, that can directly or indirectly distract them and, at the same time, affect their mode of operation [9-10, 26-27]. These tests concern both the impact of radio, navigation or mobile phone use in various traffic situations [28-31].

Many publications present research aimed at describing the driver behaviour, which in consequence may enable development of relatively simple tools to diagnose the driver profile and their mental inclination to specific, negative behaviours [32]. Important in this regard are studies aimed at understanding the intentions of a driver [33-39].

With reference to the scope of the tests implemented, their analyses may be carried out based on both simple and very complicated methods [40].

Given the complexity of the driver profile, scientists quite often use both simple measurable indicators and more complex ones [41-42]. Quite simple parameters include, for example, vehicle position, its velocity [34, 43] or acceleration [44-47]. There are publications in which the position of control elements is analysed, e.g. the position of accelerator pedal [16, 26, 48] or the service brake. In publication [37], the criteria for assessment of a driver in three types of behaviour were defined: stop, driving and braking. In [49], were classified the operating conditions of vehicles during the urban and extra-urban driving, with simultaneous determination of the traffic jam and dynamic driving.

Author of [50] assesses the acceleration value based on questionnaires. Based on them, three types of city bus rides were defined: comfortable, standard and uncomfortable. In the described tests, the level of uncomfortable longitudinal acceleration was already estimated at 1.5-2.75 m/s^2. The risk analysis of the driver's work during the bus driving is described in detail in [51].

In publication [22], authors proposed a system designed to identify drunk drivers, based on a mobile phone and an acceleration sensor, which assesses drivers by comparing the way in which certain manoeuvres were made with their performance patterns. In [24] and [52] authors developed the concept of a system, which was to determine typical and aggressive drivers based on the Smartphone sensors (accelerometer, gyroscope, magnetometer, GPS, video) for detection, recognition and recording. Use of inertial sensors for similar purposes is described in [15]. Authors in [53] attempt to assess the driver aggressiveness based on the vehicle velocity and position of the accelerator and service brake pedals. In these tests, the vehicle's inertial sensors were used and, using the CAN bus, a driver profile was developed. The authors indicated that braking and passing better characterize the driver's style than the acceleration manoeuvres.

Some behaviour of different drivers during the urban driving was indicated in [54]. The analyses related to emissions showed that the average velocity and deceleration range was lower in the peak hours compared to off-peak hours. As a rule, male drivers used higher acceleration values than women and a higher percentage of driving time in the highest acceleration classes. Women, on the other hand, had a higher percentage of time in the lowest acceleration class. The difference was particularly evident in the residential area. The study showed no major differences in average velocity for both genders, except for one type of street, where men drove faster than women.

This work is part of a larger study to develop a method for parametric assessment of drivers, based on continuous measurement of longitudinal and lateral body accelerations. Values of these accelerations are affected by many factors. In order for them to be used to assess drivers, it is necessary to precisely identify those factors the impact of which on acceleration values and variability is greatest and to "deduct" in some way that impact leaving only the impact of driver's skill, experience, temper and driving technique.

One such factor is certainly the type of car used by a driver. It is known that acceleration on acceleration, deceleration at braking, as well as lateral acceleration during the curvilinear motion of a good-class passenger car with a high-power engine, will be higher (with a sense of comfort for passengers) than, for example, a city bus with some passengers standing. Then the high centre of inertia gives a feeling of discomfort even with relatively low lateral acceleration when cornering, driving on a roundabout, etc.

The second important factor affecting the acceleration values and variability is the road. It can certainly be expected that the same driver, driving the same car, will use different velocities and accelerations, depending on whether he or she is driving on an expressway or an intercity route but of lower class (e.g. single carriageway), or in an urban traffic. This will be affected by factors, such as the number of carriageways, number of lanes on a given carriageway, length of straight sections, traffic organisation and intensity, etc. The impact study of this particular factor is the subject of this work.

2 Methodology of measurements

The test route ran from Kielce to Cracow and back and was 110 km long. During the tests, a number of parameters were measured to assess how the same driver drives the vehicle under different road conditions. The vehicle's route was recorded in detail by the Globtrak™ system, which allows, among other things, to record the GPS track. The route is shown in Figure 1.

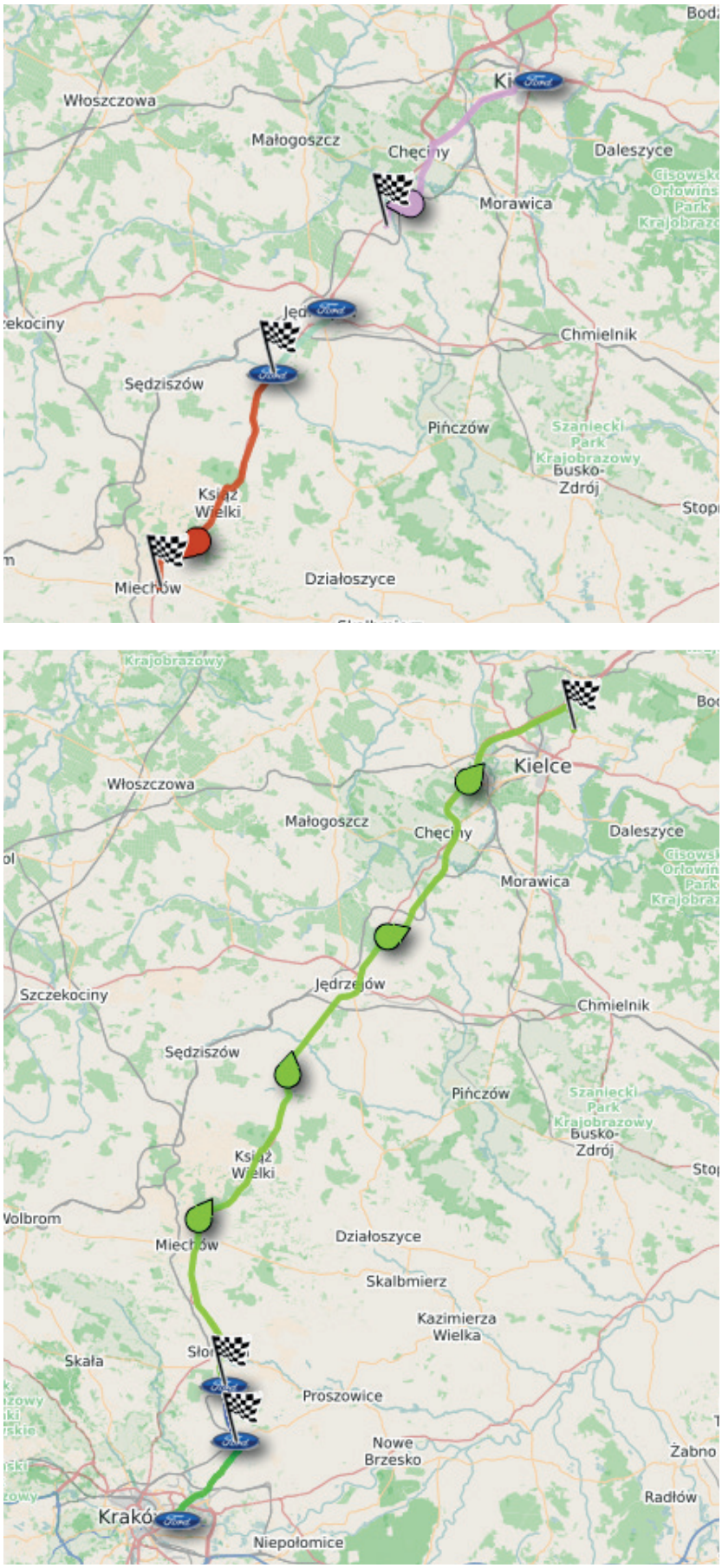


Figure 1 *The Kielce-Cracow-Kielce route from the Globtrak™ system*



Figure 2 *View of the Ford Transit test vehicle*



Figure 3 *Test apparatus used for testing; a) S-350 Corrsys Datron® optoelectronic sensor, b) Kistler® 3 axis TAA linear acceleration sensor*



Figure 4 *Data acquisition system; a) uEEP 12 Datron® Acquisition Station; b) Control tablet with ARMS® software*

The driver behaviour test in the real traffic conditions were performed with Ford Transit test vehicle shown in Figure 2.

The estate Ford Transit (the 4th generation) (9 seats) with complete vehicle kerb weight of 2070 kg had an engine capacity of 2198 cm^3 and the power of 92 kW. It was loaded with a weight of 320 kg.

3 Measuring equipment characteristics

To determine the parameters characterizing the route, the test vehicle was equipped by specialist equipment, which included, among others:

- S-350 Corrsys Datron ® optoelectronic sensor designed for measuring the vehicle motion parameters - enabling measurement of longitudinal velocity (up to 250 km/h) and vehicle lateral velocity and torque steer, additionally equipped by a compact display of motion parameters (Figure 3a),
- Kistler® TAA 3-axis linear acceleration sensor (Figure 3b) with a measuring range of +/- 3 g,
- uEEP 12 Datron® data acquisition station (Figure 4a) with control tablet and software (Figure 4b) [55-56].

Due to the need to accurately determine the vehicle motion parameters that were to be used to characterise the driver behaviour, the data was recorded simultaneously at a frequency of 10 Hz.

Table 1 *Vehicle velocity in different driving stages*

stage no	speed (km/h)			travel time (s)
	average	maximum	minimum	
1	26.4	74.4	0	1200
2	89.2	130.6	20.6	2800
3	48.5	99.0	0	1500
4	16.6	67.3	0	1900
5	24.1	64.3	0	2200
6	57.9	93.7	6.3	2800
7	109.0	127.2	42.1	2200
8	50.7	80.6	0	200

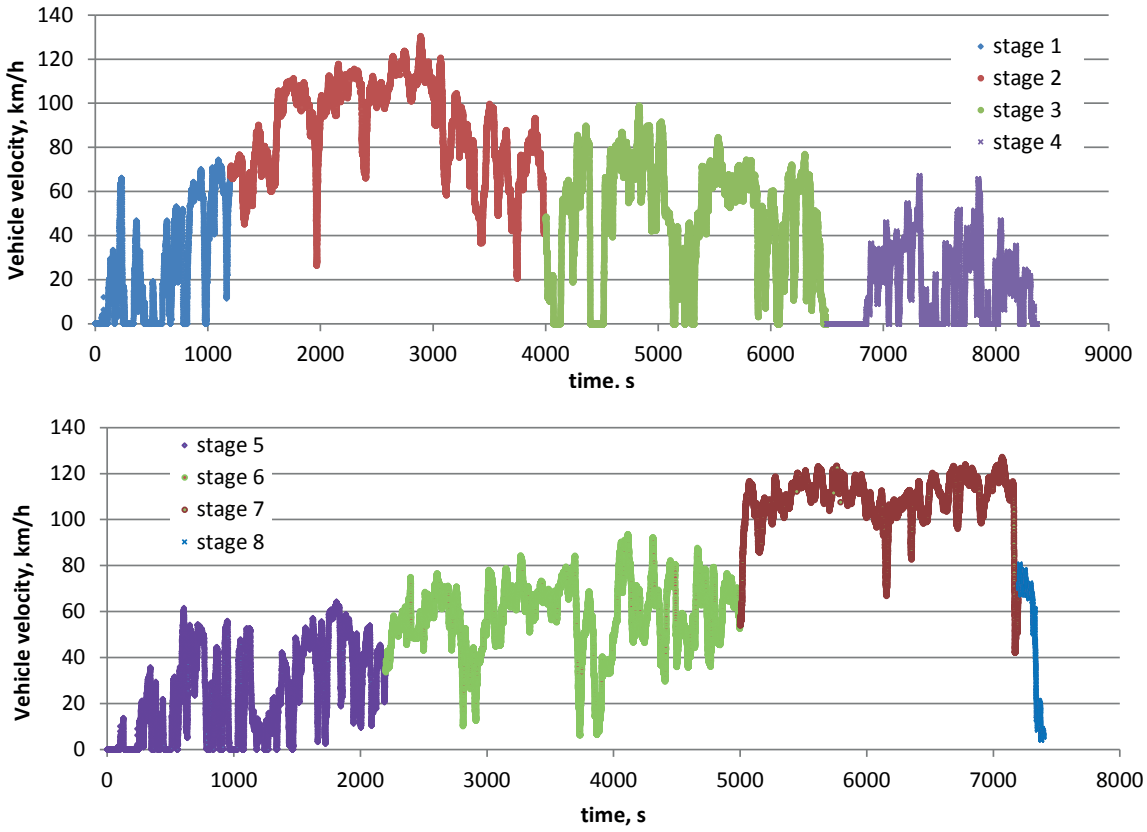


Figure 5 *Driving velocity values on the Kielce - Cracow route (stages 1-4), Cracow - Kielce (stages 5-8)*

4 Measurement results

As a result of measurements, changes in the vehicle's driving parameters were recorded. The section of the analysed route between the cities of Kielce and Cracow was divided into stages, characterised by different traffic conditions.

These conditions applied to:

- Stage 1 - departure from Kielce (urban traffic);
- Stage 2 - expressway (extra-urban drive - fast dual carriageway);
- Stage 3 - driving on the approach road to Cracow (suburban road),
- Stage 4 - driving in Cracow (urban traffic);
- Stage 5 - exit from Cracow (urban traffic);
- Stage 6 - driving on the exit road from Cracow (suburban road);
- Stage 7 - driving of the expressway to Kielce (extra-urban drive - fast dual carriageway);
- Stage 8 - driving in Kielce (urban drive);

The vehicle velocities and travel times of the section in each stage are shown in Table 1.

The measured values of the spot velocity, divided into the above presented driving stages, are shown in Figure 5.

The longitudinal acceleration values obtained are summarised in Table 2. Figure 6 shows the recorded longitudinal acceleration values. Positive values refer to acceleration on acceleration and negative values (deceleration) at braking.

Table 2 *Longitudinal acceleration in individual driving stages*

stage no	maximum (m/s²)	minimum, (m/s²)
1	2.33	-4.19
2	2.18	-2.68
3	2.76	-4.09
4	2.15	-3.37
5	2.92	-3.58
6	2.33	-3.64
7	1.39	-2.85
8	1.37	-1.82

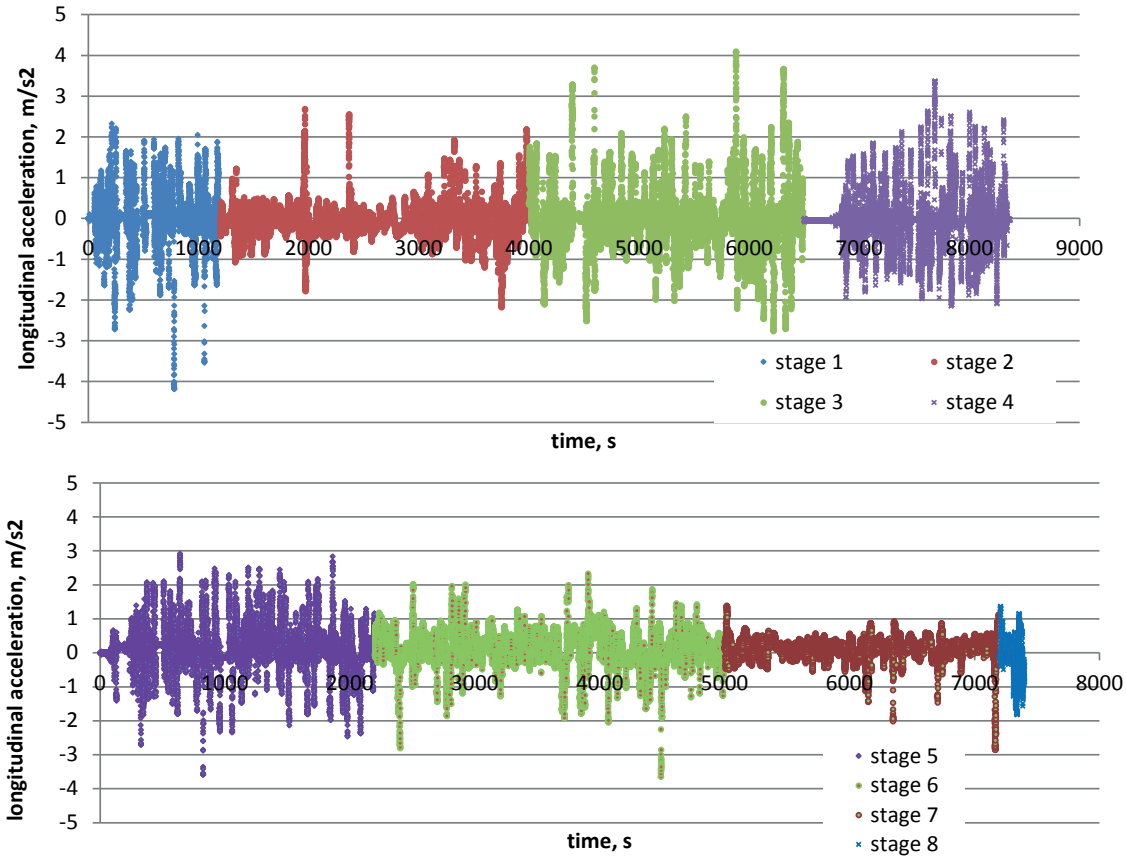


Figure 6 *Recorded lateral acceleration values on the Kielce - Cracow route (stages 1-4), Cracow - Kielce (stages 5-8)*

Values of the lateral acceleration are summarised in Table 3.

Figure 7 shows the recorded values of lateral acceleration.

5 Analysis of results

Figure 8 shows the frequency of particular longitudinal acceleration values on the analysed routes. If one treats the values intended for the entire route as one dataset, it can be assumed that the acceleration values in the range of 0.5 to -0.5 m/s² dominate in the prevailing time of the Kielce - Cracow - Kielce drive, as over 77%. This range was distinguished because it can be conventionally called driving at a constant velocity. During the actual driving at a constant velocity, accelerations also occur depending on e.g. terrain configuration (e.g. downhill and uphill slopes), a gentle increase in velocity by several or more km/h to a new higher constant value, etc.

While driving, more than 14-17% is positive acceleration 0.5 to 3 m/s² obtained during acceleration. Positive acceleration values indicating a very intense start above 3 m/s² were not recorded, which is an additional confirmation of the "calm" driving style of the tested driver.

In the case of negative accelerations (deceleration during deceleration and braking) values in the range of 0.5 to - 4 m/s² were recorded only in nearly 5-8% of the

Table 3 *Lateral acceleration in individual driving stages*

stage no	maximum (m/s²)	minimum (m/s²)
1	1.78	-2.71
2	2.06	-2.25
3	3.11	-3.35
4	1.78	-2.79
5	1.93	-3.06
6	2.48	-3.06
7	2.23	-2.34
8	1.39	-2.40

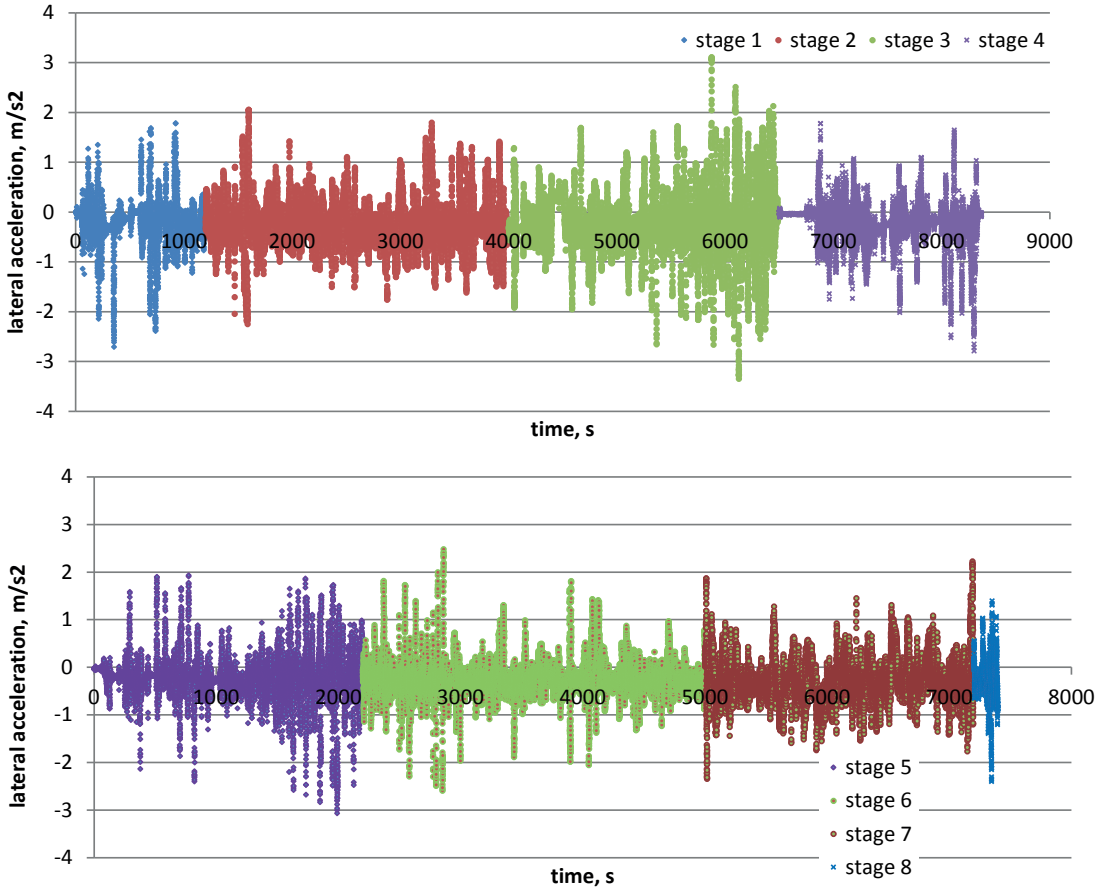


Figure 7 *Recorded longitudinal acceleration values on the Kielce - Cracow route (stages 1 -4), Cracow - Kielce (stages 5-8)*

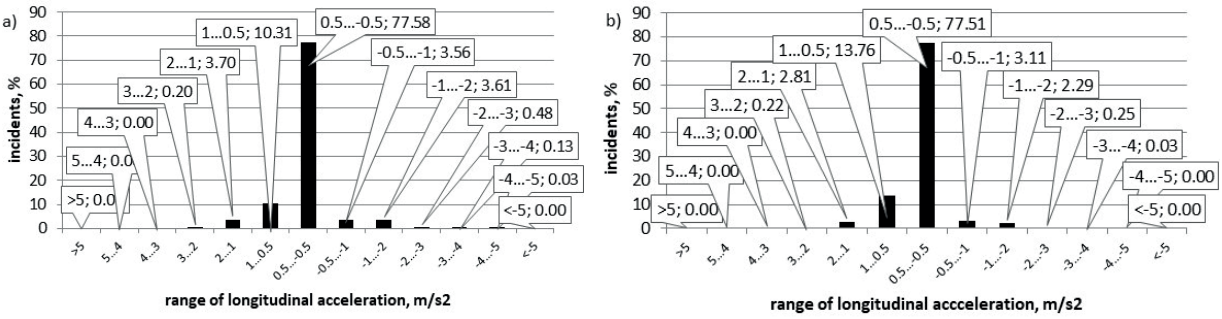


Figure 8 *Frequency of longitudinal acceleration ranges; a) for stages 1 - 4, b) for stages 5 - 8*

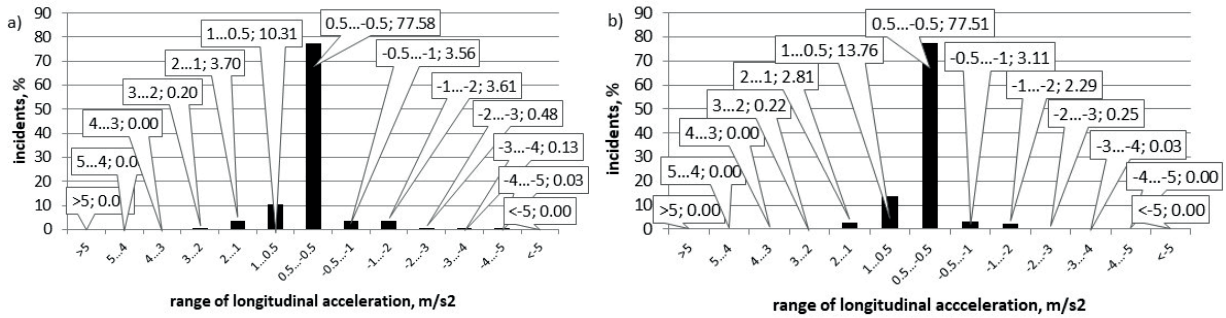


Figure 8 *Frequency of longitudinal acceleration ranges; a) for stages 1 - 4, b) for stages 5 - 8*

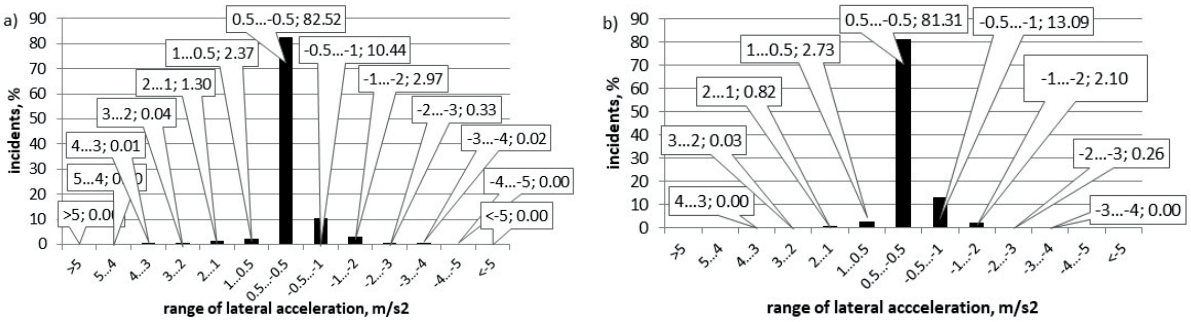


Figure 9 *Frequency of lateral acceleration ranges: a) for stages 1 - 4, b) for stages 5 - 8*

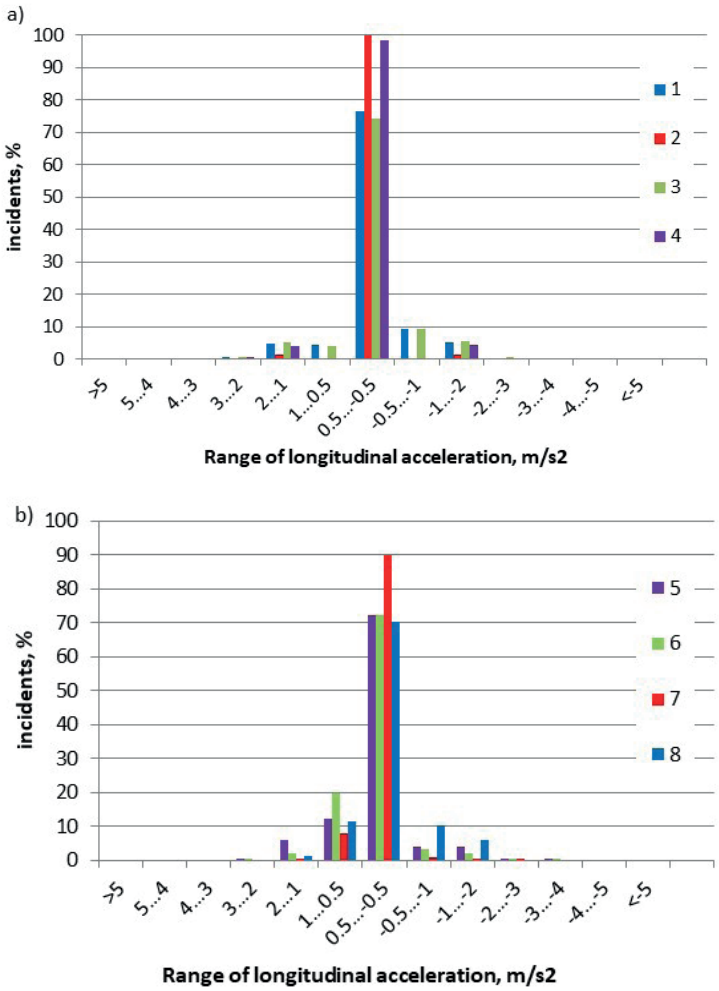


Figure 10 *Ranges of longitudinal acceleration values in individual stages of the route; a) stages 1 - 4, b) stages 5 - 8*

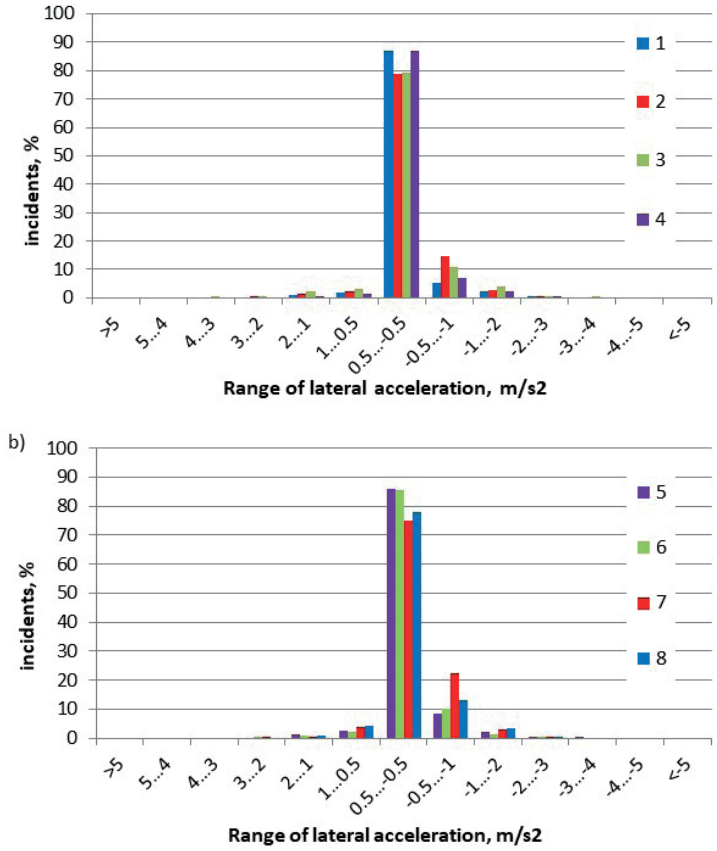


Figure 11 *Frequency of the lateral acceleration ranges; a) for stages 1 - 4, b) for stages 5 - 8*

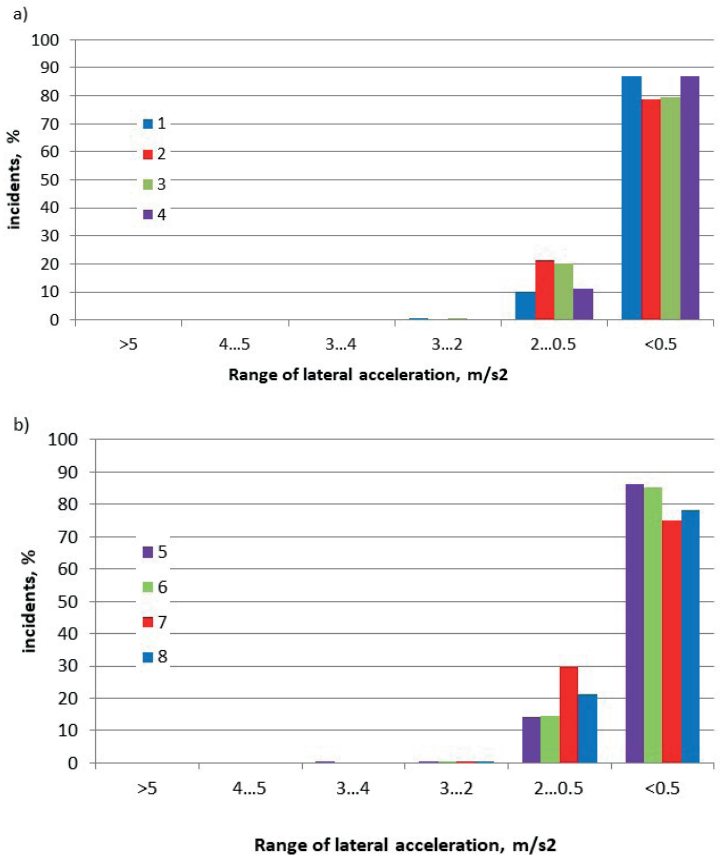


Figure 12 *Summary of absolute ranges of the lateral acceleration*

total driving time. Interestingly, there was not a single case in which the deceleration values would exceed 4 m/s^2, i.e. intensive braking. Figure 9 shows the frequency of different lateral acceleration values during driving. Positive and negative values indicate the direction of acceleration. Values in the range - 0.5 to 0.5 m/s^2 were recorded in more than 82 % of driving time.

Considering the differences in the way the route is presented in Figure 5 (velocity profiles - very clear velocity differences at individual stages), one may ask the question: what differences will occur when the route is divided into individual stages. Values of longitudinal accelerations along the test section are shown in Figure 10.

As one can see, driving with a longitudinal acceleration range of - 0.5 - 0.5 m/s^2 took place during the predominant driving time. The highest shares were recorded for the suburban and expressway driving, which means that in such conditions driving is the smoothest. During the urban drive - stage 1 (city of Kielce) and stage 4 (city of Cracow) - very similar shares of the driving time with such acceleration values of 75 % were recorded.

If these ranges are analysed using the lateral acceleration value of - 0.5 - 0.5 m/s^2 as the value considered to be "normal, smooth drive", an analysis of the frequency of absolute values may be performed. Considering direction of the lateral acceleration, it can be regarded as pointless, since it results from the road route. The absolute values are presented in Figure 12.

6 Conclusion and summary

The basic traffic parameters, presented in graphs and tables, show that the road type has a much greater impact on values and variability of the driving velocity than on accelerations, both longitudinal and lateral. Taking as a reference point the lowest average value given in Table 1, v = 16.6 km/h (urban traffic - Cracow), the highest value of the average velocity that was recorded in section 7 (expressway) is as much as 6.5 times higher. This is of course the consequence of a very different route and traffic conditions. However, with the same variation in routes and traffic conditions, variation in acceleration is many times lower. The highest acceleration of the car (given in Table 2) is only 113 % higher than the lowest value in the table. The deceleration variation (deceleration during braking, given in the same table) is slightly higher, i.e. 130 %, but it is also much less than the velocity variation. In the lateral accelerations, given in Table 3, a plus or minus symbol indicates a lateral acceleration in the right or left direction, which is due to the route profile and not to the nature of the drive. One can, therefore, merge these values using an absolute value. With this approach, the highest lateral car acceleration (given in Table 3) is only 141 % higher than the lowest value in this table, so the variation of these accelerations is also much lower than the velocity variation.

To sum up this part of the conclusion, it can be stated that values and variability of the driving velocity characterize the type of the road much more than the driving technique of the driver.

In analysis of the longitudinal accelerations, a range from - 0.5 to 0.5 m/s^2 was identified, which the authors, based on the preliminary analysis, conventionally treated as driving at a constant velocity. During the actual driving at a constant velocity, such slight accelerations occur depending on the terrain configuration (e.g. downhill and uphill slopes), a gentle increase in velocity by a few or more km/h to a new higher constant value, etc. The share of accelerations from this range, shown in Figure 8, was almost identical for the route in both directions and amounted to about 77.5 % on this route. Figure 10 shows the same distribution of accelerations as in Figure 8, but with the separation of individual sections of different roads. The largest shares of this "calm driving" were, as expected, on the expressway (sections 2 and 7) and amounted to 84 % and 90 %, respectively, i.e. deviated from the average (77.5 %) by 8 % and 16 %. It is interesting to note that the share of this "quiet drive" (due to the acceleration criterion) was very similar in the remaining six driving sections and ranged between 70 % and 77 % (see Figure 10).

Values of the positive accelerations above 3 m/s^2, indicating a very intensive start-up, were not recorded. There were also no decelerations exceeding 4 m/s^2, i.e. intensive braking, along the entire route. These two facts and the high proportion of accelerations from -0.5 to 0.5 m/s^2 indicate a "calm" driving style of the tested driver.

In analysis of the lateral accelerations, as in the case of longitudinal accelerations, a range of - 0.5 to 0.5 m/s^2 was identified. Based on the preliminary analyses, the authors concluded that these lateral acceleration values testify to smooth cornering and smooth overtaking, passing, or changing lane manoeuvres, which can also be referred to as "calm driving." The share of lateral accelerations from this range shown in Figure 9 was very similar for the route shown in the graph of the route in both directions and was approx. 82.2 % and 81.3 % on this route, i.e. 81.75 % on average for the entire trip. Figures 10 and 11 show the same distribution of accelerations as in Figure 9, but with the separation of individual sections of different roads. The share of this conventional "calm drive"' (due to the lateral acceleration criterion) was very similar in all eight driving sections and ranged between 74.9 % and 87.1 % and deviated from the average value by - 8.4 % and +6.5 %, respectively.

No lateral accelerations of more than 3 m/s^2 were found in seven of the eight sections of the route shown in the graphs. Only on section 3 several cases exceeding this value, but not exceeding 4 m/s^2, were registered.

Acknowledgements

The research was carried out as part of the Innovative system research project supporting the motor vehicle insurance risk assessment dedicated to UBI (Usage Based Insurance) No. POIR.04.01.04 00 0004/19 00 financed by the National Centre for Research and Development.

References

[1] AF WAHLBERG, A. E. Some methodological deficiencies in studies on traffic accident predictors. *Accident Analysis and Prevention* [online]. 2003, **35**(4), p. 473-486. ISSN 0001-4575. Available from: https://doi.org/10.1016/S0001-4575(02)00025-8

[2] HAKAN, A. Driver fatigue and accidents - can visual sensitivity predict drivers ability to drive safely? *Proceedings of the Human Factors and Ergonomics Society Annual Meeting* [online]. 2000, **44**(20), p. 3267-3270. ISSN 2169-5067, eISSN 1071-1813. Available from: https://doi.org/10.1177/154193120004402011

[3] BAUMLER, H. Reaction time in traffic - part I., (in German). *Verkehrsunfall und Fahrzeugtechnik*. 2007, **11**, p. 300-307. ISSN 0724-2050.

[4] BAUMLER, H. Reaction time in traffic - part II., (in German). *Verkehrsunfall und Fahrzeugtechnik*. 2007, **12**, p. 334-340. ISSN 0724-2050.

[5] BAUMLER, H. Reaction time in traffic - part III. (in German). *Verkehrsunfall und Fahrzeugtechnik*. 2008, **1**, p. 22-27. ISSN 0724-2050.

[6] GREEN, M. How long does it take to stop? Methodological analysis of driver perception-brake times. *Transportation Human Factors* [online]. 2000, **2**(3), p. 195-216. ISSN 1093-9741. Available from: https://doi.org/10.1207/STHF0203_1

[7] TORNROS, J. Effect of driving speed on reaction time during motorway driving, *Accident Analysis and Prevention* [online]. 1995, **27**(4), pp. 435-442. ISSN 0001-4575. Available from: https://doi.org/10.1016/0001- 4575(94)00084-Y

[8] AHLSTROM, C., ANUND, A., FORS, C., ÅKERSTEDT, T. The effect of daylight versus darkness on driver sleepiness: a driving simulator study. *Journal of Sleep Research* [online]. 2018, **27**(3), e12642. eISSN 1365-2869. Available from: https://doi.org/10.1111/jsr.12642

[9] DI MILIA, L., KECKLUND, G. The distribution of sleepiness, sleep and work hours during a long distance morning trip: a comparison between night-and non-night workers. *Accident Analysis and Prevention* [online]. 2013, **53**, p. 17-22 ISSN 0001-4575. Available from: https://doi.org/10.1016/j.aap.2013.01.003

[10] JURECKI, R. Influence of the scenario complexity and the lighting conditions on the driver behaviour in a car-following situation. *The Archives of Automotive Engineering - Archiwum Motoryzacji* [online]. 2019, **83**(1), p. 151-173. eISSN 2084-476X. Available from: https://doi.org/10.14669/AM.VOL83.ART11

[11] GUZEK, M. Simplex and complex reaction time of male drivers in various age - results of research with use of reflexometer. *The Archives of Automotive Engineering - Archiwum Motoryzacji*. 2014, **65**(3), p. 19-28. eISSN 2084-476X.

[12] ANDRZEJEWSKI, M., NOWAK, M. The influence of the driving style according to the principles of eco-driving on the emission of toxic substances from a light utility vehicle. *Autobusy - Technika, Eksploatacja, Systemy Transportowe* [online]. 2019, **24**(6), p. 33-37. ISSN 1509-5878, eISSN 2450-7725. Available from: https://doi.org/10.24136/atest.2019.121

[13] BIELACZYC, P., PAJDOWSKI, P., SZCZOTKA, A. Analysis of the impact of drivers' driving styles on emissions and fuel consumption. Czasopismo Techniczne. Mechanika. 2004, **101**, p. 87-94. ISSN 1897-6301.

[14] SZCZOTKA, A., PUCHALKA, B., BIELACZYC, P. Impact of driver's driving style on the uncertainty of emissions measurements on a chassis dynamometer. *Autobusy - Technika, Eksploatacja, Systemy Transportowe*. 2018, **226**(12), p. 675-679. ISSN 1509-5878, eISSN 2450-7725.

[15] VAN LY, M., MARTIN, S., TRIVEDI, M. M. Driver classification and driving style recognition using inertial. In: *2013 IEEE Intelligent Vehicle Vehicles Symposium (IV): proceedings* [online]. IEEE. 2013. ISSN 1931-0587, p. 1040-1045, Available from: https://doi.org/10.1109/IVS.2013.6629603

[16] VARHELYI, A., HJALMDAHL, M., HYDEN, C., DRASKOCZY, M. Effects of an active accelerator pedal on driver behaviour and traffic safety after long-term use in urban areas. *Accident Analysis and Prevention* [online]. 2004, **36**(5), p. 729-737. ISSN 0001-4575. Available from: https://doi.org/10.1016/j.aap.2003.06.001

[17] SPALDING, T. J. W., KISS, J., KYBERD, P., TURNER-SMITH, A., SIMPSON, A. H. Driver reaction time after total knee replacement. *The Journal of Bone and Join Surgery* [online]. 1994, **8**(76-B), p. 754-756. ISSN 2049-4394, eISSN 2049-4408. Available from: https://doi.org/10.1302/0301-620X.76B5.8083265

[18] MITAS, A., BUGDOL, M., RYGULA, A. The psychophysiological conditionings of driver's work under the aspect of traffic safety. *Transport Problems* [online]. 2009, **4**(1), p. 87-94. ISSN 1896-0596, eISSN 2300-861X.

[19] MADELEY, P., HULLEY, J.L., WILDGUST, H., MINDHAM, R. H. Parkinson's disease and driving ability. *Neurol Neurosurg Psychiatry* [online]. 1990, **53**(7), p. 580-582. ISSN 0022-3050, eISSN 1468-330X. Available from: https://doi.org/10.1136/jnnp.53.7.580

[20] HINDMARCH, I. Psychomotor function and psychoactive drugs. *British Journal of Clinical Pharmacology* [online]. 2004, **58**(7), p. 189-209. eISSN 1365-2125. Available from: https://doi.org/10.1111/j.1365-2125.2004.02279.x

[21] OGDEN, J. D., MOSKOWITZ, H. Effects of alcohol and other drugs on driver performance. *Traffic Injury Prevention* [online]. 2004, **5**(3), p. 185-198. ISSN 1538-9588, eISSN 1538-957X. Available from: https://doi.org/10.1080/15389580490465201

[22] BENDERIUS, O., MARKKULA, G.,·WOLFF, K., WAHDE, M. Driver behaviour in unexpected critical events and in repeated exposures - a comparison. *European Transport Research Review* [online]. 2014, **6**(1), p. 51-60. ISSN 1866-8887. Available from: https://doi.org/10.1007/s12544-013-0108-y

[23] JURECKI, R., STANCZYK, T. L. Driver model for the analysis of pre-accident situations. *Vehicle System Dynamics* [online]. 2009, **47**(5), p. 589-612. ISSN 0042-3114, eISSN 1744-5159. Available from: https://doi.org/10.1080/00423110802276028

[24] JURECKI R., STANCZYK T. Driver reaction time to lateral entering pedestrian in a simulated crash traffic situation. *Transportation Research Part F, Traffic Psychology and Behavior* [online], 2014, **27**, p. 22-36. ISSN 1369-8478. Available from: https://doi.org/10.1016/j.trf.2014.08.006

[25] KAYSI, I. A., ABBANY, A. S. Modeling aggressive driver behavior at unsignalized intersections. *Accident Analysis and Prevention* [online]. 2007, **39**(4), p. 671-678. ISSN 0001-4575. Available from: https://doi.org/10.1016/j.aap.2006.10.013

[26] AUGUSTYNOWICZ, A. Recognition of driver intentions based on analysis of the instantaneous position of the accelerator pedal. In: International Automotive Conference Konmot-Autoprogres: proceedings. Vol. 1. Motor Vehicles. 2004. p. 59-66.

[27] KRUSZEWSKI, M. *Methods of assessing distraction of inexperienced drivers using fuzzy logic* (in Polish). Ph.D. thesis. Warsaw: Politechnika Warszawska, 2019.

[28] AMADO, S., ULUPINAR, P. The effects of conversation on attention and peripheral detection: is talking with a passenger and talking on the cell phone different? *Transportation Research Part F: Traffic Psychology and Behaviour* [online]. 2005, **8**(6), p. 383-395. ISSN 1369-8478. Available from: https://doi.org/10.1016/j.trf.2005.05.001

[29] DAI, J., TENG, J., BAI, X., SHEN, Z., XUAN, D. Mobile phone based drunk driving detection. In: 4th International Conference on Pervasive Computing Technologies for Healthcare: proceedings [online]. IEEE. 2010. ISBN 978-963-9799-89-9, p. 1-8. Available from: https://doi.org/10.4108/ICST.PERVASIVEHEALTH2010.8901

[30] MOHEBBI, R., GRAY, R., TAN, H. Z. Driver reaction time to tactile and auditory rear-end collision warnings while talking on a cell phone. *Human Factors* [online]. 2009, **51**(1), p. 102-110. ISSN 1093-9741. Available from: https://doi.org/10.1177/00187208 09333517

[31] NILSSON, L., ALM, H. *Effects of mobile telephone use on elderly drivers' behaviour including comparisons to young drivers behaviour* [online]. Linkoping: Statens Vag - och Trafikinstitut., VTI sartryck 176, 1991. ISSN 1102-626X. Available: http://www.diva-portal.org/smash/record.jsf?pid=diva2%3A672100&dswid=9029

[32] BARTECKI, K., AUGUSTYNOWICZ, A. Use of a partially recurrant neural network to classify the driver's driving style. In: *Process and system diagnostics / Diagnostyka procesow i systemow* (in Polish). KORBICZA, J., PATANA, K., KOWALA, M. (eds.). Warszawa: Akademicka Oficyna Wydawnicza EXIT, 2007. ISBN 978-83-60434-31-4. p. 417-424.

[33] FRENCH, D. J., WEST, R. J., ELANDER, J. WILDING, J. M. Decision-making style, driving style and self-reported involvement in road traffic accidents. *Ergonomics* [online]. 1993, **36**(6), p. 627-644. ISSN 0014-0139, eISSN 1366-5847. Available from: https://doi.org/10.1080/00140139308967925

[34] MERKISZ, J., PIELECHA, J., PIELECHA, I. Impact of driver style of driving on the environmental performance of the vehicle. *Logistyka,* **2***,* 2010, p. 1910-1920. ISSN 1231-5478.

[35] MIERLO, J., MAGGETTO,, G., BURGWAL, E., GENSE, R. Driving style and traffic measures - influence on vehicle emissions and fuel consumption. *Proceedings of the Institution of Mechanical Engineers, Part D, Journal of Automobile Engineering* [online]. 2004, **218**(1), p. 43-50. ISSN 0954-4070, eISSN 2041-2991. Available from: https://doi.org/10.1243/095440704322829155

[36] RYGULA, A., Driving style identification method based on speed graph analysis. In: 4th International Conference on Image Analysis and Biometrics and International Conference on Kansei Engineering and Affective Systems: proceedings [online]. 2009. ISBN 978-0-7695-3692-7. Available from: https://doi.org/10.1109/ICBAKE.2009.51

[37] SMOLEN, P., STAROWICZ, W. The concept of a driver's driving style assesing system in road freight transport. *Transport Miejski i Regionalny*. 2018, **8**, p. 18-23. ISSN 1732-5153.

[38] VAN MIERLO, J., MAGGETTO, G., VAN DE BURGWAL, E., GENSE, R. Driving style and traffic measures-influence on vehicle emissions and fuel consumption. *Proceedings of the Institution of Mechanical*

Engineers, Part D: Journal of Automobile Engineering [online]. 2004, **218**(1), p. 43-50. ISSN 0954-4070, eISSN 2041-2991. Available from: https://doi.org/10.1243/095440704322829155

[39] GUIHE, Q., YULONG, L., MINGKUI, N., ANLIN, G., YISONG, D. Estimation of road situations and driver's intention in automotive electronic control system. In: International Vehicle Electronics Conference: proceedings. IEEE. 1999. p. 199-201.

[40] AUGUSTYNOWICZ, A., BROL, S. Use of continuous wavelet transform for estimating the driver profile in urban traffic conditions. *The Archives of Automotive Engineering - Archiwum Motoryzacji*. 2007, **4**, p. 293-307. eISSN 2084-476X.

[41] MERKISZ J., ORSZULAK, B. Initial analysis of the driver's driving style parameters recording. *Logistyka*. 2015, **3**, p. 3210-3214. ISSN 1231-5478.

[42] WANG, J., LU, M., LI, K. Characterization of longitudinal driving behavior by measurable parameters. *Transportation Research Record* [online]. 2010, **2185**(1), p. 15-23. ISSN 0361-1981, eISSN 2169-4052. Available from: https://doi.org/10.3141/2185-03

[43] LAJUNEN, T., KAROLA, J., SUMMALA, H. Speed and acceleration as measures of driving style in young male drivers. *Perceptual and Motor Skills* [online]. 1997, **85**(1), p. 3-16. ISSN 0031-5125, eISSN 1558-688X. Available from: https://doi.org/10.2466/pms.1997.85.1.3

[44] AF WAHLBERG, A. E. The relation of acceleration force to traffic accident frequency: a pilot study. *Transportation Research Part F: Traffic Psychology and Behaviour* [online]. 2000, **3**, p. 29-38. ISSN 1369-8478. Available from: https://doi.org/10.1016/S1369-8478(00)00012-7

[45] MERKISZ, J., PIELECHA, J., TARKOWSKI, S. On-board recorders of traffic parameters and their application to assess comfort in city buses. *Autobusy - Technika, Eksploatacja, Systemy Transportowe*. 2012, **13**, p. 300-305. ISSN 1509-5878, eISSN 2450-7725.

[46] REYMOND, G., KEMENY, A., DROULEZ, J., BERTHOZ, A. Role of lateral acceleration in curve driving: Driver model and experiments on a real vehicle and a driving simulator. *Human Factors* [online]. 2001, **43**(3), p. 483-495, ISSN 1093-9741. Available from: https://doi.org/10.1518/001872001775898188

[47] TAKAHASHI, H., KURODA, K. A study on mental model for inferring driver's intention. In: 35th IEEE Conference - Decision and Control: proceedings [online]. IEEE. 1996. ISBN 0-7803-3590-2. Available from: https://doi.org/10.1109/CDC.1996.572826

[48] HJALMDAHL, M., VARHELYI, A. Speed regulation by in-car active accelerator pedal: effects on driver behavior. *Transportation Research Part F, Traffic Psychology and Behavior* [online]. 2004, **7**(2), p. 77-94. ISSN 1369-8478. Available from: https://doi.org/10.1016/j.trf.2004.02.002

[49] KROPIWNICKI, J. Classification of vehicle operating conditions using the proportion of engine idling time. *Autobusy - Technika, Eksploatacja, Systemy Transportowe*. 2011, **12**, p. 204-209. ISSN 1509-5878, eISSN 2450-7725.

[50] MERKISZ, J., TARKOWSKI, S. Dynamic factors and their impact on the subjective sense of comfort in city buses. *Postepy Nauki i Techniki*. 2012, **14**, p. 169-178. ISSN 2080-4075.

[51] WOJTYTO, D., RYDZ, D. Risk assessment for the task in the context of the bus driver's work process. *Autobusy - Technika, Eksploatacja, Systemy Transportowe* [online]. 2018, **220**(6), p. 1284-1288. ISSN 1509-5878, eISSN 2450-7725. Available from: https://doi.org/10.24136/atest.2018

[52] JOHNSON, D. A., TRIVEDI, M. M. Driving style recognition using a smartphone as a sensor platform. In: 14th International IEEE Conference on Intelligent Transportation Systems ITSC: proceedings [online]. IEEE. 2011. p. 1609-1615. Available from: https://doi.org/10.1109/ITSC.2011.6083078

[53] KUDZIA, K., STOPA, S. Algorithm to determine the cost-effectiveness of a driving style based on data from car diagnostic systems. *Logistyka*. 2015, **4**, p. 4320-4326. ISSN 1231-5478.

[54] ERICSSON, E. Variability in urban driving patterns. *Transportation Research Part D: Transport and Environment*. 2000, **5**(5), p. 337-354. ISSN 1361-9209. Available from: https://doi.org/10.1016/S1361-9209(00)00003-1

[55] JURECKI, R., STANCZYK, T. L. Analyzing driver response times for pedestrian intrusions in crash-imminent situations. In: 11th International Scientific and Technical Conference on Automotive Safety: proceedings [online]. 2018. p. 1-7, Available from: https://doi.org/10.1109/AUTOSAFE.2018.8373339

[56] JURECKI R., STANCZYK T., JASKIEWICZ M. Driver's reaction time in a simulated, complex road incident. *Transport* [online]. 2017, **32**(1), p. 44-54. ISSN 1648-4142, eISSN 1648-3480. Available from: https://doi.org/10.3846/16484142.2014.913535

CLASSIFICATION OF THE SOCIO-PSYCHOLOGICAL ASPECTS OF PROTECTING SOFT TARGETS: A CASE STUDY FOR EVACUATION OF THE RAILWAY TERMINALS

Alena Šplíchalová[1,*], Tomáš Karásek[1], Tomáš Apeltauer[2]

[1]Faculty of Social Sciences, Charles University, Prague, Czech Republic
[2]Faculty of Civil Engineering, Brno University of Technology, Brno, Czech Republic

*E-mail of corresponding author: alena.splichalova@vsb.cz

Resume
Current crisis management approaches to protect soft targets make assumptions about average visitors/listeners/viewers or passengers. They do not give much consideration to impacts of diversity of potentially evacuated persons with regard to socio-psychological parameters/factors that may lead to practical problems and complications during the evacuation itself. At the same time, the soft target operators have various means of machine vision tools at their disposal, but do not use these records for more thorough analysis of evacuation planning needs. Based on this observation, the article identifies and analyzes the socio-psychological aspects that may significantly affect behavior and decisions of persons during the evacuation and thus total evacuation time.

Article info
Received 18 September 2020
Accepted 24 November 2020
Online 30 March 2021

Keywords:
evacuation,
socio-psychological aspects,
protection of soft targets,
station terminal,
bomb threat

Available online: https://doi.org/10.26552/com.C.2021.3.F71-F82

ISSN 1335-4205 (print version)
ISSN 2585-7878 (online version)

This is an open access article distributed under the terms of the Creative Commons Attribution 4.0 International License (CC BY 4.0), which permits use, distribution, and reproduction in any medium, provided the original publication is properly cited. No use, distribution or reproduction is permitted which does not comply with these terms.

1 Introduction

Protection of persons, which temporarily are using certain public buildings or spaces, i.e. soft targets, are protected through the preventative measures, e.g. systems of physical protection, passive barriers, etc. These measures prevent emergency events from occurring within infrastructure and public spaces. That is why they must be kept fully functional and up-to-date, especially through the integration of dynamic parameters, application of newly obtained knowledge [1] or systematic searches and rectification of any shortcomings [2]. This knowledge can then be implemented and used for crisis management information systems [3], which will ensure timely and effective protection of individuals. Once these systems are disrupted or fail, then it is necessary to resort to other means to protect the populace, i.e. to evacuate them from places affected by emergency events.

One of the basic tasks of population protection is to evacuate people during emergencies and to ensure their subsequent shelter and emergency survival. As an organizational measure subject to legal regulations and technical standards, evacuations ensure the timely response of a population to a threat or emergency event, minimizing loss of life and injuries [4]. An evacuation consists of a set of activities ensuring the relocation of persons in a given order, according, to priority from places threatened by an emergency event to predetermined safe places [5]. The ability to safely evacuate and effective calculate the number of people evacuated is essential for planning, designing and subsequently operating infrastructure [6]. Of course, in practice one finds that the measures currently required by law do not always provide the support that people need in buildings during an emergency event [7].

Large railway stations with complicated architecture are common in today's integrated railway networks. In this transportation infrastructure, evacuation plans are commonly designed using timeline analysis comparing Available Safe Egress Time (ASET) and Required Safe Egress Time (RSET) with approved scenarios. This approach, however, does not take much account of a basic variable, which is the behavior and decision-making of people during the evacuation itself and likewise, directly before it. In recent years, research has been conducted into human behavior during evacuations [8-9] and the results have been applied to sophisticated computer systems. However, this research was conducted on a sample of mostly healthy people that did not reflect a diverse composition of people.

ASET/RSET timeline analysis was developed over 30 years ago and therefore should be revised to apply to the extensive and structurally complicated infrastructure

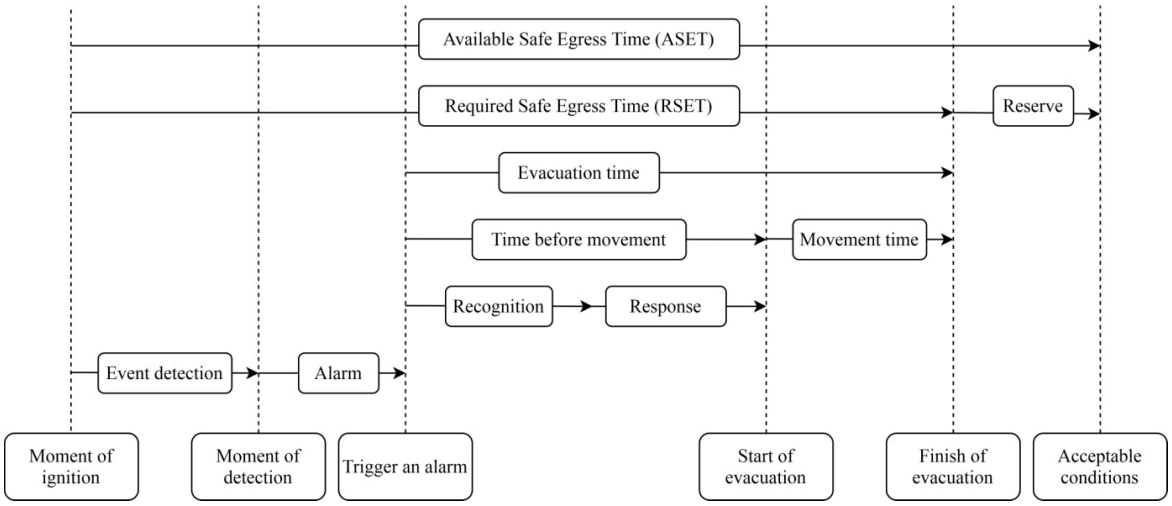


Figure 1 *Relationship between individual components of the evacuation process and its length [13]*

of today [10]. One of the ways it can be updated is to incorporate the heterogeneous behavior of persons so that models not only consider the response of healthy people, but especially people with limited orientation and movement and seniors, who fundamentally affect evacuation time. Likewise, psychonomy also has a significant impact on the behavior or people when responding to an emergency [7]. Based on these facts, the current conventional approach to calculating evacuation time must be augmented with scientific knowledge in this area.

In the context of the above, the goal was to define factors affecting the total evacuation time according to the well-known ASET/RSET approach and then point out the possible gaps, deviations or shortcomings of this approach that fundamentally impact the total evacuation time. Particular attention was given to the socio-psychological aspects of the evacuated persons and their impact on the total evacuation time.

2 Technical factors determining evacuation time (ASET/RSET)

The safety of visitors and people in buildings is defined by an evaluation based on a set of acceptance criteria. These criteria are to a considerable degree expressed by occupancy limits of visitors who may potentially be exposed to the effects of an emergency [11]. Safety during an emergency event is ensured by evacuation, where the decisive factor is the amount of time left to safely exit (time to unsustainable conditions) and the amount of time required to safely exit (building evacuation time). The basic concept when evaluating the safety of people in a building is to determine the time required for people to escape safely from the space and pass-through escape routes to a safe place before the conditions that endanger their health and lives occur [12]. This is calculated through ASET/RSET methods that determine the safety of travelers. It is a simple time-based approach where both parameters are dependent on several variables that follow from the nature of the emergency event, the character of the building and the composition and behavior of the persons evacuated. An assessment of the safe exit time is fundamental for organizing the evacuation of people in buildings, structures, or generally enclosed spaces [13].

A basic approach when analyzing effectiveness of an evacuation itself is the location and movement of people in the space examined [14]. The requirement of the safe exit and sufficient protection is defined as the difference between Available Safe Egress Time (ASET) and Required Safe Egress Time (RSET). This ratio must always be maintained, i.e. RSET < ASET. If this condition is met, the safe exit of persons is completed before conditions become dangerous [15].

The ASET, or the time for which safe conditions for travelers are guaranteed, is generally assessed using analytical equations or models simulating adverse events. In the event of a fire, it is suitable for preliminary and routine risk assessment of an adverse event due to its simple and rapid use [16]. It is determined from the moment when the effects of the emergency event reach the thresholds prescribed in the acceptance criteria. In contrast, the RSET is a variable based on an analysis of the time required by travelers to safely escape the impacts of the emergency event [11]. The RSET is often estimated on a simple technical level, taking little account of factors caused by human behavior. The RSET, or the time required to safely exit, is the sum of time to detect and react to an alarm, plus movement. The relationship between both quantities is shown in Figure 1.

The conventional ASET/RSET approach was founded on the simple concept of a two-layer zone model [17]. This model only expresses the period of unsustainable conditions for individual rooms and the evacuation time is evaluated in the same way. Nevertheless, this approach is still used today for much larger and more complicated building complexes without the slightest modification, even though the adequacy

of this approach is only occasionally discussed and not addressed in detail [11]. Since the inception of the ASET/RSET approach, a number of more sophisticated calculations methods have appeared that go beyond the framework of basic calculations. Today, complicated computer modelling of evacuation dynamics has become an integral component of simulation models and not only in a two-dimensional representation. These models also incorporate other factors affecting the RSET such as distance, overcrowding, visibility, proximity of exits to their destination or distribution of exits [18]. The concept for calculating the ASET/RSET, however, has not been adapted to this development. Continued use of the current ASET/RSET approach under these conditions could lead to significant shortcomings and inaccurate calculations, which would lead to deviations from the intended scope of purpose of providing a basic benchmark for assessing exit safety, originally proposed by Cooper [11].

For example, in the area of the fire safety, according to Babrauska et al. [19], the ASET/RSET concept is considered intrinsically defective and its use reduces the fire safety of travelers in a building. According to the authors, the concept ignores any differences in the physical abilities and condition of the people being evacuated and takes a robot-like approach to people's decision making. In the overwhelming majority of cases, evacuation time is influenced by the composition of people, their decision-making, the social relationships between them, injured people etc. These additional aspects of evacuation are considered in the computer tools already mentioned. In most cases, these tools consider the nature of the space, individual attributes, the distribution of emergency exits and possible loss of route due to the incident. These models may also include factors that significantly affect the behavior of people and their decision-making process. However, if such factors are included at all, they are very general and behavior of the people being evacuated is oversimplified [20]. Knowledge regarding the behavior of people during an evacuation and their response to emergency events is limited regardless of approach. This shortcoming stems from the lack of a comprehensive conceptual model for the decision-making and behavior of evacuees during the emergency event [12]. There is also little literature available on viable alternatives to this simplified manner of evaluating the safe escape [11].

The literature also mentions possible modifications and adaptations of the current approach. One possibility is a simple revision, consisting in the modification of the ASET to ASUT, i.e. the available time that an area can be safely used for escape and RSUT, the required time for safely using an area for escape [11]. This change considers the longest possible duration of the evacuation itself, the time when an area is last used by an occupant. This simple revision enables designers to take into consideration detailed information from more advanced simulation models. Similarly, Schroder et al. [21] consider use of the ASET/RSET ambiguous and therefore propose a map representation of this approach. The maps are generated by spatial evaluation of quantities, yielding a difference map representing safety reserve. This approach helps to determine the evacuation time in multi-dimensional or risk-based analyses. Another person taking an innovative approach to the ASET/RSET was Sime [22], who in his work began to combine and unify aspects of psychology, architecture, engineering and facility management through the concepts of occupancy, occupants and passenger location. Another modification, the primary goal of which is to bridge the divide between psychology and engineering, is occupant response shelter escape time (ORSET).

The aforementioned modifications of the ASET/RSET approach can decrease uncertainty in a design based solely on performance. It has been shown that such an approach is insufficient and it is therefore necessary to focus the future research on the aspects that significantly affect evacuation time. The most important aspects, contributing to major deviations from the planned evacuation time, are composition of the evacuees, their human behavior, response time and decision-making.

3 Socio-psychological aspects of evacuation

As already mentioned above, the process of evacuation is characterized by technical factors such as spatial requirements (i.e. width, length of narrow places, number of escape routes, etc.) and the related speed of people's movement. It is also important when calculating the RSET to include person-related factors (i.e. individual physical condition, age, mental state etc.), their geometry, as well as required assistance or orientational ability [23]. The aforementioned aspects have a fundamental impact on the movement behavior of evacuees.

Another important group of factors affecting the RSET are the socio-psychological aspects. In current models these aspects are taken into account too generally and, in most cases, homogeneously, if they are taken into account at all. Very rarely are evacuees viewed as a heterogenous group of persons, capable of making different decisions based on perception of the environment and individual personal characteristics. It follows from the above that evacuation models do not take into consideration the variability of evacuee composition and therefore do not take into account possible delays in the response time. Based on this fact, social psychology has gradually been applied to the process of calculating evacuation time, since human behavior during this phase is an important factor from a survival perspective [7].

The social psychology is one of the basic psychological disciplines that strives to understand and also explain the thought and behavior of individuals influenced by the actual, perceived or anticipated presence of

Table 1 *Three components for the fire response performance model [7]*

human features	building features	fire features
individual features	engineered features	perceptual features
• personality	• lay out	• visual features
• knowledge & experience	• installations	• smelling features
• powers of observation	• materials	• audible features
• powers of judgement	• compartments	• tangible features
• powers of movement	• size of building	
social features	situational features	fire growth rate
• affiliation (e.g. family)	• focus point	smoke yield
• task fixation	• occupant density	toxicity
• role/responsibility	• ease of way finding	heat
	• building evacuation team	
	• maintenance	
situational features		
• awareness		
• physical position		
• familiarity with layout		

others. Social psychology deals with behavior of an individual in a social environment. This discipline can also be understood as the study of individuals in their interactions with others and the interplay of individual thoughts, feelings, emotions and habits [24]. Social psychology thus examines the question to what degree the behavior of an individual is influenced by behavior of others (relatives, society, groups of people, etc.), meaning that it examines the behavior of individuals with respect to social stimuli in the surroundings [25-26], whether individuals become members of a social group and how they function in these groups. This is therefore an interdisciplinary understanding that derives the laws, development, changes and nature of interpersonal behavior. Social psychology can be defined as the actions people take based on their perception of a situation, their intention to act and considerations ensuing from crowd behavior [7].

Scientific research into human behavior during the adverse events is relatively new. Since the beginning of the 20th century there have been a number of monitored evacuation studies along with investigations of catastrophes in various types of infrastructure [18, 27-28]. Many studies have also been carried out [7, 29-31] showing that the sociological and psychological aspects of human behavior significantly affect the time required for evacuation. These studies have also confirmed an interaction between evacuees, buildings and the course of various emergencies. These three components are presented in Table 1 for the case of a fire.

Kobes [7] defines three component areas that have a fundamental impact on the RSET. The first is human features, which have a direct and primary effect on the level of response to an emergency event and are examined from the perspective of both individuals (individual characteristics) and groups (social and situational characteristics). Another major component is building features, which define the evacuated space and provide crucial information for selecting escape routes. The final area is, in this case, fire features. Here, the characteristics and subsequent development of the emergency event are crucial.

4 Factors influencing the behavior/decision making of people during an evacuation

Understanding the human behavior and decision making during the evacuation process becomes an important aspect of increasing infrastructure safety and ensuring the reliable movement of people. The very movement of heterogeneous groups of people and their interaction is important to properly design buildings and reasonably predict the course of an evacuation [32]. Empirical data on behavior during an evacuation, its effectiveness and the spread of an emergency event is scarce. There are numerical simulations to determine available and required safe exit periods [33-37], however, these are founded on imprecise homogeneous data and ideal groups of individuals. For these reasons, it is necessary to devote increased attention primarily to those factors that significantly affect the behavior and decision-making of people during the evacuation period.

People's behavior is the result of their perception, interpretation and decision-making process, which is influenced by external and internal factors [38-39]. External factors or factors that characterize and shape the building environment (for example, type of a building, number, location and width of emergency exits, location of stairways, application of evacuation signs, bottlenecks, etc.) only affect human behavior to a certain degree. However, internal factors, i.e. human characteristics, are considered as the key factors that determine response to the effects of emergency

events [36]. Kobes [7] claims that individual, social and situational traits are critical, while individual elements can further be broken down into physiological and psychological characteristics [6]. Most authors agree that human characteristics significantly affect people's behavior and have a more significant impact on people's decision making than external factors. For this reason, the following text is devoted only to internal or socio-psychological factors.

4.1 Physiological individual traits

The socio-psychological aspects affect people's decision-making, their search and selection of evacuation routes, the speed and movement of evacuees and fundamentally also affect the RSET. These aspects are characterized by the individual abilities of individuals in combination with the environment in which they find themselves. Important individual physiological characteristics include the composition of people in the evacuation space, their roles, age, gender, mental capacity and body weight. The evacuation time is also influenced by crowd density and percentage of people unable to find an escape route without assistance, presence of people with strollers, etc. [6, 22-23, 32, 40].

4.2 Psychological individual traits

The psychological characteristics of people are also important. These factors include people's cognitive and emotional states. Severe stress or, conversely, refusal to acknowledge the life-threatening events, prevents effective evacuation. Likewise, inaction, apathy or children dependent on other people prevent survivors from evacuating [6, 41]. The relationship between the speed of movement and emotional state has been derived using a theory of extreme values [42]. One must also not to forget the specific characteristics of individuals, which include [43]:

- Instincts - Instincts influence the innate pattern of behavioral response to certain stimuli. A person can act instinctively without even being aware of it. When under the great stress, people tend to follow their instincts as the most primitive response when making split second decisions.
- Experience - Based on previous situations (knowledge of safety procedures, fire safety training, etc.), it is possible to derive a relatively standard routine and then apply it to situations in the future.
- Limited rationality - This assumes decision-making based on evaluation of the alternatives in terms of their implications for preferences, i.e. searching for possibilities; anticipation of consequences; consideration of each consequence with respect to preferences and selection of the most appropriate option.

A relationship between intelligence and evacuation success was also confirmed and it was shown that specific personal characteristics tend to have a small effect on evacuation efficiency. In contrast, psychological states (anxiety, depression, stress, etc.) have a large negative impact on cognitive function, which is essential for an effective evacuation [41]. The field that deals with discovering the laws governing human behavior is psychometry [44]. Three personal traits in particular are important in this approach [7]:

- Leader/follower (active/passive) - This personal trait is very important. Most people during evacuations are followers who do not react to danger signals, but rather wait on others before they start to act. To the contrary, a leader in stress situations is able to make effective decisions. In most cases, leaders are the people who are organizationally responsible for the building based on their roles or positions.
- Resistance to stress - too much physical stress leads can overload one's capacity for processing information and can disrupt cognitive processes (as an individual reacts to the given situation) [45].
- Belief in self-efficacy - to what degree does a given person believe in himself or herself? This affects the efforts they make and the time required to act if they encounter an obstacle.

4.3 Social traits

Actions and decision-making are very strongly influenced by the social bonds existing between individual persons that create groups and shape interpersonal distance. These ties have a significant impact on behavior of the groups formed, which tend to move in mutual agreement and leave areas together [43]. Decisive social characteristics include interaction between the people present, the degree to which tasks are performed and the role of people in the building. In most cases, people tend to work together and respond as a group for as long as possible instead of acting individually. This fact is enhanced if strong social bonds exist between people (family, partners) [7]. All of these aspects impact the course of the evacuation, the response time and decision-making. If people become separated from each other, e.g. a family, this fact can lead to opposing movement and prevent the flow of the crowd as a whole, which may disrupt the permeability of emergency exits [43]. People who are part of a group tend not to make decisions for themselves, but rather wait on the response and decision of others [46]. This fact is supported by the generally accepted notion that an individual in a crowd usually acts differently than when alone [47].

4.4 Situational traits

The last group of factors that influence the behavior of people is associated with situational characteristics

Table 2 *Impact of the socio-psychological aspects on RSET*

socio-psychological aspects		components of the RSET evacuation process		
		recognition time	response time	movement time
individual physiological traits	role	X	X	
	age	X		X
	cognitive ability		X	
	body weight			X
individual psychological traits	instinct	X	X	
	experience	X		X
	limited rationality		X	X
	emotional state /resistance to stress		X	X
	leader/follower	X	X	X
	belief in self-efficacy			X
social traits	interpersonal distance		X	
	strength of social bonds	X	X	X
situational traits	awareness of emergency	X	X	
	physical position of person		X	X
	knowledge of building layout		X	X

including awareness, physical location and knowledge of the building layout [7]. Awareness of an adverse event means certain knowledge about the possible course of the emergency or how it would tend to develop. It is important to mention that awareness is dependent on the alertness of people, which may be reduced by fatigue or consumption of alcohol or narcotics [48]. Physical position means the present position of a person (standing, walking, sitting or lying). The layout of the building and especially knowledge of the layout significantly affects decisions on selecting evacuation routes. Analysis of observed phenomena clearly shows that most people leave buildings along the route they know (usually the main entrance) and thus ignore alternatives that may be more effective [43].

In addition to the aspects above, Sime [49] considers one of the most important aspects to be occupancy, which defines the relationship between people and the environment. This is based on research on human behavior during emergencies and evacuations and research in environmental behavior and environmental psychology. Sime [22] further claims that a person is different in each and every physical (and social) setting and situation. Each person is limited by the conditions and amount of knowledge and action provided by various social, organizational and physical conditions and environments occupied by people over the course of time.

The socio-psychological aspects and behavior of people during evacuation are currently part of most computer programs simulating evacuation conditions in fire safety engineering and crowd safety using the RSET [50-52]. With help of these most advanced, three-dimensional and intelligent computer tools it is possible to predict behavior to a certain degree [46, 53]. The main limitation of these sophisticated systems is the assumption of homogeneity, which presumes that people will react to specific stimuli in a similar manner [54]. Another limiting factor is the technical data describing the movement characteristics of evacuees. This system input data is generally based on young and healthy populations and often does not take into account indisposed people. Yet, the current composition of the population and demographic trends confirm the growing number of handicapped individuals and older or generally less mobile people [55]. In addition to the effects of aging, these people suffer from impaired perception, reduced information processing and reduced mobility [56]. While technical computer evacuations models do exist to estimate movement times of people and their evacuation behavior, these are poorly described and quantified and adopt simplified behavioral assumptions. Thus, this data is highly unrealistic and can provide inaccurate results [43, 57]. It is necessary to enrich all this data with a population structure that is diverse to yield more accurate calculations and ensure evacuation to a safe place. Based on the above, it is essential to apply the socio-psychological aspects to the process of calculating the total evacuation time, since these aspects have a significant impact on the speed, accuracy, efficiency and effectiveness of decision-making.

4.5 Influence of the socio-psychological aspects on evacuation time

It follows from the above that the socio-psychological aspects are a very significant component affecting the reaction time and decision-making process of evacuees, thus affecting the total time required to relocate people to a safe space. Table 2 below presents a qualitative comparison of select psychological aspects

Table 3 *Values of evacuation condition coefficients according to CSN 73 0802 [62]*

evacuees	unprotected escape route
able to move independently	1.0
with limited mobility	1.5
unable to move independently	2.0

Table 4 *Calculation of the preliminary evacuation time according to [62]*

parameters of preliminary evacuation time	value of individual parameters
length of escape route	150 m
speed of evacuee movement	20 $m.min^{-1}$
number of evacuated persons	6000
coefficient of evacuation conditions*	1.25
unit capacity of escape lane	40
number of escape lanes	8
estimated evacuation time	29 min

* *This value was adjusted based on the variability of evacuated persons*

that significantly impact components of the RSET evacuation process.

The recognition time can be described as the time it takes for a person/group of persons to identify and assess the severity of an emergency event according to certain features. The response time is the time it takes for people to react to the severity of an emergency event and the related need to take certain steps leading to subsequent evacuation. The movement time is the time it takes for people to move from an evacuation zone to emergency exits and then to the evacuation center. From Table 2 it follows that the socio-psychological aspects have a significant impact on people's decision-making process in all the phases of evacuation and therefore fundamentally affect total evacuation time. Based on a qualitative comparison of individual components it is possible to identify the most important socio-psychological aspects, including the role of leader/follower and the strength of social bonds. These aspects were then used in the case study.

5 Case study of application of the socio-psychological aspects during the evacuation of a railway terminal

To verify the theory based on current data on the socio-psychological aspects and their practical application, a hub in the transportation infrastructure of the Czech Republic was chosen. Since this is a public space with a very high concentration of people during the day and sometimes also at night, the building in question may be considered a soft target. Specifically, it is a soft target in the transportation category and interchange sub-category [58]. This element was chosen based on its significance, scope, purpose, reliability and assessment of its critical nature [58-59]. This element is interconnected with other systems. Its disruption or failure would have serious implications to the system itself and significant consequences to other critical infrastructure sectors [60]. The area selected is one of the busiest railway stations in the Czech Republic, but for reasons of safety remains anonymous. The station handles an average of 70,000 travelers a day [61]. The complex is quite extensive, consisting of platforms, passages, underground and above-ground floors, stores, restaurants, a concourse and passenger service areas. Given this fact, in this case study the focus was only on the concourse building consisting of one above-ground floor and three underground floors.

In the building there are several contract carriers along with a large number of shops. There are also restaurants, fast food, grocery stores, bookstores, information booths, clothing stores and other passenger services. Travelers not only use this space to access platforms but they also wait here for trains to arrive and depart. Because of this, a large number of people are often gathered here, which is one of the reasons why this building in particular was selected. It is a location with large groups of people and the probability of an attack is greater here [58]. The case study examines the evacuation of the main station due to a violent attack, specifically, a booby-trapped explosive device placed in the station. According to the risk analysis performed [58], this threat is classified as a secondarily significant risk and security against this type of emergency is low.

The anticipated evacuation time is calculated according to Formula 1, where the value for s only represents the values of coefficients determined according to standards [62] and does not reflect the socio-psychological aspects:

$$t_u = \frac{0.75 \cdot l_u}{v_u} + \frac{E \cdot s}{K_u \cdot u}, \tag{1}$$

where: t_u = estimated evacuation time; l_u = length

of escape route; v_u = speed of evacuee movement; E = number of persons evacuated; s = evacuation conditions coefficient; K_u = unit capacity of escape lane; u = number of escape lanes.

These calculations include only the minimal physiological aspects of the persons evacuated, such as able-bodied individuals, persons with reduced mobility or persons unable to move independently. This calculation approach also does not consider the specifics of individuals (i.e. passengers, employees, passenger escorts, etc.), their percentage representation in the total number of evacuees and psychological or social traits. These aspects, however, do affect the total evacuation time.

For calculations were used the coefficient input values given in Table 3, which are set out in CSN 73 0802 [62]. Table 4 then presents values needed to calculate the preliminary evacuation time according to current standards [62].

The simplified calculation of evacuation time carried out is merely an illustrative estimate of anticipated evacuation time. Fictitious values were used in this calculation. The subsequent evacuation time was calculated to be 29 minutes, although this does not include the socio-psychological aspects that enter into all the phases of evacuation (recognition, response and movement time). Based on a survey of the literature, it is presumed that that the inclusion of these aspects would increase the evacuation time. This fact is mainly due to the coefficient of evacuation conditions, which, however, currently only reflects the ability of evacuees to move independently (see Table 3).

In the context of currently identified socio-psychological aspects (see Table 2), the factors determining the coefficient of evacuation conditions are expanded in the following manner:

$$s = f(s_{spo}; s_{fyz}; s_{psy}; s_{soc}; s_{sit}), \quad (2)$$

where: s_{spo} = ability of people to move; s_{fyz} = physiological traits; s_{psy} = psychological traits; s_{soc} = social traits; s_{sit} = situational traits.

The basic parameter s is logically expanded by four variables, i.e. the socio-psychological aspects, affecting evacuation time. The current value of the coefficient of evacuation conditions (see Table 3) is retained, although its impact on the total value of the parameter is considerably lower. The percentage share of the proposed parameters cannot be clearly defined under the current conditions, especially due to a lack of professional studies on human behavior during evacuation. At present, studies do exist showing that individual aspects impact evacuation time, e.g. it has been demonstrated that up to 73% of people evacuate with one or more member of a group and 80% of these are family members [63]. Nevertheless, this and similar research does not determine the significance or mutual comparison of individual aspects. This fact represents a gap in research that must be addressed in the future.

Another condition that must be met by parameter s is its total value, which lies within a closed interval of <1, 2> but must not exceed the upper limit of two. This value represents the movement time of people incapable of independent movement, i.e. double the evacuation time of people capable of independent movement, that is set by the standard [62]. When maintaining the parameters of Table 4 and setting the highest possible values for the coefficient of evacuation conditions, it can be concluded that the estimated evacuation time should not be more than 43 minutes. The time difference between calculations (29, 43), represents the increase in evacuation time after expanding parameter s. These 14 minutes represents the variability and percentage share of the socio-psychological aspects.

6 Conclusion

Evacuation is the primary way of protecting soft targets and other types of buildings (e.g. structures and property used for education, social care, health care, culture, public administration, public safety etc.) [64-65], and above all the people inside them in the event of an emergency event [66]. The correct and accurate estimation of evacuation time is essential for ensuring the relocation of people to a safe place in the life-threatening and dangerous conditions. This fact is also the primary challenge for researchers developing evacuation simulations and people responsible for building and operating infrastructure.

The time interval for determining the total evacuation time is commonly determined according to the formula for calculating the RSET. Although this tool has been used for many years, under current conditions it is ineffective due to major shortcomings. Estimated evacuation time calculated according to this approach does not reflect the human factors that enter into the evacuation process. These socio-psychological aspects of human behavior and subsequent decision-making significantly affect the time required to evacuate people. This claim is backed by experimental and post-incident studies that imply patterns of human behavior. Research has shown, however, that these formulas are generally obtained from homogeneous groups of people that are not variable and do not reflect the actual composition of the populace. In this context, it is necessary to focus research on the diverse composition of the population and examine the specifics of people unable to move without assistance, people with limited mobility, senior citizens, etc.

The article also presents a source of information, systematically performed research analysis that serves as a basis for further development of simulation tools necessary to determine the total evacuation time. This article points out the shortcomings of using the current calculation approach according to the RSET and the need to update it. The current calculation

process must also incorporate the socio-psychological aspects affecting the behavior and decision-making of people. Based on the above, it is necessary to address this issue and develop a complete and comprehensive conceptual model of human behavior and decision-making during evacuations. This model would have a major impact on training and education and would also enable complete behavioral patterns of behavior to be incorporated into the simulation tools. In the future, it would also be desirable to create a better methodology or incorporate artificial intelligence and machine vision in the evacuation calculation process, making it possible to obtain the real-time evacuation estimates. The systems developed should use measurements and data based on knowledge of psychological methodology and mathematical statistics to maximize their predictive power. In the context of the above, classification of the socio-psychological aspects is an important input variable for the further development of tools and optimization of evacuation procedures.

Acknowledgments

This work was supported by the Technology Agency of the Czech Republic [grant number TL02000352].

Reference

[1] REHAK, D., SENOVSKY, P., HROMADA, M., LOVECEK, T., NOVOTNY, P., Cascading impact assessment in a critical infrastructure system. *International Journal of Critical Infrastructure Protection* [online]. 2020, **30**, p. 125-138 [accessed 2020-10-11]. ISSN 1874-5482. Available from: https://doi.org/10.1016/j.ijcip.2018.06.004

[2] RISTVEJ, J., ONDREJKA, R., SIMAK, L., LOVECEK, T., HOLLA, K., LACINAK, M., SURINOVA, L., JANOSIKOVA, M., Simulation technologies in risk prevention within crisis management. In: 30th European Simulation and Modeling Conference ESM 2016: proceedings. Vol. 2016. ISBN 978-907738195-3.

[3] VICHOVA, K., HROMADA, M., REHAK, D. The use of crisis management information systems in rescue operations of fire rescue service of the Czech Republic. *Procedia Engineering* [online]. 2017, **192**, p. 947-952 [accessed 2020-10-11]. ISSN 1877-7058. Available from: https://doi.org/10.1016/j.proeng.2017.06.163

[4] JAKUBCOVA, L., URBAN, R., KOMASOVA, S., BRICHCIN, P. Crisis management and psychology of evacuees: parameters for streamlining evacuation planning for soft target operators (in Czech). *Security Theory and Practice* [online]. 2020, **1**(2020), p. 3-34 [accessed 2020-10-11]. ISSN 1801-8211, eISSN 2571-4589. Available from: https://veda.polac.cz/?page_id=6004

[5] Decree of the Ministry of the Interior 380 of 22 August 2002 on the preparation and implementation of tasks for the protection of the population (in Czech).

[6] CHEN, S., DI Y., LIU S, WANG, B. Modelling and analysis on emergency evacuation from metro stations. *Mathematical Problems in Engineering* [online]. 2017, 2623684 [accessed 2020-10-11]. ISSN 1024-123X, eISSN 1563-5147. Available from: https://doi.org/10.1155/2017/2623684

[7] KOBES, M., HELSLOOT, I., DE VRIES, B., JOS G.P. Building safety and human behaviour in fire: a literature review. *Fire Safety Journal* [online]. 2010, **45**(1), p. 1-11 [accessed 2020-10-11]. ISSN 0379-7112. Available from: https://doi.org/10.1016/j.firesaf.2009.08.005

[8] ZHANG, J., SEYFRIED, A. Quantification of bottleneck effects for different types of facilities. *Transportation Research Procedia* [online]. 2014, **2**, p. 51-59 [accessed 2020-10-11]. ISSN 2352-1465. Available from: https://doi.org/10.1016/j.trpro.2014.09.008

[9] GEOERG, P., SCHUMANN, J., BOLTES, M., HOLL, S., HORMANN, A. The influence of physical and mental constraints to a stream of people through a bottleneck. *Collective Dynamics* [online]. 2020, **5**(2020), p. 246-252 [accessed 2020-10-11]. ISSN 2366-8539. Available from: http://dx.doi.org/10.17815/CD.2020.57

[10] KU, Y.C., CHOW, W.K, YUE, T.K. Fire evacuation in a large railway interchange station. In: 11th Asia-Oceania Symposium on Fire Science and Technology: proceedings [online]. Singapore: Springer, 2018. ISBN 978-981-32-9139-3. Available from: https://doi.org/10.1007/978-981-32-9139-3_18

[11] POON, S. L. A Dynamic approach to ASET/RSET assessment in performance based design. *Procedia Engineering* [online]. 2014, **71**(2014), p. 173-181 [accessed 2020-10-11]. ISSN 1877-7058. Available from: https://doi.org/10.1016/j.proeng.2014.04.025

[12] KULIGOWSKI, E. D., GWYNNE, S. M., KINSEY, M. J., HULSE, L. Guidance for the model user on representing human behavior in egress models. *Fire Technology* [online]. 2017, **53**(2), p. 649-672. [accessed 2020-10-11]. ISSN 0015-2684, eISSN A1572-8099. Available from: https://doi.org/10.1007/s10694-016-0586-2

[13] TOSOLINI, E., GRIMAZ, S., PECILE, L.C., SALZANO, E. People evacuation: simplified evaluation of available safe egress time (ASET) in enclosures. *Chemical Engineering Transactions* [online]. 2012, **26**, p. 501-506. [accessed 2020-10-11]. ISSN 1974-9791. Available from: https://doi.org/10.3303/CET1226084

[14] APELTAUER, T., BENES, P., VRANA, L. Application of advanced models of human movement and fire dynamics for safe evacuation of people and risk analysis (in Czech) [online] [accessed 2020-10-11]. 2015. Available from: https://www.profesis.cz/files/dokumpdf/ruzne/r7-2metodikapdf.pdf

[15] FORELL, B., KLUPFEL, H., SCHNEIDER, V., SCHELTER, S. Comparison of evacuation simulation models Aseri, building Exodus, FDS+Evac and PedGo applied to an auditorium. In: Pedestrian and Evacuation Dynamics: proceedings [online] [accessed 2020-10-11]. 2012. Available from: https://doi.org/10.13140/2.1.5156.6725

[16] TOSOLINI, E., GRIMAZ, S., SALZANO, E. A Sensitivity analysis of available safe egress time correlation. *Chemical Engineering Transactions* [online]. 2013, **31**, p. 223-228 [accessed 2020-10-11]. ISSN 1974-9791. Available from: https://doi.org/10.3303/CET1331038

[17] COOPER, L. Y. A concept for estimating available safe egress time in fires. *Fire Safety Journal* [online]. 1983, **5**(2), p. 135-144 [accessed 2020-10-11]. ISSN 0379-7112. Available from: https://doi.org/10.1016/0379-7112(83)90006-1

[18] HAGHANI, M., SARVI, M. Human exit choice in crowded built environments: Investigating underlying behavioural differences between normal egress and emergency evacuations. *Fire Safety Journal* [online]. 2016, **85**, p. 1-9 [accessed 2020-10-11]. ISSN 0379-7112. Available from: https://doi.org/10.1016/j.firesaf.2016.07.003

[19] BABRAUSKAS, V., FLEMING, J. M., RUSSELL, D. B. RSET/ASET, a flawed concept for fire safety assessment. *Fire and Materials* [online]. 2010, **34**(7), p. 341-355 [accessed 2020-11-10]. ISSN 1099-1018. Available from: https://doi.org/10.1002/fam.1025

[20] GWYNNE, S. N. V. Translating behavioural theory of human response into modelling practice. Technical report [online] [accessed 2020-10-11]. 2012. Available from: https://tsapps.nist.gov/publication/get_pdf.cfm?pub_id=912794

[21] SCHRODER, B., ARNOLD, L., SEYFRIED, A. A map representation of the ASET-RSET concept. *Fire Safety Journal* [online]. 2020, **115**, 103154 [accessed 2020-10-11]. ISSN 0379-7112. Available from: https://doi.org/10.1016/j.firesaf.2020.103154

[22] SIME, J. D. An occupant response shelter escape time (ORSET) model. *Safety Science* [online]. 2001, **38**(2), p. 109-125 [accessed 2020-10-11]. ISSN 0925-7535. Available from: https://doi.org/10.1016/S0925-7535(00)00062-X

[23] GEOERG, P., BLOCK, R., HEISTER, W., HOLL, S., PULM, A., HOFMANN, A. A score regarding the need for assistance - considering pedestrians with impairments in evacuation planning. In: 5th Magdeburg Fire and Explosion Prevention Day: proceedings [online] [accessed 2020-10-11]. 2017. Available from: http://dx.doi.org/10.978.300/0562013

[24] YOUNG, K. *Handbook of social psychology*. 2. ed. London: Kegan Paul, Trencil Trubner and Co. Ltd., 1957. ISBN-13 978-0710032379.

[25] JONES, E. E., GERARD, H. B. *Foundations of social psychology*. New York - London- Sydney: John Willey and Sons. Inc., 1967. ISBN 0-471-44906-7.

[26] SHERIF, M., SHERIF, C. W. *An outline of social psychology*. 2. ed. New York: Harper, 1956.

[27] MCCONNELL, N. C., BOYCE, K. E., SHIELDS, J., GALEA, E. R., DAY, R. C., HULSE, L. M. The UK 9/11 evacuation study: analysis of survivors' recognition and response phase in WTC1. *Fire Safety Journal* [online]. 2010, **45**(1), p. 21-34 [accessed 2020-10-11]. ISSN 0379-7112. Available from: https://doi.org/10.1016/j.firesaf.2009.09.001

[28] JEON, G. Y., KIM, J. Y., HONG, W. H., AUGENBROE, G. Evacuation performance of individuals in different visibility conditions. *Building and Environment* [online]. 2011, **46**(5), p. 1094-1103 [accessed 2020-10-11]. ISSN 0360-1323. Available from: https://doi.org/10.1016/j.buildenv.2010.11.010

[29] FAHY, R., PROULX, G. Toward creating a database on delay times to start evacuation and walking speeds for use in evacuation modelling. In: 2nd International Symposium on Human Behaviour in Fire: proceedings [online] [accessed 2020-10-11]. 2001. Available from: https://nrc-publications.canada.ca/eng/view/accepted/?id=4fef7a5e-f184-408a-b11f-3ffbf2a61ddf

[30] GWYNNE, S., BOYCE, K. Engineering data. In: *SFPE Handbook of fire protection engineering.* New York, NY: Springer, 2016. ISBN 978-1-4939-2565-0, p. 2429-2551.

[31] GEOERG, P., POLZIN, M. R., SCHUMANN, J., HOLL, S., HOFMANN, A. Small-scale studies on evacuation characteristics of pedestrians with physical, mental or age-related disabilities. In: 3rd European Symposium on Fire Safety Science: proceedings [online] [accessed 2020-10-11]. 2018. Available from: http://juser.fz-juelich.de/record/858301

[32] GEOERG, P., SCHUMANN, J., HOLL, S., BOTLES, M., HOFMANN, A. The influence of individual impairments in crowd dynamics. *Fire and Materials* [online]. 2020, **2** [accessed 2020-10-11]. ISSN 1099-1018. Available from: https://doi.org/10.1002/fam.2789

[33] KONNECKE, R., SCHNEIDER, V. Evacuation from underground railway stations - available and required safe egress time for different station types and general evaluation criteria. In: Pedestrian and Evacuation Dynamics 2005: proceedings. Berlin: Springer, 2007. ISBN 978-3-540-47064-9, p. 363-368.

[34] TISSERA, P. C., CASTRO, A., PRINTISTA, A. M., LUQUE, E. Evacuation simulation supporting high level behaviour-based agents. *Procedia Computer Science* [online]. 2013, **18**(2013), p. 1495-1504 [accessed 2020-10-11]. ISSN 1877-0509. Available from: https://doi.org/10.1016/j.procs.2013.05.317

[35] BURSTEDDE, C., KLAUCK, K., SCHADSCHNEIDER, A., ZITTARTZ, J. Simulation of pedestrian dynamics using a two-dimensional cellular automaton. *Physica A: Statistical Mechanics and its Applications* [online]. 2001, **295**(3-4), p. 507-525 [accessed 2020-10-11]. ISSN 0378-4371. Available from: https://doi.org/10.1016/S0378-4371(01)00141-8

[36] CABOVA, K., APELTAUER, T., OKRINOVA, P., WALD, F. Application of fire and evacuation models in evaluation of fire safety in railway tunnels. In: Building up Efficient and Sustainable Transport Infrastructure 2017: proceedings. Vol. 236. Materials Science and Engineering. 2017. ISSN 1757-8981.

[37] MOZER, V., OSVALD, A., LOVECEK, T., FANFAROVA, A., VRABLOVA, L. Fire safety in tunnels forming part of critical infrastructure. In: International Carnahan Conference on Security Technology ICCST: proceedings. Vol. 2013. Montreal, QC, Canada: Institute of Electrical and Electronics Engineers Inc., 2013. ISBN 978-147990889-9.

[38] ZHAO, X., LOVREGLIO, R., NILSSON, D. Modelling and interpreting pre-evacuation decision-making using machine learning. *Automation in Construction* [online]. 2020, **113**, 103140 [accessed 2020-10-11]. ISSN 0926-5805. Available from: https://doi.org/10.1016/j.autcon.2020.103140

[39] KULIGOWSKI, E. D. Modeling human behavior during building fires. National Institute of Standards and Technology - Technical Note 1619 [online] [accessed 2020-10-11]. 2008. Available from: http://citeseerx.ist.psu.edu/viewdoc/download?doi=10.1.1.462.3209&rep=rep1&type=pdf

[40] LOVREGLIO, R., RONCHI, E., NILSSON, D. A model of the decision-making process during pre-evacuation. *Fire Safety Journal* [online]. 2015, **78**, p. 168-179 [accessed 2020-10-11]. ISSN 0379-7112. Available from: https://doi.org/10.1016/j.firesaf.2015.07.001

[41] VORST, H. C. M. Evacuation models and disaster psychology. *Procedia Engineering* [online]. 2010, **3**, p. 15-21 [accessed 2020-10-11]. ISSN 1877-7058. Available from: https://doi.org/10.1016/j.proeng.2010.07.004

[42] KHOLSHEVNIKOV, V. V., SHIELDS, T. J., BOYCE, K. E., SAMOSHIN, D. A. Recent developments in pedestrian flow theory and research in Russia. *Fire Safety Journal* [online]. 2008, **43**(2), p. 108-118 [accessed 2020-10-11]. ISSN 0379-7112. Available from: https://doi.org/10.1016/j.firesaf.2007.05.005

[43] PAN, X., HAN, CH. S., DAUBER, K., LAW, K. H. Human and social behavior in computational modeling and analysis of egress. *Automation in Construction* [online]. 2006, **15**(4), p. 448-461 [accessed 2020-10-11]. ISSN 0926-5805. Available from: https://doi.org/10.1016/j.autcon.2005.06.006

[44] VERWEY, W. B. Theory of psychological functions and cognitive ergonomics: connected? (in Dutch). *Tijdschrift voor Ergonomie*. 2004, **29**(2), p. 4-9. ISSN 0921-4348

[45] PROULX, G. A stress model for people facing a fire. *Journal of Environmental Psychology* [online]. 1993, **13**, p. 137-147 [accessed 2020-10-11]. ISSN 0272-4944. Available from: https://doi.org/10.1016/S0272-4944(05)80146-X

[46] KULIGOWSKI, E. D., PEACOCK, R. D., HOSKINS, B. L. A review of building evacuation models - technical note 1680 [online] [accessed 2020-10-11]. 2010. Available from: https://tsapps.nist.gov/publication/get_pdf.cfm?pub_id=906951

[47] BRAUN, A., MUSSE, S., OLIVEIRA, L. D., BODMANN, B. Modeling individual behaviors in crowd simulation. In: 16th International Conference on Computer Animation and Social Agents: proceedings. 2003. ISBN 0-7695-1934-2, p. 143-148.

[48] BRUCK, D. The who, what, where and why of waking to fire alarms: a review. *Fire Safety Journal* [online]. 2001, **36**(7), p. 623-639 [accessed 2020-10-11]. ISSN 0379-7112. Available from: https://doi.org/10.1016/S0379-7112(01)00025-X

[49] SIME, J. D. What is environmental psychology? Texts, content and context. *Journal of Environmental Psychology* [online]. 1999, **19**(2), p. 191-206 [accessed 2020-10-11]. ISSN 0272-4944. Available from: https://doi.org/10.1006/jevp.1999.0137

[50] GWYNNE, S., GALEA, E. R., OWEN, M., LAWRENCE, P. J., FILIPPIDIS, L. A review of the methodologies used in the computer simulation of evacuation from the built environment. *Building and Environment* [online]. 1999, **34**, p. 741-749 [accessed 2020-10-11]. ISSN 0360-1323. Available from: https://doi.org/10.1016/S0360-1323(98)00057-2

[51] KULIGOWSKI, E. D. Review of 28 egress models. In: Proceedings of the Workshop on Building Occupant Movement during Fire Emergencies [online] [accessed 2020-10-11]. 2005. p. 66-88. Available from: https://pdfs.semanticscholar.org/89e0/045d33aeaeaebd6be346eaccb9b403193e9a.pdf

[52] SANTOS, G., AGUIRRE, B. E. A critical review of emergency evacuation simulation models. In: Proceedings of the Workshop on Building Occupant Movement during Fire Emergencies [online] [accessed 2020-10-11]. 2005. p. 25-50. Available from: https://pdfs.semanticscholar.org/89e0/045d33aeaeaebd6be346eaccb9b403193e9a.pdf

[53] PELECHANO, N., MALKAWI, A. Evacuation simulation models: challenges in modeling high rise building evacuation with cellular automata approaches. *Automation in Construction* [online]. 2008, **17**(4), p. 377-385 [accessed 2020-10-11]. ISSN 0926-5805. Available from: https://doi.org/10.1016/j.autcon.2007.06.005

[54] KULIGOWSKI, E. D. Predicting human behavior during fires. *Fire Technology* [online]. 2013, **49**, p. 101-120 [accessed 2020-10-11]. ISSN 0015-2684, eISSN 1572-8099. Available from: https://doi.org/10.1007/s10694-011-0245-6

[55] GEOERG, P., BERCHTOLD, F., GWYNNE, S. M. V., BOYCE, K. E., HOLL, S., HOFMANN, A. Engineering egress data considering pedestrians with reduced mobility. *Fire and Materials* [online]. 2019, **39**(2), p. 759-781 [accessed 2020-10-11]. ISSN 1099-1018. Available from: https://doi.org/10.1002/fam.2736

[56] GEOERG, P., HOFMANN, B. A., PULM, A. Evacuation dynamics under consideration of vulnerable pedestrian groups. In: 14th International Fire Science and Engineering Conference: proceedings. Vol. 1. London: Royal Holloway College, 2016. ISBN 978-0-9933933-1-0.

[57] KULIGOWSKI, E. D., GWYNNE, S. M. V. The need for behavioral theory in evacuation modeling. In: Pedestrian and Evacuation Dynamics 2008: proceedings. Berlin: Springer, 2010. ISBN 978-3-642-04504-2, p. 721-732.

[58] APELTAUER, T., HROMADA, M., KOTKOVA, D. Risk analysis of the Prague main railway station as a soft target in different attack scenarios (in Czech). Brno: Brno University of Technology, 2020.

[59] REHAK, D., SLIVKOVA, S., PITTNER, R., DVORAK, Z. Integral approach to assessing the criticality of railway infrastructure elements. *International Journal of Critical Infrastructures* [online]. 2020, **16**(2), p. 107-129 [accessed 2020-10-11]. ISSN 1475-3219, eISSN 1741-8038. Available from: https://doi.org/10.1504/IJCIS.2020.107256

[60] REHAK, D., NOVOTNY, P. Bases for modeling the impacts of the critical infrastructure silure. *Chemical Engineeging Transactions* [online]. 2016, **53**, p. 91-96 [accessed 2020-10-11]. ISSN 2283-9216. Available from: https://doi.org/10.3303/CET1653016

[61] LEITNER, B., REHAK, D., KERSYS, R. The new procedure for identification of infrastructure elements significance in sub-sector railway transport. *Communications - Scientific Letters of the University of Zilina* [online]. 2018, **20**(2), p. 41-48 [accessed 2020-10-11]. ISSN 1335-4205, eISSN 2585-7878. Available from: http://komunikacie.uniza.sk/index.php/communications/article/view/86

[62] CSN 73 0802: Fire protection of buildings - non-industrial buildings (in Czech). Prague: Office for Technical Standardization, Metrology and State Testing, 2009.

[63] MAWSON, A. R. Understanding mass panic and other collective responses to threat and disaster. *Psychiatry* [online]. 2005, **68**(2), p. 95-113 [accessed 2020-10-11]. ISSN 0033-2747, eISSN 1943-281X. Available from: https://doi.org/10.1521/psyc.2005.68.2.95

[64] LOVECEK, T., Present and future ways of physical property protection. *Communications - Scientific Letters of the University of Zilina* [online]. 2008, **10**(1), p. 35-39 [accessed 2020-10-11]. ISSN 1335-4205, eISSN 2585-7878. Available from: http://komunikacie.uniza.sk/index.php/communications/article/view/1028

[65] SIMAK, L., RISTVEJ, J. The present status of creating the security system of the Slovak Republic after entering the European Union. *Journal of Homeland Security and Emergency Management* [online]. 2009, **6**(1), 20 [accessed 2020-10-11]. ISSN 1547-7355. Available from: https://doi.org/10.2202/1547-7355.1443

[66] ZAGORECKI, A., RISTVEJ, J., COMFORT, L. K., LOVECEK, T. Executive dashboard systems for emergency management. *Communications - Scientific Letters of the University of Zilina* [online]. 2012, **14**(2), p. 82-89 [accessed 2020-10-11]. ISSN 1335-4205, eISSN 2585-7878. Available from: http://komunikacie.uniza.sk/index.php/communications/article/view/751

THE METHODOLOGY TO EVALUATE A RESCUE AND TRAINING PHANTOM FOR THE ROAD RESCUING ORGANIZED BY POLICE OFFICERS AS EXEMPLIFIED BY CRASH KELLY

Pawel Gromek*, Mariusz Nepelski

The Main School of Fire Service, Warsaw, Poland

*E-mail of corresponding author: pgromek@sgsp.edu.pl

Resume

The paper presents a methodology to evaluate a rescue and training phantom for road rescuing organized by Police officers. The methodology is exemplified by the Crash Kelly phantom, static and dynamic functionalities of which seem to be more frequently implemented in the road safety training processes. It stems from a morphological analysis, focusing on the quality of rescue activities, emergency resources' adequacy and the training levels. In addition, experts' evaluation allows to examine phantoms using 6 practically determined criteria, expressing their strengths and weaknesses in analysed context.

The results introduce Crash Kelly as a reference training equipment for Police officers dedicated to rescue victims after the road accidents. Basing on the research results, practical training guidelines are formulated.

Article info

Received 7 September 2020
Accepted 14 December 2020
Online 28 April 2021

Keywords:

road safety,
training,
phantom,
police,
rescue

Available online: https://doi.org/10.26552/com.C.2021.3.F83-F95

ISSN 1335-4205 (print version)
ISSN 2585-7878 (online version)

This is an open access article distributed under the terms of the Creative Commons Attribution 4.0 International License (CC BY 4.0), which permits use, distribution, and reproduction in any medium, provided the original publication is properly cited. No use, distribution or reproduction is permitted which does not comply with these terms.

1 Introduction

According to the World Health Organisation (WHO), approximately 1.35 million people die in road accidents on a yearly basis, while the relevant economic effects of such ones, in the case of the majority of states, consume as much as 3% of their Gross Domestic Products (GDP) [1]. The Sustainable Development Goals (SDGs), set forth by the United Nations Organisation (UN), address the aforementioned factors as they refer, among others, to the provision of life in health and the promotion of prosperity (SDG3), the erection of resistant infrastructure, promotion of common and sustainable industrialization and development of innovations (SDG9), as well as making the cities accessible, safe, resistant and developed in a sustainable manner (SDG11) [2-3]. Their interpretation remains under the influence of progressive enhancement of transportation in developing countries [4].

One of the practical measures to reduce the risk of road accidents (the risk understood as a road safety level factor [5-7] and an indirect implementation of the SDGs) includes educational activities - directed towards the commonly enhanced awareness of the rules of conduct in the case of road accidents (including the first aid), as well as training actions dedicated to such services, which professionally handle adverse events.

While focusing on the latter case, it should be underlined that the said trainings include predominantly emergency response teams and the units of the fire service (in Poland, such ones being included into the State Firefighting Rescue System - SFRS). They are undoubtedly associated with providing medical assistance in the case of road accidents. Bearing in mind the following context, training activities dedicated towards Police officers, a subsequent link (apart from the emergency response teams and the fire service units) to complement the question of the so-called first responders, constitutes a theoretical and practical gap. The said groups of entities react as first when human lives and health are jeopardised. The importance of the previously mentioned gap has been underlined by the implementation of the project financed by the National Centre for Research and Development in Poland, entitled "A simulator to support the training for Police officers in performing the actions at the scene of a road accident (No DOB-BIO9/06/01/2018 [8-9]). The main objective of the project included development of a simulator, which would make it possible to obtain practical skills to carry out the actions at the scene of a road accident. It has been assumed that the simulator in question ought to support the training process for Traffic Police officers with regards to typical and non-typical situations (e.g. mass events, supporting the emergency units) and combine virtual and real worlds. The key element of the said combination was to implement the rescue and training phantoms into the

training process dedicated to Police officers.

The following article presents partial outcomes of the designing works described as the products of the project no I.2 *The Technical and operational requirements for the module responsible for the implementation of 3 rescue and training phantoms into the didactic process* [10] as well as number III.6 entitled: *The Report on the examinations over the module responsible for the implementation of 3 rescue and training phantoms into the didactic process* [11]. They refer to the methodology used to evaluate the rescue and training phantoms for the road rescuing organized by Police officers.

Due to the practicality of its application in the course of the training process, with an intention to maximize its realism, the methodology has been realized with the rescue and training phantom of Crash Kelly type as an example. The examinations were carried out within the period between February-June 2020 by the experts team from the Main School of Fire Service in Warsaw (Poland) (MSFS).

The findings obtained throw light on capabilities and implementation range for the evaluated phantom with regards to the training process intended for Police officers worldwide, based on the commonly available training equipment and reference scenarios of road accidents.

2 Methodology

2.1 Formulation of the examination scenarios

Formulation of the examination scenarios constitute the first stage in implementation of the methodology for evaluation of the rescue and training phantom within the analysed context. As assumed, they will allow to present idealized fragments of the reality, which could serve as the background in the training processes for Police officers devoted to providing the first aid under the circumstances of road accidents. The scenarios themselves can come in great numbers [12]. Close links to the real conditions of the state of emergency, corresponding to formal requirements, are desirable from a practical perspective [13] and allow to limit the scenario quantity and their variants to the optimal level.

Basically, the examination scenarios ought to be formulated based on the regulations, which impose the norms over the issue of medical assistance provision by Police officers in road incidents. Hence, they must include the wording of the following documents:

1. The Act dated 24th August 1991 on fire protection (i.e. the Journal of Laws from the year 2020, item. 961).
2. The Act dated 8th September 2006 on the State Medical Rescue Service (i.e. the Journal of Laws from the year 2020, item. 882).
3. Enactment of the Minister of Internal Affairs dated 3rd July 2017 on the detailed organization of the State Firefighting Rescue System (Journal of Laws from the year 2017, item 1319)
4. Ruling no 36 of the Police Commander in Chief dated 14th November 2017 regarding the tasks to be carried out by the Police in emergency situations (Journal of Laws of the Police Headquarters from the year 2017, item 73)
5. Decision no 168 of the Police Commander in Chief dated 22nd May 2019 on the basic vocational training programme (Journal of Laws of the Police Headquarters from the year 219, item 83)
6. Decision no 472 of the Police Commander in Chief dated 18th November 2013 regarding the traffic specialist course programme - general part (Journal of Laws of the Police Headquarters, item 95, from the year 2014, item 61 and from the year 2017, item 83)
7. Decision no 229 of the Police Commander in Chief dated 27th July 2016 regarding the syllabus for the specialist course on the provision of the first aid (Journal of Laws from the year 2016, item 35)
8. The principles for the organization for medical rescuing within the national rescue and fire system. Headquarters of State Fire System, Warsaw 2013.

The outcomes of the analysis, with regards to the aforementioned normative documents, make it possible to get acquainted with the permissible, proper circumstances, the range and manners of operations. They additionally ameliorate to define the factors, which determine the formulation of examination scenarios, while respecting the quality of actions taken with regards to medical assistance, the level of trainings received by Police officers, as well as the adequacy of resources at disposal for the said formation at the scene of an incident. Figure 1 demonstrates their morphological recognition.

One of the factor groups seems to have the strongest impact over the formulation of scenarios under the examined context in quantitative approach. This includes the degree of adequacy for Police resources, which arrive at the scene of an event. Taking such one into account makes us consider three predominant variants of scenarios:

1. Single event variant - during which one person being a participant of the event was injured.
2. Numerous event variant - when more than one injured person was registered, however the total number of casualties does not exceed capabilities of resources from safety entities being on site (including the Police).
3. Mass event variant - if more than one injured person was registered and the total number of casualties exceeds capabilities of resources from the safety entities being on site (including the Police).

2.2 Analysis of the phantom functionality

The formulation of examination scenarios shall determine the general frameworks for examinations

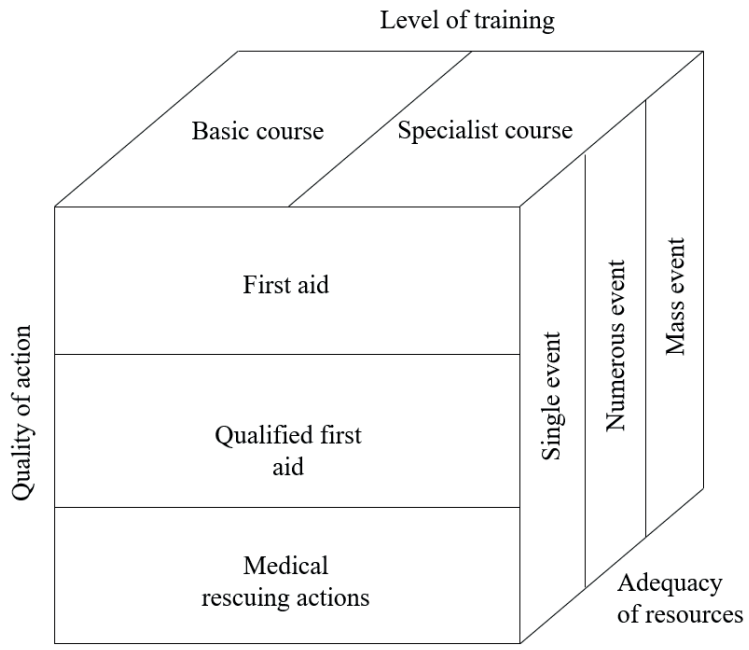


Figure 1 *Morphological recognition of factors that determine the formulation of examination scenarios*

of the rescue and training phantom. It has been assumed to be relatively detailed as far as its wording is concerned. Its adjustment to the real conditions remains indispensable, bearing in mind the operationalization of the training process for the Police officers. Hence, the analysis of the rescue and training phantom functionality ought to constitute a consecutive step in the methodology. It will provide a detailed description of the technical constraints for the training process.

Based on the peculiarities of the training process in the first aid, the functionalities of the rescue and raining phantom may be divided into the following categories:

1) Static functionalities,
2) Dynamic functionalities.

The static functionalities are related to an invariant character of the equipment location and position during the implementation of the didactic process. They refer to modifications in the phantom design and the degree to which a body position of an injured person has been represented. They are demonstrated by a system of joints and soft parts of the rescue and training phantom, which determine the mobility ranges for the head and limbs.

On the other hand, the dynamic functionalities are related to the range within which the location and position of equipment during the didactic process can be altered. They refer to a possibility of simulation for emergency response evacuation, as well as placing and sitting the phantom in an optimal position due to rescuing actions to be performed.

Both of the types determine practical capabilities for using the training equipment. They may limit the original number of examination scenarios only to such ones, which will be technically viable.

2.3 Evaluation methods for the phantom functionalities

Bearing in mind the authors' experience in rescuing operations, as well as the outcomes of the hitherto completed designing works, it has been stated that functionalities of the rescue and training phantom should be considered from the perspective of its static and dynamic equivalents. As it has been mentioned already, the first case includes the questions related to an invariant character of the equipment location and position, while implementing the training process in contrast to the latter group of functionalities.

Due to the peculiarities in the training for Police officers, regarding the first aid provided in road incidents, static functionalities include:

1) S1: the degree to which an injury is represented;
2) S2: the degree to which a body position of an injured person is represented.

The degree of an injury representation means the phantom's potential to realistically visualize the effects of a road incident over an injured person - the effects conditioned by a precise examination scenario and determining the necessity to take up the relevant rescuing actions. The degree to which an injury is represented may be evaluated in line with a check list, considering the levels of an injury representation degree set forth by Table 1.

The degree to which a body position of an injured person is represented means the compliance of the road incident effect translating into the said person's position found - the position in which the phantom should be placed when the rescuing actions are commenced (directly after the Police officers have appeared at the scene of a road incident).

Table 1 *The levels for evaluation of an injury representation degree*

criterion level	description of meanings for an evaluation criteria having been met
1	The lack of realism in the injury representation with reference to given conditions of an examination scenario. Phantom's usage ought to be limited to being a teaching aid of the situational background.
2	The phantom represents an injury with reference to given conditions of an examination scenario to a degree that allows for it to be used as a teaching aid with noticeable support from an instructor (real aid in performing the recuing actions).
3	The phantom represents an injury with reference to given conditions of an examination scenario to a degree that allows for it to be used as a main teaching aid with the minimum support from an instructor (coordination of the rescuing actions performance)
4	The phantom represents an injury fully with reference to given conditions of an examination scenario. It may be used to perform full simulation of the sequencing for the rescuing action required under given circumstances.

Table 2 *The levels for evaluation of a body position of an injured person representation*

criterion level	description of meanings for an evaluation criteria having been met
1	The lack of realism in representation of a body position for an injured person with reference to given conditions of an examination scenario. Phantom's usage ought to be limited to being a teaching aid of the situational background.
2	The phantom represents a body position of an injured person with reference to given conditions of an examination scenario to a degree that allows for it to be used as a teaching aid with noticeable support from an instructor (real aid in performing the recuing actions)
3	The phantom represents a body position of an injured person with reference to given conditions of an examination scenario to a degree that allows for it to be used as a main teaching aid with the minimum support from an instructor (coordination of the rescuing actions performance only)
4	The phantom represents fully a body position of an injured person with reference to given conditions of an examination scenario.

Table 3 *The evaluation levels for representation of the possibility to transfer from a danger zone to a safe zone*

criterion level	description of meanings for the evaluation criterion having been met
1	The lack of possibility to transfer the phantom from a danger zone to a safe zone.
2	A possibility to transfer the phantom from a danger zone to a safe zone with the lack of possibility to continue the rescuing actions within a simulation.
3	A possibility to transfer the phantom from a danger zone to a safe zone while the continuation of rescuing actions is secured once the phantom has been prepared for the simulation again.
4	A possibility to transfer the phantom from a danger zone to a safe zone while the continuation of rescuing actions is secured without further delay.

The degree to which a body position of an injured person represented may be evaluated in line with a check list, considering the levels of a body position of an injured person representation degree set forth by Table 2.

Due to peculiarities in the training for Police officers, regarding the first aid provided in road incidents, dynamic functionalities include:

1) D1: the degree to represent the possibility to transfer from a danger zone to a safe zone (as understood by emergency response evacuation)
2) D2: the degree to represent the possibility to place in the position suitable to provide the first aid
3) D3: the degree to represent the realism of rescuing actions execution
4) D4: the degree to represent the possibility to alter the phantom's position while providing the first aid.

The degree to represent the possibility to transfer from a danger zone to a safe zone ought to be analysed, while bearing in mind the necessity to carry out the emergency response evacuation for an injured person from the place where they have been found within a danger zone due to the life-threatening circumstances having been detected. This implies the promptness of evacuation activities including the transfer of the phantom from one place (associated with the danger zone) to another spot (understood as the location of the safe zone or a place within such one). The evaluation of the representation degree may be performed by means of a check-list, taking into consideration the degrees of the relevant representation set forth by Table 3.

The degree to represent the possibility to place in the position suitable to provide the first aid ought to be associated with the potential to represent the commonly applied rescue positions (e.g. recovery position, supine position) and the position in which an injured person has been found. In any case, the necessity to stabilize the injured person's cervical spine must be assumed.

Table 4 *The evaluation levels for the representation degree of the possibility to place in the position suitable to provide the first aid*

criterion level	description of meanings for the evaluation criterion having been met
1	The lack of a possibility to place the phantom in the position suitable to provide the first aid.
2	A possibility to place the phantom in the position suitable to provide the first aid without a possibility to transfer the phantom from a danger zone to a safe zone, even having previously prepared it for transportation.
3	A possibility to place the phantom in the position suitable to provide the first aid with a possibility to transfer the phantom from a danger zone to a safe zone having prepared it for transportation beforehand.
4	A possibility to place the phantom in the position suitable to provide the first aid and a possibility to transfer the phantom from a danger zone to a safe zone.

Table 5 *The evaluation levels for the representation degree of the realism to perform rescuing actions*

criterion level	description of meanings for the evaluation criterion having been met
1	Rescuing actions are performed arbitrarily only.
2	Rescuing actions are performed in a simplified manner resembling its real counterpart only functionally.
3	Rescuing actions are performed in line with the procedures and are represented in a quasi-real manner.
4	Rescuing actions are performed in line with the procedures and represented in a real manner.

Table 6 *The evaluation levels for the representation degree of a possibility to alter the phantom's position while performing the first aid*

criterion level	description of meanings for the evaluation criterion having been met
1	The lack of a possibility to alter the phantom's position while providing the first aid.
2	A possibility to alter the phantom's position while providing the first aid and the lack of possibility to continue the performance of rescue actions within a simulation.
3	A possibility to alter the phantom's position while providing the first aid with the continuation of recue action performance having prepared the phantom for the simulation again.
4	A possibility to alter the phantom's position while providing the first aid with immediate continuation of rescue action performance.

Evaluation of the representation degree for the possibility to place in the position suitable to provide the first aid may be performed by means of a check-list, taking into consideration degrees of the relevant representation set forth by Table 4.

The degree to represent the realism of rescuing action execution constitutes one of the most important evaluation parameters as it impacts directly the effectiveness of the entire didactic process including the first aid implemented by Police officers. The said realism should be demonstrated by the required compression force of the chest and respiratory resistance during the CPR, the inertia of individual phantom components during its transposition, characteristics of various injuries, application of various types of dressing and stabilizations, as well as by other questions that could contribute to the realism of the simulation with the use of the phantom. The evaluation of the representation degree for the realism of rescuing action execution may be performed by means of a checklist, taking into consideration the degrees of the relevant representation set forth by Table 5.

Altering the phantom's position while providing the first aid may be determined by the necessity to perform the preliminary examination, to place it in the position suitable to provide the first aid, to introduce a temporary change in the assumptions for the didactic process scenarios as well as the necessity to retake the rescue actions or the sequences of such ones. In any of the said cases, the phantom ought to keep injury simulations in place together with dedicated dressings and stabilizations. Evaluation of the representation degree for a possibility to alter the phantom's position while providing the first aid may be performed by means of a check-list, taking into consideration the degrees of the relevant representation set forth by Table 6.

3 Examination outcomes

3.1 Examination scenarios

The relevant scenarios remain the background for the examinations as they represent the reference circumstances during which the Police officers provide medical assistance in the road accidents. They have been formulated based on the analysis of the normative documents, based on the circumstances set forth therein, the range and the manner of action, respecting the requirements regarding the quality of actions in medical

aid imposed by such ones and the level of training received by the Police officers, as well as the adequacy of Police resources at the scene of an event [10-11]. Combined with the operational experience demonstrated by the MSFS staff, the following examination scenarios have been formulated:

1) Scenario 1 - while driving a car within an urban area, a vehicle driver sustained a heart attack, during which he pulled down on a pavement located directly at the street along which he was driving. Some passers-by of different ages (children and adults) were at the pavement. There was one passenger (an adult) in a car, apart from the driver.

a) Variant 1.1. - Police officers are the witnesses of the road incident. There are no victims among the passer-bys (the passenger and the people on the pavement). The injured person (the driver) - an adult person, unconscious, breathing maintained, cardiac arrest. A single road incident, served by one Police patrol, without any support from other safety entities.

b) Variant 1.2. - Police officers are the first representatives of the safety units at the scene of a road incident. Except for an emergency call, the witnesses have not provided any assistance to the injured persons. The first of them, the driver, is an adult, unconscious, cardiac arrest, respiratory arrest. The other injured person (the only pedestrian being present at the scene of the event, hit by a vehicle while stopping), an adult, conscious, broken lower limb, contused wounds of the lower and upper limbs. A numerous road incident, served by one Police patrol, without any support from others safety entities.

c) Variant 1.3. - Police officers are the first representatives of the safety entities at the scene of a road incident. The first injured person (the driver) is an adult, unconscious, respiratory and cardiac arrest. The other injured person (a pedestrian hit by a vehicle driven by the incident perpetrator), a child, conscious, broken lower limb, contuse wounds of the lower and upper limbs. The third injured person (a passenger), an adult, conscious, injuries of the chest and broken nose (nose bleeding due to hitting a dashboard with the head as he had his seatbelts unfastened), cognitive shock. A mass road incident served by one Police patrol, without any support from other safety entities.

2) Scenario 2 - while going by a 5-seat car outside the urban area (national road), there were 6 persons inside the vehicle (the driver and 5 passengers). The passengers aged 16-19 years old, under the strong influence of alcohol and turned aggressive towards one another. Uncontrolled movements from the passengers made the driver lose control over the vehicle.

a) Variant 2.1. - Police officers are the witnesses of the road incident including the vehicle skidding. While attempting to control the skid by the driver, one of the rear door opened and one person fell out of the vehicle. There are no victims among the passer-bys. The injured person (a passenger) is an adult, unconscious, breathing and blood circulation maintained, limb scratches. A single road incident served by two Police patrols, without any support from other safety entities.

b) Variant 2.2. - Police officers are the first representatives of the safety entities at the scene of a road incident including vehicle's going off the road and bumping into a tree located at the hard shoulder. The first injured person (the driver) is an adult, unconscious, respiratory and cardiac arrest, open fracture of the lower limb. Another injured person (the passenger taking the front seat), an adult, unconscious, breathing and blood circulation maintained, penetrating injury of the chest. Two injured persons (passengers), under-aged, in cognitive shock. Numerous road incident, served by two Police patrols, without any support from other safety entities.

c) Variant 2.3. - Police officers are the first representatives of the safety entities at the scene of the road accident - a head-on collision of a car with six passengers with another car approaching from the opposite direction, having 4 passengers on-board (two adults and two children). The first injured person (the driver of the vehicle with 6 passengers), an adult, unconscious, respiratory and cardiac arrest, another injured person (the driver of the vehicle with 4 passengers), an adult, unconscious, open fracture of the lower limb, cardiac and respiratory arrest. Other participants in the incident in a cognitive shock. Mass road incident, served by two Police patrols, without any support from other safety entities.

3) Scenario 3 (variant 3.0.) - While riding a two-wheeled vehicle (a motorcycle) outside the urban area (a provincial road through the forest), the driver and the passenger sustained a health impairment due to a collision with a deer running across the road. Police officers are dispatched to support an emergency response team. There are no victims among the passer-bys or outsiders. The first injured person (the driver) is an adult, conscious, breathing and blood circulation maintained, fractures of the lower limbs, contused wounds. The other injured person (the passenger), an adult, unconscious, cardiac and respiratory arrest, open fracture of the upper limp, contused wounds of the upper and lower limbs.

4) Scenario 4 (Variant 4.0.) - Difficult external conditions (mist, wet roadway, night) contributed to a multiple crash on the national road involving 4 cars. One of the vehicles caught fire due to the crash and fuel line breaching. Consequently, an emergency response team, 2 units of the NEFS and



Figure 2 *Preview image of the Crash Kelly-type phantom (courtesy of ETC-PZL Aerospace Industries Co. Ltd.)*

2 Police patrols were dispatched to the scene as the first rescue line. Police officers are dispatched to support the emergency response team and two NEFS units. There are no victims among the passer-bys. The first injured person (the driver of the car in fire) is an adult, unconscious, cardiac and respiratory arrest, the second-degree burns of the upper limbs. The second injured person (a passenger of the car in fire), an adult, unconscious, the second-degree burns of the face, cardiac and respiratory arrest. Additionally, 4 injured persons - participants of the incident (drivers and passengers of the other vehicles) are adults, conscious, with contused wounds, as well as one injured person, a child, unconscious, cardiac and respiratory arrest.

3.2 Functionalities of the Crash Kelly phantom

The Crash Kelly-type phantom constitutes a very common didactic aid due to the physical representation of human body - the representation reaching the degree to meet the didactic requirements regarding the first aid, qualified first aid and medical rescuing actions to be performed under the circumstances of a road incident, to name just a few its features. In comparison to other types of phantoms, its fitness for the purpose results from the offered possibilities to simulate a wide spectrum of scenarios, including, both, cardiac pulmonary resuscitation (CPR) and also related to repositioning of an injured person, as well as the performance of other rescue actions.

Figure 2 shows an image of the Crash Kelly -type phantom.

In line with the manufacturer's manual, the Crash Kelly-type phantom is intended to acquire skills regarding oral intubation, nasal intubation, finger intubation, EOA/PTL intubation, intubation by Combitube® breathing tube, intubation of the right main bronchus, insertion of the oropharyngeal tube, "ambu bag - valve-mask" ventilation, suctioning techniques, sensing the carotid pulse, extracting the injured person as well as basic principles for patient's transportation [14].

Based on the training performed, the following static functionalities of the Crash Kelly phantom have been identified:

1. Within the modification of the phantom construction:
a) non-injectable thigh pads (right and left) allowing to simulate open fracture of the femur, as well as a foreign matter in the thigh,
b) replaceable foot module with visualization of a crush wound with traumatic amputation of the little toe,
c) foot attachment with visualization of toes' crush wound,
d) replaceable crus module with the visualization of a tibia contused wound,
e) non-injectable forearm pad allowing to simulate an open fracture,
f) replaceable palm module with the visualization of a finger and metacarpus crushing,
g) replaceable palm and forearm module with visualisation of the I, II and III degree burns,
h) rubber attachment for a forearm and palm with visualisation of the I, II, III degree burns,
i) rubber attachment for a torso with the visualization of the marks after safety belts,
j) rubber attachment for a torso with visualisation of the wound dehiscence marks,
k) rubber attachment for the head with visualisation of a foreign matter intrusion,
l) a possibility of wound staging,
2. with reference to a simulated body positions of an injured person:
a) a possibility to be placed at the driver's seat with the head tilted forward,
b) a possibility to be placed at the driver's eat with the head tilted backward slightly,
c) a possibility to be placed on the floor in an upright position,
d) a possibility to be placed on the floor in a rear support position,
e) a possibility to be placed on the floor in a front-

supported position,

f) a possibility to be placed on the floor in a non-physiological position.

In the course of the training completed, the following dynamic functionalities of the Crash Kelly phantom have been identified:

1. a possibility to apply Rautek's grip in its version with partial head stabilisation,
2. a possibility to apply Rautek's grip in its version without the head stabilisation,
3. a possibility to simulate the stabilisation of cervical spine with the sitting position of an injured person (e.g. inside the car), without the need to reposition an injured person outside the vehicle involved in a road incident,
4. a possibility to tilt the head back in order to clear the upper respiratory tract and to simulate the protection of the said section against additional injuries by the manual stabilization of the injured person's head,
5. a possibility to push the lower mandible upwards,
6. a possibility to perform simplified CRP with organoleptic verification of the ventilation effectiveness,
7. a possibility to alter the phantom's position while providing the first aid (the system of joints and the limbs),
8. dimensions and weight necessitating the performance of selected medical assistance actions by more than one person.

All the static and dynamic functionalities directly influence the adequacy of the Crash Kelly-type phantom with regards to the training expectations.

3.3 Outcomes of the functional evaluation

Bearing in mind the extents to which Police officers perform rescue actions and the conditions corresponding to individual examination scenarios, the following phantom's functionalities have been defined, required with reference to such scenarios:

1) Within scenario 1:

a) for Variant 1.1.:

- W1.1.-U1: Stabilisation of the cervical spine of an injured person remaining inside a car.
- W1.1.-U2: Preliminary examination of an injured person remaining inside a car.
- W1.1.-U3: Physical repositioning of an injured person remaining inside a car from the vehicle (or its mock-up) to the final destination, where the first aid will be provided.
- W1.1.-U4: Stabilisation of the cervical spine of an injured person, as well as the CPR.
- W1.1.-U5: Moving an injured person to a spine board.

b) for Variant 1.2.:

- W1.2.-U1: Stabilisation of the cervical spine of an injured person remaining inside a car.
- W1.2.-U2: Preliminary examination of an injured person remaining inside a car.
- W1.2.-U3: Physical repositioning of an injured person remaining inside a car from the vehicle (or its mock-up) to the final destination, where the first aid will be provided.
- W1.2.-U4: Stabilisation of the cervical spine of an injured person as, well as the CPR W1.2.-U5: Stabilisation of a broken limb.
- W1.2.-U6: Dressing the wounds.
- W1.2.-U7: Moving an injured person to a spine board.

c) for Variant 1.3.:

- W1.3.-U1: Stabilisation of the cervical spine of an injured person remaining inside a car.
- W1.3.-U2: Preliminary examination of an injured person remaining inside a car.
- W1.3.-U3: Physical repositioning of an injured person remaining inside a car from the vehicle (or its mock-up) to the final destination, where the first aid will be provided.
- W1.3.-U4: CPR.
- W1.3.-U5: Stopping the haemorrhage.
- W1.3.-U6: Moving an injured person to a spine board.

2) Within Scenario 2:

a) for variant 2.1.:

- W2.1.-U1: Stabilisation of the cervical spine.
- W2.1.-U2: Preliminary examination of an injured person.
- W2.1.-U3: Dressing the wounds.
- W2.1.-U4: Placing in a supine position in order to secure thermal comfort.
- W2.1.-U5: Periodical evaluation of the injured person's state.
- W2.1.-U6: Moving an injured person to a spine board.

b) for Variant 2.2.:

- W2.2.-U1: Stabilisation of the cervical spine.
- W2.2.-U2: Preliminary examination of an injured person.
- W2.2.-U3: Stabilisation of cervical spine and CPR.
- W2.2.-U4: Stabilisation of a broken limb with simultaneous stabilization of the driver's cervical spine.
- W2.2.-U5: Dressing the wounds (open fracture of the lower limb) and monitoring of the injured driver's state.
- W2.2.-U6: Monitoring of the injured driver's state.
- W2.2.-U7: Moving the injured driver to a spine board.

c) for Variant 2.3.:

- W2.3.-U1: Preliminary examination of the injured driver.
- W2.3.-U2: Physical repositioning from the vehicle (or its mock-up) to the final destination, where the first aid will be provided.

Table 7 *Outcomes of examinations for scenario elements*

	S1	S2	D1	D2	D3	D4
W1.1.-U1	4	4	4	3	4	4
W1.1.-U2	3	3	4	3	2	4
W1.1.-U3	4	4	4	4	3	3
W1.1.-U4	3	3	4	3	3	4
W1.1.-U5	4	4	4	4	3	4
W1.2.-U1	4	4	4	3	4	4
W1.2.-U2	3	3	4	3	2	4
W1.2.-U3	4	4	4	4	3	3
W1.2.-U4	3	4	4	3	3	4
W1.2.-U5	3	2	3	3	3	4
W1.2.-U6	4	3	3	3	3	3
W1.2.-U7	4	4	4	4	3	4
W1.3.-U1	4	4	4	3	4	4
W1.3.-U2	3	3	4	3	3	4
W1.3.-U3	4	4	4	4	3	3
W1.3.-U4	3	3	3	3	3	3
W1.3.-U5	4	4	3	3	3	3
W1.3.-U6	4	4	4	4	3	4
W2.1.-U1	4	4	4	3	4	4
W2.1.-U2	3	3	4	3	3	4
W2.1.-U3	4	4	3	3	3	3
W2.1.-U4	4	4	3	4	3	4
W2.1.-U5	2	4	4	4	2	4
W2.1.-U6	4	4	4	4	3	4
W2.2.-U1	4	4	4	3	4	4
W2.2.-U2	3	3	4	3	3	4
W2.2.-U3	3	3	3	3	3	3
W2.2.-U4	2	3	3	3	3	3
W2.2.-U5	2	4	4	3	3	3
W2.2.-U6	2	4	4	3	2	4
W2.2.-U7	4	4	4	4	3	4
W2.3.-U1	3	3	4	3	3	4
W2.3.-U2	4	4	4	4	3	3
W2.3.-U3	3	3	3	3	3	3
W2.3.-U4	4	4	4	4	3	4
W3.0.-U1	4	4	4	3	4	4
W3.0.-U2	3	4	3	3	3	3
W3.0.-U3	2	4	4	3	2	4
W3.0.-U4	4	4	4	4	3	4
W4.0.-U1	3	4	3	3	3	4
W4.0.-U2	3	4	3	3	3	3

- W2.3.-U3: CPR.
- W2.3.-U4: Moving the injured driver to a spine board.

3) Within Scenario 3 (for Variant 3.1.):

- W3.0.-U1: Stabilisation of the cervical spine.
- W3.0.-U2: Dressing the wounds.
- W3.0.-U3: Current monitoring of the injured driver's state.
- W3.0.-U4: Moving the injured driver to a spine board.

4) Within Scenario 4 (for Variant 3.1.):

- W4.0.-U1: Dressing the burns.

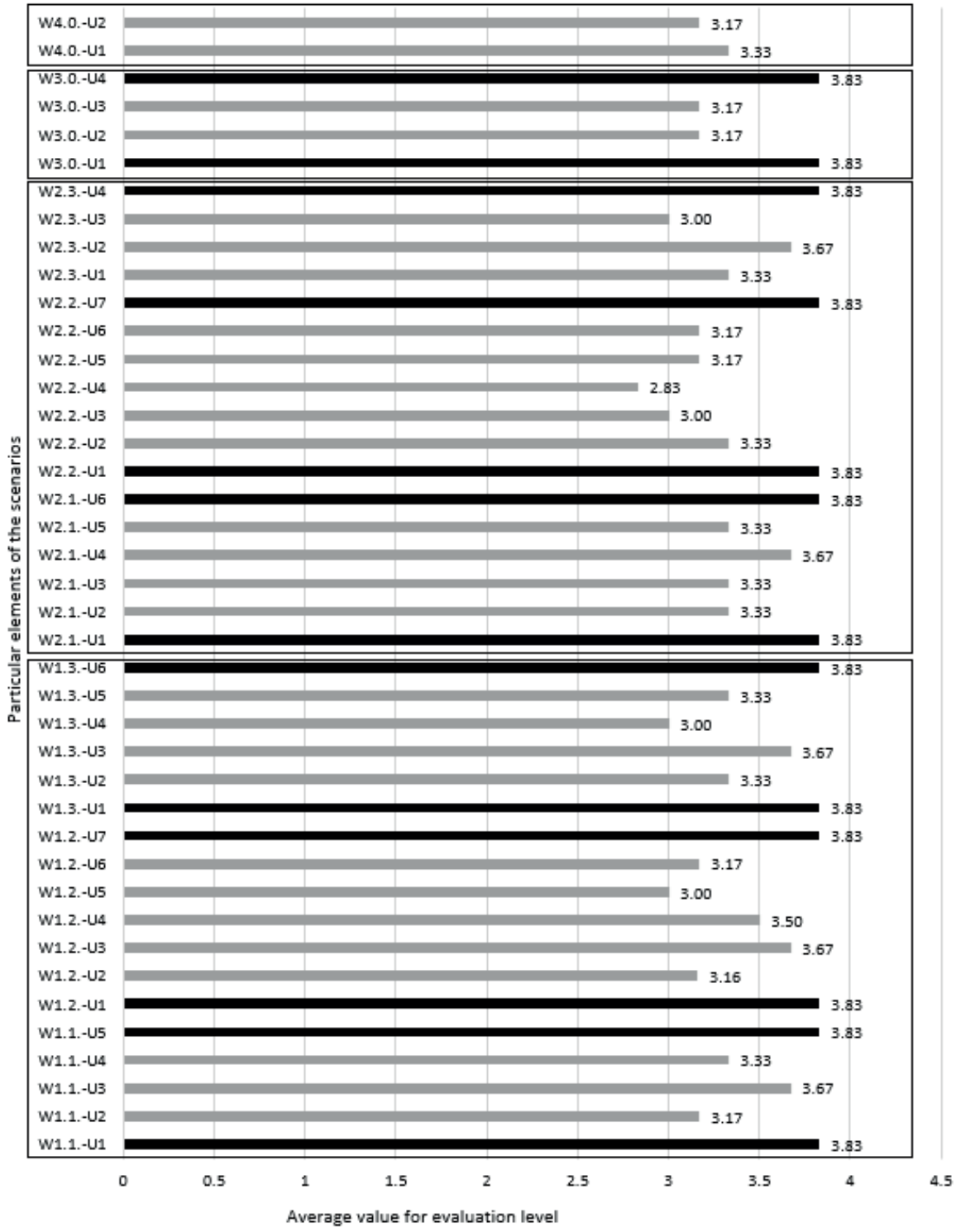


Figure 3 *Average values of evaluation level for particular elements of scenario, considering all the static and dynamic functionalities*

- W4.0.-U2: Dressing the wounds.

Subsequently, individually defined phantom's functionalities, required with reference to individual examination scenarios, have been seen in relation to individual reference functionalities. This allowed to achieve the Crash Kelly phantom functionality evaluation matrix within the context subjected to analysis. The evaluation has been performed in the course of two training sessions. Table 7 demonstrates their outcomes.

The phantom capabilities and the implementation range in the context of particular scenarios elements can be expressed by arithmetic averages of evaluation levels for particular scenario elements, considering all the static and dynamic functionalities. The values are presented in Figure 3.

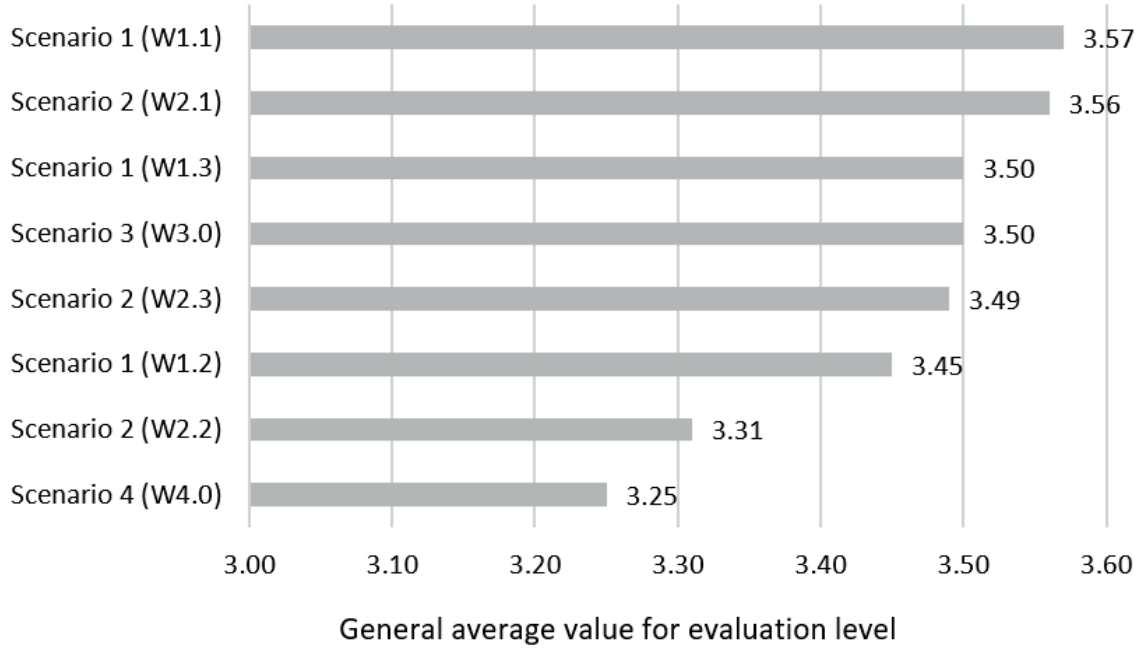


Figure 4 *General average values of evaluation level for particular variants of scenarios, considering all the static and dynamic functionalities*

The brackets indicate elements ascribed to particular scenarios. The black columns mean the highest calculated average values of evaluation levels for the scenario elements.

One can notice the highest usability of the phantom for activities, which begin and finalize the rescue procedure. There are stabilisation of the injured driver (also inside the car) and moving him/her from the danger zone with use of the spine board. This reflects the phantom elements (head, torso, legs and arms) and its general specification (weight, size, movement possibilities). In addition, in these cases the phantom is desirable as an independent didactic mean.

The lowest usability is observed in the case of stabilisation of a broken limb, stabilization of the driver's cervical spine and CPR. The first two are consequences of the phantom functional movement limitations in elbows and neck. The third one stems from the Crash Kelly's only general adaptation to CPR. In these cases, the phantom cannot be the only one didactic mean during road safety trainings. One may even consider eliminating it from the training support at these rescue procedure steps.

Other values express relatively balanced implementation ranges for particular scenarios elements, which are understood as the rescue procedure steps. They show the steps when the phantom should or could be supported by other didactic means and manners as well as directly by the trainer.

Taking into account all the outcomes of the examinations allows to present a general arithmetic averages of evaluation levels for particular scenarios variants, considering all the static and dynamic functionalities. They are presented in Figure 4.

Three groups of scenarios can be enumerated. The first one is characterised by the highest general average values of evaluation level and regard W1.1. and W2.1. The second group is comprised by W1.3., W3.0., W2.3. and W1.2. They present the lower values for evaluation levels. W2.2. and W4.0 constitute the last group, with the lowest values. Nevertheless, there are small differences in values inside and between the groups. This indicates that phantoms can be implemented in all of the scenarios. Detailed implementation manners should correspond to the previously described results for particular scenarios elements (see Figure 3).

4 Conclusions and training recommendations

The high degree of usefulness in the didactic process, regarding the provision of the first aid by Police officer in the case of road incidents, has been reported for the Crash Kelly phantom. The said equipment can be applied in all the examination scenarios. Its usefulness refers to all the variants within the aforementioned scenarios. The Crash Kelly phantom bears a great value when being implemented with reference to such rescue actions like stabilization of an injured person's cervical spine, physical repositioning of an injured person remaining inside a car away from the vehicle (or its mock-up) to the final destination where the first aid will be provided, moving an injured person to a spine board and dressing the wounds characteristic for the road incidents. However, the implementation values related to dressing the wounds and stabilizing the limbs, characteristic for the road incidents, lose their significance when a sudden change in the training scenario assumptions must be

introduced, for they may lose adhesion (together with the relevant dressings and stabilizers) to the material, which the phantom has been made of.

Phantom's "rigidness" and the aforementioned limited adhesion restrict the possibility to place it in every position (especially non-physiological position). Hence, it is recommended to limit changes in the didactic process to the ones regarding the sudden emergency evacuation (without the continuation of the originally specified rescue actions), placing the phantom in the position suitable for the CPR and on a spine board. In the case when the spectrum of rescue actions has been quite limited, the Crash Kelly phantom may be applied to train various techniques of emergency evacuation, involving one or two trainees. A periodical evaluation of an injured person's state ought to be limited to the most evident injuries only. The phantom's design makes it impossible to identify all symptoms of internal injuries (e.g. filling up the abdomen cavity or a thigh with blood, capillary refill). The phantom's design does not allow to place it in a safe position. Hence, the necessity to include injured person's monitoring into the scenarios and provide the paramedics with oropharyngeal tubes and other elements allowing for clearing the upper respiratory tract. Stabilisation of the broken limbs should be regarded as one of the last rescue actions to be taken and emergency evacuation should not be introduced afterwards accompanied by additional rescue actions due to an unacceptable risk of wound dressing loosening and limb stabilization removal.

The Crash Kelly phantom allows for the use of a self-inflating bag, an oropharyngeal tube, a laryngeal tube, a laryngeal mask of i-gel type as well as other elements intended for more advance rescue actions than just first aid. Therefore, it is useful in the course of the simulations involving the cooperation between various safety entities, especially from the so-called rescue triangle (Police, entities of NEFS and the entities of the State Medical Rescue system).

It is possible to provide additionally a staging set to improve the realism of the injuries. The degree of injury representation remains at its peak when the phantom does not change its position in the course of the scenario.

The degree to represent the body position of an injured person bears the greatest importance in the case of an analysis regarding the bodily position found by Police officers at the very beginning of the simulation. The degree to represent a possibility to transfer from a danger zone to a safe zone is related to emergency evacuation. The degree to represent the position suitable for providing first aid is to a great extent related to the first rescue actions to be performed (direct dependence).

Acknowledgement

The article was written in the framework of the project entitled *„Simulator supporting police officers performing duties at the scene of a traffic incident"* DOB-BIO09/06/01/2018 with the value of PLN 8,276,259.00 PLN, funded by the National Centre for Research and Development under the contest 9/2018. Project implemented in a research consortium composed of: Police Academy in Szczytno (the project leader), The Main School of Fire Service, General Tadeusz Kosciuszko Military University of Land Forces, Institute of Safety of Technologies „MORATEX", ETC-PZL Aerospace Industries Sp. z o. o.

References

[1] Mobility and transport. Road safety - European Commission [online] [accessed 2020-06-25]. Available from: https://ec.europa.eu/transport/road_safety/index_en

[2] Transforming our world: the 2030 agenda for sustainable development. Resolution adopted by the General Assembly on 25 September 2015 - United Nations [online] [accessed 2020-06-25]. Available from: https://www.eea.europa.eu/policy-documents/resolution-adopted-by-the-general

[3] Report of the Inter-agency and Expert group on sustainable development goal indicators - United Nations [online] [accessed 2020-06-25]. Available from: http://ggim.un.org/knowledgebase/KnowledgebaseArticle51479.aspx

[4] MAKKA, K., STACHOVA, D., KAMPOVA, K. Assessment of the mobile risk source in road transport. *Communications - Scientific Letters of the University of Zilina* [online]. 2019, **21**(1), p. 68-73 [accessed 2020-02-28]. ISSN 2585-7878, eISSN 2585-7878. Available from: http://komunikacie.uniza.sk/index.php/communications/article/view/1169/1133

[5] HOLLA, K. Dealing with key terms in risk analysis and phenomenon of uncertainty in this process. *Communications - Scientific Letters of the University of Zilina* [online]. 2007, **9**(4), p. 59-61 [accessed 2020-02-28]. ISSN 2585-7878, eISSN 2585-7878. Available from: http://komunikacie.uniza.sk/index.php/communications/article/view/1157

[6] SIMAK, L., RISTVEJ, J. The present status of creating the safety system of the Slovak Republic after entering the European Union. *Journal of Homeland Safety and Emergency Management* [online]. 2009, **6**(1), 20 [accessed 2020-06-26]. ISSN 1547-7355. Available from: https://doi.org/10.2202/1547-7355.1443

[7] HOLLA, K., RISTVEJ, J., MORICOVA, V., NOVAK, L. Results of survey among SEVESO establishments in the Slovak Republic. *Journal of Chemical Health Safety* [online]. 2016, **23**(2), p. 9-17 [accessed 2020-06-26]. ISSN 1871-5532. Available from: http://dx.doi.org/10.1016/j.jchas.2015.03.003

[8] List of formally approved applications. Competition no: 9/2018 to execute a finance scientific research and developmental works in favour of the national defence and safety - The National Centre for Research and Development [online]. Available from: https://www.ncbr.gov.pl/fileadmin/Obronnosc/9_2018/Lista_wnioskow_pozytywnie_ocenionych_pod_wzgledem_formalnym_BIO9.pdf

[9] DWORZECKI, J. Road safety in Poland, the Czech Republic and Slovakia. Presentation of international research results. *ASEJ Scientific Journal of Bielsko-Biala School of Finance and Law* [online]. 2019, **23**(2), p. 5-13 [accessed 2020-06-26]. ISSN 1871-5532. Available from: https://doi.org/10.5604/01.3001.0013.6513

[10] The technical and operational requirements for the module responsible for the implementation of 3 rescue and training phantoms into the didactic process. Product no I.2 for the project entitled: a simulator to support the training for police officers in performing the actions at the scene of a road accident (No DOB-BIO9/06/01/2018).

[11] The report on the examinations over the module responsible for the implementation of 3 rescue and training phantoms into the didactic process. Product no III.6 of the project entitled: a simulator to support the training for police officers in performing the actions at the scene of a road accident (No DOB-BIO9/06/01/2018). 2020.

[12] WROBEL, R. Scenario building for adverse events / Budowa scenariuszy zdarzen niekorzystnych. In: *The chosen issues of civil planning in crisis management system in Poland / Wybrane zagadnienia z zakresu planowania cywilnego w systemie zarzadzania kryzysowego RP* (in Polish). 1. ed. Jozefow: Wydawnictwo Centrum Naukowo-Badawczego Ochrony Przeciwpozarowej - Panstwowego Instytutu Badawczego, 2014. ISBN 978-83-61520-23-8, p. 323-326.

[13] PRZETACZNIK, R. Fire protection training methodology / Metodyka ksztalcenia w zakresie ochrony przeciwpozarowej. In: *Hazards recognition. Social-didactics issues for firefighters who solicit officers' posts related to commanding rescue actions / Rozpoznawanie zagrozen. Zagadnienia spoleczno-dydaktyczne dla strazakow ubiegajacych sie o zajmowanie stanowisk oficerskich zwiazanych z kierowaniem dzialaniami ratowniczymi* (in Polish). Warszawa: Wydawnictwo Szkoly Glownej Sluzby Pozarniczej, 2012. ISBN 978-83-88446-35-1, p. 211-213.

[14] Crush Kelly manual. USA: Laerdal Medical, 2015.

ASSESSMENT OF STATIC RESILIENCE OF OBJECTS IN THE RAIL TRANSPORT

Zdeněk Dvořák*, Nikola Chovančíková, Katarína Hoterová, Michal Szatmári

Department of Technical Science and Informatics, Faculty of Security Engineering, University of Zilina, Slovak Republic

*E-mail of corresponding author: zdenek.dvorak@fbi.uniza.sk

Resume

Resilience is the ability of an object to retain its basic functions in the case of adverse events from an external or internal environment. Adverse events can jeopardize the operation of an object or cause it to become completely inoperable. The assessment of static resilience should be dealt with mainly by objects that are included in local, regional, national, and international critical infrastructure. Critical infrastructure is the basis of today's modern functioning society.

The paper is focused on design of the static resilience evaluation of objects in the rail transport. The proposed method of static resilience assessment is based on safety pillars and is applied in a case study to a specific object of the rail transport. This approach is original in the conditions of the Slovak Republic.

Article info

Received 11 December 2020
Accepted 18 December 2020
Online 13 May 2021

Keywords:

rail transport,
resilience,
safety pillars,
critical infrastructure

Available online: https://doi.org/10.26552/com.C.2021.3.F96-F108

ISSN 1335-4205 (print version)
ISSN 2585-7878 (online version)

This is an open access article distributed under the terms of the Creative Commons Attribution 4.0 International License (CC BY 4.0), which permits use, distribution, and reproduction in any medium, provided the original publication is properly cited. No use, distribution or reproduction is permitted which does not comply with these terms.

1 Introduction

The quality of the state's transport system is crucial for development of all the sectors of the national economy and, at the same time, for an adequate quality of life. The most developed countries in the world are constantly building their transport infrastructure. An example is China, where 750 meters of a new highway are built every hour. The well-built and continuously maintained point, line and area facilities of the transport infrastructure are the basis for providing logistics activities for companies, transport services for the population and defence for the state. In the new European strategy for 2021-2030, „security and resilience" is one of the six defined thematic groups. The transport system of the state consists of several types of transport. The article will pay attention to rail transport and focus mainly on rail infrastructure [1].

One of the monitored parameters of the quality, safe and modern infrastructure is its resilience. Resilience represents the ability of an element to absorb, adapt and quickly recover the activity of the element, namely an object, as a result of an adverse event. In practice, one encounters adverse events of a natural and anthropogenic environment. Adverse events can lead to significant disruption in functioning of individual facilities in the rail transport [2].

Importance of the rail transport in Slovakia lies in its connection with pan-European corridors and its use in national as well as international transport of passengers and goods. Because of the key importance of the rail transport at the national and international level, it is necessary to focus on assessment of its static resilience.

Resilience is a way to increase the safety/security of facilities belonging to the rail infrastructure. By quantifying the static resilience, the facility operator can obtain the necessary information about the individual evaluated areas and to detect deficiencies promptly, to which he can react in advance. The paper is focused on design and testing of the static resilience evaluation of selected objects in rail transport. From the point, line and area objects, the article has focused on the area object - the railway station.

As part of the draft static resilience assessment, safety pillars were used that can comprehensively cover several safety areas. By increasing the level of resilience, it is possible to ensure their functioning, respectively maintaining the basic functions in the case of an adverse event and thus does not interfere with functioning of other elements of the system that are interconnected with them.

2 Institutional and juridical frame of critical infrastructure

Today's society often has to deal with threats that arise in the external or internal environment. Their

influence disrupts functioning of processes in the affected element, or their influence can lead to the complete failure of ongoing processes, on which other elements and the company itself depend. Objects without which the state's economy cannot function properly are included among the elements of critical infrastructure. Critical infrastructure is a set of elements whose damage or failure can have a negative impact on the population and the economy of the state. Council Directive 2008/114/EC of 8 December 2008 on the identification and designation of European Critical Infrastructure and the assessment of the need to improve their protection defines critical infrastructure Art. 2 *„as a component, system or part thereof located in the Member States, which is necessary for the maintenance of the fundamental functions of society, health, protection, safety, quality of life of the population from an economic and social point of view and the disruption or destruction of which would have serious consequences in the Member State due to the impossibility of maintaining these functions"* [3].

Within the European Union, there is a European Railway Agency (hereinafter ERA). The ERA ensures better functioning of the rail infrastructure and contributes to the efficient functioning of the Single European Railway Area. The ERA acts as a superior body to help coordinate the necessary changes leading to the creation of a single European railway area. In the field of safety, it aims to develop a harmonized approach to rail infrastructure safety, develops a technical and legal framework to remove technical barriers, improves the availability and use of rail infrastructure information, issues vehicle authorizations and single safety certificates [4].

The ERA's activities also include the provision of the Common Safety Methods (hereinafter CSM) application. Each rail line, rail infrastructure manager and entity in charge of maintenance should ensure that all suppliers and other parties working on the rail system implement risk control measures. To that end, they should apply the threat monitoring methods set out in the CSM. These methods are applied through contractual arrangements. As these agreements are an essential part of the rail infrastructure safety management system, they should be available on request from the ERA. Member States are obliged to cooperate in safety management. Common safety targets and the CSM applications have been gradually introduced [5].

The CSMs are further specified in general methods of risk assessment, risk monitoring and safety. They also focus on the management system requirements, on supervision and on the fulfilment of safety objectives [6].

Each national critical infrastructure is unique and represents a set of elements that are closely interconnected. For the needs of application of Directive 2008/114 / EC into the Slovak legal environment that is Act no. 45/2011 Coll. on Critical Infrastructure, which represents the legal framework for critical infrastructure in Slovakia. The law defines the basic requirements associated with the issue of critical infrastructure. An important part of this research is Annex no. 3 to Act no. 45/2011, which contains a list of sectors and subsectors [7]. Within the transport sector, there is a railway subsector, which is the subject of this contribution. The rail infrastructure is very important from the point of view of Slovakia's transport system because it is a part of the Pan-European transport corridors. The detailed specification of the rail transport subsector in Act no. 45/2011 Coll. is not mentioned, but its further definition can be found in the National Program for Protection and Defense of Critical Infrastructure in the Slovak Republic from 2008 (hereinafter National Program). The National Program is the only document that closer specifies the rail transport subsector and other subsectors, as well. The National Program lists elements of critical infrastructure in the conditions of rail transport, such as important rail junctions, fuel depots, electrical substations enabling the supply of electrified lines and others. Furthermore, the National Program also states the method of protection of these elements. The protection of the rail infrastructure elements is ensured through the human factor, technical means and adoption of measures to reduce risks, i.e. reducing vulnerability [8].

In relation to the issue of critical infrastructure in Slovakia, it is necessary to mention the methodological guidelines, which are of a recommendatory nature and supplement Act no. 45/2011. The first document that precisely covers the area of safety/security measures is Methodological guideline no. 29014 / 2014-1000-53190 MH SR on safety/security measures for the protection of critical infrastructure elements in the energy and industry sectors. The methodological guideline deals with the protection of critical infrastructure elements. The Annex defines the zones and a description of their safety for specific elements of critical infrastructure in the energy and industry sectors [9]. The second document is Methodological guideline no. 1321 / 2011-1020 of the Ministry of Economy of the Slovak Republic on the protection of sensitive information on critical infrastructure and on the manner of handling this information. In practice, the methodological guideline is supplemented by other legal documents related to information security [10]. It is also important to mention Act no. 69/2018 Coll. on Cyber Security and on Amendments to Certain Acts, which is connected with the issue of critical infrastructure and the protection of elements itself.

Maintaining the continued functioning of the critical infrastructure elements is not just about complying with legislation and recommendations. Objects included in critical infrastructure must focus on several areas that could affect their operation. Disruption of the the elements function can be caused by various risks, which need to be detected as soon as possible when they cannot yet cause massive damage to functions of the object [11]. A possible way to identify the sources of these risks

is through the process of assessing the level of static resilience. By determining the level of resilience, one can detect weaknesses that can cause the element to fail. The subsequent part of the paper is devoted to approach to the resilience issue and the method of evaluating the static resilience of elements included in the railway subsector.

Under Act No. 513/2009 Coll. on railways, safety is addressed in Article I in the fifth part. This section defines the safety of the railway system. The railway safety system consists of *„safety requirements for the railway system as a whole for its subsystems, including the operation of the railway infrastructure and traffic management, as well as for synergies between the infrastructure manager and railway undertakings and other entities affecting the safety of the European Union rail system"* [12].

The law further states that in determining the minimum level of safety/security, the risks associated with:

- passengers,
- the staff of the infrastructure manager and railway undertakings, as well as the staff of supply services for the railway system,
- road users at level crossings, pedestrians at crossings and other persons, without prejudice to the applicable legislation concerning the liability of the party to the accident,
- persons moving unauthorisedly in the perimeter of the track and in the premises of the infrastructure manager,
- societal risks [13].

The Ministry of Transport and Construction of the Slovak Republic (hereinafter MinDop) is a state administration body of the Slovak Republic, which, within its defined competence, also performs activities in the field of rail transport [13-14]. Within the organizational structure, the safety of the rail system is handled by the Crisis Management and Cyber Security Department.

The Transport Authority of the Slovak Republic (hereinafter DU SR) also falls under the competence of the MinDop. The DU SR according to Act no. 402/2013 Coll. on the Office for the Regulation of Electronic Communications and Postal Services and the Transport Authority is divided into the following three divisions:

- Railways and Railways Transport Division,
- Civil Aviation Division,
- Inland Navigation Division [15].

For the needs of the article, which focuses on the rail infrastructure, division of the rail and transport on the rail is described in more details. This division is legally governed mainly by Act no. 514/2009 Coll. on railways, Act no. 258/1993 Coll. on the Railways of the Slovak Republic and Act no. 259/2001 Coll. about Railway's Company Slovakia a.s. The Division of Rail and Transport on Rail is divided into basic sections, namely:

- regulation, permits and licenses on rail,
- safety and interoperability of subsystems,
- state professional technical supervision [16].

At the end of the analytical part on institutions and the juridical framework, the goal of this research is described. As a part of the ongoing research, controlled interviews were conducted with five employees of MinDop, DU SR and Railways of the Slovak Republic (hereinafter ZSR). During these interviews, the interest of the practice in the results of research in the field of resilience was confirmed. Given the expected challenges for the period 2021-2030 in the field of transport, the attention of researchers is focused on the area of „security and resilience". Within the framework of the long-term cooperation of the University of Zilina with institutions and companies in the field of transport, current problems and challenges for the needs of practice have always been solved within the research. As a part of the current applied research, this is based on projects that have been realized in the past decades, research is currently directing mainly towards the area of effective use of information and communication technologies. The researchers intend to create an expert information system which, using the 5G networks, SMART solutions and the Internet of Things, will bringthe unbiased information in real-time to support traffic management and support planned maintenance and renewal, for the needs of the rail infrastructure manager objective. The main goal of applied research for the needs of the rail infrastructure manager is to create a theoretical apparatus and software product, which will be tested and verified in cooperation with the ZSR as a tool for the new safety dispatching of the ZSR [17].

3 Literature review

The first major source was a US document in 2013 focusing on the overall framework of risks, vulnerabilities and resilience. The framework for creating the Resilience Measurement Index, real-time data collection, self-calculation and presentation of Resilence Measurement Index results was presented for the first time [18].

Next is the 2015 ETH Zurich document - Measuring Critical Infrastructure Resilience: Possible Indicators. The authors defined here the absolute and relative assessments of resilience. They focused on potential critical infrastructure resilience assessment indicators and made a significant contribution to definition of the resilinece index for the Swiss critical infrastructure [19].

Nan and Sansavini focused on the individual phases of resilience - absorption, adaptation and recovery. They were the first to publish an integrated metric for system resilience quantification and a hybrid modeling approach for representing the failure behavior of infrastructure systems [20].

Kozine, Petrenj and Trucco were focused on research approach that is capabilities-based, where a capability is defined as a combination of assets, resources and routines

specifically arranged to accomplish a critical task and assure a key objective. Another benefit is in defining the intra and inter-institutional capabilities, which are grouped into clusters according to the resilience phase (preventive, absorptive, adaptive and reconstruction). The result of their research is the interconnection of technical, operational, social and economic systems [21].

A complex approach to assessing resilience has been addressed by Rehak et al. in [22].They developed the Critical Infrastructure Elements Resilience Assessment methodology (hereinafter CIERA). Their contribution is a description of a complex approach to assessing technical and organizational resilience, as well as identifying of weak points in order to strengthen the resilience [22].

In the USA the Presidential Policy Directive-Critical Infrastructure Security and Resilience calls for proactive and coordinated efforts to strengthen and maintain a functioning, secure and, above all, resilient critical infrastructure [23]. Robust systems would help to reduce the likelihood of adverse events, or allow the element to respond effectively in the case of an adverse event.

There is no universal definition of resilience that can be applied to all the research areas. In practice, one may encounter application of this term in various scientific disciplines, such as psychology, economics, medicine, environmental sciences and safety. The critical infrastructure area uses the definition: *„resilience is the ability to absorb, adapt and / or recover rapidly from a potential adverse event"* [24].

In general, it can be stated that resilience is the ability to adapt to foreseeable or unexpected adverse events [25]. In addressing the issue of resilience in the rail transport, attention needs to be paid to researc.

Besinovic in [26] has defined the resilience of the rail infrastructure as the ability of the system to provide services under normal conditions, as well as to resist, absorb, react quickly and recover from adverse events. Author explored the possibilities of measuring and quantifying resilience. The acquired knowledge should form a mainstay in understanding the requirements related to the resilience of rail infrastructure. There is scope for a better understanding of possible applications for resilience assessment and design of resilient rail transport systems.

Deloukas and Apostolopoulou addressed the static and dynamic resilience in transport in [27]. The paper is composed to assess the urban transport resilience. The practical demonstration was applied to the Athens metro. Authors constructed the risk scenarios for the risk of an attack on the metro, which took into account the static and dynamic resilience of urban transport. The static resilience is related to robustness, i.e. the ability of the urban transport system to absorb the effects of the adverse event and to retain its basic functions, i.e. enabling the transport of persons when the section is decommissioned. In the static resilience, the focus is on replacing the metro with other modes of transport, such as bus lines. The dynamic resilience has focused on the rapid recovery of the damaged infrastructure and resuming of the transport services.

Adjetey-Bahun et al. presented a new approach to dealing with adverse events in [28], the concept of resilience, which allows not only to measur the ability of the system to absorb failures but to obtain information about the ability to build speed, as well. That is not a traditional approach to risk management that focuses on the probability and consequences of events. Part of the authors' work is a simulation model for quantification of resilience in public transport systems, which have integrated subsystems, e.g. telecommunication, organizational. The model was subsequently applied to the Paris rail transport system. Following its application, they concluded that the rail transport system remained resilient even when train speeds were reduced.

The issue of transport infrastructure resilience is also being addressed by the European Commission, which has launched the RESIST project, which is funded by the EU's research and innovation program in 2020, [29]. The project has taken a holistic approach to the strengthen road critical infrastructure. The primary goal of the RESIST project is to create a methodology and tools for risk analysis and management focused primarily on highway construction. The methodology and proposed tools should be applied to all the extreme natural and man-made adverse events. The aim is to increase the resilience of the transport infrastructure and protect the interests of users and operators of European transport infrastructure. Although the project is primarily focused on transport infrastructure, it provides a lot of information that can be used in research activities related to the rail transport, as well.

When examining information sources from specialist publications and websites, the researchers concluded that the issue of assessing the static resilience in the rail transport has not been comprehensively addressed so far, so there is a latitude for new ideas and innovations that would shift the issue of critical infrastructure protection in Slovakia and world ahead.

In the above-mentioned information sources and juristic acts, attention is paid only to some parts of this research. To move the knowledge further, the attention of researchers should be focused on a new method of quantitative evaluation of static resilience of objects in rail transport, which is based on predefined indicators in individual areas of safety.

Based on the research carried out at the researchers' workplace, the safety pillars were gradually defined based on relevant and objectively measurable indicators; pillars of safety, which allow to comprehensively cover the functioning of the most important parts of safety and security in the building. If one can quantify the level of individual areas, one can detect shortcomings and then take measures that will increase the resilience and safety of the element. Each safety pillar should have identified indicators to assess the area. Hofreiter

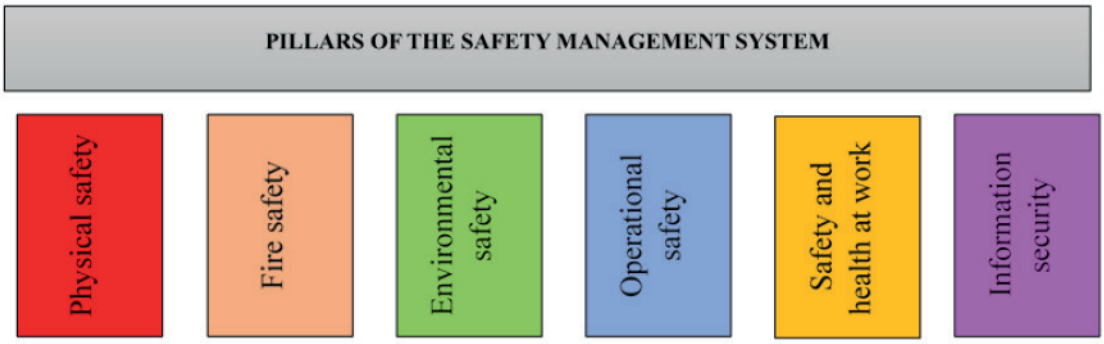


Figure 1 *Pillars of the safety management system*

Table 1 *Example of the design of indicators within the individual pillars*

design of indicators					
physical safety	fire safety	environmental safety	operational safety	safety and health at work	information security
unauthorized entry into the premises of the reference object	fire alarm	periodicity of drainage system inspection	occurrence of a malfunction of the system for proving identity check-in	expertise of employees	security of passwords
unauthorized access to the reference object	availability of firefighting equipment directly in the building	noise pollution	development of security plans	handling of hazardous substances	defining access to information
application of image surveillance systems in a reference object	smoke and heat removal equipment	the threat to the building by floods	prevention of fault events in the system	control of use of the PPE and control of their condition at the workplace	operating system updates
time for overcoming perimeter protection and approaching the reference object	level of fire safety	amount of annual investments aimed at environmental protection	development of an analysis aimed at prevention of major accidents	regular health and safety training	regular inspections of accession measures
time of overcoming the mantle protection of the reference object and penetration into the object	damage to the building due to fire	certification of the environmental management system according to the ISO 14001 standard	IRS response time to an adverse event	impact of the work environment on quality of the employees‘ health	operating system software protection
time to overcome spatial protection and approach the protected interest	degree of protection of escape routes	creation of environmental reporting	risk of electricity interruption	expertise of employees	performing an internal security audit

and Byrtusova dealt with safety indicators in[30] where they defined indicators as data, respectively data files, expressing the state of the system. The authors stated that indicators can express the normal, desired state of the system, or the transition of the system to a state of increased instability, predictability and manageability Durech also followed up on the issue of safety indicators in his dissertation and proposed a method of effective evaluation of the rail station safety using the safety indicators [31].

A holistic approach needs to be taken when creating a new resilience assessment procedure. In practice, this means that when examining a certain issue, it is necessary to focus on the whole as a whole, not just on certain parts. As stated by authors in [32], which focuses on resilience engineering, resilience are the

Table 2 *Example of the individual indicators evaluation*

pillar	indicator	indicator description	value
physical safety	time for overcoming perimeter protection and approaching the reference object	a) The reference object is at a distance of 200 m from the fence, the fence is 2 m high and equipped with other wire, the fence is still equipped with detection systems based on optical cables that send a signal via a communicator to the CPD receiver (centralized protection desk). The overcoming time is estimated at 10 min or more.	3
		b) The reference building is at a distance of 100 m from the fence, the fencing is 2 m high, the building has regular detours with its SBS. The overcoming time is estimated at 5 min.	2
		c) The reference object is at a distance of 10 m from the fence, the fence is not in good technical condition, its height is 1.5 m. The overcoming time is estimated at 1 min.	1
fire safety	level of fire safety	a) The building has fire indicators in each room with a connection to the sprinkler; escape routes meet the requirements for a protected escape route, the fire protection plan is developed and methodical exercises take place once every six months to optimize the reaction and rescue process.	3
		b) The building has fire indicators in each room, the sprinkler is not installed within the reference building, the reaction to elimination of fire must be performed by an employee using fire extinguishers, the fire protection plan is prepared and revisions are carried out together with methodical exercises.	2
		c) The building has fire indicators only in places where there is a risk of fire, the sprinkler is not installed and the elimination of the fire must be performed by a worker using fire extinguishers; the fire protection plan is prepared by law, methodical exercises are performed irregularly.	1
environmental safety	certification of the environmental management system according to the ISO 14001 standard	a) The building holds the ISO 14001 certification.	3
		b) The object partly works according to the ISO 14001 standard or tries to obtain the given certification.	2
		c) The facility does not work in the environmental field with any standard.	1
operational safety	development of an analysis aimed at the prevention of major accidents	a) Analyses are prepared in accordance with internal regulations and look for better ways to innovate, employees are fully acquainted with the analysis. Analyses are performed once a year.	3
		b) Analyses are prepared in accordance with internal regulations every two years, no better ways are sought to innovate the current situation, employees are partially familiar with the analysis.	2
		c) Analyses are not prepared, i.e. employees are not notified.	1
safety and health at work	regular health and safety training	a) Trainings have an annual regular interval, lasting one full working time with a final verification of the employee‘s state of knowledge.	3
		b) The trainings have an annual regular interval, lasting one full working time without a final examination.	2
		c) Trainings do not have a regular interval set by law and therefore employees show shortcomings in the field of health and safety awareness.	1
information security	operating system software protection	a) The reference object has a paid updated software platform (anti-virus program) to prevent intrusion into the operating system and the data contained in it.	3
		b) The reference object has a paid non-updated software platform (antivirus program) to prevent intrusion into the operating system and the data contained in it.	2
		c) The reference object has a publicly available software platform (anti-virus program) to prevent intrusion into the operating system and the data contained in it.	1

Table 3 *Final expression of static resilience*

total summary value	verbal expression	description
100%-92%	excellent level of resilience	A reference object characterized by an excellent level of resilience can withstand adverse events from external and internal environments without interruption or significant restrictions. The object has identified only minimal deficiencies in its system, which do not represent sources of risks that could affect its operation.
91%-75%	good level of resilience	A reference object characterized by a good level of resilience can withstand and maintain basic functions in the case of adverse events from external and internal environments. Deficiencies have been identified in the facility's system that may be a potential source of risks that could further affect its resilience and its functioning could be jeopardized in the future if the preventive measures are not taken.
below 75%	unsatisfactory level of resilience	A reference object characterized by an unsatisfactory level of resilience is not able to maintain its basic functions in the case of adverse events from external and internal environments. The system contains several shortcomings, which result in a reduction in the resistance of the object.

means, methods and technologies to overcome adverse events with the least possible harm and the subsequent construction of a system that will stronger and prepared for adverse events that may arise in the future. The safety environment analysis usually focuses on specific threats. Authors tried to establish a way of thinking that allows to manage all kinds of adverse events. Assessing the resilience of objects requires harmonization of knowledge in the field of safetty and resilience [32].

Enache and Letia paid attention to the rail infrastructure, which is characterized by complex safety and security systems supporting its management and monitoring, [33]. The authors stated that rail systems must maintain their resilience and ensure safety requirements without reducing efficiency. The proposed method is based on *Object Enhanced Time Petri Nets models*, which can simultaneously describe behaviour of all the components integrated into the infrastructure. The paper contains an example of application for a part of the rail system, safety and resilience of which were then analyzed.

The indicators can be specifically designed for the evaluated area and thus provide unique results. In connection with the safety indicators, several scientific publications have been published. Renard and Charles have focused their attention on underground system, which take into account the specifics of e.g. tunnels, automatic pilots, platform doors and others, [34]. A classification of safety indicators to identify information was subsequently introduced at a national level in France.

The above-detailed analysis of scientific information sources provides several findings. First, the issue of resilience research in scientific information sources is represented. Second, the authors bring theoretical knowledge linked to practical applications in several countries. Thirdly, the changing natural and social environment require a new set of boundaries for the resilience of transport infrastructure objects. The above findings and conclusions, in the area of the institutional and legal framework, imply an objective need for applied research. The following part of the article is focused on the demonstration of possible use of the safety pillars in the static resilience evaluation.

4 Evaluation of the static resilience of buildings in the rail transport

The static resilience assessment should be a comprehensive tool that can evaluate the areas located in each building or element of critical infrastructure. The method for the static resilience evaluation is based on application of the safety pillars, Figure 1. Specific indicators for the area of the rail transport are proposed for each pillar, Table 1. The proposed method of assessing the static resilience would be a comprehensive tool for the rail infrastructure objects, such as bridges, tunnels, stations, transhipments, etc. [35]

Each indicator shown in Table 1 is characterized in detail in Table 2. The indicators located in each area are evaluated by a quantitative scale from 1 to 3. In our case, the point value 3 is (excellent) assigned to the indicator, which is fully represented in the evaluated reference object. A point value of 2 (good) is assigned to the indicator if it does not meet all the requirements contained in the first point and a point value of 3 (excellent) cannot be assigned to it. A point value of 1 (unsatisfactory) is assigned if the indicator does not meet the requirements contained in the previous points. As 6 pillars were chosen and each of them has 6 indicators, this means that the maximum achieved quantitative sum represents a total of 108 points on the evaluation scale of 1 to 3. If the individual pillars are evaluated by expert estimation, one can sum them up and then calculate the level of static resilience in percent, according to:

$$I_p = \frac{100}{I_k} \times \sum I_j \,, \tag{1}$$

where:

$\sum I_j$ = the sum of the quantitative evaluations of the indicators for the reference object,

I_k = maximum value of quantitative evaluation of indicators,



Figure 2 *Indoor and outdoor environment of the Zilina railway station [37]*

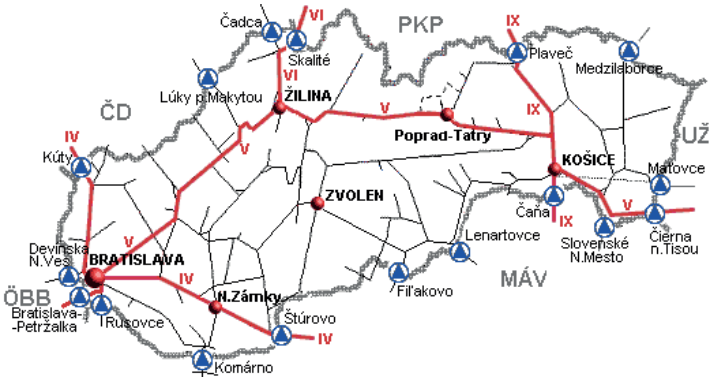


Figure 3 *Pan - European rail corridors [38]*

I_p = percentage expression of static resilience for the reference object.

Six pillars are currently proposed in each area, with the corresponding descriptions, Table 2. To ensure accurate outputs and their application in practice, it is proposed to create at least 30 indicators in each area, which would be characterized in detail. For the purpose of this article, one indicator is assigned to each area for better visualization of the structure of the proposed procedure, which is shown in Table 2.

The above description of selected safety indicators had to be evaluated. In co-operation with the practice, questionnaires were created for security experts, where they were to comment on the overall safety assessment. Based on these findings, the values determined by the experts were averaged. A value in percentage terms of 92 to 100 was determined as an excellent level. A range of 75 to 91 percent was set as a good level. Values below 75 percent were determined to be unsatisfactory. The total level of static resilience is determined by summing up all the assigned quantitative values and their subsequent percentage expression according to Table 3.

Through analysis of available information sources from Slovak Republic, it can be stated that the issue of assessing the static resilience of the rail infrastructure has not yet been addressed and in connection with the issue of resilience, there are no records of its solution, either. In the case of information sources from abroad, it can be stated that the issue of resilience is being actively developed and as regards the solution of the rail infrastructure resilience, several scientific works are devoted to it. This paper is devoted to design of a method for evaluating the static resilience of infrastructure facilities through application of the safety pillars, which are evaluated. As mentionedabove, creation of several indicators is required to ensure application of the proposed procedure. The proposed number of indicators in each area is 30. The next section of the paper presents a case study, which aims to clarify the process of evaluating the static resilience of the chosen reference object.

Table 4 *Evaluation of static resistance of Zilina railway station*

evaluation of static resilience		
pillars	name of the indicator	indicator value
physical safety	unauthorized entry into the premises of the reference object	1
	unauthorized access to the reference object	1
	application of image surveillance systems in a reference object	2
	time for overcoming perimeter protection and approaching the reference object	1
	time of overcoming the mantle protection of the reference object and penetration into the object	1
	time to overcome spatial protection and approach the protected interest	2
fire safety	fire alarm	3
	availability of firefighting equipment directly in the building	2
	smoke and heat removal equipment	3
	level of fire safety	3
	damage to the building due to fire	3
	degree of protection of escape routes	2
environmental safety	periodicity of drainage system inspection	3
	noise pollution	3
	the threat to the building by floods	3
	amount of annual investments aimed at environmental protection	2
	certification of the environmental management system according to the ISO 14001 standard	1
operational safety	creation of environmental reporting	2
	the occurrence of a malfunction of the system for proving identity? check-in	2
	development of security plans	2
	prevention of fault events in the system	3
	development of an analysis aimed at prevention of major accidents	3
	IRS response time to an adverse event	3
	risk of electricity interruption	3
safety and health at work	expertise of employees	3
	handling of hazardous substances	3
	control of the PPE use and control of their condition at the workplace	3
	regular health and safety training	3
	impact of the work environment on the quality of employee health	2
	expertise of employees	3
information security	security of passwords	3
	defining access to information	3
	operating system updates	2
	regular inspections of accession measures	2
	operating system software protection	3
	performing an internal security audit	2
sum of quantitative evaluation of indicators for the reference object		86
the total sum of the quantitative evaluation of the indicators for the reference object		108
percentage expression of the static resilience for the reference object		79.63%

5 Case study

The case study aims to present a method of evaluating the static resilience of buildings located in the sub-sector of the rail infrastructure. In Table 4 are shown the safety pillars, including the individual indicators and the assigned quantitative values on the scale 1 to 3. Table 4 does not describe individual indicators in terms of their scope. The reference object, which was decided to draw attention to and apply the proposed method of the static resilience assessment, is the rail station in Zilina. In Figure 2 is shown the surroundings and the interior of that rail station. The importance lies in the transport of people and goods within the national infrastructure and it is also the most important railway transport node, Figure 3, which is a part of the two pan-European corridors, namely:

- corridor No. V. - Bratislava - Zilina - Cierna n/T - state border Slovakia/Ukraine – Lvov,
- corridor No. VI. - Balt - Warszawa - Zwardon - state border Poland/Slovakia - Cadca - Zilina [36].

Subsequently, Table 4 presents expert estimation and analysis of the internal and external environment values for the indicators set here. Then the values of the indicators are added and the level of resilience of the evaluated reference object is expressed as a percentage. The resilience level is determined according to Table 3, in which the respective levels are defined.

The evaluated reference object within the proposed method of static resilience evaluation reached the total part of the values of indicators 86. Subsequently, the value by mathematical operation according to Equation (2) was expressed as a percentage to 79.63%, which means that the object reached only a good of the resilience level. It follows that the object can withstand and maintain basic functions in the case of adverse events from the external and internal environment. Deficiencies were identified in the system of the building, which may be a potential source of risks that could further affect its resilience and if the preventive measures are not taken, its functioning could be endangered in the future.

6 Results and discussion

The main goal of the article was to present the current results of applied research focused on the rail transport infrastructure resilience. Results of a detailed analysis of the institutional and juridical framework, together with the European Union‘s transport strategy, clearly confirm the current need for research in the areas of green and smart solutions. The EU‘s main goal for sustainable mobility by 2050 is to be climate neutral. In addition to research into the new vehicle propulsion, it is necessary to focus on smart solutions for transportation technology and increase safety with a vision of zero fatalities. This must be facilitated by the newly understood resilience of transport infrastructure [39].

Here is considered the current need to address the resilience of transport and transport infrastructure in a way to be scientifically supported by research articles. Examples from various countries and best practices from the real practice of developed countries are an inspiration for the continuous improvement of the solutions presented here. One of the challenges for the ZSR, as the administrator of the rail infrastructure, is to build a safety/security dispatching center, which would continuously monitor the specified safety and security parameters. The new modern information and communication technologies give a chance for solutions that would measure values of the selected indicators in the real state and show them in clear security maps (GIS applications) using the three traffic light colors; when the state is excellent (green), when there are partial problems (orange) and when there is a big problem (red).

Another result is the solution to challenges posed by the changing security environment - changes in the natural and social environment. Researchers primarily relied on results of the European research projects focusing on the extreme effects of weather on transport [40]. As a part of results of these projects, the new directions were defined how to cope with these extreme weather events [41]. The measures were directed mainly to quality maintenance, monitoring and timely repairs of selected transport facilities.

One can also include, as one of the results, a long-term focus on a comprehensive solution to safety issues [42]. The search for a multidisciplinary and multi-level solution brings effective and comprehensive proposals for the safety pillars with a link to relevant and measurable safety indicators. Security research has been a part of the EU‘s scientific research activities for more than 10 years.

In addition, some countries have conducted their own national security research. The current situation with the Covid-19 virus pandemic in Slovakia documents the need to reconsider the already divided division of science in Slovakia. If the company is to cope with all the similar safety and security challenges in the long term - pandemics, fundamental changes in weather extremes and other safety and security challenges, it is necessary to address scientific projects not only at the transnational but also at the national and even regional and local levels.

7 Conclusions

This article was aimed at approaching the issue of the critical infrastructure and importance of ensuring the functioning of elements included in the critical infrastructure system in the case of the impact of adverse events from the external and internal environment. The aim of the paper was to propose a method of static resilience assessment, which was designed for objects in the rail infrastructure, which can be included

in elements of the critical infrastructure. Previous research has pointed to an active solution to the issue of resilience of transport infrastructure, especially abroad. The Slovak Republic does not have any tools that would solve this particular issue. There is a latitude for new ideas and approaches that would move the issue of the resilience assessment forward. The proposed method of the static resilience evaluation represents the initial phase. Ensuring the informative value and the possibility of applying this method in practice requires even more discussions with experts who would be able to eliminate the shortcomings of the proposed method of assessing resilience using the selected pillars and their indicators with a specific description.

The main goal of the researchers is, in cooperation with partners from state institutions, companies and other research institutes, to create a usable application for practice, which will be the basis for the future safety/security dispatching of the Railways of the Slovak Republic.

References

[1] ECTRI strategy 2021-2030. Brussel: ECTRI, 7.12.2020.

[2] REHAK, D., SLIVKOVA, S., PITTNER, R., DVORAK, Z. Integral approach to assessing the criticality of railway infrastructure elements. *International Journal of Critical Infrastructures* [online]. 2020, **16**(2), p. 107-129. ISSN 1475-3219, eISSN 1741-8038. Available from: https://doi.org/10.1504/IJCIS.2020.107256

[3] Council Directive 2008/114/EC of 8 December 2008 on the identification and designation of European critical infrastructures and the assessment of the need to improve their protection - Europa [online] [accessed 2020-06-20]. Available from: https://op.europa.eu/sk/publication-detail/-/publication/ba51b03f-66f4-4807-bf7d-c66244414b10

[4] Mission, vision and values - Europa [online] [accessed 2020-06-25]. Available from: https://www.era.europa.eu/agency/mission-vision-and-values_en

[5] Directive (EU) 2016/798 of the European Parliament and of the Council of 11 May 2016 on railway safety [online] [accessed 2020-07-11]. Available from: https://eur-lex.europa.eu/legal-content/en/TXT/?uri=CELEX%3A32016L0798

[6] Common Safety Methods - Europa [online] [accessed 2020-07-12]. Available from: https://www.era.europa.eu/activities/common-safety-methods_en

[7] Law No. 45/2011 about critical infrastructure - Zakonypreludi[online] [accessed 2020-09-21]. Available from: https://www.zakonypreludi.sk/zz/2011-45

[8] National program for critical infrastructure protection and defense in the Slovak Republic condition - Mhsr [online] [accessed 2020-10-11]. Available from: https://www.mhsr.sk/uploads/files/c2CSdqQ5.pdf

[9] Methodology guidance n. 29014/2014-1000-53190 MH SR about security measures for the protection of critical infrastructure elements in the energy and industrs sectors - Economy [online] [accessed 2020-7-05]. Available from: https://www.economy.gov.sk/uploads/files/J4Vom9oj.pdf

[10] Methodology guidance n. 1321/2011-1020 Ministry of Economy of the Slovak Republic about protection of sensitive infromation on critical infrastructure and about method of manipulation with this infromations - Economy [online] [accessed 2020-09-01]. Available from: https://www.economy.gov.sk/uploads/files/v2vsqfd4.pdf

[11] DVORAK, Z. Crisis Management decision support system in railway infrastructure company. In: 18th International Conference Transport Means: proceedings. 2014. p. 169-172.

[12] Law No. 513/2009 about railways - Zakonypreludi [online] [accessed 2020-09-01]. Available from: https://www.zakonypreludi.sk/zz/2009-513#cl1-cast5)

[13] HOTEROVA, K. Safety plan of the selected railway infrastructure object. Diploma thesis. Zilina: University of Zilina, Faculty of Security Engineering, 2018.

[14] HOTEROVA, K., DVORAK, Z., BLAHO, P. Objectification of criteria for a critical infrastructure element in the rail transport sub-sector. *Transportation Research Procedia* [online]. 2019, **40**, p. 1349-1355. ISSN 2352-1465. Available from: https://doi.org/10.1016/j.trpro.2019.07.187

[15] Law n. 402/2013 about Office for regulation of electronis communications and Postal Services and Transport Office - Slov-lex [online] [accessed 2020-10-05]. Available from: https://www.slov-lex.sk/pravne-predpisy/SK/ZZ/2013/402/20131204.html)

[16] Transport Office of the Slovak Republic: transport on railways - Drahy [online] [accessed 2020-08-12]. Available from: http://drahy.nsat.sk/uvod/zakladne-informacie-2/)

[17] DVORAK, Z., LEITNER, B., MILATA, I., NOVAK,L. SOUSEK,R. Theoretical background and software support for creation of railway transport model in crisis situations. In: 14th World Multi-Conference on Systemics, Cybernetics and Informatics WMSCI 2010: proceedings. Vol. III. 2010. p. 343-347.

[18] PETIT, F., BASSETT, G., BLACK, R., BUEHRING, W. A., COLLINS, M. J., DICKINSON, D. C., FISHER, R. E., HAFFENDER, R. A., HUTTENGA, A. A., KIETT, M. S., PHILLIPS, J. A., THOMAS, M., VESELKA, S. N., WALLACE, K. E., WHITEFIELD, R. G., PEERENBOOM, J. P. Resilience measurement index: an indicator of critical infrastructure resilience. ANL/DIS-13-01. Argonne National Laboratory, U.S. Department of Energy [online]. Available from: https://www.researchgate.net/publication/299528136_Resilience_Measurement_Index_An_Indicator_of_Critical_Infrastructure_Resilience

[19] Risk and resilience report 9. Measuring critical infrastructure resilience: possible indicators - Center for Security Studies ETH Zurich [online] [accessed 2021-01-04]. 2015. Available from: https://css.ethz.ch/content/dam/ethz/special-interest/gess/cis/center-for-securities-studies/pdfs/SKI-Focus-Report-10.pdf

[20] NAN, C, SANSAVINI, G. A quantitative method for assessing resilience of interdependent infrastructures. *Reliability Engineering and System Safety* [online]. 2017, **157**, p. 35-53. ISSN 0951-8320. Available from: https://doi.org/10.1016/j.ress.2016.08.013

[21] KOZINE, I., PETRENJ, B., TRUCCO P. Resilience capacities assessment for critical infrastructure distribution: the READ framework (part 1). *International Journal of Critical Infrastructures* [online]. 2018, **14**(3), p. 199-220. ISSN 1475-3219, eISSN 1741-8038. Available from: https://doi.org/10.1504/IJCIS.2018.094405

[22] REHAK, D., SENOVSKY, P., HROMADA, M., LOVECEK, T. Complex approach to assessing resilience of critical infrastructure elements. *International Journal of Critical Infrastructure Protection* [online]. 2019, **25**, p. 125-138. ISSN 1874-5482. Available from: https://doi.org/10.1016/j.ijcip.2019.03.003

[23] Presidential policy directive-critical infrastructure security and resilience [online] [accessed 2020-09-21]. Available from: https://obamawhitehouse.archives.gov/the-press-office/2013/02/12/presidential-policy-directive-critical-infrastructure-security-and-resil

[24] National infrastructure advisory council - Critical infrastructure resilience final report and recommendations [online] [accessed 2020-09-15]. Available from: https://www.cisa.gov/sites/default/files/publications/niac-critical-infrastructure-resilience-final-report-09-08-09-508.pdf

[25] Resilience framework for critical infrastructures - Sintef [online] [accessed 2020-10-02]. Available from: https://www.sintef.no/globalassets/project/nexus/tesis-leire-labaka.pdf

[26] BESINOVIC, N. Resilience in railway transport systems: a literature review and research agenda. *Transport Reviews* [online]. 2020, **40**(4), p. 457-478. ISSN 1464-5327. Available from: https://doi.org/10.1080/01441647.2020.1728419

[27] DELOUKAS, A., APOSTOLOPOULOU, E. Static and dynamic resilience of transport infrastructure and demand: the case of the Athens metro. *Transportation Research Procedia* [online]. 2017, **24**, p. 459-466. ISSN 2352-1465. Available from: https://doi.org/10.1016/j.trpro.2017.05.082

[28] ADJETEY-BAHUN, K., BIRREGAH, B., CHATELET, E., PLANCHET J. L. A model to quantify the resilience of mass railway transportation systems. *Reliability Engineering and System Safety* [online]. 2016, **153**, p. 1-14. ISSN 0951-8320. Available from: https://doi.org/10.1016/j.ress.2016.03.015

[29] Resilient transport infrastructure to extreme events - Resistproject [online] [accessed 2020-10-21]. Available from: https://www.resistproject.eu/

[30] HOFFREITER, L., BYRTUSOVA, A. *Safety indicators*. Zlin: Radim Bacuvcik-Verbum, 2016. ISBN 978-80-87500-82-8.

[31] DURECH, P. Safety management of railway infrastructure object. Dissertation thesis. Zilina. 2020.

[32] THOMA, K., SCHARTE, B., HILLER, D., LEISMANN, T. Resilience engineering as part of security research: definitions, concepts and science approaches. *European Journal for Security Research* [online]. 2016, **1**, p. 3-19. ISSN 2365-1695. Available from: https://doi.org/10.1007/s41125-016-0002-4

[33] ENACHE, M. F., LETIA, T. S. Approaching the railway traffic resilience with object enhanced time Petri nets. In: 23rd International Conference on System Theory, Control and Computing: proceedings [online]. IEEE, 2019. ISSN 2372-1618. Available from: https://doi.org/10.1109/ICSTCC.2019.8885878

[34] RENARD, A., CHARLES, J. Underground railways in France: follow-up of safety indicators. *Transportation Research Procedia* [online]. 2016, **14**, p. 3342-3349. ISSN 2352-1465. Available from: https://doi.org/10.1109/ICSTCC.2019.8885878

[35] CHOVANCIKOVA, N., HOTEROVA, K. Indicators as a tool for assessing the pillars of the safety management system. *The Science for Population Protection* [online]. 2020, **12**(1), p. 1-12. ISSN 1803-635X. Available from: http://www.population-protection.eu/prilohy/casopis/42/367.pdf

[36] Modernization of railway corridors - Cvut [online] [accessed 2020-08-30]. Available from: https://www.fd.cvut.cz/projects/k612x1rz/prace/sk.pdf

[37] Railway station Zilina - Zilina-gallery [online] [accessed 2020-08-30]. Available from: https://zilina-gallery.sk/picture.php?/9964/category/763

[38] Railway corridors 2004 - Rail [online] [accessed 2020-08-30]. Available from: https://www.rail.sk/arp/slovakia/present/korid04.htm

[39] The 2021-2030 Integrated national energy and climate plan - Europa [online] [accessed 2020-10-20]. Available from: https://ec.europa.eu/energy/sites/ener/files/documents/ro_final_necp_main_en.pdf

[40] Risk analysis of infrastructure networks in response to extreme weather - Cordis [online] [accessed 2020-11-02]. Available from: https://cordis.europa.eu/project/id/608166/reporting

[41] TITKO, M., HAVKO, J., STUDENA, J. Modelling resilience of the transport critical infrastructure using influence diagrams. *Communications - Scientific Letters of the University of Zilina* [online]. 2020, **22**(1), p. 102-118. ISSN 1335-4205, eISSN 2585-7878. Available from: https://doi.org/10.26552/com.C.2020.1.102-118

[42] LEITNER, B., LUSKOVA, M., O´CONNOR, A., VAN GELDER P. Quantification of impacts on the transport serviceability at the loss of functionality of significant road infrastructure objects. *Communications - Scientific Letters of the University of Zilina* [online]. 2015, **17**(1), p. 52-60. ISSN 1335-4205, eISSN 2585-7878. Available from: http://komunikacie.uniza.sk/index.php/communications/article/view/393/363

TRANSPORT RISK IDENTIFICATION AND ASSESSMENT

Jaroslava Kubáňová, Iveta Kubasáková*

Department of Road and Urban Transport, Faculty of Operation and Economics of Transport, University of Zilina, Zilina, Slovak Republic

*E-mail of corresponding author: iveta.kubasakova@fpedas.uniza.sk

Resume

The transport process is characterized by transport operations and the relationships between them, the route, the time of transport and the type of product transported. One of these parameters is the degree of risk associated with a possible disruption of the transport process. Therefore, this article aims to present the possibility of calculating the degree of risk on the selected transport route. The risk level is calculated on based on the actual risk incidents on the transport route.

Article info

Received 14 January 2021
Accepted 19 January 2021
Online 20 May 2021

Keywords:

crime,
transport,
risk matrix,
measure

Available online: https://doi.org/10.26552/com.C.2021.3.F109-F115

ISSN 1335-4205 (print version)
ISSN 2585-7878 (online version)

This is an open access article distributed under the terms of the Creative Commons Attribution 4.0 International License (CC BY 4.0), which permits use, distribution, and reproduction in any medium, provided the original publication is properly cited. No use, distribution or reproduction is permitted which does not comply with these terms.

1 Introduction

The transport and logistics industry provide one of the most important services of the modern globalized and interconnected world. Since the beginning of 2020, more and more countries around the world have closed their borders and restricted traffic and travel in order to prevent the outbreak of coronaviruses (COVID-19) pandemic, thus creating barriers to international trade and transport. The pandemic affects almost every dimension of economic activity and individuals around the world. Due to the outbreak of coronavirus, the supply chains are limited in the logistics and transport industries, although they are different in the air, freight and maritime sectors. Nevertheless, the risk incidents occur that negatively affect the transport processes.

1.1 Global cargo crime trends

According to new research, the insurance company has the largest cargo theft in the world in the field of freight transport, whether it is a criminal activity during the transport or in a parking lot. In the following Figure 1 one can see a comparison of the total criminal activity in transport for selected years in the EMEA region. Most crimes occurred in Germany, France and the United Kingdom.

If one looks at the type of criminal activity, shown in Figure 2, one can notice that the most common criminal activities are theft from vehicle, theft of vehicle, theft of container or robbery. This is followed by theft from facility, fraudulent pick up, hijacking, etc.

There are different ways of parking on roads in Europe, in compliance with the Regulation 561/2006 or the AETR agreement (required rest of professional drivers), [2]. Some use regular public car parks, others park on the side of roads, while those more responsible rely on security car park services. The biggest problem is parking in unsecured parking lots. One can see in Figure 3 the number of attacks at unsecured parking places. Drivers use unsecured parking areas because there are few safe parking lots around the world. Their number in this period is 7500, which is absolutely insufficient with the growing number of road freight transport.

Risk identification

Identified risks along with their respective mitigation measures are:

- hijacking - the use of force (armed or unarmed), threat or intimidation to kidnap the driver in order to take the vehicle,
  - ❑ impact: loss of cargo, monetary loss, customer dissatisfaction, crew injury,
  - ❑ measures: insurance, safety parking spot, security equipment, training,
- robbery - the use of force (armed or unarmed), threat or intimidation in order to steal shipments/ cargo while employees, guards or drivers are present and coerced to allow access (open doors), hand over goods, hand over vehicle,
  - ❑ impact: loss of cargo, monetary loss, customer

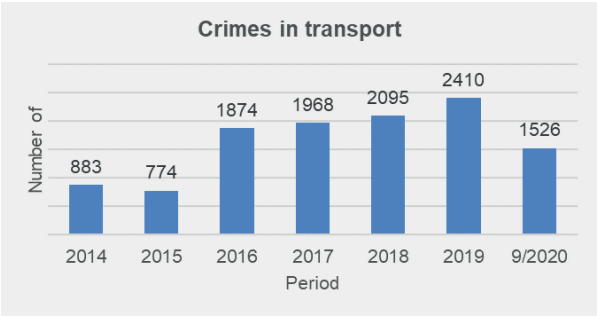


Figure 1 *Number of crimes in transport in EMEA region [1]*

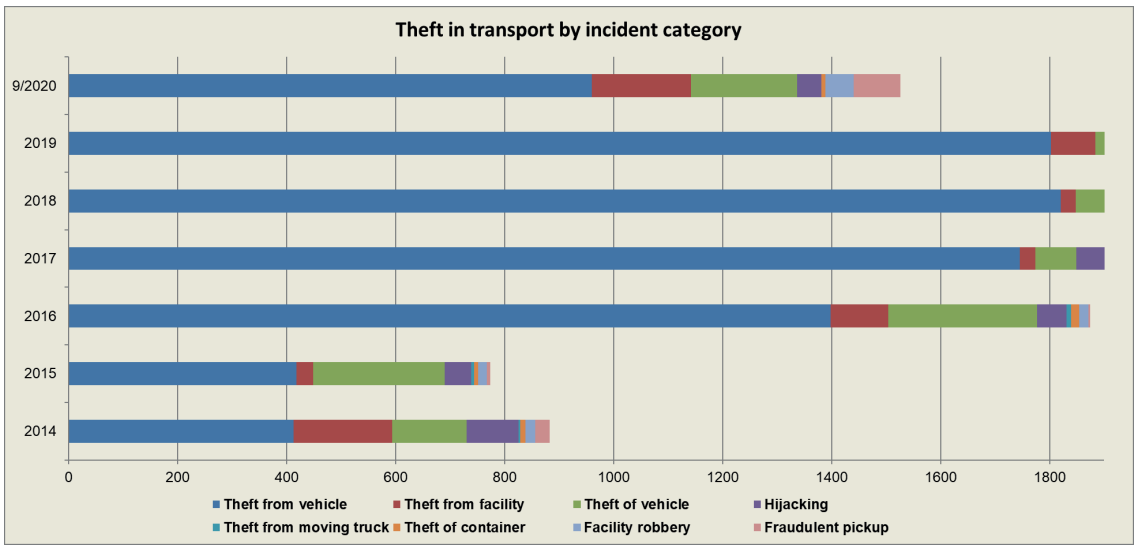


Figure 2 *Theft in transport by incident category [1]*

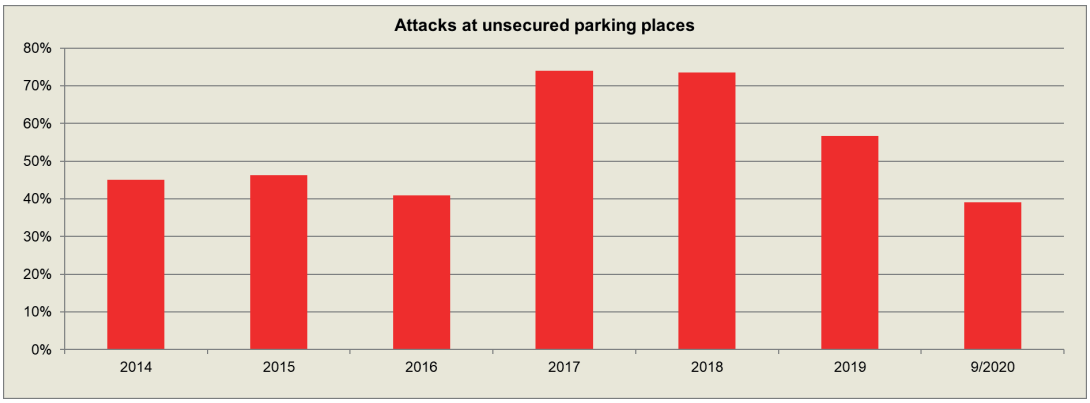


Figure 3 *The number of attacks at unsecured parking places [3]*

dissatisfaction, crew injury,
- ❑ measures: insurance, safety parking spot, security equipment, training,

- theft - general term for wrongful taking of property without the owner's willful consent,
  - ❑ impact: loss of cargo, monetary loss, customer dissatisfaction,
  - ❑ measures: insurance, training, safety parking spot, security equipment, trailer door monitoring,
- fraud - theft by deception; offense of deliberately deceiving another in order to damage them - usually, to obtain property or services from the victim unjustly,
  - ❑ impact: loss of cargo, monetary loss, customer dissatisfaction,
  - ❑ measures: insurance, training, verification of documents, verification of shipper [4-7].

1.2 Risk assessment matrix

The purpose of the risk assessment is to analyse and evaluate the identified risks to determine whether they need to be treated. Diagrams or matrices can be used to illustrate risks (See Table 1). This matrix is an example in which risks are assigned priority classes

Table 1 *Risk assessment matrix [7]*

	risk category			
likelyhood / frequency	I catastrophic	II critical	III marginal	IV negligible
frequent	1	3	7	13
likely	2	5	9	16
occasional	4	6	11	18
remote	8	10	14	19
unlikely	12	15	17	20

risk index	risk acceptance category
1 - 5	not acceptable
6 - 9	not desirable
10 - 17	acceptable with extra control
18 - 20	acceptable with no extra control

Table 2 *Matrix of losses and frequency [7]*

	losses and violence			
losses / frequency	catastrophic loss > 100 001 €	critical 100000 € < loss < 25001 €	marginal 25000 € < loss < 1001 €	negligible loss < 1000 €
frequent > 4.75	1	3	7	13
likely 3.5< li <4.75	2	5	9	16
occasional 2.25 < li < 3.5	4	6	11	18
remote 1 < li < 2.25	8	10	14	19
unlikely < 1	12	15	17	20

created by a combination of their acceptability and consequences. Such tables must be adapted to the needs of a particular organization or risk assessment objective. This risk assessment matrix contains hazards, which are categorized relatively to their degree of criticality among

- Catastrophic
- Critical
- Marginal
- Negligible,

based on their consequences in the activity under investigation. Since the frequency of each potential occurrence is important factor, this assessment risk matrix can be used to codify the risk assignment, which in conjunction with the risk assessment table present the total picture of the threats that company faces, their consequences and likelihood of occurrence [7] (see Table 2).

The risk assessment matrix is characterized according to the colour scheme that best describes the desired security level for each risk situation.

Beyond the qualitative calculation of the likelihood of occurrence for a catastrophic event, there is also the capability for quantitative computation of such a figure, in the case that the valid statistical data are recorded. Furthermore, the use of modern specialized statistical methods and models can offer significant increase in reliability of the calculation of the risk frequency of risks, with a dramatic contribution in the overall reliability of the risk assessment under examination. It is obvious that the calculated risk frequency is a crucial factor. Combined with the factor of Criticality, an organization can find out how urgent a certain risk is and then deal with it, according to the priority it assigns to that risk [8-10].

1.3 Risk assessment for transport route

For effective route planning and scheduling, it is necessary for the employees of the transport department to participate in the preparation of the distribution plan, or at least to know and understand it. The vehicle routing and planning process must meet the following objectives:

- maximizing the payload of a vehicle (by maximizing vehicle fill out and back) and maximizing vehicle utilization (by maximizing the number of loaded journeys per vehicle);
- minimizing distance (e.g., minimizing overlapping deliveries) and minimizing time (e.g., minimizing motionless time); and
- meeting the customer requirements in terms of costs, services and time and meeting the legal requirements in terms of vehicle capacity and driver hours [1, 11-13].

If the dispatcher wants to plan a safe transport for the driver, he must consider:

- date and place of loading,
- date and place of unloading,
- type of road infrastructure (highways, urban and

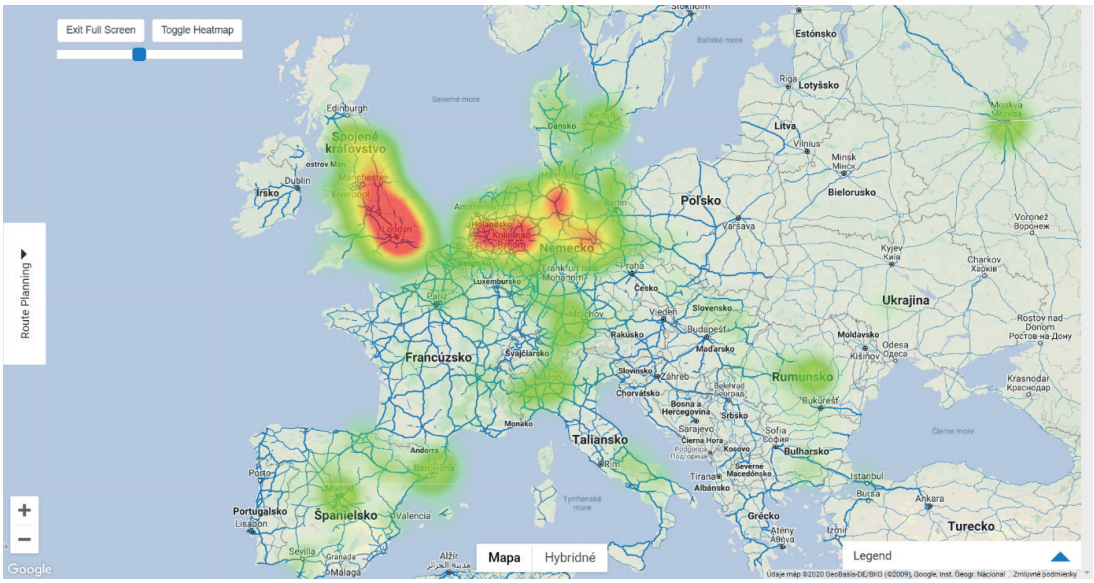


Figure 4 *The intensity of cargo crimes in the Europe in February 2020 [15]*



Figure 5 *The type of crimes in World in 2020 [3]*

rural roads),
- secure parking available,
- driving time restriction,
- risk assessment.

The road infrastructure is important due to the different speed limits and capabilities in place. If it is possible, for the highly valued transportations highways are preferred.

As mentioned above, during the transport, the driver is exposed to several types of risks [7]:
- theft,
- robbery,
- hijacking,
- fraud, etc.

One needs to make a category table of risk:

Incident type:
- Category I - hijacking, robbery, fraud
- Category II - vehicle theft
- Category III - theft from vehicle
- Category IV - other theft (theft of container, theft from facility, …)

Modus operandi:
- Category I - forced stop, violence
- Category II - deceptive stop
- Category III - intrusion
- Category IV - deception

Average monetary loss (€):
- Category I - Loss > 100 001 €
- Category II - 25 001 € < Loss < 100 000 €
- Category III - 1001 € < Loss < 25 000 €
- Category IV - Loss < 1 000 €

Likelihood Index:

This index is calculated based on the following formula:

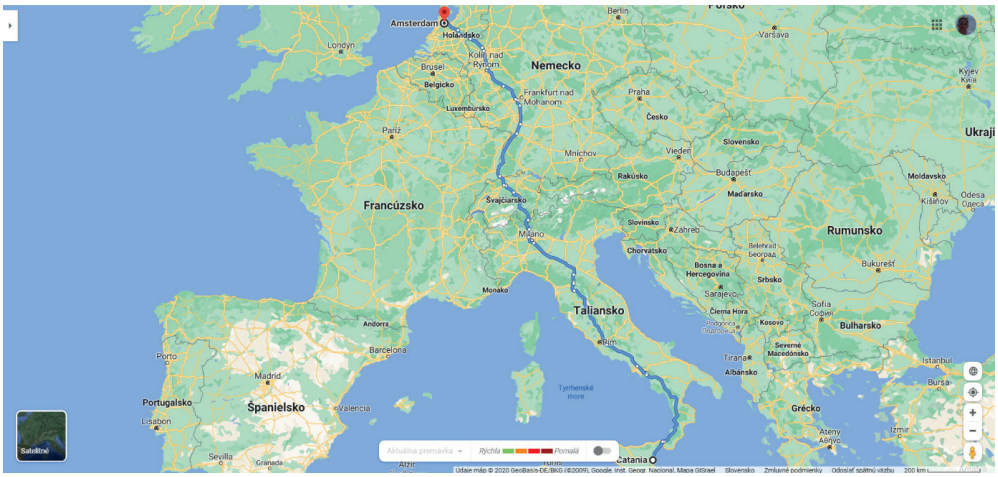


Figure 6 *The first transport route from Catania to Amsterdam [3]*

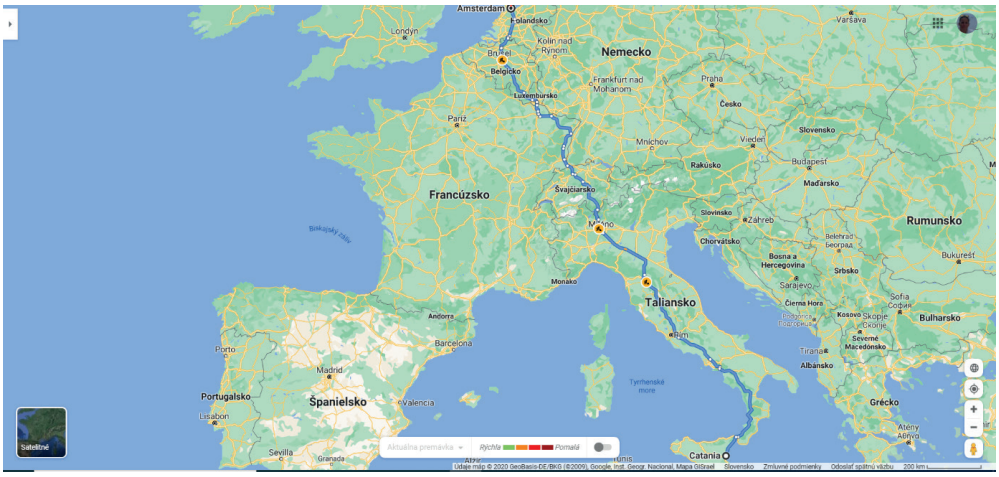


Figure 7 *The second transport route from Catania to Amsterdam [3]*

$$\text{likelyhood index} = \frac{\text{index/years}}{\text{km/100}} = \frac{\text{index} * 100}{\text{km} * \text{years}}, \qquad (1)$$

where:
km - the length of the route in km,
incidents - the number of incidents across the route,
years - the time period that includes the incidents [7].

1.4 Route planning

If the carrier wants to plan the transport with regard to safety, he must know the applications that will help him in this. One of them is the TAPA IIS database focused on the safe truck parking places. In addition to information about safety truck parking places, the IIS database also provide information about security incidents classified by several categories, including:

- burglary,
- fraud,
- hijacking,
- robbery,
- theft (theft from vehicle, theft from facility, theft of vehicle, truck theft) [1, 14].

Modus operandi:

- deception,
- deceptive stop,
- forced stop,
- fraud,
- internal,
- intrusion,
- pilferage,
- violent [9, 15].

In Figures 4 and 5 one can see the IIS heatmap tool, wich shows the intensity and type of the cargo crimes in the UK and the Netherlands in the month of February 2020.

The following example shows how the risk of criminal activity could be reduced by planning a transport route [16]. Two routes from Catania to Amsterdam (see Figures 6 and 7) were chosen. The characteristics of the individual routes are given below.

The data needed for calculation were taken from the IIS Database provided by TAPA. All incidents are reported by the TAPA EMEA members only. For the public, data from the database are provided only for the last 90 days. The complete database is only for members who pay for membership every year. The

Table 3 *Matrix of the first and second route information*

	kms	countries	incidents	likelihood index	average loss (€)	risk index
route 1	2416	4	92	7.616	68 000	10
route 2	2445	6	54	4.744	156 000	8

92 * 100 / 2416 * 0.5 = 7.616

58 * 100 / 2445 * 0.5 = 4.744

number of accidents on selected routes is for the first half of 2020 (see Table 3).

2 Results and discussion

From the case study one can evaluate the following conclusions:

Route 1:

Risk index: 10

Through:

- Italy, Switzerland, Germany, Netherland

Countries crossed: 4

Distance: 2416 km

Estimated total duration: 66 hours

Short breaks: 45 min - 4

Long breaks: > 45 min - 3

Number of incident: 92

Likelihood index: 7.616

According to the likelihood index, this risk is classified as Frequent.

Assessment Methodology:

Average money loss: 68 000 € from incident reporting money loss.

Category II

Risk acceptance category: **Not acceptable**

Incident type: 64 % of incidents reporting Incidents type are recorded as Theft from vehicle

Category III

Risk Acceptable category: **Not desirable**

Modus operandi: 68 % of incidents reporting a modus operandi are recorded as Deception.

Category IV

Risk Acceptable category: **Acceptable with extra control**

According to the above, route 1 is ranked at 3 for money loss, 7 for incident type and 13 for modus operandi.

Route 2:

Risk index: 8

Through:

- Italy, Switzerland, France, Luxemburg, Belgium, Netherland

Countries crossed: 6

Distance: 2445 km

Estimated total duration: 67.75 hours

Short breaks: 45 min - 5

Long breaks: > 45 min - 3

Number of incident: 54

Likelihood index: 4.744

According to likelihood index, this risk is classified as Likely.

Assessment Methodology:

Average money loss: 156 000 € from incident reporting money loss.

Category I

Risk acceptance category: **Not acceptable**

Incident type: 49 % of incidents reporting Incidents type are recorded as Theft from vehicle

Category III

Risk Acceptable category: **Not desirable**

Modus operandi: 53 % of incidents reporting a modus operandi are recorded as Intrusion.

Category III

Risk Acceptable category: **Not desirable**

According to the above, route 2 is ranked at 2 for money loss, and 9 for incident type and modus operandi.

3 Conclusions

After comparing the two routes, one could come to the following conclusions:

Route 1 is categorized as Not acceptable (3), Not desirable (7) and Acceptable with extra control (13). Route 2 is categorized as Not acceptable (2), Not desirable (9), Not desirable (9).

Route 1 is shorter and scored the same as route II in two categories - Average money loss and Incident type, but in Modus operandi category has an acceptable with extra control. Route 2 is longer and lead across six countries, so probability of the delay at the border is greater.

The security route risk assessment should always be a part of the route planning activity. The road risk assessment applies the standard risk assessment approach to many hazards associated with driving for work, including journey length, allowing enough time for the journey, arrangements to take a break, driving posture, route choice and thinking of alternatives to driving. The risk assessment is beneficial for carriers and their customers and can lead to prevention of possible losses from the risk accidents.

Acknowledgement

This paper was developed with support of a project: MSVVS SR - VEGA No. 1/0245/20 Poliak, M.: Identification of the impact of a change in transport related legislation on the competitiveness of carriers and carriage safety.

References

[1] IIS key glossary - Tapa Emea [online]. Available from: https://www.tapa-global.org/intelligence/iis-data-resource/iis-key-glossary.html

[2] Regulation (EC) no 561/2006 on the harmonisation of certain social legislation relating to road transport and amending Council Regulations (EEC) No 3821/85 and (EC) No 2135/98 and repealing Council Regulation (EEC) No 3820/85 [online]. Available from: https://eur-lex.europa.eu/legal-content/EN/TXT/HTML/?uri=CELEX:32006R0561&qid=1621250039404&from=SK

[3] Tapa Emea [online]. Available from: https://www.tapa-global.org/login.html?redirect _url=%2Fiis.html

[4] HLATKA, M., STOPKA, O. STOPKOVA, M.: Proposal of innovative flooring options for marine containers. *Nase More* [online]. 2018, **65**(4), p. 174-179. ISSN 0469-6255, eISSN 1848-6320. Available from: https://doi.org/10.17818/NM/2018/4SI.2

[5] KONECNY, V., SEMANOVA, S., GNAP, J., STOPKA, O. Taxes and charges in road freight transport - a comparative study of the level of taxes and charges in the Slovak Republic and the selected EU countries. *Nase More* [online]. 2018, **65**(4), p. 208-212. ISSN 0469-6255, eISSN 1848-6320. Available from: https://doi.org/10.17818/NM/2018/4SI.8

[6] BARTUSKA, L., STOPKA, O., LIZBETIN, J. Methodology for determining the traffic volumes on urban roads in the Czech Republic. In: 19th International Scientific Conference on Transport Means 2015: proceedings. 2015. ISSN 1822-296X, p. 215-218.

[7] LAIMOS, P., CHRONOPOULOS, M., LAIMOU, CH. White paper route risk assessment methodology [online]. 2020. Available from: https://docplayer.net/196079896-White-paper-route-risk-assessment-methodology-securing-your-mobility-document-date-march-2020-address-information.html

[8] KUBASAKOVA, I., SULGAN, M., KUBANOVA, J.: *Logistics for freight forwarding and road transport / Logistika pre zasielatelstvo a cestnu dopravu* (in Slovak). 2. ed. Zilina: University of Zilina, EDIS, 2020. ISBN 978-80-554-1700-4.

[9] POLIAK, M., SIMURKOVA, P., CHEU, K.: Wage inequality across the road transport sector within the EU. *Transport Problems* [online]. 2019, **14**(2), p. 145-153. eISSN 2300-861X. Available from: https://doi.org/10.20858/tp.2019.14.2.13

[10] BYRNE, J. Disabilities in tertiary education. In: *Voices of a margin*. ROWAN, L., MCNAMEE, J. (ed.). Rockhampton: CQU Press, 1994. ISBN 1875902066.

[11] POLIAK, M., POLIAKOVA, A. Relation of social legislation in road transport on driver's work quality. In: *Tools of Transport Telematics TST 2015* [online]. MIKULSKI, J. (ed.). Communications in Computer and Information Science, vol. 531. Cham: Springer, 2015. ISBN 978-3-319-24576-8, eISBN 978-3-319-24577-5, p. 300-310. Available from: https://doi.org/10.1007/978-3-319-24577-5_30

[12] SZYMANEK, A.: "Road Safety Sequence" - A New Concept of the Road Safety Management in Poland. *Communications - Scientific Letters of the University of Zilina* [online]. 2021, **23**(1), p. F1-F10. ISSN 1335-4205, eISSN 2585-7878. Available from: https://doi.org/10.26552/com.C.2021.1.F1-F10

[13] Roadsec [online]. 2019. Available from: https://www.roadsec.eu/

[14] SIKOROVA, A., BESTA, P., DUBRAVOVA, P., PROSICKY, P., KISSOVA, K., MACHOVA, K.: Lack of stocks risk reduction. *Acta Logistica* [online]. 2017, 4(3), p. 9- 13. ISSN 1339-5629. Available from: https://doi.org/10.22306/al.v4i3.8

[15] Time for action - Tapa Emea [online]. Available from: https://www.tapa-global.org/information/latest-news-views.html

[16] KAMPF, R., HLATKA, M., GROSS, P. Optimisation of distribution routes: a case study. *Communications - Scientific Letters of the University of Zilina* [online]. 2021, **23**(1), p. A62-A73. ISSN 1335-4205, eISSN 2585-7878. Available from: https://doi.org/10.26552/ com.C.2021.1.A62-A73

PREVENTION OF MAJOR ACCIDENTS OF MOBILE RISK SOURCES

Katarína Mäkká[1,*], Katarína Kampová[1], Jacek Dworzecki[2]

[1]Faculty of Security Engineering, University of Zilina, Zilina, Slovakia
[2]Faculty of Security Sciences, Military University of the Land Forces in Wroclaw, Wroclaw, Poland

*E-mail of corresponding author: katarina.makka@fbi.uniza.sk

Resume
At present, the issue of public safety in the production and manipulation of hazardous chemicals deserves more attention, since various major accidents such as fires, explosions and toxic gas releases take place frequently. The issue of prevention of emergency events has become more and more topical. The growing amount of hazardous substances transported leads to increased risk of emergencies. In order to reduce this risk in the transport of hazardous substances, a number of technical, operational, traffic and safety conditions and requirements must be fulfilled. These all contribute to the reduction of hazards and risks. The aim of the presented article was to determine the extent of the danger zone in the event of a gasoline leak due to a traffic accident in a built-up urban area with a high frequency of traffic and population movement.

Article info
Received 15 December 2020
Accepted 14 January 2021
Online 21 May 2021

Keywords:
dangerous goods,
emergency accident,
fuels,
mobile risk source,
prevention,
road transport

Available online: https://doi.org/10.26552/com.C.2021.3.F116-F122

ISSN 1335-4205 (print version)
ISSN 2585-7878 (online version)

This is an open access article distributed under the terms of the Creative Commons Attribution 4.0 International License (CC BY 4.0), which permits use, distribution, and reproduction in any medium, provided the original publication is properly cited. No use, distribution or reproduction is permitted which does not comply with these terms.

1 Introduction

Dangerous substances and articles are those which, by their nature, properties or conditions, may endanger the safety of persons, animals or the environment. The road transport of these substances must be carried out in accordance with the European Agreement concerning the International Carriage of Dangerous Goods (ADR). Hazardous chemicals and their transport are a significant mobile source of risk, especially due to the difficult prediction of their occurrence [1]. The transport routes are planned with regard to the starting and destination point of transport, time requirements of the customer to perform the transport, legislative restrictions related to the choice of route and optimization of a vehicle operation and driver‘s work. An essential determinant is the economics of transport, which significantly influences the decision-making of entities involved in the transport process and can have a significant impact on the degree of risk in transport. In the case of mobile sources of chemicals, a hazardous area is created along the transport routes.

In this context, the issue of prevention of major accidents is developing dynamically. Major accidents are significant events in the life of a society in particular its effects on human health, property or the environment. To prevent such major industrial accidents, many developed countries, including the US and EU, have implemented emergency management systems ranging from accident prevention, emergency preparedness and emergency response to accident relief [2].

The issue of prevention of major accidents, associated with the release of hazardous substances, is becoming a much-discussed professional public worldwide. At present, attention is being paid to mobile sources of risk, which are increasing the number of accidents during the transport of dangerous goods, namely: assessing the risks of spent fuel transportation and storage [3], evaluation of the safety level of fuel transportation [4], quantitative risk analysis of life safety and financial loss for road accident of fuel cell vehicle [5].

2 Analysis of the current situation in the field of security of fuel distribution

Road traffic accidents with the consequent release of hazardous substances endanger people‘s lives, property and the environment worldwide. The prevention and control of these accidents is drawing a growing attention from the whole society [6]. Therefore, the issue of prevention of such events and the resulting application of preventive measures come first. The European Union seeks to regulate this environment and set rules for all the transport participants, i.e. sender, carrier and consignee, as well as for other participants (e.g. loading, packing, filling organization, tank container operator, etc.). One of these instruments is the European

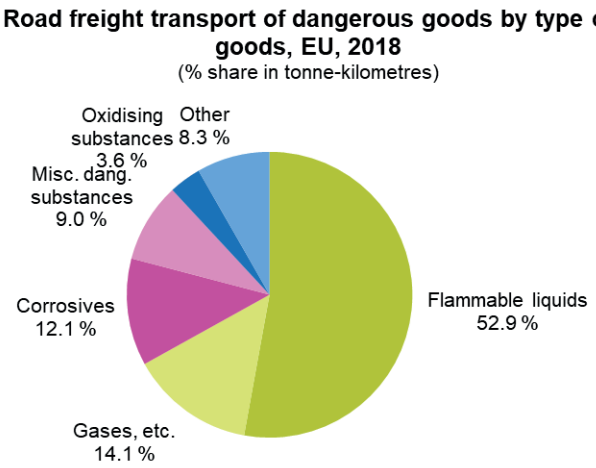


Figure 1 *Road freight transport of dangerous goods by type of goods in Europe [10]*

Agreement concerning the Transport of Dangerous Goods by Road (ADR), which was concluded on 30 September 1957 in Geneva under the auspices of the United Nations Economic Commission for Europe and entered into force on 29 January 1968, [7].

This Agreement was amended by the Protocol of Amendment to Article 14, paragraph 3, in New York on 21 August 1975, and entered into force on 19 April 1985, [8].

The ADR agreement has two technical annexes „Annex A and Annex B".

Pursuant to Article 2 of the ADR, dangerous goods, which have been excluded from carriage pursuant to Annex A may not be accepted for international carriage, whereas the international carriage of other dangerous goods may be authorized only after completion of:

- the conditions set out below in Annex A for these dangerous goods, with a special focus on their packaging and labeling requirements;
- the conditions set out below in Annex B, with particular reference to the requirements of the construction, equipment and operation of vehicles transporting these dangerous goods.

Annexes A and B have been regularly revised on a two-year cycle since the entry into force of the ADR.

Currently, contracting parties to the ADR are: Albania, Andorra, Austria, Azerbaijan, Belgium, Belarus, Bosnia and Herzegovina, Bulgaria, Cyprus, Czech Republic, Croatia, Denmark, Estonia, Finland, France, Georgia, Germany, Greece, Hungary, Iceland, Ireland, Italy, Kazakhstan, Latvia, Liechtenstein, Lithuania, Luxembourg, Malta, Montenegro, Morocco, Netherlands, Nigeria, North Macedonia, Norway, Poland, Portugal, Republic of Moldova, Romania, Russian Federation, San Marino, Serbia, Slovakia, Slovenia, Spain, Sweden, Switzerland, Tajikistan, The Republic of Uzbekistan, Tunisia, Turkey, Ukraine, United Kingdom of Great Britain and Northern Ireland.

Each Member State has adopted the ADR into its national law or has its own national rules. The ADR applies to transport operations carried out in the territory of at least two of the above Contracting Parties.

According Bernatik, the assessment of mobile risk sources is not yet prescribed by law in the European Union [9]. However, the transport of dangerous substances represents a particular hazard above all to the densely populated areas of urban zones, where releases of toxic or flammable substances into the air may endanger the health and/or lives of many inhabitants. To date, the evaluation of consequences of accidents from the mobile risk sources has been dealt with only haphazardly and not in detail.

2.1 Quantities of dangerous goods transported in the EU in 2018

Statistical data, directly related to the transport of dangerous goods, are available on the website of the European Statistical Office Eurostat. Between 2014 and 2018, most Member States of EU registered increase in transport of dangerous goods.

Figure 1 shows the types of dangerous goods in EU road freight transport in 2018. The largest specific productgroup was „flammable liquids", taking over more than half of the total (52.9 %). Two other groups, „gases (com-pressed, liquefied or dissolved under pressure)" and „corrosives", accounted for 14.1 % and 12.1 % respectively.There were very small changes compared to previous years, the distribution between product groups remained quite similar over time. The above statistical data show that the largest group in terms of

Table 1 *Selected accidents of tankers*

state	the cause of the accident	consequences
Iran (2004)	accident of a tanker carrying 18,000 liters of petrol	the explosion killed 200 people and injured 100 people
Africa (2006)	tank overturning and subsequent explosion	the explosion killed 35 people who tried to pump petrol from a crashed tank
Nigeria (2007)	the 33,000-liter tank crashed and subsequently exploded	the explosion killed at least 89 people and injured about 100 people
India (2007)	a jeep crashed into a diesel tank.	eleven people died in the crash, four suffered serious injuries
Iraq (2007)	a fuel tank exploded near a gas station	the explosion killed at least 50 people and injured 60
Czech Republic (2007)	traffic accident of a tanker transporting diesel	leakage of 30,000 liters of diesel. the oil got into the groundwater and into the stream, which is located near the crash site
Slovak Republic (2018)	the driver, for not identified reasons, went out of the way to the field	overturned the fully loaded tanker (30 000 liters of fuels), 33-year-old driver died
Italy (2018)	a tanker truck with petrol exploded after rear-ending a stopped truck	at least two people were killed, up to 70 injured and part of the raised expressway collapsed in the fireball

transported amount are flammable liquids (up to 52.9%) In the following text it is dealt with this specific group of hazardous substances.

2.2 Examples of some emergency events in the transport of fuels by road in the world and in the Slovak Republic

The most common causes of traffic accidents, according to long-term statistics from various countries, are:

- human in 85% of cases,
- the traffic route is the primary cause in 10% of cases,
- the means of transport is a source of accidents in about 5% of cases.

There are often several factors involved in accidents [1]. Although the competent authorities, carriers and drivers, pay the close attention to safety issues and compliance with the standards, rules and regulations laid down for the transport of road transport fuels, we are sometimes informed of accidents involving tanks carrying diesel, petrol or other dangerous substances. So far, accidents or incidents have occurred during the transport of petroleum products, which resulted in a vehicle fire, contamination of the surroundings with petroleum products, or groundwater contamination. The following accidents are well known (see Table 1).

An example of more recent accident in the transport of hazardous substances is the overturning and subsequent explosion of a tanker carrying 4,000 gallons of aviation fuel (15,000 liters). This event happened on February 20, 2020 in Indianapolis. The fire spread about 500 feet causing severe, catastrophic damage to the pavement and both sides of the bridge. The accident resulted in the death of the tanker driver.

A photo from the Indiana Department of Transportation (see Figure 2) shows wreckage after a fuel tanker overturned and caught fire at the intersection of interstates 70 and 465 on Indianapolis' east side on Thursday, Feb. 20, 2020.

3 Case study

The aim of the case study is to determine the extent of the danger zone in the event of a gasoline leak in a built-up urban area with a high frequency of traffic and population movement. Examples of the above-mentioned emergency events also prompted elaboration of a study focusing on urban development with a high concentration of inhabitants. The consequences of such events can cause injury or death to a large number of people.

In the Slovak Republic, fuels are the most often transported by road by the road tankers of a tractor with a semi-trailer [12]. Individual tank sets are multi-chamber (up to 6 separate chambers) with the possibility of transporting individual types of fuel at once, in different volumes, from 20,000l up to 50,000l.

For the purpose of the case study, an emergency



Figure 2 *A tanker overturned and caught on fire in the intersection of I-465 and I-70 on Indianapolis' east side on Thursday, Feb. 20, 2020 [11]*

Table 2 Survey of modeling results program TerEx

consequences of an emergency scenario	danger zones	(m)
Pool fire	first degree burns at a distance from the flame (m)	118
	failure of steel strength at a distance from the flame (m)	15
	10 % mortality from the tank	68
	50 % mortality from the tank	58
Plume atmospheric stability D / F	danger to persons from direct cloud impact	19/37
	serious damage to buildings	44.5 / 43.5
	danger to persons outside the building from serious injuries	66.5 / 57.5
	danger to persons through window glass	124 / 94.5
BLEVE (Boiling Liquid Expanding Vapor Explosion)	maximum diameter of the fireball (m)	99
	1st degree burns	479
	10 % mortality from the tank	259
	50 % mortality from the tank	209
	failure of steel strengthat a distance from the flame (m)	99

scenario was modeled: during the transport of gasoline, the entire transported amount of gasoline leaked from the tank in a built-up urban area with a high frequency of traffic and population movement. Estimated population density at the accident site 160 persons/ha. Source of risk: tank with a volume of 46 m^3, transported amount of petrol: 36,800 kg.

Currently, there are many software products available that allow scenario building and risk assessment [13-14]. Software products are based on physical models, they allow to take into account the influence of working conditions, properties of leaking substances and environmental influences on the extent of damage and contamination, which not only speeds up the calculation but also refines the data obtained [15].

The simulation tools TerEx was chosen for the purpose of simulating the consequences of an emergency event connected with the leakage of transported fuels.

The consequences of the emergency scenario were modeled in two representative types of weather conditions:

- normal air stability 4th class = D, medium wind speed - 5 $m.s^{-1}$ (most common conditions during the year),
- very stable conditions 1st class = F, wind speed low - 1.7 $m.s^{-1}$ (worst dispersion, affected largest area - the worst case scenario).

In the event of an emergency, associated with the leakage of the entire amount of gasoline from the tank, a risk for potential fatality would be for a person at a distance of 68 m from the crashed tank (see Table 2). The number of people at risk of an emergency was calculated from:

$$N = A \cdot P_D, \quad (1)$$

where: „N" is the number of persons at risk,
„A" is the total affected area (affected area) [ha],
„P_D" is the population density in the affected area [number of persons / ha].

Given the population density (160 inhabitants per hectar), 11.3 people will be potentially fatally injured. During the initiation and subsequent explosion of the escaped vapor cloud, the consequences of the explosion are worse in the case of atmospheric stability type F.

3.1 Preventive measures implemented by the management of transport companies

Transport and delivery of fuel to the customer requires compliance with international and national regulations, safety and especially the timeliness of delivery. This time pressure can cause non-compliance with the specified regulations at some stage of the fuel transport.This can ultimately lead to an emergency in the transport process and consequently endanger life, health, property and the environment. The rapid action can minimize the negative effects of emergencies and thus the degree of threat to the population in the vicinity of their occurrence.

One way to reduce the risks arising from the fuel distribution process is to comply with the prescribed operating and transport conditions, set by the ADR agreement by the participants in the transport process (i.e. consignor, transporter, consignee, vehicle manufacturer) and compliance with safety regulations when handling fuel (during the filling, dispensing fuel). However, even the best regulations will not prevent accidents and incidents in the road transport. It is only during the liquidation of traffic accidents that insufficient compliance with the above regulations is detected. Not enough attention is paid to:

- vehicle markings (incorrectly used or missing warning signs),
- the correct and accurate classification of the substance being transported in Class 3,
- vehicle equipment (prescribed mandatory equipment),
- permissible mass of the vehicle with fuel,
- readiness, professionalism and training of the driver transporting fuel.

According to an interview with an employee of a transport company that deals with the fuel transport, in the past, in the liquidation of traffic accidents or during the inspection activity, they were fully convinced that insufficient attention was paid to the above-mentioned important regulations, e.g. insufficient marking of consignments, missing warning signs and inscriptions of technical marking, inaccuracy in the classification of dangerous substances, poor storage conditions, deficiencies in the use of transport packaging.

If one discusses the accident in the transport of fuels, the most common cause of accidents is considered to be the human factor, namely:

- Inexperienced driver - insufficient control of the complexity and specificity of the liquid substances transport in tanks. Employers should therefore entrust the transport of fuel-trained drivers with sufficient experience,
- Driver fatigue caused by failure to observe the prescribed driving and rest times,
- Wrong declaration in the consignment note, which can make it difficult to deal with an emergency.

The driver's readiness to deal with an emergency, the assessment of the situation and the subsequent decision on appropriate measures, as well as their precise implementation, would ensure that the emergency would not cause extensive loss of life, health, property or the environment.

Based on a summary of the above causes of accidents, the conclusion was drawn that it is important for the fuel companies to employ drivers with many years of experience and experience in driving a tank. Driving a tank truck is an art. But even here the principle applies that the talent and courage alone are not enough. The art of safe and reliable driving with fuels is acquired through many years of practice and constant learning. Investing in drivers' education and training pays off for the company. Although the training consists of final tests and examinations, this does not ensure that the tank driver will comply with the regulations.

All these findings and negative experiences from the past should lead the transport companies to improve transport services and increase safety of the fuel transport. It is therefore important to inform, educate the drivers and all the workers who handle hazardous materials, in the form of conferences, seminars and training. These are ways to avoid unnecessary damage, loss, endangerment of lives, environmental pollution or major disasters.

4 Conclusion

The issue of the safe transport of fuels is currently becoming very disscussed worldwide. The aim of the presented article was to point out to the need to prevent major accidents of mobile sources of risks. The impuls for preparation of the case study were the recent emergency events associated with the leakage and subsequent explosion of transported flammable liquids in the densely populated areas of urban zones with a high concentration of population.

Based on the model calculations, the zones of danger to the population in the event of a leak of the transported flammable liquid substance were determined. Based on the simulation of selected emergency scenarios, it is possible to imagine the danger posed to the surroundings by a tank truck with petrol with a volume of 46 m^3.

Therefore, the issue of prevention has recently come to the fore. Dangers associated with use of the fuel transport must be anticipated and identified in time, but, above all, through appropriate preventive and mitigation measures it is necessary to prevent their possible negative effects.

Acknowledgment

This paper is a result of the science project „VEGA 1/0173/21 Research of measures implemented by security managers in the organizations related to the occurrence and spread of COVID-19 and in other emergency situations“.

References

[1] MOZER, V., LOVECEK, T., VELAS, A., MAKOVICKA, L. Fire safety and security threats identification and elimination. *Advanced Materials Research* [onine]. 2014, **1001**, p. 306-311. ISSN 1022-6680, eISSN 1662-8985. Available from: https://doi.org/10.4028/www.scientific.net/AMR.1001.306

[2] LEE, K., KWON, HM., CHO, S., KIM, J., MOON I. Improvements of safety management system in Korean chemical industry after a large chemical accident. *Journal of Loss Prevention in the Process Industries* [online]. 2016, **42**, p. 6-13 [accessed 2020-05-19]. ISSN 0950-4230 Available from: https://doi.org/10.1016/j.jlp.2015.08.006

[3] MIRAE, Y., ROBBY, CH., BO, G. K., BELAL, A., JAEHYUN, H., SANGHOON, L., HYUN G. A software tool for integrated risk assessment of spent fuel transportation and storage. *Nuclear Engineering and Technology* [online]. 2017, **49**, p. 721-733 [accessed 2020-05-18]. ISSN 1738-5733. Available from: https://doi.org/10.1016/j.net.2017.01.017

[4] ZHONGYANG, L., CHUNHUA, CH., SHENGPENG, Y., BIN, W., LIJUAN, H., JIN, W., YICAN, W. Safety evaluation of spent fuel road transportation based on weighted nearest neighbor method. *Annals of Nuclear Energy* [online]. 2019, **127**, p. 412-418 [accessed 2020-05-22]. ISSN 0306-4549. Available from: https://doi.org/10.1016/j.anucene.2018.12.036

[5] SUN, K, LI, Z. Y. Quantitative risk analysis of life safety and financial loss for road accident of fuel cell vehicle. *International Journal of Hydrogen Energy* [online]. 2019, **44**, p. 8791-8798 [accessed 2020-05-21]. ISSN 0360-3199. Available from: https://doi.org/10.1016/j.ijhydene.2018.10.065

[6] REHAK, D, SENOVSKY, P., HROMADA, M. LOVECEK, T. Complex approach to assessing resilience of critical infrastructure elements. *International Journal of Critical Infrastructure Protection* [online]. 2019, **25**, p. 125-138 [accessed 2020-05-19]. ISSN 1874-5482. Available from: https://www.sciencedirect.com/science/article/pii/S1874548218301744

[7] United Nations. European Agreement concerning the Transport of Dangerous Goods by Road (ADR) [online] [accessed 2020-05-18]. 2019. eISBN 978-92-1-004891-0, p. 668. Available from https://www.adr.sk/dohoda-adr-2019/.

[8] Council of Europe. Protocol of Amendment to Article 14, paragraph 3 of the European Agreement of 30 September 1957 concerning the International Carriage of Dangerous Goods by Road [online] [accessed 2020-05-18]. 1975. p. 3. Available from://oemmndcbldboiebfnladdacbdfmadadm/https://unece.org/DAM/trans/danger/publi/adr/Protocole_e.pdf

[9] REHAK, D., BERNATIK, A., NOVOTNY, P. Preference risk assessment of hazardous substances road transportation. In: European Safety and Reliability Conference Safety and Reliability ESREL 2014: Methodology and Applications: proceedings. 2014. ISBN 978-1-138-02681-0, p. 1671-1676.

[10] Road freight transport of dangerous goods by type of goods in Europe [online] [accessed 2020-05-18]. Available from: https:// ec.europa.eu>eurostat>images

[11] A tanker overturned and caught on fire in the intersection of I-465 and I-70 on Indianapolis‘ east side on Thursday, Feb. 20, 2020 [online] [accessed 2020-05-20]. Available from: https://eu.indystar.com/picture-gallery/news/2020/02/20/jet-fuel-tanker-explodes-on-citys-east-side/4823811002

[12] REHAK, D, SENOVSKY, P., HROMADA, M. LOVECEK, T., Novotny, P. Cascading impact assessment in a critical infrastructure system. *International Journal of Critical Infrastructure Protection* [online]. 2018, **22**, p. 125-138 [accessed 2020-05-20]. ISSN 1874-5482. Available from: https://www.sciencedirect.com/science/article/pii/S1874548215300251

[13] RISTVEJ, J., ONDREJKA, R., SIMAK, L., LOVECEK, T., HOLLA, K., LACINAK, M., SURINOVA, L., JANOSIKOVA, M. Simulation technologies in risk prevention within crisis management. In: European Simulation and Modelling Conference ESM ´2016 -Modelling and Simulation: proceedings. 2016. ISBN 978-90-77381-95-3, p. 327-330.

[14] SIVAKOVA, L., LOVECEK, T. Modelling and simulation of crisis phenomena as a new tool for research and training in visegrad countries. *Key Engineering Materials* [online]. 2017, **755**, p. 346-352. ISSN 1662-9795. Available from: https://doi.org/10.4028/www.scientific.net/KEM.755.346

[15] JANTOSOVA, A., DOLNAK, I., DADO, M. An overview of vehicular ad hoc networks. In: 17th IEEE International Conference on Emerging eLearning Technologies and Applications ICETA 2019: proceedings. 2019. ISBN 978-1-7281-4967-7, p. 305-308.

komunikácie
COMMUNICATIONS

VEDECKÉ LISTY ŽILINSKEJ UNIVERZITY
SCIENTIFIC LETTERS OF THE UNIVERSITY OF ZILINA

VOLUME 23 Number 3

https://doi.org/10.26552/com.J.2021.3

Author guidelines

- All papers have to deal with the topic of transport and be submitted strictly within one of the listed subtopics. Please, refer to list of topics and subtopics here and indicate it clearly when submitting your paper.
- Submitted papers must be unpublished and must not be currently under review for any other publication.
- Manuscripts written in good English must include abstract and keywords also written in English. The abstract should not exceed 10 lines. Please provide minimum three up to maximum seven keywords which express the principal topics of the paper.
- Submitted manuscripts should not exceed 20 pages including figures and graphs.
- Submission should be sent by e-mail – as an attachment – to the following address: komunikacie@uniza.sk.
- The author‘s exact mailing address, full names, E-mail address, telephone or fax number, the name and address of the organization and workplace (also written in English) must be enclosed.
- For all manuscripts a double-blind peer review by at least two independent reviewers and language correction is mandatory.
- After reviewing and incorporating the editor‘s comments, the final draft (before printing) will be sent to authors for final review and minor adjustments.

The full author quidelines are available at:
http://komunikacie.uniza.sk/index.php/communications/guidelines

Editor-in-chief:
Branislav HADZIMA - SK

Associate editor:
Jakub SOVIAR - SK

Executive editor:
Sylvia DUNDEKOVA - SK

Honorary members:
Otakar BOKUVKA - SK
Jan COREJ - SK (in memoriam)
Milan DADO - SK
Pavel POLEDNAK - CZ

Editorial board:
Greg BAKER - NZ
Abdelhamid BOUCHAIR - FR
Pavel BRANDSTETTER - CZ
Mario CACCIATO - IT
Jan CELKO - SK
Andrew COLLINS - GB
Samo DROBNE - SI
Erdogan H. EKIZ - MA
Michal FRIVALDSKY - SK
Juraj GERLICI - SK
Vladimir N. GLAZKOV - RU
Ivan GLESK - GB
Mario GUAGLIANO - IT
Andrzej CHUDZIKIEWICZ - PL
Jaroslav JANACEK - SK
Zdenek KALA - CZ
Antonin KAZDA - SK
Michal KOHANI - SK
Jozef KOMACKA - SK
Matyas KONIORCZYK - HU
Tomas LOVECEK - SK
Frank MARKERT - DK
Jaroslav MAZUREK - SK
Marica MAZUREKOVA - SK
Vladimir MOZER - CZ
Jorge Carvalho PAIS - PT
Peter POCTA - SK
Maria Angeles Martin PRATS - ES
Pavol RAFAJDUS - SK
Che-Jen SU - TW
Giacomo SCELBA - IT
Janka SESTAKOVA - SK
Eva SVENTEKOVA - SK
Eva TILLOVA - SK
Anna TOMOVA - SK
Franco Bernelli ZAZZERA - IT

Address of the editorial office:
University of Zilina
EDIS – Publishing House
Univerzitna 8215/1
010 26 Zilina, Slovakia

E-mail: komunikacie@uniza.sk

Individual issues of the journal can be found on:
http://komunikacie.uniza.sk

Each paper was reviewed by two reviewers.

Journal is excerpted in **SCOPUS** and **EBSCO host**.

Published quarterly by University of Zilina
in EDIS – Publishing House of University of Zilina

Registered No: EV 3672/09

ISSN (print version) 1335-4205
ISSN (online version) 2585-7878

ICO 00397 563

July 2021